Ivan S. Gutzow · Jürn W.P. Schmelzer

The Vitreous State

Thermodynamics, Structure, Rheology, and Crystallization

Second Edition

Springer

The Vitreous State

Ivan S. Gutzow • Jürn W.P. Schmelzer

The Vitreous State

Thermodynamics, Structure, Rheology, and Crystallization

Second Edition

Springer

Ivan S. Gutzow
Institute of Physical Chemistry
Bulgarian Academy of Sciences
Sofia
Bulgaria

Jürn W.P. Schmelzer
Institut für Physik
Universität Rostock
Rostock
Germany

ISBN 978-3-642-34632-3 ISBN 978-3-642-34633-0 (eBook)
DOI 10.1007/978-3-642-34633-0
Springer Heidelberg New York Dordrecht London

Library of Congress Control Number: 2013934285

Preface

The first edition of the present monograph was met with interest by the glass science community, and at the end of 1996, it was practically already completely sold out and, thus, open for preparation of a second edition. However, in the following 15 years to come, we, both authors of the first edition, were involved with a variety of projects connected with experimental applications and even with the technical realization of some of the ideas developed in our book. Particular attention was given also by both of us to further theoretical generalizations of the results already achieved. In particular, both authors were involved with the study and with the development of problems, connected with the very essence of the theory forming the basis for the understanding of the glass transition, of the apparent kinetic stability, and of segregation processes and crystallization of glass-forming systems. In some respect, these were projects connected with the application of glasses as a very specific material and particular physical state of matter.

In the first edition of the present book, already the conviction was expressed that common, e.g. silicate glasses are only the most popular, the experimentally most frequently investigated, and, in many respects, the theoretically best-known representatives of matter in this particular state, the vitreous state. This notion was one of the leading ideas in writing the first edition of our book: analyzing the state of common glasses supplies us simultaneously with valuable information on many other systems in which matter exists as a particular frozen-in immobilized state. Thus, it was to be expected that results, obtained on common glasses, could be of use in many other fields of science. In this respect, the evidence obtained with technical glasses and especially with simple model glasses could and can be, so we hope, applied also to the vitreous-like states of matter in cases, when experimental analysis and theoretical modeling are more difficult or even impossible. Here we have first to mention the particular cases of *unusual* glasses, like vitreous ice, or of aqueous solutions with particular biological properties, allowing even life to be frozen-in into the vitreous-like state of absolute anabiosis. It is well known that there are even proposals to consider cosmic objects like black holes or the excited state of light in lasers like being in physical situations similar to those existing in common glasses. Let us mention also the case of comets: according to present-day

knowledge, the kernel of comets is constituted of vitreous ice. If this is so, it would turn out that 99.9 % of water in the universe as a whole is not to be found in the form of the common water of our oceans but exists as vitreous ice. In speaking about such seemingly extreme cases of systems with vitreous-like behavior or vitreous-like states, it becomes evident how significant in fact can be the knowledge and especially the lack of knowledge in investigating glasses and glassy systems.

The years after 1995 have been a time in which many well-known specialists in the field of glass science devoted their efforts to the development of ideas or models to describe vitreous states in a general way. Here first we have to mention ideas based on modeling glass-like systems in terms of statistical mechanics, for example, based on general concepts like mode-coupling theory, energy landscape approaches, models based on extended lattice hole approaches (with nonsymmetric two-minima energetic wells), and many others. The results obtained with most of these statistical physics models were however in many respects disappointing: some of the results even contradicted experiment; others gave only commonly known information. This is the reason why the efforts of several scientific groups were mainly concentrated on the development of ideas connected with the phenomenology, that is, with thermodynamics and overall kinetics of glass transition in terms of the more general formulation of thermodynamics, especially of the thermodynamics of irreversible processes in its simplest, linear formulations. Out of the cooperation of both authors of the present monograph in the time elapsing between 1995 and 2012, more than 40 common publications have been developed. They have been published in the international literature, and most of them are devoted to the analysis of the thermodynamic state, the structure, and the crystallization of glass-forming systems. We have prepared in the same time (in cooperation with two Russian colleagues, Oleg V. Mazurin and Alexander I. Priven, and two Bulgarian coworkers, Boris P. Petroff and Snejana V. Todorova) also a second monograph (J. W. P. Schmelzer and I. S. Gutzow, “Glasses and the Glass Transition”, Wiley-VCH, 2011) where the interested reader can find summarized and further developed many of the problems initiated and formulated in the first edition of the present book. A brief account of these new developments, going at part widely beyond the results presented in latter monograph, can be found here in Chap. 14 and in several footnotes to the text of the present second edition. Particular efforts of both authors were also concentrated on the development of thermodynamic problems connected with phase formation in glass forming systems; in the framework of this subject, one of the present authors (J.W.P.S.) developed an approach, to which particular attention is given in the second part of the above-mentioned Chap. 14.

Thermodynamics is the science which has to decide where to put and how to describe any state of matter. This is the reason why this great phenomenological approach is used in the present book. However, thermodynamics was classically derived as a science describing only systems in equilibrium and in predicting changes, which can and have to take place between different equilibrium states, for example, when one of them is more stable than the other. On the other hand, vitreous states, as proven already by the first investigations of the thermodynamics of glasses, are nonequilibrium states: this is their particular and most striking

characteristics. Sometimes this particular feature of glasses is expressed in terms of ergodicity and non-ergodicity: in the sense that glasses are non-ergodic systems. However, in doing so, it is usually forgotten that even the definition of ergodicity is at present open to discussion: this is why the use of the more generally defined notion of equilibrium and nonequilibrium seems to be more appropriate to the present authors at least to define a particular state in terms of properly understood, defined, and accepted notions. It is known and discussed in details in Chap. 5 of the first edition of our monograph that the investigations, which led to the conclusion that glasses are nonequilibrium, systems that is, non-thermodynamic bodies were reached in the beginning of the 1920s in connection with the efforts to verify Nernst's heat theorem and the third principle of thermodynamics by several of the most outstanding representatives of twentieth century classical thermodynamics. This problem is also summarized in Chap. 14, and its development represents an exciting scientific story retold by the present authors in two contributions cited there. It was F. Simon who proposed a remarkable approximation which has given the possibility to describe for a number of purposes with sufficient accuracy both glass transition and the thermodynamic properties of glasses. This approximation, governing the development of ideas and their treatment and development into what can be called the initial phenomenological theory of glass, was for more than 90 years adopted in glass science. This approximation of F. Simon was taken as a leading tool and the main idea in writing the first edition of the present book and in developing the ideas described there. We hope that this development, we decided to perform beginning with the 1990s, showed the really great advantage of Simon's approximation. We described in its framework the glass transition itself, vapor pressure and solubility of glasses, influence of the conditions of vitrification on glass properties, relaxation, stabilization, and crystallization of glass-forming systems: all this is given in the first edition of our book.

But the reader will also see how our efforts also indicated the deep limitations of Simon's approximation, the estimate of errors, introduced by it in both scientific thinking and prediction: to this is devoted a particular publication of both authors, also mentioned in Chap. 14. It turned out that the development of the basic idea of Simon's approximation also brought with it the further developments out and beyond of it, to which the efforts of the present authors lead as a logical consequence. And this consequence was that the second phenomenological stage in the theory of glass transition and in the description of glasses has to be the generic application to this problems of the following, the nonequilibrium stage of thermodynamics itself, of the development of thermodynamics, already several times mentioned in the present preface, into the thermodynamics of irreversible processes, as it was developed by scientists like De Donder, Prigogine, de Groot, and many others.

As indicated with the title of our book, our intention was and is also to continue the idea of another great scientist of mid twentieth century, Gustav Tammann, who proposed to treat glasses out of mysticism as a physical state, although as a *particular* physical state, and this was what also gave the title to his little famous booklet with the German title *Der Glaszustand*. We tried with the first edition of our

monograph to continue not only a tradition introduced by Tammann in the title of our book, but also to follow a remarkable idea formulated by this great scientist.

In adopting this idea and assuming irreversible thermodynamics to be the key, allowing one to open a new way of the description of glass transition and description of glasses, we had also to introduce into our book a generalized summary of essential basic thermodynamics in the form we thought that it is most convenient to be applied to glass science. It is introduced in the first chapters of the first edition of our book and gives not only essentials of thermodynamics, but also, what seemed to be even more necessary to the present authors, the direct applications of classical thermodynamics in the form of Simon's approximations to vitreous states and the necessary preparation for the second step: to go beyond classical thermodynamics. From the point of view of classical thermodynamics the kinetics of nucleation, of crystallization, and of phase transitions in glasses were treated in great details. The strict employment of thermodynamics led us to a further development of Gibbs model of the thermodynamics of nucleation. In this respect, we would like to acknowledge the close cooperation, in particular, of V. V. Slezov, A. S. Abyzov (Kharkov, Ukraine), V. G. Baidakov, G. Sh. Boltachev (Yekaterinburg, Russia), V. M. Fokin (St. Petersburg, Russia), and E. D. Zanotto (Sao Carlos, Brazil). Treating both vitrification and stabilization of glasses and the crystallization of glass-forming systems strictly and consequently in the framework of thermodynamics – in both its classical and newer formulations – is one of the features, in which most probably our book differs from most textbooks and monographs devoted to glass science.

In trying to open thermodynamic thinking and application of thermodynamics to glasses even to beginners in glass science, we introduced in the first two chapters of the book a thermodynamic introduction beginning with the essentials of classical thermodynamics and continuing further on to what we thought was necessary for the next and decisive step of any-one interested in glass science, including the thermodynamics of nonequilibrium. This basic idea was noticed by our readers and, we may even say, appreciated by many of our colleagues. In Chap. 3 of our book moreover, a direct introduction is given into the thermodynamics of irreversible processes: at least into the essentials we considered necessary to understand vitreous state and vitrification from this enlarged standpoint of thermodynamics. In this way from a beginning with the essentials of glass science and irreversible thermodynamics as they are introduced in Chap. 2 of our book and in developing ideas and methods to the third chapter, the present authors also enlarged their own possibilities to treat and analyze vitrification in the specific features of thermodynamics of irreversible processes. Beginning in 1996, both authors made the necessary efforts to develop their ideas on glass science in connection with the basic principles of thermodynamics of irreversible processes.

It is also to be noted that the first edition of this book published in 1995 was born in two series of lectures on the fundamentals of glass science given by one of the present authors in a series of courses in Bulgarian universities (at the Assen Zlatarov Technical University in Bourgas, 1985–1995 in collaboration with Dr. B. Bogdanov) and then (in 1996–2002 at the Chemical Technical University

in Sofia with Dr. I. Gugov) and after that in a joint lecture course of the two present authors at the Physical Institute of Rostock University in Germany at the beginning of the 1990s. In 1996–1999, this course of lectures was continued by I. S. Gutzow in collaboration with Prof. L. D. Pye at the Alfred College of Glass and Ceramics of the State University of New York (USA) and in 1995 also at the Federal University of Sao Carlos in Brazil. In all these lecture courses, the thermodynamic accent was always of significance in order to bring glass science to students of both theoretical physics and in engineering chemistry and ceramic materials. The generalized treatment of glasses in terms of the thermodynamics of irreversible processes was initiated by the same author (I.S.G.) by a course he had to give as several lectures at a Black Sea conference on the theory of amorphous states and the structure of glasses held in the little town of Sozopol in 1996. A resume of his lectures was published as two overview contributions given as references in Chap. 14 of the present second edition. The title of one of these papers was formulated as *The generic phenomenology of glass formation*. This title was proposed by the conference proceedings editor, a well-known American colleague, Prof. P. Boolchand.

Of even greater significance in preparing several of the publications of both authors in employing thermodynamics of irreversible processes to describe glasses and glass transitions were the conferences and lecture courses organized by one of the present authors (J. W. P. Schmelzer) annually for more than 15 years, now, at the Bogoliubov Laboratory of Theoretical Physics of the Joint Institute for Nuclear Research in Dubna (Russia), under the title *Nucleation Theory and Applications*. The presence at these conferences and the benefit of discussions with our colleagues including outstanding well-known scientists like W. Ebeling, D. H. E. Gross, V. P. Skripov, V. V. Slezov, V. G. Baidakov, V. P. Koverda, A. M. Gusak, B. M. Smirnov, A. P. Grinin, A. K. Shchekin, G. E. Norman, G. T. Guria, R. Feistel, S. A. Kukushkin, V. S. Balizkij, and colleagues from the St. Petersburg glass school like I. G. Polyakova, V. M. Fokin, B. Z. Pevzner, V. K. Leko, L. Landa, and many others were of greatest significance because practically any new idea developed by the authors was first discussed and partly even published as preprints in the proceedings of these conferences (available as pdf files via Internet at http://theor.jinr.ru/meetings/2012/nta/) and then adopted and included in following scientific publications and in the present book. In fact, several of the considerations of both authors connected with the thermodynamics of glasses were initiated by their analysis of the most significant peculiarities of crystallization of glass-forming melts discussed in the course of these conferences. It is also a great pleasure to acknowledge the financial support from the DFG, the DAAD, the Heisenberg-Landau program of the BMBF, QSIL Langewiesen (Dr. F.-P. Ludwig), the Leibniz Institute for Tropospheric Research Leipzig (Dr. O. Hellmuth), the Russian Foundation for Basic Research, and other sponsors of our activities as well as the hospitality and support of the Joint Institute for Nuclear Research in Dubna, Russia (Dr. V. I. Zhuravlev, Mrs. G. G. Sandukovskaya, Mrs. E. N. Rusakovich). We would like to express here our particular gratitude to the DFG for long-standing financial support both of the stays of J. W. P. Schmelzer in Sofia and I. S. Gutzow in Germany. One

of the authors (J.W.P.S.) would like to express his deep gratitude to the Institute of Physical Chemistry in Sofia for long-standing hospitality and for electing him as an Institute Associate Member and to the Bulgarian Academy of Science for decorating him with the Marin Drinov Medal of Honour acknowledging the very fruitful cooperation over a period of more than three decades. The other author (I.S.G.) would like to express his deep gratitude to the Alexander von Humboldt Foundation for the Humboldt Research Prize 2002–2003 assigned to him and for the possibilities it opened to him for his work at German universities. Thanks are to be expressed as well to the same organization for the grant given to Dr. J. Möller for a stay in Sofia in 2005 allowing him to perform joint work with both authors at the Institute of Physical Chemistry of the BAS. This prize allowed also one of the authors to perform joint research with Prof. C. Ruessel at the Otto-Schott Institute of the Friedrich-Schiller University in Jena. In particular, it allowed I. Gutzow et al. to perform investigations with DARA in Cologne on crystallization experiments under cosmic conditions discussed in details in Chap. 14. Here particular thanks are to be expressed to DARA for the financial support for this cosmic project. Also of significance for the development of the thermodynamic aspects of glass science problems treatment were the three Glass and Entropy Workshops, organized in 2008, 2009, and 2012 by our colleagues L. Wondraczek and R. Conradt initiated by discussions at the 21st ICG Congress in Strasbourg in 2007. In these discussions, the significance of thermodynamic thinking was brought to its full development, especially when it turned out necessary to be used in analyzing and even in rejecting not sufficiently founded opinions. J.W.P.S. would like to express his particular gratitude to the highly interesting cooperation with BASF Ludwigshafen (Dr. H. Baumgartl) on technological problems of production of polymeric foams, to Dr. F.-P. Ludwig (QSIL Langewiesen) for long-standing scientific cooperation including the analysis of a variety of problems of the technology of silicate glass production, and to Dr. O. Hellmuth for the cooperation on different aspects of the physics of the atmosphere and the influence of phase formation processes on its dynamics.

The evolution of ideas themselves, the developing knowledge of the authors in cooperation and discussion with their protagonists or antagonist gave impetus to new developments: development new to both authors and to their colleagues in many parts of glass science. This development as it took place in the last 15 years is summarized here in Chap. 14 of the present second edition of our monograph. The first publications, in this new direction were a series of papers beginning in 2000 by one of the present authors and his Bulgarian colleagues and continued in collaboration of both present authors. In the framework of these first publications we have to mention our Bulgarian colleagues V. Yamakov, F. Babalievski, and D. Ilieva and in particular our American colleague, Prof. L. David Pye. In the following period of joint developments, we have especially to mention the contributions of J. Möller, B. Petroff, S. Todorova, and I. Avramov. In this time, we had to introduce into the treatment of vitrification one of the most specific notions of thermodynamic of irreversible processes: the entropy production accompanying any irreversible process. This analysis was then continued in a series of papers by J.W.P. Schmelzer

with his German colleagues from the Polymer Physics Laboratory of C. Schick in Rostock in cooperation with T. V. Tropin from Dubna, Russia, and then with R. Pascova and quite recently in application of thermodynamics of glasses to problems of electrochemistry with L. Wondraczek and N. Jordanov. Finally, we would like to acknowledge the support of A. S. Abyzov in the course of the preparation of the present book and to N. Jordanov for similar assistance and especially in writing of Chap. 14.

In this way, the present two authors hope to have initiated and brought to a new, higher level of understanding the analysis of vitrification and of the properties of glasses in the most natural way possible: in the framework of thermodynamics of irreversible processes. It turned out that the process of glass transition can be described in a generic way out of first principles of thermodynamics of irreversible processes without introducing additional approximations. For many years, the peculiarities of glass and especially the complicated nature of its thermodynamics led many authors into the belief that new and more new *glassy* models are necessary in order to describe glass and improve the level of its understanding. Our experience shows that in fact it is not the development of more and more new models but a better understanding of the existing sound thermodynamic basis in the form of the thermodynamics of irreversible processes which is of major significance in developing a new understanding of glass science.

For several years, we performed intensive work trying to reorganize our first monograph: we tried to add several new topics and to introduce new ideas and the concepts of the thermodynamics of irreversible processes in a more advanced form into the original structure of the first edition. The realization of this task turned out to be a very difficult problem not solved by the present authors. So we tried to bring to the attention of the devoted readers of our book on the thermodynamics and the kinetics of the vitreous state in its initial formulation, adding in Chap. 14 and in several footnotes a brief account of these new developments which followed since 1996 both from our own work and in the publications of colleagues who worked in the same field of science. We have tried to summarize also in our already-mentioned second monograph most of the ideas developed in the time 1996–2010.

We hope that this way of preparing the second edition of this monograph is the most appropriate one and that most colleagues, who would like to try to begin and continue study of glasses, would like to have the original form of our first book as an introduction into thermodynamics in its essentials and especially also the application of thermodynamics and kinetics to the processes of crystallization of glasses in the form as they are given in the first edition. So following this believe and the outspoken advise of several colleagues, we decided to prepare the second edition of our book preserving its original kernel, however, extending it in adding the following parts: (i) in Chap. 14, the development of the generic way of treating glasses and glass transition in the way this was done mainly by the present authors is reviewed briefly including also new developments in the theory of phase transformation processes in glass-forming systems. (ii) With footnotes, some necessary corrections and new developments are introduced which have become apparent 15 years after the first publication. (iii) The main text is reprinted in an widely identical form as in

the first edition except minor corrections, for example, of several misprints. (iv) In the second edition, we have provided our book with an index.

We hope that in such a combination the interested reader will find the optimal way to follow the developments as they have been initiated and performed by the present authors and may be even of help to find better ways of further developing the science of glass. In this way, we hope to bring to the attention of our colleagues interested in the theory and the application of glasses a book which can be used as a bridge between classical thermodynamics and the classical way of treatment of the theory of glasses in an approximative approach following the new ideas and possibilities opened by the thermodynamics of irreversible processes. This science in the opinion of the present authors is the only theory, which indicates new ways in which all these strange physical states denoted as vitreous or glassy states may be treated from a simple and sound theoretical standpoint. For many years, glass science is never any more the story about the Egyptian queen Hatseputh (1500 BC) and the glassy beads of her necklace nor the story of fine wine glasses and even not of optical glasses: it is now more and more the new material in sun-energy convertors, of glassy quick-dissolving medicines, of frozen-in life and anabiosis, and even of a variety of processes taking place in the universe. Time has come to understand that although glass is not the fourth state of matter as proclaimed by enthusiastic glass researchers of the 1920s, it is one of the most interesting physical states, in which matter can exist. We hope that the renewed second edition of our book will help both people, experienced in glass and its problems, and newcomers, even students in materials science, in physics and in physical chemistry, to learn something new about one of the oldest materials mankind has ever employed.

Sofia, Bulgaria — Ivan S. Gutzow
Rostock, Germany, 2012 — Jürn W.P. Schmelzer

Preface to the First Edition

The present book is devoted to problems of a physically very important state of condensed matter – the vitreous state. We tried to summarize here the experimental evidence and the different theoretical approaches – structural, thermodynamic, and those of statistical physics – connected with the formation, the kinetic stability, and with the general nature of glasses as a particular physical state. In addition, a summary is given on the information available concerning processes of nucleation and crystallization of glass-forming systems; on methods of preventing or, in contrast, catalyzing crystallization in vitrifying liquids; on the kinetics of nucleation; on the modes of crystal growth in undercooled melts; and on the devitrification of glasses.

It was our aim to summarize in the present volume the basic principles and the most significant developments of a newly emerging science – glass science – and to show that, at least, in principle, any substance can exist in the vitreous state. Moreover, we have tried to demonstrate that the characteristic properties of the vitreous state may be attributed under certain conditions not only to systems with an amorphous structure (like the common glasses) but also to a number of other states of condensed matter including the crystalline one. This ambitious program includes problems and requires the application of methods from different scientific disciplines: classical thermodynamics and, in particular, the thermodynamics of irreversible processes, statistical physics, structural modeling and rheology of liquids, theory of phase formation, and crystal growth. In some cases, more advanced mathematical methods have also to be used.

Proceeding with the realization of our program, we recognized that we could not expect all our readers to be equally experienced in all of the mentioned fields. Although they have the common interest in the fundamentals of glass science, they may study or work in very different fields of science and technology. With this idea in mind, we decided to include in the respective chapters short discussions of the basic assumptions and results of different scientific approaches applied to the interpretation of experimental results concerning the structure and properties of vitreous materials. In this way, the present book may serve as an introduction into glass science from two points of view: on one hand, with respect to the basic

experimental results concerning the vitreous state and their theoretical analysis as well as to the methods applied in this respect. On the other hand, it is intended to give the reader the opportunity of following the argumentation in other more specialized books and articles on glass science that already exist and, as we hope, also those which will be written in future.

The mentioned general attitude in describing the vitreous state and its general character – the concentration on fundamental aspects and the broad scope of the discussion ranging from the introduction into basic ideas to the most recent developments – distinguishes, as we hope, the present book from any other of the existing monographs devoted to glasses, or more generally, to the description of disordered structures. The realization of such a program is, of course, a difficult task, and only the reader can decide whether we have succeeded in finding the right compromise between a resume of modern results and an introduction into the basic ideas of glass science.

Of help in this respect was a joint course of lectures we prepared and held together at the University of Rostock in 1990 as well as lecture courses on the fundamentals of glass, given by one of us at the Technical Universities of Bourgas and Sofia. Both authors have been working for years on the problems the book is devoted to. Thus, it was natural that many of our own results, obtained at part in close cooperation, are reflected in it. This long-standing cooperation also had a major impact on the way the book was prepared: in the present monograph, each chapter, any page is written by both authors, is the result of manifold repeated discussions of the respective scientific problems, of the search for the best way of outlining the respective ideas and results. In this way, of course, both of us also have to take the responsibility for any mistakes or shortcomings.

Many of the results, outlined in the book, were obtained with the help of colleagues and coworkers. We would like to express our gratitude to all our coauthors for giving permission to use their published or even as yet unpublished results. Here we have to mention, in particular, Dr. I. Avramov, Dr. J. Bartels, Dr. A. Dobreva-Veleva, Dr. E. Grantcharova, I. Gerroff, F.-P. Ludwig, Dr. M. Marinov, Dr. A. Milchev, Dr. J. Möller, E. Pancheva, Dr. E. Popov, Dr. R. Pascova, Dr. I. Penkov, B. Petrov, Prof. B. Samouneva, Dr. F. Schweitzer, Dr. H. Tietze, and Dr. I. Tomov. In the process of formation of the ideas outlined in the present book, we could benefit from numerous discussions with colleagues at the institutes, at meetings, colloquia, and conferences, from common efforts to find the most appropriate way in interpreting and understanding the properties of vitreous materials and glasses. We are indebted to many people who helped us in this way in writing the book. Here we would like to mention first Prof. R. Kaischew (Sofia), Prof. S. Christov (Sofia), Prof. H. Ulbricht (Rostock), and Prof. W. Ebeling (Berlin) who supported our work in many respects. Major parts of the results included in the book were obtained at the Institute of Physical Chemistry of the Bulgarian Academy of Sciences at a time when an atmosphere of discussion and fruitful competition had been created and maintained by a great scientist and organizer of science, the founder of the institute, Prof. Kaischew. Many of the following pages are devoted to the results in the physics of crystal growth obtained by him. We would like to express our sincere thanks to many

other colleagues from Sofia, Prof. D. Kashchiev and Prof. I. Markov; from Rostock, Prof. G. Röpke, Dr. R. Mahnke, and Dr. U. Lembke; and from the international scientific *glass and crystallization*, community, Prof. O. V. Mazurin (St. Petersburg), Prof. D. Uhlmann (Boston), Prof. L. D. Pye (Alfred University, New York), Prof. A. A. Chernov (Moscow), Prof. V. V. Slezov (Kharkov), Prof. W. Vogel (Jena), Dr. W. Goetz (Jena), Prof. W. C. Johnson (Pittsburgh), and Dr. W. Vogelsberger (Jena), who helped with ideas, suggestions, fruitful criticism, or in any other form. We would also like to commemorate here the common efforts and many results obtained with our late colleague Dr. S. Toschev. One of us would like to remember with love and appreciation the memory of his father, Prof. Stoyan Gutzow, who introduced many students and also his son to his knowledge and admiration for problems of the technology and science of glass.

As already mentioned, the present book is the result of long-standing cooperation between both authors working in different institutes. Such a cooperation could only be realized with the financial support the authors received from different organizations. In particular, we would like to express our gratitude to the Deutsche Forschungsgemeinschaft (Dr. H. Leutner, Dr. D. Schenk) as well as to the Bulgarian National Science Foundation, for giving financial support for a number of common research projects including the present monograph. We would like to thank also Mrs. Z. Ivancheva who prepared the numerous (more than 150) original figures and did an enormous amount of work in solving a number of technical problems. Last but not least, it is a pleasure for us to mention and acknowledge the patience, the understanding, and support of our families we could enjoy in the course of writing the book.

Sofia, Bulgaria — Ivan S. Gutzow
Rostock, Germany, 1995 — Jürn W.P. Schmelzer

Contents

Chapter 1
Introduction

Silicate glasses belong with pottery, ceramics and bronze to the oldest materials employed by men. This early widespread application is in some respect due to the broad distribution of glasses in nature. As an example, magmatic rocks can be mentioned, which consist to a large degree of vitreous silicates or completely amorphous natural glasses such as obsidian or amber. It is well-known, that the natural glass obsidian served as a material for the preparation of the first cutting tools of primitive men. In the ancient cultures of Central America, obsidian served as the material for the ritual knifes of high priests.

The wide distribution of glasses in nature is not due to chance. The inner part of the earth, characterized by very high values of pressure and temperature, is itself an enormous glass-forming melt. Processes of crystallization and glass-formation connected with the eruption of volcanos and the more or less abrupt cooling processes of parts of this melt determine to a large degree the course of geological processes and the structure and properties of the lithosphere. Natural glasses are widespread not only on earth but also on the moon as it became evident from the investigation of samples of lunar rocks brought to earth by the lunar expeditions (see, e.g., Pye et al. [653]).

The first applications of glasses in primitive societies for a limited number of purposes was followed by a long evolution to the modern glass industries and glass science. From the point of view of the variety of properties of glasses and the spectrum of possible applications the importance of different glasses can hardly be even estimated. The validity of this statement becomes evident if one tries to imagine for a while things surrounding us in everyday life without the components made of vitreous materials. Technical glasses like chemically resistant glass or optical glasses are also well known to everyone. Imagine, for example, a chemical plant, a physical laboratory, a car or a dwelling house without glasses or let us think about the importance of silicate glasses for optical devices, in particular, in microscopy and astronomy.

In addition to the classical oxide and particularly silicate glasses in the last decades new classes of vitreous materials have gained importance, consisting of substances or mixtures of substances for which the possibility of existence in the

I.S. Gutzow and J.W.P. Schmelzer, *The Vitreous State*,
DOI 10.1007/978-3-642-34633-0_1, © Springer-Verlag Berlin Heidelberg 2013

vitreous state was thought as being exotic or even impossible. One example in this respect are metallic glasses. Metallic glasses in a period of about 10 years were transferred from a stage of exotic research to the stage of production and world-wide technological application. Similar examples are glassy polymers or vitreous carbon, glass-forming chalcogenide or halide systems. The development of modern methods of information technology e.g. of cable TV is also based on glass, on extremely pure, defect-free vitreous fibres with particular optical properties.

With the increase of the number of substances, which can be obtained in the vitreous state, also the variety of properties and possible applications of glasses has been increased. Beyond the traditional applications in technology and science, glassy materials are also used as substitutes for biological organs or tissues, e.g., as prostheses even in ophthalmology. Glass-forming aqueous solutions with biologically relevant compositions are used as a carrier medium for the freezing-in of biological tissues. Thus, it seems that even life can be frozen in to a glass thus solving the problems of absolute anabiosis within the vitreous state. Porous silicate glass particles are used to supply nutrient solutions to microbial populations and slowly soluble glasses containing exotic oxides are used as an ecologically compatible form of micro-element fertilization.

Besides pure glasses, glass-ceramics like Pyroceram, Vitroceram, Sital – partly crystalline materials formed from devitrifying glasses – are also gaining in importance. In such materials the transformation of the melt into the desired vitrocrystalline structure is initiated by a process of induced crystallization usually caused by the introduction of insoluble dopants (crystallization cores or surfactants) into the melt. As a result heterogeneous materials are formed in which the properties of glasses and crystals are combined. In this way an astonishing variety of new materials with extreme properties and unusual possibilities of application is obtained: classical enamels, glass-ceramics (like Pyroceram) and so called glass ceramic enamels give an example in this respect.

The widespread application and development of different vitreous materials and their production was connected with a thorough study of related scientific and technological aspects, resulting in the publication of a number of monographs, devoted to special classes of vitreous materials or special technological processes like the technology of silicate glasses, glassy polymers, metallic glasses. In these books mainly specific properties of the particular glasses discussed or of the technological processes connected with their production are analyzed.

The aim of the present book is different. The specific properties of various vitreous materials are not studied in detail but the attempt is made to point out the main fundamental properties and features which are common to all glasses independent of the substrate they are formed from and the way they are produced. Hereby particular attention is directed to the specification of the thermodynamic nature of any glass independent of its composition or any other specific properties. Special glasses or technologies connected with their production will be discussed only as far as it is desirable as an illustration of general statements or conclusions.

The present monograph is structured as follows. In Chap. 2 we first give a phenomenological description of processes which can be observed during the cooling of

glass-forming melts. Properties of the melts and the glasses are described together with the way of evolution of historically important ideas and suggestions concerning the nature of the vitreous state and the mechanism of glass formation. The basic definitions, derivations and equations, required for the theoretical interpretation of the experimental results, are introduced and discussed briefly to allow even non-specialists in glass science to follow in detail the conclusions derived later. The experimental results summarized in this chapter give the basis for a test and verification of theoretical developments outlined in the subsequent parts.

A detailed analysis of the experimental results and their theoretical interpretation, given in Chap. 2, leads to the conclusion, that glasses from a thermodynamic point of view are frozen-in non-equilibrium systems. The thermodynamic description of such states and their specific thermodynamic properties is outlined in Chap. 3. This discussion is based on the general postulates of the thermodynamics of irreversible processes and, in particular, on the method of description of non-equilibrium states, developed by De Donder. The thermodynamic analysis is followed in Chap. 4 by an outline of basic ideas concerning the structure of different glasses.

Chapter 5 is devoted to statistical-mechanical model calculations of properties of glass-forming melts which allow one an interpretation of experimental observations, for example, in the framework of the free-volume theory of liquids. In Chaps. 6–10, criteria are developed to answer the question under which conditions a given substance can be brought into the vitreous state. Of major importance in this respect are problems of the kinetics of nucleation (Chaps. 6 and 7) and crystal growth (Chaps. 8 and 9) and factors determining the overall course of phase transformations in glass-forming systems (Chap. 10). These processes may be affected considerably by a primary liquid phase separation as outlined in detail in Chap. 11.

The crystallization of glass-forming melts, its initiation and control or inhibition, respectively, determines to a large degree the possibility to transform a melt into a glass or to synthesize a glass-ceramic material with a predetermined structure, degree of crystallization and desired properties. On the other hand, crystallization processes and phase transformations in glass-forming melts have served as model systems for the development and verification of different concepts concerning the kinetics of phase transformation processes also in other fields of science and technology. By both reasons the derivation of criteria of glass formation is started with a thorough discussion of the kinetics of nucleation and growth processes.

The criteria for glass formation derived in Chap. 10 show that there is no principal division between different substances with respect to the ability to be transformed into the vitreous state. For some substances the conditions for glass formation can be realized easily in laboratory, for other materials sophisticated methods, e.g., ultra-rapid cooling, vapor quenching or plasma sputtering have to be applied. For a third group of substances the criteria obtained indicate that even the most elaborated of the existing vitrification techniques developed till now with cooling rates reaching about ten millions degrees per second are not sufficient to produce a glass. There is, however, no principal limitation that with more powerful methods these substances could be also vitrified in future. From such a point of view it follows as a general consequence that the vitreous state is a possible form of existence of, in principle,

all pure substances or mixtures. In this respect, glass science is no more the description of a limited number of materials but a general theory for a state, possible for practically all substances.

The transformation of more and more materials into the frozen-in non-equilibrium state of a glass is connected also with a substantial change in the meaning of the word glass. Originally under glasses only amorphous (in the sense of non-structured) frozen-in non-equilibrium systems were understood. At present every frozen-in non-equilibrium state (non-amorphous systems included) is denoted sometimes as a glass, e.g., frozen-in crystals, crystalline materials with frozen-in magnetic disorder (spin glasses) etc.

Glass-forming melts represent a unique material also with respect to their rheological properties. In particular, in the vicinity of the transformation region from the melt to a glass glass-forming systems cannot be considered usually as classical Newtonian liquids. The specific rheological properties of glass-forming melts are of significance for most of the technological processes in glass production and also for processes of crystallization and cluster growth. This is the reason why these properties are considered in detail in Chap. 12.

As it is seen from the given overview of the contents the present book is directed to an analysis of the fundamental problems of glass science which are of importance for the understanding of the properties of glasses, in general. In this discussion of the basic ideas concerning the vitreous state the historic course of their evolution is also briefly mentioned. Hereby not a chronologically exact or comprehensive description is attempted but a characterization of the inner logic of this evolution, the interconnection of different ideas. This approach implies that in addition to the most fruitful concepts and ideas, which, as it turned out later, were real milestones in the evolution of glass science, also proposals are analyzed, which already at the time of their formulation or by the subsequent developments were shown to be incorrect or even misleading, at least, as far as it is known today. To the opinion of the authors only by such an approach can a correct picture of the evolution of science as a struggle between different or even contradicting ideas be given. On the other hand, the detailed analysis of differing proposals and the proof that some of them are not correct is of an undoubted heuristic value. Such an approach can also prevent any overenthusiasm with respect to insufficiently substantiated new hypotheses or to old already refuted ideas presented in a modern form. This was one of the leading ideas in writing the first edition of the present book. It is also followed in this second edition.

A discussion of the vitreous state and of the history of glass science would be incomplete without a short characterization of the contributions of, at least, some of the men, whose names are closely connected with the development of the modern theory of glasses. G. Tammann, O. Schott, E. Berger, I. F. Ponomaryev, A. Winter-Klein, D. Turnbull, A. A. Lebedev, E. A. Porai-Koshits and many others became well-known in science mainly by their investigations of basic properties of glasses, of the nature of the vitreous state, of the interconnections between crystallization and glass formation, of the structure of glasses. Important insights into the understanding of glass structure are due also to such outstanding

representatives of structural chemistry, in general, like V. M. Goldschmidt, G. Hägg, L. Pauling and J. Bernal. V. M. Goldschmidt was the first to develop geometrical or crystal-chemical criteria for glass formation, which allowed one the prediction of a whole new class of glass-forming systems. Based on Goldschmidt's ideas W. H. Zachariasen formulated his beautiful model of glass structure while J. Bernal, also using a geometric approach, indicated in the early 1960s the possible existence of metallic alloy glasses.

The scientific importance of problems connected with the characterization and the properties of the vitreous state as a specific physical state also becomes evident from the fact that some of the most outstanding physicists and chemists of the past century, people like W. Nernst, A. Einstein, F. Simon, L. Pauling, I. Prigogine, Ya. I. Frenkel, L. Anderson, N. Mott were involved in the study of glasses. Thus, A. Einstein in a famous article, devoted to the basic principles of statistical physics, as early as in 1914, mentioned the possibility that glasses have to be considered not as equilibrium but as non-equilibrium systems. This hypothesis was verified many years later by F. Simon, who started his investigations trying to reconcile the behavior of glasses with the Third law of thermodynamics, formulated by W. Nernst. These investigations led to a reformulation of the Third law and gave a stimulus for the extension of thermodynamics to non-equilibrium states.

G. Tammann in addition to his own pioneering work on glass properties and the process of vitrification was also the first scientist to try to summarize the basic results obtained at his time in his remarkable book "Der Glaszustand", published first in 1933. The present monograph represents an attempt to take up Tammann's approach and to summarize the basic principles and ideas of glass science, including the new developments, in one volume. Hereby we tried to follow – we hope, successfully – the advice given by Albert Einstein: "*Everything should be done as simple as possible but not simpler*".

Chapter 2
States of Aggregation, Thermodynamic Phases, Phase Transformations, and the Vitreous State

2.1 The Vitreous State: First Attempts at a Classification

From a molecular-kinetic point of view all substances can exist in three different states, as gases, liquids and solids. These three states of aggregation of matter (from the Latin word: *aggrego* – to unite, to aggregate) are distinguished qualitatively with respect to the degree of interaction of the smallest units of the corresponding substances (atoms, molecules) and, consequently, with respect to the structure and mobility of the system. Gases are characterized, in general, by a relatively low spatial density of the molecules and a relatively independent motion of the particles over distances significantly exceeding their size. The average time intervals, τ_f, of free motion in gases are considerably larger than the times of strong interaction (collisions, bound states) of two or more atoms or molecules. In a first approximation the free volume in a gas is equal to the volume occupied by the system. The molecules can be treated in a such an approximation as mathematical points (perfect gases); however, in more sophisticated models the volume, shape and the interaction of the molecules have to be accounted for. Gases are compressible; with a decreasing volume of the gas the pressure increases as expressed, e.g., for a perfect gas by Boyle-Mariotte's law.

Liquids have a significantly higher density than gases and a considerably reduced free volume. Thus, an independent translation of the building units of the liquid is impossible. The molecular motion in liquids and melts gets a cooperative character and the interaction between the particles determines to a large extent the properties of the system. Moreover, the compressibility is much smaller than for gases, simple liquids are practically incompressible. According to an approximation due to Frenkel (1946) [233] liquids can be described in the following way: the motion of the building units in a liquid can be considered as an oscillation around temporary average positions. The temporary centers of oscillations are changed after an average stay time, τ_R. The mean distance between two subsequently occupied centers of oscillation is comparable with the sizes of the molecules. Every displacement of the building units of the liquid requires thus a more or less distinct

I.S. Gutzow and J.W.P. Schmelzer, *The Vitreous State*,
DOI 10.1007/978-3-642-34633-0_2, © Springer-Verlag Berlin Heidelberg 2013

way of regrouping of the particles and an appropriate configuration of neighboring molecules, e.g., the formation of vacancies in terms of the "hole" theories of liquids to be discussed in Chap. 5. Though such a picture of the molecular motion in liquids can be considered only as a first approximation it explains both the possibility of a local order and the high mobility of the particles as a prerequisite for the viscous flow and the change of the form of the liquids.

A quantitative measure for the ability of a system to flow is the shear viscosity, η. According to Frenkel the shear viscosity, η, and the average stay time, τ_R, are directly connected. This connection becomes evident by the following equations (Frenkel (1946) [233])

$$\tau_R = \tau_{R0} \exp\left(\frac{U_0}{k_B T}\right) \tag{2.1}$$

and

$$\eta = \eta_0 \exp\left(\frac{U_0}{k_B T}\right). \tag{2.2}$$

By U_0 the activation energy for the viscous flow is denoted, k_B is the Boltzmann constant and T the absolute temperature. More accurate expressions for the temperature dependence of η will be given in Sect. 2.4.1. Nevertheless, already Eqs. (2.1) and (2.2) show in a qualitatively correct way the significant influence of temperature both on the viscosity η and the relaxation time τ_R. Liquids like gases have no own shape but acquire the shape of the vessel they are contained in. They are amorphous in the classical sense of the word, i.e., a body without its own shape (from the Greek word *morphe*: shape; *amorph*: without shape). This classical meaning of the word amorphous is different from the modern interpretation. Today amorphous bodies are understood as materials without a long range order, which is a characteristic property of crystals.

Solids in classical molecular physics were identified initially with crystals. Their structure can be understood as a periodic repetition in space of a certain configuration of particles, of a certain elementary unit. In addition to the local order, found already in liquids, a long range order is established resulting in a possible anisotropy of the properties of the crystals. The motion of the atoms consists, at least, for a perfect crystal of an oscillation around time-independent average positions. This type of motion is connected with the absence of the ability to flow and the existence of a definite shape of crystalline solids.

The properties of gases and liquids are scalar characteristics, while the periodicity in the structure of the crystals determines their anisotropy and the vectorial nature of their properties. Liquids and solid crystals belong to the so-called condensed states of matter. In condensed states the intermolecular forces cannot be neglected, in principle. This classification is, of course, useful only as a first rough division between different states of matter. It has, however, its limitations. So it was shown that some gas mixtures may undergo decomposition processes, which are the result of the interaction of the particles. Liquids can be brought continuously into the gas phase (see van der Waals (1873) [879]) and vice versa. Perfect absolutely regular

crystals do not exist in nature, moreover, under certain conditions crystals can also show some ability to flow, in particular, so-called plastic crystals. Now we also know that, besides topological disorder, also frozen-in orientational disorder even in crystals can produce a behavior similar to that observed in glasses.

Despite these limitations, one of the first questions discussed with the beginning of a scientific analysis of glasses was the problem, to which of the mentioned states glasses have to be assigned to. Experimental results indicated, on one hand, that glasses have a practically infinite viscosity, a definite shape and the mechanical properties of solids. On the other hand, typical properties of liquids can also be found in glasses: the amorphous structure, i.e., the absence of a long-range order and the isotropy of the properties.

As a solution to this problem W. Parks (1925) [623], Parks and Hoffman (1927) [624] and E. Berger (1930) [68] (see also Blumberg (1939) [85]) and subsequently other authors proposed to define the vitreous state as the fourth state of aggregation in addition to gases, liquids and (crystalline) solids. In this connection we have to mention that similar proposals have also been developed (but not accepted generally) with respect to other systems with unusual structure and properties (liquid crystals, elastomers, gels etc.) introducing the fourth, fifth and further states of matter. Already the considerable increase of the number of states of aggregation, which would follow from the acceptance of such proposals, shows that the generalization obtained with the classical division of the states of aggregation would be lost. A considerably more powerful argument against such proposals is connected with the limits for existence, stable coexistence and the possibility of a transformation between different states of aggregation.

Sometimes the partially or totally ionized state of matter, the plasma state, is denoted as the fourth state of aggregation (compare Arcimovich (1972) [18] and Frank-Kamenetzki (1963) [231]). The details of the transition of matter into the plasma state cannot be discussed here, it is very different as compared with the transformations between the different states of aggregation – gases, liquids and crystals – discussed so far. It seems also that in attributing the term fourth state of matter to the plasma state physicists are more or less emotionally influenced by the beautiful schemes of ancient Greek philosophy (e.g., Anaxagoras and, especially, Empedocles (see, e.g., J. Bernal (1957) [71]) and its four elemental forces constituting the universe: air (→ gas), water (→ liquid), earth (→ solid), fire (→ plasma)).

The modern concepts concerning the division of matter into different states of aggregation and the structural characteristics of these states stem from the molecular kinetic ideas of the eighteenth century. These ideas were supplemented by a thermodynamic analysis. Thermodynamics defines the states of aggregation as thermodynamic phases and the transition in between them as particular cases of phase transformations. This fact requires a thorough discussion of the definition of thermodynamic phases and of the thermodynamics of phase transformations as it is presented in the following section. Here we have to mention that, if we accept the point of view that states of aggregation are thermodynamic phases, we can call glasses an additional state of aggregation only, if we can prove that a glass fulfils

the requirements thermodynamics connects with the notation thermodynamic phase. Such a proof cannot be given, however, as it is shown in the subsequent sections. In order to enable a thorough analysis of these problems to be made in the following sections the basic thermodynamic ideas in this respect are outlined.

2.2 Basic Thermodynamic Relationships

2.2.1 The Fundamental Laws of Classical Thermodynamics and Some Consequences

Classical thermodynamics is based mainly on three postulates, the three fundamental laws of thermodynamics. According to the first postulate there exists a function of state U, the so-called internal energy of the system, which depends only on the actual state of the system and not on the way the system was brought into it. The change of the internal energy (First law of thermodynamics) can be expressed as (Kubo (1968) [487]; Bazarov (1976) [53])

$$dU = dQ + dA + dZ. \tag{2.3}$$

It follows that the internal energy of a thermodynamic system is changed, if energy is transferred to it from other bodies either in form of heat dQ (microscopic form of energy transfer), by work dA (macroscopic form of energy transfer) or by the transfer of some amount of matter dZ.

If one specifies the expressions for dQ, dA and dZ one obtains with the Second law of thermodynamics, Eq. (2.4),

$$dS \geq \frac{dQ}{T}, \tag{2.4}$$

the following relationship between another function of state, the entropy S, the absolute temperature T, the internal energy U, the pressure p, the volume V, the chemical potentials μ_j and the mole numbers n_j of the independent molecular species (components)

$$dU \leq TdS - pdV + \sum_j \mu_j dn_j. \tag{2.5}$$

This equation is valid only for homogeneous macroscopic bodies. Electromagnetic fields, elastic strains or surface effects are not considered here; in part, they will be discussed later.

In Eqs. (2.4) and (2.5) the equality sign holds for so-called quasi-static or reversible processes. Reversible processes are defined by the criterion that a process carried out with the system can be reversed without any variations in the states of

other thermodynamic systems to remain. Reversible processes are realized in nature if the variation in the state of the system proceeds via a sequence of equilibrium states, i.e., when the characteristic times of change of the external parameters are small as compared with the corresponding relaxation times of the system to the actual equilibrium state (quasi-static or quasi-stationary processes). Equilibrium states are distinguished by the following properties: (i) for fixed external parameters, no macroscopic processes proceed in the system, (ii) the macroscopic properties are determined only by the actual values of the external thermodynamic parameters and not by the way they are established; they do not depend on the pre-history of the system.

The second part of the first definition of an equilibrium state is needed to distinguish between true equilibrium and stationary or frozen-in non-equilibrium states, for which the evolution to equilibrium is hindered either by the superimposed boundary conditions or by the inhibition of the kinetic mechanisms responsible for approaching equilibrium. For quasi-stationary processes, Eqs. (2.4) and (2.5) may be written as

$$dS = \frac{dQ}{T}, \tag{2.6}$$

$$dU = TdS - pdV + \sum_j \mu_j \, dn_j . \tag{2.7}$$

An integration of Gibbs's fundamental equation, Eq. (2.7), yields

$$U = TS - pV + \sum_j \mu_j \, n_j . \tag{2.8}$$

From the combined First and Second laws of thermodynamics as given by Eq. (2.7) it follows that for equilibrium states the internal energy is uniquely determined by the values of S, V and n_j. If the functional dependence $U = U(S, V, n_1, n_2, \ldots, n_k)$ is known, all thermodynamic properties of the system can be determined by a derivation of U with respect to the independent variables, i.e.,

$$T = \left(\frac{\partial U}{\partial S}\right)_{V,n_j}, \qquad -p = \left(\frac{\partial U}{\partial V}\right)_{S,n_j}, \qquad \mu_j = \left(\frac{\partial U}{\partial n_j}\right)_{S,V,n_j}. \tag{2.9}$$

Thus it becomes evident, why in analogy to classical mechanics the internal energy U (and other thermodynamic functions having analogous properties) are denoted as thermodynamic potentials at the corresponding conditions.

For the analysis of the properties of different systems, including glass-forming melts, two other thermodynamic functions, the enthalpy H and the free enthalpy G (or Gibbs's free energy) are of particular importance. This is connected with the circumstances that condensed systems including glass-forming melts are usually investigated at a constant external pressure, the atmospheric pressure. The variable parameter is then the temperature of the system.

The enthalpy H is determined thermodynamically by

$$H = U + pV. \tag{2.10}$$

For a constant value of the external pressure, which is assumed to be equal to the pressure inside the system (mechanical equilibrium), Eqs. (2.3), (2.7) and (2.10) yield

$$dH = dQ + dZ. \tag{2.11}$$

Consequently, for closed systems ($dZ = 0$) and isobaric conditions ($p = \text{const.}$) the energy supplied to the system in form of heat is equal to the change of the enthalpy.

From the definition of the heat capacity at constant pressure, C_p,

$$C_p = \left(\frac{dQ}{dT}\right)_p, \tag{2.12}$$

one obtains thus

$$C_p = \left(\frac{dH}{dT}\right)_p \tag{2.13}$$

or, with Eq. (2.6),

$$C_p = T\left(\frac{dS}{dT}\right)_p. \tag{2.14}$$

Similarly one gets for the heat capacity at a constant volume C_V

$$C_V = \left(\frac{dQ}{dT}\right)_V, \tag{2.15}$$

$$C_V = \left(\frac{dU}{dT}\right)_V, \tag{2.16}$$

$$C_V = T\left(\frac{dS}{dT}\right)_V. \tag{2.17}$$

The Gibbs free energy G is defined by

$$G = H - TS \tag{2.18}$$

or

$$G = U - TS + pV \tag{2.19}$$

and with Eqs. (2.7) and (2.8)

$$dG = -SdT + Vdp + \sum_j \mu_j dn_j, \tag{2.20}$$

$$G = \sum_j \mu_j n_j \tag{2.21}$$

is obtained. In analogy to U the Gibbs free energy G is also a thermodynamic potential if this quantity is known as a function of T, p and n_j. In this case one gets similarly to Eq. (2.9)

$$S = -\left(\frac{\partial G}{\partial T}\right)_{p,n_j}, \qquad V = \left(\frac{\partial G}{\partial p}\right)_{T,n_j}, \qquad \mu_j = \left(\frac{\partial G}{\partial n_j}\right)_{p,T,n_j}. \tag{2.22}$$

The application of Eqs. (2.9) and (2.22) requires the knowledge of the functions $U(S, V, n_j)$ or $G(T, p, n_j)$, respectively. These dependencies reflect the properties of the particular system and cannot be established by pure thermodynamics. For the determination of the thermodynamic potentials of a real system either calculations based on statistical mechanics or on a distinct set of experimental measurements have to be carried out. Following the second approach one possible way consists of the experimental determination of the temperature dependence of the specific heats C_p for different values of the pressure p.

Once the dependence $C_p = C_p(p, T)$ is established experimentally, the thermodynamic functions H, S and G can be determined by (see Eqs. (2.13), (2.14) and (2.22))

$$H(p, T) = H(p, T_0) + \int_{T_0}^{T} C_p \, dT, \tag{2.23}$$

$$S(p, T) = S(p, T_0) + \int_{T_0}^{T} \frac{C_p}{T} \, dT, \tag{2.24}$$

$$G(p, T) = G(p, T_0) - S(p, T_0)(T - T_0) - \int_{T_0}^{T} dT \int_{T_0}^{T} \frac{C_p}{T} \, dT. \tag{2.25}$$

In most cases, the experimenter is interested in the knowledge of C_p, H, S and G only at atmospheric pressure.

Equations (2.23)–(2.25) hold for any arbitrary reference temperature T_0. They can be simplified based on the Third law of thermodynamics. The Third law of thermodynamics, established first by W. Nernst in 1906 (see Nernst (1918) [601]; Bazarov (1976) [53]), reads in the formulation by M. Planck (see Planck (1954) [636]; Wilks (1961) [923]) that approaching zero of the absolute temperature the entropy of a system in thermodynamic equilibrium becomes a constant, equal to S_0. This entropy value is independent of pressure or other possible thermodynamic parameters and the state of aggregation of the substance considered. Since the entropy is defined, according to Eq. (2.6), only with an accuracy of an additive constant, this constant is set according to Planck's well known proposal [636] equal to zero.

In a mathematical formulation the Third law can be written thus as

$$\lim_{T\to 0} S = 0 \tag{2.26}$$

with the consequences

$$\lim_{T\to 0} C_p = 0, \quad \lim_{T\to 0} C_V = 0, \tag{2.27}$$

$$\lim_{T\to 0}\left(\frac{\partial G}{\partial T}\right) = \lim_{T\to 0}\left(\frac{\partial H}{\partial T}\right) = 0. \tag{2.28}$$

With the Third law Eqs. (2.23)–(2.25) are simplified to

$$H(p,T) = H(p,0) + \int_0^T C_p\, dT, \tag{2.29}$$

$$S(p,T) = \int_0^T \frac{C_p}{T}\, dT, \tag{2.30}$$

$$G(p,T) = G(p,0) - \int_0^T dT \int_0^T \frac{C_p}{T}\, dT. \tag{2.31}$$

Another formulation of the Third law of thermodynamics can be given with Boltzmann's interpretation of the entropy S of a system as

$$S = k_B \ln \Omega. \tag{2.32}$$

Here Ω is the number of distinct microstates corresponding to one and the same macrostate. In such an approach, the Third law is equivalent to the statement that to the macrostate of the system for temperatures, T, tending to zero corresponds only one (or a relatively small number, cf. Fermi (1937) [203]) of microstates.

2.2.2 *General Thermodynamic Evolution Criteria, Stability Conditions and the Thermodynamic Description of Non-equilibrium States*

So far only thermodynamic systems in equilibrium states and reversible processes in between them have been discussed. In general, for systems in non-equilibrium states, the inequality

$$(dU)_{S,V,n_j} \leq 0 \tag{2.33}$$

holds. For fixed values of the entropy, the volume and the number of moles of the different components the internal energy decreases until in the equilibrium state a minimum of U is reached. Similarly one obtains for the Gibbs free energy at fixed values of p, T and n_j

$$(dG)_{p,T,n_j} \leq 0. \tag{2.34}$$

If we consider a homogeneous system and divide it artificially into two parts, specified by the subscripts (1) and (2), respectively, then the entropy S, the volume V and the mole number n_j of the whole system can be written as

$$S = S_1 + S_2, \qquad V = V_1 + V_2, \qquad n_j = n_{j1} + n_{j2}. \tag{2.35}$$

If S, V and n_j are kept constant, spontaneous deviations of S_1, V_1 and n_{j1} result in corresponding deviations of S_2, V_2 and n_{j2}, i.e.,

$$\delta S_1 + \delta S_2 = 0, \qquad \delta V_1 + \delta V_2 = 0, \qquad \delta n_{j1} + \delta n_{j2} = 0. \tag{2.36}$$

In the vicinity of equilibrium, which is characterized by a minimum of $U = U_1 + U_2$, such changes do not vary the total value of U. As a result one gets from the necessary equilibrium conditions $\delta U = 0$, e.g.,

$$\delta U = \left(\frac{\partial U}{\partial S_1}\right) \delta S_1 = \left(\frac{\partial U_1}{\partial S_1} - \frac{\partial U_2}{\partial S_2}\right) \delta S_1 = 0 \tag{2.37}$$

and (compare Eq. (2.9))

$$T_1 = T_2. \tag{2.38}$$

Similarly one obtains

$$p_1 = p_2 \qquad \text{(for planar interfaces)} \tag{2.39}$$

and

$$\mu_{j1} = \mu_{j2}. \tag{2.40}$$

In equilibrium the values of temperature, pressure and the chemical potentials are the same throughout the system.

The sufficient equilibrium criterion

$$(\delta^2 U)_{S,V,n_j} > 0 \tag{2.41}$$

may be written also as (see Kubo (1968) [487])

$$\delta S \delta T - \delta p \delta V + \sum_j \delta \mu_j \delta n_j > 0. \tag{2.42}$$

If only the temperature of a homogeneous system is changed, as a particular case one obtains

$$\left(\frac{\partial S}{\partial T}\right)(\delta T)^2 > 0 \tag{2.43}$$

and, consequently, (cf. Eqs. (2.14) and (2.17), see also Prigogine and Defay (1954) [649])

$$C_p > 0, \qquad C_V > 0. \tag{2.44}$$

Equations (2.30) and (2.44) allow one in agreement with Eq. (2.32) the conclusion that the entropy S of an equilibrium system for $T > 0$ is always positive.

Equation (2.34) shows further that, also for fixed values of p, T and n_j, in non-equilibrium processes a change of G is possible. This statement implies that the values of p, T and n_j do not determine completely the state of a non-equilibrium system. Suppose that it is necessary to introduce additional macroscopic state variables $\xi_1, \xi_2, \ldots \xi_m$, which together with p, T and n_j contain the whole information about the macroscopic properties of the corresponding non-equilibrium system. We denote these additional state variables $\{\xi\}$ as internal or structural order parameters. In such cases, G is determined by an expression of the form

$$G = G(p, T, n_j, \xi_1, \xi_2, \ldots, \xi_m). \tag{2.45}$$

Since in equilibrium G is a function of p, T and n_j, in this limiting case the additional parameters ξ_j must be also functions of p, T and n_j, i.e., the relation

$$\xi_j^{(e)} = \xi_j^{(e)}(T, p, n_1, n_2, \ldots, n_k) \tag{2.46}$$

has to be fulfilled. If the structural order parameters ξ_j are defined in such a way that they decrease with the approach to the respective equilibrium values $\xi_j^{(e)}$, we have

$$\frac{\partial G}{\partial \xi_j} \geq 0. \tag{2.47}$$

The method of description of non-equilibrium states by the introduction of additional structural order parameters was developed by De Donder (1936) [156] (see also Prigogine and Defay (1954) [649]; Leontovich (1953) [504]). This method will be used in Chap. 3 for the definition of the vitreous state and in order to introduce the so-called fictive temperature as a characteristic quantity describing the state of a glass.

2.2.3 *Phases and Phase Transformations: Gibbs's Phase Rule and Ehrenfest's Classification*

The term thermodynamic phase (from the Greek word *phasis*: form of appearance) was introduced by J.W. Gibbs (1875–1878) to characterize a definite equilibrium

form of appearance of a substance. In Gibbs's words the definition reads: "In considering the different homogeneous bodies which can be formed out of any set of component substances, it will be convenient to have a term which shall refer solely to the composition and thermodynamic state of any such body without regard to its quantity or form. We may call such bodies as differ in composition or state different phases of matter considered, regarding all bodies which differ only in quantity and form as different examples of the same phase. Phases which can exist together, the dividing surfaces being plane, in an equilibrium which does not depend upon passive resistances to change we shall call coexistent" (Gibbs (1928, p. 96) [249]).

According to this classical definition thermodynamic phases are different equilibrium forms of appearance of one and the same substance. Every thermodynamic phase is physically homogeneous and, in the absence of external fields, its thermodynamic parameters are the same in each part of the volume occupied by it. In other words, Gibbs's definition implies that a phase is characterized by one well-defined equation of state. Different thermodynamic phases may coexist in mutual contact in equilibrium; the coexisting phases are divided by interfacial boundaries, where the thermodynamic parameters of the substance change rapidly. The transformation of a substance from one phase to the other is called phase transformation.

The notation thermodynamic phase is more restrictive than the term state of aggregation. Inside a given state of aggregation a substance may exist in several different phases like, e.g., the different phases of ice or the different modifications of SiO_2 (see, e.g., Tammann (1922) [818]). A thorough discussion of these problems is given also, e.g., by van der Waals and Kohnstamm (1908) [881] and Storonkin (1967) [808].

In a thermodynamic description of a heterogeneous system, consisting of more than one, say r, phases, the thermodynamic potential G can be written as a sum of the contributions of the r phases

$$G = G_1 + G_2 + \ldots + G_r. \tag{2.48}$$

Interfacial contributions are neglected here as in the previous discussion. The necessary equilibrium conditions read then (cf. Eqs. (2.38)–(2.40))

$$T_m = T_r, \qquad p_m = p_r, \qquad \mu_{jm} = \mu_{jr}, \qquad m = 1, 2, \ldots, r-1. \tag{2.49}$$

The properties of the phase m can be determined if the functional dependence

$$G_m = G_m(T_m, p_m, n_{1m}, \ldots, n_{km}) \tag{2.50}$$

is known. According to the above given definition the properties of a phase do not depend on the total quantity. Consequently, the state of one phase is characterized by $k+1$ variables, e.g., the temperature T, the pressure p and the independent molar fractions $x_j, j = 1, 2, \ldots, k-1$. The total number of variables needed for the description of the properties of an r-phase system is, therefore, $r(k+1)$. In equilibrium between these variables $(r-1)(k+2)$ independent relationships exist (compare Eq. (2.49)). The number of independent variables or the number of

degrees of freedom is, therefore, $f = r(k+1) - (r-1)(k+2)$ or

$$f = k + 2 - r. \tag{2.51}$$

Equation (2.51) is denoted as the Gibbs phase rule. The way of derivation of this rule demonstrates once more that the notation phase as it is introduced and used by Gibbs is and has to be applied to equilibrium states only (see in this respect also [487]).

During a change of the external parameters different types of transformations of a substance from one phase into another one can be observed. The first classification of such possible types of phase transformations was proposed by P. Ehrenfest (1933) [183]. This classification will be summarized here briefly in application to one-component systems.

For a one-component closed system the change of the Gibbs free energy in a reversible process is given by (cf. Eq. (2.20))

$$dG = -SdT + Vdp. \tag{2.52}$$

Since for one-component systems $G = \mu n$ holds (see Eq. (2.21)) Eq. (2.52) may be rewritten as

$$d\mu = -sdT + vdp, \tag{2.53}$$

where s and v are the molar values of entropy and volume of the system. Equation (2.53) yields

$$s = -\left(\frac{\partial \mu}{\partial T}\right)_p, \qquad v = \left(\frac{\partial \mu}{\partial p}\right)_T. \tag{2.54}$$

Possible dependencies $G = G(T, p = \text{constant})$ and $G = G(p, T = \text{constant})$ for two different phases are shown in Fig. 2.1. Only in the point of intersection of the $G(T)$- or $G(p)$-curves the necessary conditions for equilibrium are fulfilled. For the values of p and T corresponding to the point of intersection and denoted here by T_e and p_e, a coexistence of the different phases is possible.

For fixed values of p, T and n_j spontaneous processes are connected with a decrease of the Gibbs free energy (cf. Eq. (2.34)). Consequently, in Fig. 2.1a, b the lower branches of the curves correspond to the thermodynamically preferred more stable state. In a process, e.g., of continuous heating, after T_e is reached (Fig. 2.1a), a transition from phase (2) to phase (1) is to be expected from a thermodynamic point of view. The difference of the thermodynamic potentials is a measure of the thermodynamic driving force of the process of phase transformation. The particular way and the rate such processes proceed depend on additional thermodynamic and kinetic factors discussed in detail in Chaps. 6 and 7.

Phase transformations of the form as depicted in Fig. 2.1a, b, according to the classification of P. Ehrenfest (1933) [183], are denoted as first order phase transitions. This notation originates from the fact that in an equilibrium two-phase

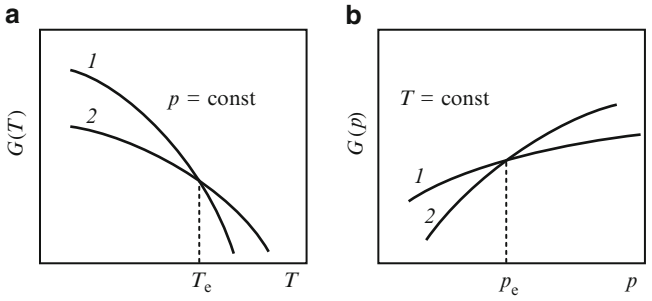

Fig. 2.1 Possible dependencies (**a**) $G = G(T, p = \text{const.})$ and (**b**) $G = G(p, T = \text{const.})$ for two different phases, specified by (*1*) and (*2*), respectively. The points of intersection of these curves determine the values of p and T for which an equilibrium coexistence of both phases is possible. A behavior of such a type is typical for first-order phase transformations according to Ehrenfest's classification

state the values of the molar Gibbs free energies g of both phases coincide, while the first derivatives with respect to p or T differ. It means that the relations

$$g^{(1)}(T, p) = g^{(2)}(T, p), \tag{2.55}$$

$$\left(\frac{\partial g^{(1)}}{\partial T}\right)_p \neq \left(\frac{\partial g^{(2)}}{\partial T}\right)_p, \qquad \left(\frac{\partial g^{(1)}}{\partial p}\right)_T \neq \left(\frac{\partial g^{(2)}}{\partial p}\right)_T \tag{2.56}$$

have to be fulfilled. Here and in the following derivations small letters always refer to molar values of the respective extensive variables.

Taking into account Eq. (2.22) the relations Eq. (2.56) are equivalent to

$$s^{(1)} \neq s^{(2)}, \qquad v^{(1)} \neq v^{(2)}. \tag{2.57}$$

It follows that if a system is transferred from one phase to another in a first-order phase transition, then the values of the entropy and volume per mole are discontinuously changed. This change is connected with a qualitative variation of the structure of the system and the release or adsorption of the latent heat of the transformation (heat of melting, heat of sublimation, heat of evaporation). It is also manifested in the discontinuous change of the molar enthalpy, h ($h^{(1)} \neq h^{(2)}$).

According to Gibbs's phase rule a one-component two-phase equilibrium system has one degree of freedom. Thus, the equilibrium value of the pressure can be considered as a function of temperature. The type of dependence $p = p(T)$ can be derived from the equilibrium condition $\mu^{(1)}(p, T) = \mu^{(2)}(p, T)$. A derivation of this equation with respect to T leads to the Clausius-Clapeyron equation

$$\frac{dp}{dT} = \frac{s^{(1)} - s^{(2)}}{v^{(1)} - v^{(2)}}. \tag{2.58}$$

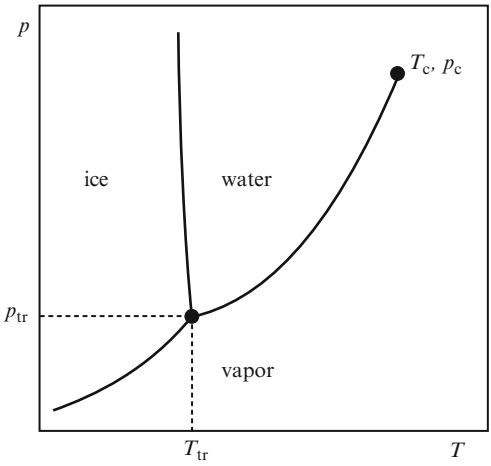

Fig. 2.2 Phase diagram for water with triple point (T_r, p_r) and critical point (T_c, p_c): $T_r = 273.17\,\mathrm{K}$, $p_r = 610.6\,\mathrm{Pa}$; $T_c = 647\,\mathrm{K}$, $p_c = 22.1 \cdot 10^6\,\mathrm{Pa}$

The difference of the molar entropies can also be expressed through the molar latent heat of the transformation q as

$$s^{(1)} - s^{(2)} = \frac{q}{T}, \tag{2.59}$$

which yields

$$\frac{dp}{dT} = \frac{q}{T(v^{(1)} - v^{(2)})}. \tag{2.60}$$

By the determination of all possible $p = p(T)$ curves representing different phase equilibria of the same substance the well-known phase diagrams are obtained. The point of intersection of three curves (triple point) corresponds to a three phase system. According to Gibbs's phase rule a three-phase equilibrium is possible only for single points in the (p, T)-plane. This conclusion is illustrated in Fig. 2.2 for the classical example of water-ice-vapor coexistence.

For second-order phase transitions both the molar free enthalpy and their first-order derivatives are the same for both phases in the transition point, while the second order derivatives differ. In addition to Eq. (2.55) we have to write

$$\left(\frac{\partial g^{(1)}}{\partial T}\right)_p = \left(\frac{\partial g^{(2)}}{\partial T}\right)_p, \quad \left(\frac{\partial g^{(1)}}{\partial p}\right)_T = \left(\frac{\partial g^{(2)}}{\partial p}\right)_T, \tag{2.61}$$

$$\left(\frac{\partial^2 g^{(1)}}{\partial p \partial T}\right) \neq \left(\frac{\partial^2 g^{(2)}}{\partial p \partial T}\right), \left(\frac{\partial^2 g^{(1)}}{\partial p^2}\right)_T \neq \left(\frac{\partial^2 g^{(2)}}{\partial p^2}\right)_T, \tag{2.62}$$

$$\left(\frac{\partial^2 g^{(1)}}{\partial T^2}\right)_p \neq \left(\frac{\partial^2 g^{(2)}}{\partial T^2}\right)_p.$$

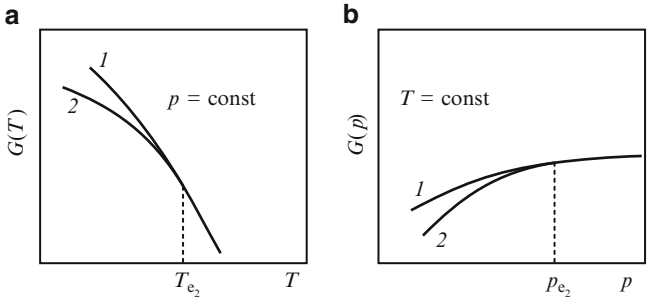

Fig. 2.3 Illustration of the (**a**) $G = G(T, p = \text{const.})$ and (**b**) $G = G(p, T = \text{const.})$ dependencies for second-order phase transformations according to the classification of P. Ehrenfest. The different phases are specified by (*1*) and (*2*), again

As a consequence it follows that in second order phase transformations no latent heat is released by the system.

The second-order derivatives of the Gibbs free energy with respect to p and T may be expressed through the thermodynamic coefficients. In general, thermodynamic coefficients describe the reaction of a system with respect to the variation of the external parameters of state. An often used set of independent thermodynamic coefficients consists of the heat capacity, C_p (cf. Eqs. (2.12)–(2.14)), the thermal expansion coefficient, α, and the isothermal compressibility, κ. The thermal expansion coefficient α and the compressibility κ are defined by (Landau and Lifshitz (1969) [495])

$$\alpha = \frac{1}{V}\left(\frac{\partial V}{\partial T}\right)_p, \qquad \kappa = -\frac{1}{V}\left(\frac{\partial V}{\partial p}\right)_T. \tag{2.63}$$

Taking into account Eqs. (2.22) and (2.63) the inequalities Eq. (2.62), characterizing second-order phase transitions, may be rewritten as

$$C_p^{(1)} \neq C_p^{(2)}, \qquad \alpha^{(1)} \neq \alpha^{(2)}, \qquad \kappa^{(1)} \neq \kappa^{(2)}. \tag{2.64}$$

Equations (2.64) indicate that second-order phase transformations, according to the classification of Ehrenfest, are connected with qualitative changes of the response of the system with respect to a change of the external parameters. An illustration of Eq. (2.62) and thus of second-order phase transitions is given in Fig. 2.3a, b. Here, as seen from the figures, in contrast to first-order phase transitions, the tangents to the curves representing both possible phases coincide in the transformation point, while the curvatures of the $G = G(T)$ and $G = G(p)$ curves differ.

For second-order phase transformations in analogy to the Clausius-Clapeyron equation, in the form as given by Eqs. (2.58) or (2.60), relations can be derived connecting the equilibrium values of pressure and temperature. Based on Eq. (2.61) or the equations

$$s^{(1)} = s^{(2)}, \qquad v^{(1)} = v^{(2)}, \tag{2.65}$$

by a derivation with respect to T one obtains

$$\frac{dp}{dT} = \frac{1}{VT} \frac{(C_p^{(1)} - C_p^{(2)})}{(\alpha^{(1)} - \alpha^{(2)})}, \tag{2.66}$$

$$\frac{dp}{dT} = \frac{(\alpha^{(1)} - \alpha^{(2)})}{(\kappa^{(1)} - \kappa^{(2)})}. \tag{2.67}$$

Since both these equations are equivalent, after an elimination of (dp/dT) a relation is obtained, connecting the changes of the thermodynamic coefficients in second-order phase transformations

$$\frac{1}{VT} \frac{\Delta C_p \Delta \kappa}{(\Delta \alpha)^2} = 1. \tag{2.68}$$

Equation (2.68) is called Ehrenfest's equation.

Formally, Ehrenfest's classification of phase transformations can be extended to define transitions of any arbitrary order in dependence on the degree of the derivatives, which become discontinuous. However, from the point of view of an experimenter investigating the structure or the reaction of a given system in dependence on the variation of some external parameters and identifying qualitative changes with phase transformations, only first (qualitative changes of the structure) and second order phase transformations (qualitative changes of the response) from Ehrenfest's classification scheme are of real physical significance.

We would also like to mention that Ehrenfest's classification is far from being complete. As it became evident by Onsager's discussion of the Lenz-Ising model (Onsager (1944) [611]), qualitative variations of the state or the reaction of a system may exist, which cannot be described in the scheme discussed so far (see, e.g., Gebhardt and Krey (1980) [246]; Gunton, San Miguel, and Sahni (1983) [283]). For a first discussion of the nature of the process of vitrification of glass-forming melts, however, the remarkably simple classification of Ehrenfest is sufficiently accurate.

To allow one a direct comparison with the behavior of glass-forming melts in the solidification range, the type of temperature dependence of the basic thermodynamic quantities in first and second order phase transformations is summarized briefly in Fig. 2.4. In first-order phase transformations a temperature dependence of the thermodynamic quantities is observed as shown in Fig. 2.4a. In addition, the Clausius-Clapeyron equation, Eq. (2.60), has to be fulfilled. Second-order phase transformations are characterized by the curves shown in Fig. 2.4b and Ehrenfest's relations (2.66)–(2.68).

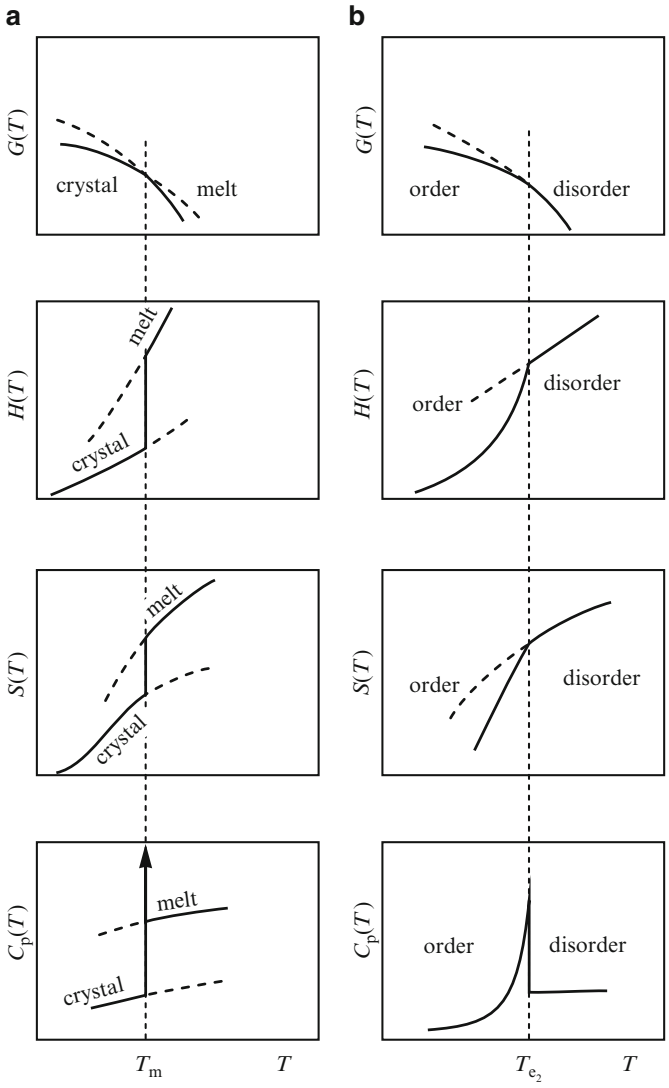

Fig. 2.4 Temperature dependence of the thermodynamic functions G, H, S and of the specific heat, C_p, of a system undergoing a first (**a**), respectively, second-order (**b**) phase transformation. As an example for first-order phase transformations the transition melt-crystal is chosen, while as an example for second order phase transformations an order-disorder transition with a λ-type C_p-curve is presented. In first-order phase transformations we have to expect $C_p \rightarrow \infty$ for $T \rightarrow T_m$ as indicated in the figure by an *arrow*. T_m is the melting temperature, T_{e2} the second-order transition temperature. With *dashed lines* the continuations of the curves into the respective region of stability of the other phase are indicated which, however, can be realized in experiments only for first-order transformations (metastable states)

2.3 Crystallization, Vitrification and Devitrification of Glass-Forming Melts: Overview on Some Experimental Results

We now consider possible types of processes which may take place in the course of cooling of the melt of a substance, which can be transformed, at least, under certain conditions into a glass. The melting temperature of the corresponding crystalline phase we denote as T_m. According to the results outlined in Sect. 2.2, T_m is at the same time the temperature, at which at a constant pressure, the liquid and crystalline phases may coexist in equilibrium.

Let us assume we have a crucible with a certain amount of a pure glass-forming melt at a temperature somewhat above the melting temperature T_m. Starting with this initial state, energy is removed in the form of heat with a constant rate from the melt. The resulting decrease in temperature is measured by a thermocouple. Possible $T = T(t)$ curves, which may be obtained in this way, are shown in Fig. 2.5.

Part (1-2) of the curve in Fig. 2.5a describes the process of cooling of the melt down to T_m. At this temperature the melt may start to crystallize. If this is the case, a time interval is found for which the external cooling is compensated by the release of the latent heat of crystallization (cf. Eq. (2.59)), resulting in a temporary constancy of temperature (part (2-3) of the curve in Fig. 2.5a). This horizontal part (2-3) is followed then by the cooling curve (3-4) of the completely crystallized material. Such behavior, when the new phase appears immediately without any measurable under-cooling, is found only in some metal melts or when in an oxide melt certain precautions are undertaken to initiate the crystallization process (i.e., introduction of seed crystals of the same substance).

In the majority of cases a more or less pronounced degree of under-cooling ΔT_{max} has to be reached, before an intensive crystallization process starts. As under-cooling the temperature difference, $\Delta T = T_m - T$, is denoted. Thus, ΔT_{max} has to be understood as

$$\Delta T_{max} = T_m - T_{min}. \tag{2.69}$$

Here T_{min} is the lowest value of the temperature which can be reached without measurable crystallization being observed. Figure 2.5b gives an example of a temperature vs time curve for such a case. Again, the part (1-2) corresponds to the cooling curve of the melt, but this time the cooling curve is extended into the metastable region (2-3), where the crystalline state and not the under-cooled melt is stable from a thermodynamic point of view. This result is the simplest demonstration of the well-known fact that in first-order phase transformations equilibrium has to be more or less exceeded to allow measurable phase changes to take place. In second-order phase transformations such an existence of a metastable phase outside the limits of its thermodynamic stability has not been observed. The thermodynamic and kinetic significance of these facts will be discussed in Chap. 3.

After a critical under-cooling, ΔT_{max}, is reached, a spontaneous crystallization process follows. The release of the latent heat accompanying the process of

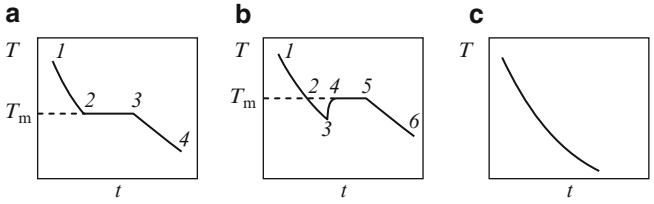

Fig. 2.5 Temperature T vs time t curves of a melt at constant cooling rates for three different situations: (**a**) the crystallization of the melt proceeds immediately below T_m; (**b**) a significant crystallization is observed only after some critical value ΔT_{max} of the undercooling is reached; (**c**) the melt is transformed into a solid without a measurable crystallization to occur

crystallization results in an increase of temperature until T_m is established, again. After completion of crystallization, the cooling curve of the crystalline phase is followed (5-6) similarly as in Fig. 2.5a. In a number of substances the possible under-cooling may be extended to considerable values, for example, 370 K for platinum, 150 K for iron melts, 20 K for gallium (see Table 2.1). The values of the undercoolings realized experimentally at normal cooling rates (10^{-1}–10^2 K s^{-1}) are usually found to be of the order $\Delta T_{max}/T_m \approx 0.2$. This value is also predicted by an empirical rule (Ubbelohde (1965) [871]; Skapski (1956b) [766]), which states that

$$\frac{T_{min}}{T_m} \approx 0.8 - 0.9. \tag{2.70}$$

This rule is valid for a large number of substances (see Table 2.1).

An example of a substance, which can be easily under-cooled, is gallium. Gallium has a melting point of about 29 °C. In accordance with the formulated empirical rule, it can be preserved as an undercooled liquid at room temperatures $T_{(room)}$ for practically unlimited periods of time ($T_{(room)}/T_m \approx 0.97$). Other substances, which have been frequently used in laboratory demonstrations as undercooled melts, are natrium thiosulfate ($Na_2S_2O_35H_2O$) and salol ($HOC_6H_4COOC_6H_5$). These substances have a melting point of about 50 °C and can be cooled down to room temperatures also without any crystallization being detected.

An inspection of Table 2.1 shows that for substances with very different compositions and structure (metals, oxides, salts, molecular liquids, polymer melts) the relative critical under-cooling, which may be achieved by normal cooling techniques, is practically the same and normally does not have values below $(0.7 - 0.8)T_m$. This applies even to melts like $NaPO_3$, lithium disilicate, glycerol, piperine, which are representatives of typical glass-forming substances. For most of the substances included in Table 2.1, an under-cooling to temperature values below T_{min} leads to immediate crystallization. It will be shown in subsequent chapters that the dramatic increase of the viscosity for $T \leq T_{min}$ observed for typical glass-formers has the consequence that crystallization may not occur in such substances for longer periods of time in this temperature region.

Table 2.1 Critical values of the under-cooling ΔT_{max}, at which an intensive crystallization is observed, for different classes of substances, provided heterogeneous nucleation is inhibited. T_m is the melting temperature and T_{min} the lowest value of temperature the substance may be transferred to under normal cooling conditions without detectable crystallization. The data are collected from: Turnbull (1950, 1952b) [859, 860], Turnbull and Cech (1950) [863], Ubbelohde (1965) [871], Chernov (1980) [132], Umanski et al. (1955) [875], Grantcharova and Gutzow (1986) [268], Penkov and Gutzow (1984) [632], Tammann (1933) [820], Tammann and Jenckel (1930) [821], and Walton (1969) [907]

First part of Table 2.1

Substance	T_m (K)	ΔT_{max} (K)	T_{min}/T_m	References
Hg	235	50	0.78	[132, 859, 860, 863]
Ga	302	36	0.87	[132, 859, 860, 863]
In	429	81	0.81	[132, 859, 860, 863]
Sn	505	105	0.79	[132, 859, 860, 863]
Bi	544	90	0.79	[132, 859, 860, 863]
Pb	610	80	0.86	[132, 859, 860, 863]
Sb	903	135	0.85	[132, 859, 860, 863]
Al	933	130	0.86	[132, 859, 860, 863]
Ag	1,234	227	0.76	[132, 859, 860, 863]
Au	1,336	190	0.82	[132, 859, 860, 863]
Cu	1,356	180	0.79	[132, 859, 860, 863]
Co	1,765	310	0.73	[132, 859, 860, 863]
Fe	1,825	295	0.84	[132, 859, 860, 863]
Pd	1,825	310	0.82	[132, 859, 860, 863]
Pt	2,042	370	0.82	[132, 859, 860, 863]
Mean value for metals:			0.81	
LiF	1,121	232	0.79	[871]
LiCl	887	186	0.79	[871]
LiBr	819	94	0.76	[871]
NaF	1,285	281	0.84	[871]
NaCl	1,073	168	0.84	[871]
NaBr	1,014	163	0.84	[871]
KCl	1,045	169	0.84	[871]
KBr	1,005	162	0.83	[871]
KJ	958	155	0.85	[871]
RbCl	990	163	0.84	[871]
CsF	955	153	0.86	[871]
CsCl	915	152	0.83	[871]
CsBr	909	162	0.82	[871]
CsF	894	206	0.78	[871]
Mean value for alkali halides:			0.82	
BF_3	144	19	0.87	[871]
Cyclopropene	145	19	0.87	[871]
Methylbromide	179	36	0.80	[871]

(continued)

Table 2.1 (continued)

First part of Table 2.1				
Substance	T_m (K)	ΔT_{max} (K)	T_{min}/T_m	References
CH_3NH_2	180	36	0.80	[871]
SO_2	198	34	0.83	[871]
$CHCl_3$	209	48	0.77	[871]
Mean value for molecular liquids:			0.82	
H_2O	273	4.4	0.85	[875]
Ge	1,231	200	0.84	[875]
NH_3	195	40	0.79	[871]
CH_3Cl	176	56	0.68	[871]
C_6H_6	278	70	0.74	[871]
CH_3Br	197	42	0.78	[871]
Thiophene	235	51	0.78	[871]
$NaPO_3$	898	189	0.79	[268]
$Li_2O\,2SiO_2$	1,313	446	0.66	[632]
Glycerol	293	57	0.80	[821]
Piperine	402	92	0.77	[820]
Mean value for glass-formers:			0.75	
CBr_4	363	82	0.78	[908]
CCl_4	251	50	0.81	[908]
White phosphor	396	116	0.71	[908]
Diphenyl	343	86	0.75	[908]
Naphtalene	353	94	0.74	[908]
Poly(ethylene)				
linear	423	55	0.87	[908]
branched	422	59	0.86	[908]
Marlex-50	505	86	0.83	[908]
Polyoxymethylene	454	84	0.82	[908]
Nylon 6	500	99	0.88	[908]
Isotactic				
Poly(propilene)	459	101	0.78	[908]
Mean value for polymers:			0.80	

Experimental evidence accumulated for more than 150 years for very different classes of substances (cf. the beautiful summary on the history of phase formation processes as it is given in the introduction to Volmer's monograph (1939) [894] or, with more details, in Ostwald's classical textbook (Ostwald (1896–1902) [616])) allow one to draw the following conclusions concerning the initiation of crystallization processes in under-cooled melts:

- The highest possible values of the under-cooling, T_{min}, can be realized experimentally only if insoluble foreign particles, which may act as centers of crystallization, or certain surface-active substances are removed from the melt. However, foreign particles are not equally active in the induction of crystallization in under-cooled melts. The highest activity with respect to initia-

tion of crystallization show seed particles of the same substance or crystallization cores with a structure and cell dimensions close to those of the evolving crystal.
- In some cases, mechanical effects (vibrations, stirring) may initiate crystallization.
- The achievable under-coolings increase by increasing the degree of dispersion of the melt. In the process of quenching of the melt, for small droplets significantly larger values of the under-cooling may be reached as compared with corresponding data for bulk samples of the same melt, which are to be expected according to Eq. (2.70).

Thus, under-coolings for water droplets of about 10^{-6} m in size may reach the order of $\Delta T \approx 40$–50 K, which is of a particular meteorological importance, and for metal melts, with a relatively high melting point, $\Delta T \approx 200$–300 K is often reported (see Table 2.1).

A relatively high degree of dispersion of the melt can be achieved, for example, by the process of pulverization of the melt in an air stream. This method, connected with a rapid quenching on cold surfaces, was introduced by Tammann as an effective method for the transformation of substances into the vitreous state (Tammann (1933) [820]; see also Fig. 2.6a). A modification of this method is shown in Fig. 2.6b.

An extension of Tammann's ideas was performed by Turnbull (1949 [858], 1952 [860]; see also Greer (1988) [274]) and consists of the emulgation of low temperature melting metals like tin, lead, bismuth, mercury etc. in silicon oil. Additional emulgators, introduced into the system, prevent the coagulation of the metallic drops. To get high temperature melting metals like iron, nickel, platinum or chromium into the dispersed state as an emulgator silicate glass-forming melts can be used. By vibrating and mixing the liquid with another appropriate substance the test liquid is dispersed into a large number of small droplets. If impurities are present in the test liquid then some of the drops will contain them while others will remain uninfluenced by such foreign crystallization cores and may be under-cooled to temperatures at which intensive homogenous nucleation occurs. Thus the increase in the degree of under-cooling in small particles is due to the absence of active foreign crystallization cores, at least, in some of the drops (Fig. 2.7a, b).

The temperature T_g, below which the under-cooled melt behaves like a solid, is denoted, according to a proposal by Tammann, as the glass transformation temperature. The solid resulting in such a cooling process without perceptible crystallization is a glass. The temperature vs time curve for the process of glassy solidification is shown in Fig. 2.5c. A horizontal part of the curve as in Fig. 2.5a, b does not exist. This feature is an indication, that the process of vitrification is not connected with the release of any latent heat and thus with a discontinuous change of the structure, the entropy and the enthalpy of the system. The systems remain spatially homogeneous and no crystallization is to be detected. For temperatures below T_g, crystallization processes of the already vitrified melt have never been observed. However, crystallization may occur, if the glass is reheated, again, to temperatures above T_g. Such a crystallization process is usually denoted as devitrification.

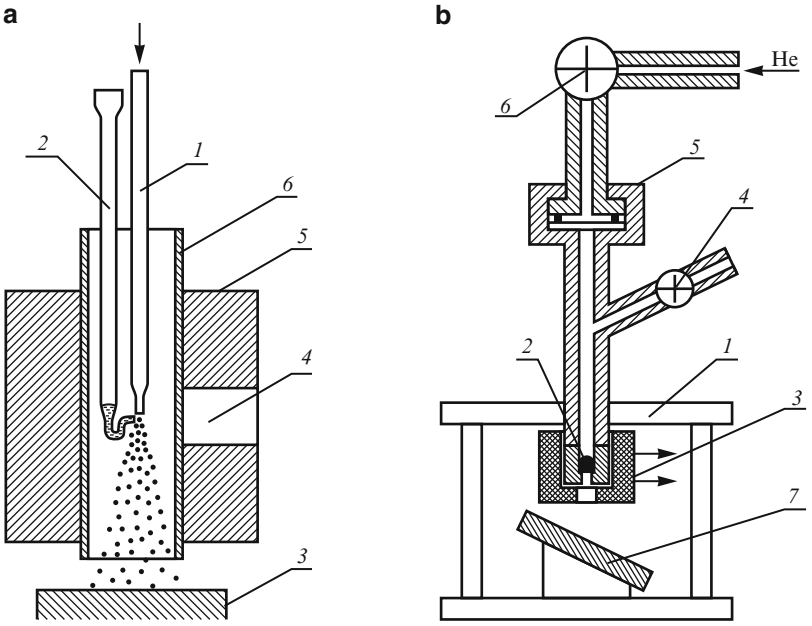

Fig. 2.6 (**a**) Tammann's atomizer for vitrification of molten salts: An inert gas (nitrogen) is passing under pressure through a tube (*1*) dispersing the molten salt contained in tube (*2*). The droplets are quenched at the metal plate (*3*) cooled by liquid nitrogen. The oven tube (*6*) as well as the tubes (*1*) and (*2*) are made of quartz glass, so that the course of the process of dispersion can be followed through the window (*4*) in the experimental device (*5*). (**b**) Modification of Tammann's atomizer: A crucible (*1*) contains a drop (*2*) of a metallic alloy molten in the oven (*3*). High pressure inert gas (He) is supplied with valve (*6*) rupturing the mylar diaphragm slit (*5*) and forces the drop at high speed onto a cooled metal plate (*7*), where it is frozen to a glass. Further metallic alloy samples are introduced into the system by the valve (*4*) (After Giessen and Wagner (1972) [253])

The existence of the glass transformation temperature T_g, of vitrification and of devitrification processes may be demonstrated more effectively as in single cooling curves, by heating or cooling runs with differential thermal analysis (DTA). The DTA-curves of a devitrifying glass at constant heating rates (usually 10 K per minute) show a well-pronounced salient point, when the temperature T_g is reached. This salient point can be used to determine T_g in a standardized procedure. Somewhat above T_g, an exothermic peak usually occurs, which corresponds to the process of devitrification. For typical glass-forming melts, which can be vitrified at normal cooling rates (i.e., not exceeding 10^{-1}–$10^{2}\,\mathrm{K\,s^{-1}}$), devitrification processes begin usually at 30–50 K above T_g. For other systems, however, like the already mentioned glass-forming metallic alloys, which are obtained only as the result of extreme cooling rates, the devitrification peak appears immediately above the T_g-discontinuity. In such cases, the peak itself gives us the possibility of determination of T_g (see Fig. 2.8).

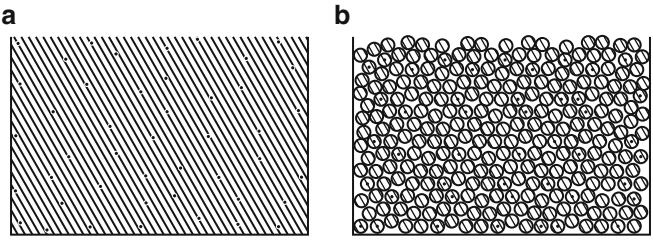

Fig. 2.7 Droplet techniques (see text): (**a**) Insoluble crystallization cores in the bulk of the melt are indicated by *black dots*. (**b**) After the dispersion of the melt, a large number of drops is formed which do not contain insoluble crystallization cores. For such drops, crystallization by homogeneous nucleation may be expected to occur

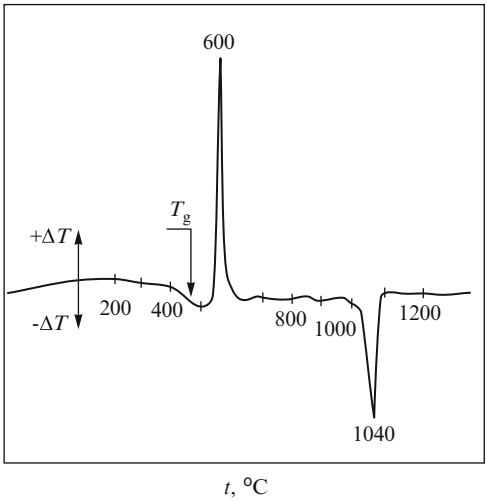

Fig. 2.8 Typical DTA-curves obtained in the process of heating of a ($Li_2O\,2SiO_2$)-glass. A crystallization peak at 600 °C is seen followed by an endothermic peak at 1,040 °C corresponding to the melting point of crystalline lithium disilicate. T_g is indicated by an inflexion point in the DTA-diagram (see Penkov and Gutzow (1984) [632])

Figure 2.9 shows the DTA-heating curve of a technical silicate glass. In the devitrification process two different crystalline phases are formed. The respective liquidus temperatures are also clearly to be seen. Particularly instructive are devitrification experiments carried out by differential-scanning calorimetry (DSC) (see Fig. 2.10). The latent heat of the crystallization or melting process can be easily determined from the areas under the crystallization or melting peaks. The discontinuity of the DTA- and especially of the DSC-curves at T_g is a direct indication that the process of glassy solidification of a melt is connected with a discontinuity in the specific heats. From these and similar experimental results it also becomes evident that the solidification of a melt into a glass is not a transformation in the sense of a first-order phase transition with a release of latent heat. It looks at a first glance more similar to a second-order phase transformation (discontinuity in C_p).

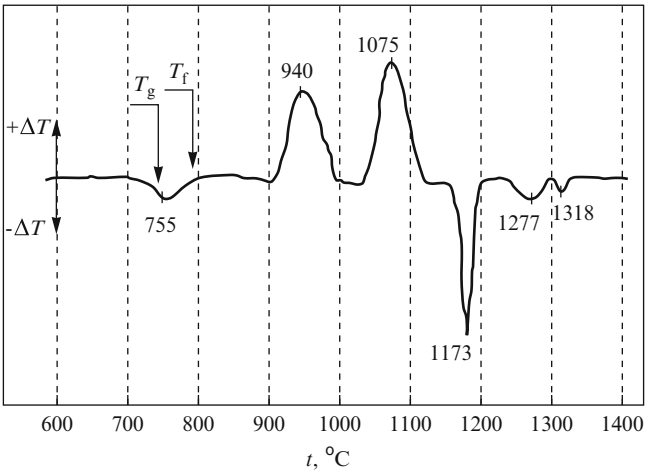

Fig. 2.9 Heating curve of a technical solidified glass-forming melt (enstatite ceramics precursor glass; after Gutzow et al. (1977) [328]). The devitrification process is manifested by two crystallization peaks at 940 and 1075 °C. The three endothermic peaks at higher temperatures correspond to the process of melting of the three different crystalline phases formed in the devitrification process. The transformation temperature and the softening point of the glass are denoted by T_g and T_f, respectively

A more extended discussion, given in the following section, shows that vitrification is described more correctly as a freezing-in process of the under-cooled melt. Here we have to mention only, that the notation glass transformation (or glass transition) temperature, proposed by Tammann, is to some extent misleading. Correct with respect to above indicated mechanism of vitrification is the proposal developed by F. Simon (1930) [756] to denote T_g as the freezing-in temperature of the glass (*Glaseinfriertemperatur* $T_e = T_g$). In English literature the "neutral" notation temperature of vitrification is preferred. It corresponds to the word *Glastemperatur* used in German literature on the physics of high polymers. However, since in technology of silicate glasses Tammann's notation glass transformation temperature is till now the most common one, it will be preferably applied here, especially, when technical glasses are discussed.

It was also first mentioned by Tammann that the value of the glass transformation temperature varies to some extent in dependence on the method of determination and, what is of principal importance, on the value of the cooling rate $q = -(dT/dt)$, reached in the in the course of vitrification of the undercooled melt: with increasing values of q higher T_g-values are obtained. Moreover, as it was also mentioned by Tammann, we have to speak more precisely of a transformation range, in which the melt is solidified into a glass. Following, again, Tammann, we will apply, in general, the notation T_f for the upper and T_g for the specification of the lower boundary of the transformation range. However, the notation T_g is mostly applied, when a standardized method of solidification is used, giving more or less reproducible values for the temperature of vitrification.

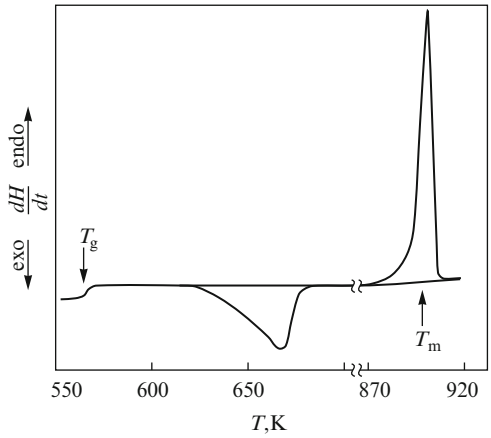

Fig. 2.10 Differential scanning calorimetry (DSC) measurements of the devitrification process of a $NaPO_3$-glass heated with a constant heating rate of 10 K min^{-1}. At T_g a salient point is observed followed by an endothermic devitrification peak. At 898 K the heat of melting of the crystalline $\alpha - NaPO_3$ phase is released. The areas under the crystallization, respectively, melting curves give the latent heat of the transformation (see also Grantcharova, Avramov, and Gutzow (1986) [271])

For typical one-component glass-forming melts and normal cooling rates the value of the glass transformation temperature, divided by the melting temperature, is usually of the order

$$\frac{T_g}{T_m} \approx \frac{2}{3}. \tag{2.71}$$

This is the so-called Beaman-Kauzmann rule (Kauzmann (1948) [440]; Beaman (1952) [55] for a first derivation of this rule see Gutzow (1972) [308]). The Beaman-Kauzmann rule was generalized by Sakka and Mackenzie (1971) [680] to multi-component systems. In this case, T_m is to be replaced by the respective liquidus temperature T_l of the system. However, for glass-forming metallic alloys the value of the ratio T_g/T_l may be considerably smaller, e.g.,

$$\frac{T_g}{T_l} \approx \frac{1}{2}. \tag{2.72}$$

For amorphous thin layers of a number of metals such as tin or gallium even considerably lower values as predicted by Eq. (2.72) are reported.

In Fig 2.11a, b (see also Table 2.2 presented in Sect. 2.5.2) according to Gutzow and Dobreva (1991) [308] distribution histograms for T_g-values of a large number of typical glass-forming melts and vitreous metallic alloys are shown. In accordance with the Beaman-Kauzmann rule for typical glass-formers, indeed, average values about $T_g/T_m \approx 0.65$ are found, while for metallic alloy glasses in addition to the peak at 0.5 a second peak at 0.3–0.4 can be noticed. The substances

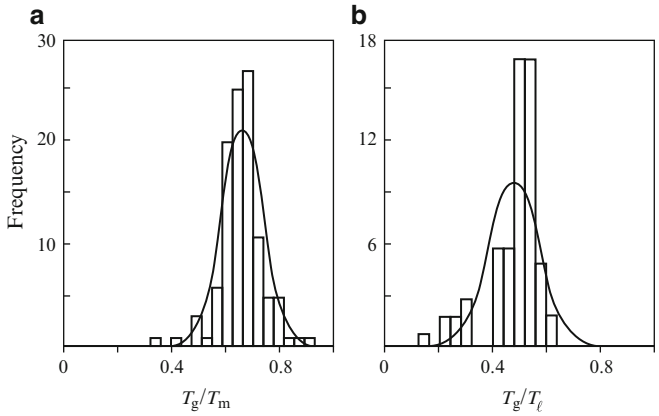

Fig. 2.11 (**a**) Frequency distribution histogram of experimentally observed T_g/T_m-values for 108 typical glass-formers with different compositions vitrified at normal cooling rates. (**b**) Frequency distribution histogram of 80 experimental T_g/T_l – values for metallic glass-forming alloys (After Gutzow and Dobreva (1991) [308])

taken into consideration in Fig. 2.11a include representatives of different types of glass-forming melts: oxides (SiO_2, B_2O_3), halides (BeF_2, ZnCl), simple borate, silicate and phosphate glasses (e.g., $Na_2O\,2B_2O_3$, $Na_2\,SiO_2$, $NaPO_3$), glass-forming organic compounds (alcohols, e.g., C_2H_5OH, CH_3OH, glycerol), organic acids and oxiacids as well as a number of more complicated aromatic organic substances. The T_g-values of practically all glass-forming organic polymer melts are also included.

Similar empirical relationships were also proposed by other authors. According to Turnbull and Cohen (1960) [865], e.g., the following equation, connecting the glass temperature T_g with the boiling temperature T_b of the substance, is valid, i.e.,

$$T_g \approx \left(\frac{1}{4} - \frac{1}{3}\right) T_b. \tag{2.73}$$

However, if one takes into consideration an additional empirical connection between T_b and T_m of the form

$$T_b \approx \frac{5}{2} T_m, \tag{2.74}$$

it turns out that Eqs. (2.73), (2.71) and (2.72) are to a large extent equivalent. For organic high polymers the glass temperature T_g depends on the average degree of polymerization, $\bar{x}$. According to Flory (1940) [215]

$$\frac{1}{T_g} \approx A + \frac{B}{\bar{x}} \tag{2.75}$$

Table 2.2 Thermodynamic properties of typical glass-forming substances: Vitrification temperature T_g, melting temperature T_m, molar melting entropy ΔS_m and molar frozen-in entropy ΔS_g (both in $\mathrm{J\,K^{-1}\,mol^{-1}}$). The ΔS_g-values are taken from: Simon and Lange (1926) [760], Gutzow (1979) [301], Nemilov (1976) [596], Timura et al. (1975) [837], Weyl and Marboe (1967, vol. 2/2, p. 1327) [919], Smith and Rindone (1961, 1962) [665, 783], Grantcharova et al. (1986a, b) [271, 272], Angell and Rao (1972) [15], Anderson (1937) [9], Tammann (1933) [820], Tammann and Jenckel (1930) [821], Tammann (1930) [819], Greet and Turnbull (1967) [276], Simon (1931) [757], Bestul and Chang (1964) [79], Kelley (1929) [447], Chen (1976) [130], Chen and Turnbull (1967) [128], and Dobreva (1992) [173]

Substance	T_m(K)	T_g(K)	T_g/T_m	ΔS_m	ΔS_g	$\Delta S_g/\Delta S_m$	References
SiO_2	1,996	1,473	0.73	9.13	3.8	0.42	[302, 596]
GeO_2	1,386	900	0.65	12.15	3.8	0.31	[596]
BeF_2	1,076	580	0.54	15.5	4.6	0.30	[596, 837]
$H_2O\,4B_2O_3$	1,132	633	0.56	111.4	29.3	0.26	[783, 919]
$Na_2O\,4B_2O_3$	1,085	689	0.63	121.1	36.4	0.30	[783, 919]
$NaPO_3$	898	550	0.61	24.7	11.0	0.44	[271]
B_2O_3	723	521	0.72	31.8	10.6	0.33	[919]
$ZnCl_2$	535	375	0.70	16.6			[783]
$H_2SO_4\,H_2O$	237	157	0.66	102.2	24.72	0.24	[15]
Se	491	303	0.62	10.89	2.9	0.27	[9, 302]
Phenolphthaleine	534	353	0.66	95.5	10.1	0.11	[302]
Betol	368	250	0.68	54.0	19.7	0.36	[820, 821]
Orthoterphenyle	329	245	0.74	51.5	22.6	0.44	[276]
Benzophenone	321	158	0.49	55.3	15.1	0.27	[820, 821]
Glycerol	291	178	0.61	62.85	19.3	0.31	[757, 821]
n-Propanol	146	95	0.65	39.0	15.9	0.41	[79]
Ethanol	156	93	0.6	31.8	10.9	0.34	[15]
Methanol	175			18.1	7.62	0.42	[15]
2Methylpentane	119	78	0.65	52.8	16.8	0.32	[79]
Butene-1	88	59	0.67	43.6	12.6	0.29	[79]
Poly(propylene)	449	259	0.58	24.3	8.0	0.33	[79]
Poly(ethyleneterephtalate)	542	342	0.63	47.9	14.3	0.30	[173]
Rubber	301	199	0.66	14.7	5.9	0.40	[79]
$Pd_{0.775}\,Cu_{0.05}-Si_{0.165}$		636			3.3		[130]
$Pd_{0.48}\,Ni_{0.32}-P_{0.20}$		585			7.5		[130]
$Au_{0.77}\,Ge_{0.136}-Si_{0.094}$	624	290	0.46	19.7	6.3	0.32	[130]
$Au_{0.814}\,Si_{0.186}$	636	290	0.45		6.3		[130]

holds. A and B are constants, specific for the considered substance.

In some respect similar to above dependencies is also the rule proposed by Tammann (1933) [820]

$$T_g \approx \left(1 - \frac{C_m}{\sqrt[3]{M}}\right) T_m. \tag{2.76}$$

Here M is the molar mass of the substance and C_m a constant, which for organic glass-forming melts has a value of about $C_m = 2$. As far as for most organic compounds $M \approx 10^2$ holds Eq. (2.76) is in fact equivalent to the Beaman-Kauzmann rule.

In the following sections the properties of glass-forming melts in the vitrification range are discussed in more detail. We start with the analysis of the temperature dependence of the viscosity, since primarily the increase of the viscosity determines the transformation of the liquid melt into a solid glass.

2.4 The Viscosity of Glass-Forming Melts

2.4.1 The Temperature Dependence of the Viscosity of Glass-Forming Melts

The first systematic studies of the viscosity of glass-forming melts were performed by Tammann. His results are summarized in his well-known monographs "Aggregatzustände" and "Der Glaszustand". Tammann carried out his investigations mainly on low melting organic model substances like salol, betol, manniol, piperine, natural resins and colophony, which can be easily transferred into the vitreous state. Based on the results of his investigations Tammann formulated elementary but very instructive concepts concerning the process of glass transition. He also formulated simple criteria for the conditions under which the quenching of a melt will lead to a glass or, vice versa, under which conditions crystallization is preferred.

It was also Tammann, who divided the process of crystallization of an undercooled melt into two consecutive stages: nucleation (characterized by the nucleation rate J, the rate of formation of centers of the crystalline phase in the bulk of the melt) and their subsequent linear growth characterized by the linear growth velocity, v. It was argued by Tammann that vitrification will occur, if in the range between T_m and T_g the temperature dependencies of the curves, representing nucleation rate J and growth rate v, respectively, do not show any significant overlapping. In contrast, an overlapping of the nucleation and growth curves will be an indication of the formation of a crystalline phase (see Fig. 2.12). According to Tammann both processes, nucleation and growth, are determined by the value of the bulk viscosity of the melt, thus underlining once more the importance of this quantity with respect to glass formation.

Since Tammann's time sophisticated methods for the determination of the viscosity of glass-forming melts and its temperature dependence have been developed and a large number of experimental data have been accumulated. Such data can be found, for example, in the classic reference book by Eitel, Pirani, and Scheel (1932) [186]. A more recent summary of properties of glasses and glass-forming

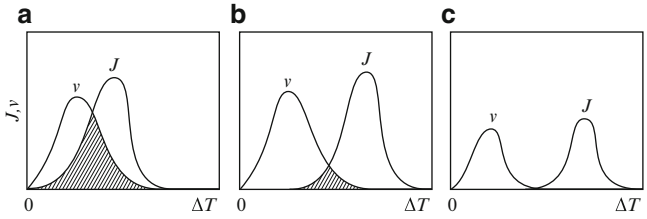

Fig. 2.12 Possible temperature dependencies of the nucleation rate, J, and the linear growth velocity, v. According to a proposal by Tammann the curve (**a**) corresponds to a melt with a low glass-forming ability while (**b**) and (**c**) refer to the opposite situation. Tammann's ideas are reformulated today in terms of the so-called TTT- (time-temperature-transformation) diagrams (see Chap. 10)

melts including viscosity data is given in the series of monographs edited by O.V. Mazurin (1973–1981, 1989, 2011) [544–546].[1]

From a physical point of view, the viscosity is a measure of the internal friction, which results from the relative motion of different layers of a liquid. If the velocity of the liquid is changed, e.g., in the x-direction, then the force F acting between the layers is given by

$$F = \eta A \frac{dv}{dx}. \tag{2.77}$$

The factor of proportionality η in Eq. (2.77) is denoted as the (shear) viscosity of the liquid, A is the surface area of the layers. Viscosity, determining the kinetics of flow of liquids, is, as discussed further on, a thermodynamic property of any liquid.

Equation (2.77) was proposed by Newton. Liquids, which can be described by such an equation with a value of η, depending on temperature and the specific properties of the liquid only, are called Newtonian liquids (see also Chap. 12). The unit "Poise" was applied earlier as the unit of the viscosity. This is the natural unit in the cgs-system. In the international system of units the corresponding quantity is Pascal second (Pas). Both quantities are related by 1 Poise = 0.1 Pas. To retain the numerical values, familiar in Poise, in the modern literature also the unit dPas is often used.

Already the first investigations of the temperature dependence of the viscosity showed that with a decrease of T a very steep increase of the viscosity is found. While at the melting temperature the viscosity seldom exceeds the value $\eta \approx 10^2$–10^3 dPas, in the transformation range its value reaches $\eta \approx 10^{13} - 10^{14}$ dPas. Examples are shown in Figs. 2.13 and 2.14 for SiO_2 melts, glycerol and selenium.

For relatively small temperature intervals the viscosity of a glass-forming melt can be described in a good approximation by an equation usually attributed to Andrade (1930, 1934) [13] and Frenkel (1934 [232], 1946 [233]) and denoted as

[1] This comprehensive information and its analysis is included and considerably extended in the SciGlass database edited by Oleg V. Mazurin and colleagues (for details see: Mazurin (2011), [545]).

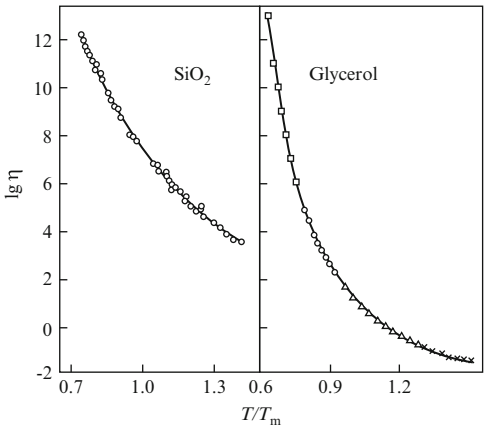

Fig. 2.13 Temperature dependence of the viscosity of two typical glass-forming substances (SiO_2 and glycerol) according to data of different authors (see Landoldt-Börnstein, vol. 2b, part 15a, Springer, Berlin, 1969, p. 120, 213 [504]). The temperature is given in relative units T/T_m, where T_m is the melting temperature

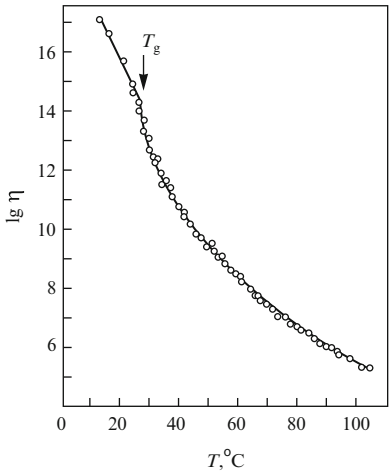

Fig. 2.14 Temperature dependence of the viscosity of selenium (c.f. Nemilov (1964) [595]; see also Rawson (1967) [657])

Andrade-Frenkel or Eyring's (1936) [193] equation

$$\eta = \eta_0 \exp\left(\frac{U_0}{k_B T}\right). \tag{2.78}$$

However, as mentioned by Andrade himself, Eq. (2.78) was first proposed as early as 1913 by de Guzman ([158], see Besborodov (1975) [80]). Frenkel gave the first elementary molecular kinetic interpretation of this equation, which was reformulated later by Eyring in terms of the absolute rate theory (see Glasstone et al. (1941) [255]).

In Eq. (2.78) U_0 is the energy (or thermodynamically more precise: the enthalpy) of activation of viscous flow, assumed to be a constant ($U = U_0$), and η_0 a temperature independent constant. Experimental results, plotted in so-called Arrhenius coordinates log η vs $(1/T)$, do not give, however, a straight line (see

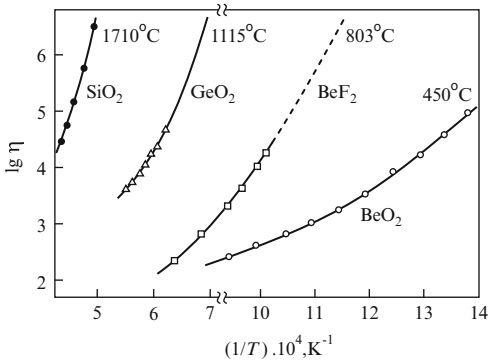

Fig. 2.15 Temperature dependence of the viscosity of typical glass-forming melts in $\log \eta$ vs $1/T$ coordinates (Mackenzie (1960) [525]; see also Rawson (1983) [657]). The temperature values given to each curve are the melting temperatures of the respective substance

Fig. 2.15), as it is to be expected from Eq. (2.78). Possible generalizations of Eq. (2.78) are connected with the introduction of a temperature dependent activation energy $U(T)$ leading to

$$\eta = \eta_0 \exp\left[\frac{U(T)}{k_B T}\right]. \tag{2.79}$$

Experiments show that with decreasing temperature an increase of $U(T)$ is observed, generally, so that the condition

$$\left(\frac{dU}{dT}\right) \leq 0 \tag{2.80}$$

is fulfilled. As shown in further developments given below in this book, this condition is of upmost importance in determining the process of glass transition. The simplest temperature dependence of the activation energy, satisfying Eq. (2.80), is given by the linear combination

$$U(T) = U'_0 - U_1 T, \tag{2.81}$$

where U'_0 and U_1 are constants (Kanai and Satoh (1954) [428]).

According to Eq. (2.78), the slope of the derivative $d(\log \eta)/d(1/T)$ gives directly the activation energy, U_0. However, for temperature dependent activation energies this is not the case. In contrast, $U(T)$ in Eq. (2.79) is determined by the differential equation Eq. (2.82) as

$$\frac{d \ln \eta}{d(1/T)} = \frac{1}{k_B T}\left\{U(T) + \frac{1}{T}\frac{dU(T)}{d(1/T)}\right\}. \tag{2.82}$$

It is evident that for temperature dependent activation energies $U(T)$ cannot be determined directly by an Arrhenius plot but only via Eq. (2.79) as

$$U(T) = k_B T(\ln \eta - \ln \eta_0). \tag{2.83}$$

A number of equations of the form of Eq. (2.79) which fulfil the condition Eq. (2.80) were proposed by different authors. Most of them give a temperature dependence closer to experimental results than the linear approximation Eq. (2.81) due to Satoh and Kanai.

Here dependencies are summarized which are distinguished both by the accuracy of description of experimental results as well as by the possibility of interpreting them in the framework of statistical model theories of liquids. The most well-known equation of this type is the Vogel-Fulcher-Tammann (VFT) equation

$$\eta = \eta_0 \exp\left(\frac{U_0^*}{k_B(T - T_\infty)}\right). \tag{2.84}$$

Here η, U_0^* and T_∞ are empirical constants specific to the substance considered.

The Vogel-Fulcher-Tammann equation was independently proposed by the three men giving this equation their names. Vogel (1921) [887] developed it based on investigations of the temperature dependence of the viscosity of greases, Fulcher (1925) [239] by an analysis of the $\eta(T)$-course of silicate glasses and Tammann (with Hesse (1926) [822]) based on experiments with glass-forming organic substances. If the choice of the three constants in Eq. (2.84) is carried out appropriately from measurements of values of the viscosity at sufficiently different values of temperature and viscosity (e.g., $\log \eta \approx 2 - 4, \log \eta \approx 6 - 8, \log \eta \approx 12 - 13$), then the VFT-equation describes the viscosity in the whole temperature range, characterized by changes of the viscosity by ten orders of magnitude, with an accuracy better than 10 %.

For $T \to T_\infty$, according to the VFT-equation, the viscosity tends to infinity. This is the reason for the usual notation T_∞ for one of the constants in Eq. (2.84). The VFT-equation corresponds to a temperature dependent activation energy of the form

$$U(T) = U_0^* \frac{T}{(T - T_\infty)}, \tag{2.85}$$

which also tends to infinity for $T \to T_\infty$.

The analysis of a large number of experimental data shows that for most of the typical glass-forming substances (oxide glasses, silicate glasses, organic high polymers) in a good approximation

$$\frac{T_\infty}{T_m} \approx 0.5 \tag{2.86}$$

holds (Gutzow (1975) [297]). For glass-forming metallic alloys usually a somewhat lower value

$$\frac{T_\infty}{T_l} \approx 0.33 \tag{2.87}$$

is obtained. If one takes into account Eq. (2.71) then Eq. (2.86) may be written also as

$$\frac{T_\infty}{T_g} \approx \frac{3}{4}. \tag{2.88}$$

Equivalent to the VFT-equation is a relation widely used in the rheology of glass-forming organic high polymers named WLF-equation after Williams, Landel and Ferry ((1955) [924], see also Ferry (1961) [204]). According to the WLF-equation the relaxation time, τ, or the characteristic frequency of motions, $\omega = 2\pi/\tau$, of the building units of the melt in the vicinity of T_g can be calculated by (Donth (1981) [179])

$$\log\left(\frac{\omega}{\omega^*}\right) = \frac{C_1(T - T^*)}{(C_2 + (T - T^*))}. \tag{2.89}$$

The parameters ω^* and T^* are arbitrarily chosen reference values, the constants C_1 and C_2 depend on the choice of the reference state. Equation (2.89) can be transformed into the VFT-equation by a simple substitution of variables (see Gutzow (1972) [294]).

It is of principal importance that both the VFT- and WLF-equations can be derived in the framework of the free volume theories of liquids. According to this theory, the free volume $\nu(T)$ determines the viscosity via (see Chap. 12)

$$\eta = \eta_0 \exp\left(\frac{B_0}{\nu(T)}\right). \tag{2.90}$$

Here B_0 and η_0 are constants, again.

Equation (2.90) is called the Doolittle equation (Doolittle (1951) [180]; Bueche (1962) [109]). It can be considered as a generalization of an empirical expression, proposed many years ago by Batchinski (1913) [50],

$$\eta = \frac{\eta_0}{\nu(T)}. \tag{2.91}$$

Another equation with a temperature dependent activation energy was proposed by Cornelissen, van Leeuwen and Waterman (1957 [140], see Bezborodov (1975) [80])

$$\eta = \eta_0 \exp\left(\frac{A}{T^n}\right), \tag{2.92}$$

corresponding to an activation energy of the form

$$U(T) = \frac{k_B A}{T^{n-1}}. \tag{2.93}$$

Here η_0, A and n are three constants characteristic for a given melt. Evstropev and Skornyakov (see Skornyakov (1955) [767]) showed that the temperature dependence of the viscosity can be described in terms of Eq. (2.93) with $n = 2$ for temperatures higher than the liquidus temperature T_l with a very satisfactory

accuracy. In such a way the three constants in Eqs. (2.92) and (2.93) are reduced to only two. Recently, a derivation of an equation of the form of Eq. (2.92) has been developed in the framework of a new molecular model of viscous flow in glass-forming melts (Avramov and Milchev (1988) [26]).

Finally, we mention an equation, proposed by the well-known physico-chemist le Chatelier (1924) [502] and by Waterton (1932) [913] (see, again, Bezborodov (1975) [80])

$$\eta = \eta_0 \exp\left[b_0 \exp\left(\frac{U^*}{k_B T}\right)\right]. \tag{2.94}$$

This equation gives a particularly steep temperature dependence of the viscosity. It was applied by Schischakov (1954) [687] to a number of glass-forming systems and is denoted sometimes also as Schischakov's equation. In contrast to Eq. (2.84), Eqs. (2.92) and (2.94) do not predict a divergence of the viscosity for finite values of temperature but only for T tending to zero. A derivation of Eq. (2.94) from a statistical point of view is possible applying the hole theory of liquids (Sanditov, Bartenev (1982) [683]).

Sometimes equations are also used for the interpretation of experimental results which represent combinations of the expressions discussed above, e.g.

$$\eta = \eta_0 \exp\left(\frac{U_0}{k_B T}\right) \exp\left(\frac{B_0}{T^n}\right), \tag{2.95}$$

$$\eta = \eta_0 \exp\left(\frac{U_0}{k_B T}\right) \exp\left(\frac{B_0}{(T - T_\infty)}\right), \tag{2.96}$$

i.e., combinations of a Frenkel type temperature dependence with equations providing a steeper temperature course. Equation (2.95) was proposed by Fulcher (1925) [239] while Eq. (2.96) is due to Macedo and Litovitz (1986) [524]. Since the number of constants in such combinations of equations is increased to four, it is not a surprise that, by using them, the description of experimental results can be achieved with a higher accuracy.

The above mentioned and similar combined equations have been found in a more or less empirical manner. However, from a theoretical point of view, combinations of equations of the considered form with two different exponential temperature dependencies may reflect different sides of the mechanisms of the viscous flow: for example, separation of the individual diffusing units from their neighbors as the first step followed by a translation over certain distances into an appropriate vacancy (see, e.g., the discussion in Sanditov and Bartenev (1982) [683]). In this respect equations of the form of Eq. (2.79) are less general since they describe only one side of the complicated process of viscous flow.

Finally, we would like to mention that Eq. (2.77) with a value of the viscosity depending only on temperature and the specific properties of the liquid, is itself only an approximation, valid for medium values of the viscosities and velocities of the viscous flow. Generalizations of Eq. (2.77) and the significance of Non-Newtonian flow in vitrification kinetics and phase transformations in glass-forming melts will be discussed in Chap. 12.

2.4.2 Technological Significance of the Viscosity

The temperature dependence of the viscosity of glass-forming melts is also of an exceptional technological significance, in particular, for processes of purification and homogenization of the melt, styling and thermal treatment of the already formed glass products. It determines the temperature range, in which one method of machining or the other may be applied. In glass technology usually a division between short and long glasses is made in dependence on the steepness of increase of the viscosity in the transformation range. Usually in technological processes long glasses with a moderate increase of viscosity are preferred, since they are less vulnerable with respect to small temperature changes. Unfortunately, some of the most important technical glasses behave as short glasses, which leads to a number of technological difficulties in their fabrication. As extremely short materials metallic glass-forming alloys have to be considered, which require the application of very specific methods of vitrification and glass-processing (splat cooling and ultra-rapid spinning methods).

In glass technology the transformation temperature T_g is usually identified with a value of the viscosity of the order of 10^{13} dPas. The upper value of the vitrification range T_f (Tammann's softening temperature) corresponds to approximately 10^{11} dPas. In glass-processing one of the most important forms of treatment is the annealing of a glass in order to remove strains produced in the course of formation and manufacturing of the glass. This process may be carried out in a distinct temperature range. T_g corresponds to the upper limit of this interval. It is denoted, therefore, in the technological literature also as the upper annealing point. Above T_g the form of the glass changes and crystallization processes may occur.

The lowest value of the temperature at which the annealing process can be realized in glass-processing, the lower annealing point T_a, corresponds to a viscosity of 10^{14} dPas. At the upper annealing temperature T_g strains, which may exist in the glassy material, relax over a period of about 10–15 min, while at T_a optically measurable strains disappear only after 10–15 h. The value of the temperature T_a for technical silicate glasses is found to be usually 10–15 K below T_g. Below T_g and T_a the highly viscous frozen-in melt can be considered, at least, in technological respect, as a solid. Usually, it is assumed that a solid is characterized by a viscosity of the order 10^{15} dPas or even higher. The transformation temperature T_g and the softening temperature T_f corresponding to the lower and upper boundaries of the transformation range, are usually determined by dilatometric measurements (see Fig. 2.16). At T_g in the dilatometric curves a salient point is observed, while at T_f the material breaks down. At the Littleton softening point $\eta \approx 2 \cdot 10^8$ dPas holds.

Further important from a technological point of view temperature values of a glass-forming melt are the flow point, corresponding to a viscosity of $7 \cdot 10^4$ dPas (the Lillie flow point) or 10^4 dPas (Dietzel and Brückner (1955–1957) [167–169]), the viscosity range for glass blowing ($\log \eta \approx 3 - 5$), the seal point ($\log \eta \approx 6$), where an adhesion of the melt on metals becomes possible. The Littleton softening

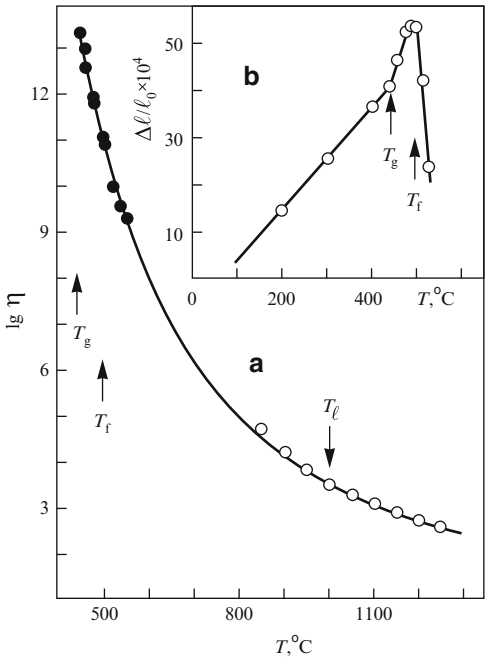

Fig. 2.16 Temperature dependence of the viscosity η (**a**) and dilatometric curve of a lithium disilicate enamel melt (**b**) (see Penkov and Gutzow (1984) [632]). The salient point in the dilatometric curve determines T_g, while at T_f the sample breaks down. A comparison with the viscosity vs temperature curve shows that T_g corresponds to $\log \eta \approx 13$ and T_f to $\log \eta \approx 11$ (η in dPas)

point corresponds to the lower limit of temperature for which a crystallization of glass-forming melts may, as a rule, still be observed.

2.4.3 Temperature Dependence of Molecular Properties Connected with the Viscosity

From the viscosity of a melt, which can be measured in a relatively simple way, the temperature dependence of other quantities connected with the viscosity can be determined. Though some of the relations which are discussed in the following are in part only a qualitative estimate, they can be helpful, nevertheless, for obtaining a first insight into the temperature dependencies of a number of parameters important for the processes of vitrification or crystallization. Two of these quantities are the self-diffusion coefficient of the building units of the melt D_0 and the impingement rate Z, i.e., the number of collisions of molecules of the melt with a unit area of some hypothetical surface, embedded in it.

According to Stokes's law the force acting on a sphere with a diameter d_0 moving with a velocity v can be expressed by

$$F = 3\pi\eta d_0 v. \tag{2.97}$$

If one applies this equation to the motion of a molecule in the melt then, following Einstein's approach for the description of Brownian motion, the following relation is obtained (see Einstein (1905) [187]; Hodgdon and Stillinger (1993) [372])

$$D_0 = \frac{k_B T}{3\pi\eta d_0}. \tag{2.98}$$

In terms of Eyring's absolute rate theory a more correct derivation can be given leading to (Glasstone, Laidler, and Eyring (1941) [255])

$$D_0 = \frac{k_B T}{\eta d_0}. \tag{2.99}$$

Equation (2.99) is of the same form as Eq. (2.98), however, with a somewhat smaller numerical factor of about one order of magnitude. Applying in addition Einstein's relation

$$|\Delta\mathbf{r}|^2 = 2Dt, \tag{2.100}$$

connecting the diffusion coefficient of a Brownian particle with the square of the displacement $\Delta\mathbf{r}$ from the initial position occupied at $t = 0$, then one may also write

$$D_0 \approx \frac{d^2}{\tau_R}. \tag{2.101}$$

Now we can use the idea that here τ_R is Frenkel's average stay time for a particle of the melt at a given position and d is the average displacement connected with a jump to a new position. Usually, it can be assumed that d is of the order of the size of building units of the liquid ($d \approx d_0$), which gives

$$D_0 \approx \frac{d_0^2}{\tau_R}. \tag{2.102}$$

Equations (2.99)–(2.102) yield

$$\tau_R \approx \frac{d_0^3 \eta}{(k_B T)}. \tag{2.103}$$

Compared with the exponential dependence of the viscosity on temperature, the terms linear in T can be considered practically as constants. Thus, η also determines according to Eqs. (2.102) and (2.103) the temperature dependence of the relaxation time τ_R and the self-diffusion coefficient D_0 of the melt.

From the phenomenological equations, describing the rheological properties of highly viscous liquids, developed by Maxwell, Kelvin and Voigt (see Chap. 12), the macroscopic relaxation time of a melt τ_R is connected with the viscosity by

$$\tau_R = \frac{\eta}{G^*}. \tag{2.104}$$

The factor of proportionality G^* in above Eq. (2.104) has the dimension and the physical meaning of a modulus of elasticity. A comparison with Eq. (2.103) leads us to the conclusion that highly viscous melts can be considered as elastic bodies, characterized by a modulus of elasticity of the order

$$G^* \approx \frac{k_B T}{d_0^3} \approx \frac{k_B T}{v_m}, \tag{2.105}$$

where v_m is the average volume per particle of the melt.

An elementary estimation of the impingement rate, Z, and its connection with the viscosity can be given in the following way. If $\langle v \rangle$ is the average of the absolute value of the velocity of translation of the melt particles and c the average number of particles per unit volume, then Z can be expressed in analogy to the collision frequency in gases (see Chap. 6) as

$$Z = \frac{1}{4} c \langle v \rangle. \tag{2.106}$$

For condensed systems

$$c \approx \frac{1}{v_m} \approx \frac{1}{d_0^3} \tag{2.107}$$

holds, while the average velocity of molecular translation in a liquid may be written in accordance with Frenkel's model as

$$\langle v \rangle \approx \frac{d_0}{\tau_R}. \tag{2.108}$$

Equations (2.106)–(2.108) yield

$$Z \approx \frac{1}{d_0^2 \tau_R} \tag{2.109}$$

or

$$Z \approx \frac{k_B T}{d_0^5 \eta}. \tag{2.110}$$

It is obvious that the equations outlined in this section have to be considered only as qualitative estimates. For highly structured molecules, which are far from having a spherical shape, additional steric factors have to be introduced, in particular, for the calculation of the effective value of the impingement rate. The effective number of collisions $Z^{(eff)}$ can be defined as the ratio ς of the total number of molecular collisions Z, which results in an incorporation of the colliding particle into the aggregate of an evolving crystalline phase. Thus, we may write $Z^{(eff)} = \varsigma Z$. According to its definition the parameter ς has values in the range $0 \leq \varsigma \leq 1$. Despite the mentioned limitations experiments show that the expressions derived describe the temperature dependence of D_0, Z and τ_R with a reasonable accuracy, sufficient for a large number of applications.

2.5 Thermodynamic Properties of Glass-Forming Melts

2.5.1 Temperature Dependence of the Heat Capacities

In the transformation range with the decrease of temperature not only a dramatic increase of the viscosity of the melt is observed, but all properties of the under-cooled melt change to those of the corresponding glass. It was, again, Tammann who started the investigations of the temperature dependence of the thermodynamic properties of glass-forming melts in the vitrification range (cf. also Winkelmann and Schott (1894) [926]). First measurements of the mechanical properties were performed (thermal expansion coefficient, hardness etc.) applying as usual for this remarkable investigator relatively simple but instructive methods.

Of considerable importance for the understanding of the physical nature of the vitreous state in addition to viscosity data are measurements of the variation of the caloric properties of glass-forming melts in the transformation range. As discussed in Sect. 2.3 the process of vitrification is not connected with a plateau in the $T = T(t)$-curves (compare Fig. 2.5c). This behavior, as already mentioned, is an indication that the transformation of the melt into a glass is not connected with a discontinuous change of the entropy or enthalpy of the system. However, DTA and DSC-curves exhibit an inflexion point in the $C_p(T)$-curves at T_g in the process of glass heating. This feature is an indication for an abrupt change of the specific heat, the second derivative of the thermodynamic potential G at T_g.

This type of behavior is illustrated in Fig. 2.17 for the classical case of glycerol, which is used as an example also in the following figures to illustrate the change of the thermodynamic properties of glass-forming melts in the vitrification range. These and all subsequent investigations of the temperature dependence of the specific heat of glass-forming substances carried out in different laboratories in the last 80 years have shown the same typical s-shaped decrease of the specific heat of the under-cooled melt, first observed for glycerol and silica.

The first measurements of caloric properties of glass-forming substances were initiated by W. Nernst in connection with the desired verification of the Third law of thermodynamics proposed by him in 1906 (see Nernst (1918) [601]; Simon (1930 [756], 1956 [759]); Eitel (1954) [185]). Nernst expected that the Third law of thermodynamics and its consequences can be applied to all forms of condensed matter – liquids, crystals and glasses.

In the classical studies, carried out by Witzel (1921) [930], Simon and Lange (1926) [760], the specific heats of silica glass, of the corresponding crystalline phase (quartz, cristobalite and tridymite) and the glass-forming melt were measured. The choice of SiO_2 was not very suitable, since the measurements had to be carried out over a range of temperatures of about 2000 K, from the melting point of cristobalite (1983 K) to temperatures of liquid hydrogen. To comprise this interval, four different calorimetric methods had to be used. At the same time also measurements with the much more convenient substance glycerol were performed by Gibson and Giauque (1923) [252], Simon and Lange (1926) [760] (see Fig. 2.17). The melting

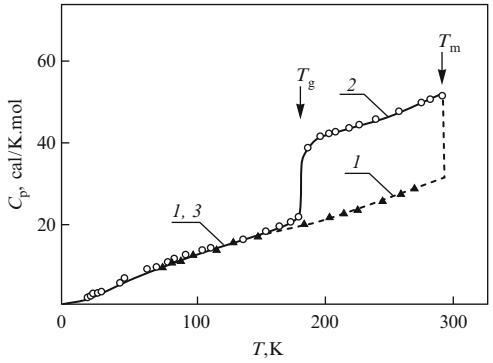

Fig. 2.17 Typical $C_p = C_p(T)$ curves for the fluid ($C^{(f)}$), crystalline ($C^{(c)}$) and vitreous forms of a substance, here presented as an example for glycerol. The values of the specific heats for the crystalline state (*1*) are specified by *black triangles*, the curve for the undercooled melt (*2*) and the glass (*3*) by *white circles* (Data are taken from the measurements of Gibson and Giauque (1923) [252], Simon and Lange (1926) [760], summarized in [311])

point of glycerol is about $T_m \approx 298\,\mathrm{K}$, while T_g is of the order $T_g \approx 193\,\mathrm{K}$ and only one crystalline phase of this substance exists (silica, in contrast, is known to have six crystalline modifications). In both cases it is thanks to F. Simon that the measurements were extended down to the lowest temperatures achievable at that time, to those of liquid helium. Soon after that similar C_p-measurements on low melting glass-forming substances were carried out by Tammann and other investigators (organic compounds, ionic melts, metallic alloys, silica, see Fig. 2.18). At present the results of C_p-measurements on about 150 substances are known. Qualitatively always the same s-shaped curves were obtained for the temperature dependence of this quantity.

Curves of the type given in Figs. 2.17 and 2.18 can be obtained reproducibly at moderate cooling rates. With an increase in the cooling rate the jumps in the $C_p(T)$-curves and, consequently, T_g are found at higher temperatures. A first example in this respect is supplied by the results of the measurements of Zhurkov and Levin (Fig. 2.19, [957], see also Kobeko (1952) [461]). Quantitatively the dependence connecting cooling rate q and glass transformation temperature T_g is given by the Bartenev-Ritland equation

$$\frac{1}{T_g} = A - B\log(q), \qquad q = -\frac{dT}{dt}, \tag{2.111}$$

where A and B are constants.

In Fig. 2.20 another kinetic effect in vitrification is demonstrated. One and the same glass sample, vitrified with different cooling rates, is heated up with a constant heating velocity. The T_g-values obtained differ as demonstrated by experiments performed by Moynihan with a simple inorganic glass.

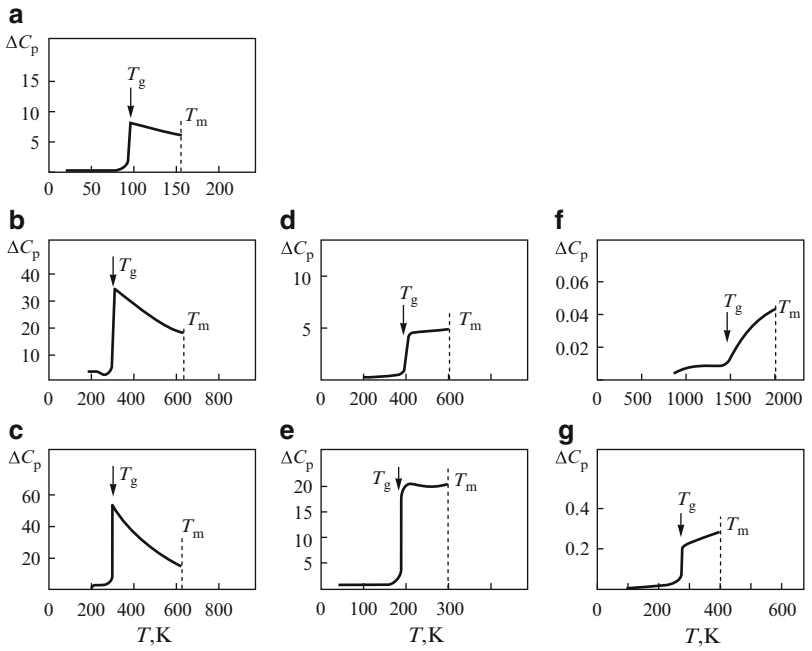

Fig. 2.18 Temperature dependence of the difference of the specific heats ΔC_p melt-crystal of a number of glass-forming melts in the $(T_m - T_g)$-region measured by different authors (see Gutzow (1975) [297]; Gutzow and Grantcharova (1985) [311]). The substances are: (**a**) methanol; (**b**) metglass (Au/Si); (**c**) metglass (Au/Ge/Si); (**d**) $ZnCl_2$; (**e**) glycerol; (**f**) SiO_2; (**g**) glycose

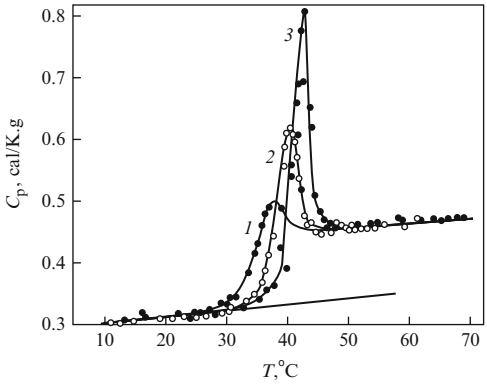

Fig. 2.19 $C_p(T)$-curves obtained in the process of heating of a glass-forming organic polymer melt for different heating rates according to the measurements of Zhurkov and Levin ((1950) [957], see also Kobeko (1952) [461]). Curve (*1*) corresponds to a heating rate of 0.1 K min^{-1}, curve (*2*) to 0.4 K min^{-1} and curve (*3*) to 1.5 K min^{-1}

The Bartenev-Ritland equation and the experimental results underlying it are of importance in two different aspects. First, it becomes evident, that the process of vitrification cannot be considered as an equilibrium phase transformation, e.g., in the sense of the Ehrenfest classification. For equilibrium phase transformations the

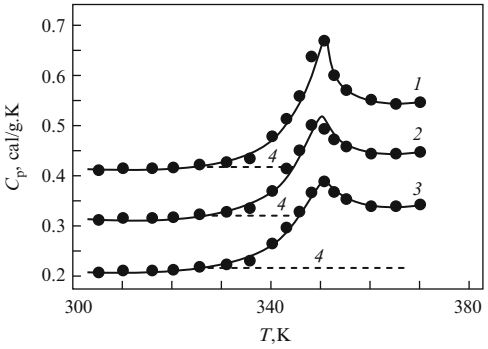

Fig. 2.20 Influence of the thermal history on the $C_p(T)$-curves measured in the heating process of a vitrified substance ($0.4Ca(NO_3)_2\ 0.6KNO_3$). The melt was quenched with different cooling rates ((*1*): 0.62 K min^{-1}; (*2*): 2.5 K min^{-1}; (*3*): 10 K min^{-1}). In all considered cases the melt is heated with the same heating rate 10 K min^{-1} (Moynihan et al. (1976) [581]; see also Mazurin (1986) [543])

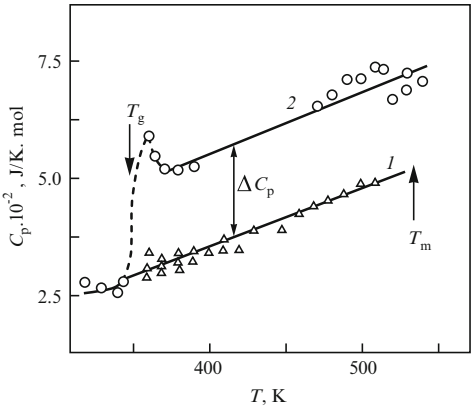

Fig. 2.21 Temperature dependence of the specific heats of crystalline (*1*) and amorphous (*2*) phenolphthalein as determined by differential scanning calorimetric measurements in heating runs (After Grantcharova et al. (1986) [268])

transition temperature is a well-defined quantity, which does not depend on kinetic factors.

Equation (2.111) shows, moreover that the dependence of the glass transformation temperature upon cooling rate is of a logarithmic form. This result has the consequence that significant variations of the cooling rates are required to reach measurable variations of the properties of the solidified to a glass melt. Moreover, experiments show that with an increase of the cooling rate a peak in the $C_p(T)$-curves develops in the vicinity of T_g as it is also seen on Fig. 2.20. A kinetic derivation of Eq. (2.111) and a discussion of the origin of this peak will be given in Chap. 3 in the framework of the kinetic theory of vitrification, developed by a number of authors, and, in particular, by Volkenstein and Ptizyn ((1956) [892]; see also Volkenstein (1959) [891]) (see also Fig. 2.21).

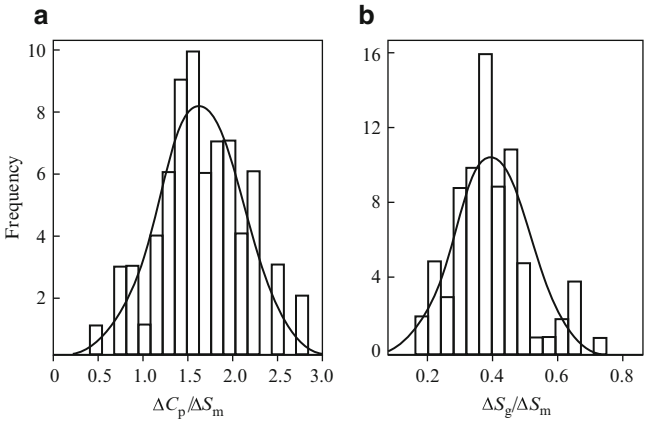

Fig. 2.22 Frequency distribution of (**a**) experimentally determined $\Delta C_p(T_g)/\Delta S_m$-values and (**b**) $\Delta S_g/\Delta S_m$-values for 80 typical glass-forming systems for which the respective thermodynamic measurements have been reported. Experimental data are taken from Kauzmann (1948) [440], Gutzow (1972) [293], Privalko (1980) [650], Wunderlich (1960) [934]; see Gutzow and Dobreva (1991) [308]. According to these results the most probable value of the ratio $\Delta S_g/\Delta S_m$ equals 0.38 and for the ratio $(\Delta C_p(T_g)/\Delta S_m) \approx 1.5$ follows as expressed by Eq. (2.112)

It was further shown by Wunderlich (1960) [934] based on an analysis of the then existing experimental results on about 45 substances (mainly organic and organic high polymers) that the ratio $\Delta C_p(T_g)/\Delta S_m$ is, generally, of the order

$$\frac{\Delta C_p(T_g)}{\Delta S_m} \approx 1.5, \tag{2.112}$$

indicating a certain universality in the caloric behavior of different substances. On Fig. 2.22 the validity of Eq. (2.112) is illustrated taking into consideration practically all known for today data on $C_p(T)$-measurements of glass-forming substances (Gutzow and Dobreva (1991) [308]).

2.5.2 *The Temperature Dependence of the Thermodynamic Functions*

According to Eqs. (2.29)–(2.31) the temperature dependence of the thermodynamic functions of glass-forming melts can be expressed directly through C_p. In addition, the values of the enthalpy H and the free enthalpy G have to be known, at least, for one temperature. Instead of the potentials H, G or S of the respective states we will discuss the differences between these quantities for the liquid or vitreous states compared with the corresponding crystalline phase. These differences are denoted

in the following by

$$\Delta H = H^{(f)} - H^{(c)} \qquad \Delta H_g = H^{(g)} - H^{(c)}, \tag{2.113}$$

$$\Delta G = G^{(f)} - G^{(c)} \qquad \Delta G_g = G^{(g)} - G^{(c)}, \tag{2.114}$$

$$\Delta S = S^{(f)} - S^{(c)} \qquad \Delta S_g = S^{(g)} - S^{(c)}. \tag{2.115}$$

The subscripts f, g, c refer to the liquid (f), vitreous (g) and crystalline (c) states of the considered substance, respectively.

Denoting further by ΔG_m and ΔS_m the values of these quantities at the melting point (free enthalpy and entropy of melting) Eqs. (2.23)–(2.25) may be rewritten (identifying the arbitrary reference value of temperature T_0 with the melting temperature T_m) in the form

$$\Delta S(T) = \Delta S_m - \int_T^{T_m} \frac{\Delta C_p}{T}\, dT, \tag{2.116}$$

$$\Delta H(T) = \Delta H_m - \int_T^{T_m} \Delta C_p\, dT, \tag{2.117}$$

and with $G = H - TS$ (Eq. (2.18)) we have to write

$$\Delta G(T) = \Delta H(T) - T\Delta S(T). \tag{2.118}$$

As a result, we obtain (see also Eq. (2.25))

$$\Delta G(T) = \Delta S_m(T_m - T) - \int_T^{T_m} dT \int_T^{T_m} \frac{\Delta C_p}{T}\, dT. \tag{2.119}$$

In Eq. (2.119), ΔG_m was set equal to zero since for $T = T_m$ the free enthalpies of the liquid and crystalline phases coincide (compare Sect. 2.2.3).

If one takes, moreover, into consideration the experimental fact that $\Delta C_p \approx 0$ for $T < T_g$ (see Figs. 2.17 and 2.18), then Eqs. (2.116)–(2.119) may be approximated for $T < T_g$ by

$$\Delta S(T) = \Delta S_m - \int_{T_g}^{T_m} \frac{\Delta C_p}{T}\, dT, \tag{2.120}$$

$$\Delta H(T) = \Delta H_m - \int_{T_g}^{T_m} \Delta C_p\, dT, \tag{2.121}$$

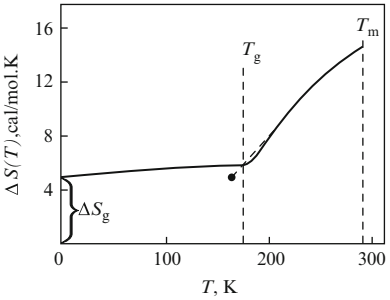

Fig. 2.23 Temperature dependence of the entropy difference of glycerol for the liquid and the glass (After Simon (1931) [757]). In contradiction to Nernst's Third law of classical thermodynamics the zero point entropy difference is not equal to zero but has a finite positive value $\Delta S(0) \approx \Delta S(T_g)$. With a *dashed line* the entropy value of the glass is given as obtained by Oblad and Newton (1937) [609] as the result of prolonged annealing (See also Fig. 2.34). The *black dot* corresponds to a temperature of 174 K

$$\Delta G(T) = \Delta S_m(T_m - T) - \int_T^{T_m} dT \int_{T_g}^{T_m} \frac{\Delta C_p}{T}\, dT. \tag{2.122}$$

Since according to Eq. (2.116)

$$\Delta S(T_g) = \Delta S_m - \int_{T_g}^{T_m} \frac{\Delta C_p}{T}\, dT \tag{2.123}$$

holds, Eq. (2.120) is equivalent to

$$\Delta S(T) = \Delta S(T_g) \equiv \Delta S_g = \text{const.} \qquad \text{for} \quad T < T_g. \tag{2.124}$$

It follows that the entropy of a glass has a nearly constant value for $T < T_g$ and, moreover that the entropy of the glass is not equal to zero for T tending to zero.

Following F. Simon, the behavior of S as a function of T is shown in Fig. 2.23 for glycerol calculated from the $C_p(T)$-course of this substance (Fig. 2.17). Similarly, we obtain that for $T < T_g$ the relations

$$\Delta H(T) = \Delta H(T_g) = \Delta H_g, \qquad \Delta H_g = \text{const.} \quad \text{for} \quad T < T_g, \tag{2.125}$$

$$\Delta G(T) = \Delta H(T_g) - T\Delta S(T_g) \qquad \text{for} \quad T < T_g, \tag{2.126}$$

are fulfilled (see also Fig. 2.24). These equations are, again, in contradiction to the Third law of thermodynamics, in particular, with its consequences expressed through Eq. (2.28). In contradiction to Eq. (2.28) and the Third law we obtain

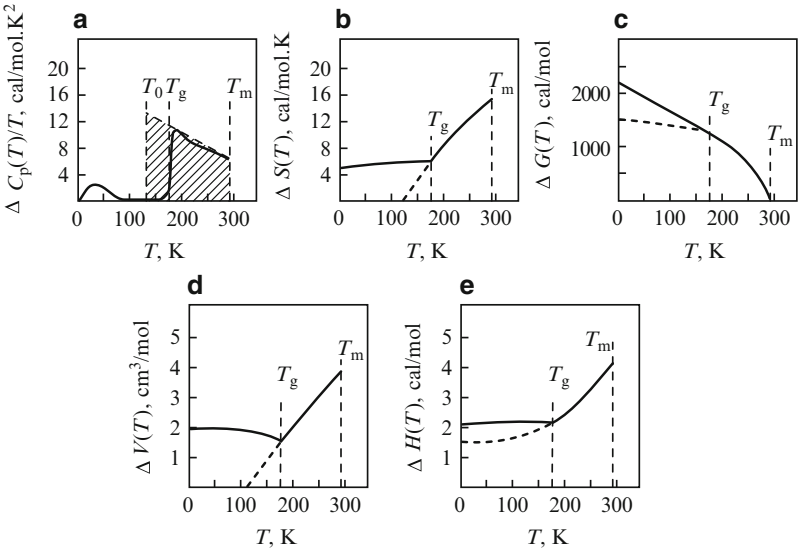

Fig. 2.24 Temperature dependence of some thermodynamic functions of glycerol calculated from measurements of the specific heat (compare Fig. 2.17) and of the densities of the liquid, vitreous and crystalline states of glycerol: (**a**) Reduced specific heat difference (the shaded area from T_m to T_0 gives the entropy of melting of glycerol according to Eq. (2.116)); (**b**) entropy; (**c**) Gibbs free energy; (**d**) molar free volume (the curve is given based on density measurements); (**e**) enthalpy. By a *dashed line* extrapolations of the thermodynamic functions of the undercooled melt into the region below T_g are given. The curves for the undercooled melt and the glass are specified by *full lines* (According to data by Simon for a.), b.), c.), e.) and by Schulz for d.))

$$\lim_{T\to 0}\frac{\partial}{\partial T}(\Delta G) = -\Delta S(T_g) < 0, \tag{2.127}$$

$$\lim_{T\to 0}\frac{\partial}{\partial T}(\Delta G) \neq \lim_{T\to 0}\frac{\partial}{\partial T}(\Delta H), \qquad \lim_{T\to 0}\frac{\partial}{\partial T}(\Delta H) = 0. \tag{2.128}$$

From these considerations the construction shown in Fig. 2.25b is found, which is to be compared with Nernst's $\Delta G(T)$- and $\Delta H(T)$-curves (Fig. 2.25a, Nernst (1918) [601]).

All the experimental results known at present show that considerable values of the thermodynamic functions H, G and S are frozen-in in the vitreous state. If the glass is solidified at normal cooling rates then in the average the relations

$$\frac{\Delta S_g}{\Delta S_m} \approx \frac{1}{3}, \tag{2.129}$$

$$\frac{\Delta H_g}{\Delta H_m} \approx \frac{1}{2} \tag{2.130}$$

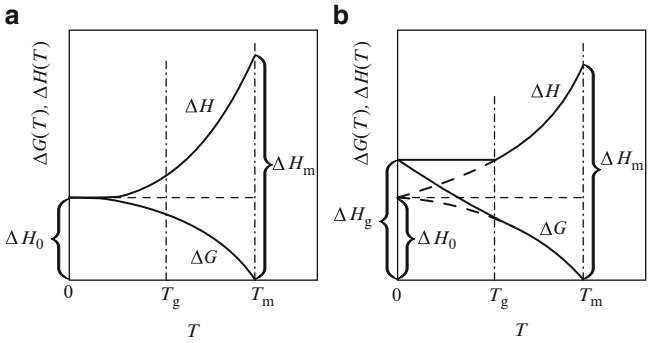

Fig. 2.25 (**a**) Temperature dependence of the enthalpy (ΔH) and the Gibbs free energy (ΔG) difference melt-crystal for an equilibrium system obeying the Third law of thermodynamics (Nernst's $\Delta H, \Delta G$-diagram); (**b**) Temperature dependence of the enthalpy and the Gibbs free energy for a vitrifying system *(full curves)* according to Simon (1956) [759]. The temperature course one would expect from the Third law of thermodynamics is indicated by *dashed curves*. ΔH_0 is the zero-point enthalpy difference for the two different equilibrium states of the same substance (melt and crystal), ΔH_g the zero-point enthalpy difference between the glass and the undercooled melt. Note also that for equilibrium systems $(d(\Delta H)/dT) = (d(\Delta G)/dT) = 0$ is obtained for $T \to 0$, while for a glass the relations $(d(\Delta H)/dT = 0)$ and $(d(\Delta G)/dT) < 0$ hold

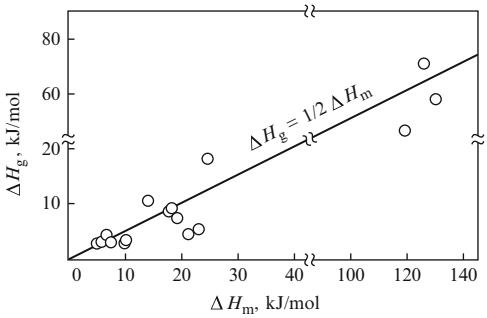

Fig. 2.26 Dependence of the molar frozen-in enthalpy ΔH_g of glass-forming melts on the molar heat of melting ΔH_m. The *black dots* are obtained by dividing both the ΔH_g- and the ΔH_m-values by two

are fulfilled (Gutzow (1971) [313]; Gutzow and Dobreva (1991) [308]; cf. Figs. 2.22b and 2.26).

For a proof of the outlined generalizations of experimental results thermodynamic properties of different glass-forming melts are summarized in Tables 2.2–2.4. Typical glass-forming melts like $SiO_2, GeO_2, Be_2O_3, NaPO_3$, alkali-borates and ethanol are included as well as glass-forming molecular substances like *n*-propanol, benzophenone, phenolphthalein or metallic alloy systems, which form glasses at higher cooling rates. The following conclusions can be drawn from these experimental results:

- Even for glass-forming substances with a very different structure the ratio T_g / T_m is given in a good approximation by Kauzmann's rule (compare Eq. (2.71)).

Table 2.3 Thermodynamic properties of representative glass-forming substances: Change of the molar specific heat ΔC_p at the vitrification temperature T_g and the ratio $\Delta C_p(T_g)/\Delta S_m$. The $\Delta C_p(T_g)$-values are taken from: Wunderlich (1960) [934], Grantcharova et al. (1986a, b) [268, 271], Angell and Rao (1972) [15], Dobreva (1992) [173], and Chen and Turnbull (1967) [128]

Substance	$\Delta C_p(T_g)$ ($\mathrm{J\,K^{-1}mol^{-1}}$)	$\Delta C_p(T_g)/\Delta S_m$	References for $\Delta C_p(T_g)$
B_2O_3	41.9	1.25	[934]
$H_2SO_4\,3H_2O$	175.6	1.72	[934]
$NaPO_3$	50	2.02	[271]
$ZnCl_2$	20.9	1.26	[15]
Se	14.7	1.33	[934]
$CaNO_3\,4H_2O$	230.4	2.40	[15]
Phenolphthalein	190	2.0	[272]
Glycerol	88	1.41	[934]
Ethanol	31.8	1.21	[934]
2Methylpentane	66.6	1.26	[934]
Butene-1	66.2	1.50	[934]
2-3Dimethylpentane	66.6	1.71	[934]
Poly(styrene)	24.3	1.5	[934]
Poly(ethylenetherephtalate)	76	1.6	[173]
$Au_{0.77}Ge_{0.136}Si_{0.094}$	23.5	1.19	[128]

Exceptions to this rule are found for metallic glass-forming alloys, for which considerably lower (T_g/T_m)-ratios are observed.

- With respect to the $\Delta C_p/\Delta S_m$, $\Delta S_g/\Delta S_m$ and $\Delta H_g/\Delta H_m$ ratios the regularities, expressed through Eqs. (2.112), (2.129) and (2.130), are verified. Moreover, also the deviations from the average values can be noticed (see also Figs. 2.22, 2.25b and 2.26, where all experimental data, known at present, are summarized).

It can be seen that for more complex substances ($NaPO_3$, phenolphthalein) the deviations from the average values are particularly significant. This tendency is a characteristic feature of polymer systems as can also be seen from the experimental data compiled by Privalko (1980) [650]. Possible explanations of the relative stability of the ratios discussed above as well as of the observed deviations for some classes of substances will be given in Chap. 5 on the basis of molecular models of glass-forming melts.

A natural measure of the instability of the vitreous state with respect to the crystalline phase is the difference in the Gibbs free energy ΔG of both states of the substance. With Eqs. (2.126), (2.129) and (2.130) we obtain

$$\frac{\Delta G(T)}{T_m \Delta S_m} = \left(\frac{1}{2} - \frac{T}{3T_m}\right) \quad \text{for } T < T_g. \tag{2.131}$$

The largest value of ΔG is reached thus for T tending to zero, it is equal to

Table 2.4 Thermodynamic properties of glass-forming substances: Molar enthalpy of melting ΔH_m and molar value of ΔH_g for selected glass-forming melts. Data are collected from the following references: Weyl and Marboe (1967, 2/2 p. 1327) [919], Smith and Rindone (1961) [783], Eitel (1952) [184], Brizke and Kapustinski (1949) [105], Anderson (1937) [9], Tammann (1933) [820], Angell and Rao (1972) [15], Chen and Turnbull (1967) [128], Mandelkern (1964) [528], and Dobreva (1992) [173]

Substance	ΔH_m kJ mol^{-1}	ΔH_g kJ mol^{-1}	$\Delta H_g/\Delta H_m$	References
B_2O_3	24.7	18.3	0.74	[783, 919]
SiO_2	14.3	10.5	0.72	[184]
Se	6.7	4.4	0.65	[9, 105]
Ethanol	4.98	2.68	0.54	[820]
n-Propanol	5.72	2.895	0.51	[820]
$Na_2O\,4B_2O_3$	130.4	58.3	0.45	[783, 919]
$LiO_2\,2B_2O_3$	120.4	46.4	0.39	[783, 919]
$H_2O\,4B_2O_3$	126.5	72.6	0.57	[783, 919]
Benzophenone	17.9	8.5	0.48	[820]
Glycerol	18.3	8.7	0.48	[820]
Poly(ethyleneterephtalate)	25.9	12.9	0.50	[173]
Betol	19.2	7.4	0.38	[820]
2Methylpentane	6.9	3.9	0.46	[15]
$ZnCl_2$	10.0	3.1	0.31	[15]
$H_2SO_4\,3H_2O$	23.3	5.1	0.22	[15]
$Ca(NO3)_2\,4H_2O$	21.6	4.3	0.20	[15]
$Au_{0.77}Ge_{0.136}Si_{0.094}$	10.6	6.3	0.59	[128]

$$\Delta G(T \to 0) = \frac{1}{2} T_m \Delta S_m. \tag{2.132}$$

From Boltzmann's dependence Eq. (2.32) furtheron

$$\frac{\Delta S_m}{\Delta S_g} = \ln(\Omega_m)/\ln(\Omega_g) \tag{2.133}$$

is obtained, resulting with Eq. (2.129) in

$$\Omega_g = \sqrt[3]{\Omega}_m. \tag{2.134}$$

The transition to the vitreous state occurs, therefore, then, when the number of possible microscopic configurations Ω, corresponding to the the same macrostate, reaches at normal cooling rates a value, given by Eq. (2.134), which is nearly the same for all glass-forming substances. This state of increased molecular disorder is retained down to temperatures approaching absolute zero. This result is a violation of the Third law of thermodynamics. Summarizing the above given thermodynamic results we have to conclude:

- At $T \approx T_g$ in the vitrified melt considerable ratios of the values of the enthalpy and entropy of melting are frozen in. These frozen-in values of the thermodynamic potentials remain nearly constant in the further cooling of the substance down to absolute zero. According to Boltzmann's relation (Eqs. (2.32) and (2.133)) this property is connected with a relatively high degree of configurational disorder retained in the glass.
- The Third law of thermodynamics formulated by W. Nernst does not hold for glasses. In particular, according to the Third law the temperature derivatives of H and G disappear for $T \rightarrow 0$, while for glasses this is not the case (compare Eq. (2.128)). Thus, at least, in principle a glass could be used to measure temperature differences for $T \rightarrow 0$, which is excluded by the Third law.

The results, outlined in this chapter, were so surprising that many distinguished physicists and chemists doubted initially the validity of the experimental findings (see, e.g., Nernst's comments from 1918). However, all the experiments carried out in subsequent years always confirmed these results.

2.5.3 *Alternative Methods of Determination of Caloric Properties of Glass-Forming Melts*

The determination of the thermodynamic potentials of glasses based on specific heat measurements is accompanied by tedious experiments over, in general, large temperature ranges. Thus a simpler method of their evaluation is, if possible, desirable. An alternative approach is also of use to exclude systematic errors possibly connected with the one specific method applied so far.

One possible method of direct determination of the frozen-in value of the enthalpy difference ΔH_g consists of the measurement of the heat of chemical reactions if the substance reacts once as a glass and another time as a crystal. Care has to be taken that the same reaction products are formed in both cases. One known example in this respect is the measurement of the reaction heat of quartz and the corresponding silica glass in hydrofluoric acid according to the scheme

$$SiO_2 + 4HF \rightarrow SiF_4 + 2H_2O + Q. \tag{2.135}$$

ΔH_g can be determined then by

$$\Delta H_g = Q_{glass} - Q_{crystal}, \tag{2.136}$$

where Q_{glass} and $Q_{crystal}$ are the respective heats of reaction.

Usually the solution of silicate glasses in hydrofluoric acid is carried out in platinum calorimeters (Eitel (1954) [185]). Similar experiments can be also performed with water soluble glasses or with vitrified metallic alloys dissolved

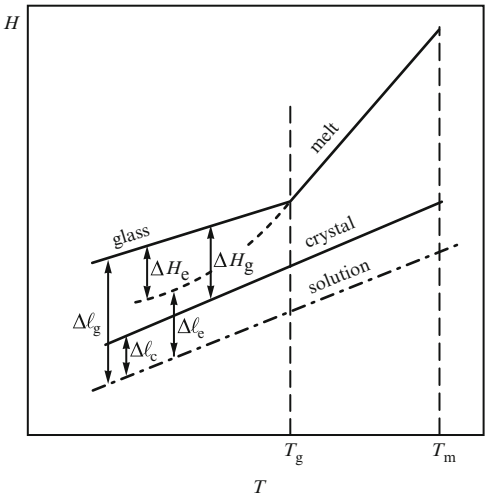

Fig. 2.27 Schematic illustration of the method of determination of ΔH_g by dissolution experiments with glasses. Δl_g and Δl_c are the heats of dissolution of the glass and the crystal, respectively. Δl_e is the heat of dissolution of the under-cooled melt, ΔH_e the enthalpy difference between glass and under-cooled melt

in acid solutions and other appropriate solvents. Schematically this method is illustrated in Fig. 2.27.

An interesting variation of this method of determination of ΔH_g by dissolution experiments was developed by Jenckel and Gorke ((1952) [408]; see also Haase (1956) [338]). According to the proposal of these authors not the heats of dissolution and swelling of a crystalline polymer, which is difficult to prepare, are measured, but the heats of dissolution for the vitreous state Δl_g and the respective under-cooled melt Δl_e are compared (see Fig. 2.27). This method can be applied only when in between the melt and the solution there is practically no energetic difference (the enthalpy of dissolution of the melt must be equal to zero); in this case $\Delta l_g = \Delta H_g$ holds.

Another method of estimation of ΔH_g consists of the measurements of the heat of combustion of the crystalline and glassy forms of organic substances, e.g., of vitreous carbon and graphite in a calorimetric bomb. The disadvantage of this method is connected with the necessity of determining ΔH_g as the difference of two comparatively large quantities, which yields relatively large uncertainties in the values of ΔH_g. A comparison of ΔH_g, obtained by $C_p(T)$-measurements, with the above discussed alternative estimates, shows a coincidence, verifying once more the results outlined earlier.

Two further methods, which can be applied directly for a determination of ΔH_g and ΔS_g, are measurements of the temperature dependence of the solubility and the vapor pressure of a glass and a crystal formed of the same substance. It is to be expected that both the solubility and the vapor pressure of the vitreous material are higher than the corresponding values of the crystalline phase. From this difference, the Gibbs free energy can be immediately calculated.

In a similar way, measurements of the electromotoric force of an electric element in which a suitable conducting glass is used as the cathode, while the anode

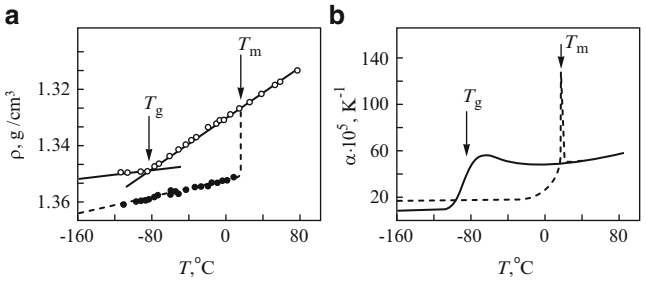

Fig. 2.28 Density (**a**) and coefficient of thermal expansion (**b**) of vitrifying glycerol as a function of temperature according to the measurements by Schulz (1954) [740]. *White circles* in Fig. 2.29a are experimental data for liquid and vitreous glycerol, *black dots* refer to the crystalline phase. In Fig. 2.28b the full curve represents the temperature dependence of the coefficient of thermal expansion α for the melt respectively the glass, while the *dashed curve* refers to the crystal. Note the sigmoidal change of α at T_g and the discontinuity of α_{cryst} at the melting temperature T_m

consists of the crystalline phase of the same substance, can be applied for a direct calculation of $\Delta G(T < T_g)$. However, these methods are associated with additional peculiarities which cannot be discussed in detail here (see Sect. 3.12; Gutzow (1981) [304]; Grantcharova and Gutzow (1986) [268]).

2.5.4 *The Change of Mechanical, Optical and Electrical Properties in the Transformation Range*

Already the first systematic investigations of glass-forming systems showed that in addition to the heat capacity, other thermodynamic coefficients such as the thermal expansion coefficient or the compressibility also exhibit a jump in the typical *s*-shaped form on vitrification. One example is given in Fig. 2.28, where the thermal expansion coefficient α (see Eq. (2.63)) for glycerol is shown as a function of temperature according to the dilatometric measurements of Schulz (1954) [740]. The $\alpha(T)$-curves are determined by the temperature dependence of the molar volume v or the molar density. These $v = v(T)$-curves exhibit a typical salient point at T_g (see, e.g., Fig. 2.28).

Intensive investigations, in particular, of organic polymeric glasses showed that the transformation to a glass is initiated usually at an actual value of the relative free volume, which corresponds to, approximately, 11–12 % of the relative free volume of the melt at the melting temperature. Hereby the relative free volume is determined by $(v_f - v_c)/v_c$. v_f and v_c are the molar volumes of the fluid and crystalline phases, respectively. These experimental results encouraged Simha and Boyer (1962) [753] to formulate the idea that the process of glassy solidification has to be considered as a freezing-in process of a constant value of the free volume (iso-free volume theory of vitrification). For other classes of glass-forming melts at normal cooling rates,

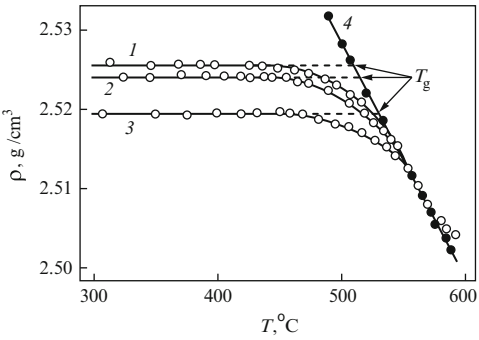

Fig. 2.29 Temperature dependence of the density of a borosilicate glass measured for three different cooling rates. (*1*): 1 K min^{-1}; (*2*): 2 K min^{-1}; (*3*): 10 K min^{-1}; (*4*): annealing curve. It can be seen that T_g increases with an increasing cooling rate (Ritland (1954) [667])

e.g., for SiO_2, GeO_2, BeF_2, Ar_2S_3, approximately constant values of the relative free volume about 18–20 %, frozen-in in the glass, could be observed. For vitreous metallic alloys the corresponding value is equal to 8–10 %. A summary of results in this respect is given in Table 2.5.

A possible interpretation of these results was given by model experiments performed by Scott (1960) [741]. Stimulated by a suggestion of J. Bernal (1959 [72], 1964 [74]), Scott tried to model the structure of liquids by a random packing of steel spheres of equal size. The volume occupied by the ensemble of equally sized spheres in the most dense hexagonal crystalline packing is about 74 % of the total volume available, while for the so-called dense, respectively, loose random packings 68 % and 63 % were obtained. These values correspond to relative free volumes, referred to the dense hexagonal packing, between 28 % and 17 %, and – as was pointed out by Gutzow (1962) [288] – to the free volume found in typical glass-forming substances.

These model experiments are not only instructive from a structural point of view. They show in addition the close connection between mobility and free volume (cf. also the Doolittle or Batchinski equations, Eqs. (2.90) and (2.91)). As found for the $C_p(T)$-curves, the value of the transformation temperature T_g depends on the cooling rate in the same way as predicted by the Bartenev-Ritland equation (2.111) (compare Figs. 2.19 and 2.29). A similar result is shown also in Fig. 2.30. Since any thermodynamic coefficient can be represented as a second-order derivative of an appropriately chosen thermodynamic potential glass-formation processes also show, with respect to mechanical properties, a similarity with second-order equilibrium phase transformations.

An equivalent behavior is also found for electric properties of glass-forming melts, e.g., for the dielectric constant ϵ. Figure 2.31 shows ϵ as a function of temperature for a vitrifying glycerol melt. It is seen from Fig. 2.31 that the significant variation in ϵ is found practically at the same temperature as for the coefficient of thermal expansion, α, and the heat capacity, C_p (Figs. 2.17 and 2.29). Since ϵ can be represented as (Landau and Lifshitz (1967) [493])

Table 2.5 Relative occupied volume β of various glasses, calculated from the densities ρ or the packing densities ψ of the glass (g) and the respective crystalline phase (c). The value of β is calculated either by $\beta = \rho_g/\rho_c$ from the density ratio of the glass versus crystal or by $\beta = \psi_g/\psi_c$ from the respective packing densities. The density data are taken from: Simha and Boyer (1962) [753], Dietzel and Poegel (1953) [171], Sternberg et al. (1989) [799], Cargill (1975) [122], Chen and Turnbull (1968) [129], and Zanotto and Müller (1991) [948]. For further details see also Gutzow (1979) [301]

Substance	Structure of the crystal	ρ_g (g cm^{-3})	ρ_c (g cm^{-3})	ψ_g	ψ_c	β
	Organic linear polymers [753]					
	Various					0.89
	Inorganic glass-forming polymers [753]					
As_2O_3		3.70	4.15			0.89
GeS_2	Hexagonal	2.69	3.0			0.89
Se	Hexagonal	4.28	4.82			0.89
$PbSiO_3$		5.98	6.49			0.92
Li_2SiO_3	Orthorhombic	2.34	2.52			0.93
	Network glass-formers [171, 799]					
SiO_2	Hexagonal					
	quartz-like	2.20	2.65			0.83
GeO_2	Hexagonal					
	quartz-like	3.63	4.28			0.85
BeF_2	Hexagonal					
	quartz-like	1.98	2.37			0.84
$AlPO_4$ [171]	Hexagonal					
	(berlinite)		2.64			0.84
$GaPO_4$	Hexagonal					
	quartz-like	2.37	2.72			0.87
P_2O_5 [948]		2.37	2.72			0.87
B_2O_3 [948]		1.84	2.46			0.74
	Vitreous metallic alloys [122, 129]					
	(Co-P; Fe-P-C; Pd-Si; Ni-Pd-P; Cu-Pd-Si)					
				0.68	0.74	0.92
AuGeSi [129]	Hexagonal					
[122]	close packing			0.64	0.74	0.89
	Bernal-Scott mechanical models of equally-sized spheres					
Loose-random	Hexagonal					
packing	close packing			0.61	0.74	0.82
Dense-random	Hexagonal					
packing	close packing			0.64	0.74	0.86

$$\epsilon = 4\pi \left(\frac{\partial^2 G}{\partial E^2} \right)_{T,p,n_j} + 1, \tag{2.137}$$

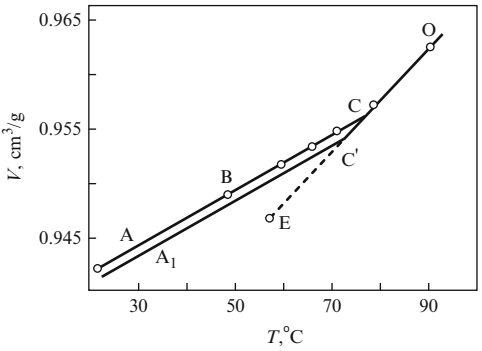

Fig. 2.30 Volume vs. temperature curves in the process of vitrification of polystyrene at different cooling rates. The curve (*A*,*B*,*C*,*O*) corresponds to a process of rapid quenching, the curve *(A_1-O)* to a cooling rate of 0.2 K min^{-1}, while curve *(E-O)* is obtained after a prolonged annealing (Alfrey et al. (1943) [8]). In this way, the curve *(E-O)* approaches the equilibrium values

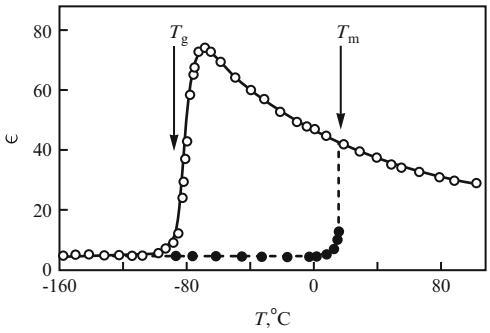

Fig. 2.31 Temperature dependence of the dielectric constant ϵ of liquid and vitreous glycerol *(circles)*. *Black dots* refer to the crystalline state (after Ubbelohde (1965) [871]). Note the analogy in the $\epsilon(T)$-dependence with the $\alpha(T)$- and $C_p(T)$-curves of the same substance

the similarity to other thermodynamic coefficients is obvious. E in Eq. (2.137) is the absolute value of the electric field vector. Thus, it turns out that the mechanical, caloric and electrical coefficients of vitrifying systems are abruptly changed in the vitrification range. This similarity of the behavior of the thermodynamic coefficients to the respective course in second-order phase transformations led Boyer and Spencer (1944 [96], 1945 [97], 1946 [98]) to the idea of interpreting vitreous solidification as a kind of second-order phase transformations. However, this suggestion cannot be accepted, since, as mentioned by Boyer and Spencer themselves, a thermodynamically defined value of T_g does not exist. In contrast, T_g in all considered cases depends on the cooling rate.

In addition, the combination of the jumps in the thermodynamic parameters $\Delta\alpha$, $\Delta\kappa$ and ΔC_p, written in form of Ehrenfest's equation Eq. (2.68), gives a nearly constant value also for vitrification processes (see Davies and Jones (1953) [153]; Moynihan (1976) [580]). However, this constant is not equal to unity, as is the case for second-order equilibrium phase transformations, but is greater than one and varies, in dependence on the specific properties of the vitrifying substance, usually

between 2 and 5 (see also Chap. 3). Further details concerning empirical aspects of the thermodynamics of the glass transition can be found in a paper by Angell and Sinicha (1976) [16].

2.6 Conclusions: The Nature of the Vitreous State

Summarizing the results of the previous sections we may formulate the following main conclusions characterizing the glass transition and the nature of the vitreous state:

1. The transition range between the under-cooled liquid and the glass is characterized by the absence of a heat of transformation, by jumps in the values of the thermodynamic coefficients corresponding to second-order derivatives of the thermodynamic potential G and by a steep increase of the viscosity followed by a break-point at T_g.
2. The discontinuities in the values of the thermodynamic parameters do not obey Ehrenfest's equation Eq. (2.68). They follow a similar but not identical dependence derived by Prigogine and Defay and discussed here in Sect. 3.8.
3. The glass transition does not take place at a fixed value of external thermodynamic parameters (p, T) but depends on kinetic factors like the cooling rate.
4. The Third law of thermodynamics and some of its consequences, as they are known for equilibrium systems, fail for the vitreous state.

The properties (2)–(4) lead to the conclusion that the glass transition cannot be interpreted in terms of any thermodynamic phase transformation according to Ehrenfest's classification. Taking into account the considerations of Sect. 2.1 it is, therefore, not reasonable to consider glasses as a state of aggregation or a phase in the classical sense as discussed above. A solution of the problems concerning the nature of the vitreous state and its deviation from the Third law of thermodynamics was given first by F. Simon (1930) [756]. In this way, a significant and useful approximation was introduced in glass science. Simon proposed to consider glasses as kinetically frozen-in thermodynamically non-equilibrium states. Due to the sharp increase in the viscosity relaxation processes in the melt towards equilibrium become so slow in the transformation range that they cannot follow the variation of the external parameters. Thus, a certain molecular configuration is frozen-in in the glass, which results in the relatively high values of ΔS and ΔH, remaining approximately constant for $T < T_g$ (Eqs. (2.125) and (2.126)). Simon's proposal excludes glasses from the framework of classical thermodynamics, since thermodynamics is applicable in its classical form only to equilibrium systems. Glasses do not obey, according to this interpretation, the Third law because they are non-thermodynamic systems in the classical sense.

Thus thermodynamics is not violated by the existence and the particular thermodynamic behavior of glasses, but glasses, as any other frozen-in states, cannot be

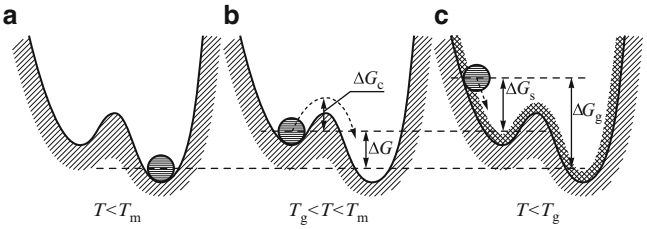

Fig. 2.32 Mechanical analogy for an interpretation of the differences between the stable at $T < T_m$ crystalline state (**a**), the metastable melt (**b**) and the glass below T_g (After Simon and Jones (1949) [409]). In this mechanical analogy the crystalline state corresponds to an absolute minimum of the potential well, the under-cooled melt to a higher local minimum. In order to be transferred from the metastable to the stable crystalline state the system has to overcome a potential barrier ΔG_c. ΔG is the thermodynamic driving force of crystallization. The glass is represented in this analogy by a ball glued to the wall of the potential well above the minimum (**c**). Crystallization is commonly preceded by stabilization processes, the thermodynamic force of stabilization ΔG_s is also indicated

treated quantitatively in the framework of classical thermodynamics. This peculiar non-thermodynamic nature of glasses has to be accounted for in analyzing glass properties and in the definition of the vitreous state. In this sense, Simon's statement requires a generalization of the definition of the vitreous state given first by Tammann. Tammann stated that glasses are *under-cooled solidified melts* (see also Tammann (1933) [820]). This definition is as a first step correct but not sufficient since nothing is said about the specific thermodynamic state of glasses. In discussing Tammann's definition it has also to be pointed out, that glasses at present are obtained not only by the under-cooling of melts but also by a variety of other methods, e.g., vapor deposition. Also from such a point of view Tammann's original definition has to be generalized. Several general definitions of the vitreous state are discussed in Chap. 3 (Sect. 3.15).

Simon gave an illustration of his ideas on the nature of the vitreous state in the form shown in Fig. 2.32. This figure demonstrates the difference between the crystalline state, thermodynamically stable for $T < T_m$, the corresponding metastable under-cooled melt and the glass. At $T < T_m$ the metastable liquid melt is, as any other metastable system, stable with respect to small fluctuations but unstable with respect to sufficiently large deviations from the initial state. Such sufficiently large changes initiate the transition to the thermodynamically favored crystalline phase. In glasses, as will be demonstrated in Chaps. 3 and 6, the thermodynamic driving forces towards the respective equilibrium state are far from zero. Moreover, it can be shown that the thermodynamic driving force for crystallization in a glass is even higher than for the respective under-cooled melt. The particular nature of glasses as frozen-in non-equilibrium states is represented in Fig. 2.32 by a ball glued to the wall of the potential well.

Simon's point of view is verified by a number of additional facts, not mentioned so far. The first of these facts was an experiment conceived by Simon and carried

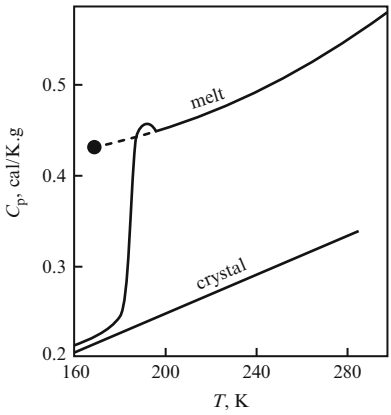

Fig. 2.33 Specific heats of under-cooled glycerol obtained at normal cooling rates *(full curve)* and after prolonged annealing (72 h at 174 K *(dashed curve)*). With the value of ΔC_p obtained by the annealing procedure the dotted S-values in Fig. 2.23 are calculated

out by Oblad and Newton ((1943) [609]; see Fig. 2.33). It is based on the following argumentation. If the scenario proposed by Simon is valid, then a decrease in the cooling rate should lead to a decrease of the values in enthalpy and entropy, frozen-in during the transformation to a glass. It was in fact shown by Newton and Oblad with glycerol that slow cooling processes extended over several months led in fact to a decrease of the residual entropy (see Fig. 2.23). Due to the steep increase in viscosity and the resulting exponential increase in the time, required to carry out the measurements, such an extension of the experimental investigations of the under-cooled melt below the value of T_g, corresponding to normal cooling rates ($q \approx 10^{-2} - 10^{2}$ Ks^{-1}), is possible for very narrow temperature intervals, only. Thus, the extension to even lower temperatures can be carried out only based on carefully performed interpolations of the curves, consistent with the principles of thermodynamics, or on statistical mechanical investigations of model systems.

For moderate deviations from T_g, the values of $\Delta S(T)$ corresponding to the metastable melt, can be approximated by a linear extrapolation of the curve determined in the range $T_g < T < T_m$ (see Fig. 2.23). However, if one extends such a linear interpolation to absolute zero, negative values of the entropy of the fictive under-cooled melt below T_g for temperatures tending to zero are obtained (Fig. 2.34). Such a possibility is in conflict with classical thermodynamics, in particular, with the Third law, according to which ΔS tends to zero for temperatures approaching zero (cf. Eqs. (2.26)–(2.28)). It also has to be excluded from the point of view of the statistical interpretation of entropy (see Boltzmann's equation Eq. (2.32)) since it would correspond to a number of microscopic realizations Ω of such a state less than one. This extrapolation was carried out by Kauzmann (1948) [440]; it is known as Kauzmann's paradox and repeatedly discussed in the subsequent literature. Kauzmann himself, as it is evident from his paper, was fully aware of the inadmissibility of such a linear extrapolation and proposed it only as a paradoxical possibility (Kauzmann (1948) [440]).

Another, at a first glance, paradoxical result, giving rise to prolonged discussions in the literature (see, e.g., Blumberg (1939) [85]), was connected with erroneous

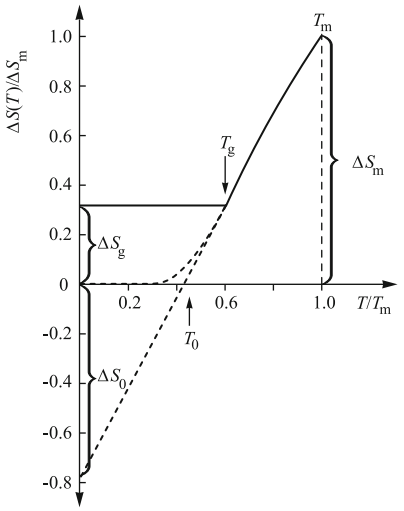

Fig. 2.34 $\Delta S(T)$ curves for glycerol and Kauzmann's paradox: The *solid line* represents the under-cooled metastable liquid (for $T_g < T < T_m$) and the vitreous state (for $T < T_g$). The *dashed curve* is an inadmissible linear extrapolation of the $\Delta S(T)$-dependence for the melt down to absolute zero. Only such an unrealistic linear extrapolation yields negative values of the entropy for $T \rightarrow 0$. Thermodynamically forbidden consequences and paradoxa do not occur for more realistic thermodynamically self-consistent extrapolations of the properties of the fictive under-cooled melt as shown, e.g., by the second *dashed line*. The temperature is given in relative units T/T_m. T_0 is the temperature for which ΔS becomes practically equal to zero

$\Delta S(T)$-determinations by Tammann (1922) [818], based on $C_p(T)$-measurement of glycerol. Due to an error in the calculations Tammann was led to the conclusion that there may exist a point of intersection of the $S(T)$-curves of the glass and the under-cooled melt. In this way, it seemed to be possible that the thermodynamic potential of the frozen-in glass may be lower for some substances (Tammann mentioned glycerol) as compared with the respective value for the undercooled melt. This led Tammann (1930) [819] further to the conclusion that under certain conditions the glass is more stable from a thermodynamic point of view than the undercooled melt. The error in Tammann's calculations was first mentioned by Simon. Tammann agreed with Simon's criticism (Tammann and Jenckel (1930) [821]) and gave a correction of his previous incorrect statements. Despite these facts, Tammann's first erroneous conclusions entered some text-books on glass science and appear in literature from time to time even today.

A second point to be mentioned, giving additional support to Simon's ideas, is the behavior of glasses in devitrification processes. If a glass is heated slowly after reaching sufficiently low values of the viscosity first a relaxation into the actual metastable equilibrium can be observed, before eventually, the transition to the stable crystalline state occurs. The isothermal relaxation of a glass into the corresponding metastable under-cooled liquid is denoted in glass science as

stabilization. The stabilization of the non-equilibrium glass always precedes the crystallization of the under-cooled melt. This is a typical feature of the process of evolution from frozen-in disordered to equilibrium states.

A third point supporting Simon's concept is the structural isomorphy of the vitreous state compared with the liquid melt from which it originated. This isomorphism is supported by X-ray measurements, IR-spectra and other methods of structural investigations. Further arguments in favor of Simon's interpretation are the possibility to derive the Bartenev-Ritland equation and relations similar to Ehrenfest's equation based on the interpretation of vitrification as a kinetically determined freezing-in process. This approach led to a theoretical development which is known in literature as the kinetic theory of vitrification. The respective derivations are given here in Chaps. 3 and 5.

Chapter 3
Non-equilibrium Thermodynamics and the Kinetics of Glass Transition and Stabilization

3.1 The Thermodynamic Description of Non-equilibrium States: Introduction

The preceding discussion in Chap. 2 concerning the nature of the vitreous state has led us to the conclusion that glasses are frozen-in non-equilibrium systems. Non-equilibrium systems cannot be described in the framework of classical thermodynamics, which is restricted in its scope to equilibrium states and quasi-static processes proceeding in between them. Nevertheless, as already mentioned in Sect. 2.2.2, a thermodynamic description can also be given for non-equilibrium states, in general, and glasses as frozen-in non-equilibrium states, in particular. This treatment is based on the introduction of additional structural order-parameters ξ_i in analogy to chemical reaction coordinates in classical thermodynamics.

The introduction of such additional parameters of state is carried out usually in the framework of the thermodynamics of irreversible processes employing a formalism developed by De Donder (1938) [155]. The details of this approach are described in a number of well-known monographs. Among them we would like to mention especially the books of Prigogine and Defay (1954) [649] and of Leontovich (1953) [504]. The original formulation of De Donder's ideas may be found also in De Donder monograph published first in 1936 (De Donder and van Rysselberghe [156]; cf. also [157]).

The application of De Donder's approach to vitrification processes was initiated by Davies and Jones (1953) [153] and Kanai and Satoh (1954, 1955) [428] with the aim of giving a description of stabilization processes in glasses. Cooper (1971) [152] used this method for a definition of the vitreous state while Grantcharova and Gutzow (1986) [268] applied it for the analysis of the problem of the vapor pressure and solubility of glasses. In two recent publications by Gutzow and Dobreva (1991 [308], 1992 [310]) this method was also used for a determination of the dependence of the vitrification parameters on cooling rate.

In the course of the mentioned and similar investigations it has become evident that for an accurate description of glasses as frozen-in non-equilibrium states, a

I.S. Gutzow and J.W.P. Schmelzer, *The Vitreous State*,
DOI 10.1007/978-3-642-34633-0_3, © Springer-Verlag Berlin Heidelberg 2013

different number of reaction parameters has to be introduced in dependence on the desired degree of accuracy of description and the complexity of the investigated substance. Besides one or even more parameters portraying the topological order (or disorder), additional reaction coordinates are needed for a description of the degree of completion of chemical reactions or molecular transformations taking place in the melt (variation of the degree of polymerization, of molecular configuration etc.) or corresponding to different states of mobility of the building units (rigidity or flexibility of chain folding polymers etc.) of the considered system.

It is difficult to give a comprehensive answer to the question of how many parameters ξ_i have to be introduced for a proper description of the state of the considered system (see e.g., Moynihan (1976) [580]; Nemilov (1988) [598]). It has even been stated that it is, in principle, impossible to have more than one independent structural order parameter for a glass. This statement is based on the argument that different equilibration processes in glasses are interconnected. Thus, if statistical models of a glass are formulated involving several order parameters, one has to check whether these parameters are indeed independent or not. A mathematical criterion to prove the independence of different order parameters is given below.

From the experience with more or less realistic lattice-hole models of vitrifying melts (see, for example, Gibbs and Di Marzio (1956) [251]; Gibbs (1960) [250]; Gutzow (1977 [298], 1979 [302]); Milchev and Gutzow (1982) [561]; Petrov, Milchev, and Gutzow (1994) [634]) obtained in recent years it has become evident that, in general, three structural parameters are needed to define, with a sufficient degree of quantitative accuracy, the thermodynamic state of a simple or polymer glass-forming melt. One parameter is needed for the description of the topological disorder (i.e., the free volume of the melt), one parameter describes the degree of complexity of the building units of the system (i.e., the degree of polymerization or aggregation of the building units), while one additional parameter reflects the probability of the building units to exist in different conformations with respect to the degree of flexibility, e.g., of the polymer chains or other molecular aggregates. In some statistical models these parameters are indeed independent variables. However, models have also been developed in which the flexibility or the configuration of the units constituting the melt depend on the free volume of the liquid. In such cases, between the three above mentioned parameters connections exist and they cannot be considered any more as independent quantities.

The introduction of more than one structural order parameters was also considered for a long time as a necessary requirement in order to obtain realistic values for the already mentioned Prigogine-Defay ratio (see Prigogine and Defay (1954) [649] and the analysis of Rehage and Borchardt (1973) [658], Moynihan (1976) [580] and Nemilov (1988) [598]). The Prigogine-Defay ratio is a relation similar to the Ehrenfest equation describing properties of second-order equilibrium phase transformations (see Eq. (2.68)). However, for a demonstration of De Donder's method and the derivation of the basic qualitative results attempted here we restrict ourselves in describing vitrifying systems to only one structural parameter ξ. We assume, that this parameter describes in some generalized way all the essential

structural and configurational disorder of the vitrifying melt. By definition, the parameter ξ may have values in the range $0 \leq \xi \leq 1$. Hereby, $\xi = 0$ corresponds to a state of complete order (crystal), while $\xi = 1$ is the state of complete disorder. Thus, the introduction of the structural order parameter allows us to give a unified description of the structure of the under-cooled melt, the glass and also the respective crystalline phase of the substance.

From a mathematical point of view the introduction of additional structural order parameters requires an extension of the fundamental equation of thermodynamics. If we choose the pressure p, the temperature T and the reaction coordinates ξ_1, $\xi_2 \ldots \xi_m$ as independent variables, Gibbs's fundamental equation may be written in the form (compare Eqs. (2.20) and (2.45))

$$dG = -SdT + Vdp + \sum_i \frac{\partial G}{\partial \xi_i} d\xi_i . \tag{3.1}$$

It is assumed from the very beginning that the number of moles of the different components is constant (closed system). The criterion that two order parameters ξ_i and ξ_j are independent can be formulated in the following way (see Nemilov (1988) [598])

$$\frac{\left(\frac{\partial V}{\partial \xi_i}\right)_{p,T}}{\left(\frac{\partial S}{\partial \xi_i}\right)_{p,T}} \neq \frac{\left(\frac{\partial V}{\partial \xi_j}\right)_{p,T}}{\left(\frac{\partial S}{\partial \xi_j}\right)_{p,T}} . \tag{3.2}$$

In the thermodynamics of irreversible processes the state functions, A_i, conjugate to the structural order parameters, ξ_i, are denoted as affinities with respect to the generalized reactions described by ξ_i. They are defined by

$$A_i = -\left(\frac{\partial G}{\partial \xi_i}\right)_{p,T,\xi_j} \tag{3.3}$$

(compare Prigogine and Defay (1954) [649]). Introducing the affinities A_i into Eq. (3.1) we obtain

$$dG = -SdT + Vdp - \sum_i A_i \, d\xi_i . \tag{3.4}$$

For the case of only one structural parameter this equation is simplified to

$$dG = -SdT + Vdp - A \, d\xi . \tag{3.5}$$

The affinity has the meaning of the thermodynamic driving force of the respective restructuring process. It is defined in such a way that the signs of A and $d\xi/dt$ coincide for spontaneous equilibration processes.

Equation (3.5) allows us to give a simplified description of the metastable melt as well as of the frozen-in system, the glass. It will be used in the subsequent

sections for a discussion of different properties of glasses. In particular, analytical expressions will be derived, describing the dependence of the thermodynamic properties of the glass on cooling rate in vitrification. A derivation of the Prigogine-Defay ratio is also given here in Sect. 3.8. It will be shown further that the approach outlined is also a convenient method to treat different problems of the kinetics of stabilization, of the vapor pressure and solubility of glasses.

3.2 Structural Order Parameters and Thermodynamic Functions of Vitrified Systems

As outlined in Sect. 3.1 in the framework of De Donder's method any thermodynamic characteristic Φ of a system becomes a function not only of pressure p, temperature T and the number of moles of the independent components n_j but also of one or more additional structural order parameters, ξ_i. Taking into account only one additional order parameter and assuming the number of moles of the independent components and the pressure to be constant, we have to write

$$\Phi = \Phi(T, \xi). \tag{3.6}$$

In equilibrium the structural order parameter ξ is a single-valued function of the state variables (compare Eq. (2.46)) and under the discussed conditions a function only of temperature, i.e.,

$$\xi^{(e)} = \xi(T). \tag{3.7}$$

In equilibrium, in addition, the following relations have to be fulfilled (compare Eq. (2.47))

$$\left(\frac{\partial G_f(T,\xi)}{\partial \xi}\right)_{p,T} = 0\,, \qquad \left(\frac{\partial^2 G_f(T,\xi)}{\partial \xi^2}\right)_{p,T} > 0. \tag{3.8}$$

Equation (3.8) determine the equilibrium value of $\xi = \xi^{(e)}$. The subscript f refers to the (fluid) under-cooled melt.

However, when the state of the system is abruptly changed (e.g., by rapid quenching), its structure, described by the parameter ξ, cannot follow the alterations of temperature immediately. In such cases, at lower temperatures the melt remains frozen-in in a state of disorder, characterized by the value ξ^* of the order parameter corresponding to a different temperature T^* as compared with the value of temperature T established in the course of the rapid cooling process. For such a sudden quench and if the relaxation processes in the final state can be neglected, we can assume that ξ^* corresponds to the structure of the initial state before the quench and is determined by the initial temperature T^*, i.e.,

$$\xi^* = \xi(T^*). \tag{3.9}$$

For this non-equilibrium state, not Eq. (3.8) holds but

$$\left(\frac{\partial G(T,\xi=\xi^*)}{\partial \xi}\right)_{p,T} \neq 0. \tag{3.10}$$

If the order parameter ξ is larger than its equilibrium value, then the derivative in Eq. (3.10) is positive (compare Eq. (2.47)).

From a mathematical point of view, the notation "frozen-in" reads

$$\left(\frac{d\xi}{dt}\right) = 0. \tag{3.11}$$

This equation holds for $T < T^*$. Since ξ is constant for $T < T^*$ we may also write

$$\frac{d\xi}{dT} = 0 \qquad \text{for} \qquad T < T^*. \tag{3.12}$$

From Eqs. (3.6) and (3.9) we may conclude that the thermodynamic functions and the thermodynamic properties of the vitrified melt, i.e., the glass, are functions of the form

$$\Phi_f(T < T^*) \equiv \Phi_g = \Phi(T,\xi^*). \tag{3.13}$$

Here and further the subscript g specifies the properties of the glass. In the subsequent derivations we will omit the superscript $*$ in ξ^*, specifying by ξ the actual state of disorder and by $\xi^{(e)}$ the respective equilibrium value of ξ.

The temperature T^*, corresponding to the state of disorder ξ, is usually denoted as Tool's fictive temperature or the structural temperature of the respective glass (see also Tool and Eichlin (1931) [845]). Tool derived his ideas concerning the introduction of a fictive temperature as a measure of the state of disorder of the glass on an empirical basis (from the analysis of the densities of glasses frozen-in at different cooling rates). This concept has been proven generally to be of great heuristic value and is used nowadays not only in the scientific analysis but also in the discussion of technological aspects of the vitrification process (see, e.g., Mazurin (1986) [543]).

In reality, the freezing-in process takes place in a relatively broad temperature range, the already mentioned "transformation region" of the glass. However, following Simon's proposal (Simon (1931 [756, 759]) we can assume that at temperatures $T > T_g$ the under-cooled melt behaves as a metastable system in an internal thermal equilibrium, while at $T < T_g$ the melt is frozen-in to a glass. In such a simplified treatment $T^* = T_g$ holds, where T_g is the conventional glass transition temperature. However, even after the system is vitrified to a glass, evolution processes in the system may take place resulting in a change of the structure and thus of the value of the order parameter ξ. Consequently, the fictive temperature corresponding to the respective value of the order parameter also varies in time. Such processes, which proceed, of course, on large time scales, are discussed in detail in Sect. 3.9.

For vitrification processes in glass-forming melts the freezing-in temperature T^* varies with the conditions of the vitrification process. With an increase in the cooling

rate, it is moved to higher values. Consequently, the properties of the glass may also vary in dependence on the cooling rate in broad ranges (see Gutzow and Dobreva (1991 [308], 1992 [310])). Taking into account, that the thermodynamic state of the vitrifying melt is determined (for p = constant) by the two independent variables T and ξ, the total differential of any thermodynamic function of the melt may be expressed as

$$d\Phi_f(T,\xi) = \left(\frac{\partial \Phi_f}{\partial T}\right)_{p,\xi} dT + \left(\frac{\partial \Phi_f}{\partial \xi}\right)_{p,T} d\xi. \tag{3.14}$$

Since according to the adopted definition for the crystalline phase (specified by the subscript (c)) the order parameter ξ is to be taken equal to zero the analogous expression for the crystal reads

$$d\Phi_c = \left(\frac{\partial \Phi_c}{\partial T}\right)_p dT. \tag{3.15}$$

From the definition of the specific heat at constant pressure (Eqs. (2.12)–(2.14)) we have for a quasistatic process taking place with the melt (ξ is a function of temperature as determined by Eq. (3.7))

$$C_p^{(f)} = \left(\frac{\partial H_f}{\partial T}\right)_{p,\xi} + \left(\frac{\partial H_f}{\partial \xi}\right)_{T,p} \left(\frac{d\xi}{dT}\right)_p, \tag{3.16}$$

while for the crystalline phase

$$C_p^{(c)} = \left(\frac{\partial H_c}{\partial T}\right)_{p,\xi=0} \tag{3.17}$$

holds. Equation (3.17) defines the contribution to the specific heat due to the vibrations of the particles around their respective equilibrium positions, the phonon contributions. For a crystal these phonon contributions coincide practically with the total value of the specific heat, i.e.,

$$C_p^{(c)} = C_p^{(phon)}. \tag{3.18}$$

The specific heat of the melt in an internal equilibrium is determined according to Eq. (3.16) by two contributions. While the first term has the same structure as the expression for $C_p^{(c)}$ the second term in Eq. (3.16) is connected with variations of the structure of the under-cooled melt. The first term in Eq. (3.16) we may identify, consequently, with the phonon contribution while the second term refers to the configurational part of the specific heat of the melt. This conclusion yields the following expression for the configurational part of the specific heat (see Prigogine and Defay (1954) [649])

$$C_p^{(conf)}(T) = \left(\frac{\partial H_f}{\partial \xi}\right)_{p,T} \left(\frac{d\xi}{dT}\right). \tag{3.19}$$

Approximately, we may identify the phonon contributions of the specific heat of the equilibrium melt and the crystal, which yields

$$C_p^{(phon)} = \left(\frac{\partial H_c}{\partial T}\right)_{p,\xi=0} \approx \left(\frac{\partial H_f}{\partial T}\right)_{p,\xi}. \tag{3.20}$$

Using the previously mentioned approximations, we may express the specific heat of the melt as the sum of the phonon and the configurational parts, where the phonon contribution may be identified with the specific heat of the crystalline phase, as

$$C_p^{(f)} = C_p^{(phon)} + C_p^{(conf)}. \tag{3.21}$$

In such an approach the difference between the specific heats of the melt and the crystal $\Delta C_p(T)$ is determined by the configurational contribution $\Delta C_p^{(conf)}$:

$$C_p^{(f)} = C_p^{(c)} + \Delta C_p(T), \tag{3.22}$$

$$\Delta C_p(T) = C_p^{(conf)}. \tag{3.23}$$

Based on the knowledge of the specific heat difference and the thermodynamic functions of the crystalline phase with the general thermodynamic relationships, outlined in Chap. 2, all thermodynamic functions of the melt may be determined (compare Eqs. (2.113)–(2.123)). It follows as a consequence that according to Eq. (3.22) any thermodynamic characteristic of the melt Φ_f can be expressed as the sum of two terms, corresponding to the phonon and the configurational parts of the respective distribution function of the system

$$\Phi_f = \Phi_f^{(phon)} + \Phi_f^{(conf)} \tag{3.24}$$

or, approximately,

$$\Phi_f(T) = \Phi_c(T) + \Delta\Phi(T), \tag{3.25}$$

$$\Delta\Phi(T) = \Phi_f^{(conf)}. \tag{3.26}$$

One additional example in this respect is the thermal expansion coefficient α introduced with Eq. (2.63),

$$\alpha_f = \frac{1}{V}\left(\frac{\partial V}{\partial T}\right)_p = \frac{1}{V}\left[\left(\frac{\partial V}{\partial T}\right) + \left(\frac{\partial V}{\partial \xi}\right)_{p,T}\left(\frac{d\xi}{dT}\right)_p\right]. \tag{3.27}$$

The difference between the coefficients of thermal expansion of the melt and the crystal may be expressed, thus, as

$$\Delta\alpha = \alpha_f - \alpha_c = \frac{1}{V}\left(\frac{\partial \Delta V}{\partial T}\right)_p, \tag{3.28}$$

and with the same argumentation as in the derivation of Eq. (3.20), we arrive at

$$\Delta\alpha = \left(\frac{\partial \omega}{\partial \xi}\right)_{p,T}\left(\frac{d\xi}{dT}\right)_p = \alpha^{(conf)}, \tag{3.29}$$

$$\omega = \frac{V_f - V_c}{V_c}. \tag{3.30}$$

By ω the relative free volume of the melt is denoted. This quantity plays a decisive role in statistical lattice-hole models of vitrifying melts (free volume theories of vitrification, see Chap. 5).

Upon vitrification the system is frozen-in and according to Eq. (3.12) the configurational contributions to the thermodynamic coefficients of the vitrified melt become equal to zero, e.g.,

$$\Delta C_p(T) = C_p^{(conf)}(T) = 0 \qquad \text{for} \qquad T < T^*, \tag{3.31}$$

$$\Delta\alpha(T) = \alpha^{(conf)}(T) = 0 \qquad \text{for} \qquad T < T^*, \tag{3.32}$$

as it is evident from Eqs. (3.19) and (3.29). This result gives the thermodynamic explanation of the discontinuities of the thermodynamic coefficients in devitrification observed experimentally (compare Figs. 2.17, 2.28b, and 2.31). It follows, moreover that upon vitrification the configurational parts of the thermodynamic functions are frozen-in and that for $T < T_g$ the thermodynamic functions of the glass Φ_g like volume, entropy, enthalpy etc. can be expressed as

$$\Phi_g(T) = \Phi_g^{(phon)}(T) + \Delta\Phi_g \qquad \text{for} \qquad T \le T^* \tag{3.33}$$

with

$$\Delta\Phi_g(T \le T^*) = \Phi_f^{(conf)}(T \le T^*) \approx \Phi_f^{(conf)}(T^*). \tag{3.34}$$

The contributions $\Delta\Phi(T < T^*)$ are determined by the respective values at the fictive temperature T^*. They therefore depend, via the Bartenev-Ritland equation Eq. (2.111), on the cooling rate q. In the determination of $\Phi^{(phon)}$, as mentioned, the respective Φ-values for the crystalline phase can be used. Of particular importance for the determination of the thermodynamic properties of glasses is the knowledge of the $S(T)$-dependencies, since the entropy is directly connected with the configurational order of the vitrifying melt. It follows from these considerations that the knowledge of the fictive temperature T^* or the glass-transformation temperature T_g

and the properties of the under-cooled melt for these values of temperature are of basic significance for the understanding of the thermodynamic properties of a glass.

3.3 Thermodynamic Functions of Undercooled Melts: A Simple Thermodynamic Model

Since the under-cooled melt represents, from a thermodynamic point of view, a (metastable) equilibrium system it follows from the general thermodynamic equilibrium conditions that the inequality $C_p > 0$ has to be fulfilled (compare Eq. (2.44)). The same inequality also holds for the specific heat of the crystalline form of the substance.

The particles in the melt have additional degrees of freedom connected with configurational restructuring processes and thus higher C_p-values than the crystal. The number of possibilities for such restructuring processes increases with increasing temperature. It follows that the configurational part of the entropy is also an increasing function of temperature and, consequently, the inequality Eq. (3.35) is fulfilled,

$$\Delta C_p = C_p^{(f)} - C_p^{(c)} = T\frac{d\Delta S}{dT} > 0. \tag{3.35}$$

Here ΔS is the difference between the entropies of the melt and the respective crystalline phase (compare Figs. 2.23 and 2.24).

Further consequences from Eq. (3.35) are (see Eqs. (2.13) and (2.14))

$$\left(\frac{d\Delta H}{dT}\right)_p > 0 \tag{3.36}$$

and with $\Delta G = \Delta H - T\Delta S$ (cf. Eq. (2.18))

$$\left(\frac{d\Delta G}{dT}\right)_p = -\Delta S(T) < 0, \qquad \Delta G = G_f - G_c. \tag{3.37}$$

It turns out that the differences $\Delta H(T)$ and $\Delta S(T)$ decrease with decreasing temperature while $\Delta G(T)$ increases.

From the Third law of thermodynamics additional conclusions can be drawn concerning the behavior of the discussed thermodynamic functions. In agreement with Eqs. (2.26)–(2.28) we have

$$\lim_{T\to 0} \Delta C_p(T) = 0, \tag{3.38}$$

$$\lim_{T\to 0} \frac{d\Delta S(T)}{dT} = 0, \qquad \lim_{T\to 0} \Delta S(T) = 0, \tag{3.39}$$

$$\lim_{T\to 0} \frac{d\Delta H(T)}{dT} = 0, \qquad \lim_{T\to 0} \frac{\Delta G(T)}{dT} = 0. \tag{3.40}$$

Moreover, from the relation connecting G, H and S (Eq. (2.18)) immediately Nernst's classical formulation of the Third law of thermodynamics equation (3.41) is obtained, i.e.,

$$\lim_{T\to 0} \Delta G(T) = \lim_{T\to 0} \Delta H(T) = 0 \tag{3.41}$$

(compare Fig. 2.25).

Classical thermodynamics does not specify the value of temperature below which Eqs. (3.38)–(3.41) are fulfilled. We denote this particular value, below which $\Delta S(T) = 0$ holds, by T_0 and determine it through the extrapolation of the $\Delta S(T)$-curves in the range $T_g < T < T_m$ to temperatures below T_g. Extrapolations of the $\Delta S(T)$- and $\Delta H(T)$-curves for the fictive under-cooled melt into the temperature region below T_g, where the substance is frozen-in to a glass, were carried out first by Kauzmann (1948) [440], who used a linear extrapolation, and later by Angell and Rao (1972) [15] and Gutzow and Grantcharova (1985) [311]. These extrapolations indicate that for typical glass-forming melts the ratio T_0/T_m equals $1/2$, while for vitrifying metallic alloys $T_0/T_l \approx 1/3$ holds. T_l is as in Eq. (2.72) the liquidus temperature of the melt.

The general thermodynamic condition for a two-phase equilibrium state melt-crystal in first-order phase transformations consists of (see Eq. (2.55))

$$\lim_{T\to T_m} \Delta G(T) = 0, \tag{3.42}$$

where T_m as usual denotes the melting temperature. However, the differences in S and H remain, in general, finite at the melting temperature (see Eq. (2.57)) and we have

$$\Delta S(T_m) = \Delta S_m > 0, \tag{3.43}$$

$$\Delta H(T_m) = \Delta H_m = T_m \Delta S_m > 0, \tag{3.44}$$

where ΔS_m and ΔH_m are the entropy and enthalpy of melting, respectively.

Equations (3.35)–(3.44) are general thermodynamic requirements for any realistic model describing the temperature dependence of the thermodynamic properties of metastable under-cooled melts. In the following derivations the simplest, as we believe, of such models is developed, which, at the same time, allows one a realistic interpretation of the properties of under-cooled glass-forming melts and of the frozen-in melts, the glasses.

We start the discussion by first establishing the temperature course of the Gibbs free energy G in the temperature range from absolute zero to T_m. By a Taylor expansion of $\Delta G(T)$ in the vicinity of T_m we obtain

$$\Delta G(T) = \left(\frac{\partial \Delta G(T)}{\partial T}\right)_{T=T_m} (T - T_m) + \frac{1}{2}\left(\frac{\partial^2 \Delta G(T)}{\partial T^2}\right)_{T=T_m} (T - T_m)^2 + \ldots \tag{3.45}$$

and with the first of Eqs. (2.22) and (2.14)

$$\Delta G(T) = T_m \Delta S_m \left(1 - \frac{T}{T_m}\right) - \frac{T_m \Delta C_p(T_m)}{2} \left(1 - \frac{T}{T_m}\right)^2. \tag{3.46}$$

For an abbreviation of the following notations the reduced temperature

$$\theta = \frac{T}{T_m} \tag{3.47}$$

is introduced. With this notation Eq. (3.46) may be transformed into

$$\Delta G(T) = T_m \Delta S_m (1 - \theta) \left[1 - \frac{\Delta C_p(T_m)}{2\Delta S_m}(1 - \theta)\right]. \tag{3.48}$$

It is evident from Eq. (3.48) that the $\Delta G(T)$-course is determined to a large degree by the value of the parameter a_0, defined by

$$a_0 = \frac{\Delta C_p(T_m)}{\Delta S_m}. \tag{3.49}$$

With $a_0 = 2$, Eq. (3.48) gives the well-known approximation

$$\Delta G(T) = T_m \Delta S_m \theta (1 - \theta), \tag{3.50}$$

proposed by Hoffman (see Gutzow (1977) [298]; Hoffman (1958) [375]). For $a_0 = 1$

$$\Delta G(T) = \frac{1}{2} T_m \Delta S_m (1 - \theta^2) \tag{3.51}$$

is found (Gutzow and Dobreva (1991) [308]), while the classical approximation due to J.J. Thomson

$$\Delta G(T) = T_m \Delta S_m (1 - \theta) \tag{3.52}$$

corresponds to $a_0 = 0$.

An analysis, performed by Gutzow and Grantcharova (1985) [311] (see also Battezatti and Garrone (1984) [51]; Dubey and Ramanchandrao (1984/1985) [181]) shows that the ratio $\Delta C_p(T_m)/\Delta S_m$ varies for most of the typical glass-forming substances, in particular, for hydrogen-bonded organic melts, oxide glass-forming substances, silicates and borates in the range between 1.5 and 2. However, for metallic alloy glass-formers this ratio is $a_0 \approx 1$, while for pure metals its value is so low that the relation $\Delta C_p(T_m)/\Delta S_m \approx 0$ can be used. In this way, the three approximations mentioned find an application for different classes of glass-forming melts. It turns out, moreover that the value of the thermodynamic parameter a_0 defines which type of glasses the particular substance belongs to.

The simplest, and at the same time sufficiently accurate assumption which may be used for the determination of the thermodynamic properties of glass-forming melts and which is at the same time in agreement with all above mentioned general

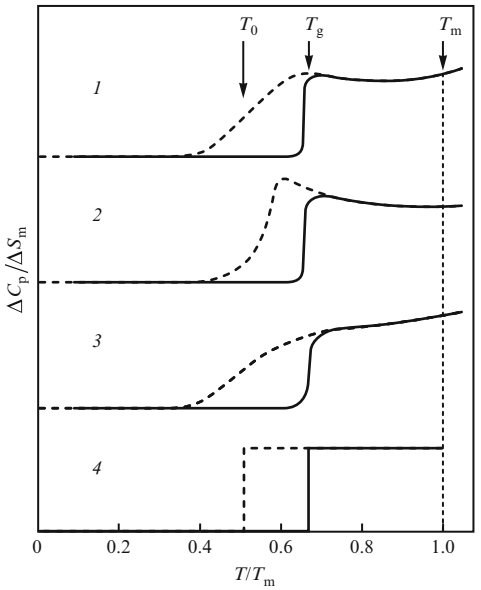

Fig. 3.1 Illustration of the approximation made with Eq. (3.54). The *curves*, specified by (*1*), (*2*) and (*3*), correspond to different experimentally observed $\Delta C_p(T)$-dependencies (compare also Fig. (2.18)). *Full lines* represent the directly measured curves for the metastable under-cooled melt for temperatures $T > T_g$ and the glass, while the *dashed curves* refer to the most probable continuation of the equilibrium dependencies into the region of the fictive equilibrium melt below T_g. In (*4*) the construction corresponding to the simplified thermodynamic model equation (3.53) is shown for comparison

thermodynamic requirements, consists of

$$\frac{\Delta C_p(T)}{\Delta S_m} = \left\{ \begin{array}{lll} a_0 = \text{constant} & \text{for} & \theta_0 \le \theta \le 1 \\ 0 & \text{for} & 0 \le \theta \le \theta_0 \end{array} \right\} . \tag{3.53}$$

Equation (3.53) has been proposed and discussed in detail by Gutzow (1977) ([298], see also Gutzow (1981) [303]; Gutzow and Dobreva (1991) [308]). Figure 3.1 gives an illustration of the type of approximation made with Eq. (3.53). As a special case, in Fig. 3.2 this approximation is applied to glycerol as a typical representative of a glass-forming melt (cf. also Figs. 2.17, 2.18, and 2.21).

With the approximation Eq. (3.53) for ΔC_p and the discussed general thermodynamic relationships Eqs. (2.120)–(2.122) the following set of equations can be derived for the configurational part of the thermodynamic functions of an under-cooled melt:

$$\frac{\Delta S(T)}{\Delta S_m} = \left\{ \begin{array}{lll} 1 + a_0 \ln \theta & \text{for} & \theta_0 \le \theta \le 1 \\ 0 & \text{for} & 0 \le \theta \le \theta_0 \end{array} \right\} , \tag{3.54}$$

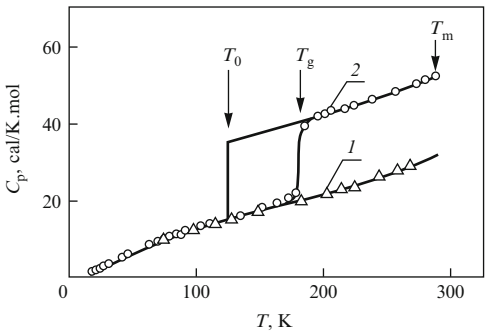

Fig. 3.2 $C_p(T)$-curves for the liquid, crystalline and vitreous forms of glycerol (compare Fig. 2.17). In addition to the experimental data the curve resulting from the assumption Eq. (3.53) is shown by a *full line*

$$\frac{\Delta H(T)}{T_m \Delta S_m} = \left\{ \begin{array}{lll} 1 - a_0(1-\theta) & \text{for} & \theta_0 \le \theta \le 1 \\ 1 - a_0(1-\theta_0) & \text{for} & 0 \le \theta \le \theta_0 \end{array} \right\}, \tag{3.55}$$

$$\frac{\Delta G(T)}{T_m \Delta S_m} = \left\{ \begin{array}{lll} (1-a_0)(1-\theta) - a_0 \theta \ln \theta & \text{for} & \theta_0 \le \theta \le 1 \\ (1-a_0)(1-\theta_0) - a_0 \theta_0 \ln \theta_0 & \text{for} & 0 \le \theta \le \theta_0 \end{array} \right\}. \tag{3.56}$$

As mentioned, the value of $\theta_0 = (T_0/T_m)$ is determined by the condition

$$\Delta S(T_0) = 0. \tag{3.57}$$

Thus, with Eq. (3.54), we obtain for T_0 the following expression

$$T_0 = T_m \exp\left(-\frac{1}{a_0}\right). \tag{3.58}$$

For a large number of glass-forming melts the assumption $\Delta C_p(T) = \text{constant}$ is a quite accurate approximation (see, for example, the $\Delta C_p(T)$-curve for glycerol presented in Figs. 2.17, 2.18 and 3.2). In other cases, when a monotonically increasing or decreasing $\Delta C_p(T)$-dependence is observed (see Figs. 2.18 and 3.1), then $\Delta C_p(T)$ may be replaced by $\Delta C_p(T_g)$ corresponding to the average value of $\Delta C_p(T)$ in the temperature range $T_0 < T < T_m$. In this case the general equation for the determination of ΔS_m (see Eq. (2.30)) gives

$$\Delta S_m = \int_0^{T_m} \frac{\Delta C_p(T)}{T}\, dT \approx \int_{T_0}^{T_m} \frac{\Delta C_p(T)}{T}\, dT \approx \Delta C_p(T_g) \ln\left(\frac{T_m}{T_0}\right), \tag{3.59}$$

which is equivalent to Eq. (3.58).

From the preceding discussion it is evident that the simplest possible temperature course of the thermodynamic functions of glass-forming melts should have the form shown in Fig. 3.3. In the framework of the outlined simplified model it turns out that the ratio $\Delta C_p/\Delta S_m$ is the major and at the same time the only structural order parameter determining the thermodynamic properties of glass-forming systems.

3.4 Some Simple Geometrical Considerations

In a simplified form, approximated by straight lines, the $\Delta S(T)$- and $\Delta H(T)$-curves from Fig. 3.3 are shown on Fig. 3.4. Upon vitrification the configurational parts of both functions are frozen-in resulting in a representation of these functions in Fig. 3.4 by straight lines parallel to the (T/T_m)-axis for $T < T_g$.

According to the Beaman-Kauzmann rule [55, 440] (Eq. (2.71)) $T_g/T_m \approx 2/3$ holds. The linear extrapolation of the entropy difference $\Delta S(T)$ into the temperature region below T_g gives for typical glass-forming melts

$$T_0 = \frac{1}{2} T_m \tag{3.60}$$

or

$$T_0 = \frac{3}{4} T_g. \tag{3.61}$$

Here T_0 is in fact also the value of temperature for which the viscosity η of the melt reaches the asymptotic value $\eta \to \infty$, found by extrapolating the temperature dependence of the viscosity (i.e., $T_0 = T_\infty$ in the VFT-equation Eq. (2.84)).

Equations (3.60) and (3.61) follow from the geometrical construction shown in Fig. 3.4 (triangles T_0, T_g , b and T_0, T_m, a), according to which

$$\frac{\Delta S_g}{\Delta S_m} = \frac{T_g - T_0}{T_m - T_0} = \frac{T_g(1 - T_0/T_g)}{T_m(1 - T_0/T_m)} \tag{3.62}$$

holds. Taking into account the mentioned experimental results (compare Eq. (2.129))

$$\frac{\Delta S_g}{\Delta S_m} \approx \frac{1}{3}, \tag{3.63}$$

Eq. (3.62) gives with Eq. (2.71) directly Eq. (3.60).

The $\Delta H(T)$-dependence differs from the $\Delta S(T)$-curve, since we have to introduce into the geometrical illustration an initially unknown quantity, the zero-point enthalpy ΔH_0. Based on Fig. 3.4b the following additional relation can be derived (triangles e, f, g and d, f, h)

$$\frac{\Delta H_g - \Delta H_0}{\Delta H_m - \Delta H_0} = \frac{T_g - T_0}{T_m - T_0}. \tag{3.64}$$

With the values of the ratios T_g/T_m and T_0/T_m established thus and the value of the ratio $\Delta H_g/\Delta H_m$ (compare Eqs. (2.71), (3.60) and (2.130)), known from experiment, this expression can be used for a determination of ΔH_0. We obtain

$$\Delta H_0 = \frac{1}{4} \Delta H_m \tag{3.65}$$

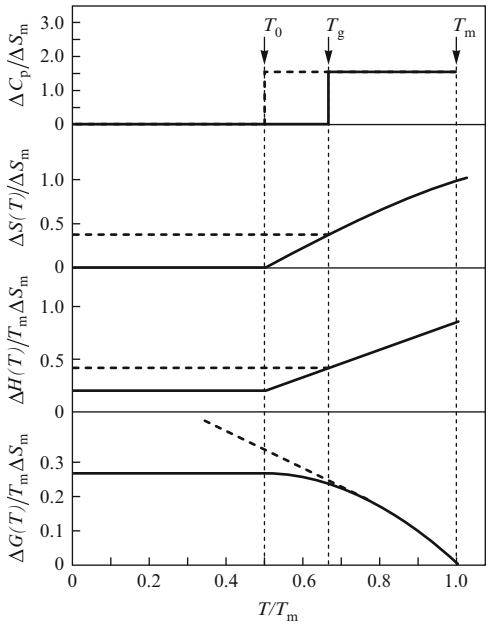

Fig. 3.3 Temperature course of thermodynamic functions of the metastable under-cooled melt calculated with the approximation Eq. (3.53) and the resulting relations Eqs. (3.54)–(3.56) *(full curves)*. Hereby the parameter a_0 was set equal to $a_0 = 1.5$, corresponding to the most probable value of this ratio for typical glass-formers. By *dashed curves* the respective dependencies for the glass are given (see Sect. 3.5 and Eqs. (3.67)–(3.70), derived there)

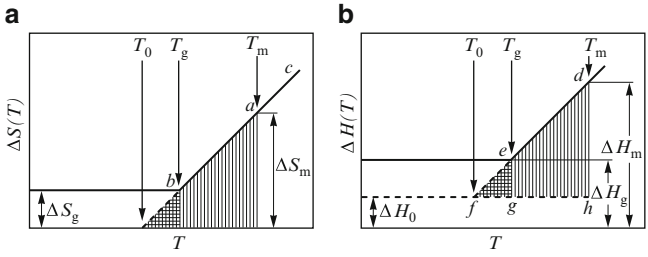

Fig. 3.4 Linearized representation of the $\Delta S(T)$ and $\Delta H(T)$ dependencies for an estimation of T_0 and ΔH_0 (see text)

or

$$\Delta H_0 = \frac{1}{2}\Delta H_g. \tag{3.66}$$

This result (Eq. (3.65)) is in agreement with Eq. (3.55), when the mentioned typical values of T_0 and $a_0 = 1.5$ are substituted into it.

3.5 Thermodynamic Functions of Vitrified Melts

According to the formalism, developed in Sect. 3.2, we have to expect that below the respective vitrification temperature the values of ΔC_p and $\Delta\alpha$ drop to zero. For the thermodynamic functions of the glass we have (cf. Eq. (3.34))

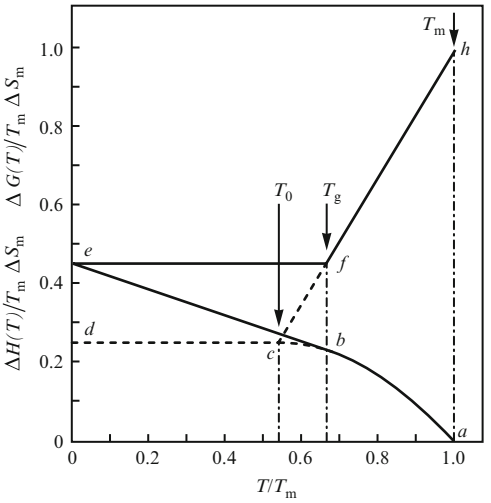

Fig. 3.5 Temperature dependence $\Delta H(T)$ and $\Delta G(T)$ for the under-cooled melt and the glass according to Eqs. (3.55)–(3.56), (3.68) and (3.70). *Curves (abcd)* and (*hfcd*) correspond to the metastable equilibrium state of the melt while (*abe*) and (*hfe*) refer to the glass

$$\Delta S(T)|_{T<T^*} = \Delta S(\xi^*) = \text{const.} = \Delta S_g, \tag{3.67}$$

$$\Delta H(T)|_{T<T^*} = \Delta H(\xi^*) = \text{const.} = \Delta H_g, \tag{3.68}$$

$$\omega(T)|_{T<T^*} = \omega(\xi^*) = \text{const.} = \omega_g, \tag{3.69}$$

i.e., constant values of the configurational entropy, enthalpy and free volume of the system. With Eq. (2.18) we obtain for the thermodynamic potential $\Delta G(T)$ the relation

$$\Delta G(T)|_{T<T^*} = \Delta H_g - T\Delta S_g. \tag{3.70}$$

Equation (3.70) shows that for every glass irrespective of the particular value of ξ (i.e, irrespective of the particular value of the fictive temperature T^* and the corresponding cooling rate) we always have to expect a linear increase of ΔG_g with decreasing temperature, since with the above equation

$$\frac{d\Delta G_g}{dT} = -\Delta S_g < 0 \tag{3.71}$$

holds. This type of temperature dependence of the thermodynamic functions for $T < T_g$ is in conflict with the Third law of thermodynamics (compare, e.g., with Eqs. (3.39) and (3.40)). For $T \to 0$ we obtain from Eq. (3.70)

$$\lim_{T\to 0} \Delta G_g(T) = \Delta H_g. \tag{3.72}$$

With the equations above, we may now construct the temperature course of the thermodynamic properties of the vitrifying melt in the whole temperature range from $T = 0$ to the melting temperature T_m of the substance (see Figs. 3.3 and 3.5). As shown in Figs. 3.2 and 3.3, $\Delta C_p(T)$ displays in a first approximation a

discontinuity at T_g (or T^*), while $\Delta S(T)$ and $\Delta H(T)$ both exhibit salient points at T_g. From above discussions the $\Delta G_g(T)$-curve is obtained for $T < T_g$ as a straight line tangent to the corresponding curve for the under-cooled melt at $T = T_g$. In a more extended form the same construction is shown in Fig. 3.5 for ΔG and ΔH. In addition to the already mentioned dependencies this figure gives also an illustration of Eq. (3.72).

The conclusions illustrated in the figures lead to the implication that Tool's temperature can be determined both from the salient points of the temperature dependence of the thermodynamic functions ($\Delta S(T)$- and $\Delta H(T)$-curves) as well as from the discontinuities of the thermodynamic coefficients ($\Delta C_p(T)$ and $\Delta\alpha(T)$). Another method consists in the determination of T^* from the temperature course of $\Delta G(T)$. As demonstrated in Figs. 3.3 and 3.5 in the $\Delta G(T)$-diagram, the vitrification temperature is determined as the temperature at which the $\Delta G_g(T)$-curve tangents the $\Delta G(T)$-curve of the equilibrium melt. Other methods of determination of Tool's temperature can be based on the investigation of the temperature dependence of kinetic quantities such as viscosity, as discussed in detail in Mazurin's monograph (Mazurin (1986) [543]) and in Chap. 12.

3.6 Thermodynamics and the Kinetics of Vitrification in Terms of Simon's Approximation

A fundamental kinetic criterion for glass-formation can be formulated in the form that at the temperature of vitrification the time of molecular relaxation τ_R has to be of the same order as the characteristic observation or stay time Δt for the process considered, i.e.,

$$\tau_R \approx \Delta t \qquad \text{for} \qquad T = T_g. \tag{3.73}$$

For a glass the ratio $\tau_R/(\Delta t)$ is a very large number, while for the liquid in the vicinity of the melting temperature T_m

$$\tau_R \approx (10^{-12} - 10^{-13})\text{s} \tag{3.74}$$

is to be expected, resulting in very small values of the ratio

$$Dh = \frac{\tau_R}{\Delta t}. \tag{3.75}$$

This ratio was introduced by Reiner (1964) [660], a well-known specialist in the field of rheology, and is denoted by him as Deborah's number (see also Stevels (1971) [800]).[1]

[1] Instead of the approach followed here, we developed recently a model-independent formulation of the glass transition criterion not employing the concept of the Deborah number (Schmelzer (2012) [700]). In this general model-independent approach, we introduced similarly to the presented in

According to Reiner, the notation Deborah's number stems from a Biblical text where the Judge Deborah (a prophetess, the wife of Lepidoth, who judged Israel in those ancient times) says "*The earth trembled ... and the mountains melted from before the Lord*" (The Bible; Old Testament; (King James Version); Judges 5:5).

---

the book approach a characteristic relaxation time, τ_R, defined via

$$\frac{d\xi}{dt} = -\frac{1}{\tau_R(p,T,\xi)}(\xi - \xi_e), \qquad q = -\frac{dT}{dt},$$

and a characteristic time scale of change of temperature, τ_T, as

$$\frac{dT}{dt} = -\frac{1}{\tau_T}T, \qquad \tau_T = \left\{\frac{1}{T}\left|\frac{dT}{dt}\right|\right\}^{-1}.$$

So, provided change of temperature and change of the structural order parameter would proceed by the same laws, the respective characteristic time scales could be then compared directly. The criterion for glass-formation is given then by the condition that both time scales are of the same order of magnitude, i.e.,

$$\tau_R \cong \tau_T \qquad \Longrightarrow \qquad \left\{\frac{1}{T}\left|\frac{dT}{dt}\right|\tau_R\right\}\Big|_{T=T_g} \cong C, \qquad C \cong 1.$$

Indeed, as stressed in detail in the cited paper, classical equilibrium thermodynamics implies (as one of the conditions of its applicability) the fulfillment of the conditions $\tau_R \ll \tau_T$ while in the frozen-in non-equilibrium state, the glass, the inequality $\tau_R \gg \tau_T$ holds. Latter equation specifies thus by necessity the transition region between equilibrium liquid and glass for the case that the glass transition is induced by a change of temperature. This general criterion contains above mentioned particular criteria for glass formation as special cases. Moreover, above given criterion can be extended straightforwardly to any other cases of glass-formation introducing similarly to the case considered here characteristic times of change of pressure, external field etc.

This criterion immediately leads also to the appropriate conditions for glass formation in application to dynamic glass transitions – glass-like transitions at periodic external perturbations. Indeed, dynamic glass transitions may proceed at the change of the state of the system with some characteristic frequency, ν, or angular frequency, $\omega = 2\pi\nu$, by varying the frequency of external perturbations. For such cases, the equilibrium value of the structural order parameter is varied in above equation as

$$\xi_e \propto \exp(i\omega t).$$

The characteristic time, τ_D, of change of the respective equilibrium state, ξ_e, can be determined then via the set of equations

$$\frac{d\xi_e}{dt} = i\omega\xi_e, \qquad \frac{d\xi_e}{dt} = -\frac{1}{\tau_D}\xi_e, \qquad i\omega = -\frac{1}{\tau_D}.$$

Taking the absolute value, we arrive at

$$\tau_D\omega \cong 1.$$

The criterion for glass-formation at dynamic glass transitions can be written consequently as

$$\tau_R \cong \tau_D \qquad \Longrightarrow \qquad \omega\tau_R \cong 1.$$

In other words, in above relation for the kinetic criterion of glass-formation in cooling and heating processes, (q/T) has to be replaced by ω (for a more detailed discussion, see also Chap. 14).

This statement implies that for the long observation times possible only for God the mountains, having a permanent shape for a human being with his very restricted observation times, are rapidly changing.

Taking the derivative of Eq. (3.73) with respect to temperature results in (see also Cooper and Gupta (1982) [146])

$$\frac{d\tau_R}{dT} = -\frac{1}{q}, \tag{3.76}$$

where the cooling rate q is introduced as

$$q = -\frac{dT}{dt}. \tag{3.77}$$

Applying this definition it follows that q is a positive quantity for cooling experiments.

If the already discussed expression

$$\tau_R = \tau_{R0} \exp\left(\frac{U(T)}{k_B T}\right) \tag{3.78}$$

is used for the description of the temperature dependence of the relaxation time (compare Eq. (2.1) and Sect. 2.4.1) we have

$$\frac{d\tau_R}{dT} = \tau_R \frac{d}{dT}\left(\frac{U(T)}{k_B T}\right). \tag{3.79}$$

When the activation energy U is considered, approximately, as a constant ($U = U_0$) this expression is simplified to

$$\frac{d\tau_R}{dT} = -\tau_R \frac{U_0}{k_B T^2}. \tag{3.80}$$

Eqs. (3.76) and (3.80) yield

$$q\tau_R = \frac{k_B T^2}{U_0} \tag{3.81}$$

The starting equation Eq. (3.73), upon which the derivation is based, holds for $T \approx T_g$. Consequently, in Eqs. (3.78) and (3.81) we have to replace T by T_g resulting, finally, in

$$q\tau_R(T_g) = \frac{k_B T_g^2}{U_0} = C_0 \tag{3.82}$$

Above equation $q\tau_R(T_g) = C_0$ with $C_0 = \text{const.}$ is usually denoted as the Frenkel-Kobeko equation (Bartenev (1966) [45]). Hereby C_0 in Eq. (3.82) is found by Bartenev to be of the order $C_0 \approx (1\text{–}5)$ K for typical glass-formers.

Taking the logarithm from both sides of Eq. (3.82) we obtain further

$$\frac{1}{T_g} = \frac{2.3k_B}{U_0}\log\left[\frac{k_B T_g^2}{U_0\tau_{R0}}\right] - \frac{2.3k_B}{U_0}\log(q). \tag{3.83}$$

With the notations

$$C_0 = \frac{k_B T_g^2}{U_0}, \qquad C_1 = C_2\log\left(\frac{C_0}{\tau_{R0}}\right), \qquad C_2 = 2.3\frac{k_B}{U_0} \tag{3.84}$$

Eq. (3.83) may be rewritten in the form

$$\frac{1}{T_g} = C_1 - C_2\log(q). \tag{3.85}$$

Equation (3.85) is the well-known Bartenev-Ritland equation (Bartenev (1951) [44]; see also Bartenev (1966) [45]; Ritland (1954) [667]). In terms of the dimensionless variable θ it may be rewritten in the form

$$\frac{1}{\theta_g} = \left(\frac{2.3k_B T_m}{U_0}\right)\left[\log\left(\frac{C_0}{\tau_{R0}}\right) - \log(q)\right] \tag{3.86}$$

or

$$\theta_g = \frac{\epsilon^{(*)}}{\left[\log\left(\frac{C_0}{\tau_{R0}}\right) - \log(q)\right]}, \qquad \epsilon^{(*)} = \frac{U_0}{2.3k_B T_m}, \tag{3.87}$$

where τ_{R0} is the period of eigenvibrations of the building units of the melt. It is a practically temperature independent quantity with values of the order 10^{-12}–10^{-13} s. Consequently, the term $\log(C_0/\tau_{R0})$ is nearly constant. It turns out that θ_g depends mainly on the cooling rate q and the value of $\epsilon^{(*)}$ which reflects the properties of the considered substance. The dependence $\theta_g = \theta_g(q)$ is shown for different values of $\epsilon^{(*)}$ in Fig. 3.6 (Gutzow and Dobreva (1991) [308]).

The analysis of experimental data shows furthermore (Turnbull, Cohen (1960) [865]; Gutzow (1975) [297]; Gutzow, Avramov, and Kästner (1990) [331]), that the ratio $U_0/k_B T_m$ is also a constant for large classes of glass-forming melts. For glass-forming inorganic oxides this ratio has values of the order 15–20. For metals and halides considerably lower values from 5 to 10 are found. With realistic parameter values corresponding to typical glass-forming substances ($U_0/(k_B T_m) \approx$ 15–20, respectively, $\epsilon^{(*)} \approx 6$ to 8; $C_0 \approx 1$ to 5 K; $\tau_{R0} \approx (10^{-12} - 10^{-13})$ s) and a cooling rate $q \approx 10^2\,\mathrm{Ks}^{-1}$ an estimate for θ_g of the order 0.5–0.7 is obtained in agreement with the Beaman-Kauzmann rule. An alternative derivation of Eq. (3.82) was given by Volkenstein and Ptizyn (1956) [892] in the framework of a kinetic model of vitrification with two energetic levels (see Sect. 12.6).

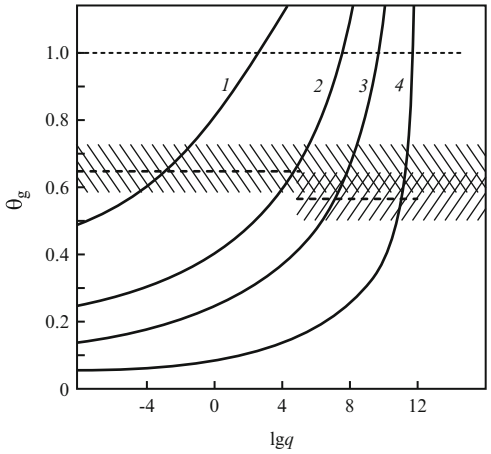

Fig. 3.6 Dependence of the reduced vitrification temperature θ_g on the cooling rate q for different values of the parameter $\epsilon^{(*)}$ according to Eq. (3.87). *Curves* (*1*), (*2*), (*3*) and (*4*) correspond to values $\epsilon^{(*)} = 10$, 5, 3 and 1, respectively. The *dashed lines* indicate the mean values for the experimentally observed θ_g-data for typical glass-formers ($\theta_g \approx 2/3$) and glass-forming metallic alloys ($\theta_g \approx 1/2$). The *shaded areas* correspond to the region of the standard deviation of the experimental data (cf. Fig. (2.11))

A generalization of the derivation of the Bartenev-Ritland equation has also been developed for the case that, instead of the constant activation energy U_0, a temperature dependent function $U(T)$ is employed (see Gutzow and Dobreva (1992) [310]). In this case, U_0 can be identified, approximately, with $U(T_g)$.

3.7 Dependence of the Thermodynamic Properties of Glasses on Cooling Rate

From the knowledge of the temperature dependence of the thermodynamic functions of the metastable glass-forming melt and the dependence of the temperature of vitrification on cooling rate q it is, in principle, possible to determine the configurational part of the thermodynamic functions of the glass for any q. If, e.g., the thermodynamic model, discussed in Sect. 3.3 (Eqs. (3.54)–(3.56) and (3.67)–(3.70)), and the Bartenev-Ritland equation as given by Eqs. (3.85) or (3.87) are applied, the following dependencies can be obtained (Gutzow and Dobreva (1991) [308])

$$\frac{\Delta S_g(q)}{\Delta S_m} = 1 + a_0 \ln \theta_g(q), \tag{3.88}$$

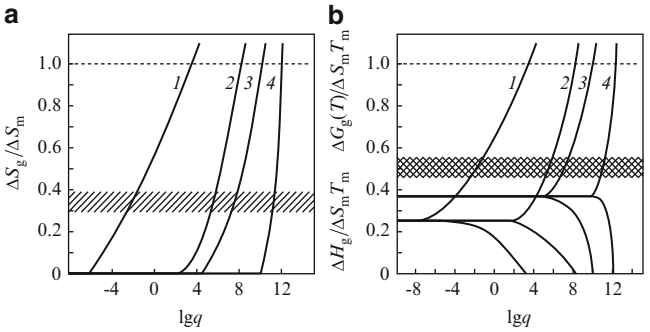

Fig. 3.7 Dependence of the frozen-in values of (**a**) the reduced configurational entropy $\Delta S_g/\Delta S_m$ (according to Eq. (3.88)) and of (**b**) the configurational enthalpy $\Delta H_g/(T_m \Delta S_m)$ *(upper set of curves)* as well as of the reduced free enthalpy $\Delta G_g(T)/(T_m \Delta S_m)$ *(lower set of curves)* (according to Eqs. (3.89) and (3.90)) on cooling rate q. The values of the kinetic and thermodynamic parameters, corresponding to the different curves, are: (*1*) $\epsilon^{(*)} = 10$, $a_0 = 1.5$ (typical oxide glass-former); (*2*) $\epsilon^{(*)} = 5$, $a_0 = 1.5$ (typical organic glass-forming melt); (*3*) $\epsilon^{(*)} = 3$, $a_0 = 1$ (metallic alloy glass or binary halide); (*4*) $\epsilon^{(*)} = 1$, $a_0 = 1$ (metallic melt). The *shaded area* indicates the region of the standard deviation of the experimental $\Delta S_g/\Delta S_m$- (cf. Fig. 2.22) and $\Delta H_g/\Delta H_m$-values (cf. Eq. (2.130))

$$\frac{\Delta H_g(q)}{T_m \Delta S_m} = 1 - a_0(1 - \theta_g(q)), \tag{3.89}$$

$$\frac{\Delta G_g(q)}{T_m \Delta S_m} = (1 - a_0)(1 - \theta_g(q)) - \theta a_0 \ln \theta_g. \tag{3.90}$$

Similar expressions can be derived also for the mechanical properties of glasses, provided the respective temperature courses for the under-cooled metastable melt are known.

Figure 3.7a,b illustrate the dependence of the thermodynamic functions of the vitrifying melt on cooling rate for different values of the thermodynamic structure factor a_0 and the kinetic parameter $\epsilon^{(*)}$ according to Eqs. (3.88)–(3.90). These figures show that for every pair of parameter values $(q, \epsilon^{(*)})$ similar $\Phi(q)$ curves are obtained.

It can be demonstrated that the specific rheological properties of glass-forming melts, in particular, the exponential dependence of the viscosity on temperature, transfer the influence of cooling rate on the thermodynamic properties of the glasses onto a logarithmic scale. Only significant variations in the cooling rate result in measurable variations of the frozen-in structure and the properties of the glass. This result explains the relative reproducibility of the properties and of the structure of glasses under varying technological vitrification conditions.

The dependencies, given above, and also the curves presented in Fig. 3.7a,b show, moreover that for each class of glass-forming melts (i.e., for every pair of parameters a_0 and $\epsilon^{(*)}$) a range of cooling rates exists, for which a nearly linear functional

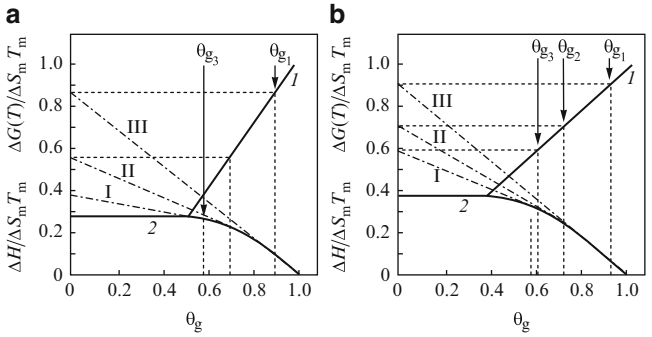

Fig. 3.8 Temperature dependence of $\Delta G(T)$, $\Delta G_g(T)$ and $\Delta H(T)$ in reduced coordinates: (**a**) $a_0 = 1.5$, $\epsilon^{(*)} = 10$; The lines *I, II* and *III* and the respective glass temperatures correspond to cooling rates $\log q = -1.9$, $\log q = -1.3$ and $\log q = -4.2$; (**b**) $a_0 = 1$, $\epsilon^{(*)} = 3$; They refer to $\log q = 9.7$, $\log q = 8.7$ and $\log q = 7.9$ (q in Ks^{-1}). By *full lines* the temperature dependence of the metastable under-cooled melt is shown, while the *dashed-dotted curves* represent the $\Delta G_g(T)$-dependence of the glass

dependence $\Delta\Phi$ vs $\log(q)$ is observed. For typical glass-formers this is the range of the normal cooling rates (10^0–10^2) Ks^{-1}. For metallic glass-forming alloys this range corresponds to extreme cooling rates and can be realized only in so-called splat-cooling experiments with quench rates from 10^6 to 10^8 Ks^{-1}.

From Fig. 3.7a it is also evident that below the mentioned range of cooling rates vitrification does not take place, in fact, since the degree of frozen-in disorder would correspond to a ratio $\Delta S_g/\Delta S_m = 0$. With the above given most probable values of the parameters $\epsilon^{(*)} = 10$ and $a_0 = 1.5$, as they are to be expected for typical glass-formers, and at normal cooling rates values $\Delta H_g/\Delta H_m \approx 0.52$ and $\Delta S_g/\Delta S_m \approx 0.35$ are found, again, in agreement with experimental evidence.

Figure 3.8 gives the $\Delta G_g(T)$-, $\Delta G(T)$- and $\Delta H(T)$-dependencies in reduced coordinates for different cooling rates. As can be seen, different curves are obtained resulting in a fan-like structure of the $\Delta G_g(T)$-functions. These quantities determine the deviations from equilibrium in glasses resulting from different cooling rates.

As already mentioned, the highest possible value for the deviation of the entropy of the glass compared with the under-cooled melt is of the order $(\Delta S_g/\Delta S_m) \approx 2$. Figure 3.7 shows that only for very extreme cooling rates this limit can be surpassed substantially. Moreover, a comparison of the ΔS_g-values for solids with defect structures, prepared by other possible methods (e.g., milling, grinding, disintegration to nanometer sizes, introduction of foreign atoms or molecules) verifies that this limit cannot be surpassed substantially even with the most effective known at present methods of preparation of frozen-in non-equilibrium states.

On the other hand, in agreement with Eqs. (2.129), (2.130) and (3.70) it turns out that $\Delta G_g/(T_m \Delta S_m)$ cannot exceed $1/2$ (see also Fig. 3.8). Consequently, the value $1/2$ specifies the state with the highest possible deviation from equilibrium. These

findings characterize the possibilities and the limits of processes of vitrification as methods of producing solids with an increased free energy. The existence of such an upper limit for the degree of disorder of glasses gives also a limitation to the possibilities of preparation of solids with an enhanced chemical reactivity, as will be discussed in Sect. 3.13.

3.8 The Prigogine-Defay Ratio

As shown in the preceding chapters, the process of vitrification is connected with discrete jumps in the thermodynamic coefficients, for example, in the specific heat C_p, the compressibility κ and the isothermal expansion coefficient α. Following Prigogine and Defay in this chapter a relation is deduced connecting the jumps ΔC_p, $\Delta\alpha$ and $\Delta\kappa$ observed in the process of vitrification of a glass-forming melt.

The derivation is based on Eq. (3.5) and the expression for the change of the affinity A as a function of T, p and ξ resulting from it. This expression reads (see Prigogine and Defay (1954) [649] for the derivation)

$$dA = \frac{A + h_{p,T}}{T}\, dT - v_{p,T}\, dp + a_{p,T}\, d\xi. \tag{3.91}$$

Here the notations

$$a_{p,T} = \left(\frac{\partial A}{\partial \xi}\right)_{p,T} = -\left(\frac{\partial^2 G}{\partial \xi^2}\right)_{p,T}, \tag{3.92}$$

$$v_{p,T} = \left(\frac{\partial V}{\partial \xi}\right)_{p,T}, \qquad h_{p,T} = \left(\frac{\partial H}{\partial \xi}\right)_{p,T} \tag{3.93}$$

are used.

If one considers not A but ξ as the dependent and T, p and A as the independent variables, Eq. (3.91) may be rewritten as

$$d\xi = \frac{1}{a_{p,T}}\, dA - \frac{A + h_{p,T}}{T a_{p,T}} dT + \frac{v_{p,T}}{a_{p,T}}\, dp. \tag{3.94}$$

By assumption, ξ is a function of A, T and p. Its total differential has the form

$$d\xi = \left(\frac{\partial \xi}{\partial A}\right)_{p,T} dA + \left(\frac{\partial \xi}{\partial T}\right)_{p,A} dT + \left(\frac{\partial \xi}{\partial p}\right)_{A,T} dp. \tag{3.95}$$

A comparison between Eqs. (3.94) and (3.95) yields

$$\left(\frac{\partial \xi}{\partial A}\right)_{p,T} = \frac{1}{a_{p,T}}, \tag{3.96}$$

$$\left(\frac{\partial \xi}{\partial T}\right)_{A,p} = -\frac{A + h_{p,T}}{T a_{p,T}}, \tag{3.97}$$

$$\left(\frac{\partial \xi}{\partial p}\right)_{A,T} = \frac{v_{p,T}}{a_{p,T}}. \tag{3.98}$$

According to Eqs. (2.13) and (3.16) we may write for the under-cooled metastable melt

$$C_p = C_{p,\xi} + \left(\frac{\partial H}{\partial \xi}\right)_{p,\xi} \left(\frac{d\xi}{dT}\right)_p. \tag{3.99}$$

With Eqs. (3.96)–(3.98) and $A = 0$ (the melt is in an internal equilibrium state) we obtain

$$C_p = C_{p,\xi} - \frac{h_{p,T}^2}{T a_{p,T}}. \tag{3.100}$$

Similarly, we may write

$$\left(\frac{\partial V}{\partial p}\right)_T = \left(\frac{\partial V}{\partial p}\right)_{T,\xi} + \left(\frac{\partial V}{\partial \xi}\right)_{p,T} \left(\frac{d\xi}{dT}\right)_p. \tag{3.101}$$

Taking into account the equality of mixed derivatives of different order of any function of state, in particular, of G (Theorem of Schwarz, see, e.g., Fichtenholz (1966) [205]), we have

$$\frac{\partial^2 G}{\partial p \partial \xi} = \frac{\partial^2 G}{\partial \xi \partial p}. \tag{3.102}$$

It follows, therefore, from Eq. (3.5) that the relation

$$\left(\frac{\partial V}{\partial \xi}\right)_{p,T} = -\left(\frac{\partial A}{\partial p}\right)_{T,\xi} \tag{3.103}$$

is fulfilled. Moreover, with the thermodynamic identity

$$\left(\frac{\partial A}{\partial p}\right)_{T,\xi} = -\left(\frac{\partial A}{\partial \xi}\right)_{p,T} \left(\frac{\partial \xi}{\partial p}\right), \tag{3.104}$$

derived by Prigogine and Defay (1954) [649], from Eqs. (3.92), (3.101), and (3.103) the relation

$$\left(\frac{\partial V}{\partial p}\right)_T = \left(\frac{\partial V}{\partial p}\right)_{T,\xi} + a_{p,T} \left(\frac{\partial \xi}{\partial p}\right)_T^2 \tag{3.105}$$

is obtained. With the definition of the compressibility κ (Eq. (2.63)) we obtain, finally,

$$\kappa = \kappa_\xi - \frac{v_{p,T}^2}{Va_{p,T}}. \tag{3.106}$$

For the coefficient of thermal expansion (Eq. (2.63)) the similar expression

$$\alpha = \alpha_\xi - \frac{v_{p,T} h_{p,T}}{VTa_{p,T}} \tag{3.107}$$

can be derived easily based on Eq. (3.27).

The first terms on the right hand sides of Eqs. (3.100), (3.106) and (3.107) describe the values of the thermodynamic quantities for the frozen-in melt, i.e., for the case when ξ is constant. The second terms refer to the contributions, connected with the change of the structure of the melt, respectively, with the variations of the structure parameter ξ. The jumps of the thermodynamic coefficients upon vitrification can be expressed, thus, as

$$\Delta C_p = \frac{h_{p,T}^2}{Ta_{p,T}}, \qquad \Delta\kappa = \frac{v_{p,T}^2}{Va_{p,T}}, \qquad \Delta\alpha = -\frac{v_{p,T} h_{p,T}}{VTa_{p,T}}. \tag{3.108}$$

Consequently, by a combination of these equations a relation equivalent in form to Ehrenfest's result, Eq. (2.68),

$$\frac{1}{VT}\frac{\Delta C_p \Delta\kappa}{(\Delta\alpha)^2} = 1 \tag{3.109}$$

is obtained.

We would like to underline once more that this result does not imply that the glass transition has to be considered as an example of second-order equilibrium phase transformations. In addition to the already mentioned arguments (cf. Sect. 2.6) conflicting with such a classification, this conclusion is also supported by the experimental finding that, although the ratio of the thermodynamic coefficients, written in the form of Eq. (3.109), has nearly the same value for different classes of glass-forming melts, this value may vary, in general, in the range from 1 to 5. This statement follows from experimental findings summarized by Davies and Jones (1953) [153], Moynihan et al. (1976) [580], Moynihan and Gupta (1978) [577] and Nemilov (1988) [598]. Examples in this respect are B_2O_3 with a value of the ratio 4.7, 40 mol % $Ca(NO_3)_2$ 60 mol % KNO_3 with 4.5, glycose (3.7), rubber (8.3), poly(vinylacetate) (2.2) and polystyrene (16).

Deviations from Eq. (3.109) can be explained by the introduction of more than one order parameter into the description of freezing-in phenomena as shown by Meixner (1952) [554] and Davies and Jones (1953) ([153]; see also Moynihan and Gupta (1978) [577]; Rehage and Borchardt (1973) [658]; Nemilov (1988) [598]). No theoretical explanation for such a deviation from unity can be given, if vitrification is considered as a special example of second-order equilibrium phase transformations. In this sense, the mentioned deviations are an additional indication

that vitrification is not a second-order phase transformation but a freezing-in process. Moreover, the existence of the mentioned deviations can also be considered as a strong indication that in most cases of real glass-forming melts more than one independent order parameter has to be introduced to describe properly the structure of the melt and the resulting in the course of vitrification glass.[2]

3.9 Kinetics of Stabilization Processes

The foregoing discussion has shown that in accordance with Simon's idea, glass is a frozen-in non-equilibrium state characterized by a larger Gibbs free energy than the respective value for the metastable melt at the same temperature. In terms of the kinetic coefficients describing transport properties of the substance it implies that the self-diffusion coefficient D of the structural units has very low values. Since the self-diffusion coefficient is connected via Eq. (2.98) with the viscosity very large values of the viscosity have to be expected for a glass.

However, though the mobility of the basic units constituting a glass have very low values this quantity is, nevertheless, not equal to zero and slow changes of the state of the glass, slow relaxation processes of the system to the state of the metastable melt may take place and, in fact, are found in experiments. Such processes are usually denoted as stabilization of the glass and schematically shown in Fig. 2.32. Due to the slow relaxation processes the structure of the glass and the structure parameter ξ change and as the result also the value of the fictive temperature T^* varies in time. It follows, moreover that the respective vitrification temperature T_g may be identified with T^* only in cases when relaxation processes for the

[2]In the analysis performed in the present book, Simon's model of the glass transition is employed. In such approach, indeed, Eq. (3.109) is obtained as an estimate for the value of the Prigogine-Defay ratio provided one structural order parameter is employed for the description of the system under consideration. However, in 2006, we have developed for the first time an alternative theoretical treatment (Schmelzer and Gutzow (2006) [706]). In this alternative approach, glass-forming systems are described by only one structural order-parameter, again. However, in contrast to previous approaches to the derivation of this ratio, the process of vitrification has been treated not in terms of Simon's simplified model as a freezing-in process proceeding at some sharp temperature, the glass-transition temperature T_g, but in some finite temperature interval accounting appropriately for the non-equilibrium character of vitrifying systems in this temperature range. As the result of the theoretical analysis, we find, in particular, that the experimentally measured values of the Prigogine-Defay ratio have to be generally larger than one for vitrification in cooling processes. Quantitative estimates of the Prigogine-Defay ratio are given utilizing a mean-field lattice-hole model of glass-forming melts and shown to be in good agreement with experimental data. Some of the statements as outlined in the present section, in particular. the statement that it is necessary to introduce more than one structural order parameters in order to interpret the experimental values of the Prigogine-Defay ratio, are, consequently, not correct any more. The analysis initiated in 2006 has been extended by us further in the following references: Tropin et al. (2011) [856], Tropin et al. (2012) [857], and Schmelzer (2012) [700] (for a more detailed discussion, see also Chap. 14).

considered intervals of observation are negligible. The aim of the present section consists in the theoretical description of such stabilization processes. Hereby, we apply a phenomenological approach based on the linear thermodynamics of irreversible processes (see also Moynihan and Lesikar (1981) [578]).

In the framework of this theoretical approach, thermodynamic fluxes J are introduced, which characterize processes (flows) in the system. The thermodynamic quantities which are the cause of such processes are called, in analogy to classical mechanics, thermodynamic forces. They are usually denoted by X. For the case under consideration that the structure of the system is described by only one generalized scalar structural order parameter ξ (see Sect. 3.1) the flux J may be expressed as

$$J = \frac{d\xi}{dt}, \tag{3.110}$$

while the force X is a, in general, not known function of the affinity A of the process under investigation, i.e.,

$$X = f(A). \tag{3.111}$$

If the affinity is equal to zero, i.e., $(\partial G/\partial \xi) = 0$ (Eq. (3.3)), we have an equilibrium with respect to variations of the structural parameter ξ and the thermodynamic driving force X is also equal to zero, i.e.,

$$X(A = 0) = f(0) = 0 \tag{3.112}$$

holds. The equilibrium value of ξ for given values of p and T we denote as $\xi^{(e)}$, again (compare Eq. (3.7)).

A truncated Taylor expansion of $f(A)$ in the vicinity of $A = 0$, including only terms linear in A, results in

$$\frac{d\xi}{dt} = LA, \qquad L = \left(\frac{\partial f(A)}{\partial A}\right)_{A=0}. \tag{3.113}$$

Restricting ourselves in the expansion of $f(A)$ to linear terms in A we are working in the framework of the linear thermodynamic theory of irreversible processes. This theory is valid for relatively small deviations of the state of the system from the corresponding equilibrium state. The parameter L in Eq. (3.113) is denoted as Onsager's coefficient. It has the meaning of a mobility coefficient connected with the considered structural change and has to be considered in the applied phenomenological approach as an empirical phenomenological quantity.

From Eq. (3.3) we have (see also Haase (1963) [339]; Popoff (1953, 1954) [639])

$$A = -\left(\frac{\partial G}{\partial \xi}\right)_{p,T}. \tag{3.114}$$

This equation allows us to rewrite Eq. (3.113) in the form

$$\frac{d\xi}{dt} = -L\left(\frac{\partial G}{\partial \xi}\right)_{p,T}. \tag{3.115}$$

Equation (3.115) exhibits another interesting analogy to the description of the motion of mechanical bodies. Changes in the state of the substance are connected linearly with the thermodynamic driving force, which may be expressed as the derivative of the respective thermodynamic potential G for the considered state in the same way as the change of the velocity of a mechanical body is connected with the gradient of the respective mechanical potential.

Suppose, a system is in a frozen-in state characterized by the value ξ of the structural order parameter and a corresponding value of the fictive temperature T^*. T^* is different from the actual temperature T and the value of the order parameter ξ differs also from the respective value $\xi^{(e)}$, which it would have in the equilibrium state. Introducing the quantity D instead of the Onsager coefficient L

$$\frac{D}{RT} = L, \tag{3.116}$$

denoted as the diffusion coefficient for the considered process of structural reorganization, we obtain from Eq. (3.115) the following expression for the change of the structure parameter ξ

$$\frac{d\xi}{dt} = -\frac{D}{RT}\left(\frac{\partial G}{\partial \xi}\right)_{p,T}. \tag{3.117}$$

(Different possibilities for introducing kinetic coefficients into the description of processes of structural evolution are discussed, e.g., in Smirnov (1966) [782]; Kirkaldy and Young (1987) [453] or Bartels et al. (1990) [42]). If the thermodynamic potential G is expressed not as a molar quantity but refers to one particle, then RT has to be replaced by $k_B T$.

Since we are considering states in the vicinity of a (metastable) equilibrium state, a Taylor expansion of the derivative $(\partial G/\partial \xi)$ including second-order terms results in

$$\left(\frac{\partial G}{\partial \xi}\right)_{p,T} = \left(\frac{\partial G}{\partial \xi}\right)_{p,T,\xi^{(e)}} + \left(\frac{\partial^2 G}{\partial \xi^2}\right)_{p,T,\xi^{(e)}} (\xi - \xi^{(e)}). \tag{3.118}$$

From the equilibrium condition (minimum of G) we obtain (cf. Eq. (3.8))

$$\left(\frac{\partial G}{\partial \xi}\right)_{p,T,\xi=\xi^{(e)}} = 0. \tag{3.119}$$

Moreover, the second-order derivative of G with respect to ξ is positive.

Eqs. (3.117)–(3.119) yield

$$\frac{d\xi}{dt} = -\frac{D}{RT}\left(\frac{\partial^2 G}{\partial \xi^2}\right)_{p,T,\xi=\xi^{(e)}} (\xi - \xi^{(e)}). \tag{3.120}$$

With Eq. (3.121)

$$\tau = \frac{1}{\dfrac{D}{RT}\left(\dfrac{\partial^2 G}{\partial \xi^2}\right)_{p,T,\xi=\xi^{(e)}}} \tag{3.121}$$

a quantity with the dimension of time is usually introduced. This quantity τ is denoted as the relaxation time of the considered process (Haase (1963) [339]; Prigogine and Defay (1954) [649]). By applying this notation Eq. (3.120) reads

$$\frac{d\xi}{dt} = -\frac{(\xi - \xi^{(e)})}{\tau}. \tag{3.122}$$

The solution of Eq. (3.122) can be written in the form

$$\xi(t) = \xi^{(e)} + (\xi(0) - \xi^{(e)}) \exp\left(-\frac{t}{\tau}\right), \tag{3.123}$$

which allows us to express the rate of change of ξ also as

$$\frac{d\xi}{dt} = \frac{(\xi^{(e)} - \xi(0))}{\tau} \exp\left(-\frac{t}{\tau}\right). \tag{3.124}$$

In terms of the applied above notations (cf. Eq. (3.11)) a frozen-in state corresponds thus to very large relaxation times ($\tau \to \infty$).

In the case of relaxation of glass-forming melts it is usually assumed that τ in Eqs. (3.121)–(3.124) is proportional to the viscosity or the time of molecular relaxation τ_R of the melt (Davies and Jones (1953) [153]; Kanai and Satoh (1955) [428]). With this reasonable assumption τ may be written (compare Eqs. (2.1), (2.79), and (2.80)) in the form

$$\tau = \tau_0 \exp\left(\frac{U}{k_B T}\right), \qquad \frac{dU}{dT} \leq 0, \tag{3.125}$$

where τ_0 is a constant, which can be identified with the time of molecular eigenvibrations τ_{R0} introduced earlier.

Dependencies of the form, as expressed by Eq. (3.122), can also be obtained for other thermodynamic quantities Φ, which are determined by the value of the structural order parameter ξ. In equilibrium a single-valued functional dependence $\Phi^{(e)} = \Phi(\xi)$ or $\xi^{(e)} = \xi(\Phi)$ exists. Since we are interested in states not far from equilibrium, in the vicinity of the actual state, these dependencies can be considered as monotonic functions as shown, for example, in Fig. 3.9 by a full curve.

By a rapid quench, the melt can be brought into a non-equilibrium state characterized by $\xi(0)$ and the respective initial value of Φ, denoted as $\Phi(0)$. This initial state is marked in the figure by a black dot. The spontaneous stabilization process is characterized by a decrease of ξ indicated in Fig. 3.9 by an arrow. If,

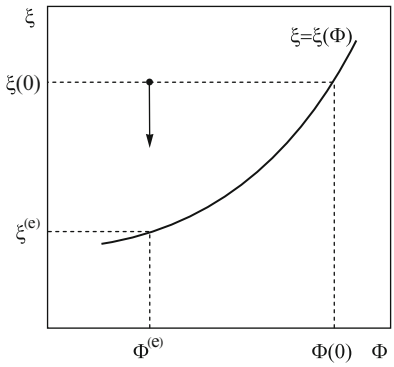

Fig. 3.9 Illustration for the derivation of Eq. (3.127) (see text)

as assumed, the order parameter ξ determines the actual value of Φ also for the process of stabilization, a relation can be found, connecting the time dependencies of ξ and Φ. From the mentioned figure we obtain in a linear approximation

$$\frac{\xi(t) - \xi^{(e)}}{\Phi(t) - \Phi^{(e)}} = \left(\frac{\partial \xi}{\partial \Phi}\right)_{\Phi = \Phi^{(e)}}. \tag{3.126}$$

With Eq. (3.122) we may write

$$\frac{d(\Phi - \Phi^{(e)})}{dt} = -\frac{(\Phi - \Phi^{(e)})}{\tau}. \tag{3.127}$$

This differential equation has similar solutions as for ξ (cf. Eq. (3.123)).

Relaxation processes of all quantities, which are determined by the value of the order parameter ξ, are governed, consequently, by the same kinetic equation and the same time of relaxation τ. In particular, this conclusion also holds for the fictive temperature T^*. According to Eq. (3.127) we obtain for this special case

$$\frac{d(T^* - T)}{dt} = -\frac{(T^* - T)}{\tau} \tag{3.128}$$

or (since T is kept constant during the considered stabilization process)

$$\frac{dT^*}{dt} = -b\frac{(T^* - T)}{\eta}, \tag{3.129}$$

b being a constant interrelating the viscosity η and the time of molecular relaxation τ (see Eq. (2.104)). An equivalent equation was introduced into glass science on an empirical basis by Tool, Hill and Eichlin (1925, 1931) [845, 846] and Tool (1946) [844]. It can be seen that this equation follows directly from the theoretical approach outlined in this chapter.

The equations predict, moreover that the evolution to the final state should be symmetric independent of the direction of approach, i.e., whether the initial state

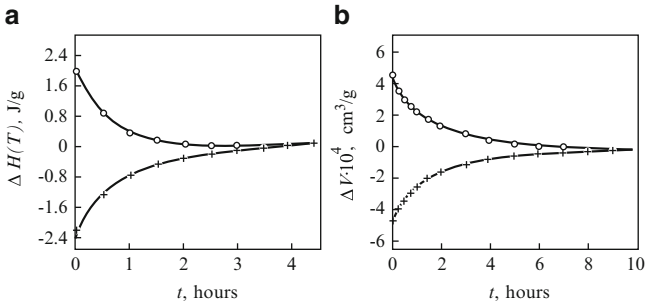

Fig. 3.10 Experimental curves for the relaxation of vitrified glass-forming melts in the vicinity of T_g (After Davies and Jones (1953) [153]): (**a**) Relaxation of the enthalpy of glycerol at a temperature $T = 185$ K; (**b**) Relaxation of the volume of glucose at a temperature $T = 304$ K; *Crosses*: Approach to equilibrium from below, *Circles*: Approach to equilibrium from above

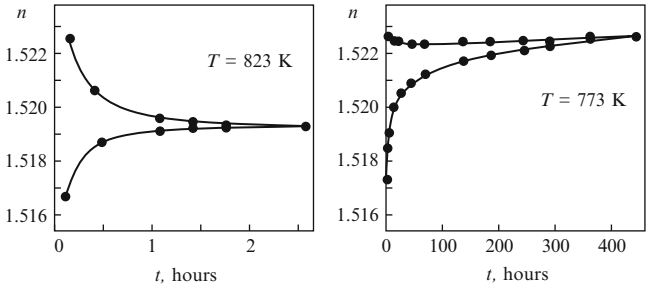

Fig. 3.11 Relaxation of the coefficient of refraction n of an optical borosilicate glass according to the measurements of Winter-Klein (1943) [929] for two different values of temperature as indicated in the figure. Note that in this figure the approach to equilibrium from a higher value of the fictive temperature is given by the *lower curves*, while the *upper curves* correspond to initially lower values of the fictive temperature

of the considered thermodynamic quantity corresponds to values higher or lower compared with the respective equilibrium value. However, though in some cases this symmetry is indeed observed (compare Fig. 3.10) in most experimental situations a different behavior may also be found (Fig. 3.11). In the simplest form such effects can be described in the following way.

As exemplified by Fig. 3.11 a non-symmetrical approach to equilibrium is found as the rule for initially large deviations from this state. In such cases, the linear approximation in the Taylor expansion of the function $f(A)$ (cf. Eq. (3.113)) is not sufficient and has to be replaced by a more accurate expression keeping higher-order terms. In the next approximation we thus obtain

$$\frac{d\xi}{dt} = LA + L_1 A^2 + \ldots, \qquad L_1 = \frac{1}{2}\left.\frac{\partial^2 f}{\partial A^2}\right|_{A=0} \tag{3.130}$$

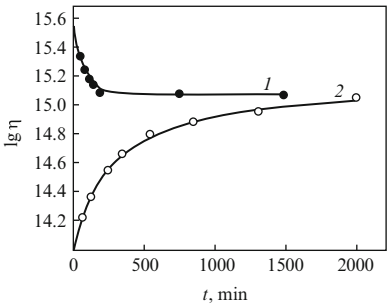

Fig. 3.12 Stabilization of kinetic properties of glass-forming melts: Viscosity vs time curves for two samples of a silicate glass with the same composition but different thermal histories heat treated at 486 °C (After Lillie (1933) [512]). Curve (*1*): Glass sample equilibrated before stabilization at a lower temperature (478 °C); Curve (*2*): Glass sample quenched before stabilization from temperatures considerably above 486 °C to room temperatures and brought to 486 °C afterwards. By such treatment the lower viscosity values corresponding to initially higher temperatures are frozen-in in the sample. Note that in both cases the same equilibrium value of the viscosity is approached with time

or

$$\frac{d\xi}{dt} = LA\left(1 + \frac{L_1}{L}A + \ldots\right). \tag{3.131}$$

Proceeding in the same way as in the derivation leading to Eq. (3.122) one gets

$$\frac{d\xi}{dt} = -\frac{(\xi - \xi^{(e)})}{\tau^{(*)}} \tag{3.132}$$

with

$$\tau^{(*)} = \frac{\tau}{\left(1 + \frac{L_1}{L}A + \ldots\right)}. \tag{3.133}$$

The parameters L and L_1 are constants, determined by the derivatives of the function $f(A)$ in the equilibrium state $A = 0$ (cf. Eqs. (3.113) and (3.130)). It follows that $\tau^{(*)}$ has different values above ($\xi > \xi^{(e)}$, $A < 0$) and below ($\xi < \xi^{(e)}$, $A > 0$) equilibrium, as far as the term $L_1 A/L$ is comparable in magnitude with unity (compare also Eq. (3.5) and the comments to it).

It follows from Eq. (3.133) that the effective value of τ is a function not only of temperature (cf. Eq. (3.125)) but also of A or ξ, respectively, the fictive temperature T^*. With increasing values of the fictive temperature, corresponding to structures of the metastable under-cooled melt for higher values of temperature T, the relaxation time decreases. Consequently, the following inequality should hold

$$\tau^*(T^* < T) > \tau^*(T^* > T). \tag{3.134}$$

Thus, the approach to equilibrium from a fictive temperature below the actual temperature T is expected to proceed more slowly than in the opposite situation.

Moreover, at the same time, the new concept of the non-equilibrium viscosity of glass-forming melts is introduced, since, as can be seen, not only the thermodynamic quantities but also the kinetic parameters describing glasses and glass-forming melts deviate from the respective equilibrium values. The necessity of introducing non-equilibrium values of the viscosity was demonstrated for the first time convincingly by Lillie (1933) [512]. Lillie measured directly the change of the viscosity during stabilization for two different cases, when the equilibrium was approached from above and from below (see Fig. 3.12). These ideas were developed further in a paper by Narayanaswami (1971) [592] who introduced the concept of frozen-in values of the activation energy of viscous flow (see also Avramov et al. (1987) [29]; Avramov and Gutzow (1990) [24]). A detailed discussion of this approach is given in Chap. 12.

3.10 Temperature Dependence of the Thermodynamic Driving Force of Stabilization

In Sect. 3.3 an expression was derived for the difference of the free enthalpy of a substance in the states of an under-cooled melt and of a crystal in the vicinity of the melting point T_m (Eq. (3.48)). This enthalpy difference can be considered also as the thermodynamic driving force for crystallization. As already mentioned, crystallization is usually preceded by stabilization processes, i.e., the approach to the respective metastable equilibrium state as schematically illustrated in Fig. 2.32. The calculation of the thermodynamic driving force of this process is the aim of the present section.

We proceed first in the same way as in Sect. 3.3, i.e., by expanding the difference in the free enthalpy this time in the vicinity of the glass transformation temperature and taking into account that similarly to second-order equilibrium phase transformations, both the potentials G as well as their first-order derivatives with respect to the independent variable (the temperature T) coincide at T_g (compare Sects. 3.3 and 3.4). Denoting the thermodynamic driving force of stabilization by $\Delta G_s(T)$ we may write

$$\Delta G_s(T) = G_g(T) - G_f(T), \tag{3.135}$$

$$\Delta G_s(T_g) = 0 \tag{3.136}$$

and similarly for the entropy difference

$$\Delta S_s(T) = S_g(T) - S_f(T), \tag{3.137}$$

$$\Delta S_s(T_g) = 0. \tag{3.138}$$

A Taylor expansion of $\Delta G_s(T)$ in the vicinity of T_g yields, thus, with the first of Eq. (2.22) and with Eq. (2.14)

$$\Delta G_s(T) = \frac{\Delta C_p(T_g)}{2T_g}(T_g - T)^2, \tag{3.139}$$

$$\Delta C_p(T_g) = C_p^{(f)}(T_g) - C_p^{(g)}(T_g) \approx C_p^{(f)}(T_g) - C_p^{(c)}(T_g). \tag{3.140}$$

Equation (3.139) was first derived by Mazurin, Filipovich and Shultz (1977) [547]. This expression can be applied, at least, approximately, for any temperature $T \leq T_g$. For $T > T_g$ it is expected to be of physical relevance only for observation times, Δt, considerably smaller than the time of molecular relaxation, $\tau(T)$.

Introducing the reduced temperature $\theta = T/T_m$, Eq. (3.139) yields

$$\Delta G_s(T) = \frac{1}{2}\frac{\theta_g \Delta C_p(T_g)}{\Delta S_m}\left(1 - \frac{\theta}{\theta_g}\right)^2. \tag{3.141}$$

In an alternative approach we may express $\Delta G_s(T)$ as the difference between $\Delta G_g = G_g - G_c$ and $\Delta G = G_f - G_c$ in the form (see Fig. 3.13)

$$\Delta G_s(T) = \Delta G_g(T) - \Delta G(T). \tag{3.142}$$

Applying this equation we may determine $\Delta G_s(T)$ via ΔG_g and $\Delta G(T)$. For $\Delta G(T)$ we may use any function valid in the whole temperature range from $T = 0$ to $T = T_m$, in particular, the thermodynamic model outlined in Sect. 3.3 (Eq. (3.56)).

With Eq. (3.70), written as

$$\frac{\Delta G_g}{T_m \Delta S_m} = \frac{\Delta H_g}{T_m \Delta S_m} - \theta \frac{\Delta S_g}{\Delta S_m} \tag{3.143}$$

and Eqs. (3.54) and (3.55) we obtain

$$\frac{\Delta G_s(\theta)}{T_m \Delta S_m} = a_0(\theta_g - \theta) - a_0 \theta \ln\left(\frac{\theta_g}{\theta}\right) \qquad \text{for} \qquad T_0 < T < T_g, \tag{3.144}$$

$$\frac{\Delta G_s(\theta)}{T_m \Delta S_m} = a_0(\theta_g - \theta_0) - \theta(1 + a_0 \ln \theta_g) \qquad \text{for} \qquad 0 < T < T_0, \tag{3.145}$$

where in the determination of T_0, again, the relation Eq. (3.58) was used. The logarithmic term in Eq. (3.144) can be expanded into a Taylor series. For this purpose we rewrite the logarithmic term as

$$\ln \frac{\theta_g}{\theta} = \ln\left(\frac{\theta + (\theta_g - \theta)}{\theta}\right) = \ln\left(1 + \frac{(\theta_g - \theta)}{\theta}\right) \tag{3.146}$$

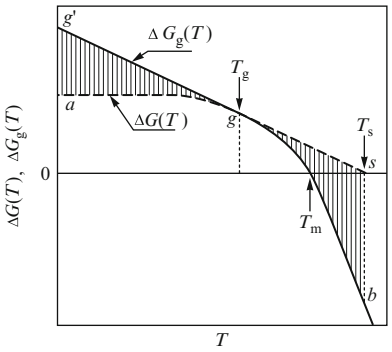

Fig. 3.13 Temperature dependencies of the differences of the Gibbs free energies between the vitreous and crystalline states (ΔG_g) and between the under-cooled melt and the crystal (ΔG) (schematically, after Gutzow, Pye, and Dobreva (1994) [335]): Curve *(a,g,T_m,b)*: Difference of the Gibbs free energy $\Delta G(T)$ between the under-cooled melt and the crystal according to Eq. (3.56). Below T_g the curve is given by a *dashed line* referring to the fictive under-cooled melt. These states can be realized in experiments only for observation times $\Delta t/\tau(T_g) \to \infty$ (compare Eq. (3.75)). Curve *(g',g,s)*: Difference of the Gibbs free energies between the glass and the crystal according to Eq. (3.70). Above T_g the curve is given by a *dashed line*. Such states can be realized in experiments only for observation times $\Delta t/\tau(T_g) \to 0$. The values of the difference $\Delta G_s = \Delta G_g - \Delta G$ are indicated by *vertical lines*. Note the asymmetric course of this difference for larger deviations from T_g. With T_s the particular temperature value is specified, for which ΔG_g becomes equal to zero

and get, consequently,

$$\ln \frac{\theta_g}{\theta} \approx \frac{\theta_g - \theta}{\theta} - \frac{1}{2}\left(\frac{\theta_g - \theta}{\theta}\right)^2 + \ldots \tag{3.147}$$

Substituting this expression into Eq. (3.144) for values near T_g Eq. (3.141) is obtained, again.

For typical glass-forming systems the relations $\theta_g = 2/3$ and $a_0 = 3/2$ hold and Eqs. (3.144) and (3.145) yield

$$\frac{\Delta G_s(\theta)}{T_m \Delta S_m} \approx 1 - 0.9\theta + \frac{3}{2}\theta \ln \theta \qquad \text{for} \qquad T_0 < T < T_g, \tag{3.148}$$

$$\frac{\Delta G_s(\theta)}{T_m \Delta S_m} \approx \frac{1}{4} - \frac{2}{5}\theta \qquad \text{for} \qquad 0 < T < T_0, \tag{3.149}$$

while for the same class of substances

$$\frac{\Delta G_g(\theta)}{T_m \Delta S_m} = \frac{1}{2} - \frac{1}{3}\theta \tag{3.150}$$

is fulfilled (compare Eqs. (3.63), (3.70) and (2.130)).

A comparison of Eqs. (3.148)–(3.149) shows that the thermodynamic driving force of crystallization of the under-cooled melt for $T < T_g$ always exceeds ΔG_s, e.g., for $\theta = 1/2$ we have $\Delta G_g/\Delta G_s(T) \approx 10$. Moreover, it can be verified from Fig. 3.13 that for $T \leq T_g$ the inequality $\Delta G_g > \Delta G > \Delta G_s(T)$ holds, i.e., the thermodynamic driving force for crystallization of the glass is always greater than the thermodynamic driving force of crystallization of the under-cooled melt. For temperatures $T > T_g$ in the vicinity of T_m the thermodynamic driving force of stabilization $\Delta G_s(T)$ can be larger than ΔG, if the ΔG_g-curve is prolonged to such high temperature values.

The knowledge of the thermodynamic driving force of crystallization, respectively, of stabilization allows one conclusions concerning the stability of the considered state of the substance. At the same time, it allows us to make conclusions concerning the kinetics of these processes. As shown in Sect. 3.9, the basic relation describing relaxation processes in the vicinity of equilibrium states is given by Eq. (3.117). Approximately, we may replace the derivative in Eq. (3.117) by the ratio of the differences $\Delta G = G(\xi) - G(\xi^{(e)})$ and $\Delta\xi = \xi - \xi^{(e)}$. Moreover, since $G(\xi)$ is the thermodynamic potential of the vitrified melt, it can be identified with the actual value of G_g. Thus, we obtain, finally,

$$\frac{d\xi}{dt} = -\frac{D}{k_B T}\left(\frac{\Delta G_s}{\Delta\xi}\right) \qquad \text{with} \qquad \Delta G_s(T) = G_g - G_f \tag{3.151}$$

and with Eq. (3.126) (for the particular case $\Phi = T^*$)

$$\frac{d(T^* - T)}{dt} = -\frac{D}{k_B T}\left(\frac{\Delta G_s(T)}{T^* - T}\right)\frac{1}{a^2}, \qquad a = \left(\frac{\partial\xi}{\partial T^*}\right)_{T^*=T}. \tag{3.152}$$

With Eq. (3.141) for ΔG_s, again, an expression of the form of Eq. (3.129) (Tool's equation) is found.

3.11 Experimental Results

The first experimental investigations of stabilization phenomena in glasses in the vicinity of T_g were directed to the analysis of variations in time of the specific volume and quantities like density, coefficient of refraction and other properties connected with it. Classical examples in this respect are shown in Figs. 3.10 and 3.11 (relaxation of the molar volume of glucose according to Davies and Jones (1953) [153] and change in the coefficient of refraction in a technical glass according to Winter-Klein (1943) [929]). From this first period of experimental investigations, we would also like to mention the results of Tool, Hill and Eichlin (1925, 1931) [845, 846], Ritland (1954) [667], Kanai and Satoh (1954, 1955) [428], Daragan (1952)

[152] and additional measurements carried out by Winter-Klein (1943) [929] and Davies and Jones (1953) [592]. More recent results were reported by Moynihan et al. (1971 [581], 1976 [154,579]) and Narayanaswami (1971) [592]. These authors analyzed caloric properties and, in particular, the relaxation of the enthalpy of vitrified melts (see also Bergmann, Avramov et al. (1985) [69]; Scherer (1986) [686]).

It is evident from the results presented in Figs. 3.10 and 3.11 that for relatively small deviations from equilibrium really a symmetric approach to equilibrium is found. The same conclusion can be drawn to a large extent also with respect to the time evolution of the coefficient of refraction, at least, for relatively high temperatures (see Fig. 3.11). However, for lower temperatures a significant deviation from such a simplified picture is observed. Particularly interesting examples in this respect are the solubility and the vapor pressure of glasses. These topics will be discussed below.

We want to mention also that far below T_g very slow processes of structural transformation, so-called secular changes, have been observed, which do not seem to fit into the outlined theoretical approach (see Morey (1954) [574]; Schönborn (1955) [731]; Charles (1971) [127]; Cooper (1982) [153]). Such variations are of particular importance for thermometry as described in more detail by Scholze (1965, 1967) [732] and Gutzow (1962) [315]. It has been observed that for alkali lime silicate glasses containing a high percentage of sodium and potassium oxides, such variations caused a measurable depression of the zero point of mercury thermometers at temperatures 200–300 K below T_g. In a famous investigation, carried out by Schott (1891) [734], it was shown that such secular density changes are practically suppressed for compositions of the glass containing only sodium or potassium.

It was established empirically that the change δl of the zero point of the thermometric scale can be described as

$$\delta l = A \log\left(\frac{t}{t_0}\right) + B, \tag{3.153}$$

where A, B and t_0 are constants. For polymer systems it was found that similar processes are connected with variations in the conformation of the molecules. At present, there is no satisfactory structural theory for such secular changes in technical glasses, although the experimental evidence has been known for a long time (for an overview on attempts in this direction see, e.g., Hunt (1993) [385]; Hodge (1994) [373]). Possibly, this type of behavior could be connected with the simultaneous relaxation of more than one structural order parameter, which is not reflected in the simple scheme as described above. In such cases, transformations could occur even then when the main order parameter connected with the free volume of the vitrified melt is frozen-in. Another theoretical approach to an understanding of secular changes could be based on a non-linear description of the viscous flow of glass-forming melts, as it will be discussed in Chap. 12.

3.12 Vapor Pressure and Solubility of Glasses

The classical methods used for the determination of the thermodynamic functions of glass-forming melts and glasses are based on measurements of the temperature dependence of the specific heats of the respective substances (see Sects. 3.3–3.5). Here and in the following section another method will be discussed which interrelates the thermodynamic functions of glasses with the vapor pressure, the solubility and the chemical reactivity (or affinity) of vitreous substances. The agreement of experimental results and theoretical predictions for these properties gives an additional proof of the expressions for the thermodynamic potentials, derived in Sects 3.3 and 3.5.

The problem of the very existence of a well-defined value of the vapor pressure and solubility of frozen-in systems like glasses has given rise to prolonged discussions in literature. Frequently the opinion was expressed that these quantities cannot be attributed to non-equilibrium systems like a vitrified melt. The development of the discussions around this problem over many years can be followed in the literature beginning with van der Waals and Kohnstamm (1908) [881], Simon (1937) [758], Fowler and Guggenheim (1939, pages 228–229, [225]), Haase (1956, pages 304, 564, [338]) and Kritchevski (1970, pages 400–405, [486]).

The origin of the problem of whether the mentioned quantities have well-defined values for a glass is due to the fact that classical thermodynamics gives us the possibility of determining vapor pressure, solubility and affinity only for systems in an internal thermodynamic equilibrium state. Thus the only way out of this conceptional difficulty seemed to consist of adopting a statistical-mechanical approach, which, as mentioned first by L. Boltzmann, can be applied to determine the thermodynamic functions of equilibrium as well as of non-equilibrium states of matter (see Boltzmann (1896–1898) [87]). Such a point of view was used in their argumentation also by van der Waals and Kohnstamm (1908) [881]. Authors like Schmolke (1931) [730] argued, moreover that even to a metastable system no definite value of the vapor pressure may be assigned.

The main postulate, underlying the thermodynamic definition of vapor pressure, solubility and chemical affinity of a glass, applied here, is the following: These quantities are determined by the respective values of the thermodynamic functions of the metastable under-cooled melt at the freezing-in temperature $T = T^*$. This approach was first proposed by Gutzow in 1972 [294] and developed further by Grantcharova and Gutzow in 1986 [268]. The basic assumption implies, as pointed out first by Simon (1937) [758] that the process of condensation/evaporation (or dissolution/recondensation) can lead to a transformation of the structure and the properties of the glass in the direction of the state corresponding to the metastable under-cooled melt for the actual value of temperature T. Consequently, such quantities like vapor pressure and solubility should also change slowly with time. However, vapor pressure and solubility of glasses have typically relatively low values and often the mentioned and bulk relaxation phenomena may be neglected for the actual times of observation. In these cases practically constant values of vapor

pressure and solubility are measured. For example, the condensation coefficient of vitreous As_2O_3 is of the order 10^{-5}–10^{-9}, the vapor pressure of vitreous SiO_2 and of other typical glasses has values below 10^{-40} Torr (see also Gutzow (1972) [294]; Knacke and Stranski (1952) [459]; Stranski and Wolf (1951) [811]; Bestul and Blackburn (1960) [78]).

For a derivation of conclusions from the above formulated general definition we make the simplest possible assumptions with respect to the properties of the vapor phase (perfect gas composed of the same particles as the glass sample) or the solution (perfect solution). These assumptions are reasonable since both the vapor pressure and the solubility of glasses have, as mentioned, relatively low values. Generalizations can be found in the papers by Gutzow (1972) [294] and Grantcharova and Gutzow (1986) [268]. We consider first the problem of the vapor pressure of a glass. The extension to the solubility can be performed straightforwardly.

From the equilibrium conditions for a one-component solid with a chemical potential μ_c in contact with its vapor (μ_v) (compare Eq. (2.40))

$$\mu_c(p_c, T) = \mu_v(p_c, T) \tag{3.154}$$

and the similar relation for the liquid-vapor coexistence

$$\mu_f(p_f, T) = \mu_v(p_f, T) \tag{3.155}$$

we obtain with the expression for the chemical potential μ_v of a one-component perfect gas at pressure p

$$\mu_v(p, T) = \mu_v(p_0, T) + RT \ln\left(\frac{p}{p_0}\right) \tag{3.156}$$

(p_0 is some reference value of the pressure, e.g., the atmospheric pressure, R the universal gas constant) the following relation interconnecting p_f, p_c and the difference in the molar values of the Gibbs free energy ΔG for both considered phases

$$\mu_c(p_c, T) = \mu_v(p_0, T) + RT \ln\left(\frac{p_c}{p_0}\right), \tag{3.157}$$

$$\mu_v(p_f, T) = \mu_f(p_0, T) + RT \ln\left(\frac{p_f}{p_0}\right), \tag{3.158}$$

$$\frac{\Delta G}{RT} = \ln\left(\frac{p_f}{p_c}\right), \qquad \Delta G = \mu_f - \mu_c, \tag{3.159}$$

(see, e.g., also Simon (1926, 1927) [754, 755]). p_f and p_c are the equilibrium pressures of the liquid and the crystalline phase for the actual value of temperature T.

If one applies Eq. (3.159) to the under-cooled and to the vitrified melt, we get as special cases

$$\ln\left(\frac{p_f}{p_c}\right) = \frac{\Delta G}{RT}, \qquad \Delta G = G_f - G_c, \tag{3.160}$$

$$\ln\left(\frac{p_g}{p_c}\right) = \frac{\Delta G_g}{RT}, \qquad \Delta G_g = G_g - G_c. \tag{3.161}$$

ΔG and ΔG_g in the above expressions can be determined by Eqs. (3.56) and (3.70). With these expressions we obtain

$$\ln\left(\frac{p_g}{p_c}\right) \approx \frac{\Delta S_m}{R}\left(\frac{1}{2\theta} - \frac{1}{3}\right), \tag{3.162}$$

$$\ln\left(\frac{p_f}{p_c}\right) \approx \begin{cases} \dfrac{\Delta S_m}{2R}\left(1 - \dfrac{1}{\theta} - 3\ln\theta\right) & \text{for} \quad \theta_0 \le \theta \le 1 \\ \dfrac{\Delta S_m}{4R\theta} & \text{for} \quad 0 \le \theta \le \theta_0. \end{cases} \tag{3.163}$$

Eqs. (3.160)–(3.163) allow one the determination of the vapor pressure of the under-cooled metastable melt and the glass, provided the temperature dependence of the vapor pressure of the gas in equilibrium with the crystalline phase is known.

Eqs. (3.160) and (3.161) yield further

$$\ln\left(\frac{p_g}{p_f}\right) = \frac{\Delta G_s}{RT}. \tag{3.164}$$

It is evident from Eq. (3.164) that the vapor pressure of a glass, determined in the above mentioned sense, always exceeds the vapor pressure of the metastable under-cooled melt. The difference is determined by the actual value of the thermodynamic driving force of stabilization $\Delta G_s(T)$ (Eqs. (3.144) and (3.145)). A substitution of these expressions into Eq. (3.164) yields

$$\ln\left(\frac{p_g}{p_f}\right) = \begin{cases} \dfrac{\Delta S_m}{R}\left(\dfrac{1}{\theta} - 0.9 + \dfrac{3}{2}\ln\theta\right) \\ \dfrac{\Delta S_m}{R}\left(\dfrac{1}{4\theta} - \dfrac{2}{5}\right) \end{cases} \tag{3.165}$$

A qualitative illustration of the temperature course of p_f, p_c and p_g is shown in Fig. 3.14.

Taking into account that $\Delta G_s(T)$ depends on the cooling rate, it follows that the vapor pressure of a glass also depends on it. Moreover, as discussed in Sect. 3.9, relaxation processes of the glass result in a change of the fictive temperature and, consequently, also in a variation of $\Delta G_s(T)$ and p_g, approaching with time the value

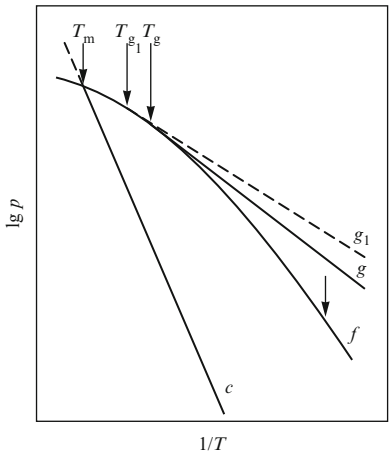

Fig. 3.14 Temperature dependence of the vapor pressure of a crystal specified by (c), the under-cooled melt (f) and the glass (g), frozen-in at two different temperatures T_g and T_{g1} ($T_{g1} > T_g$). The change of the vapor pressure of the glass upon stabilization is indicated by an *arrow*. It is evident from the figure and the respective equations, that at $T = T_g$ no discontinuity of the log p vs $1/T$-dependencies occurs

of the under-cooled metastable melt. This change of p_g is indicated in Fig. 3.14 by an arrow.

Quantitatively, the time dependence of $\Delta G_s(T)$ can be described according to Eq. (3.127) by

$$\frac{d(\Delta G_s(T))}{dt} = -\frac{\Delta G_s(T)}{\tau} \tag{3.166}$$

with the solution

$$\Delta G_s(t) = \Delta G_s(0) \exp\left(-\frac{t}{\tau}\right). \tag{3.167}$$

A substitution into Eq. (3.164) yields

$$\ln\left(\frac{p_g}{p_f}\right) = \frac{\Delta G_s(0)}{RT} \exp\left(-\frac{t}{\tau}\right). \tag{3.168}$$

For small deviations of p_g from p_f by a Taylor-expansion of the logarithmic term in Eq. (3.168) one obtains (compare Eqs. (3.146) and (3.147))

$$\frac{p_g - p_f}{p_f} \approx \frac{\Delta G_s(0)}{RT} \exp\left(-\frac{t}{\tau}\right). \tag{3.169}$$

Assuming a perfect solution glass/solvent the process of dissolution of glasses may be discussed in a totally equivalent form. The only change in the equations derived above consists in a replacement $p_g \to c_g$, $p_f \to c_f$ and $p_c \to c_c$, where by c_g, c_f and c_c the solubilities of the substance in the form of the glass, the under-cooled melt and the crystal are denoted. In particular, we may write

$$\ln\left(\frac{c_f}{c_c}\right) = \frac{\Delta G}{RT}, \tag{3.170}$$

$$\ln\left(\frac{c_g}{c_c}\right) = \frac{\Delta G_g}{RT}, \tag{3.171}$$

$$\ln\left(\frac{c_g}{c_f}\right) = \frac{\Delta G_s}{RT}. \tag{3.172}$$

Again, based on the knowledge of ΔG and ΔG_g the respective values of the solubility can be determined and vice versa.

So far vapor pressure and solubility of glasses and their variations in time have been discussed connected only with bulk variations of the state of the considered sample. In addition to such processes of bulk relaxation the possible existence of time dependent changes of the glass/vapor or glass/solution interface has also to be taken into account. If variations of the glass-vapor or glass-solution interface determine to a large extent the vapor pressure or the solubility, then there is indeed no point in assuming well-defined values of vapor pressure or solubility of a glass, as it was assumed by Simon (1937) [758]. Such surface variations are the result of evaporation/recondensation processes leading to a removal of the kinetic barrier of the stabilization process from the non-equilibrium state of the glass to the respective under-cooled melt.

Generally, it can be expected, however, that the evolution of the interface of the system is also directed to a state corresponding to the structure of the fictive metastable melt. Thus, the equations describing the time dependence of the discussed thermodynamic quantities will be of the same form as for the bulk changes but possibly with a different relaxation time, τ_{surf}. For glass-vapor interfaces it has to be expected, as discussed by Grantcharova and Gutzow (1986) [268] that τ_{surf} is of the same order as τ_{bulk}. For glass-solution interfaces most probably $\tau_{surf} < \tau_{bulk}$ holds. In the case of a glass-solution interface a penetration of the solvent into the surface layer of the glass may also occur. This effect is analyzed in detail by Harvey et al. (1986 [349], 1987 [348]). Moreover, for high supersaturations also crystallization processes may take place at the interface (for the glass-vapor interface see, for example, Stranski and Wolf (1951) [811] and for the glass-solution interface Grantcharova and Gutzow (1986) [268]). The influence of interfacial effects in the determination of the vapor pressure and the solubility may be suppressed, if in the investigation of these quantities the interface is permanently renewed. This procedure was followed by Grantcharova and Gutzow (1986) [268] who succeeded by this method in measuring definite values of the solubility of phenolphthalein glasses.

Experimental results concerning vapor pressure and solubility of glasses are relatively scarce. Practically only one more detailed measurement of the vapor pressure of a simple one-component typical oxide glass-forming substance is known, referring to the orthorhombic and the tetragonal crystalline modifications of P_2O_5 and their under-cooled melts (see Hill et al. (1943) [359]). By using the results of Hill et al. (1943) [359] in coordinates $\ln(p_f/p_c)$ vs $(1 - \theta^{-1} - 3\ln\theta)$ straight lines are obtained in agreement with the theoretical prediction as expressed by Eq. (3.163) (see Fig. 3.15). The experimental results lead, when compared with

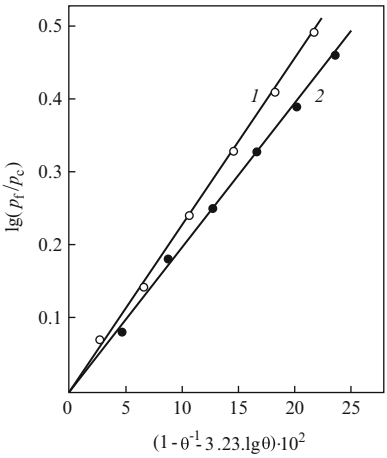

Fig. 3.15 Temperature dependence of the vapor pressure of under-cooled P_2O_5 in coordinates referring to Eq. (3.163). The experimental data are taken from Hill et al. (1943) [359]. *White points* specify the vapor pressure of orthorhombic P_2O_5 while *black dots* refer to tetragonal P_2O_5. Unfortunately, measurements have been carried out only for two temperatures just above T_g

the theoretical predictions, to reasonable values of the entropies of melting $\Delta S_m =$ 17.8 and 20.8 e.u. for both considered modifications.

An additional important aspect to be noted here is the convex character of the log p_f vs 1/T curve as to be expected from the theoretical predictions. Of particular interest are also measurements of the vapor pressure of liquid, crystalline and vitrified thin argon films performed quite recently (Kouchi and Kuroda (1990) [477], see Fig. 3.16). The results are significant in two aspects, since (i) for the first time a noble gas has been vitrified, and (ii) the temperature dependence of the vapor pressure of a simple substance in the three condensed states has been determined.

Vitrification of argon was achieved by the mentioned authors by vapor quenching at 10 K with an extremely high effective cooling rate corresponding to $10^{16}\,\mathrm{Ks}^{-1}$. In a next step of the experimental investigation the sample was heated with a rate $2\,\mathrm{K\,min}^{-1}$, corresponding to the rates of vitrification (10^1–$10^2\,\mathrm{Ks}^{-1}$) used in the standardized determination of T_g. Thus, T_g was found to be equal to about 20 K.

This experimental result coincides with a previously given theoretical estimate, based on the analysis of the rheological properties of this substance (Gutzow, Kashchiev, and Avramov (1985) [330]). Above T_g a rapid process of crystallization of the argon films is observed which leads to a completely crystalline structure of the sample. The vapor pressure of the resulting crystalline phase corresponds to the value for fcc-argon. Similar curves were obtained by Kouchi (1987) [476] also for thin films of water both for the vitreous and the crystalline states of the substance (for a further discussion see Grantcharova and Gutzow (1993) [270]).

In Fig. 3.16 also a fit of the vapor pressure curve for the amorphous argon film is given based on Eq. (3.161). The best fit is obtained if the value of the fictive temperature is set equal to $T^* = T_m$. Taking into account the Bartenev-Ritland equation Eq. (2.111) and also Fig. 3.6 such a result appears to be quite natural for the applied extremely high cooling rates. With Eq. (3.143) we get for this special case

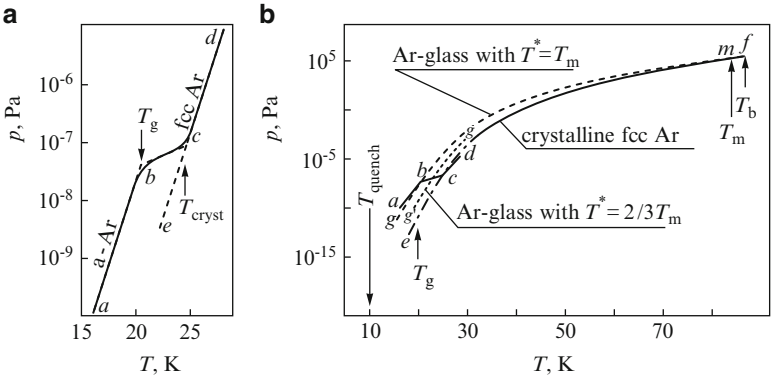

Fig. 3.16 Temperature dependence of the vapor pressure of liquid, crystalline and vitrified argon films (Grantcharova and Gutzow (1993) [270]): (**a**) Experimental data for the vapor pressure of vitreous and crystalline argon films reported by Kouchi and Kuroda (1990) [477]. Amorphous argon films (curve (*1*)) were obtained by vapor quenching at 10 K. When heated with a rate of 2 K min^{-1} at a temperature of about 20 K stabilization and crystallization processes occur which result in the formation of a crystalline fcc structure. Above 25 K the vapor pressure of the crystalline argon is measured (curve (*2*)). (**b**) Determination of the fictive temperature T^* of vitreous argon films: Vapor pressure curves for crystalline (curve (*1*)) and liquid (curve (*2*)) argon according to the measurements of Kouchi and Kuroda and reference data. Curve (*3*) corresponds to the vapor pressure of the under-cooled liquid argon according to Eq. (3.161). T_m is the melting point of argon, T_g the conventional vitrification temperature and T^* is Tool's fictive temperature for the vitrified argon. T^* corresponds to effective quenching rates of 10^{16} Ks^{-1} employed in the experiment

$$\Delta G_g(T) = T_m \Delta S_m (1 - \theta). \tag{3.173}$$

If this expression is substituted into Eq. (3.161) the dashed line in Fig. 3.16b is found. For comparison, in this figure a vapor pressure curve for vitreous argon is also given, when the fictive temperature T^* is assumed to be considerably lower than T_m (dashed-dotted curve). It can be seen that this curve cannot fit the relatively high values of the vapor pressure of vitreous argon measured in Kouchi's and Kuroda's experiments.

Measurements of the vapor pressure of two-component glasses are reported by Scholze and Gliemeroth (1964) [733], Hackenberg and Scholze (1970) ([341], H_2O in a Na_2SiO_3 H_2O-glass) and Überreiter et al. (1962, 1964, 1966) ([869], benzene in an organic high polymer). In both cases, the $\log p$ vs. $1/T$ curve follows the theoretical predictions. Überreiter and Bruns (1964) [869], moreover, mentioned a change in time of the vapor pressure into the direction of the value for the respective under-cooled melt, when the glass is tempered for prolonged times in the vicinity of T_g (see Fig. 3.17). This result is of principal interest, since it gives a direct evidence of relaxation processes in glasses as predicted first by Simon (1937) [758]. However, a quantitative analysis of the results of Scholze et al. and Überreiter et al. requires a more detailed thermodynamic description of vitrification and relaxation in multi-component systems which goes beyond the scope of the present discussions (see also Gutzow (1972) [294]; Grantcharova and Gutzow (1986) [268]).

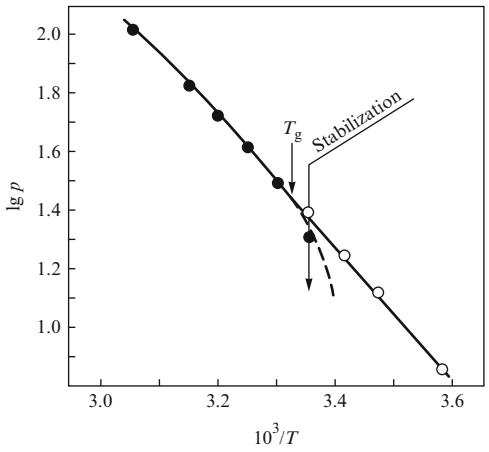

Fig. 3.17 Change of the vapor pressure of a glass-forming solution of polyvinylcarbosolon in benzene in an annealing process near T_g according to the measurements of Überreiter and Bruns (1964) [870]. The results are a direct illustration of the existence of relaxation processes in glasses towards the respective metastable equilibrium. *Black dots* refer to the vapor pressure of the under-cooled metastable melt while *circles* indicate the vapor pressure of the glass. An *arrow* describes the direction of change of the vapor pressure of the vitrified sample in the process of stabilization after 5 months annealing at a temperature 296 K

Of even greater importance for the verification of the outlined theoretical approach is the comparison of dissolution experiments with the same substance in the form of the metastable under-cooled melt, in the vitreous and in the crystalline states. The expected higher solubility of glasses can be of technological importance and attracted the attention already many years ago. As examples in this respect the work of Nacken (1945) [589] with SiO_2 and of Kolb (1969) [463] with selenium can be mentioned (see also Smakula (1962) [780]). This interest is connected with the possible realization of an isothermal synthesis of monocrystals from solutions, where the vitreous solid serves as the source of constant supersaturation.

Experimental data on the solubility of vitreous systems are given in Fig. 3.18 (Grantcharova and Gutzow (1986) [268]). It can be shown that the values of the molar enthalpy and entropy of melting, calculated from the solubility data and the theoretical equations Eqs. (3.170)–(3.172) ($\Delta H_m = 18.4\,\mathrm{kJ\,mol^{-1}}$, $\Delta S_m = 9.2\,\mathrm{J\,K^{-1}\,mol^{-1}}$ for SiO_2) are in reasonable agreement with the values of these parameters obtained from calorimetric measurements ($\Delta H_m = 13.2\,\mathrm{kJ\,mol^{-1}}$, $\Delta S_m = 9.2\,\mathrm{J\,K^{-1}\,mol^{-1}}$; Witzel (1921) [930], see also Eitel (1952) [184]). From a methodological point of view of considerable interest are the results on solubility measurements of phenolphthalein (Grantcharova and Gutzow (1986) [268]). Phenolphthalein (PhPh) exists in only one orthorhombic crystalline modification. Moreover, UV-spectral analysis reveals that the solutions of the crystalline and vitreous forms of this substance are formed by the same structural unit, the PhPh-molecule.

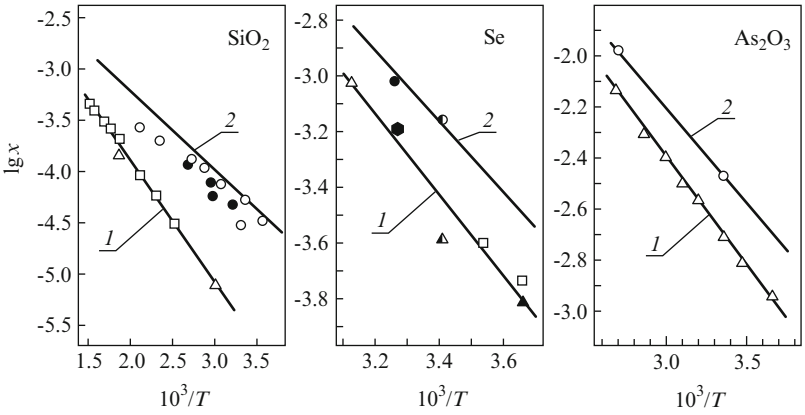

Fig. 3.18 Experimental results on the solubility of simple inorganic glass-forming systems in coordinates corresponding to Eqs. (3.170)–(3.172). As a measure of the solubility the molar fraction x of the solute in the solution is chosen. The curves refer to SiO_2 in water (*triangles and squares* – solubility of quartz; *black and white dots* – solubility of amorphous samples, according to experimental data compiled by Iler (1979) [386]), Se in CS_2 (*triangles, squares and hexagons* – solubility of crystalline monocline Se according to Mitcherlich (1855) [565], Ringer (1912) [666] (see Gmelins Handbuch der anorganischen Chemie, 8th edition, No. 10, 1952, p. 257 [256, 257]); *black and semiblack circles* – amorphous Se according to Rammerlsberger and Shidai (Gmelins Handbuch, No. 10, p. 257 [256, 257])), As_2O_3 in water (*triangles* – solubility of crystalline cubic As_2O_3 according to experimental data by Anderson and Story (1923) [11] (see also Gmelins Handbuch, 8th edition, No. 17, p. 278 [256, 257]), *white circles* – solubility of vitreous As_2O_3 according to a determination by Winkler (1885) (Gmelins Handbuch, p. 278 [256, 257]), Landolt-Börnstein, Zahlenwerte und Funktionen, part II, 2b, 6th edition, Springer, 1962). In all three cases the straight line is a fit through the experimental data as it would have been expected from the outlined theoretical equations (see Eq. (3.171)) by using the caloric data

In Fig. 3.19 dissolution curves are shown for PhPh in water both for vitreous and crystalline samples of the substance and for two different temperatures. For the crystalline substance the approach to saturation can be described satisfactorily as a diffusion limited process in terms of Nernst's kinetic equation (see Nielsen (1964) [603])

$$\frac{dc}{dt} = \frac{D_0 A_s}{\delta}(c^{(e)} - c). \tag{3.174}$$

Here D_0 is the diffusion coefficient of the solute molecules in the solvent, δ the thickness of the diffusion layer and A_s the surface area of the solid/solution interface.

Introducing a relaxation time τ_N via

$$\tau_N = \frac{\delta}{D_0 A_s}, \tag{3.175}$$

Eq. (3.174) may be rewritten in the same form as Eq. (3.122)

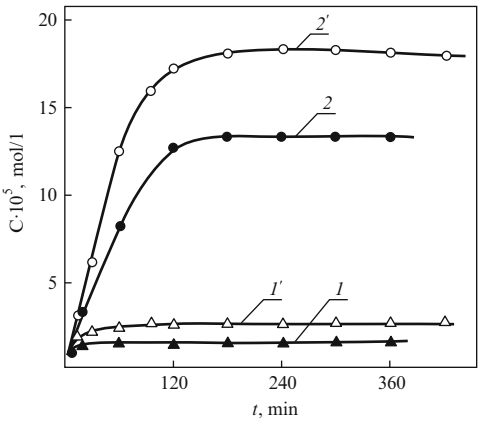

Fig. 3.19 Kinetics of dissolution of phenolphthalein in water in the absence of crystallite precipitation: curves (*2*) and (*2′*) – dissolution of the glass at temperatures 13 and 22 °C, respectively; curves (*1*) and (*1′*) – dissolution of the crystalline phase at the same conditions (Grantcharova and Gutzow (1986) [268])

$$\frac{d(c - c^{(e)})}{dt} = -\frac{(c - c^{(e)})}{\tau_N}, \tag{3.176}$$

underlining the similarity between structural relaxation of glasses and kinetics of dissolution (approach to thermodynamic equilibrium, respectively, metastable equilibrium). The saturation plateau in the dissolution curves can be identified with the respective equilibrium solubility. In the same figure, the dissolution curves of the glass are also given. They follow Nernst's equation Eq. (3.174) as well. This coincidence gives us the right to speak, in the same sense as it was done for crystals, about definite values of the solubility of the glass, since, as it can be seen, the saturation value remains, again, constant for the considered observation times. In terms of Eq. (3.122) this result means that for the considered experimental conditions τ is practically equal to infinity.

In Fig. 3.20 the results of determination of the solubility of phenolphthalein at different values of temperature are given. It is found that the solubility of the glass does not change in all considered cases for the characteristic times of dissolution experiments. From the slope of the straight lines in Fig. 3.20 Grantcharova, Avramov and Gutzow (1986) [271] determined the frozen-in values of the enthalpy and the entropy of the glass as $\Delta H_g = (11.7 \pm 1.3)\,\mathrm{kJ\,mol^{-1}}$ and $\Delta S_g = (19.6 \pm 5.4)\,\mathrm{J\,mol^{-1}\,K^{-1}}$.

Determinations of these quantities, based on specific heat measurements performed with a differential scanning micro-calorimeter (compare Fig. 2.21), gave the following values: $\Delta H_g = (13.8 \pm 1.3)\,\mathrm{kJ\,mol^{-1}}$ and $\Delta S_g = (10.1 \pm 4.6)\,\mathrm{J\,mol^{-1}\,K^{-1}}$ for the same substance. Taking into account the relatively high scattering in the determination of these quantities by the caloric measurements (up to 10–15 %) the agreement between the results obtained in the two different ways can be considered as quite satisfactory.

In performing the solubility experiments with phenolphthalein Grantcharova and Gutzow (1986) [268] encountered difficulties known also from other similar experiments with glasses. When the solubility of the glass exceeds considerably the

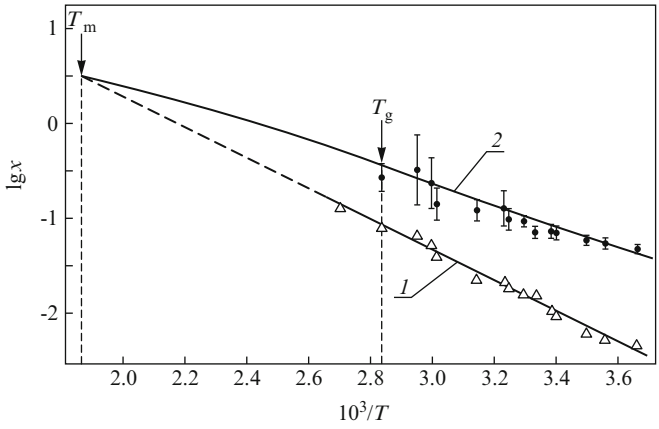

Fig. 3.20 Temperature dependence of the solubility of vitreous and crystalline phenolphthalein in water according to Grantcharova and Gutzow (1986) [268] (*triangles*: solubility data for the crystal; *circles*: solubility data for the glass). The straight line (*1*) through the crystal solubility data and its extension (*dashed curve*) is obtained by a least square fit. Curve (*2*) through the solubility data of the vitreous sample is drawn according to theoretical expectations (cf. Eq. (3.163)). x multiplied with 10^{-5} gives the molar fraction of PhPh in the solution

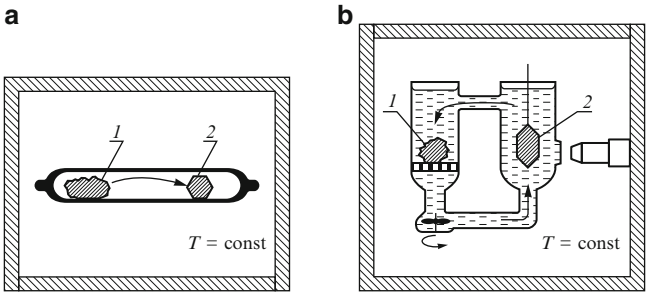

Fig. 3.21 Schematic illustration of the crystal growth experiments at a constant temperature, when vitreous solids are used as the source of constant supersaturation: (**a**) via the gas phase (vapor pressure of the glass); (**b**) via the solution (solubility of the glass). In both cases by (*1*) the glass and by (*2*) the growing single crystal is denoted

solubility of the crystal, the solutions become highly supersaturated with respect to crystallization and a spontaneous precipitation occurs. This effect is undesirable, if the growth of a single crystal from the solution is attempted as tried by Nacken. This was also the reason, why Nacken's experiments directed to an isothermal synthesis of quartz under hydrothermal conditions failed (see the criticism of Nacken's work given by Smakula (1962) [780]). Choosing temperature values only slightly below T_g, Grantcharova and Gutzow (1986) [268] were able to obtain in the experiments an isothermal growth of PhPh-crystals from aqueous solutions in which the supersaturation was sustained by the dissolution of the glass. Under

these conditions the supersaturation was sufficiently low not to cause precipitation (see Fig. 3.21 for a schematic representation of monocrystal growth experiments by dissolution or evaporation of glasses).

3.13 Affinity of Chemical Reactions Involving a Vitreous Reagent

The higher values of the molar Gibbs free energy of a substance in the vitreous state as compared with that of the under-cooled melt or of the crystalline phase also result in higher values of the chemical reactivity. This is another problem of the thermodynamics of glasses which can be treated in the same way as vapor pressure and solubility of glasses (see also Gutzow (1974) [296]; Grantcharova and Gutzow (1986) [268]).

We consider a heterogeneous chemical reaction in the gas phase described by

$$\alpha_E E + \alpha_1 A_1 + \alpha_2 A_2 + \ldots \rightleftharpoons \beta_1 B_1 + \beta_2 B_2 + \ldots, \tag{3.177}$$

taking place at constant pressure and temperature ($T < T_g$). It is supposed that the solid component E participates in it once as a crystal and another time as a glass. More precisely, it is assumed that in the heterogeneous gas reactions not the solid itself takes part but its vapor characterized by the vapor pressure p_E. Consequently, the course of the chemical reaction may be different depending on the vapor pressure of the gas being in contact either with the crystal or the glass.

The stoichiometric coefficients in the above reaction are denoted, for the initial reagents, by α_i and α_E (α_E refers to the vapor in equilibrium with the solid) and β_i for the reaction products. The degree of completion of a chemical reaction can be described, again, by a variable ξ. In terms of ξ the change of the number of moles of the different components is expressed as

$$dn_i = \nu_i \, d\xi \qquad \begin{cases} \nu_i = \{-\alpha_E, -\alpha_i\}, \ \nu_i < 0 & \text{for the reactants} \\ \nu_i = \beta_i \qquad\qquad\quad \nu_i > 0 & \text{for the reaction products} \end{cases} \tag{3.178}$$

and for the change of the Gibbs free energy in a chemical reaction we may write (for $p = \text{const.}$, $T = \text{const.}$)

$$dG = \sum_i \mu_i \, dn_i = d\xi \sum_i \mu_i \, \nu_i . \tag{3.179}$$

According to Eqs. (3.5) and (3.179) the affinity A of the considered process can be written as

$$A = -\sum_i \nu_i \, \mu_i \,. \tag{3.180}$$

To derive further conclusions, we express first the chemical potentials μ_i of the different components of the gas mixture through their values μ_i^0 for the pure substance at a reference pressure p_0 and a temperature T, the molar fractions x_i and the activity coefficients f_i as

$$\mu_i(p, T, x_1, x_2, \ldots) = \mu_i^0(p_0, T) + RT \ln\left(x_i \, f_i \, \frac{p}{p_0}\right). \tag{3.181}$$

A substitution into Eq. (3.180) yields

$$A = -\left[\sum_i \mu_i^0(p_0, T)\nu_i + RT \sum_i \nu_i \ln\left(x_i \, f_i \, \frac{p}{p_0}\right)\right]. \tag{3.182}$$

With the notation

$$K(T) = \exp\left\{-\frac{\sum_i \mu_i^0(p_0, T)\nu_i}{RT}\right\} \tag{3.183}$$

we obtain for the equilibrium state ($A = 0$, compare Eq. (3.5))

$$K(T) = \left\{\prod_i (x_i \, f_i)^{\nu_i}\right\} \left(\frac{p}{p_0}\right)^{\sum_i \nu_i}. \tag{3.184}$$

This equation is the general form of the well-known mass action law. It shows that the equilibrium vapor pressure of the different components is uniquely determined by the actual value of temperature. For a mixture of perfect gases ($f_i = 1$, $p_i = p x_i$) this equation can be written (in a more extended form applying the original notations Eq. (3.178)) as

$$K(T) = \frac{\prod_i (p_i)^{\beta_i}}{\prod_i (p_i)^{\alpha_i} (p_E)^{\alpha_E}} (p_0)^{(-\sum_i \nu_i)}. \tag{3.185}$$

Similar equations can be formulated if the chemical reactions proceed in solution.

The equilibrium constant $K(T)$ of the chemical reaction is expressed according to Eq. (3.183) through the chemical potentials of the pure components, taking part in the chemical reaction, at the temperature T and the reference pressure p_0. It is only a function of temperature. Moreover, it follows directly that the ratio $\sigma_E = K_g / K_c$ can be written in the form

$$\sigma_E = \frac{K_g(T)}{K_c(T)} = \exp\left\{\frac{\alpha_E}{RT}\left[\mu_{E0}^{(g)}(p_0, T) - \mu_{E0}^{(c)}(p_0, T)\right]\right\}. \tag{3.186}$$

Here by g and c the reaction constants for the reaction in contact either with the glass or the crystal are specified.

The difference in the chemical potentials can be expressed through the difference of the molar values of the free enthalpy between the glass and the crystal as (for $p_0 = p$)

$$\mu_{E0}^{(g)}(p, T) - \mu_{E0}^{(c)}(p, T) = \Delta G_g. \tag{3.187}$$

With Eq. (3.161) these results allow one a direct estimation of the temperature dependence of the equilibrium constant $K_g(T)$, when the respective expression for the reaction taking place in contact with the crystalline solid is known. We get

$$K_g(T) = K_c(T)\left(\frac{p_g}{p_c}\right)^{\alpha_E}. \tag{3.188}$$

Since $p_g > p_c$ holds, the equilibrium constant of the considered chemical reaction is always higher, when the solid takes part in the chemical reaction as a glass.

In reference literature usually the necessary data can be found, needed for the calculation of K_c, e.g., by Ulich's method (see Karapetyanz (1975) [432]). Equation (3.188) gives thus a simple method for the estimation of the equilibrium constant of a chemical reaction taking place with the participation of the glass, if ΔH_g and ΔS_g are known or estimated according to theoretical approaches similar to those outlined in Sect. 3.5. Such calculations can be of use in deriving the equations describing thermodynamic and kinetic properties of chemical transport processes taking place with vitreous solids or for the design of isothermal monocrystal growth with chemical transport reactions (see Schaefer (1962) [684] and for a more detailed discussion Grantcharova and Gutzow (1986) [268]).

3.14 Location of the Vitreous State in the (p, T)-Diagram

In Chap. 2 (Fig. 2.2), the equilibrium phase diagram for water is given. The different curves in this (p, T)-diagram correspond to two-phase equilibria for liquid water, its vapor and normal ice. For water the specific volume of the solid is larger than the respective value for the liquid. This specific property results in negative slopes of the melting curve. For most substances, however, the opposite situation is found as reflected in Fig. 3.22.

In Fig. 3.22, in addition to the equilibrium vapor pressure curves also their extensions into the one-phase regions of the solid and the liquid phases are given. These extensions reflect the vapor pressure curves for the metastable condensed states of the substance. The areas, bounded by the lines (ac) and (af), respectively,

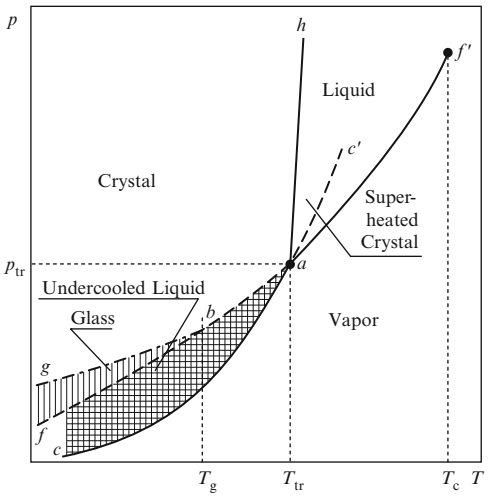

Fig. 3.22 Phase diagram for a glass-forming substance with triple point T_{tr}, critical point T_c and $p(T)$-curves for the vapor pressure of both the equilibrium and metastable phases: Curve (cac'): Vapor pressure of the stable crystal (ca) and the superheated crystal (ac') (provided such a state can be realized in experiments); curve (faf'): Vapor pressure curves of the liquid in thermodynamic equilibrium with the vapor (af') and for the under-cooled melt (af); curve (ah): Melting curve of the crystal; curve (bg): Vapor pressure curve of the vitrified melt. *Vertical bars* specify the possible location of the vitreous state in the phase diagram for a given value of the temperature of vitrification T_g. The *double shaded area* corresponds to the metastable under-cooled liquid

(ac') and (ah), correspond to regions of the possible existence of a superheated solid and an under-cooled liquid (double shaded region).

If we suppose that the considered substance can be vitrified to a glass at the temperature of vitrification T_g, then the vapor pressure of the glass in dependence on temperature T can also be introduced into the (p, T)-diagram. According to Eq. (3.164) this curve is located above the respective (p, T)-dependence for the metastable liquid and is tangent to it at $T = T_g$ (see also Fig. 3.14).

In Fig. 3.22 only the part of the vapor pressure curve of the glass, corresponding to temperatures $T < T_g$, is given (line (bg)). The region in the phase diagram, bounded by the curves (bg) and (bf), can be considered, consequently, as the field of possible existence of the substance in the vitreous state. It is marked by vertical lines. In agreement with the Bartenev-Ritland equation Eq. (2.111) for higher cooling rates T_g is transferred to higher values of temperature and the region in the (p, T)-space with the possible existence of the glass is increased. Vice versa, for very slow cooling processes this area shrinks to zero. In this way, it is once again evident that glasses cannot be considered as an equilibrium state of aggregation. The area allocated to the vitreous state in the (p, T)-diagram is determined not only by the material parameters of the substance but also on the kinetics of the process of vitrification.

3.15 Discussion

It has been shown by the foregoing analysis that in the framework of the thermodynamics of irreversible processes even in the simplest approach, when only one structural order parameter ξ is used, numerous results may be obtained, which describe the experimental findings quite satisfactorily, at least, qualitatively. Let us recall, for example, that in a very general and non-contradictory way the discontinuities in the thermodynamic coefficients can be explained, as well as the dependence of the thermodynamic properties of glasses on cooling rate. The agreement with experimentally observed results for simple and for polymer glass-forming melts is even better than it could be expected in advance from such a simplified treatment. This result gives confidence that the applied approach could be also of use for the description of freezing-in and stabilization processes of disordered structures of a more general nature than those considered so far. In this respect systems with magnetic disorder (spin glasses) or even different forms of vitrified life (frozen-in cells or even organs) could be mentioned.

However, the method applied so far also has its shortcomings. Firstly, we have confined the analysis to the consideration of only one structural order parameter. As mentioned in the first section of this chapter, the introduction of more than one order parameter is essential not only for a quantitatively more correct description of the experimental results (cf., e.g., the discussion concerning the Prigogine-Defay ratio in Sect. 3.8). It can be shown, moreover, that essential qualitative features, e.g., hysteresis effects in heating and cooling, can be adequately described only if more than one order parameter is applied for the description of vitrification. A thorough discussion of this topic can be found in the monograph by Mazurin (1986) [543] (see also Kovacs et al. (1977) [478]; Avramov and Milchev (1988) [26]).

The temperature of vitrification T_g was also determined within the mentioned simplified approach. Taking into account hysteresis effects different values of T_g can be found for heating and cooling runs. A thorough discussion of these topics is given by Bartenev (1966) [53], Kovacs et al. (1977, 1979) [478, 479], Mazurin (1986) [543], Avramov and Gutzow (1988) [24] and Avramov, Gnappi, and Montenero (1992) [33]. A more rigorous standard way of definition of glass transition temperatures will be analyzed in Chap. 12 in connection with the discussion of the rheology of glasses. Further, if larger deviations from equilibrium occur, then the introduction of non-linear equations in describing the kinetics of relaxation and the properties of vitrifying systems is essential. With Eqs. (3.130)–(3.134) we made an attempt to give such a more accurate description for stabilization processes of vitrified glass-forming melts.

The analysis of vapor pressure, solubility and affinity of glasses, outlined in Sects. 3.12 and 3.13, has, as mentioned, also a direct technological significance in developing methods of mono-crystal synthesis. However, their main importance from a theoretical point of view is that the experiments discussed verify the existence of well-defined values of solubility or vapor pressure of a glass and the prescription how these quantities can be defined and measured. It is evident that the only way

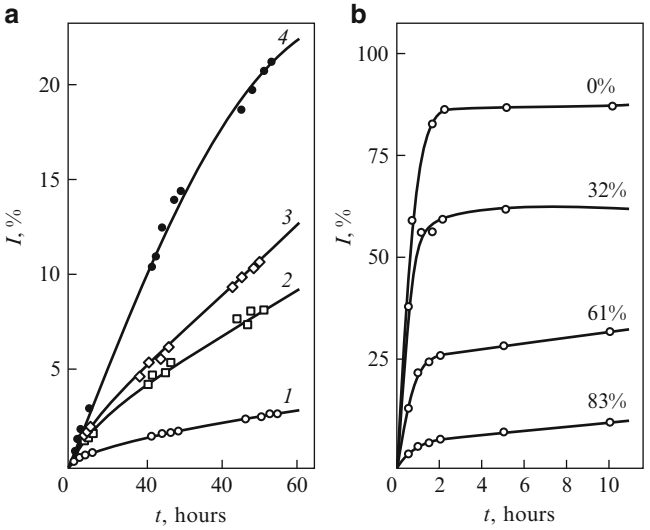

Fig. 3.23 Solubility of different modifications of silica in a 0.1 normal NaOH aqueous solution at 298 K in dependence on time: (**a**) Kinetics of dissolution of quartz (*1*), cristobalite (*2*), tridymite (*3*) and SiO_2-glass (*4*) (Berman, Patterson (1961) [70]); (**b**) Kinetics of dissolution of tribochemically amorphisized quartz with different degrees of crystallinity x (given as the parameter to each curve) in dependence on time (Steinike et al. (1978) [797], see also Heinicke (1984) [352])

they can be determined consists of identifying them with the limiting values of the solubility vs time (or vapor pressure vs time) curves. In this analysis, the necessary precautions have to be undertaken (introduction of new virgin samples or creation of fresh surfaces by milling the substance during the process of dissolution, inhibition of crystallization) in order to obtain reproducible results.

The outlined experimental findings show, moreover that the approach in the theoretical determination of these quantities, connecting vapor pressure and solubility of a glass with ΔG_g, is also consistent with the caloric determinations of ΔG_g. In this way, experimental data on solubility or vapor pressure may be used for a determination of ΔG_g. Moreover, measurements of the solubility and the vapor pressure of glasses may also serve as a method to follow experimentally structural changes taking place in the glass in the course of thermal or other methods of treatment. In this respect the results of the measurements of the kinetics of dissolution of photoactive amorphous substances (chalcogenide glasses) in alkaline aqueous solutions can be mentioned (see Mitkova and Boncheva-Mladenova (1987) [566]; Ivanova and Boncheva-Mladenova (1979) [388]).

Another example in this respect are the experimental investigations of Steinike et al. (1978) [797] of the course of amorphization of initially crystalline quartz powders under the influence of different mechano-chemical treatments (see Fig. 3.23). It is interesting to note that from the solubility of the powders amorphisized in such a

way thermodynamic parameters are obtained which are in good agreement with the respective values for vitreous silica obtained by the classical methods of preparation from the melt.

A related problem of great interest is the possibility of forming vitreous condensates from the vapor phase or from solutions. This process is reverse of evaporation or dissolution of a glass discussed so far. It was again Tammann (see Tammann and Starinkevich (1913) [823]) who first obtained vitreous condensates from the vapor phase. We would also like to mention the existence of a large amount of evidence that the amorphous mineral hyalite can be considered as the vitreous SiO_2 precipitate formed under geological hydrothermal conditions.

Based on the results outlined in the present chapter the definition of the vitreous state can be given in a more precise form than it has been done before. We propose the following definition:

> Glasses are thermodynamically non-equilibrium kinetically stabilized amorphous solids, in which the molecular disorder and the thermodynamic properties corresponding to the state of the respective under-cooled melt at a temperature T^* are frozen-in. Hereby T^* differs from the actual temperature T.

It is evident that the definition outlined above adopts, in principle, Tammann's argumentation (glasses are under-cooled frozen-in liquids). It also accounts for Einstein's and Simon's ideas, identifying the vitreous state with a particular non-equilibrium state of matter. The definition is at the same time narrower and more precise since it gives us the possibility of distinguishing glasses from other non-equilibrium states of matter. The definition formulated above does not imply moreover that glasses are formed only by rapid quenching of a melt. If an amorphous solid is prepared, e.g., by vapor quenching or electrolyte deposition it can be also denoted as a glass, if its structure and thermodynamic properties correspond to a state of a real or fictive melt of the substance at some definite value of temperature T^*. Thus, conceptional difficulties existing in the application of previous definitions in discussing, e.g., vapor quenching as a method to produce a glass do not occur in this approach. The new definition may be formulated also in the more general form:

> Any thermodynamically non-equilibrium (amorphous or crystalline) solid can be denoted as a glass when a state of order or disorder is frozen-in in it corresponding to an equilibrium state which is possible for higher temperatures (or any other values of the external parameters).

Such a generalization includes into the class of glasses also those crystalline solids in which a particular type of atomic, molecular or electronic structural disorder is frozen-in corresponding to equilibrium configurations at higher temperatures (e.g., the mentioned already spin- or quadrupole glasses, frozen-in disordered crystals (see, e.g., Haase (1963, p. 560) [339]). The outlined definition is applicable also without restrictions to systems characterized by negative values of the absolute

temperature, a problem, which may be also of principal significance, as pointed out in a paper by I. Gutzow, J. Schmelzer, I. Gerroff, Unpublished.[3]

In the preceding chapters a thermodynamic description of vitrification processes and the properties of glasses was given. Looking back to the problems discussed and the results obtained a remark made by Earl C. Kelley (1947) [446] for a similar situation comes into mind: "We have not succeeded in answering all our problems - indeed we sometimes feel we have not completely answered any of them. The answers we have found have only served to raise a whole set of new questions. In some ways we feel that we are confused as ever, but we think we are confused on a higher level and about more important things".

In part the limitations in tackling the problems raised by us are due to the fact that the approach, used in the preceding chapters, is of a phenomenological nature and does not allow one to specify neither the number of necessary structural order parameters nor the microscopic processes connected with vitrification and stabilization. The more detailed microscopic approach requires the knowledge of the basic features concerning the structure and statistical methods of description of glasses. These topics will be discussed in Chaps. 4 and 5.

[3]The second formulation as discussed here connects the definition of glasses with the properties of the initial system thermodynamic equilibrium at the initial values of the thermodynamic control parameters. Having in mind the way of description of glasses via a set of structural order parameters as discussed in detail in the present chapter, one could also propose as a next step in advancing about a next step in advancing definitions of glasses as:

> Glasses are thermodynamically non-equilibrium kinetically stabilized amorphous or non-amorphous solids characterized, in addition to the f equilibrium thermodynamic state variables, by one or more structural order parameters $\{\xi_j\}$ and use by a generalized equation of state, in the form
>
> $$\Phi = \Phi(p, T, \{n_i\}, \{\xi_j\}).$$
>
> In equilibrium, the structural order parameters are unambiguously defined by the value of the thermodynamic state parameters; in the vitreous state, they have values determined by the concrete glass transition process.

Such a statement fully separates the definition of the vitreous state from the way glasses are conventionally formed.

Chapter 4
General Approaches to the Description of the Structure of Glasses

4.1 Introduction

Taking into account the great variety of substances with extremely different compositions, known to exist in the vitreous state, it seems impossible at a first glance even to formulate such a problem like the general description of the structure of glasses. Moreover, as we already know, even from a given melt with a definite composition glasses with different properties and structures can be prepared by varying the cooling rates.

For many years, in the discussion of the structure of glasses in most textbooks devoted to the vitreous state only the structure of oxide and, in particular, of silicate glasses is analyzed. This is due, on one hand, to historic reasons, connected with the early widespread application of such glasses and, on the other hand, because oxide glasses represent, in fact, a striking example for a large variety of possible structures. Thus, an extended discussion is required to describe the structural properties of oxide glasses in a more or less comprehensive way. Other glass-forming systems, for which thorough structural investigations have been performed, are metallic glass-forming alloys and organic polymer glass-forming systems. A number of cases of structure determinations for glasses with more exotic compositions have also to be mentioned. In this connection, metallic, halide and chalcogenide glasses are of particular interest.

In line with the general approach of the present book we will not attempt to give a precise description of the structure of particular glasses but would like to summarize in the following sections structural hypotheses and results of structural investigations which allow one to draw more or less general conclusions concerning the structural principles of glasses, valid for any type or, at least, for large classes of glass-forming systems. From a historical point of view the first such a general principle was developed by the Norwegian crystal-chemist G.V. Goldschmidt. This is the reason why we start the discussion with his ideas.

I.S. Gutzow and J.W.P. Schmelzer, *The Vitreous State*,
DOI 10.1007/978-3-642-34633-0_4, © Springer-Verlag Berlin Heidelberg 2013

4.2 Goldschmidt's Rule

Goldschmidt noted in 1926 that for binary ionic glass-formers (oxides, halides, chalcogenides) there exists a distinct correlation between the ability of a substance to form a glass and the ratio of its anionic (R_a) and cationic (R_c) radii. According to Goldschmidt's ratio criterion for typical glass-formers the inequality

$$0.2 < \frac{R_c}{R_a} < 0.4 \tag{4.1}$$

has to be fulfilled (Goldschmidt (1926) [262]). A review of early comments concerning Goldschmidt's rule can be found in glass-science literature of his time (see, e.g., Blumberg (1939) [85]). The further development of crystallochemical ideas in glass-formation, which originated from Goldschmidt's criterion, is discussed in a number of more recent monographs (see, e.g., Salmang (1957) [681]; Rawson (1967) [657]; Scholze (1965, 1977) [732]; Feltz (1983) [202]) and original publications (Poulain (1981) [643]). Goldschmidt's rule is equivalent to the statement that the anions (O, F) have to be able to arrange themselves around the smaller cations (Si, Ge, Be, Al, etc.) in a tetrahedral order (see, e.g., Fig. 4.1).

Goldschmidt's criterion is an interesting suggestion. For the first time a hypothesis was formulated which should be applicable to any system consisting of anions and cations. Substances like SiO_2, GeO_2, P_2O_5, As_2O_3, BeF_2 and many others, indeed, fulfil the requirements of this rule. Goldschmidt's criterion gave, moreover, the impetus for the synthesis of a whole new class of glass-forming substances. It opened the wide field of beryllium fluoride based glasses, the first of them being synthesized by Goldschmidt himself. Goldschmidt concluded from the criterion formulated by him, that beryllium fluoride, being structurally similar to SiO_2, should be not only a typical glass-former, but has to be expected to possess crystalline modifications similar to those of SiO_2. Later it was found, indeed that BeF_2 has quartz-like, tridymite-like and cristobalite-like crystalline modifications (Roy et al. (1950) [673]; Jahn and Thilo (1953) [399]). Goldschmidt termed BeF_2-glasses structurally weakened glasses as compared with the silicate glasses, since for one and the same cation-anion ratio a lower interatomic binding energy is to be expected in silicates, if one takes into account the lower valency of beryllium as compared with silicon (compare Be − F with O = Si = O). On the other hand, Goldschmidt predicted the existence of glass-forming systems he called structurally strengthened, in which for the same R_c/R_a ratio a larger bonding energy is found as compared with SiO_2 (Al ≡ N, Si≡C). One excellent example in this respect are nitrides (e.g., aluminium nitrides). Indeed, amorphous aluminium nitride thin films and Al ≡ N-oxinitride bulk glass samples were formed in recent years in fulfilment of Goldschmidt's predictions (Mackenzie and Zheng (1992) [526]).

Despite its mentioned advantages in addition to its simplicity and geometric visuality, it has to be also noted, however that Goldschmidt's criterion is far from being generally valid. This remark is true even in application to ionic substances. A large number of ionic substances exists for which Goldschmidt's ratio criterion is

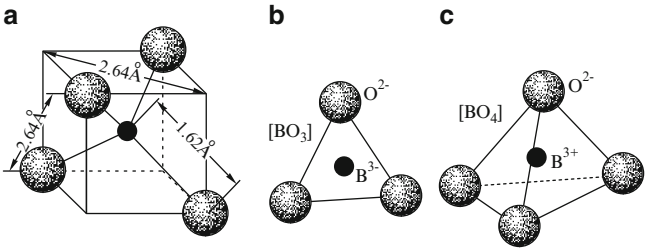

Fig. 4.1 Tetrahedral structure elements which represent the basic units of the structure of oxide glasses according to Goldschmidt's rule: (**a**) SiO_2-tetrahedron, (**b**) and (**c**) boron oxide in a trigonal and a tetragonal configuration

fulfilled, but the substances are not glass-formers. The best known example in this respect is beryllium oxide BeO; most of the halides are also excluded from this rule. Goldschmidt's approach can be also criticized from a more general point of view. In the derivation of his criterion Goldschmidt treated the classical glass-forming oxides as purely ionic substances while, according to present-day concepts of inorganic chemistry, to any ionic bond also a certain percentage of covalent bonding has to be attributed. For the Si − O bond in silicates this percentage of covalent bonding is approximately 50 % and in phosphates, the percentage of covalent bonding reaches 60 %. For the C − C bonds of organic substances even more than 80 % covalency is expected. It turns out, consequently that Goldschmidt's original idea is strictly speaking applicable only to substances like ionic halides, where the ionic character of bonding dominates (see also Pauling (1948) [629]; Scholze (1965, 1977) [732]; Rawson (1967) [657]).

It is remarkable, nevertheless that despite these limitations, Goldschmidt's rule still gives a key to the understanding of the structure of glasses. In fact, all classical glass-forming substances obey Goldschmidt's rule. Thus, it is evident that Goldschmidt's original ideas have to be supplemented by additional restrictions. This was done by Zachariasen in 1932.

4.3 Zachariasen's Criteria for Glass-Formation

The next major step in developing geometrical criteria for glass-formation and in the clarification of the structure of glasses was made in a beautiful form by Zachariasen (1932, 1933) [941–943] based on his random network hypothesis of glass structure (see also Rawson (1967) [657]; Hinz (1970) [363]). Zachariasen formulated three remarkable rules specifying the additional structural requirements, under which a tetrahedral arrangement of anions around smaller cations leads to glass-formation. In this way, Goldschmidt's main idea was reformulated by Zachariasen in a more precise form. Zachariasen stated that only such cations are glass-formers:

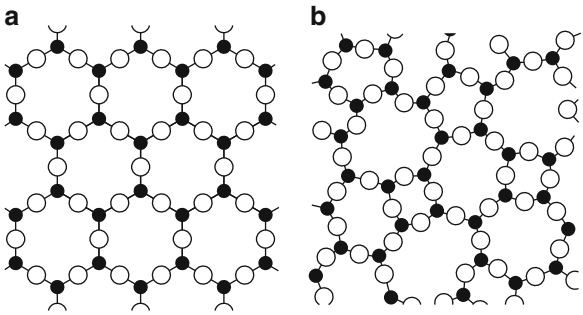

Fig. 4.2 The structure of (**a**) quartz and (**b**) silica glass in a two-dimensional representation according to Zachariasen

- Which have valencies larger than one and outer shell electronic configurations resembling those of the respective noble gases located in the same row of the periodic system of elements. However, the most significant supplement to Goldschmidt's ideas, formulated by Zachariasen, consists of the statement that
- Tetrahedral structures result in glass-formation only in cases, when the tetrahedra may form either linear chains of infinite length or two-, respectively, three-dimensional networks. Moreover,
- The tetrahedra have to be interconnected only by their vertices, not by their edges or faces.

In a second approach Zachariasen and Warren (Warren and Biscoe (1938) [911]; Warren (1937, 1941) [909, 910]) applied the mentioned crystal-chemical concepts for the specification of the structure of two- and multi-component oxide and, in particular, silicate glasses. In this connection the division of substances into network formers (glass-formers; in more recent literature also the notation glass promoters is used) and network modifying oxides (network modifiers) was introduced. According to Zachariasen "*an oxide glass is formed, firstly, if the sample contains a high percentage of cations, which are surrounded by oxygen tetrahedrons or oxygen triangles; second, if these tetrahedrons or triangles share only their vertices with each other, and, third, if some oxygen atoms are linked to only two such cations and do not form further bonds with other cations . . . All oxide glasses must contain appreciable amounts of various glass-forming cations or other cations, which are able to replace them isomorphically*". A two-dimensional example for a structure of the type as suggested by Zachariasen is shown in Fig. 4.2.

The division of oxides into network formers (SiO_2, GeO_2, P_2O_5, As_2O_3 etc.) and network modifiers has entered every textbook on glass science and technology. Modifiers, according to Zachariasen and Warren (see, also Rawson (1967) [657]; Scholze (1965, 1977) [732]; Hinz (1970) [363]) are to be divided into two classes, in bridging (i.e., two-valent earth alkali oxides: CaO, ZnO, MgO) and in non-bridging (NaO, CaO, etc.) oxides. This simple scheme, developed by Zachariasen and Warren, allows us to explain in a qualitative way the influence of different oxides on the properties of silicate glasses. As examples in this respect, the introduction of bridging oxides can be connected with the increase of the viscosity of the melt, while

univalent modifiers (e.g., alkali oxides) strongly reduce properties such as hardness, chemical durability, temperature of vitrification and result also in an increase of the molar volume. Moreover, the introduction of non-bridging oxides can be interrelated with the formation of "long" glasses with respect to the temperature dependence of the viscosity (see Sect. 2.4.1).

Alkali modifier atoms, according to Zachariasen, have to fit into the relatively large holes in the tetrahedral network. This is the reason, why modifiers are, in general, large ions with a low charge (Na^+, Cs^+, K^+, Zn^{2+}, Pb^{2+} etc.). Two additional prepositions underlying implicitly Zachariasen's approach should also be mentioned:

- The energy of the amorphous state is assumed to be practically the same as for the crystal.
- The univalent network modifiers are supposed to be distributed randomly in the structure.

Zachariasen expected, moreover that the isoenergetic increase of the entropy in the transformation of the substance into a glass can be considered as some kind of thermodynamic stabilization of the vitreous state. Taking into account the experimental result $\Delta H_g = (1/2)\Delta H_m$ and the conclusions concerning the nature of the vitreous state, discussed in Chaps. 2 and 3, the energetic considerations of Zachariasen cannot be accepted from a present day point of view. The second of the mentioned additional prepositions in Zachariasen's approach concerning the spatially random distribution of the network modifiers, is also highly improbable due to energetic considerations. In fact, it was not verified by experimental evidence.

Further developments and additional critical remarks with respect to Zachariasen's ideas may be found in the already cited monographs (Rawson (1967) [657]; Scholze (1965, 1977) [732]; Hinz (1990) [363]). However, it is remarkable that more than 80 years after its development Zachariasen's geometric approach is still of great scientific importance (or as it is said in a reappraisal of Zachariasen's work: "*The melody still lingers on*" (Cooper (1982) [145])). Geometrical considerations similar to those of Goldschmidt and Zachariasen also underly the structural criteria for glass-formation developed later on by Bernal. However, before we can go over to the discussion of these criteria, we have to describe an alternative development to Zachariasen's model which was proposed historically even earlier than Zachariasen's random network model: Lebedev's crystallite hypothesis of glass structure.

4.4 Lebedev's Crystallite Hypothesis of Glass Structure

According to the crystallite hypothesis in its original form silicate glasses are to be considered as agglomerates of submicroscopic crystallites, which are formed either of one of the crystalline modifications of SiO_2 or consist of solid solutions of these modifications with other components. Following this hypothesis glasses are micro-multi-phase and micro-heterogeneous in their structure. These peculiarities in the

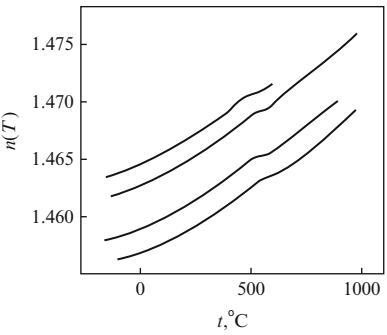

Fig. 4.3 Change of the coefficient of refraction, n, with temperature in an optical glass. Note the peculiarities in the temperature range between 400 and 500 °C, which according to Lebedev have to be connected with the $(\alpha \rightarrow \beta)$-transformation in quartz crystallites in the glass

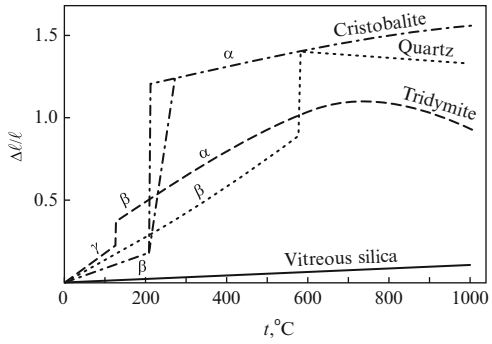

Fig. 4.4 Dilatational effects in different silica modifications corresponding to discontinuities in heating curves of silica glasses (According to Porai-Koshits (1989) [641])

structure should have a number of consequences with respect to the properties of the glass which should give one the possibility of an experimental verification of its premises.

The crystallite hypothesis was developed by A.A. Lebedev (1921) [500] (cf. also [192]). However, similar ideas were also expressed as early as 1835 by Frankenheim, by le Chatelier in the investigation of the viscosity of glass-forming melts, by Randall, Ruxby, and Cooper (1930) [655]. The term crystallite hypothesis was coined in 1937 also by Lebedev [501] (for a historic survey see Porai-Koshits (1955 [640], 1989 [641])). Lebedev came to his ideas based on the analysis of the temperature dependence of the coefficient of refraction, $n(T)$, for a number of optical silicate glasses. It was found in these experiments that in the temperature range from 400 to 500 °C peculiarities were observed in the (n vs. T)-curves and subsequently also in other properties of silicate glasses (see Porai-Koshits (1955) [640] and Figs. 4.3 and 4.4). Lebedev connected the observed discontinuities with the $(\alpha - \beta)$-transformation of the expected quartz-crystallites in the glass, which is known to occur in this temperature range (see Fig. 4.4).

Later it was found that the mentioned effect is less pronounced for quenched samples of the same composition. It is completely absent in SiO_2-glass obtained by vapor quenching (so-called vitreosil). It became evident also, that in quenched samples the quartz crystallites are present in a lower percentage, in vapor quenched vitreous materials they are completely absent. This difference is the reason why

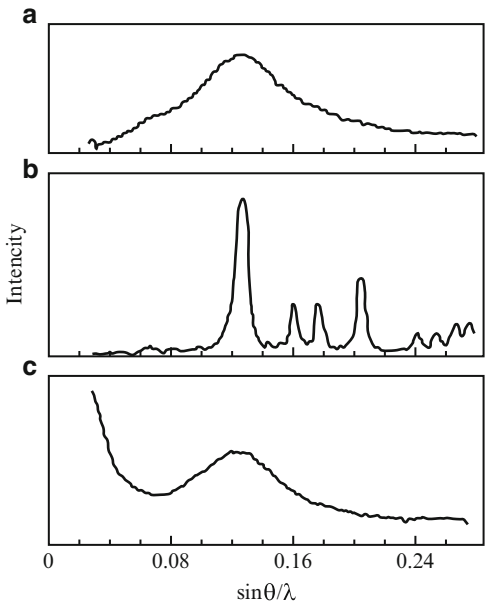

Fig. 4.5 Intensity curves obtained by X-ray measurements for (**a**) quartz-glass, (**b**) cristobalite and (**c**) a silica gel

on heating quenched SiO_2-glass samples, effects due to the transformation of the low-temperature modification are less pronounced in experiments or why such effects do not occur at all in such cases as in vitreosil. By thorough experimental investigations, Tudorovskaya succeeded in finding similar effects in the (n vs. T)-curves, however, less pronounced, in the temperature ranges 85–120 °C, 140–165 °C and 180–210 °C, which correspond to the ($\alpha \rightarrow \beta$)-transformations of the other two crystalline modifications of SiO_2, tridymite and cristobalite.

It was expected that the decision concerning the question which of the both mentioned approaches is more appropriate, either the crystallite hypothesis or Zachariasen's random network model, could be given by X-ray methods of structural analysis. These methods had shown their power just at that time, i.e, the end of the 1920s, in the determination of the structure of crystalline solids. However, it was found that for amorphous structures and, in particular, for silicate glasses, X-ray analysis is a far less convincing method than when used for crystalline solids. While for crystalline solids the structure may be determined more or less unambiguously from X-ray measurements, the determination of the structure of amorphous materials is a very complicated problem. Particularly for glasses, this method meets serious difficulties both of an experimental and theoretical nature.

The primary result of such structural investigations are X-ray patterns, which give the intensity of the radiation in dependence on the scattering angle, θ. In Fig. 4.5, typical examples of such curves are shown for quartz glass (a), cristobalite (b) and silica gel (c). The aim in the interpretation of such curves consists of the determination of the spatial distribution of atoms and molecules, giving the same X-ray patterns. This problem can be solved both for crystalline and amorphous

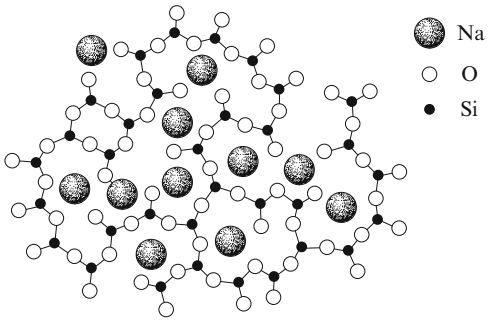

Fig. 4.6 A two-dimensional representation of the structure of a sodium silicate glass according to Warren

substances in two ways. In the first approach based on the intensity curves the spatial structure is determined by using an appropriate mathematical algorithm (Fourier transformations). The second method – of trial and error – consists of the preposition of some hypothetical structure of the investigated object, the determination of the intensity curve corresponding to this model and the comparison with the experimentally observed patterns.

For a determination of the structure of glasses in most cases the second approach was employed. As the basic assumption for the determination of glass structure it was supposed initially, that the glass can be considered as an agglomerate of small crystallites as proposed, e.g., by Randall et al. (1930) [655]. It follows that in the first attempts at structure determination of glasses the crystallite hypothesis was used as the starting point. The estimation of the sizes of the expected crystallites was based on the theory of scattering of X-ray radiation by fragmented crystallites (measurements of line broadening), developed by Scherrer in 1918 and applied by him to a number of micro-crystalline materials. The main diffusive maximum observed in the intensity curves of glasses was interpreted in these first investigations (see Randall et al. (1930) [655]) as the result of the scattering of an ensemble of cristobalite crystallites with a size of the order 10^{-7} cm.

Another method of treatment of the experimental results, which is based from a mathematical point of view on Fourier's integral analysis, was developed by Debye and Menke (1931) [160] and Zernicke and Prins (1927) [456]. For applications to amorphous structures, this theory was developed further by Warren. Warren's method is still the basis for modern investigations of glass structure (see Kitaigorodski (1952) [456]). Warren and coworkers applied this method to a number of silicate glasses and came to opposite conclusions concerning the structure of glasses: Glasses have to be described in the framework of Zachariasen's random network model. A two-dimensional representation of the structure of sodium silicate glasses according to Warren is shown in Fig. 4.6.

In discussing his results Warren mentioned that, provided the crystallite hypothesis is correct, the size of the crystallites should be only slightly larger than a single unit cell. At these small dimensions, however, the concept of crystallinity ceases to have any meaning (see also Rawson (1967) [657]). In the analysis of quartz glass Warren came to the following more definite conclusions. The distance between two

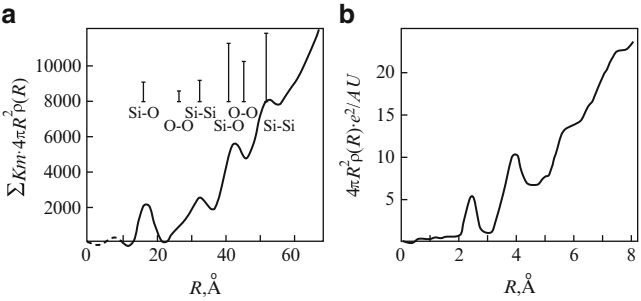

Fig. 4.7 Radial distribution function of atomic density in quartz glass (**a**) and in a $Ge_{0.42}Se_{0.58}$ glass (**b**) as obtained from *X*-ray diffraction studies (Bienenstock (1977) [81])

silicon atoms in the Si – Si-bond equals 3.24 Å, which is characteristic for an edge to edge tetrahedral bonding. The general distribution of the bond lengths Si – Si, Si – O and O – O corresponds to a slightly deformed and widened infinite tridymite skeleton, in which, however, no long range order is found. For distances exceeding 6 Å the maxima reflecting long range order disappear (see Fig. 4.7a). A similar structure is found also for vitreous boron oxide, for sodium silicate, lead silicate and borate glasses (see also Fig. 4.7b for a substance with a more exotic composition).

If partially ordered domains of the glass with cristobalite or quartz-like structures are in fact responsible for the mentioned peculiarities in the temperature dependence of the coefficient of refraction, observed upon heating of silicate glasses, then the height of the peaks could give a measure of the percentage of quartz-like structural units in the sample. Such an estimate was performed by Appen, it gave an upper value of only 10^{-4} for the molar fraction of crystalline material actually present in the glass. If one remembers that the size of one of such crystalline domains is of the order 15–20 Å (as found both by the opponents and the followers of the crystallite hypothesis), it follows, that such regions are practically of no significance in determining, e.g., the thermodynamic properties of the glass. They have to be taken into account only if so-called structurally sensitive properties such as the strength of glasses are analyzed (see, e.g., Gutzow (1964) [291]).

The results obtained by Warren and coworkers and similar ones are usually considered as the verification of Zachariasen's structural hypothesis and this is, indeed, to a large extent the case. It seemed that after Warren's *X*-ray investigations silicate glasses cannot be considered any more as an agglomerate of crystallites. On the contrary, it seemed to be proven that the glass is formed by an infinite aperiodic network, for which the average distances between the atoms are near to the respective values for the crystalline phase. However, as it turned out later on, a large number of unresolved problems remained, and in the solution of these problems the crystallite hypothesis in its modified modern versions may be helpful. One of such modifications is schematically illustrated in Fig. 4.8.

Warren himself obtained an *X*-ray intensity curve for a pyrex glass heat-treated at a temperature 430 °C for about 731 days in which one very sharp maximum and

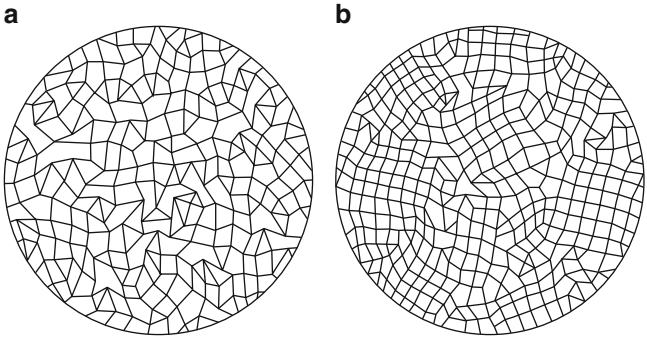

Fig. 4.8 Schematic representation of an amorphous structure based on the Zachariasen-Warren random network model (**a**) and of later reformulations of the crystallite hypothesis (**b**)

a number of additional less expressed maxima could be observed. This result can be interpreted in such a way that in the process of annealing of a glass at relatively high temperatures a process of structural reorganization takes place and the formation of micro-heterogeneities is observed, which are difficult to be interpreted in terms of Zachariasen's theory. Even more interesting are the results of Valenkov and Porai-Koshits (see Porai-Koshits (1955) [641]) on sodium silicate glasses. These experiments showed that during heat treatment of the glass the X-ray patterns are transformed continuously from a form typical for the vitreous state to a curve referring to a crystalline structure.

In Fig. 4.9a, a X-ray intensity curve is shown for a vitreous Na_2SiO_3-sample, the curves (b), (c) and (d) refer to the same sample after 1–3 h of heat treatment at 430 °C, while curve Fig 4.9e refers to the totally devitrified crystalline Na_2SiO_3. The maxima due to crystalline meta-silicate can be seen, which are only indicated slightly in the untempered glass, as well as the approach to X-ray patterns which are typical for the crystalline structure. Thus, on Fig. 4.9 the evolution from the amorphous state via pre-crystalline structural changes – corresponding in some way, may be, to structures and states anticipated by the crystallite hypothesis – is transformed to the crystalline state. Similar experiments were performed also by other investigators with a large number of glasses. The results are equivalent to those mentioned above. They indicate that a continuous change from structures of the type I to type II as given in Fig. 4.9 is possible.

The discussion connected with the random network hypothesis and its relation to the crystallite model of glass structure led to numerous experimental investigations. It can be even said that the broad application of small-angle X-ray scattering methods in glass science originates from the numerous attempts to verify one of the discussed structural hypotheses for silicate glasses. In the further development, different X-ray techniques were directed to the verification of the existence of inhomogeneities both in one- and multi-component glasses (see Porai-Koshits (1989) [641]). It is now confirmed that in dependence on the method of synthesis and thermal history of the samples, inhomogeneities in the density or composition

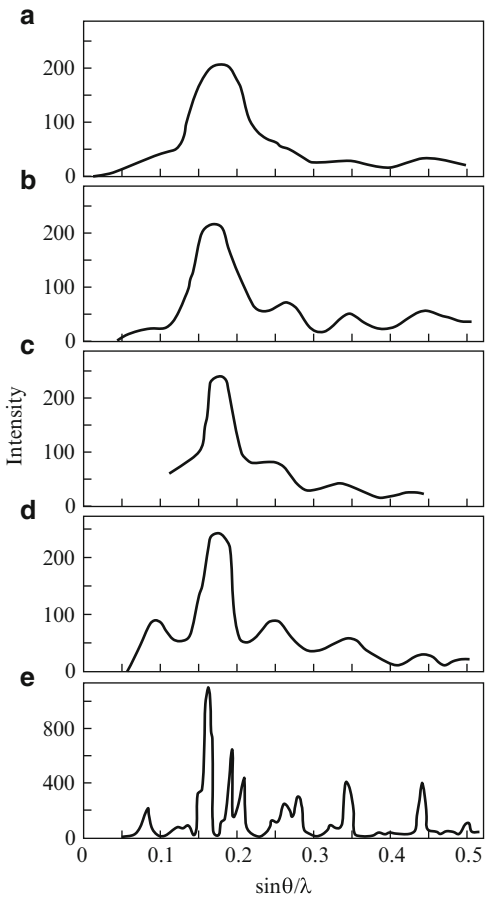

Fig. 4.9 Intensity curves for a sodium silicate glass according to Valenkov and Porai-Koshits (see text): (**a**) original glass; (**b**), (**c**), (**d**) sample heat treated at 430 °C for 1–3 h, (**e**) crystalline sample with the same composition

may be observed, ranging in size from several Å to considerably larger values. In most cases, such inhomogeneities may be interpreted as the result of liquid-liquid phase separation processes in the system.

Of principal importance are the recent results obtained in this respect by a number of Russian investigators (see, again, Porai-Koshits (1989) [641]), demonstrating the existence of density inhomogeneities in glasses of only several Å in size. These inhomogeneities could be explained theoretically as frozen-in homophase density fluctuations in the bulk of the glass sample (see Filipovich (1987) [208]; Porai-Koshits and Golubkov (1979) [642]). However, frozen-in homophase fluctuations and compositional inhomogeneities can hardly by called crystallites in the original sense of the term as introduced by Lebedev.

The outlined results are verified also by another method of structural investigations, i.e. neutron scattering, so that considerable doubts have been accumulated to consider complete randomness as the only paradigm in specifying the structure

of glasses (see, e.g., Gaskell (1992) [241]). As was also pointed by Porai-Koshits, it is impossible to answer the problem of the structure of glasses applying only one or two methods of structural investigations, e.g., X-ray and neutron scattering. For a comprehensive analysis and in order to obtain more or less unambiguous results a large number of different and complementary methods has to be applied. In fact, modern investigations of glasses require a combination of different scattering methods (X-ray, neutron scattering) with other methods of structural investigations like nuclear magnetic resonance (see, e.g., Bray et al. (1960 [102], 1983 [103], 1987 [101]), infrared spectroscopy (Simon and Litke (1960) [761]), optical methods of investigation, electron microscopy, electron magnetic resonance, modern X-ray microprobe studies, calorimetric methods (see, e.g., Hinz (1970) [363]). The critical analysis of the crystallite hypothesis shows that crystallites in the original sense, as anticipated by le Chatelier and Lebedev, were, in general, not found in silicate glasses. They appear only as the result of crystallization treatments, as shown in Fig. 4.9. It is, however, interesting to note that amorphous substances exist, like, e.g., the so-called vitreous carbon (cf. e.g. [794]), synthesized in recent years, which represent examples for systems in which the original ideas of the crystallite hypothesis of glass structure may be fulfilled.

Vitreous carbon is formed in the process of thermal destruction (pyrolysis) of carbon-rich organic compounds in an inert atmosphere at temperatures up to 2000°C. Structural investigations showed that this material can be described as an amorphous structure in which up to several percent of the material is embedded in the amorphous matrix in form of graphite-like crystallites with dimensions up to 70–80 Å. This is an example, how an interesting idea may find an unexpected application.

4.5 The Bernal-Polk Model

Bernal's model was developed originally in order to describe the structure of liquids. However, since glasses according to the already given definition can be considered as frozen-in non-equilibrium systems with a configurational disorder corresponding to an equilibrium structure of the melt at higher temperatures as compared with the actual temperature, this model is applicable also for the discussion of the structure of glasses. Bernal's geometric approach to the description of the structure of liquids is based on the geometry of packing of equally sized spheres. It can be considered as a continuation of the work of Barlow (1898) [37] (see also Wunderlich (1973) [935]), who described the symmetry of crystalline structures in terms of close packing of spheres.

It is known that in hexagonal or face-centered cubic close packing of equally sized spheres the volume occupied by the spheres is about 74 % of the total volume of the system. It means that about 26 % of the volume in such a three-dimensional closest crystalline-like packing is free (see Fig. 4.10a, b). It is to be expected that the packing density of randomly distributed ensembles of equally sized spheres

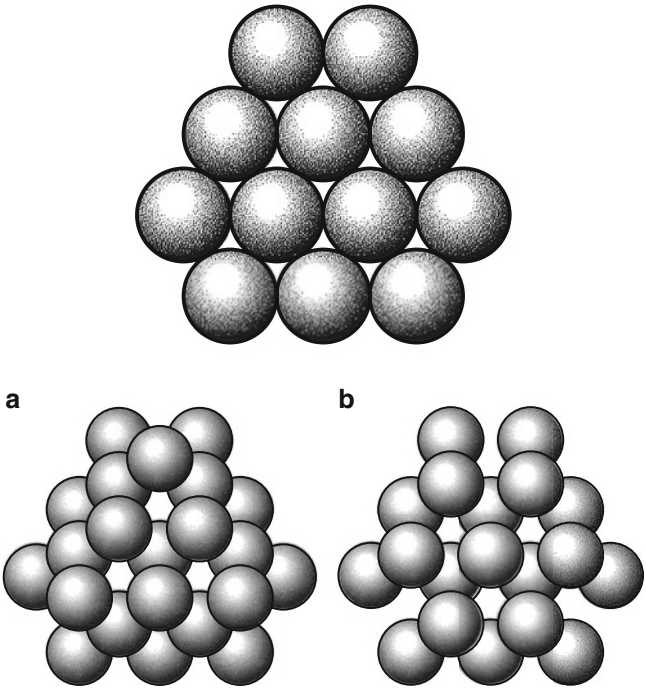

Fig. 4.10 Ensemble of equally-sized spheres in a two-dimensional close packing (*top*) and in three-dimensional (*bottom*) (**a**) cubic and (**b**) hexagonal close packing

should have values lower as compared with the regular crystalline-like arrangement of spheres. Thorough experimental investigations in this respect were performed by Scott (1960) [741], who followed ideas, proposed earlier by Bernal (1959 [72], 1960 [73], 1964 [74]). Scott filled rigid containers of volume V_x with equally-sized steel spheres (ball bearings). By using containers with different volumes and extrapolating the results to $V_x \to \infty$ (or, equivalently, $1/\sqrt[3]{V_x} \to 0$) Scott avoided finite size effects in the determination of the packing densities (see Fig. 4.11).

The free volume for any of the arrangements of the steel spheres was determined by introducing an appropriate liquid (oil) into the container, filled with the ensemble of spheres. Two different shaking procedures were applied generating different configurations of the spheres in the containers. As the result two more or less defined spatial arrangements of the spheres were obtained: the so-called dense random and loose random packing. In the described way it was established that the fraction of the volume occupied by the spheres in the dense random packing equals 0.64, while for the loose random packing a value of 0.61 was found. The difference in the free volumes (in per cent) for the random packing (36 % and 40 %, respectively) and the close regular crystalline-like packing (26 %) is a measure of the increased free volume in a random array of equal spheres. Different shaking procedures in the model experiment can be identified with different temperatures

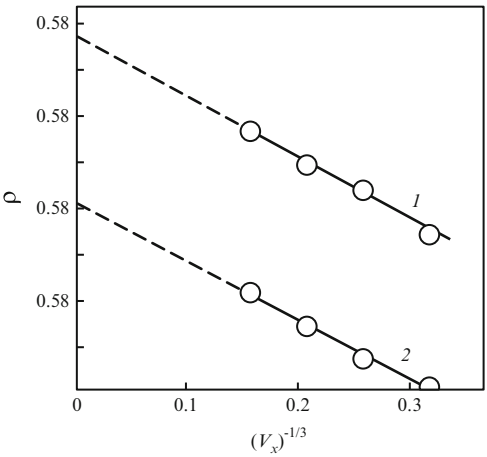

Fig. 4.11 Results of Scott's experiments with containers of volume V_x filled with equally sized spheres. The extrapolation to zero gives the packing density ρ for $V_x \to \infty$: (*1*) dense random packing; (*2*) loose random packing

of the liquid, respectively, with different freezing-in (or fictive) temperatures of the glass (compare Table 2.5). As it was mentioned by Gutzow (1964) [291] and pointed out briefly already in Chap. 2, the two different densities in the random packing of equal spheres observed by Scott correspond, approximately, to packing densities found in real glass-forming systems. For example, glasses of typical network formers (SiO_2, BeF_2) have a free volume higher by 18–20 % than the packing density of the respective crystal. For organic polymers this value equals 10–12 % (see also Simha and Boyer (1962) [753]; Gutzow (1964) [291], (1972) [294]) and here the data given in Table 2.5. These estimates show that Bernal's model may give a key to the understanding of some of the general features concerning the structure of any glass.

The next step in the further development of above discussed geometric ideas was also made by Bernal. It was connected with the analysis of the distribution of free volumes and the coordination numbers in model experiments, again, with random ensembles of equally sized spheres (Bernal (1960) [73]; Bernal and Mason (1960) [75]). Bernal and Mason analyzed the contact numbers sphere to sphere and the distribution of coordination numbers. An analysis was also made of the size distribution of holes in the investigated model random structures. It turned out that in such ensembles, approximately, 18–20 % of the free volume consists of octahedral voids of a size of about 0.2–0.4 R in diameter, where R is the radius of the spheres. The analysis of the experimental results showed further that along with hexagonal coordinations also an increased percentage of pentagonal arrangements of the building units of the randomly arranged model systems (which consisted of non-gluing plastilin spheres) was found. The significance of above mentioned findings consists in the following. If to a liquid, constituted of relatively large nearly spherical atoms, e.g., of metal atoms, 20 atom % of smaller atoms are added fulfilling the above mentioned geometric requirements to fit into the octahedral holes, then a system with a higher packing density and a more stable structure could be formed.

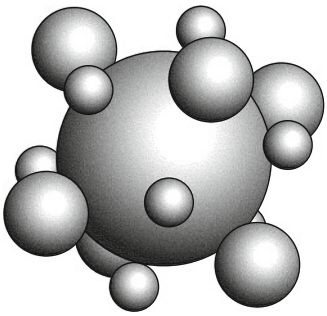

Fig. 4.12 A sphere in a cubic close packing of equally sized spheres surrounded by 6 (8) spheres of different sizes occupying the voids in the structure (Belov (1947) [63]). The figure gives an illustration of the basic idea of the Bernal-Polk model

This consequence from Bernal's model of liquids was drawn by Polk (1970) [638] (Fig. 4.12; see also Sadoc et al. (1973) [679]). It led to the formulation of composition requirements for a possible glass-formation in substances not vitrified so far, in metallic alloy systems (see Cohen and Turnbull (1961) [138]) and to the synthesis of a first generation of metallic alloy glasses. Subsequently, metallic alloy glasses were obtained for Au − Si (Cohen and Turnbull (1961) [138]), Pd − S, Au − Ge − Si, Co − C, Fe − C and other systems (see Giessen and Wagner (1972) [253]). A more detailed description of the properties of metallic alloy glasses and their technical applications as well as further developments in this respect may be found, e.g., in Chen (1977) [131], Luborsky (1983) [516], Güntherodt and Beck (1981) [284].

Different to the hexagonal face-centered packing of spheres discussed so far other crystalline-like arrangements of equally-sized spheres are characterized by lower values of the packing density δ as compared with the already mentioned value $\delta = 0.74$ for the hexagonal close packing. This statement is illustrated by the following summary of packing densities of possible spatial structures of ensembles of spheres of equal size characterized by different coordination numbers, z, and different types of symmetry (see Hilbert and Cohn-Vossen (1932) [356]; Rouse Ball and Coxeter (1961, 1974) [669]; Zhdanov (1961) [956]): (i) hexagonal close packing with a coordination number $z = 12$: $\delta = \pi/(3\sqrt{2}) \approx 0.74$; (ii) tetragonal arrangement with $z = 10$: $\delta = 2\pi/9 \approx 0.70$; (iii) cubic volume centered packing with $z = 8$: $\delta = \pi\sqrt{3}/8 \approx 0.68$; (iv) simple cubic packing with $z = 6$: $\delta = \pi/6 \approx 0.52$; (v) cubic diamond-like packing with $z = 4$: $\delta = \pi\sqrt{3}/16 \approx 0.34$. No model experiments exist to show what the increase of free volume would be for a randomized packing of the crystalline-like structures of lower symmetry (ii)–(v) as compared with the hexagonal close packing. Such types of packing are difficult to realize in model experiments, because the hexagonal close packing is the natural way in which a system of equal spherical structure elements is arranged. The situation is different for systems with directed bonding, as it was demonstrated first by Dietzel and Deeg (1957) [170] in model experiments with floating spheres containing tiny magnets.

However, taking into account the data in Table 2.5, where the results of the packing densities in the vitreous state for substances with different crystal structures are summarized, it seems that for vitrified random structures always an

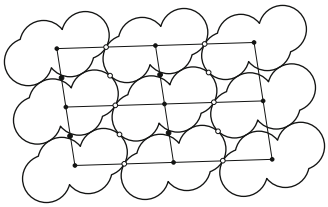

Fig. 4.13 Close packing of molecules with complex shape according to Kitaigorodski (1955) [457]. Note the small fraction of free volume as compared with close packing of equally sized spheres

approximately 15 % higher free volume is frozen-in as compared with the respective regular arrangement. It has also to be mentioned that for packing of spheres or other structural elements of different sizes higher packing densities can be found than the limiting value 0.74 for an ensemble of equal spheres (see, e.g., in this respect Haynes (1975) [350], Barlow (1898) [37] and Wunderlich (1973) [935]). The same conclusion is valid for non-symmetric equally sized molecules (Kitaigorodski (1955) [457] and Fig. 4.13). In these cases packing densities of crystalline-like arrangements up to $\delta \approx 0.9$ may be realized.

Taking into account the conclusions by Polk and his application of the Bernal model to vitrification of metallic alloy systems, it becomes evident that the existence of structural units of different sizes is the origin for the relatively high values of the packing density of metallic alloys as compared with typical glass-forming systems (see, again, Table 2.5). Bernal's approach found an application also in the consideration of the structure of crystalline and vitreous silicates. According to Whittaker (1967) [920] silicates can be considered as an ensemble of nearly close packed O^{2+} ions, where the octahedral voids in between them are filled by silicon cations. Additional ions may be distributed more or less randomly in the structure. According to Whittaker, upon vitrification of molten silicates a random packing of O^{2+} ions is frozen-in in a similar way as in the experiments of Scott (1960) [741].

Independent of the particular application and the special features of Bernal's model a very general conclusion can be drawn from it. In every liquid or solid amorphous structure different types of structural elements may be found even if they are constituted initially of identical primary units. Already for the particular case of an ensemble of non-aggregating equally sized spheres we have to distinguish, for example, between spheres with pentagonal, hexagonal and tetragonal coordinations (see Figs. 4.14 and 4.16).

In Fig. 4.14 a two-dimensional representation of a close packing of equal spheres is shown. When the relative free volume is increased (i.e., the packing density is diminished) pentagonal structural units appear (Fig. 4.14b). From a thermodynamic point of view this result implies that those amorphous structures are preferred which for similar values of energy are characterized by higher values of the entropy. This conclusion verifies to some extent ideas proposed many years before Bernal's considerations by G. Hägg ((1935) [343]; see also Scholze (1965, 1977) [732]). At

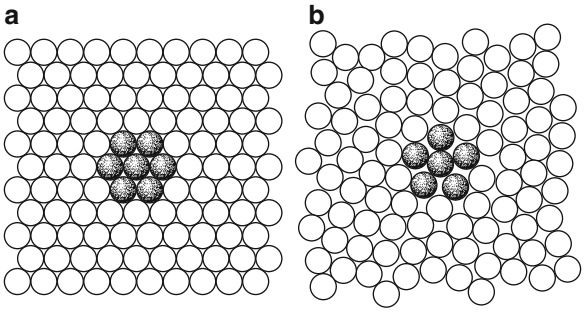

Fig. 4.14 Random packing of equal spheres according to Bernal: (**a**) Crystalline-like close packing: Only hexagonal symmetry connected with a coordination number 6 in a two-dimensional representation is observed; (**b**) Evolution of structural elements with a coordination number 5 and pentagonal symmetry in a random close packing

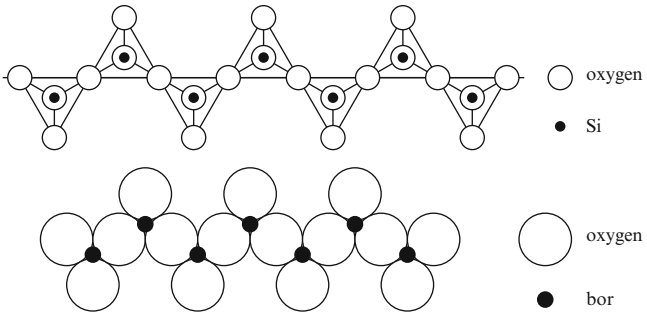

Fig. 4.15 Possible types of chains in oxide glasses (According to Hägg)

part in contradiction to Zachariasen's approach and partially in verification of his ideas Hägg suggested that only those structures tend to form a glass, in which a tendency to aggregation is found or to the formation of polymer-like uni-, two- or three-dimensional networks exists resulting in the formation of different structural units (see Fig. 4.15 as an illustration of possible types of linear anionic structure elements in inorganic glasses).

Similar proposals have been made also by a number of other investigators. Here, in particular, Berger (1930) [68] and Botvinkin (1938) [94] have to be mentioned. Many years ago, Botvinkin, for example, even developed a semi-quantitative theory of vitrification starting with the basic idea of a temperature dependent degree of polymerization (or aggregation) of the primary monomeric building units of the melt. According to Botvinkin's approach the process of vitrification is connected with the completion of the polymerization process, i.e., T_g corresponds to the particular state of the substance where the degree of polymerization reaches infinity. Taking into account the results given in Chaps. 2 and 3 (in particular, the Bartenev-Ritland equation) such an approach cannot be accepted, since it would imply that vitrification has to occur always at one and the same temperature. Nevertheless,

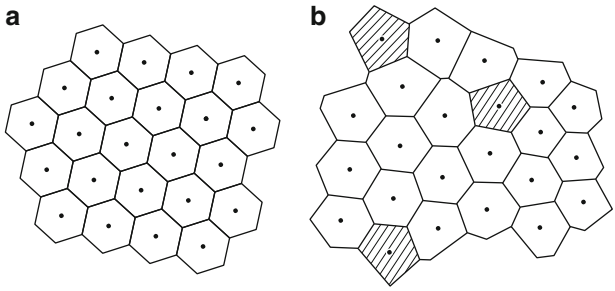

Fig. 4.16 Illustration of Voronoi polyhedra describing the structure of glasses: (**a**) Regular polyhedra forming a crystalline structure; (**b**) Structure of a two-dimensional liquid modeled by distorted regular polyhedra (Voronoi polyhedra). Note the appearance of pentagons in addition to hexagons

Botvinkin's basic idea has been fruitful in developing a number of present day models of vitrification.

Similar ideas that glasses are most easily formed, when structurally different polymorphic modifications are produced by aggregation or polymerization have been also been expressed in later times in a more or less qualitative way by Goodman (1975) [264] and Cahn (1975, 1983) [116,117]. The conclusion that aggregation and polymerization processes are of great importance in the thermodynamics of most of the glass-forming melts is verified by statistical-mechanical model considerations of glass-forming substances (see Chap. 5).

4.6 Further Developments: Voronoi Polyhedra, Polymerization and Aggregation

Crystalline structures can be described as a regular arrangement of identical polyhedra in space. In a modification of this idea to liquids and glasses, Bernal and Finney suggested to describe the structure of simple liquids by filling the space with so-called Voronoi polyhedra (Finney and Bernal (1967) [209]; Finney (1977) [210]). Voronoi polyhedra are a generalization of the classical regular polyhedra. They represent irregularly distorted polyhedra of different types. A schematic two-dimensional illustration of the possibility of describing regular and irregular structures by using polyhedra of different types is given in Fig. 4.16.

Of particular importance for portraying the structure of simple liquids are, according to Bernal, pentagonal structural elements. This idea that pentagonal structural elements prevail in simple liquids, was used in order to construct amorphous structures by a system of neighboring pentagons. More generally noncrystalline cluster models have been developed based on the idea that noncrystallographic growth patterns of clusters may exist with tetrahedral, pentagonal and icosahedral

symmetries, which are more stable than fcc-crystallites with the same number of atoms (Hoare and Pal (1971) [371]; Hoare (1976) [369]). Such high-density (low energy) clusters may be expected to evolve under certain conditions preferably but they cannot be extended infinitely.

In more recent publications (see Hoare and Barker (1977) [370]; Gaskall et al. (1977) [242] and Gupta and Cooper (1992) [285]) different variants of construction of amorphous structures by using distorted polytops are given together with the advantages and limitations of this method. Another of Bernal's previously mentioned ideas, namely that structural units of different sizes are a necessary prerequisite for an understanding of the structure of liquids and glasses, was formulated earlier in a qualitative form by Fajans ((1949) [194]; see also Scholze (1965, 1977) [732]; Thilo et al. (1964) [832]; Vogel (1979) [889]) for the development of a model of the structure of a group of exotic binary glass-forming systems (alkali and earth alkali nitrate glasses).

It is known that none of the alkali or earth alkali nitrates forms a one-component glass at standard cooling rates. However, binary mixtures of alkali and earth alkali oxides are typical glass-forming systems and are easily vitrified into stable glasses. Fajans explained this increased glass-forming ability of binary systems assuming that in a mixture of alkali and earth alkali nitrates the large alkali cations are deformed by the interaction with the small higher charged earth alkali cations. Similar explanations have also been developed in attempts to understand glass-formation in other exotic systems like binary melts of AgJ and CsJ, where, again, due to the existence of the large deformable Cs-cations and of the small Ag-cations irregular structures may be formed (Nishii et al. (1985) [604]). This exotic system is the representative of a new family of halide glasses which is expected to lead to a new generation of optical wave guides (Hu et al. (1983) [382]; Lucas (1989) [519]). Variations of the idea that distinct structural units with five-fold symmetry may play a decisive role in forming the structure of liquids were also developed by Frank (1952) [228] and Tilton (1957) [836], who used an icosahedra model.

In inorganic glass-forming systems typical polymer structures have been found, in particular, in meta-phosphates and borates. Due to the property of boron to establish bonds with three oxygen atoms in the formation of boric acids in borates networks of the composition $n[BO_2]$ evolve. These networks are formed by the anions $n[BO_2]^{2-}$, where in between the B- and O-atoms partly covalent bonds are established (see Figs. 4.1b, c and 4.15). A similar anionic polymer-like structure is also developed in alkali meta-phosphates, in calcium meta-phosphate and other earth-alkali phosphates. It is assumed, that the existence of anionic chains with a low mobility is the origin for the large viscosity of borate melts and their ability to vitrify easily. It has been also pointed out that a tendency for glass-formation and higher viscosities is shown only by those inorganic melts in which the formation of anionic chain structures is possible. Besides the already mentioned cases further interesting examples are pentafluorides and platinum-halides (Wells (1975) [915]; Gutzow et al. (1990) [331]). The formation of cyclic structural units is also a typical feature of inorganic glass-forming melts (e.g., S_8, Se_6, $Na_3[P_3O_9]$ etc.). According

to the already mentioned hypothesis by Hägg aggregation and formation of complex structural units is a prerequisite for glass-formation.

When applying this idea to silicate melts, it has to be taken into account that the properties of the ionic structural elements in silicates depend on the relative ratio Si : O in the composition of the melt. If this ratio equals 0.25, then isolated tetrahedra of orthosilicate type dominate. Linear $n[SiO_3]_2^-$-chains develop if the ratio Si : O equals 0.33; for larger values of this ratio two-dimensional layers develop. Consequently, it is to be expected and in fact verified by experiments that in silicate melts of intermediate composition intermediate forms of the mentioned structures are also present. In considering the ability of a melt to form larger structural units and to be vitrified to a glass, the type of bonding and the type of aggregation of the elementary units of which the system is composed of has to be taken into account.

As already mentioned for typical oxide glass-formers the bonds between the positively charged atoms and the oxygen ions are only 40–50 % ionic. The increase in the ratio of covalent bonding contributes significantly to the relative stability of complex anions in the melt and, thus, in the respective glass. For organic high polymers the C − C-bonding energy is 10–15 % ionic and 85–90 % covalent. This property explains the increased stability of polymer structures in these organic substances compared with inorganic glasses.

In water soluble phosphate glasses the polymeric structural elements are so stable that they can be detected by paper chromatography after dissolution of the glasses in appropriate aqueous solvents. Paper chromatography of condensed phosphates was developed to a high level of perfection by Thilo and Grunze (1953) [280] and many other investigators in the 1960s. For a summary of earlier results in this field see the monograph of van Wazer (1958) [882]. In this sense alkali phosphate glasses of meta-phosphate and more alkaline composition allowed one the first direct proof for the existence of linear anionic chains of the type

$$(O - \underset{\underset{O}{\|}}{P} - O - \underset{\underset{O}{\|}}{P} - \ldots)_n$$

in glasses (Westmann and Crowther (1954) [917]; Grunze and Thilo (1953) [280]; for its size-distributions see Jost (1962) [413]; Jost and Wodtcke (1962) [414]). In the so-called Graham's glass $(NaPO_3)_x$ anionic chains with a degree of polymerization of up to 300 PO_4 structural units have been found. The relatively high stability of phosphate anionic complexes in aqueous solutions also permitted the application of other chemical and physico-chemical methods of analysis, well-known from organic polymer physics and chemistry (end-group titration, centrifugation).

The existence of polymeric structures in the less soluble alkali earth-phosphate glasses was also proven mainly by paper chromatography (see Schulz and Hinz (1953) [740]; Abbe et al. (1974, 1976) [1, 2]) by using more aggressive solvents than water (e.g., aqueous solutions of acetic acid). In a series of papers Goetz et al. (1972 [259], 1977 [260]) developed a method for dissolution and chromatography of silicates using appropriate solvents. As a result of these investigations anionic

chains in metasilicates were also detected and the distribution functions for anionic structural elements were established.

In addition to the mentioned optical and infrared investigations other methods of verification of the existence of polymer-like structures have also been used. One of such methods was proposed by Tarassov (1945, 1946, 1956) [824, 825]. Tarassov calculated the spectrum of vibrations of solids consisting of linear chains or two-dimensional network structures. He came to the conclusion that for low temperatures ($T \rightarrow 0$) the specific heat C_p of a solid with such an unisodesmic structure should behave like

$$C_p \sim T \qquad \text{(for linear chains)} \tag{4.2}$$

$$C_p \sim T^2 \qquad \text{(for two-dimensional networks)} . \tag{4.3}$$

These dependencies differ from the well-known expression obtained by Debye ($C_p \sim T^3$) for three-dimensional isodesmic network structures. The indirect proof of the existence of linear chains in the sample, proposed by Tarassov, is based on the measurement of the temperature dependence of the specific heat. If a linear dependence of the form given by Eq. (4.2) is found, then this result is to be interpreted in the sense that the sample is composed to a large extent of linear chains or chain-like aggregates. Numerous investigations carried out by Tarassov and coworkers showed that in all glasses of the type B_2O_3, SiO_2, As_2O_3, Sb_2O_3 and, in particular, in meta-borates, meta-phosphates and meta-silicates a high percentage of anionic structural units are aggregated in chain-like elements. Such chains were also found in elemental glasses like Se, in glasses of the composition Se – Te and in many other systems.

For the description of the structure of Na_2SiO_3-glasses, Tarassov proposed a scheme as presented in Fig. 4.17. If the alkaline character of the meta-silicate glass is increased, then the length of the chains decreases. If, vice versa, the percentage of SiO_2 introduced into the melt is increased, the chains become connected by bridges.

Of particular interest are also the investigations of the crystalline and amorphous forms of selenium (Krebs (1958) [484]; Richter (1972) [664]; Wells (1975) [915]). While two of the crystalline modifications of selenium consist of cyclic Se_8 molecules, the hexagonal metallic form of this element is constituted of infinite helical –Se – Se – Se–chains. X-ray and neutron scattering analysis show that vitreous selenium contains the same helical chains as the metallic form of the substance together with cyclic structural elements consisting of six to eight selenium atoms. The relative percentage of occurrence of the mentioned structural elements depends on temperature and on the way the vitreous sample is produced. Similarly, X-ray investigations of alkaline B_2O_3-glasses and melts allow one the conclusion that, both in the melt and in the glass, planar chains are formed.

The evidence summarized above is of importance for the understanding of the structure of glasses and, in particular, also for the description of the kinetics of devitrification. Two limiting cases of this process may be distinguished, called

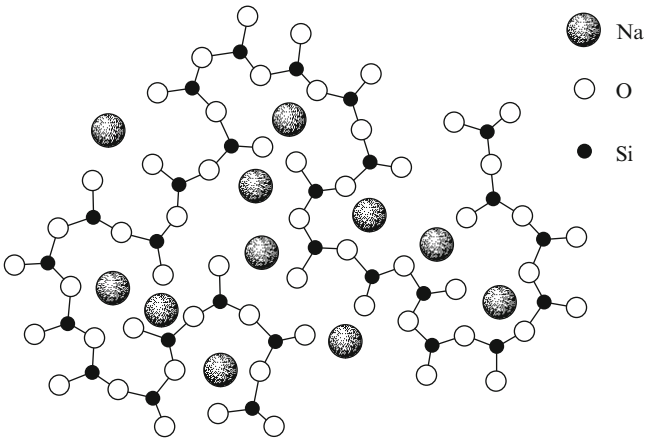

Fig. 4.17 Structure of $NaSiO_3$ according to Tarassov (see text): Note the similarity between the models of the structure shown here and in Fig. 4.6. However, in the present figure the structure is formed by one infinite chain

non-reconstructive and reconstructive crystallization. These two different mechanisms of devitrification are characterized by:

- Non-reconstructive: reorganization and ordering of structural elements already existing in the melts,
- Reconstructive: devitrification, preceded by processes of molecular reconstruction, i.e., by the formation of the basic elements of the crystalline structure, which are absent (or present only in a limited amount) in the initial melt.

The kinetics of devitrification depends significantly upon the particular mechanism involved in the considered process. A more detailed description of the devitrification kinetics of glasses is given in Chaps. 6 and 7.

4.7 Homogeneous Versus Heterogeneous Models for the Structure of Glasses

In the foregoing discussion concerning the structure of glasses, the question was posed as to whether multi-component glasses should be considered as intrinsically homogeneous or as heterogeneous systems. According to Zachariasen's model in two- or more-component silicate glasses the distribution of cations and anions is of random character. This assumption leads to the consequence that macroscopic regions do not exist in glasses enriched in the composition by some of the components. However, *X*-ray investigations of the structure of alkali-silicate glasses led to a different conclusion. According to these investigations, in most cases, domains in the glass sample exist with an increased content of SiO_2, while in

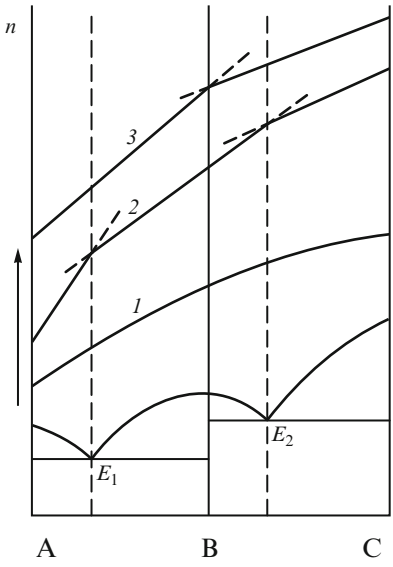

Fig. 4.18 Possible types of dependencies property n versus composition according to Demkina (1958) [163] (see text)

other parts alkali oxides prevail. For a summary of results in this respect see the already mentioned monographs by Vogel (1979) [889], Scholze (1965, 1977) [732] and Feltz (1983) [202]. Of particular interest in this respect are investigations of Na_2O/SiO_2-glasses, for which it was observed that domains with compositions are formed which are expected to occur for the given boundary conditions according to the equilibrium phase diagram. Dietzel (1949) [166] (see Scholze (1965, 1977) [732]) suggested that such behavior is always to be expected for any multi-component glass.

A similar structural micro-heterogeneity was assumed from the very beginning in the crystallite hypothesis of silicate glass structure. Consequently, in the discussion of the merits and disadvantages of the crystallite hypothesis the related problem was also analyzed, namely what the effect of the assumed micro-heterogeneity on the macroscopic properties of multi-component glasses would be. Knowing the significance of such effects, it should be possible to decide which of the proposed models of glass structure is more correct. Let us assume, for example that we have two glass-forming oxides A and C, which may form some chemical compound B of a definite composition. In Fig. 4.18 the lowest curve shows a possible equilibrium phase diagram of such a binary system with two eutectic points E_1 and E_2. If Zachariasen's approach to glass structure and its properties is correct then the dependence property vs. composition should be of the type as given by curve 1. If, however, in the glass sample aggregation complexes of a definite composition are formed resulting in some heterogeneity in the structure of the glass, then a salient point in the curves property, (n), versus composition is to be expected, at least, at some singular points in the phase diagram.

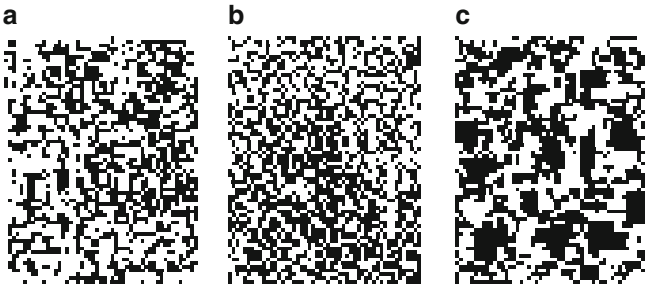

Fig. 4.19 Micro-heterogeneities in glasses modeled by distributions of black and white squares according to a classical picture given by Laves: (**a**) system with a relatively slight aggregation of white squares, (**b**) statistical random distribution, (**c**) pronounced clustering (See Vogel (1979) [889])

Some authors, for example Evstropyev, expected that such a change in the properties occurs at the composition B (curve 3 in Fig. 4.18), corresponding to the formation of B-compounds while other authors who also preferred the crystallite theory of glass structure (Kumanin, Demkina), in agreement with Botvinkin (1938) [94] expected a behavior of the type shown with the broken line (2) in the same Fig. 4.18, i.e., a discontinuous change in the properties at the eutectic points E_1 and E_2. Experimental results and a thorough discussion of related topics may be found in the monograph by Demkina (1958) [163].

The question concerning the most probable form of the property versus composition curves for glasses is not only of theoretical interest in giving criteria for the proper choice of the correct model of glass structure but also of technological significance. However, it is difficult to decide experimentally, which of the discussed dependencies is the correct one. This is due to the fact that the expected effects involved are small compared with the scattering of data in the experimental determination of the properties of the glass. From a practical point of view it is often more convenient to describe the property versus composition dependence by one continuous curve of the type (1). Thus, measurements of the discussed type cannot give a conclusive answer to the question which of the proposed models has to be preferred. On the other hand, cases are also known, when the inhomogeneity is expressed to such a degree that it is possible to assume two different micro-phases as constituting the glass.

An example in this respect are borosilicate glasses. In such glasses one of the micro-phases, the borate phase, may be removed by dissolution. The SiO_2-matrix remaining after such a process forms then a porous structure which may be transformed by heat treatment into the SiO_2-rich vycor glass. In some cases the regions of inhomogeneity may reach such a size ($\sim$ 600 Å) that they are just below the limits where an optical darkening is found. In other cases, these regions are too small to reach the limits of detectability for the applied method ($\sim$ 20 Å) (see also Figs. 4.19 and 4.20). In some glasses, such micro-heterogeneities are not found at all. The development of micro-heterogeneities in multi-component glasses

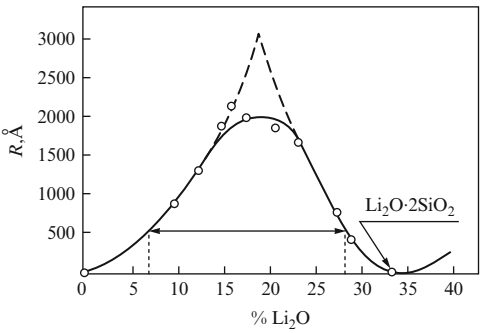

Fig. 4.20 Dependence of the average size of micro-segregation complexes formed in an inorganic glass-forming system (in Li_2O/SiO_2-glasses) on composition. The optically detectable region of immiscibility is indicated by the horizontal bar (Vogel (1979) [889])

on heat treatment is usually connected with the process of liquid-liquid micro-phase separation and is discussed here in more detail later. The problems of liquid-liquid immiscibility in glasses have been analyzed mainly for silicate glasses but phase separation processes have been also found in chalcogenide and metallic glass-forming systems.

4.8 Superstructure of Real Glasses

It has been established experimentally that the mechanical strength of crystalline materials is significantly lower than the theoretical predictions derived from the energy of the molecular bonds. A similar situation is also found for glasses, where the ratio between the measured and the theoretically determined values of the mechanical strength is of the order 1 : 20 (Stanworth (1950) [793]).

The experiments for the determination of the mechanical strength of NaCl single crystals in saturated NaCl aqueous solutions carried out by Yoffe showed that the decrease of the mechanical strength of solids is connected with microcracks at the surface of the samples. Such microcracks (or Griffith's cracks) were proven to exist for different systems, including glasses. It was shown that the increase in the mechanical strength of glass fibers with a decrease in their radius observed experimentally is connected with the decrease in the number of surface cracks (Bartenev (1984) [46]). This is also the reason why fibers leached with fluoride acid, a process for removing the defective surface layer of the glass, have a higher strength. It is also known that coating the surface of the glass fibers with hydrophobic materials preserves the initial relatively high strength for a long time (the formation of surface cracks due to atmospheric influences is considerably reduced).

It was also expected by some authors that in addition to the existence of surface cracks, the whole volume of the glass sample contains cracks and inhomogeneities (see Schischakov (1954) [687]). It was supposed, e.g. that similarly to crystalline solids some mosaic-like structure may be found in glasses. In this direction, Smekal

developed the idea that silicate glasses may be composed of individual grains. This proposal is equivalent to the assumption of a system of cracks in the bulk of the vitreous sample. Smekal estimated that the average size of such grains should be about 0.1 μm.

Opinions were also expressed that the existence of such cracks is the reason for the permeability of glasses to gases, in particular, to noble gases (see, for example, also the data collected in the monograph by Slavianski (1958) [772]). There exist, in fact, experimental results (see Schischakov (1954) [687]) indicating that silicate glasses in contact with aqueous solutions form SiO_2-rich colloidal silica suspensions with particle sizes of the order 10^{-3} to 10^{-5} cm. It has to be mentioned, however that for most of above discussed effects, alternative explanations can be given. Consequently, the existence of a grain-like superstructure of silicate glasses is a question open to discussion. The only well-established result is the decrease in the strength of the glass caused by surface cracks.

4.9 Structure of Organic High-Polymer Glasses

Organic glass-forming melts were the first models used by Tammann and his coworkers in order to demonstrate the nature of vitrification and to study the properties of glasses. Tammann used low melting organic molecular substances such as salicine, piperine, glycose and natural resins like colophony, shellac etc. His approach to the investigation of the vitreous state was followed by other investigators in this field (see, e.g., Parks (1925) [623]; Parks and Huffman (1927)) using similar substances as the subjects of investigation. Some of these substances, in particular glycerol, served as the model for which, for the first time, the variations of the thermodynamic functions upon vitrification were analyzed in detail (see Chap. 2). In more recent investigations, again, organic glass-forming systems were studied in order to understand the process of vitrification and the specific rheological properties of glasses and glass-forming melts (see, e.g., Ubbelohde (1965) [871]).

A first review of the thermodynamic properties of organic glasses was given by Kauzmann (1948) [440]; later results were summarized by Wunderlich (1960) [934] (for C_p) and by Privalko (1980) [650] (entropy measurements). Results on the mechanical properties of organic model glasses were reviewed by Eitel, Pirani, and Scheel (1932) [186]. Tammann's own results were summarized in his monograph (1933) [818]. In the course of further experimental investigations it was proven that, as a rule, aggregation and polymerization processes take place in the melt of organic glass-forming substances. A review of this topic was given in Kobeko's book (1952) [461].

Glass-forming organic high-polymer melts and the glasses formed from them were also subjected to intensive studies (for reviews see the monographs by Wunderlich (1973, 1976, 1980) [935]; Keinath, Miller, and Rieke (1985) [442]; Mandelkern (1964) [528]; Großberg and Chochlov (1989) [277]). As the result of polymerization and poly-condensation processes a distribution of macromolecules

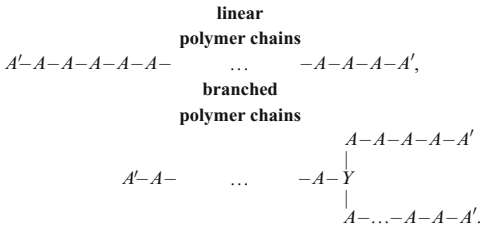

Fig. 4.21 Two possible types of polymers chains: linear and branched polymers

develops in such systems, the mean degree of polymerization reaching values of the order $n \sim 10^5$ and the molecular mass 10^6. The kinetics of polymerization processes and the nature of the resulting chain distributions in organic high polymers were investigated from the very beginning of polymer chemistry (see, e.g., Flory (1936, 1943) [215, 218]; Schulz (1936,1937,1940) [737]). The methods developed for organic polymers were applied later also to the analysis of anion polymerization in phosphates (Jost (1962) [414]; Jost and Wodtcke (1962) [413])) and silicates. For a review of the methods and results in this field see Balta and Balta (1976) [35].

In physical chemistry of polymerization one may distinguish between linear and branched polymers. Examples in this respect are shown in Fig. 4.21. Here A is some segment of the chain, while by A' an end group of the chain is denoted. Furthermore, between two or more polymer chains bridges may be formed, which result in a strengthening of the polymer structure. A classical example in this respect is the vulcanization of rubber. In rubber the strengthening is due to the formation of cross links between the chains. Cross linking may reach such an extent that it becomes possible to speak of trimeric cross-linked polymers.

The application of thermodynamics and statistical physics to polymer melts requires the solution of a very difficult problem. In considering the structure of low molecular substances the knowledge of the topological order, e.g., described in terms of Bernal's model, is more or less sufficient for a characterization of the system under investigation. Similarly, for systems with non-spherical building units (compare Fig. 4.13) in addition to the way of ordering of the centers of the primary building units, their mutual orientation has to be specified. However, for polymers the length of the polymer chains becomes so large that the conformation of the molecule itself is the subject of a separate statistical-mechanical treatment, the conformational statistics of polymer molecules.

The conformational statistics of linear polymer chains was developed mainly in the framework of the Flory-Huggins lattice models (see Flory (1943) [218]; Stewart (1953, 1955) [801]; Gibbs (1960) [250]; Milchev and Gutzow (1981) [560]). In addition to the conformational properties of polymer molecules their ability to allow one a more or less free rotation around the C − C-bonds is of importance. In this way, the conformations of organic chain molecules depend on the flexibility of the C − C-chains in the substance under investigation. For polymer chains with nearly perfect flexibility, chain folding of the molecules themselves and formation of links between them determine to a large extent the thermodynamic properties and the

rheology of the system. Chain folding is also of particular significance in deriving specific models for nucleation and crystal growth in organic polymer glass-forming systems.

In comparing inorganic polymer glass-forming substances with typical organic polymer glass-formers two significant differences have to be mentioned:

- In most cases the stiffness of the inorganic chains like $-Se-Se-Se-$, $-Te-Te-Te-$ or $-P-O-P-O-P-$ is much higher than that for organic polymers.
- The average degrees of polymerization in inorganic systems are restricted usually to an order $\bar{x} < 100$; in polymer chemistry such degrees of polymerization are considered as relatively low ones and are called oligomeric systems.

An analysis of the structure of polymers based on statistical-mechanical methods shows that the most stable configuration of the flexible polymer molecule in solution consists of a particular coil-like structure (see, e.g., the analysis given by Flory (1943) [218] or by Bueche (1962) [109]). Moreover, based on the above mentioned model considerations, properties may be explained resulting from the existence of long chains in the sample. One example in this respect is the super-elasticity found, e.g., in rubber and other elastomers.

Comparing the summary of results concerning the structure of organic high-polymers with the discussion given in the preceding section, it is evident that analogies exist with respect to the basic mechanisms of structure formation. In particular, this refers to the possibility of formation of long chains of the repeatable structural units. For inorganic glasses the chains are usually of anionic nature. In such glasses, cross links are intermediated by earth alkali and other bivalent cations. The existence of such cross-links connected with the significantly reduced ability of a free rotation around the Si – O – Si or P – O – P-bonds results in a considerably more strengthened and inelastic structure, although the basic structural elements in organic and inorganic polymers are similar. These differences are, of course, of gradual character and may be diminished by a variation of the external constraints. For example, even for typical inorganic high polymers at low temperatures the rotation around the $-C-C-$bonds is significantly reduced (e.g., at low temperatures rubber can be obtained as a solid). On the other hand, inorganic glasses exist which show similarities in structure and properties to rubber-like polymers (inorganic glass-forming elastomers like polynitrilchloride).

An intermediate position between both types of chains discussed – linear and branched chains – as elements of the structure of glasses are taken up by aggregation complexes. Aggregation complexes are formed in under-cooled melts and detected in glasses of low-molecular organic substances like, e.g., the alcohols and glucose. In the process of under-cooling of the melt in such liquids more or less stable aggregates are formed. The bonds between the different structural elements are hydrogen bonds. To some extent such additional polymerization also has to be considered in organic polymer chains (“living chains”). It is interesting to remember, in this connection, the aggregation theory developed by Botvinkin (1938) [94]. It seems likely that the prerequisites underlying Botvinkin’s theory are fulfilled, may be to a large extent, in the cases discussed above.

Continuing the discussion of similarities and differences in the structure of organic and inorganic glasses, it is also of interest that for glasses stabilized by hydrogen bonds, the ratio of such bonds below T_g does not change (Volkenstein (1955) [891]). This particular example shows that below T_g not only topological changes but also all types of structural reorganization processes connected with chemical reactions are frozen-in. The stability of anionic chains in inorganic glass-forming melts can vary to a large degree. Probably, such chains are most stable in the previously discussed phosphate glasses since the anions remain as individual units even in aqueous solutions and separated from the cations. Organic polymer molecules exist separately and remain stable in solution. However, there are also cases for which the solution is connected with a dissociation, in such cases, the solution is to be considered to be a polyelectrolyte.

Basically, as was underlined by Thilo (1955, 1958) [829–831], a strong division between polymeric and non-polymeric anions cannot be made. For example, even the anion $[SO4]_2^-$ can be considered with some right as a polymeric anion, although it is classified usually into the group of inorganic complexes. In the process of poly-condensation and polymerization molecules with different molecular masses and different degrees of condensation or polymerization are formed. Hereby, it turns out that the degree of polymerization and the effective length of the chains is determined by size-distributions similar to those derived by Flory (1943) [218] and Schulz (1936, 1937, 1940) ([737]; see also Gutzow (1964) [291]). From these size distributions, a mean degree of poly-condensation (or polymerization) may be calculated. It seems probable (see, e.g., Goodman (1975, 1977) [264,265] and Hägg (1935) [343]) that for the realization of the vitreous state, the existence of molecules with different sizes is required as a necessary precondition. This preposition is founded on the idea that the formation of a regular crystalline structure from elements of different sizes is hardly realizable.

Of importance for the possibility of transformation of a given melt into the vitreous state is obviously also the length of the chains. For sufficiently large molecules, a folding or formation of coil-like structures is to be expected, which inhibits crystallization. In general, steric factors of a very different nature may be of significant importance for the possibility of obtaining a substance as a glass (see also Eldrigde et al. (1993) [189]). It is known, for example that non-linear isomers of a compound can be under-cooled more easily than the respective normal linear polymers (see Kobeko (1952) [461]). On one hand, such steric factors diminish the mobility of the molecules, on the other hand, with the increase of the complexity of molecular configurations its stability in the under-cooled melt and the vitreous state is facilitated: the entropy in the free energy expression is increased.

For some inorganic polymer systems the analogies to organic polymers with respect to the structure are striking. One example of such a case is plastic sulfur $-S-S-S-S-S-$ with the structural unit $-S-$. From PCl_5 and NH_4Cl the already mentioned poly-nitrile polymers with rubber-like properties may be synthesized, described by the structural formula

$$[\ldots - \underset{\underset{Cl}{|}}{\overset{\overset{Cl}{|}}{P}} = N - \ldots]_n$$

Also of interest is the process of crystallization of high-polymers. Typical organic polymers are easily under-cooled. The mechanism of crystallization for such classes of substances consists either of the parallel arrangement of parts of the chains to each other (theory of Gerngross et al. (1930) [248]) or in the formation of a chain-folded structure. Both mechanisms are discussed in details in Chap. 6.

Here we would like to mention only that in both cases one and the same molecule takes part at the same time in the formation of the regular as well as of the irregular amorphous structure (see also Kobeko (1952) [461]; Geil (1965) [247]; Wunderlich (1973) [935]; Price (1969) [646] and Hoffman (1968) [379]). A more realistic chain-folding mechanism of crystallization of organic polymer substances was proposed by Keller (1957, 1959) [443, 444] and Fischer (1957) [211]. In Keller's theory it is supposed that the regular folding of the polymer chains have a length determined by the supersaturation and thus by temperature.

4.10 Reconstructive and Non-Reconstructive Crystallization

For under-cooled melts of simple substances the crystal has the same molecular structure and composition as the melt and crystallization can be considered as a purely physical process. However, the preceding discussion has revealed that in many cases, the melt and the crystalline phase may be constituted of different structural units. It seems that this is the case in most of the phosphate and silicate glass-forming systems in which the melt (and the glass) are formed of a variety of different anionic structural elements which have to be transformed upon devitrification into the building units corresponding to the respective crystalline phase.

In Figs. 4.22 and 4.23 based on paper chromatography experiments, the transformations are shown taking place in the melt upon devitrification in a well-known model glass, Graham's glass $(NaPO_3)_x$, and a sodium phosphate glass of another more alkaline composition ($Na_8P_6O_{19}$) (Gutzow (1979) [302]). For Graham's glass, the melt and the glass are constituted mainly of chain anions $-PO-PO-$ with an average degree of polymerization of the order 100 and by approximately 10 % cyclic phosphate anions, trimetaphosphate (P_3O_9) and tetrametaphosphate (P_4O_{12}) anions. Upon devitrification the orthorhombic $\alpha-NaPO_3$ is formed, constituted of benzene-like anions (P_3O_9). This is a classical example of reconstructive crystallization of anionic chains, which was investigated in great detail (Gutzow (1962, 1979) [289, 302]).

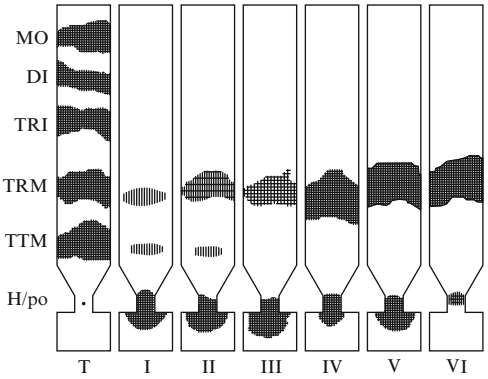

Fig. 4.22 Change of anionic composition of $NaPO_3$-glass semolina samples with an average size of the particles from 0.75 to 1 mm during heat treatment at 320 °C as revealed by paper chromatography: (*T*): Chromatogram with the reference substance; (*I*): Initial glass; (*II*): Sample after 20 min of heat treatment; (*III*): Sample after 80 min of heat treatment; (*IV*): Sample after 145 min of heat treatment; (*V*): Sample after 200 min of heat treatment; (*VI*): Sample after 360 min of heat treatment. The reference substances are: Mo: monophosphate anion; Di: diphosphate; TRI: triphosphate; TRM: trimetaphosphate; TTM: tetrametaphosphate; H/po: high polymer. Out of the initial melt, constituted of high-polymeric and trimetaphosphate anions (P_3O_9), crystalline $\alpha - NaPO_3$ is formed, comprising $Na_3[P_3O_9]$-complexes, only

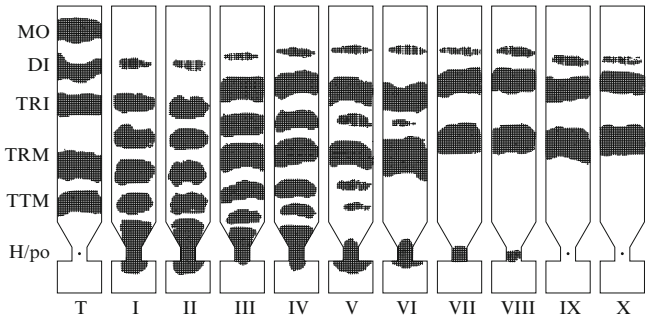

Fig. 4.23 Filter paper chromatograms of hexaphosphate glass ($Na_8P_6O_{19}$) semolina samples with an average size of the particles ranging from 0.75 to 1 mm after different times of heat treatment at 330 °C: (*T*): Reference substance; (*I*): Initial glass; (*II*): Sample after 20 min of heat treatment; (*III*): Sample after 40 min of heat treatment; (*IV*): Sample after 60 min of heat treatment; (*V*): Sample after 80 min of heat treatment; (*VI*): Sample after 140 min of heat treatment; (*VII*): Sample after 160 min of heat treatment; (*VIII*): Sample after 180 min of heat treatment; (*IX*): Sample after 200 min of heat treatment; (*X*): Sample after 360 min of heat treatment; (*I–III*): Formation of linear $Na_3P_3O_{10}$; (*IV–VIII*): Formation of cyclic $Na_3(P_3O_9)$; (*IX*), (*X*): Complete crystallization

In the sodium metaphosphate glass and the corresponding melts, a distribution of anion oligomers exists which may be transformed into two crystalline structures, either the linear ($NaPO_3$, Kuroll's salt) or the cyclic ($Na_3[P_3O_9]$). In glasses with a composition of pyrophosphates of bivalent metals a distribution of different ions is

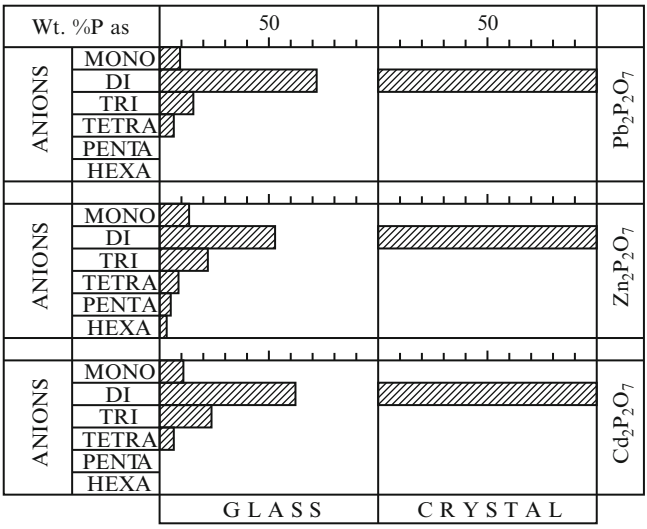

Fig. 4.24 Anionic composition of pyrophosphates of bivalent metals (as glasses and as crystals) according to filter paper chromatographic data of Schulz and Hinz (1955) [740]

also frozen-in. This effect was shown by filter chromatography by Schulz and Hinz (1955) [740]. In each of the cases considered, these glasses give crystals made up of pyrophosphate anions only.

Paper chromatography also gives us the possibility of investigating the structure of vitreous thin films formed by vapor quenching of $NaPO_3$ on a substrate maintained at temperatures $T < T_g$. The changes upon heat treatment in thin vitreous $NaPO_3$-films thus obtained are similar to those shown in Figs. 4.22 and 4.23 (see Gutzow et al. (1976) [327]). In such experiments with thin films, the advantages of paper chromatography as a method of investigation are obvious. Only a few micrograms of the substance are usually needed to produce paper chromatograms of the type shown in Figs. 4.22–4.25 (see also Grunze (1965) [278]; Grunze and Thilo (1953) [280]).

A similar experiment was also performed with pyrophosphates and silicates as demonstrated in Figs. 4.23 and 4.24. In these figures, the anionic composition of pyrophosphates and vitreous Pb_2SiO_4 and of the resulting crystalline substance after devitrification are shown (see Goetz et al. (1970, 1977) [259, 260]). A similar change in the anionic structure was also observed in the process of crystallization of $LiPO_3$-glasses (Avramov et al. (1979) [27]) which is an interesting analog of $NaPO_3$. In this system the melt and the resulting glass are also constituted of chain phosphate oligomers and of ring anions ($Li[P_3O_9]$). However, these structural units are transformed upon devitrification into an asbestos-like crystal constituted of linear chains with a degree of polymerization $n \to \infty$.

Similar processes of molecular reconstruction also have to take place in the crystallization of selenium and chalcogenide glasses. However, the investigation

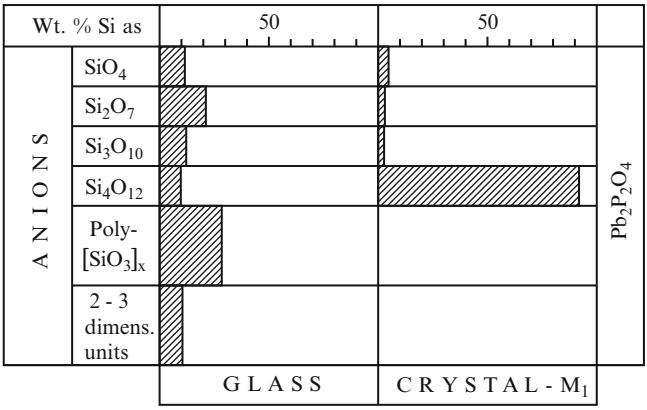

Fig. 4.25 Composition of vitreous and crystalline Pb_2SiO_4 according to Goetz et al. (1977) [259]

of such processes in these systems is connected with significant experimental difficulties when compared with phosphates, where paper chromatography gives an easy method for determination of structural changes in the anionic part of the system. Molecular or anionic reconstruction may considerably inhibit crystallization processes and it can be an additional factor determining the kinetic stability of under-cooled melts.

A thermodynamic criterion for the similarity or dissimilarity between the melt and the crystal is the value of the entropy of melting. In cases of structural similarity between the melt and the crystal (metallic melts, melts of noble gases), the molar entropy of melting is of the order $\Delta S_m \approx (1-2)$ R. In cases, where a reconstructive crystallization takes place, considerably higher values ($\Delta S_m \approx (5-10)$ R) are found. The only glass formed up to now which can be described as an ensemble of frozen-in billiard balls is the already mentioned vitreous argon obtained in the form of thin amorphous films by Kouchi and Kuroda (1990) [477]. These films are very unstable and, as already discussed, transform easily at $T > T_g$ into the respective fcc-crystalline structure. In all other cases, more complicated structures and a more complicated mechanism of crystallization is to be expected. A schematic illustration of possible types of crystallization processes discussed here is given in Fig. 4.26.

4.11 The Hierarchy of Disorder and the Structure of Glasses

In discussing the structure of amorphous solids, in general, and of glasses, in particular, we have met different types of disorder. Firstly, we have to mention

- The topological disorder in the spatial arrangement of the centers of the repeating structural units,
- The orientational disorder with respect to the mutual orientation of molecules of complex shape,

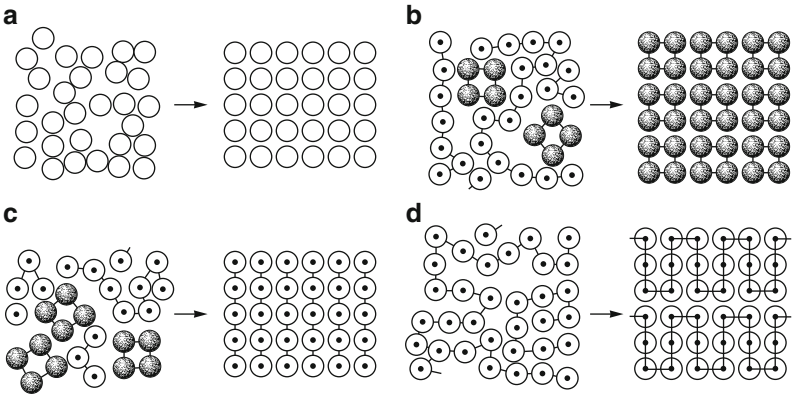

Fig. 4.26 Schematic representation of melt crystallization of substances with different structures: (**a**) Crystallization of a simple melt without structural changes of the building units of the substance (metals, inorganic network polymers); (**b**) crystallization with structural reconstruction: formation of crystals constituted of low molecular cyclic units from melts with polymer and cyclic structural elements ("crystalline" cyclic structural elements are shadowed); (**c**) crystallization with second-type structural reconstruction: formation of high-polymeric crystals from a melt containing cyclic and oligomeric chains (cyclic structural units are shadowed, again); (**d**) crystallization of chain folding organic polymers

- The conformational disorder of chain-like molecules constituted of a large number of identical structural units.

In most cases, these three forms of disorder are expected to occur in real glasses and their existence has been verified, in fact, by X-ray and other methods of structural analysis. Only in systems like the already mentioned argon glass is a topological disorder solely of the first type found.

An example of a system with a frozen-in orientational disorder are the so-called frozen-in molecular crystals (CO_2) (Haase (1956) [338]; see also Westerhoff and Feile (1990) [916]), where two or more energetically similar mutual orientations of non-symmetric molecules are frozen-in. Westerhoff and Feile described a number of frozen-in systems which can be denoted as orientational glasses. Flory discussed a model system consisting of flexible polymer chains with different possible conformations. This system can be frozen-in to form a glass which can be called Flory's glass (see also Milchev and Gutzow (1982) [561]). In such Flory-glasses only conformational disorder is frozen-in. In most of the real glasses as discussed so far, all three types of molecular disorder are usually found. In dependence on the particular structure one or the other may of course dominate.

In the theoretical description of disorder in such real glass-forming systems in the framework of existing statistical-mechanical models, it is usually assumed that the different forms of disorder are reflected by three more or less distinct additive contributions to the entropy of the system. Hereby, topological disorder may be described in terms of free volume theories as discussed in Chap. 5. For the analysis

of orientational and conformational disorder, lattice models are usually applied (see also Chap. 5).

Up to now, we have discussed only the types of disorder connected with the spatial arrangement of the atomic or molecular building units of the system. However, employing the more general definition of the vitreous state, given in Chap. 3, a frozen-in disorder not connected with the spatial arrangement of the atoms or molecules of the substance may also be used to define a glass. Classical examples in this respect are spin-glasses or quadrupole glasses. Here the spatial arrangement of the building units of the substance may be far from being in an amorphous state. Most magnetic substances are indeed crystalline. However, in magnetic materials different types of orientational disorder may be frozen-in, connected with the electronic subsystem of the sample under consideration. Examples in this respect are the so-called Ising- and Heisenberg-glasses. As Ising-glasses systems are termed with only two possible orientations of spins while the term Heisenberg-glasses is usually attributed to systems in which any orientation of the spins is possible and may be frozen-in (Ziman (1979) [960]).

Spin glasses represent an interesting example for a glass also from a theoretical point of view in the following respect. So far we have always dealt, when discussing vitreous samples, with positive values of the actual temperature T and the fictive temperature T^*. However, spin-systems represent an example in which states may exist which have to be characterized by negative values of the absolute temperature (Bazarov (1976) [53]; Kittel (1969) [458]). Consequently, by rapid quenching, such states with negative values of T may be frozen-in resulting in glasses with negative values of the fictive temperature. The peculiar properties of such glasses with negative fictive temperatures and the kinetics of stabilization of them is discussed in detail elsewhere (I. Gutzow, J. Schmelzer, I. Gerroff, Unpublished). Under certain conditions, e.g., by the application of strong magnetic fields a disorder may be frozen-in in the electronic structure (in the Fermi gases or Fermi-liquids). The systems obtained in such a way may be denoted as Fermi glasses (see also Ziman (1979) [960]).

In a similar way, one may also speak about other types of glasses connecting the disorder, e.g., with the properties of colloidal subsystems of the material. Experimental examples in this respect are solids (glasses or crystals) in which the disorder of submicroscopic metallic colloids is frozen-in. A classical example in this respect are gold particles with colloidal dimensions frozen-in and determining the remarkable optical properties of gold ruby glasses. The physical nature of gold ruby was initially recognized by Faraday. Thus, systems with a frozen-in disorder in colloidal dimensions may be called Faraday glasses. A similar example is the disorder caused by a frozen-in subsystem of vacancies in a crystal.

In a system vitrified to a glass not only a physically disordered state may be frozen-in but also chemical states and structures, corresponding to a chemical equilibrium at higher values of temperature. Examples in this respect are frozen-in amorphous S_2-condensates (the normal structures below the freezing-in temperature being S_8-rings and higher polymers), thin amorphous layers of condensed phosphates (Gutzow and Avramov (1981) [307]). The process of annealing of such

amorphous structures includes relaxation processes connected with the formation of the structural units which are stable for the actual values of pressure and temperature. Interesting examples in this respect are discussed in a paper by Gutzow et al. (1976) [327], where the process of annealing of thin amorphous $NaPO_3$-films obtained by vapor quenching is investigated. As evident from the latter mentioned experimental investigation, the classification of possible types of disorder in three-dimensional structures can also be extended to include two-dimensional systems, which similarly to the respective crystalline structures may be characterized by peculiarities as compared with the respective bulk samples. For a more detailed discussion of specific aspects of two-dimensional disorder and two-dimensional glasses see, e.g., Schreiber, Ottomeier (1992) [736], Volkmann, Knorr (1989) [893], You et al. (1986) [937], Wiekert et al. (1987) [921]. Two-dimensional amorphous films are usually formed by vapor quenching if the quenching rate is sufficiently high to prevent the formation of the respective crystalline phases.

Many years ago, it was claimed by Semenov (see Chap. 11, Gutzow and Avramov (1981) [307]) that condensation of two-dimensional amorphous films always precedes the formation of crystalline layers. This prediction was based on the consideration of a two-dimensional van der Waals-equation of state. In this sense, the formation of crystalline layers requires the existence of intermediate two-dimensional liquid and frozen-in two-dimensional vitreous structures. It follows that the possible existence of vitreous and crystalline two-dimensional states is closely interconnected. For one-dimensional systems, it is known (e.g., Landau and Lifshitz (1969) [494]), that phase transformations in them cannot occur. However, there seems to be no restriction that one-dimensional glasses could exist (e.g., orientational disorder in a system of particles located along a linear scratch in a solid matrix). As the highest form of frozen-in disorder, presumably, vitrified samples resulting from a rapid quenching of biological solutions (living cells, plant and animal tissues) have to be considered. In this way, we may speak about life frozen-in to a glass. In such frozen-in biological solutions we have to expect a combination of very different forms of disorder, e.g., topological and configurational disorder, frozen-in chemical non-equilibrium states and frozen-in metabolic processes. If a vitrified biological system can be reversed to its initial high-temperature state by an appropriate annealing then obviously it would be possible to resolve the problem of absolute anabiosis within the vitreous state. A number of additional important biological and even technical applications could be suggested in this case. For a comprehensive analysis of possible types of disorder and the possibilities of its description the reader is referred to the already mentioned monograph by Ziman (1979) [960].

4.12 Discussion

As mentioned in the introduction, the aim of the present chapter is not to give a detailed description of a particular glass but to summarize some of the approaches to an understanding of the structure of glasses, in general. In summarizing the

structural models discussed in the previous sections it can be concluded that there seems to be one common feature to all of them: They are in fact models of random close packing of equal or different building units. As we know, Barlow's principle of close packing determines the possible crystalline structures. Similarly, the application of this principle to disordered states, as proposed by Bernal, seems to give the most general key to describing vitreous structures (see also Hoare (1976) [369]; Cargill (1976) [123]).

Silicates and phosphates, halides and metallic alloys, organic molecular glasses can be described in terms of ordered or disordered close packing of structural elements. In vitrified melts a state of random close packing is frozen-in in which a relatively high percentage of free volume (from 10 % for organic polymer systems to 15–20 % for oxide glasses) is fixed. This point of view makes it possible to understand and generalize the geometric and crystal-chemical criteria of glass-formation formulated by Goldschmidt, Zachariasen, Polk and many other authors. The problems connected with the crystallite hypothesis, which for many years gave an impetus for various experimental investigations of glasses, are in fact not problems of the structure of glasses, but are connected with the superstructure of substances in the vitreous state. Crystallite-like formations can be verified in any glass and they can be, as it is the case for vitreous carbon, the typical structural element in many vitreous substances including silicate glasses. However, the extent of detectable crystallization and of structural inhomogeneities in glasses is more or less caused by their prehistory, method of synthesis and thermal treatment. In this sense, crystallites are not the essential structural elements of glasses.

The results outlined in the preceding sections demonstrate the significance of processes of aggregation (poly-condensation, polymerization, association) in undercooled melts and in describing the structure of glasses. Processes of aggregation significantly change the thermodynamic behavior of glass-forming melts, as will be discussed in the next chapter, and increase dramatically the viscosity of the system. Thus, they are an absolutely necessary element in describing and understanding the structure of glass-forming systems. In this sense, the ideas of Hägg and of Goodman have to be recalled again. This is also the reason why in the next chapter such statistical models are discussed in detail in which the attention is focused on processes of polymerization and aggregation.

A more detailed discussion of the structure of particular glasses than given here can be traced in a number of monographs. A systematic survey of the structure of inorganic glass-forming systems (silicates, oxides, chalcogenides, halides, nitrates, phosphates, sulfates) is given, for example, in Rawson's and Feltz's monographs (Rawson (1967) [657]; Feltz (1983) [202]). A large number of different systems are also reviewed in the series of proceedings of the Russian school of glass science, edited by Porai-Koshits. An extended discussion of the problems connected with the crystallite hypothesis of glass structure may also be found there. An analysis of the possibilities of electron microscopic investigations on the superstructure of glasses and the verification of the existence of micro-heterogeneities in glasses by electron microscopy is given in Vogel's monograph (1979) [889]. A survey of modern problems of the structure of non-crystalline materials may be found also

in the proceedings of the conference on physics and chemistry of glasses held in Cambridge in 1976 (Gaskall (1977) [242]; cf. also [91]). Particular emphasis on the verification of polymer structures in glasses is given in the monograph on the physical chemistry of glasses by Balta and Balta (1976) [35].

In considering the structure of oxide, halide or silicate glasses up to now only glasses have been discussed in which one and the same anion (phosphate, silicate, fluoride) is combined with one or several cations. From a structural point of view such glasses may be termed as mono-anionic glasses. In most of the of modern technical glass-forming systems different oxide anions are present. Moreover, poly-anionic systems, in which the anionic skeleton is built up of different anions become more and more important. Main representatives of these new classes of glasses are oxynitride, oxycarbide and oxyhalide glasses. The synthesis of such glasses is connected with the development of unexpected structures and technical applications. A review of these modern developments is given by Mackenzie and Zheng (1992) [526].

Speaking about the structure of glasses, it is usually stated that glasses are characterized by a short range order similar to that of the respective crystalline substance but a long range order is missing. There also exists, however, a class of non-stoichiometric crystalline phases (e.g., tellurium oxides such as $SrTe_5O_{11}$) in which, in contrast, the short range order is distorted but a nearly perfect long-range crystalline-like order is retained. These peculiar systems are called anti-glasses by Burckhardt and Trömel (1983) [111] (see also Trömel (1988) [855]). In these two papers, typical X-ray patterns of crystals are shown, however, the IR-spectra exhibit a peak broadening characteristic for liquids and glasses. Thus, the short range structure of these peculiar systems can be treated in terms of frozen-in atomic oscillations in the otherwise perfect crystalline lattice. However, up to now, caloric data for these substances are not available. This is another example demonstrating the truth of the words expressed by one of the experts in the field of the structure of glasses (Finney (1977) [210], p. 35): "*For non-crystalline phases . . ., in general, it is only our imagination that limits our models of homogeneous and heterogeneous amorphous structures*".

Chapter 5
Statistical Physics of Under-cooled Melts and Glasses

5.1 Introduction: Summary of Attempts at Modeling the Liquid State

In the foreword to a collection of papers, edited by the well-known Russian academician V.L. Bonch-Bruevich, he wrote: "*The study of disordered materials - liquids, glasses, strongly alloyed superconductors - belongs to the 'hot spots' of contemporary solid state physics. The reasons for this are two and both are equally important and incentive. Firstly, the needs of technology have to be mentioned. Modern electronics calls for materials with such a rich and non-trivial combination of properties that all the superpure crystals, which served mankind with fidelity so many years, are already insufficient to fulfil the needs. Second, we have to take into account also the intrinsic logic of scientific evolution. From perfect gases to perfect crystals and to different types of disordered structures of condensed systems - this is the logical way of evolution of the physics of many-particle systems*" (Bonch-Bruevich (1970) [88]). As we will see, this logical way of evolution of condensed matter physics is exhibited very clearly, in particular, in the development of different statistical-mechanical model approaches to the description of liquids, glass-forming melts and glasses.

The statistical-mechanical or microscopic description of the liquid state, its relation to other states of matter and of the kinetic processes taking place in liquids are very complicated problems. As a first step in this direction the analysis of van der Waals has to be mentioned, leading to the formulation of the equation of state named after him (van der Waals (1873) [879]). This equation reads (for one mole of the substance)

$$\left(p + \frac{a}{v^2}\right)(v - b) = RT. \tag{5.1}$$

The result of van der Waals is based on an assumption which is denoted today as the mean field approach. It is the basis of a large class of statistical-mechanical model considerations of different systems including substances in the liquid state. In van der Waals' approach, the interaction of the molecules is accounted for by a term

I.S. Gutzow and J.W.P. Schmelzer, *The Vitreous State*,
DOI 10.1007/978-3-642-34633-0_5, © Springer-Verlag Berlin Heidelberg 2013

a/v^2, while the effect of the volume of the molecules on the behavior of the liquid is described by the parameter b.

In a general form, the problem of the microscopic description of the liquid state was formulated first by Eger and Mie (see, for example, Moelwyn-Hughes (1972) [567]). Different attempts in this direction were developed by Frenkel (1946) [233]. In Frenkel's monograph a summary of earlier work in describing liquids based on van der Waals like approaches may also be found. After this initial period a number of model investigations were carried out in an empirical or semi-empirical manner. In these attempts a qualitative or even a semi-quantitative description of the properties of liquids was achieved. In this direction we have to note especially the group of cell or lattice-models of the liquid state. In these models another method was chosen for the analysis: the liquid state is investigated by introducing appropriate deviations from a virtual crystalline-like structure. However, in such an approach, the lattice structure superimposed from the very beginning affects, of course, the results of the model analysis. Moreover, problems arise in the description of short-range order and transport processes in liquids could not be modeled, in principle, in the original versions of this approach. Further examples for earlier theoretical attempts in describing the liquid state can be found in the paper by Lennard-Jones and Devonshire (1939) [503] and Eyring's monograph (see Glasstone, Laidler, and Eyring (1941) [255]).

A further line in the development of microscopic models of the liquid state is connected with ideas to describe appropriately the increased free volume of liquids by introducing unoccupied cells (holes) or vacancies into the virtual lattice. This approach can be used in describing the structure not only of simple but also of more complicated liquids like, for example, polymer systems. As examples in this respect the models of Flory (1942 [217], 1949 [219], 1956 [220]), Gibbs and DiMarzio (1958) [251], Gutzow (1962a,b [288, 289], 1977 [298]), Milchev and Gutzow (1981 [560], 1982 [561]), and Milchev (1983) [557] may be noted. The concept of holes and the belief in the dominant effect of the free volume in describing the properties of the liquid state stems from another classical model, the hole model of liquids, proposed initially by Frenkel and Eyring. A beautiful description of the basic ideas underlying this approach, its inner logic and the attempts of Altair and Fürth to advance it to a quantitative description of liquids may be also found in Frenkel's already cited monograph. Hole and vacancy models were also applied in order to describe the rheological properties of liquids (Frenkel (1946) [233]; Hirai and Eyring (1959) [365]) and, in particular, the temperature dependence of the viscosity. Other classes of models employed for a more or less accurate description of the properties of liquids consist of the so-called two-energy-level models (see Angell and Rao (1972) [15]; Rao and Angell (1972) [656]) and in approaches, where mathematical formulations of Bernal's and Finney's ideas concerning the structure of liquids, as discussed in Chap. 4, are attempted to be performed (see, e.g., Mutaftschiev and Bonissent (1977) [587]).

In discussing microscopic approaches for an understanding of the properties of liquids, also an idea proposed originally by Bresler (1939) [104] and developed

further, again, by Frenkel is of particular interest. In this approach two types of order parameters are introduced, one reflecting short-range order, the other the long-range order of the system under consideration. In the lattice and lattice-hole models, the liquid state is described taking as the starting point a real or virtual crystalline-like state. Liquid-like behavior in the model is achieved by introducing a temperature-dependent number of holes into the lattice. Thus, transport properties and the general rheological behavior of liquids can also be modeled in accordance with existing experimental evidence. One of the main aims in most of the theoretical attempts is to establish unified models allowing one to incorporate both the liquid-gas and the melt-crystal transitions into the description of liquids. However, till now no approach exists where this goal is realized in a straightforward way.[1] As mentioned by Green (1952) [273] in contemporary models the liquid passes through the melting point without "knowing" about the existence of a crystalline state.

In discussing the models of liquids summarized briefly above, it can be mentioned first that a majority of them are really excellent products of imagination and theoretical thinking. Nevertheless, for some of them grave shortcomings remain. Thus, for most of the mentioned approaches an adequate theoretical formulation in terms of the general methods of the statistical theory of the liquid state, i.e., in terms of the partition function of the system does not exist. Moreover, an estimation of the significance of the approximations introduced is often impossible. So a large number of these models have to be considered only as fruitful semi-empirical attempts to describe the structure and properties of liquids in molecular terms.

An exception to this is represented by the class of cellular, lattice or lattice-hole models of the liquid state. For these models due to the efforts made, in particular, by Kirkwood (1950) [454] and Rowlinson and Curtiss (1951) [671] (see also Hirschfelder, Curtiss, and Bird (1954) [366]) it was possible to specify mathematically the nature of the approximations made and their quantitative significance. A summary of the formalism of the statistical mechanical approach required for the microscopic description of the properties of liquids and the theoretical foundation of lattice and cell-models is given in the subsequent sections.

5.2 Statistical Physics of Liquids: Basic Equations

As it is discussed in detail in the respective courses on statistical physics, in order to give a microscopic interpretation of the properties of macroscopic bodies, in general, and of liquids, in particular, the partition function Z of the system has to be calculated. For a macroscopic one-component system, consisting of N particles, the

[1]The failure to develop such unified models may have a deep theoretical origin as discussed in detail by V.P. Skripov and coworkers (Skripov and Baidakov [768]; Skripov and Faizullin [769]; Skripov and Faizullin [770]). It is reflected in the absence of a spinodal in melt crystallization as established by cited here authors.

partition function $Z(T, V, N)$ can be expressed as (see, e.g., Sommerfeldt (1937) [786]; Becker (1964) [58]; Mayer and Goeppert-Mayer (1946) [541])

$$Z(T, V, N) = \frac{1}{h^{3N} N!} \int \dots \int \exp\left(-\frac{H(q, p)}{k_B T}\right) dq_1 \dots dp_{3N}. \tag{5.2}$$

Here $H(q, p)$ or, in a more extended form, $H(q_1, q_2, \dots, q_{3N}, p_1, p_2, \dots, p_{3N})$, is the Hamilton function of the system, $\{q_i\}$ are the generalized coordinates and $\{p_i\}$ are the generalized momenta (see, e.g., Schmelzer (1992) [692]), specifying the microscopic state of the considered N-particle system.

If the partition function $Z(T, V, N)$ is known, the Helmholtz free energy $F(T, V, N)$ may be calculated via (Becker (1964) [58])

$$F = -k_B T \ln Z. \tag{5.3}$$

The Helmholtz free energy F is, generally, defined as

$$F = U - TS, \tag{5.4}$$

and similarly to the respective equations, derived in Sect. 2.2.1, we have

$$F = -pV + \sum_i \mu_i n_i \tag{5.5}$$

and

$$dF = -SdT - pdV + \sum_i \mu_i \, dn_i. \tag{5.6}$$

From Eq. (5.6) we obtain

$$S = -\left(\frac{\partial F}{\partial T}\right)_{V, n_i} \tag{5.7}$$

and with Eqs. (5.3) and (5.4)

$$S = k_B \left[\ln Z + T \frac{\partial}{\partial T}(\ln Z)\right], \tag{5.8}$$

$$U = k_B T^2 \frac{\partial}{\partial T}(\ln Z). \tag{5.9}$$

Similarly, from the partition function Z also the thermal equation of state of the considered macroscopic body may be calculated. In fact, from Eq. (5.6) we obtain

$$p = -\left(\frac{\partial F}{\partial V}\right)_{T, n_i}, \tag{5.10}$$

resulting with Eq. (5.3) in

$$p = k_B T \frac{\partial}{\partial V}(\ln Z). \tag{5.11}$$

With $H = U + pV$ and $G = U - TS + pV$ we have, consequently,

$$H = k_B T \left[T \frac{\partial}{\partial T}(\ln Z) + V \frac{\partial}{\partial V}(\ln Z) \right], \tag{5.12}$$

$$G = -k_B T \left[\ln Z - V \frac{\partial}{\partial V}(\ln Z) \right]. \tag{5.13}$$

It follows that all the difficulties in giving a microscopic interpretation of the properties of macroscopic bodies are connected with the determination of the partition function, Z. If Z is known, the set of above equations automatically defines the thermodynamic functions of the system.

According to Eq. (5.2) for a determination of Z the Hamiltonian $H(q, p)$ of the system has to be known. In classical mechanics for the considered case of a one-component system consisting of N particles $H(q, p)$ is shown to be of the form

$$H(q_1, \ldots, p_{3N}) = \sum_{i=1}^{3N} \frac{p_i^2}{2m} + U_N(q_1, q_2, \ldots, q_{3N}) \tag{5.14}$$

or, equivalently,

$$H(\mathbf{r}_1, \mathbf{r}_2, \ldots, \mathbf{r}_N, \mathbf{p}_1, \mathbf{p}_2, \ldots, \mathbf{p}_N) = \sum_{i=1}^{N} \frac{(\mathbf{p}_i)^2}{2m} + U_N(\mathbf{r}_1, \mathbf{r}_2, \ldots, \mathbf{r}_N). \tag{5.15}$$

In Eqs. (5.14) and (5.15), m is the mass of a single particle, as generalized coordinates Cartesian coordinates are chosen. Integration over all components of the momenta results in

$$Z = \left(\frac{2\pi m k_B T}{h^2} \right)^{\frac{3N}{2}} \frac{Q}{N!} \tag{5.16}$$

with

$$Q = \int_V \ldots \int_V \exp\left\{ -\frac{U_N(\mathbf{r}_1, \ldots, \mathbf{r}_N)}{k_B T} \right\} d\mathbf{r}_1 \, d\mathbf{r}_2 \ldots d\mathbf{r}_N. \tag{5.17}$$

It follows that Eqs. (5.3), (5.9), (5.11), (5.12) and (5.13) may be reformulated in terms of the configurational part Q of the partition function Z. For the Helmholtz free energy F we get immediately

$$F = -k_B T \left[\ln Q - \ln N! + \frac{3}{2} N \ln \left(\frac{2\pi m k_B T}{h^2} \right) \right] \tag{5.18}$$

and with Stirling's approximation

$$\ln N! \approx N(\ln N - 1), \tag{5.19}$$

valid for large values of N, the thermodynamic function F can be written in the form

$$F = -k_B T \ln Q + N k_B T \left[\ln N - 1 - \frac{3}{2} \ln \left(\frac{2\pi m k_B T}{h^2} \right) \right]. \tag{5.20}$$

In the absence of interactions between the different particles ($U_N = 0$), as it is assumed for a perfect gas, the configurational part of the partition function can be directly calculated. As the result one obtains

$$Q = V^N. \tag{5.21}$$

Denoting by F_0 the free energy in the absence of interactions between the molecules we may write, consequently,

$$F_0 = -N k_B T \ln \frac{V}{N} - N k_B T \left[1 + \frac{3}{2} \ln \left(\frac{2\pi m k_B T}{h^2} \right) \right]. \tag{5.22}$$

Similarly, we obtain from Eq. (5.9)

$$U = \frac{3}{2} N k_B T + k_B T^2 \frac{\partial}{\partial T} (\ln Q). \tag{5.23}$$

Denoting by U_0 the internal energy in the absence of molecular interactions in the system as a special case

$$U_0 = \frac{3}{2} N k_B T \tag{5.24}$$

is found. Finally, for the thermal equation of state we get from the relation Eq. (5.11)

$$p = k_B T \frac{\partial}{\partial V} (\ln Q) \tag{5.25}$$

and for a system of non-interacting particles ($p = p_0$)

$$p_0 = \frac{k_B T N}{V}, \tag{5.26}$$

which is the well-known expression for the thermal equation of state of a perfect gas.

The outlined equations can be easily generalized to the case of a multi-component system. Instead of above given equations we have to write, now

$$Z = \frac{1}{h^f \prod_i N_i!} \int \ldots \int \exp\left(-\frac{H(p,q)}{k_B T}\right) dq_1 dq_2 \ldots dq_f dp_1 dp_2 \ldots dp_f. \tag{5.27}$$

With

$$H = \sum_i \frac{(\mathbf{p}_i)^2}{2m_i} + U_N(q_1, q_2, \ldots, q_f), \tag{5.28}$$

the following expression for Z is obtained

$$Z = Q \prod_i \left(\frac{2\pi m_i k_B T}{h^2}\right)^{\frac{3N_i}{2}} \frac{1}{N_i!}, \tag{5.29}$$

where Q is given by

$$Q = \int \ldots \int \exp\left(-\frac{U_N(q)}{k_B T}\right) dq_1 dq_2 \ldots dq_f. \tag{5.30}$$

Here f is the total number of degrees of freedom of the system ($f = 3\sum_i N_i$), N_i the number of particles of the different components and m_i the mass of a particle of the i-th component.

A simple model of non-interacting oscillators can also be used to derive the thermodynamic functions and the equations of state of a perfect crystal. In the partition function of both the perfect crystal and the perfect gas the determination of Q can be carried out straightforwardly. However, for liquids (as well as for real gases) the evaluation of Q is a very difficult task. This is the reason, why the microscopic description of liquids causes enormous problems. It follows that all model statistical treatments of liquids can be described in terms of more or less suitable approximative attempts only. The approximations for the determination of Q have to guarantee that an integration of the basic equations is possible and either numerical or analytical results for the temperature dependencies of the thermodynamic properties of the system can be obtained.

The particular case of a system of non-interacting particles considered with Eqs. (5.22), (5.24) and (5.26) corresponds to the model of a perfect gas. This model is employed as one of the starting points for the statistical-mechanical description of real gases. Models of real gases have been used also, however, with limited success, for the description of the properties of liquids. On the other hand, for crystalline solids the model of an absolutely perfect crystal is applied as the basis for the derivation of the macroscopic properties of real crystals starting from microscopic considerations. Models of the crystalline state can also be taken as the starting point for the development of another class of approaches to the liquid state, the cellular or lattice models of liquids. This approach is characterized in the next sections. Up to now a specific model of liquids does not exist but only the gas or crystalline-like models are developed in attempting to establish the properties of liquids.

Another fundamental method for deriving the thermodynamic characteristics of liquids is based on the possibility of expressing them through the radial distribution function (Zernicke and Prins (1927) [953]; Fisher (1961) [212]). This method is of considerable interest since it allows one the determination of the thermodynamic properties of the liquid using the results of X-ray or neutron structural investigations. However, this method merely gives a connection between thermodynamic and structural measurements and is not a way of microscopic modeling the liquid state.

5.3 Cell or Lattice Models of Liquids

As a first step in simplifying the problem of the calculation of the configurational part of the partition function the potential energy of the system of N interacting particles constituting the liquid is expressed usually as the sum of the contributions only of pair-interactions in the form

$$U_N(\mathbf{r}_1, \mathbf{r}_2, \ldots, \mathbf{r}_N) = \sum_{1 \le i < j \le N} \varphi(|\mathbf{r}_i - \mathbf{r}_j|). \tag{5.31}$$

For the specification of the potentials, φ, of the pair-interactions different proposals have been developed. The most well-known expression of such functions is the Lennard-Jones potential, given by the equation

$$\varphi(r) = 4\varepsilon \left[\left(\frac{a}{r}\right)^{12} - \left(\frac{a}{r}\right)^{6} \right] \qquad \text{with} \qquad r = |\mathbf{r}_i - \mathbf{r}_j|. \tag{5.32}$$

The course for the $\varphi(r)$-function and the meaning of the parameters ε and a are illustrated in Fig. 5.1.

The Lennard-Jones potential is a representative of a more general class of interaction potentials, proposed earlier by Mie (see, e.g., Moelwyn-Hughes (1972) [567]),

$$\varphi(r) = 4\varepsilon \left[\left(\frac{a}{r}\right)^{m} - \left(\frac{a}{r}\right)^{n} \right]. \tag{5.33}$$

Here m and n are natural numbers with $m > n$. Mie's potential and other types of pairwise interactions often used in modeling liquids are illustrated in Fig. 5.2. The analytical expressions for the different curves given in this figure are summarized below (see also Soules (1990) [787])

$$\text{Hard spheres} \qquad \varphi(r) = \begin{cases} 0 & r > a \\ \infty & r \le a \end{cases} \tag{5.34}$$

$$\text{Point center of repulsion} \qquad \varphi(r) = br^{-\delta} \tag{5.35}$$

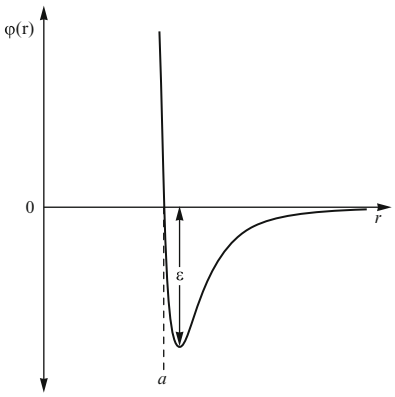

Fig. 5.1 Illustration of the course of the Lennard-Jones potential and the meaning of the parameters a and ε used in it

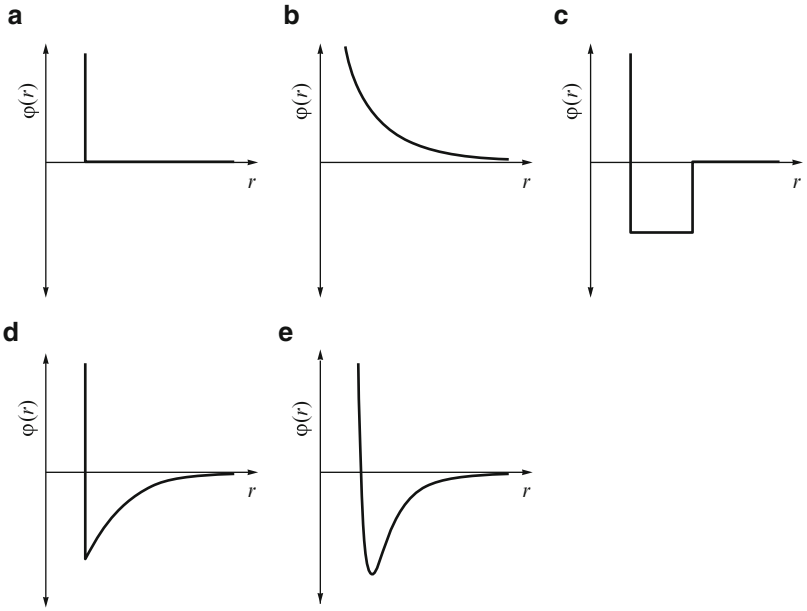

Fig. 5.2 Schematic representation of other often used pair-interaction potentials: (**a**) Hard spheres; (**b**) point center of repulsion; (**c**) rectangular potential well; (**d**) Sutherland potential; (**e**) Lennard-Jones or Mie-potential

Reactangular potential-well

$$\varphi(r) = \begin{cases} \infty & r \leq a \\ -\varepsilon & a < r < R \\ 0 & R \leq r \end{cases} \tag{5.36}$$

Sutherland potential

$$\varphi(r) = \begin{cases} \infty & r \leq a \\ -cr^{-\gamma} & r > a \end{cases}. \tag{5.37}$$

As seen from these equations, the more realistic cases of interaction potentials may be written in the form

$$\varphi(r) = \varepsilon f\left(\frac{r}{a}\right). \tag{5.38}$$

Dealing only with pairwise interactions, the configurational part of the partition function may be expressed, in general, as

$$Q = \int \dots \int \exp\left[-\frac{\sum\limits_{1\le i<j\le N} \varphi(|\mathbf{r}_i - \mathbf{r}_j|)}{k_B T}\right] d\mathbf{r}_1 \dots d\mathbf{r}_N. \tag{5.39}$$

For the particular expressions of the interaction potentials which may be written in the form given by Eq. (5.38) we have (in Cartesian coordinates)

$$Q = \int \dots \int \exp\left\{-\frac{\varepsilon}{k_B T} \times \right. \tag{5.40}$$

$$\left. \times \sum_{1\le i<j\le N} f\left(\sqrt{\frac{(x_i - x_j)^2 + (y_i - y_j)^2 + (z_i - z_j)^2}{a^2}}\right)\right\} dx_1 \dots dz_N.$$

Introducing the reduced variables

$$x_i^{(r)} = \frac{x_i}{a}, \qquad y_i^{(r)} = \frac{y_i}{a}, \qquad z_i^{(r)} = \frac{z_i}{a}, \tag{5.41}$$

Eq. (5.40) yields

$$Q = a^{3N} \int \dots \int \exp\left\{-\frac{\varepsilon}{k_B T} \times \right. \tag{5.42}$$

$$\left. \times \sum_{1\le i<j\le N} f\left(\sqrt{(x_i^{(r)} - x_j^{(r)})^2 + (y_i^{(r)} - y_j^{(r)})^2 + (z_i^{(r)} - z_j^{(r)})^2}\right)\right\} d\Gamma$$

with

$$d\Gamma = dx_1^{(r)} \dots dz_N^{(r)}. \tag{5.43}$$

The integral on the right hand side of Eq. (5.42) is, consequently, a function of $\varepsilon/k_B T$ and the volume of the system in reduced units, i.e., V/a^3. It follows that Q can be expressed as

$$Q = a^{3N} \Psi\left(\frac{k_B T}{\varepsilon}, \frac{V}{a^3}\right). \tag{5.44}$$

With the notations

$$T^{(r)} = \frac{k_B T}{\varepsilon}, \qquad V^{(r)} = \frac{V}{a^3}, \qquad U^{(r)} = \frac{U}{\varepsilon}, \qquad p^{(r)} = \frac{p a^3}{\varepsilon} \tag{5.45}$$

we obtain from Eqs. (5.23) and (5.25)

$$U^{(r)} = U^{(r)}\left(T^{(r)}, V^{(r)}\right), \tag{5.46}$$

$$p^{(r)} = p^{(r)}\left(T^{(r)}, V^{(r)}\right), \tag{5.47}$$

i.e., the law of corresponding states is fulfilled. A further discussion of the validity of the law of corresponding states, in particular, in application to noble gases can be found, e.g., in the monograph by Fisher (1961) [212]. But even with the assumption of a pairwise additivity of the interactions and the introduction of more or less realistic interaction potentials an analytical calculation of the partition function is not possible. Thus further approximations are needed.

The basic idea underlying the lattice or cell models of the liquid state is connected with the introduction of some virtual lattice for the description of the structure of liquids. It is assumed that each particle of the liquid moves only in a cell in the vicinity of a knot of the lattice. For each particle the lattice cell is formed by the neighboring particles. Translations of the molecules of the liquid from one cell to another, possible in real liquids, are thus excluded from the consideration. Taking into account that we are discussing models of liquids in application to glass-forming melts the latter limitation does not seem to be a very serious one. More serious restrictions of the validity of this approach are connected with the neglect of the short range order of the liquids and the choice of a virtual lattice or the definition of its properties. At part the difficulties with the description of the short-range order may be removed in the framework of the lattice-hole models. We shall return to these problems later.

Based on the mentioned approximations, the configurational part of the partition function may be written as

$$Q = N! Q_N^{(1)}, \tag{5.48}$$

where by $Q_N^{(1)}$ one of the possible distributions of particles of the liquid to the cells of the lattice is denoted. It is assumed hereby that each of the cells contains only one molecule of the liquid. In the next step, the true interaction potential $U_N(\mathbf{r}_1, \ldots, \mathbf{r}_N)$ is replaced by a mean field, acting on each particle in its cell. Provided all particles are located in the centers of the respective cells, forming the virtual lattice, the total potential energy is expressed as

$$U_N^{(c)} = \frac{1}{2} N E_0. \tag{5.49}$$

Here E_0 is the energy of interaction of one particle with all other molecules for the considered lattice configuration. Deviations of the positions of the particles from this regular arrangement result in a change in the interaction energy. These variations may be expressed through a potential function $\varphi(\mathbf{q})$, which is assumed to be of the same form for each particle in every cell. The ordered state is described by $\mathbf{q}_i = 0$,

$i = 1, 2, \ldots, N$. According to the definition of E_0, for this regular crystalline-like arrangement φ is equal to zero.

In general, however, we have to write

$$U_N = \frac{1}{2} N E_0 + \sum_{1 \le i \le N} \varphi(\mathbf{q}_i), \tag{5.50}$$

resulting in

$$\exp\left[-\frac{U_N(\mathbf{r}_1, \ldots, \mathbf{r}_N)}{k_B T}\right] = \exp\left[-\frac{N E_0}{2 k_B T}\right] \prod_{1 \le i \le N} \exp\left[-\frac{\varphi(\mathbf{q}_i)}{k_B T}\right]. \tag{5.51}$$

A substitution into the expression for Q yields (see Eq. (5.17))

$$Q = N! \exp\left[-\frac{N E_0}{2 k_B T}\right] \left[\int_v \exp\left(-\frac{\varphi(\mathbf{r})}{k_B T}\right) d\mathbf{r}\right]^N. \tag{5.52}$$

Here v is the volume of one of the cells, i.e.,

$$v = \frac{V}{N}. \tag{5.53}$$

With the notation

$$v_{fm} = \int_v \exp\left[-\frac{\varphi(\mathbf{r})}{k_B T}\right] d\mathbf{r} \tag{5.54}$$

we obtain, finally,

$$Z = \left(\frac{2\pi m k_B T}{h^2}\right)^{\frac{3N}{2}} \exp\left(-\frac{N E_0}{2 k_B T}\right) v_{fm}^N. \tag{5.55}$$

v_{fm} is usually denoted as the free volume referred to one particle of the liquid (see, e.g., Hirschfelder et al. (1954) [366]). In the absence of repulsive interactions ($\varphi = 0$) it is equal to $v_{fm} = v$. If the interactions, in contrast, are strong, then φ is a rapidly increasing function of $\mathbf{q}$, and the inequality $v_{fm} \ll v$ holds.

It follows that, more precisely formulated, the quantity v_{fm} is a measure of the volume free for the motion of the molecules of the liquid considered as mass-points. This more precise meaning is specified by the additional subscript m (from motion) in v_{fm} to avoid confusion with the already discussed relative free volume having the meaning of the percentage of space not occupied by the particles (compare the analysis of Bernal's ideas in Chap. 4). Obviously, both quantities are interrelated, but, at least in general, they are not identical. The free volume in Bernal's sense we denote by v_f.

Once the partition function is known, all thermodynamic quantities of the considered system may be calculated by using the equations given in the preceding

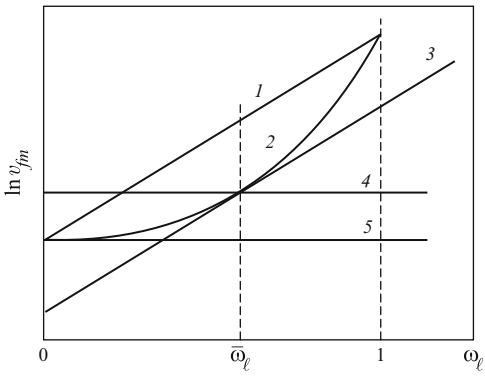

Fig. 5.3 Different types of dependencies of the generalized free volume $v_{fm}(\omega_l)$ as a function of the fraction of the holes ω_l in the first coordination shell of a molecule of the liquid according to (*1*) Ono, (*2*) Curtiss, (*3*) Rowlinson, (*4*) Hill, (*5*) Eyring

section. For the free energy we obtain, for example,

$$F = \frac{NE_0}{2} - \frac{3Nk_{BT}}{2} \ln\left(\frac{2\pi m k_{BT}}{h^2}\right) - Nk_{BT} \ln v_{fm}. \tag{5.56}$$

However, to allow one quantitative predictions, the values of the parameters E_0 and v_{fm} and their dependencies on temperature T and specific volume v and, may be, other characteristics of the liquid have to be established. By considering the liquid as a system of hard spheres with a diameter d as an estimate for v_{fm} the expression

$$v_{fm} = 8[v^{1/3} - d]^3 \tag{5.57}$$

may be obtained (Hirschfelder et al. (1954) [366]). The quantity d^3 is proportional to the constant b in van der Waals' equation of state, describing the effect of the volume occupied by the particles on the behavior of the liquid. On the other hand, the first term in Eq. (5.56) may be interconnected with the enthalpy of evaporation of the substance. It can be expressed also in terms of van der Waals' equation of state, but this time through the parameter a.

For a more straightforward estimation of v_{fm} the knowledge of the so-called mean field potential $\varphi(\mathbf{q})$ is required. In principle, this function can be determined by the solution of an integral equation, derived first by Kirkwood (1950) [454]. However, due to the difficulties in the realization of such a program $\varphi(\mathbf{q})$ is often calculated in a simpler way by expressing this function through the contributions of the pair-interaction potentials of the neighboring particles, applying, for example, the Lennard-Jones potential (see, e.g., Fisher (1961) [212]). In a further step, the outlined model can be generalized to include the effect of a reduced or an increased free volume on the thermodynamic properties of the model liquid under consideration. Hereby a dependence of the free volume v_{fm} on the relative ratio ω_l of empty cells in the first coordination shell of a molecule is introduced. Different approximations for the calculation of the v_{fm} vs ω_l dependence are discussed by Hirschfelder et al. (1954) [366] and Hill (1956) [358]. They are illustrated in Fig. 5.3. With regard

to glass-forming melts and polymer solutions the approximation $v_{fm} = \text{const.}$ is usually applied. ω_l-dependent solutions have been used up to now only in order to establish the thermal equation of state of simple liquids constituted of spherical non-associated molecules.

5.4 Lattice-Hole Models of Simple Liquids

5.4.1 General Characterization

In lattice-hole models the increased free volume of the liquid as compared with the respective crystalline form of the same substance is attributed to the existence of unoccupied cells or holes in the virtual lattice. It is assumed usually that the volume of such a hole is a constant, equal to the volume of the molecule of the liquid. Such an approximation was employed first by Eyring (see Glasstone, Laidler, and Eyring (1941) [186]) and Frenkel (1946) [234]. More sophisticated approaches have also been introduced, assuming, for example that the volume of the holes exceeds the size of the molecules (e.g., Hirai and Eyring (1958 [405], 1959 [406])). A summary of developments in this direction can be found in the monograph by Stewart (1955) [801] and in the above cited papers by Hirai and Eyring. However, practically in all further applications of lattice-hole models to glass-forming melts and polymer solutions the simplest assumption of a constant volume v_{fm} equal to the respective volume of a molecule of the liquid is employed.

By introducing the concept of holes into the model we have to determine the thermodynamic properties of the model system in a new way. In addition to the calculation of the partition function of the cell system, developed in the previous section, the contributions of the holes to the thermodynamic functions have to be specified. Thus the analysis of the problem requires, in principle, a generalization in terms of the formalism indicated with Eqs. (5.27)–(5.30) for multi-component systems. However, in considering holes as a new type of particles with definite properties the problem is usually simplified by reducing it to the calculation of the mixing contributions to the partition function in a way known from the statistical treatment of two-component solutions.

We consider here first the case of simple liquids, defining them as substances consisting of particles with a nearly spherical shape, which do not exhibit aggregation or polymerization. In application to polymer melts and solutions, attention is also concentrated on the determination of the configurational contributions to the properties of the respective liquids due to the complex structure and non-spherical shape of the molecules and their possible conformations. This is the reason why polymer melts will be treated as a second step in our analysis.

A simple method in treating binary (A-B) solutions and alloy systems was proposed in 1934 by Bragg and Williams ([99], see also, e.g., Frenkel (1946) [233]; Hill (1956) [358]) in the framework of a mean-field approach. Hereby as a

mean-field theory any model is denoted for which the calculation of the partition function and the thermodynamic quantities is based on the assumption that all possible configurations of the system have to be accounted for with the same probability and that an averaging procedure of the $A - B$-interactions is possible in determining the energy of the system. In accordance with this general approach the basic assumptions of Bragg and Williams (1934) [99] are as follows:

- The entropy is calculated directly by a determination of the number of all possible configurations corresponding to the same value of the internal energy of the system.
- The energy is determined from the molecular interactions assuming that only nearest-neighbor interactions have to be accounted for, hereby the number of particles of the different components in the first coordination shell is assumed to be given by their mean concentration in the system.

According to the first of these assumptions the specific nature of the A-B, A-A and B-B interactions is neglected in the calculation of the entropy. Thus, a possible clustering or enrichment of particles of the various components in different parts of the system is also excluded from the consideration. In this respect, the mean-field approach leads to the determination of the properties of a state of the system having the highest possible degree of disorder.

A correction of the values for the configurational part of the entropy calculated by an application of the first assumption can be carried out by the introduction of appropriate correction factors, depending on specific properties of the A-A, B-B and A-B interactions (Bethe-Guggenheim approach). A detailed discussion of this topic may be found in the books by Hill (1956) [358], Guggenheim (1952) [281], and Prigogine (1957) [647]. An argumentation of the validity of the second of the listed above assumptions is given in the monograph by Zvetkov, Esskin and S. Frenkel (1964) [962] and in different modifications in the books by Ya. Frenkel (1946) [233] and Hill (1956) [358]. A proof of the validity of this assumption is also developed in a paper by Milchev and Gutzow (1981) [560]. Considering only nearest-neighbor interactions it is shown that the partition function of a binary A-B solution in a mean-field approximation may be obtained.

5.4.2 The Classical Lattice-Hole Model

In applying the ideas outlined in the previous section to lattice-hole models of simple liquids the interaction energy between two holes and a hole and a molecule of the liquid is set equal to zero. Moreover, as an additional peculiarity compared with the commonly discussed case of a binary solution of two different components, we have to take into account that the number of holes in a liquid does not have a definite value but may change in dependence on the thermodynamic parameters like external pressure and temperature. In the subsequent derivations, we assume the number of holes, denoted by N_0, to be given first and determine its value

later on by applying the condition of thermodynamic equilibrium. The number of molecules of the liquid is denoted by N_A and is assumed to be equal to Avogadro's number. Consequently, the thermodynamic functions referred to one mole of the model substance are established in the course of the calculations.

As mentioned, the volumes occupied by one particle and a hole are assumed to be the same and denoted by v_0. Consequently, the total volume of the system can be expressed as

$$V = (N_A + N_0)v_0. \tag{5.58}$$

The molar fraction of holes ξ is given then by

$$\xi = \frac{N_0}{N_A + N_0}. \tag{5.59}$$

Here ξ is at the same time equal to the relative free volume of the system. Thus, by $(1 - \xi)$ the relative ratio of the occupied volume is given, i.e.,

$$1 - \xi = \frac{N_A}{N_A + N_0}. \tag{5.60}$$

The free volume can be considered as an additional order parameter in the sense discussed in Chap. 3. This is the reason why it is denoted as ξ.

The total number Ω of statistically distinct distributions of holes and molecules on the assumed virtual lattice is given by

$$\Omega = \frac{(N_0 + N_A)!}{N_0!N_A!}. \tag{5.61}$$

With Boltzmann's equation Eq. (2.32) the configurational part of the entropy is obtained as

$$\Delta S = k_B \ln\left[\frac{(N_A + N_0)!}{N_A!N_0!}\right]. \tag{5.62}$$

Applying Stirling's formula Eq. (5.19) we get, approximately,

$$\Delta S = -k_B\left[N_A \ln\left(\frac{N_A}{N_A + N_0}\right) + N_0 \ln\left(\frac{N_0}{N_A + N_0}\right)\right], \tag{5.63}$$

i.e., the well-known expression for the entropy of mixing. Taking into account the definition of ξ and the relation

$$R = N_A k_B, \tag{5.64}$$

connecting the universal gas constant R, Boltzmann's constant k_B and Avogadro's number N_A, we may rewrite Eq. (5.63) in the form

$$\Delta S_{mol} = -R\left[\ln(1 - \xi) + \frac{\xi}{1 - \xi}\ln\xi\right]. \tag{5.65}$$

For the considered model the energy of bonding between the holes and the molecules and the holes themselves is equal to zero. The configurational contribution to the internal energy is given, consequently, by the decrease of the number of bonds between the molecules due to the introduction of holes into the virtual lattice.

By definition of ξ the number of molecules in the system can be expressed as $(N_A + N_0)(1 - \xi)$. Moreover, the probability of finding a hole in the immediate vicinity of a molecule of the liquid is given by $z\xi$, where z is the number of nearest neighbors, i.e., the coordination number. Consequently, in the mean-field approach the change of the internal energy connected with the introduction of holes into the system, reads

$$\Delta U = \frac{1}{2} E_{AA} z (N_A + N_0)(1 - \xi)\xi. \tag{5.66}$$

Hereby by E_{AA} the energy of an A-A bond is denoted (see also Becker (1938) [57]). For one mole of the liquid we get with Eq. (5.60)

$$\Delta U_{mol} = \frac{1}{2} z E_{AA} N_A \xi, \tag{5.67}$$

or, using for the energy of hole-formation the notation

$$\Delta E_0 = \frac{1}{2} z E_{AA} N_A \tag{5.68}$$

the equivalent expression

$$\Delta U_{mol} = \Delta E_0 \xi. \tag{5.69}$$

With above equations the change of the enthalpy per mole due to the introduction of holes may be expressed as

$$\Delta H_{mol} = \Delta U_{mol} + p \Delta V_{mol}, \tag{5.70}$$

where p is the external pressure acting on the system. Hereby the change of volume may be written in the form

$$\Delta V_{mol} = N_0 v_0 = N_A v_0 \frac{\xi}{1 - \xi}. \tag{5.71}$$

Similarly, for the change of the Gibbs free energy per mole

$$\Delta G = \Delta U + p \Delta V - T \Delta S \tag{5.72}$$

the expression

$$\Delta G_{mol} = \Delta E_0 \xi + p V_0 \frac{\xi}{1 - \xi} + RT \left[\ln(1 - \xi) + \frac{\xi}{1 - \xi} \ln(\xi) \right] \tag{5.73}$$

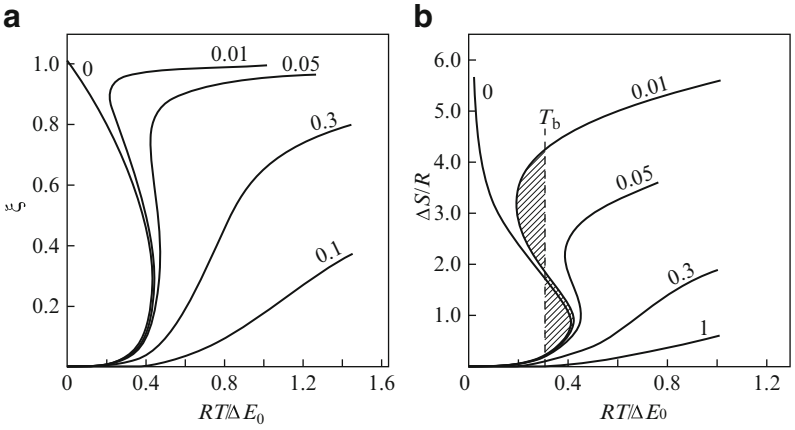

Fig. 5.4 (**a**) Temperature dependence of the order parameter ξ, reflecting the relative free volume in the system calculated according to Eq. (5.75) for different values of the ratio $(pV_0/\Delta E_0)$ indicated by the respective numbers to the curves in the figures. Note the appearance of a *s*-shaped course of the curves indicating a first-order phase transition for parameter values $(0 < pV_0/\Delta E_0) < 0.05$. (**b**) Temperature dependence of the configurational contributions to the entropy of a lattice-hole model. ΔS is obtained by a substitution of the equilibrium values of ξ (Eq. (5.75)) into Eq. (5.65). The $(pV_0/\Delta E_0)$-values are specified in the figure by giving their values as a parameter to each curve

is found. V_0 in Eq. (5.73) is the volume per mole of the substance in the absence of holes in the system.

The equilibrium value of ξ is determined according to the general thermodynamic equilibrium conditions by minimizing the Gibbs free energy ΔG (compare Sect. 2.2.2). The equilibrium condition reads here

$$\left(\frac{\partial \Delta G}{\partial \xi}\right)_{p,T} = 0, \tag{5.74}$$

resulting in

$$\xi = \exp\left[-\frac{\Delta E_0(1-\xi)^2 + pV_0}{RT}\right]. \tag{5.75}$$

The temperature course of the equilibrium value of the order parameter $\xi(T)$ is shown in Fig. 5.4a for different values of the ratio $pV_0/\Delta E_0$ indicated by the respective numbers to the curves in the figures.

From the knowledge of ξ as a function of temperature not only the temperature dependence of the density of the considered model substance can be established, but also a number of additional quantities. Taking into account that ξ represents, in fact, the probability that at one of the neighboring sites of the molecule of the liquid on the virtual lattice a hole is found, the coordination number distributions in a liquid may also be calculated (Milchev and Gutzow (1981) [560]). In this way,

a characterization of the short range order, being an essential feature of the liquid state of matter, can be given, which, as already mentioned, is impossible to perform in pure lattice or cell models.

A substitution of the temperature dependence of ξ according to Eq. (5.75) into the expressions for the configurational contributions of thermodynamic functions allows one to specify the temperature dependence of these quantities. As an example in Fig. 5.4b the temperature dependence of the entropy is shown. It is seen that for the temperature dependence of the configurational part of the entropy an s-shaped curve is found indicating the existence of a first-order phase transformation. Such an s-shaped course is always obtained for values of the parameters in the range, given by the inequality

$$0 < \left(\frac{pV_0}{\Delta E_0}\right) < 0.05. \tag{5.76}$$

The temperature of the phase transformation can be determined by Maxwell's rule of equal areas.

A more detailed analysis of this transformation (see Milchev and Gutzow (1981) [560]), in particular, the calculation of the change in the free volume connected with the transition between the two states of the system, reveals that the different states of matter described by the model correspond to the liquid and the gas phases, respectively. The second possible type of phase transformations expected for liquids and being of particular importance for the understanding of crystallization and vitrification, respectively, melting, the liquid-solid transformation, is not reflected in the model considered. It is, in fact, well-known that lattice-hole models cannot give a straightforward description both of melting and crystallization. A possible way of incorporating the melting transition into the framework of lattice-hole models is discussed in the next section.

For the liquid branch of the curves, describing the configurational contributions to the thermodynamic properties of the model substance, the fraction of holes, i.e., ξ, is a relatively small quantity. In this case, ξ may be approximated starting with Eq. (5.75) by

$$\xi = \exp\left(-\frac{\Delta E_0^{\oplus}}{RT}\right), \qquad \Delta E_0^{\oplus} = \Delta E_0 + pV_0. \tag{5.77}$$

This expression was first derived by Frenkel (1946) [234] in minimizing ΔG but omitting the term $p\Delta V$ in Eq. (5.72). It means that not the appropriate thermodynamic potential, i.e., the Gibbs free energy, but the Helmholtz free energy F was chosen for the description of the state of the system. In dealing with liquids, this difference is of no significance. However, such an (erroneous) approach fails in the attempt to model the liquid-gas transition. By applying the condition $\xi \ll 1$ the thermodynamic functions of the liquid may be approximated as follows (see also Grantcharova and Gutzow (1986) [268]; Gutzow (1989) [305]).

For the entropy we get with a Taylor-series expansion of the logarithmic terms in Eq. (5.65)

$$\Delta S(T) \cong 3R\xi(T) \tag{5.78}$$

and with Eq. (5.77)

$$\Delta S(T) \cong 3R \exp\left[-\frac{\Delta E_0^{\oplus}}{RT}\right]. \tag{5.79}$$

As a particular case, if the existence of a melting point is assumed, Eq. (5.79) reads

$$\Delta S(T_m) = \Delta S_m \cong 3R \exp\left[-\frac{\Delta E_0^{\oplus}}{RT_m}\right] \tag{5.80}$$

and combining both latter equations the expression

$$\Delta S(T) \cong \Delta S_m \exp\left[\Xi\left(1-\frac{1}{\theta}\right)\right] \tag{5.81}$$

is obtained.[2] In Eq. (5.81), again, the introduced earlier reduced temperature $\theta = T/T_m$ (cf. Sect. 3.3) and the notation

$$\Xi = \frac{\Delta E_0^{\oplus}}{RT_m} \tag{5.82}$$

are used.

[2]Instead of Eqs. (3.53) and (3.54), Eq. (5.81) can be employed also as the starting point in order to determine the frozen-in values of the entropy in the glass transition. For the case of relaxation proceeding by an Arrhenius law, θ in Eq. (5.81) has to be replaced merely by θ_g as given by the Bartenev-Ritland equation, Eqs. (3.85)–(3.87). In contrast to the results shown in Fig. 3.7, here

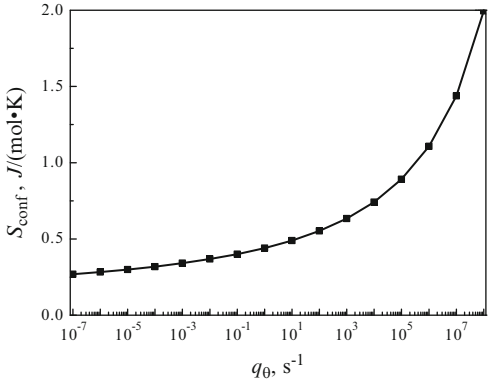

always finite values of the entropy are frozen-in for any value of the glass transition temperature in the range $T_g > 0$. Similar results are obtained as well if other relaxation laws have to be applied. An example is shown in the figure. Here relaxation is described by the Vogel-Fulcher-Tammann law ($q_\theta = d\theta/dt$; for the details see: Tropin et al. (2011) [856]).

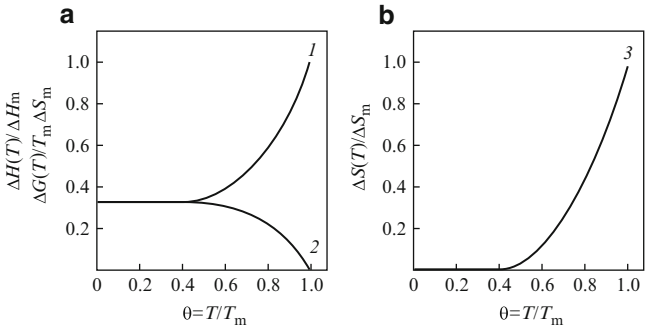

Fig. 5.5 Thermodynamic functions of under-cooled melts ((*1*) $\Delta H(T)$, (*2*) $\Delta G(T)$, (*3*) $\Delta S(T)$) calculated by a lattice-hole model as discussed in the text (Eqs. (5.81), (5.85) and (5.86)). In the calculations the value of the parameter $\Xi = 4$ has been used. This value is obtained from the enthalpy of evaporation of liquids applying Trouton's rule as discussed in more detail by Gutzow and Grantcharova (1985) [311] and Gutzow (1972) [294]

With this relation for the temperature dependencies of the configurational part of the entropy we may obtain analytical results for the configurational contributions to the other thermodynamic functions in a mean-field approximation by substituting the expressions for ξ and ΔS into Eqs. (5.69)–(5.73). In addition, from Eq. (2.14) we obtain from Eq. (5.81) for the configurational specific heat the relation

$$\frac{\Delta C_p(T)}{\theta \Delta S_m} = \Xi \exp\left[\Xi\left(1 - \frac{1}{\theta}\right)\right]\frac{1}{\theta^2}. \tag{5.83}$$

This relation can also be used in another direction, taking into account the following considerations. ΔC_p is primarily the difference between the specific heat calculated for the lattice-hole model and the pure cell model of the liquid. In this way, this quantity may also be expected to determine, to a large degree, the difference in the respective values of the liquid and the crystal. This obviously reasonable assumption allows us to calculate, in addition, the difference in the values of the Gibbs free energies and the enthalpies of the liquid and the crystal. From Eq. (2.23) we obtain, choosing as the reference temperature in the corresponding integral the value $T_0 = T_m$,

$$\Delta H(T) = \Delta H_m - \int_T^{T_m} \Delta C_p dT. \tag{5.84}$$

A substitution of Eq. (5.83) into this relation yields by a simple approximative integration (see Zeldovich and Myschkis (1965) [950]),

$$\frac{\Delta H(T)}{T_m \Delta S_m} = \left\{1 + \theta(\Xi - \theta)\exp\left[\Xi\left(1 - \frac{1}{\theta}\right)\right]\right\}\frac{1}{\Xi}, \tag{5.85}$$

$$\frac{\Delta G(T)}{T_m \Delta S_m} = \left\{1 - \theta^2 \exp\left[\Xi\left(1 - \frac{1}{\theta}\right)\right]\right\} \frac{1}{\Xi}. \tag{5.86}$$

With these equations the curves shown on Fig. 5.5 are drawn. As it can be seen from the figures, the curves are in a quite satisfactory agreement with the results outlined in Chaps. 2 and 3 (cf. Figs. 2.28, 2.24, 3.2 and 3.5). It turns out, that the values of $\Delta H(0)$ and $\Delta G(0)$ coincide as expected according to the Third law of thermodynamics. Moreover, a quite reasonable value for the zero-point enthalpy ($\Delta H(0) = (1/4)\Delta H_m$) is found. In the above results, however, the existence of a melting point T_m was introduced ad hoc via Eq. (5.84). In a more precise way the existence of a melting transition can be incorporated into the description as shown in the next section.

5.4.3 *Incorporation of the Melt-Crystal Transition into Lattice-Hole Models of Liquids*

As mentioned in the preceding section, in the framework of the discussed lattice-hole models of simple liquids the liquid-vapor transition may by described directly but not the crystal-melt transformation. In order to fulfil this gap the following procedure can be used, applied for the first time in a similar situation by Mott (1934) [576]. In this approach, the liquid is described by the model developed so far, while for the crystalline state an additional expression of the form given by Eq. (5.55) is proposed with appropriately chosen values of the parameters v_{fm} and E_0. Such a procedure corresponds to the application of Einstein's approximation for the calculation of the partition function of crystals, i.e., considering the crystal as a system of identical oscillators. The melting temperature is then determined by the point of intersection of the curves, representing the temperature dependencies of the Gibbs free energies of the model liquid and the crystal, respectively. As it became evident in the preceding section and as discussed in more detail by Milchev and Gutzow (1981) [560], such a point of intersection can be only found in a thermodynamically correct way, if the zero-point enthalpy of the model liquid and the model crystal differ, the zero-point enthalpy of the liquid being higher. In terms of the cell model applied, this statement means that different virtual lattices have to be used in describing the liquid or the crystalline states.

The difference in the zero-point enthalpy is accompanied by higher values of the volume of the liquid for $T \to 0$, i.e., we have to expect

$$\Delta H(T = 0) = \left(H_{liquid} - H_{crystal}\right)_{(T=0)} > 0, \tag{5.87}$$

$$\Delta V(T = 0) = \left(V_{liquid} - V_{crystal}\right)_{(T=0)} > 0. \tag{5.88}$$

The similarity in the differences of the values of the zero-point enthalpy and zero-point volumes is also supported by experimental findings concerning the

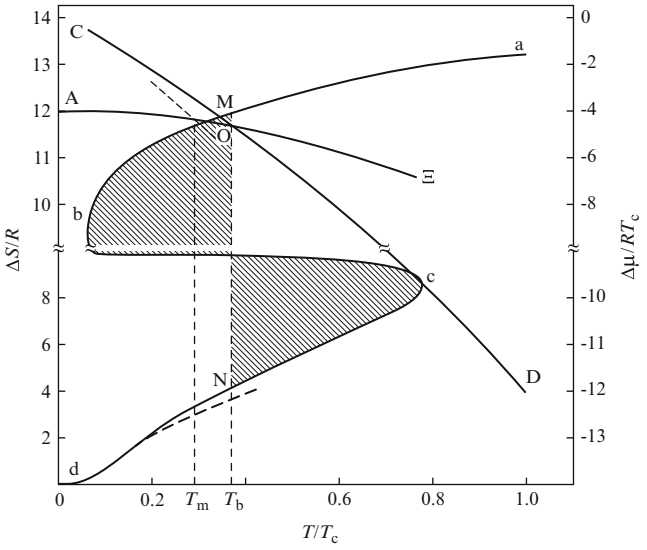

Fig. 5.6 Temperature dependence of the total entropy (S/R) (curve $(abcd)$) and of the chemical potential $(\Delta\mu/k_BT)$ of the liquid (AB), the vapor (CD) and of the crystal (EF). T_c and p_c are the critical values of pressure and temperature of the system. The *dashed curve* in the figure represents the entropy of the substance in the state of a perfect crystal using Einstein's approximation in the calculation of the partition function. By T_b the boiling point is indicated. With T_m the melting point is denoted, again, i.e., the temperature, where the $\Delta\mu$ curves of the liquid and the crystal intersect. In order to illustrate the position of the melting point more clearly the slope of the $\Delta\mu$-curve of the crystal has been increased by a factor five (For further details see Milchev and Gutzow (1981) [560])

temperature dependence of the density of liquids. Extrapolations of the density versus temperature curves of simple under-cooled liquids to $T = 0$ result in values of the zero-point density, which are about 3 % lower than the packing densities of a system of spheres (Bondi (1968) [89]), respectively, the packing densities of the crystalline state. This finding is related to the existence of different values of the energy of the two assumed virtual lattices: Higher energy values have to be assigned to the stretched lattice of the liquid.

It turns out that both statements as described by Eqs. (5.87) and (5.88), can be explained in terms of lattice-hole models by one and the same assumption, the introduction of different virtual lattices for each of the condensed states of the substance considered. It is difficult to suggest any realistic picture of the virtual lattice describing the structure of the fictive under-cooled melt in internal equilibrium at $T = 0$. However, the introduction of two such different lattices is essential, if both evaporation and melting are to be described in the framework of one and the same model. In Fig. 5.6 the temperature dependence of the entropy and

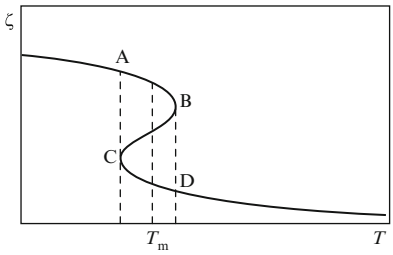

Fig. 5.7 Temperature dependence of the order parameter ζ introduced by Bresler (1939) [104]. In comparing these curves with the results shown in Fig. 5.4a note that ξ (and $1-\zeta$) describe, in fact, the order and ζ the disorder in the system

the chemical potentials is given for the model substance for all three states of matter according to an investigation performed by Milchev and Gutzow (1981) [560].

It turns out that in terms of lattice-hole mean-field models in their simplest form an adequate, at least, qualitative picture of the thermodynamic properties of stable and metastable undercooled melts, their crystalline and gaseous phases and the transformations in between them can be given. In application to the melting transition this approach is, of course, far from being a first-principles calculation. Nevertheless, these results give a useful theoretical picture for discussing crystallization, vitrification and stabilization of glasses.

5.4.4 Discussion of Some Further Developments

In further developments of lattice-hole models, additional order parameters have been introduced into the theory to describe the long-range order. In this way the possibility of a direct description of the melt-crystal transformation could be expected to be realized. One of the first attempts in this direction was performed by Bresler (1939) [104],who introduced, instead of ξ, a long-range order parameter ζ as

$$\zeta = (1-\xi)^z = \left[1 - \exp\left(-\frac{U'}{k_B T}\right)\right]^z, \tag{5.89}$$

where the energy of hole formation is given by

$$U' = U_0 + U_1\zeta. \tag{5.90}$$

The $\zeta(T)$-dependence, according to Bresler's proposal, is shown schematically in Fig. 5.7. Taking into account Fig. 5.4a, where ξ is depicted, it is seen that no qualitative improvement as compared with the results of the previous analysis is found. The sigmoid s-shaped dependence resulting from Eq. (5.89) has, again, to be interconnected with a liquid-vapor transformation. Moreover, since the way of introduction of the order parameter ζ as used by Bresler is more or less arbitrary this approach is today only of historical interest.

Another direction in developing lattice-hole models of liquids is connected with the work of Lennard-Jones and Devonshire (1939) [503]. These authors introduced two lattices, one crystalline-like and one liquid-like. However, their ΔS-curves do not have a s-shaped course and fail in this way to describe a phase transformation in the model: they correspond in fact to the ΔS vs T curve in Fig. 5.4b with $pV_0 = 0$. Due to this feature of their model and a number of ad hoc assumptions applied in the formulation of it, their investigation also has to be considered as only of historical interest (for a critical review see Frenkel (1946) [234]).

Another interesting approach is connected with the efforts of Altair and Fürth (see, again, Frenkel (1946) [234]; Moelwyn-Hughes (1972) [567]) to treat holes in liquids as really existing physical objects and to determine the internal energy and the heat of evaporation of liquids by calculating the work required for the formation of a hole of molecular dimensions in the liquid, assigning macroscopic values of the surface tension to it. This procedure is, however, open to criticism from various points of view and led to physically not meaningful results. From its basic assumptions similar to lattice-hole models are also the so-called broken bond models developed, in particular, by Angell and coworkers (see, e.g., Angell and Rao (1972) [15, 656]). In these types of models instead of the energy of hole formation the somewhat less definite concept of bond-breaking between neighboring particles is employed.

Other models like the dislocation theory of melting or the description of melting as a break-down of the modulus of elasticity are also only of historical interest in so far as they do not even give a qualitatively correct picture of this process. For other attempts to describe the structure of liquids the interested reader is referred to the respective literature (e.g., Frenkel (1946) [234]; Moelwyn-Hughes (1972) [567]; Hirschfelder et al. (1954) [366], Green (1952) [273]).

5.5 Statistical Models of Polymer Glass-Forming Systems

5.5.1 Introductory Remarks

Experimental evidence accumulated over the past 60 years shows that simple liquids in the sense introduced above, consisting of spherical monomers exhibiting no aggregation or polymerization processes, are rather the exception than the rule. Examples for simple liquids are provided by noble gases (liquid argon) and some organic liquids with a high symmetry of the molecules, e.g., tetrabromo methane. In most other liquids, as verified by X-ray analysis, infrared and Ramann-spectroscopy, with decreasing temperature processes take place which may be described in terms of aggregation, poly-condensation and polymerization.

As discussed already in more detail in Chap. 4, in organic molecular liquids aggregates and polymer-like chains are formed mainly due to H-bonding. Most typical cases in this respect are organic alcohols, oxycarbonic acids etc. H-bonding

may be verified in these cases commonly by infrared spectroscopy. A substantial experimental evidence on different processes of aggregation in under-cooled melts can be found in Kobeko's monograph (1952) [461], where a summary of classical results in this respect is given.

Even in metallic glass-forming melts, especially in the under-cooled melts of semi-metals like gallium, bismuth, antimony etc. detailed X-ray measurements and specific heat determinations have revealed the existence of dimers like Ga_2, Sb_2 and even higher-order aggregates. It was also mentioned in Chap. 4 that in organic glass-forming phosphates linear -P-O-P-O- structural elements are the main structural constituent. Similar processes of formation of branched and linear anionic chains are detected also in silicate melts and in other typical glass-forming substances (selenium, sulfur) by different methods of structural analysis.

In the preceding chapter it was already pointed out that some of the earlier investigators in glass-science even assumed that aggregation is a prerequisite of vitrification (remember, for example, the aggregation theories of vitrification of Botvinkin and Berger (Blumberg (1939) [85])). From classical physical chemistry of organic polymers it is well-known that a decrease in temperature is usually accompanied by an increase in the degree of polymerization. Hereby, the increase of the average chain-length is commonly connected with chain-branching and intra-chain bonding and may lead, finally, to the formation of a complete three-dimensional network. Compared with simple spherical primary building units of liquids a polymeric chain molecule is characterized by an increased number of possible configurations. Due to this peculiarity the existence of polymeric chains or of equivalent aggregates should considerably increase the total number of possible spatial configurations and, thus, the entropy of the system. In addition, an increase in the entropy is to be taken into account, connected with the formation of different types of structural elements and resulting in additional entropy of mixing contributions.

So far and subsequently in the following discussions, the notation conformation is used to describe the possible configurations of complex aggregative structural elements of the liquid. In general, these complex building units are formed by primary repeatable units of different types (atomic inorganic polymers like sulfur, monomeric units in organic polymers and in anionic chains). In these cases the statistical-mechanical treatment of the topological order, respectively, disorder in the liquid, which can be described in terms of free volume in lattice hole-models, has to be supplemented by a configurational statistics accounting for the different conformations of the complex building units of the melt. This can be done by generalizing the lattice-hole model outlined in the preceding sections. Different versions of Ising-type models are usually employed.

In application of Ising-models to the description of liquids the different states in the model are identified with A- (molecules of the liquid) and B-particles (holes). Models of this type were developed for a description of polymer solutions beginning in the 1930s (Flory-Huggins cell or lattice models (see Stewart (1955) [801] and also Fig. 5.8)). In the simplest form in the framework of this model conformational contributions to the thermodynamic properties may be described

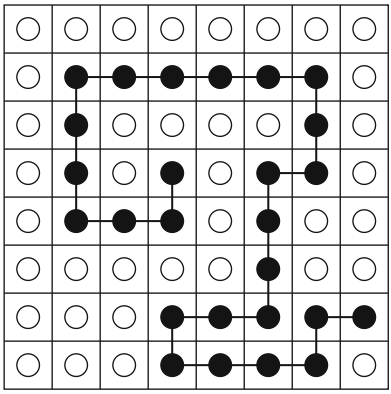

Fig. 5.8 One of many possible conformations of a flexible chain (*black points*) embedded in solute molecules (*white circles*) in a two-dimensional lattice

by using the classical mathematical solution of the problem of finding the number of possible configurations Ω of a chain consisting of n identical elements. For a two-dimensional chain ($d = 2$)

$$\Omega_{d=2} = 2^{n-1} \tag{5.91}$$

is found, while for a three-dimensional lattice ($d = 3$) with z nearest neighbors the relation

$$\Omega_{d=3} = (z-1)^{n-1} \tag{5.92}$$

is obtained. A survey of the classical literature on lattice models of polymer solutions may be found in the monographs by Flory (1943) [218], Volkenstein (1959) [891] and Prigogine (1957) [647].

Gibbs and DiMarzio (1958) ([251]; see also Gibbs (1960) [250]) were the first to apply Flory's approach to melts considering them as an ensemble of chains of different length and holes, introduced into the lattice. A similar model was also employed by Gutzow (1964) [291] and Milchev and Gutzow (1981 [560], 1982 [561]) to describe the zero-point entropy and the temperature dependence of the thermodynamic functions of glass-forming melts. In this model a possible change in the length of the chains as a function of temperature was incorporated.

In calculating the number of possible conformations of chain-like or more complicated primary units of the melt it is essential to take into account possible variations of bond-stiffness in dependence on the considered substance and thermodynamic parameters like temperature. In calculations of the stiffness of polymeric chains, a proposal made first by Flory is usually employed. It is assumed that an n-meric chain is constituted of f absolutely flexible and $(1-f)$ totally rigid bonds. If the rigidity of the chains is considered as a temperature independent quantity, then the paradoxical result is obtained that for temperatures approaching zero, negative values of the entropy for a system in a metastable equilibrium state are obtained (see Gutzow and Milchev (1981) [560]; Milchev (1983) [557]) in contradiction to

the Third law of thermodynamics. In this way it turns out that the stiffness of the polymeric chains has also to be considered as a temperature dependent quantity.

In this and similar situations, a very general premise in constructing statistical models and applying them to the description of thermodynamic properties of different systems has to be taken into account. It has to be checked always whether the models employed fulfil the requirements which follow from the three fundamental principles of thermodynamics. If this is not the case, the model has to be discarded. This criterion which statistical models have to fulfil was first formulated by L. Szilard (1929) [815] (see also J. von Neumann (1932) [897] and in application to idealized thermodynamic models by Vukalovich and Novikov (1952) [903]). Therefore, we may denote this principle as Szilard's principle; for a more popular discussion of Szilard's principle see Bennett (1987) [66]. In this way, more or less realistic lattice-hole models of under-cooled polymer or polymer-like melts can be developed, allowing us to treat three types of structural changes, namely (i) a variation in the free volume as a function of temperature, (ii) a change in the conformations of the complex units of the melt, (iii) a variation in length of the polymer chains with temperature. The second type of variation is connected with the temperature dependence of chain-stiffness.

5.5.2 Lattice-Hole Models of Polymer Liquids

In attempting to calculate the thermodynamic properties of a model polymeric liquid consisting of holes and polymeric molecules of different length and varying stiffness two approaches were applied, both originally developed by Flory. In the first approach, the probability of introduction of an i-th molecule into the lattice is examined, assuming that $(i-1)$ molecules already have been incorporated into it. In determining the possible conformations of the i-th molecule it has to be taken into account that a considerable amount of lattice places is already occupied by the molecules introduced before. Consequently, the number of mathematically possible configurations $(z-1)^{n-1}$ (compare Eq. (5.92)) has to be multiplied by a probability function depending on the ratio of already occupied to empty lattice places. This model approach is discussed in more detail in Flory's original publications (1942, 1949, 1956) [217, 219, 220] and his monograph [218] in application to polymer solutions. It is employed practically without modifications by Gibbs and DiMarzio (1958) [251] to polymer melts.

In the second of the approaches developed by Flory it is assumed that all the polymer molecules, monomeric units and holes are arranged in a first stage of the calculations to form a so-called super-chain. This super-chain is introduced then into the lattice considering it as a mathematical chain where all configurations are allowed (see Fig. 5.9). This process has to be repeated for all statistically different super-chains which can be formed out of the constituting the model system building units. After that an estimate is made to account for the effects due to possible multiple occupations of lattice sites. In making these estimates Flory used the

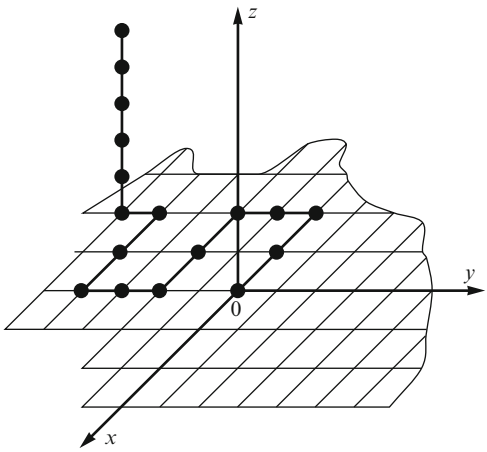

Fig. 5.9 Illustration of the second of the methods proposed by Flory for the determination of the number of possible configurations of polymeric solutions: Introduction of a polymer super-chain into a two-dimensional lattice

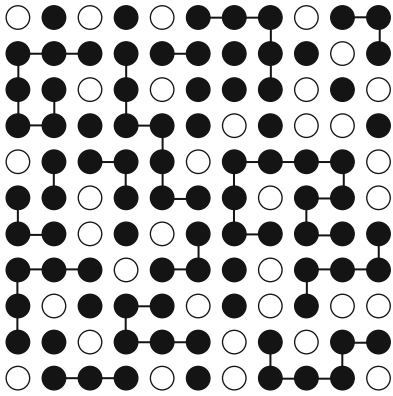

Fig. 5.10 Two-dimensional representation of a lattice occupied by holes, monomers and polymeric molecules

results of his first method. In comparing both approaches, it may be stated, that the second of the discussed methods gives an easier opportunity for the calculation of the mixing contributions of molecules of different types, i.e., in considering more complex glass-forming melts. Figure 5.10 gives a schematic two-dimensional illustration of the structure resulting when the filling-process is completed.

It has to be noticed that Flory's first approach has a serious short-coming not noticed for a long time. As pointed out by Milchev (1983) ([557]; see also Milchev and Gutzow (1981) [560]), Flory's original method in calculating the conformations of macromolecules gives negative values for the entropy at temperatures T tending to zero. Thus, it seems, as if according to Szilard's principle this method has to be abandoned as contradicting one of the fundamental laws of thermodynamics. Flory supposed, in fact, in his analysis that in the process of filling the lattice with polymer chains of different types a number of configurations cannot be realized because a certain percentage of the lattice sites are inaccessible, blocked by previously introduced molecules. In this way, Flory assumed in the model analysis a real

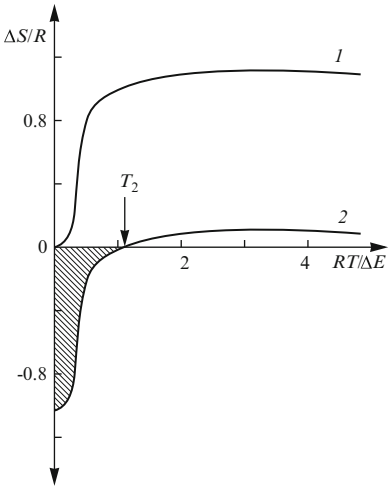

Fig. 5.11 Dependence of the configurational entropy ($\Delta S/R$) on temperature ($RT/\Delta E$) (in reduced units) for a polymer system constituted of chains of infinite length in a lattice without holes: (*1*) According to Milchev's proposal; (*2*) According to Flory's original model. The *dashed area* gives the temperature range, where Flory's model leads to negative values of the entropy in contradiction with the Third law of thermodynamics. At T_2 according to Gibbs and DiMarzio (1958) [251] a second-order phase transformation should occur

filling process of the primary units onto the lattice. This approach leads, in fact, to an underestimation of the possible number of configurations. Milchev (1983) [557] proposed an exact alternative procedure, guaranteeing that all the building units of the system (holes and polymer molecules) are introduced into the lattice. In this way results are obtained which are in agreement with the Third law of thermodynamics and Szilard's principle (Fig. 5.11). It has also to be noted that if the second super-chain method of Flory is used without his restrictive corrections (i.e., if the super-chain is introduced into the lattice like a mathematical chain according to Eq. (5.92), Gutzow (1962 [289], 1977 [298])), again, no violation of the Third law of thermodynamics is observed. An overestimation of the number of possible configurations is probably made in this way, which is, however, of no principal significance.

Going over to the derivation of the basic equations of a simple model of polymer melts we consider a three-dimensional lattice with a coordination number, z. It is assumed that, at a given temperature, from the $N + N_0$ lattice sites N sites are occupied and N_0 are vacant (or filled with holes). Again, the interaction energies between holes themselves and holes and molecules are set equal to zero. By $\bar{N}$ the total number of chain molecules is denoted characterized by an average degree of association $\bar{x}$. Denoting by N_i the number of chains with the length, x_i, we may introduce the average degree of polymerization, $\bar{x}$, as

$$\bar{x} = \frac{\sum_{i=1}^{\infty} x_i N_i}{\sum_{i=1}^{\infty} N_i}. \tag{5.93}$$

Consequently, we may write for the number of occupied places in the lattice

$$N = \bar{N}\bar{x}. \tag{5.94}$$

As in the case of simple liquids we assume, again that the number of monomers equals $N = N_A$, i.e., we are considering one mole of monomeric building units of the liquid (in German literature *Grundmol*). The individual monomeric building units in each chain are interconnected on average with $(\bar{x} - 1)$ intermolecular bonds. These bonds in the case of organic high polymers are of covalent nature. In other systems also H-bonding (organic molecular liquids), ionic bonding (inorganic anionic polymers) or metallic bonding (in under-cooled metals) play an important role.

Following Flory's approach it is assumed further that from the $(\bar{x} - 1)$ bonds of any polymer molecule, a fraction f is in an absolutely flexible state and that the remaining fraction of $(1 - f)$ bonds are in the absolutely rigid ground state. By using the second super-chain method from those described above, it can be shown (Gutzow (1962 [289], 1977 [298])) that the configurational entropy, calculated via Boltzmann's equation from the total number of distinct microscopic configurations, is given by several additive contributions, i.e.,

$$\Delta^{(conf)}S(T) = \Delta^{(\xi)}S + \Delta^{(\bar{x})}S + \Delta^{(f)}S + \Delta^{(c)}S. \tag{5.95}$$

In this equation $\Delta^{(\xi)}S$ describes the contributions to the entropy due to the free volume. This contribution is given by (compare Eq. (5.65))

$$\Delta^{(\xi)}S = -R\left[\frac{\xi}{1-\xi}\ln\xi + \frac{1}{\bar{x}}\ln(1-\xi)\right]. \tag{5.96}$$

Here, however, the relative free volume is determined by

$$\xi = \frac{N_0}{\bar{N}\bar{x} + N_0}. \tag{5.97}$$

The other contributions in Eq. (5.95) reflect (see Gutzow (1962 [289], 1977 [298]); Gutzow and Milchev (1981) [560]):

- A mixing contribution arising from the existence of chains of different length. This contribution may be written as

$$\Delta^{(\bar{x})}S = \frac{R}{\bar{x}}\left[\bar{x}\ln\bar{x} - (\bar{x}-1)\ln(\bar{x}-1)\right], \tag{5.98}$$

- A mixing contribution arising from the possible interchange of the places of f "excited" and $(1-f)$ "ground state" intermolecular bonds, described by

$$\Delta^{(f)}S = -R\left(1-\frac{1}{\bar{x}}\right)\left[f\ln f + (1-f)\ln(1-f)\right], \tag{5.99}$$

- A contribution accounting for the configurational possibilities of an $\bar{x}$-membered chain with a flexibility f, expressed in the form

$$\Delta^{(c)}S = R\left(1-\frac{1}{\bar{x}}\right) f\ln\left[\frac{(z-1)}{e}\right]. \tag{5.100}$$

It is interesting to note that the entropy ΔS is not determined by the specific form of the size distribution of the polymer molecules but only by the average characteristics of this distribution, expressed through the average degree of polymerization, $\bar{x}$.

For different processes of polymerization and poly-condensation, various size distributions have been established and verified experimentally by authors like Schulz (1936, 1937, 1940) [737, 738], Hosemann (1939) [380], Flory (1940, 1943, 1971) [216, 218, 221] and Stewart (1953, 1955) [801]. It can be shown that using any of these size distributions, one and the same equation Eq. (5.98) results for the entropy of mixing of polymer molecules of different sizes. From Eq. (5.98) it can also be seen that within the limits $\bar{x} = 1$ (simple liquid) and $\bar{x} \to \infty$ the entropy term $\Delta^{(\bar{x})}S$ vanishes. A maximum for this term is found for $\bar{x} = 2$. In this respect, it is of interest to recall that in some glass-forming metallic alloy systems, associates and aggregates with such a small average length do indeed dominate.

In addition to the entropy, the expression for the internal energy also has to be modified. Instead of Eq. (5.69) we may express the internal energy referring to one mole of monomeric units as

$$\Delta U(T) = U_0 N_0 + (U_1 f - U_2)\bar{N}(\bar{x}-1). \tag{5.101}$$

While the parameter U_0 describes, as earlier, the energy change connected with the formation of holes, U_1 denotes the energy required for the excitation of an absolutely rigid bond in the ground state. U_2 is a parameter connected with intermolecular bonding and variations in the degree of association. By substituting these expressions into Eq. (5.72), the Gibbs free energy of the system under consideration can be determined. Taking into account that we have three different order parameters ξ, $\bar{x}$ and f in this generalized model, for a determination of the equilibrium values of these quantities partial derivatives of the Gibbs free energy have to be calculated and set equal to zero for each of them. As the result of these calculations the equilibrium values of the structural order parameters of the system are obtained in the form

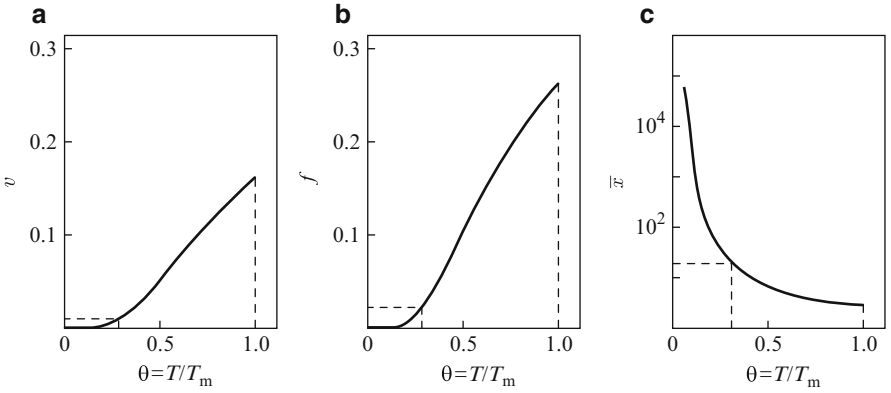

Fig. 5.12 Temperature dependencies of (**a**) the relative free volume, (**b**) the flexibility and (**c**) the mean degree of polymerization for a model melt in mean-field-approximation according to Gutzow (1979) [302]. With *dashed lines* the frozen-in values of the order parameters are indicated, corresponding to a vitrification temperature $T/T_m = 0.3$

$$\xi = \exp\left\{-\left[\frac{U_0^*}{RT} + (1-\xi)\left(1-\frac{1}{\bar{x}}\right)\right]\right\}, \tag{5.102}$$

$$f = \exp\left(-\frac{U_1^*}{RT}\right)\left[\left(\frac{z-1}{e}\right) + \exp\left(-\frac{U_1^*}{RT}\right)\right]^{-1}, \tag{5.103}$$

$$\bar{x} = 1 + \frac{1}{1-f}\left[(1-\xi)\exp\left(\frac{U_2^*}{RT}\right)\right]. \tag{5.104}$$

Here by the superscript (*) the values of the parameters U_0, U_1 and U_2 referred to one mole are specified.

In Fig. 5.12 it is illustrated, how the order parameters of a model system representing an under-cooled polymer melt vary in dependence on temperature. The respective curves are calculated using typical U_0, U_1 and U_2-values. Introducing these equilibrium values of the order parameters into Eqs. (5.96) and (5.98)–(5.100), the temperature dependence of the thermodynamic functions of the system can be obtained. Results from such calculations are given in Fig. 5.13a, b. A polymer-like model of under-cooled glass-forming melts similar to the one described above was also used by Gibbs and DiMarzio (1958 [251], 1960 [250]). Within this model the temperature dependence of the configurational entropy was calculated. It turned out that at temperatures below T_g a second-order phase transformation temperature T_2 is to be expected (cf. Fig. 5.11).

In considering these results of Gibbs and DiMarzio the following remarks have to be taken into account:

- Gibbs and DiMarzio used Flory's statistics in the original form. In order to avoid negative $S(T)$-values for temperatures approaching the zero of absolute

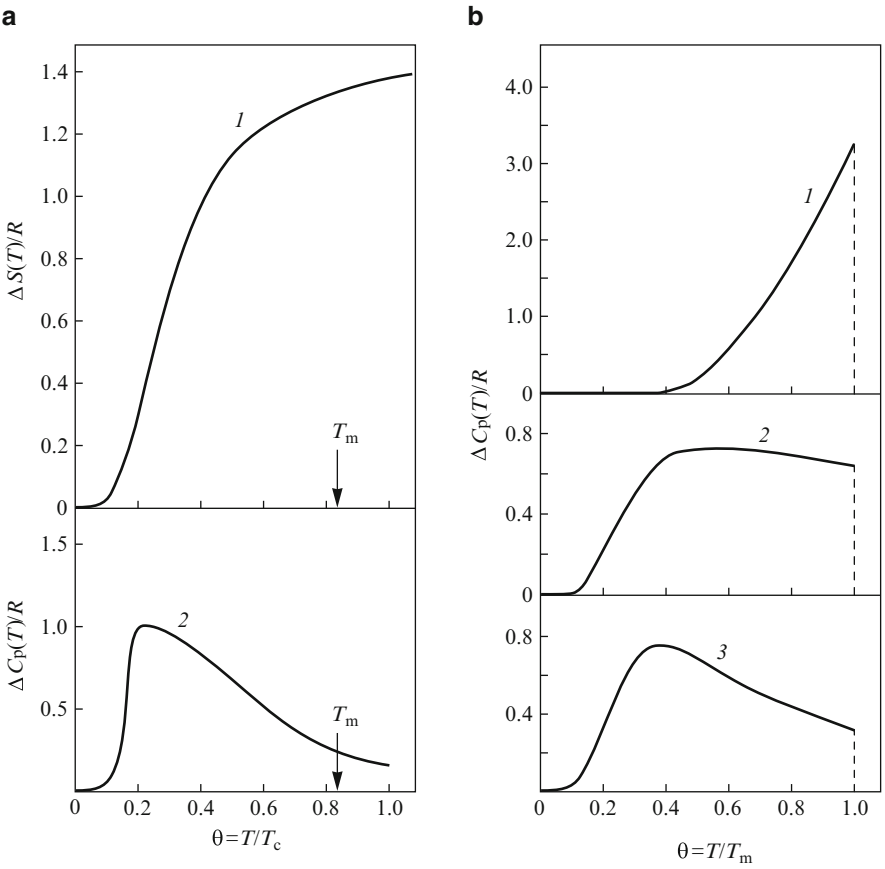

Fig. 5.13 (**a**): Temperature dependence of (*1*) the configurational entropy and (*2*) the specific heats of polyethylene (in reduced variables) calculated by Milchev and Gutzow (1981) [560] in the framework of a mean-field lattice model with energy constants reflecting the real system. (**b**): Temperature dependence of the specific heat difference ΔC_p determined by lattice-hole models in MFA-approximation for three model melts with different degrees of complexity by Petrov, Milchev and Gutzow (1996) [634]: (*1*) Simple liquid without polymerization or aggregation, (*2*) liquid with flexible linear living polymer aggregates, (*3*) liquids with very short aggregates resembling metal-like structures

temperature, a second low-temperature statistics was introduced in addition. In this way a peculiar point in the $S(T)$-curve occurs at $T = T_2$. It is seen that the existence of such a temperature T_2 and the possibility of a second-order phase transformation is obtained by Gibbs and DiMarzio to some extent artificially. The significance of this peculiarity in the $S(T)$-curves found by Gibbs and DiMarzio gave rise to prolonged discussions. A critical reappraisal of this subject can be found in papers by Gutzow (1977) [298].

- In Gibbs and DiMarzio's analysis only polymer systems with a very high degree of polymerization are considered. Further processes of aggregation including changes of polymer length are not investigated. However, for most glass-forming melts (see Chap. 4) such processes are of essential significance.

A thorough investigation of a variety of possible lattice-hole models and their features has been carried out by Gutzow (1979) [302] and more recently by Milchev (1983) [557] and Petrov, Milchev, and Gutzow (1994) [634]. By changing the values of the parameters U_0, U_1 and U_2 the structure and the thermodynamic properties of a great variety of glass-forming systems with differing structures (polymer-like, metallic, molecular glasses etc.) were investigated. The mean-field models described above in combination with Monte-Carlo simulation techniques proposed by Jarič (see Jarič, Benneman (1983) [404]; Jarič (1983) [403]) were used. The basic conclusions of the analysis can be summarized in the following way:

- The type of temperature dependence of the configurational contributions to the specific heat is determined to a large degree by the particular structure and the complexity of the building units of the model system. For simple liquids monotonically increasing concave ΔC_p-curves are found. However, if polymerization or aggregation processes are possible in the system then a ΔC_p-course with a maximum in the range $0 < T < T_m$ is generally observed. Moreover, in the range $T_g < T < T_m$ a dependence of the form $\Delta C_p =$ constant is found to be a good approximation. It turns out, consequently that measurements of the specific heats of real glass-forming systems can give information concerning the presence or absence of aggregation or polymerization processes in the melt. This approach resembles to some extent the method proposed by Tarassov, who tried to prove the existence of polymeric chains in solids also by measurements of the phonon specific heat (compare Sect. 4.6). The method described here has the advantage that it is not necessary, as in Tarassov's approach, to extend the measurements to temperatures near to absolute zero, which is a very tedious task from an experimental point of view. The analysis shows that all types of temperature dependencies of the specific heat which are observed experimentally can be modeled (cf. Figs. 2.17, 2.21, 3.2 and especially 2.18).
- The analysis of the temperature dependence of the entropy and of other thermodynamic functions shows that in the framework of mean-field theories a non-catastrophic approach to zero-entropy states is found without any indication that a second-order type phase transformation occurs. Usually the value $\Delta S = 0$ is approached for temperatures $(T/T_m) \approx 0.1 - 0.2$. In this way, computer modeling of polymeric liquids in the framework of mean-field lattice theories does not support the prediction, made by Gibbs and DiMarzio (1958) [251] and Gibbs (1960) [250], of a second-order phase transformation at a temperature T_2 below T_g.
- In applying Monte-Carlo simulations to lattice models containing flexible polymer molecules similar to those analyzed in the framework of mean-field approaches it was found in the same investigation that for certain model

structures very steep λ-like temperature dependencies of ΔC_p are observed. This result may be an indication of the possibility of the existence of an order-disorder transition at $T_2 < T_g$. It is caused by the ordering of semi-flexible polymer molecules with a temperature dependent flexibility. Further computer modeling and theoretical analysis is necessary to determine the nature of this process for which, however, no experimental evidence can be obtained since ΔC_p measurements below T_g give no information on the state of the fictive melt, but refer to the glass.

In discussing the results of the already mentioned and similar model calculations it has to be taken into account that both in mean-field-approaches as well as in Monte-Carlo simulations discrete lattices are used to describe continuous systems. This principal shortcoming of the models may significantly affect the conformational possibilities of the arrangement of the macromolecules as compared with real systems. Nevertheless, computer-modeling based on lattice models is at present the only way to prove or disprove theoretical expectations concerning the temperature dependence of the properties of glass-forming melts below the temperature of vitrification. In addition, the assumption of only linear aggregation processes may also be an oversimplification compared with real polymeric systems, where cross-linking and the formation of two- or three-dimensional structures is possible. In this sense, the application of models consisting of linear chains has to be considered only as a first step in examining processes of aggregation and polymerization and their influence on the thermodynamic properties of real glass-forming melts. Up to now no computer modeling of the process of vitrification for such complex polymer systems has been carried out, the efforts being concentrated mainly to the investigation of the temperature dependence of the thermodynamic properties of the considered system.

5.6 Configurational Statistical Determination of the Zero-Point Entropies of Glasses

5.6.1 Comparison of Theoretical and Experimental Results and the Correlation of the Entropy with the Structure of Glasses

In many respects the zero-point entropy of glasses ΔS_g is the focus where the problems of the structure, the thermodynamics and the statistical physics of the vitreous state converge to a single point. Values of the zero-point entropy greater than zero, measured experimentally, initiated the discussion concerning the nature of the vitreous state (see Chaps. 2 and 3). It was mentioned in the introduction that Albert Einstein was the first to foresee the possibility that for glasses and for solid solutions as states of constant (we would say: frozen-in) statistical disorder

zero-point entropies $\Delta S_0 > 0$ have to be expected. "*However, too little is known at present about the structure of glasses*", Einstein mentioned 1914 in the cited paper [188], "*in order to determine the possible value of their zero-point entropy*". It was also Einstein who proposed the procedure which has to be followed: The number Ω of thermodynamically distinct microstates of the system at $T \to 0$ has to be calculated and the entropy ΔS_0 has to be determined in accordance with Boltzmann's formula Eq. (2.32). The possibility that glasses may be an exception with respect to the applicability of the Third law of thermodynamics was also suggested by Lewis and Gibson (1920) [507] even before the major part of theoretical and experimental work clarifying the problem was performed.

Using Einstein's proposal first estimates of possible values of the zero-point entropy of solid solutions were given by Stern (1916) [798] and Schottky (1921) [735]. For binary solutions consisting of two types of particles with particle numbers N_1 and N_2 they obtained from

$$\Delta^{(1/2)} S(0) = k_B \ln \frac{(N_1 + N_2)!}{N_1! N_2!} \tag{5.105}$$

the following expression for the molar entropy

$$\Delta^{(1/2)} S(0) = R \ln 2, \tag{5.106}$$

provided the molar fractions of both components are equal. Similar $\Delta S(0)$-values were derived also for three-component solutions. Experimental verifications were soon found both for solid solutions as well as for molecular crystals (i.e., orientational glasses in the sense as discussed in Sect. 4.11; see Kaischew (1938) [416], Haase (1956) [338], and Levich (1954) [505]).

In a next attempt L. Pauling and R.C. Tolman (1925) [630] tried to estimate in a more general way the value of the zero-point entropy by an imagined evaporation-condensation process. The expression for the zero-point entropy of glasses was found by them to be of the form

$$\Delta S_g = R \ln a_g^{(o)}. \tag{5.107}$$

According to Pauling and Tolman "*the quantity $a_g^{(o)}$ may be regarded as the average number of ways in which a single molecule can be rearranged in the under-cooled liquid ... It is evident on the basis of this interpretation*", they continued, "*that $a_g^{(o)}$ will be a small number which increases as the complexity of the molecules increases*". It follows from this citation that Pauling and Tolman and even later – in 1939 – Fowler and Guggenheim [225] did not differentiate between under-cooled liquids and glasses; a clear distinction in this respect was made first, as mentioned in Chap. 2, by Simon (1931) [757]. However, the second part of their statement turned out to be prophetic.

A first detailed quantitative analysis of the possible values of the zero point entropy of glasses was performed by Gutzow (1962 [288], 1964 [291]). His analysis was carried out on the basis of lattice-hole models as discussed in Sect. 5.5. It was shown that the frozen-in entropy consists of several additive contributions reflecting

- The general topological disorder determined in the simplest case via the relative free volume ξ or from the relative occupied volume β as (compare Eq. (5.78))

$$\Delta^{(\xi)}S \cong 3R\xi \cong 3R(1-\beta_g), \qquad \beta_g = \frac{\rho_{glass}}{\rho_{crystal}}, \tag{5.108}$$

  where ρ_{glass} and $\rho_{crystal}$ are the densities of the glass and the liquid. Taking into account the β-values summarized in Table 2.5 ($\beta_g \approx 0.85 - 0.89$) typically $\Delta^{(\xi)}S \cong (0.4-0.6)$ R is found. For polymeric systems we have to use Eq. (5.96) instead of Eq. (5.78). For long chain molecules the second term in the brackets may be neglected and we obtain

$$\Delta^{(\xi)}S \cong -R\frac{\xi}{1-\xi}\ln\xi \cong R; \tag{5.109}$$

- The disorder of mixing of polymeric chains of different lengths. The highest value of $\Delta^{(\bar{x})}S$ is obtained for $\bar{x} = 2$, it equals (see Eq. (5.98))

$$\Delta^{(\bar{x})}S = R\ln 2. \tag{5.110}$$

  For systems with a degree of polymerization higher than oligomeric ($\bar{x} > 10$), this contribution is negligible;
- The disorder resulting from the different possible conformations of the chain molecules frozen-in at T_g and the exchange of excited and non-excited intermolecular bonds (see Eqs. (5.99) and (5.100)). In dependence on the value of the chain stiffness, f, the quantity $\Delta^{(f/c)}S = \Delta^{(f)}S + \Delta^{(c)}S$ varies in between

$$\left[0.1\ln\left(\frac{z-1}{e}\right) - 0.2\right] \leq \frac{\Delta^{(f/c)}S}{R} \leq \left[0.1\ln\left(\frac{z-1}{e}\right) - 0.1\right]. \tag{5.111}$$

  With realistic values of the coordination number z (i.e. for $z = 4$ and for $z = 12$) values in between 0 and 4R are found;
- The disorder resulting from different possible orientations. For linear molecules with two different possible orientations we get according to Eq. (5.106)

$$\Delta^{(or)}S = \mathrm{R}\ln 2. \tag{5.112}$$

It turns out that the overall configurational entropy ΔS_g cannot exceed, in general, a value of about (3 − 5)R.

Table 5.1 Comparison of theoretical estimates and experimental data for the zero-point entropy of glasses. The relative occupied volume β is calculated from the density data given in Table 2.5. The β-data for glycerol are taken from Fig. 2.28, for $NaPO_3$ from Gutzow (1970) [292]

Substance	β_g	$\Delta^{(theor)}S_g$	$\Delta^{(exper)}S_g$	Source for $\Delta^{(exper)}S_g$
SiO_2	0.83	0.51 R	0.45 R	Simon and Lange (1926) [760]
GeO_2	0.85	0.45 R	0.45 R	Nemilov (1976) [596]
BeF_2	0.84	0.47 R	0.55 R	Timura et al. (1975) [837] Nemilov (1976) [596]
$AlPO_4$	0.84	0.50 R		
$GaPO_4$	0.87	0.40 R		
P_2O_5	0.87	0.40 R		
B_2O_3	0.74	0.78 R	1.28 R	Weyl and Marboe (1967) [919]
As_2O_3	0.89	0.32 R		
GeS_2	0.89	0.32 R		
Se	0.89	0.32 R	0.35 R	Anderson (1937) [9]
Organic				
Linear polymers	0.89	0.32 R	(0.70–1.0)R	cf. Table 2.2
Vitreous				
Metallic alloys	0.9–0.95	0.30 R	(0.4–0.9)R	cf. Table 2.2
$NaPO_3$	0.99	0.03 R	1.3 R	Grantcharova et al. [268, 271]
Glycerol	0.98	0.06 R	2.3 R	Simon (1931) [757]
Bernal-Scott models				
Loose random packing	0.82	0.53 R		
Dense random packing	0.86	0.40 R		

Further it becomes evident that in agreement with the expectations of Pauling and Tolman a well-expressed correlation exists between this value and the complexity of the basic building units of the substance and the structure of the glass. For glasses where only one type of disorder dominates (simple non-associating glasses, orientational glasses) the highest possible value should not exceed R or (Rln 2) (compare Eqs. (5.109), (5.110) and (5.112)). A classical example in this respect are the network forming glasses (SiO_2, Ge_2, BeF_2, $AlPO_4$ etc.; see Gutzow (1962) [288]). As shown in Table 5.1 the theoretical estimates for this case are in good agreement with the experimental results as obtained first by Witzel (1921) [930] and Simon and Lange (1926) [760].

Based on the outlined derivations, Gutzow (1962 [288], 1964 [291]) predicted ΔS_g-values for BeF_2 and GeO_2, for which at that time experimental data were not known. In subsequent years the predictions were verified experimentally (compare Table 5.1 and the summary of experimental data given by Nemilov (1976 [596], 1977 [597])). Similar low values of ΔS_g are also found for glasses where only orientational disorder occurs (spin-glasses, frozen-in crystals (Jäckle (1981, 1986) [391, 392]; Johari (1980) [410])). In systems we denoted in Sect. 4.11 as Flory's glasses with perfect flexibility i.e. with ($f = 1$) a value $\Delta S_g \approx \mathrm{Rln}((z-1)/e)$ is to

be expected. Relatively low values of ΔS_g are found also for Se. For this substance the chain stiffness f has so low and the degree of polymerization $\bar{x}$ so high values that $\Delta^{(c/f)}S \approx 0$ holds. Of particular interest are also the estimates for $AlPO_4$ and P_2O_5, where values similar to those of SiO_2 have to be expected.

The relatively high ΔS_g-value for B_2O_3 may be considered as an indication that besides the topological also orientational and mixing contributions to ΔS_g have to be taken into account. In metallic alloy glasses mixing effects seem to be of particular importance. This result can be understood taking into account that metallic glasses are, indeed, binary or even ternary systems. As seen, moreover, glycerol and $NaPO_3$ represent exceptions from the estimates given above. They represent examples of systems where the crystal and the glass have qualitatively different structures and crystallization occurs via a reconstruction of the building units of the melt. These particular properties, also known from direct structural investigations, are reflected in Table 5.1 by β-values near to unity.

It is seen from the results outlined in Table 5.1 that with respect to the frozen-in configurational part of the entropy, lattice-hole models also allow us to derive simple (although approximative) relations giving us the possibility of calculating this quantity from known thermodynamic parameters of the system and, for this case, in particular from the relative occupied volume β. Table 5.1 shows, moreover, in accordance with Fox and Flory (1951) [226] that vitrification of simple liquids occurs in fact at nearly the same values of the free volume, corresponding in general, to the respective values of Bernal's and Scott's mechanical models of random packing of equally sized spheres. Additional support to this conclusion is given by molecular dynamic simulations of systems of hard spheres, showing that vitrification is connected with a volume densification of the system (see Kanno (1980) [429]; Gordon et al. (1976) [266]; Hoover and Ree (1968) [379]). In such simulations vitrification is shown to occur at a packing density $\Psi \cong 0.6$ which corresponds to $\beta \cong 0.89$.

5.6.2 *Further Attempts*

The further development of theoretical determinations of the zero-point entropy of glasses is characterized by a more specific account of the particular structure of the considered substance. First attempts in this respect were developed by Hicks (1966) [355], Beal and Dean (1968) [54] and Smyth (1971) [784]. Beal and Dean performed their calculations by analyzing the process of construction of a model of vitreous SiO_2, i.e., by counting the number of ways a tetrahedron can be added to a typical site of the disordered network, either

- To a site, where it is bound by its three corners (triple bonding, which can be realized by one way only),
- To a site, where it is bound by two corners (double bonding, which can be realized by one or two possibilities),

- To a site, where it is bound by only one corner (single bonding, which can be realized on average in four different ways).

As the result of the analysis the following expression for ΔS was obtained

$$\Delta S \cong R\left[\frac{\varepsilon^{\odot}}{2}\ln 1 + (1-\varepsilon^{\odot})\ln 2 + \frac{\varepsilon^{\odot}}{2}\ln 4\right] \cong R\ln 2 \cong 0.69R. \qquad (5.113)$$

The pre-factors to the logarithmic terms in Eq. (5.113) are proportional to the frequency of occurrence $\varepsilon^{\odot}$ of the respective type of bonding ($0 \leq \varepsilon^{\odot} \leq 1$). However, since approximately $\ln 2 \cong (1/2)\ln 4$ holds, the numerical result is widely independent of the actual value of this parameter. It is close to the data given in Table 5.1 for typical network formers. Beal and Dean identified this result with ΔS_g, although no proof was given for the validity of this assumption. With the same justification, an identification of this quantity with ΔS_m should also be possible.

An elaborated configurational statistics of disordered SiO_2-structures were developed by Smyth (1971) [784]. At a less advanced level a similar model was earlier proposed by Urnes (1961) [876]. Smyth calculated the total number of bonding of silicon and oxygen atoms for disordered structures having different coordination numbers with either silicon or oxygen ions. The configurational parts of the thermodynamic functions of silicate melts are determined in this approach by the presence and frequency of occurrence of different structural elements which are correlated with the composition (e.g., Na_2O/SiO_2, Si/O, etc.). However, no indication is given by the author of how the thermodynamic functions depend on temperature and other external parameters.

Theoretical attempts at a determination of ΔS_g were also carried out based on the Bernal-Scott model of liquids (see Sects. 4.5 and 4.6). One of these methods is used to calculate the number of possibilities a random sequential filling of mono-layers may be performed – by the so-called Matheson algorithm of computer modelling of random close packing (Matheson (1974) [537]; Woodcock (1976) [931]; Bonissent, Finney, Mutaftschiev (1979) [90]). In such approaches configurational entropies of the order of R are usually obtained, however, without giving a specification to what temperatures (T_g or T_m) this value should be assigned to (the packing density of the Matheson liquid equals 0.59; in the molecular dynamics studies of hard sphere systems carried out by Woodcock packing densities close to values reported by Scott are found; for the hard sphere model the glass transition is, indeed, characterized by values of ΔS_g near 1 R). Other developments are based on more or less realistic lattice-hole models of liquids as antipicated already by Cernuschi and Eyring (1939) [124]. As mentioned already, in the simplest version, when only the division between occupied and unoccupied lattice places (holes) is made, a great variety of possible local configurations can be found as illustrated in Fig. 5.14 (Milchev, Gutzow (1981) [560]).

In the framework of mean-field theories also the frequency distributions for the different configurations may be calculated (see Milchev and Gutzow (1981) [560] and Fig. 5.15). Assuming that each of the configurations shown on Fig. 5.14 represents a statistically independent structural unit the configurational entropy of

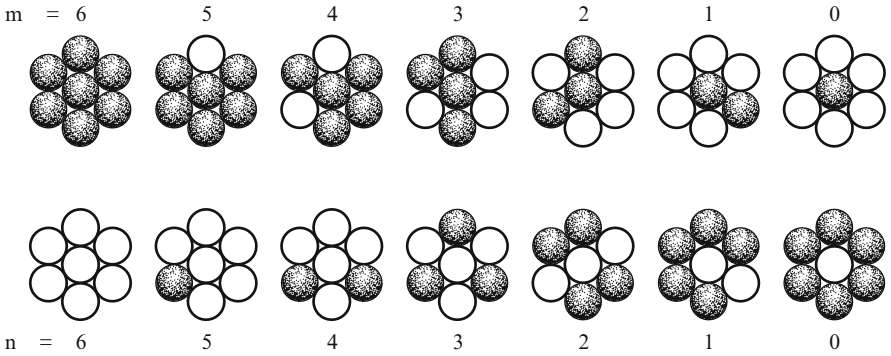

Fig. 5.14 The 14 possible local configurations in the first coordination sphere of a 2-dimensional lattice-hole model of simple liquids: Possible configurations in the vicinity of an atom (*top*) and a hole (*bottom*)

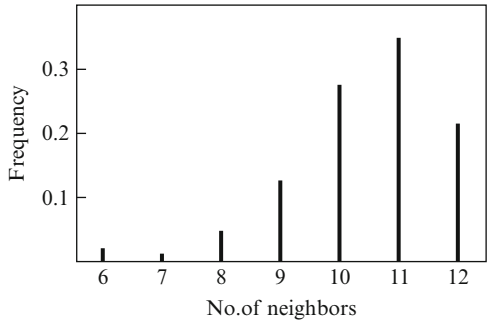

Fig. 5.15 Distribution diagram for atoms with different numbers of neighbors in the first coordination sphere of a liquid. The calculation was carried out in the framework of a mean-field approach. Parameter values were chosen referring to the properties of liquid argon in the vicinity of the melting temperature (Milchev and Gutzow (1981) [560])

the system may be calculated as a mixing entropy via

$$\Delta S^{(conf)} = \sum_i c_i \ln c_i . \tag{5.114}$$

With the distribution given on Fig. 5.15, a value $\Delta S^{(conf)}$ of the order 1.5 R is obtained close to the entropy of melting of liquid argon ($\Delta S_m \cong 1.7$ R).

By applying another method to describe the structure of liquids - in terms of the statistics of Voronoi polyhedra (see Fig. 4.16) – Barker et al. (1975) [36] also determined frequency distributions but this time of faces of the polyhedra with a given number of edges. The results obtained for temperatures near T_m are given on Fig. 5.16. Applying Eq. (5.114) again, values of the configurational entropy of the order $\Delta S^{(conf)} \cong 1.4$ R are found. Employing the empirical relation Eq. (2.129) we could expect a value of ΔS_g of the order

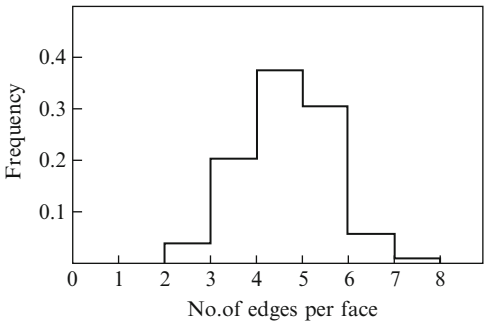

Fig. 5.16 Distribution diagram for the face frequency of Voronoi polyhedra modelling Bernal's hard sphere liquids at temperatures near T_m (After Barker et al. (1975) [36])

$$\Delta S_g \cong \frac{1}{3}\Delta S^{(conf)} \approx (0.35 - 0.4)R, \tag{5.115}$$

which agrees with alternative estimates of the frozen-in entropy of a Bernal-Scott's glass as shown in Table 5.1 and also with the results obtained by the mean-field approach.

In both of the discussed approaches – considering either different local configurations in the melt or different types of Voronoi polyhedra – the real system was replaced by a model system characterized by different structural units occurring with a defined frequency (distribution of structural units, cf. [149]). The configurational entropy was calculated then as the entropy of mixing. Such an approach can be used in very different, but of course, in part, semi-empirical ways for a description of disordered systems, in general. Let us suppose, for example that by some appropriate method, all the distances d_i between neighboring building units in an amorphous solid have been determined. For a simple mono-atomic system the mean interatomic distance $\overline{d_0}$ and the dispersion $\overline{D_0}$ can be determined then as (see, e.g., Ventzel (1969) [883])

$$\overline{d_0} = \int_{-\infty}^{+\infty} d_i f(d_i) d(d_i), \tag{5.116}$$

$$\overline{D_0} = \int_{-\infty}^{+\infty} f(d_i)(d_i - \overline{d_0})^2 d(d_i), \tag{5.117}$$

where $f(d_i)$ is the distribution function of interatomic distances. Assuming that the average coordination number in the system equals $\bar{z}$, the number of interatomic bonds for one mole of the substance equals $(\bar{z}N_A/2)$.

The entropy of mixing can be written then similarly to Eq. (5.114) as

$$\Delta^{(mixing)} S = -2\left(\frac{R\bar{z}}{2}\right) \int_0^{+\infty} f(d_i) \ln[f(d_i)]\, d(d_i). \tag{5.118}$$

Assuming a Gaussian distribution

$$f(d_i) = \frac{1}{\sqrt{2\pi\overline{D_0}}} \exp\left(-\frac{(d_i - \overline{d_0})^2}{2\overline{D_0}}\right) \tag{5.119}$$

we obtain (Ventzel (1969, p. 497) [883])

$$\Delta^{(mixing)} S = \frac{\bar{z}}{2} R \ln(2\pi\overline{D_0}). \tag{5.120}$$

For the crystal, atomic oscillations around the lattice sites cause also a relatively small dispersion in the lattice spacings. If we apply, consequently, the above equation both for the melt (characterized by $\Delta^{(mixing)}_{(m)} S$; $\overline{D_0^{(m)}}$) and the crystal ($\Delta^{(mixing)}_{(c)} S$; $\overline{D_0^{(c)}}$) we obtain

$$\Delta S^{(conf)} = \Delta^{(mixing)}_{(m)} S - \Delta^{(mixing)}_{(c)} S = \frac{\bar{z} R}{2} \ln\left(\frac{\overline{D_0^{(m)}}}{\overline{D_0^{(c)}}}\right). \tag{5.121}$$

A similar expression was derived for the first time – for the determination of the temperature dependence of the viscosity η – by Avramov and Milchev ((1988) [26]; see also Avramov (1990, 1991) [20, 21], cf. also [121]). It can be extended to the description of polymer melts, e.g., in the following way. Suppose in a system consisting initially of N_A building units (i.e., one mole) polymerization processes take place. As a result, $\bar{N}$ polymer molecules are formed with an average degree of polymerization $\bar{x}$ (compare Eqs. (5.93) and (5.94)). To each (monomeric or polymeric) molecule, two intermolecular valencies may be attributed. While in the initial state $2N_A$ valencies are present this number is reduced on average to $2N_A/\bar{x}$ in the polymerized system. The number of intramolecular bonds formed upon polymerization equals therefore $2N_A((\bar{x} - 1)/\bar{x})$.

Applying Eq. (5.114) we arrive easily at the already discussed result (Eq. (5.98)) determining the configurational entropy of a system with a given distribution of polymer chain molecules. In the same way the entropy of mixing of "ground-state" and "excited" intermolecular bonds can be calculated resulting in Eq. (5.99) as well as the conformational entropy term given by Eq. (5.100). Consequently, the full set of equations determining the configurational entropy of polymer melts may be calculated showing the strength of the described method.

Further extensions of the problems connected with the calculation of the zero-point entropy of glasses could include the analysis of the influence of defects, e.g., caused by radiation, of minor additives (Zakis (1984) [944]), micro-heterogeneities (e.g., as defined in the crystallite hypothesis (Gutzow (1964) [291]) and other possible forms of superstructure in glasses. Accounting for the logarithmic structure of the expression for the entropy of mixing, it is evident that the influence of such effects should be of minor importance except, may be, in cases like vitreous carbon,

where different structural units (amorphous and graphite like) exist in comparable amounts. The values of the entropy and of the thermodynamic functions, in general, are relatively insensitive to moderate structural changes. This effect is both a valuable advantage (when the problems of the overall structure are considered) as well as a disadvantage (since it does not allow us to decide, e.g., whether a superstructure exists or not).

In order to obtain definite results from Eq. (5.121) the values of the parameters $\overline{D_0}$ both for the crystal and the melt have to be known. One way of obtaining the required information in this respect would be to connect the ratio $(\overline{D_0^{(m)}}/\overline{D_0^{(c)}})$ with the broadening of X-ray diffraction peaks of amorphous solids as compared with the crystalline state (for details see Frenkel's monograph (1946) [234], in particular, the Prins model of structural diffusivity discussed there and also Fisher's book (1961) [212], where expressions connecting the thermodynamic properties of liquids with the radial distribution function are given). Another method could consist of expressing the mentioned ratio through the relative free volume. A detailed analysis of these problems is, however, reserved to future developments of both theory and experiment.

From the point of view of the general theory of information, entropy is a measure of the uncertainty of our knowledge of the state and the microstructure of the system (Shambadal (1963) [745]; Ventzel (1969) [883]). From such a point of view, in glasses, a residual entropy and thus a lack of information is frozen-in. An under-cooled melt corresponds to a state of temperature dependent increased informational disorder, glasses are systems with a frozen-in degree of structural information and crystals are the condensed state of matter with the highest possible degree of structural information. Stabilization of a glass is, in this sense, a process in which states with a higher degree of structural information are reached. Similarly, crystallization represents an evolution leading from states of informational uncertainty to a state with full structural information.

5.7 Specific Heats of Glasses at Ultra-low Temperatures

In discussing his own results on the C_p-measurements of SiO_2-glass Witzel (1921) [930] mentioned that there is the hypothetical possibility that below hydrogen temperatures (corresponding to the lowest temperatures 9 K reached by him) an unexpected change in the specific heats could occur, which could possibly lead to $\Delta S_0 \to 0$ at $T \to 0$ and reconcile the properties of glasses with the predictions of the Third law of thermodynamics. Simon's experiments (see Simon and Lange (1926) [760]) which were performed down to helium temperatures (4 K) seemed to exclude such a possibility.

Many years later it turned out, however that at ultra-low temperatures (below 1 K) in amorphous solids, in fact, a dramatic rise of C_p can be observed as compared with the respective value for the crystal. One of the first substances where such effects

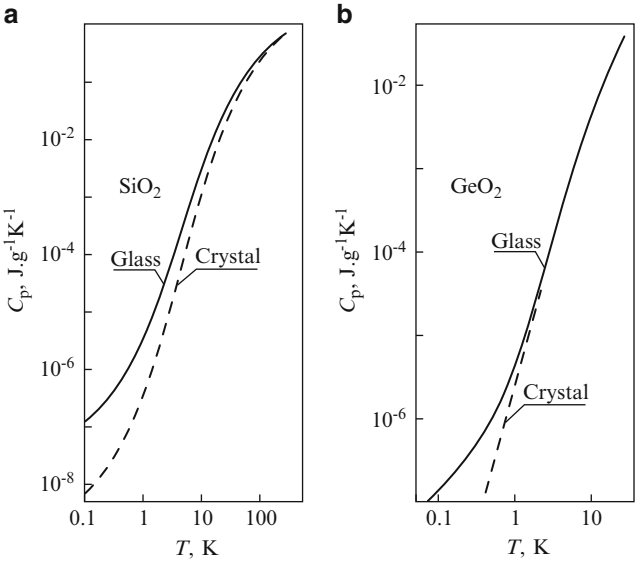

Fig. 5.17 Temperature dependence of the specific heats of (**a**) SiO_2 and of (**b**) GeO_2 at ultra-low temperatures in logarithmic coordinates. *Full lines*: Experimental data for the specific heats of the substances in the amorphous state; *dashed curves*: Experimental data for the specific heats of the crystalline phase (According to Zeller and Pohl (1971) [951])

were detected was, again, SiO_2; many others followed (see Zeller and Pohl (1971) [951]; Johari (1992) [411]). An illustration is given on Fig. 5.17. This anomaly cannot be explained in terms of classical models of phonon contributions to the specific heats.

An interpretation turned out to be possible, however, via a model of phonon assisted quantum mechanical tunneling formulated by Anderson et al. (1972) [12] and Philips (1972) [635]. According to the mentioned authors in amorphous solids localized groups of atoms are frozen-in which at ultra-low temperatures tunnel between two ground states of nearly the same energy. It turned out (see Johari (1992) [411]) that the ultra-low temperature rise of C_p is possible only in amorphous structures, it depends on the conditions of vitrification in a way similar to the dependence of the temperature of vitrification on cooling rate. It can be shown, however that the ultra-low temperature change in C_p does not affect the value of the zero-point entropy measurably. After integration over the small temperature range even a considerable change in C_p is not sufficient to result in significant variations of the thermodynamic functions of the system.

Another anomaly typical for vitrified silica glass is the negative value of its coefficient of thermal expansion α for temperatures below approximately 190 K. This negative value of α is retained down to $T \to 0$. It can be explained in terms of classical statistical physics as the result of a change in the mode of harmonic oscillations below the mentioned temperature. A thorough discussion of this effect

and a summary of the literature may be found in Novikova's monograph (1964) [607].

Further, it is interesting to note that crystalline quartz samples, totally amorphisized by heavy doses of neutron bombardment, display both anomalous effects. This result is an additional confirmation of the possibility of transforming crystals into a glass by heavy radiation damage (see also Samwer and Ettl (1994) [682]). In analyzing this process, it is to be taken into account that under neutron irradiation along the neutron tracks in the crystal temperature changes of up to 10,000 K are to be expected. In this sense the seemingly anomalous transformation quartz → glass is indeed a transformation which has to be described as a sequence crystal → superheated melt → quenched glass.

5.8 Atomistic Approach to the Kinetics of Stabilization

Lattice-hole models have been used also in different applications for the description of the properties of vitrified glass-forming melts and of the process of vitrification itself. Historically, the first attempt to describe from a microscopic point of view processes of vitrification of glass-forming melts was made by Alfrey, Goldfinger and Mark (1943) [8], who considered a glass as a lattice-hole system with a frozen-in number of holes. In a similar approach, Wunderlich (1960) [934] employed lattice-hole models of simple liquids for the calculation of the specific heats, while Hirai and Eyring (1958 [364], 1959 [365]), Bartenev (1966) [45], Bartenev et al. (1969) [49], and Sanditov and Bartenev (1982) [683] applied such models for an analysis of the viscosity and, in general, of the rheological properties of glass-forming melts.

Free-volume approaches for understanding the viscosity of liquids go back to Batchinski (1913) [50], who drew attention to the fact that the viscosity of liquids is determined primarily not by temperature but by the free volume of the liquid. Batchinski's suggestion turned out to be of great heuristic significance as will be elaborated in more detail in Chap. 12.

In the present section, we will restrict ourselves to a discussion of the atomistic interpretation of stabilization processes in the simple form given in Chap. 3 from a macroscopic point of view. As the order parameter, again, ξ is considered, describing the effect of free volume on the properties of the glass-forming melt. The freezing-in process in terms of the applied model is equivalent to a fixing of the number of holes, respectively, of the value of ξ. We will employ the notations as introduced in Chap. 3.

According to the already discussed lattice-hole model of simple liquids, the equilibrium value of the order parameter $\xi^{(e)}$ can be approximated for $T < T_m$ by Eq. (5.77). This approximation is valid since, in the considered temperature range $T < T_m$, the order parameter ξ does not exceed 0.05 ($\xi \ll 1$), (see also Hirai and Eyring (1958 [364], 1959 [365]); Dobreva and Gutzow (1994 [176])). The configurational contributions of the holes to the thermodynamic functions of simple liquids may be then written (compare Eqs. (5.69)–(5.71) and (5.73)) as

$$\Delta U \cong \Delta E_0^{\oplus} \xi, \tag{5.122}$$

$$\Delta V \cong V_0 N_A \xi, \tag{5.123}$$

$$\Delta H \cong (\Delta E_0 + pV_0)\xi, \tag{5.124}$$

$$\Delta G \cong \left[(\Delta E_0 + pV_0)\xi + RT \left(\ln(1-\xi) + \frac{\xi}{1-\xi} \ln \xi \right) \right]. \tag{5.125}$$

Suppose, the system is frozen-in at a temperature of vitrification $T^* \approx T_g$. The frozen-in structural parameter ξ can be expressed in the form

$$\xi = \exp\left[-\frac{\Delta E_0^{\oplus}}{RT^*} \right]. \tag{5.126}$$

With Eqs. (5.80) and (5.126) we may write

$$\ln\left(\frac{\xi}{\xi^{(e)}} \right) = \frac{\Delta E_0^{\oplus}}{RTT^*}(T^* - T). \tag{5.127}$$

By a Taylor-expansion of the logarithmic term the relation

$$\ln\left(\frac{\xi}{\xi^{(e)}} \right) = \ln\left(\frac{\xi^{(e)} + (\xi - \xi^{(e)})}{\xi^{(e)}} \right) \approx \frac{\xi - \xi^{(e)}}{\xi^{(e)}} \tag{5.128}$$

is obtained and applying the approximations ($T \sim T^* \sim T_g$)

$$\frac{\xi - \xi^{(e)}}{\xi^{(e)}} \approx \frac{\Delta E_0^{\oplus}}{RT_g^2}(T^* - T) \tag{5.129}$$

is found. It turns out that for relatively small deviations from the respective metastable equilibrium $\Delta\xi$ is indeed a linear function of $(T^* - T)$, as assumed by the phenomenological approach as developed in Chap. 3. However, in knowing the more exact relations connecting T^* and ξ it is possible, now, to give an estimate of the region of applicability of the linear approximation.

For silicate glasses, stabilization processes take place at temperatures 40–50 K below T_g. T_g is of the order $T_g \approx 1{,}000$ K. For organic glasses $\Delta T = T^* - T$ is of the order 10–20 K with values of T_g about 400–500 K. It turns out that for both cases, above given linear relation is a quite accurate approximation. The thermodynamic driving force for processes of stabilization, proceeding at a temperature T, may be expressed for the considered case as

$$\Delta G_s = \Delta G(T, \xi) - \Delta G(T, \xi^{(e)}). \tag{5.130}$$

A Taylor-expansion of the logarithmic terms in $\Delta G(T,\xi)$ in the vicinity of $\xi^{(e)}$ (cf. Eq. (5.125)) including second-order terms results in

$$\Delta G = (\Delta E_0 + pV_0)(\xi - \xi^{(e)}) + (\xi - \xi^{(e)})RT \ln \xi^{(e)} + \frac{RT}{2\xi^{(e)}}(\xi - \xi^{(e)})^2. \quad (5.131)$$

Taking into account Eq. (5.77) the terms linear in $(\xi - \xi^{(e)})$ vanish and Eqs. (5.130)–(5.131) yield

$$\Delta G_s = \frac{RT}{2}\xi^{(e)}\left(\frac{\xi - \xi^{(e)}}{\xi^{(e)}}\right)^2. \quad (5.132)$$

With this equation the second-order derivative $(\partial^2 \Delta G_s/\partial\xi^2)$ can be calculated which occurs in the equations of the phenomenological theory of stabilization derived in Chap. 3 (cf. Eqs. (3.120)–(3.121)). As the result one obtains

$$\left(\frac{\partial^2 \Delta G_s}{\partial \xi^2}\right)_{\xi \to \xi^{(e)}} \approx \frac{RT}{\xi^{(e)}}. \quad (5.133)$$

With this expression an atomistic interpretation of the relaxation time τ defined with Eq. (3.121) may be given as

$$\tau = \frac{\xi^{(e)}}{D}, \quad (5.134)$$

where by D the diffusion coefficient of the considered process of structural reorganization is denoted as defined by Eq. (3.116). Moreover, with Eq. (3.122)

$$\frac{d\xi}{dt} = -D\frac{(\xi - \xi^{(e)})}{\xi^{(e)}} \quad (5.135)$$

is found. Thus, the rate of change of ξ is proportional to the mobility coefficient D and the relative deviation of the order parameter ξ from its equilibrium value $\xi^{(e)}$. Moreover, taking into account the linear relationship Eq. (5.129) Tool's equation (Eq. (3.129)) is obtained as the result of the present atomistic approach.

With $\Delta C_p = T(\partial \Delta S/\partial T)$ or Eq. (3.19) we obtain

$$\Delta C_p = T\left(\frac{\partial \Delta S}{\partial \xi^{(e)}}\right)\frac{d\xi^{(e)}}{dT} \quad (5.136)$$

and

$$\Delta C_p = \frac{(\Delta E_0^{\oplus})^2}{RT^2}\xi^{(e)}. \quad (5.137)$$

A substitution of Eqs. (5.137) and (5.129) into Eq. (5.132) directly gives Eq. (3.141), again. Thus, a comparison with the results obtained by the phenomenological considerations outlined in Chap. 3 shows an expected agreement with the atomistic approach. Moreover, some of the parameters introduced phenomenologically get

a microscopic interpretation. A first attempt at giving an atomistic interpretation of stabilization phenomena was made in the above terms by Dobreva and Gutzow (1994) [176].

It can be verified in this way that in the framework of the simple atomistic model analyzed, it is possible to calculate some of the constants introduced earlier phenomenologically. We have, however, to take into account that the model employed is, in fact, a very crude description of real glass-forming melts. Thus, if we use more sophisticated models, quantitative corrections can be expected. The simple model considered also has a principal disadvantage. It cannot give, as with any two-level model of liquids with only two possible states of a lattice site and one activation energy, a description of memory effects in relaxation processes of glasses. For a quantitatively more correct description and an incorporation of such qualitatively new features, models of the type discussed here for polymer liquids are required, where three different activation energies are introduced describing hole formation, chain flexibility and association.

5.9 Model Statistical Treatments of Vitrification

The first attempts to describe the process of vitrification in molecular terms were made by Tammann (1922 [818], 1933 [820]), Botvinkin (1938) [94], Berger (1930) [68], and Alfrey, Goldfinger, and Mark (1943) [8]. Tammann connected vitrification with the freezing-in of molecular motion in the liquid, in particular, with the inhibition of the rotation of molecules. This decrease of the degree of rotational mobility should result, according to Tammann, in the discontinuity of the specific heat at the transformation temperature, T_g. Botvinkin and Berger supposed that, at T_g, temperature dependent processes of aggregation result in the formation of an infinite network which they assumed to be equivalent to the formation of the glass. Similar aggregative, polymeric or micellar approaches in vitrification can be found also in other earlier work in glass science (see e.g., Blumberg (1939) [85]). Alfrey, Goldfinger, and Mark (1943) [8], as already mentioned, considered vitrification as a freezing-in process of the fraction of holes in a lattice-hole model. The same assumption was adopted also by Hirai and Eyring (1958 [364], 1959 [365]).

The derivations outlined in the preceding sections in the framework of lattice-hole models show that, in general, the ideas discussed historically (freezing-in of free volume, inhibition of molecular motion due to increased molecular stiffness, formation of polymeric structures) are indeed of importance in vitrification. An illustration is given in Fig. 5.12. The steep variation of the three structural order parameters ξ, f and $\bar{x}$ with decreasing temperature dramatically increases the viscosity of the system and the time of molecular relaxation. Thus, it may cause vitrification. In vitrification, as indicated in the same Fig. 5.12, constant values of the structural order parameters are frozen-in. At present, however, it is difficult to decide, which of above discussed processes is the dominant one.

The first attempts to describe the kinetics of vitrification in molecular terms were made by Bartenev (1951) [44]. In the derivation of his equation the assumption is made that self-diffusion and relaxation in the under-cooled vitrified melt are determined by a single activation energy. Thus with the assumption that vitrification takes place at $\tau \approx \Delta t$ (time of observation) the Bartenev-Ritland equation can be easily derived, as shown in Sect. 3.6. A similar model, i.e., a liquid in which two states (a ground state and an activated state) of the buiding units are possible was used by Volkenstein and Ptizyn (1956) [892] to derive in a more straightforward way the Bartenev equation (given by Eq. (3.85)). In the literature (Mazurin (1986) [543]) this derivation is denoted as the starting point of the molecular kinetic theory of vitrification. Further developments and ideas connecting more complicated rheological behavior in vitrification and qualitative ways of explaining the kinetics of vitrification and especially of stabilization (the so-called stretched exponential formula for relaxation of glass-forming systems, see Chap. 12) may also be found in Mazurin's monograph (1986) [543].

As already mentioned, two-level models cannot give an explanation of memory effects in the rheology of glasses and in their behavior on annealing. This is the reason, why neither the Volkenstein-Ptizyn model nor the phenomenological treatment applying one activation energy can describe the complicated behavior of real organic and inorganic polymer glasses when they are quenched to different temperatures and are exposed afterwards to different heat treatments. In this respect, a significant step forward was made in a recent publication by Avramov and Milchev (1984) [25], in which a three-level model was used in order to obtain at least a qualitative description of memory effects in the rheology and the thermal behavior of glasses in molecular terms. Although a third level is introduced by these authors in a somewhat formal way the Avramov-Milchev model gives an indication of the necessary directions of further developments.

Of particular interest is also a new approach in the microscopic description of vitrification developed in a series of papers by Götze (1985) [261], Bengtzelius, Götze, and Sjölander (1984) [65], and Bengtzelius and Sjögren (1986) [64]. In this approach the dynamics of vitrification is described from first principles governing molecular processes and relaxation in condensed systems. It is shown that the solution of certain non-linear equations for the correlation functions of the liquids exhibits anomalies which coincide qualitatively with those known from the liquid-glass transition, described in Chaps. 2 and 3. It turns out that from such a general point of view, the liquid-glass transition can be understood as a dynamic transformation of many-particle systems from ergodic to non-ergodic behavior. Although in this approach a number of approximations and simplifications are used (for example, only one-component systems are considered) it seems also to be a fruitful direction of further research in a generalized description of vitrification processes. For a somewhat different approach and an overview on attempts of a theoretical description of the structure of substances in the condensed state including glasses see also Turski (1989)[868].

5.10 Conclusions

The results of the preceding sections show that even relatively simple lattice-hole models may give a qualitatively correct description of the temperature dependence of the thermodynamic properties of glass-forming melts, of the process of vitrification and stabilization of glasses. As mentioned in the introduction to this chapter, lattice-hole models were applied preferably, because they may be derived from the general concepts of statistical physics. Hereby, the nature of the approximations used is relatively clearly seen and also the directions of possible improvements. This is also the reason why we have used lattice models for Monte-Carlo simulations of polymer melts as first done by Jarič (1983) [404].

It has also to be noted that the molecular approaches in the description of glass-forming systems are at their very beginning (for a recent overview on atomistic modeling of polymeric systems see Monnerie and Suter (1994) [573]). This is the part of glass-science, which, when compared with other theoretical aspects of the description of the vitreous state (structure, thermodynamics, theory of nucleation and crystallization, rheology), seems to be at the lowest level of development. However, attempts in this direction reap the rewards accruing from any innovatory investigation of a scientific problem: Here the efforts of the interested scientists can still be of utmost significance and new ideas can bring the benefit of unexpected results. Nevertheless, it seems also that the time has come to bring to an end the kaleidoscopic generation of new atomistic models of liquids and glasses. Any development which is not based on the general principles of statistical physics and which cannot be derived by calculating the partition function of the system has little chances of success.

Very interesting results can be expected from computer simulations (Monte-Carlo and molecular dynamics) with the intention of studying the kinetic and structural effects in liquid-glass transitions by varying the cooling rates (see, e.g., Soules (1990) [787]; Lai et al. (1993) [491] and references cited therein). Taking into account the encouraging results obtained with the simplest but well-founded models it seems it would be fruitful to try to continue in the described way the development of simple models in order to test new ideas. In this connection we would like to recall the remarkable words of two of the greatest scientists working in the field of statistical physics – J.W. Gibbs and Ya.I. Frenkel. Gibbs noticed in 1881 in his letter to the American Academy of Arts and Sciences on the occasion of being awarded the Rumford medal (see Rukeyser (1964) [675]): "*One of the principal objects of theoretical research in any department of knowledge is to find the point of view from which the subject appears in its greatest simplicity*", while Ya. Frenkel wrote (see Frenkel (1947) [234]): "*The more complex the system is, the simpler its theoretical description should be . . . The theory should be required only to provide a correct interpretation of the more general characteristics and laws of the system . . . The theoretical physicist is in this respect like a cartoonist who does not reproduce all the details of the original, but simplifies it so as to throw*

into relief its most typical features only. Photographic precision can and should be required in the description of the simplest systems. The adequate theory of complex systems should only amount to a good caricature which emphasizes the properties that are most typical and ignores deliberately all the features which are less relevant."

Chapter 6
Kinetics of Crystallization and Segregation: Nucleation in Glass-Forming Systems

6.1 Kinetics of Phase Formation and Its Relevance for Glass Science and Technology

Processes of phase formation, of nucleation and growth of crystals are of particular significance in glass science and technology in many respects. First, the rate of crystallization of a glass-forming melt determines to a large degree the conditions under which a substance may be transformed into a glass. Thus, at least, a qualitative understanding of the factors determining the rate of formation of clusters of the new phase and their rate of growth is a prerequisite in glass-technology if the production of a homogeneous glass is desired (cf. S. Gutzow (1963) [290]). Second, in many cases the technological process requires an induced crystallization of glass-forming melts in order to produce a partly crystalline material, e.g., a glass-ceramic with a predetermined structure and properties. In this case, a prevention of crystallization is not the aim but the factors have to be known which allow one to undertake appropriate measures in order to reach an acceleration of crystallization by the introduction of certain dopants (nucleation catalysts: insoluble crystallization cores or surfactants) or other manipulations on the melt. In some cases the glassy matrix acts only as a carrier medium for substances dissolved and undergoing phase transformations in it. A classical example in this respect is the formation of photoactive silver chloride micro-crystals in photochromic glasses or the precipitation of colloidal metal particles in gold ruby glasses. Since for the desired applications of such glasses, in general, dispersions with distinct particle numbers and distributions of the newly evolving phase with well-defined characteristics have to be produced, the question has to be answered in which way the nucleation and growth process may be influenced in order to obtain the desired properties of the segregating phase. In other cases, crystallization of the major constituents of the glass-forming melt itself takes place either during its cooling to vitrification temperatures or after reheating of the already formed glass (devitrification).

In the production of glass-ceramic materials the melt and the glass are exposed to one or several more or less prolonged heat-treatments in temperature regions

I.S. Gutzow and J.W.P. Schmelzer, *The Vitreous State*,
DOI 10.1007/978-3-642-34633-0_6, © Springer-Verlag Berlin Heidelberg 2013

where maximal nucleation frequency and crystal growth rates are to be expected. This method of treatment guarantees an optimal or even maximal percentage of crystallization in the system. In contrast, in the synthesis of glassy metallic alloys or in vitrifying life in biological solutions, these temperature regions have to be passed with extreme cooling velocities (exceeding 10^2–10^6 Ks^{-1}) in order to prevent crystallization. In this way glasses with practically no crystallization centers in them can be obtained from melts with unusual or even exotic compositions. In most cases in glass-technology particular attention is devoted to the prevention of processes of liquid phase separation which is possible in multi-component glass-forming melts. Such processes cause undesirable effects in optical glasses. As mentioned by Morey (1938, [574], p. 29): *Devitrification is the chief factor which limits the composition range of practical glasses, and it is an ever-present danger in all glass manufacture and working, and takes place promptly with any error in composition or technique*.

However, there are also optical glasses and glass-ceramic materials, in which particularly important properties are obtained when, in the course of formation of the material, processes of controlled phase separation have taken place. In this way, processes of nucleation and controlled crystal growth belong to the most powerful methods of synthesis of fully crystalline, semicrystalline or vitro-crystalline materials, which are representatives of a new generation of materials. Many other examples in this respect could be given. The technological aspects determine, however, only one side of the interest in the kinetics of processes of phase formation and crystallization in glasses. On the other hand, glass-forming melts are a remarkable experimental model, as an example of metastable systems, in which processes of crystallization, of liquid phase separation and precipitation can be easily initiated and conveniently studied. This is another reason why glass-forming melts have been the source of a considerable experimental evidence on the kinetics and mechanisms of crystallization phenomena. The unusual thermodynamic properties of the vitreous state and the structural changes taking place upon crystallization of glass-forming melts have attracted the interest of theoreticians and experimenters. This interest represents an additional cause leading to numerous investigations in both theory and experiment in crystallization of glass-forming melts.

By both reasons in the following analysis, the basic ideas underlying the theoretical description of nucleation and growth of a newly formed phase, in general, and in melts, in particular, are outlined. In the first part of the discussion, we will try to formulate the basic prepositions, assumptions and postulates of the relevant theories and the most important results obtained in this field. In the derivation of the theoretical results only a sketch is given in some cases since a detailed analysis would go beyond the scope of this book. Nevertheless, for the interested reader it should be no problem to reestablish the details of the derivations based on the outline of the general ideas and the additional references given in the course of the discussion.

For a more detailed overview of basic ideas connected with phase formation processes and different applications see, e.g., the monographs by Volmer (1939) [894] and Hirth and Pound (1953) [368] as well as the review articles by Mc Donald

(1963) [548], Wegener and Parlange (1970) [914], Zettlemoyer (1969 [954], 1977 [955]), Feder et al. (1966) [198], Binder and Stauffer (1976) [83], Gunton et al. (1983) [283], Hodgson (1984) [374], and Mutaftschiev (1993) [585]. In Volmer's monograph (Volmer (1939) [894]) a remarkable outline is given concerning the historical development of the experimental investigations on phase formation and crystallization and on the concepts which led to their theoretical explanation.[1]

It was J.W. Gibbs who formulated the idea that in order to understand the experimental results accumulated in the eighteenth and nineteenth centuries on crystallization of under-cooled melts, on condensation and boiling – in all the different cases, when a new phase is formed – it is necessary and sufficient to account for the surface properties of the aggregates of the new phase emerging in the ambient system to explain the processes of phase transformation, at least, qualitatively. Gibbs arrived at this conclusion in the framework of the general thermodynamic treatment of surface properties of matter. This is the reason, why in the theoretical explanation of phase transformation processes, one has to start with an analysis of the thermodynamic properties of heterogeneous systems, in general, and specific properties of small clusters, in particular.

6.2 Thermodynamics and Nucleation Phenomena

6.2.1 Thermodynamics of Heterogeneous Systems

As already mentioned, the first comprehensive thermodynamic theory of heterogeneous systems was developed by J.W. Gibbs ((1875-1878) [249]; see also Rowlinson and Widom (1982) [672]; Schmelzer (1985) [689]; Ulbricht, Schmelzer et al. (1988) [874]). In the framework of Gibbs's theory the real system consisting of the homogeneous bulk phases and the interfacial region between the coexisting phases is replaced by an idealized model of two homogeneous bodies divided by a mathematical surface, representing the interfacial zone (Fig. 6.1). The deviations from additivity of the thermodynamic quantities are expressed through the

[1] A variety of new monographs devoted to the outline and extension of the classical concepts of nucleation and growth was published in the time since the publication of the first edition of the present book. Out of this spectrum, we would like to mention here, in particular, the following references: Kashchiev [439], Mutaftschiev [586], Milchev [558], Markov [534], Jackson [396], Kelton and Greer [450]; and a series of books edited by one of the authors (J.W.P. Schmelzer, Ed.): Schmelzer et al. [721], Schmelzer [695], Skripov and Faizullin [770], Baidakov [34], Ivanov [387], Slezov [773], Gusak et al. [286] as well as the series of workshop proceedings Schmelzer et al. [720]. For a current review on the state of affairs with respect to experimental and theoretical investigations of crystallization of glass-forming melts, see also the following articles: Fokin et al. [224], Schmelzer [696], Schmelzer [698], Zhuravlev et al. [958], Schmelzer [699], and Schmelzer and Schick [711]. Some particularly important to our point of view own contributions into this field are described briefly in the Chap. 14 and in some of the footnotes to this and subsequent chapters.

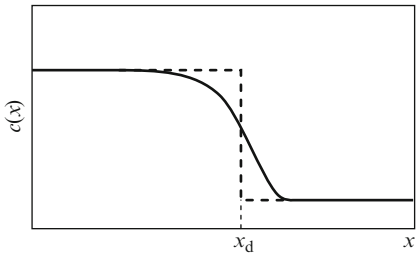

Fig. 6.1 Illustration of the basic idea used in Gibbs's approach in describing surface phenomena. By a *full curve* a possible real density profile $c(x)$ is shown, while the *dashed line* refers to Gibbs' idealized model consisting of two homogeneous parts, divided by a mathematical surface of zero thickness. Here, x_d denotes the position of the dividing surface, x being the spatial coordinate perpendicular to it

introduction of superficial quantities formally attributed to this mathematical surface (*postulate 1*). For the internal energy U, the entropy S and the mole numbers of the different components n_j we get, for example,

$$U = U_1 + U_2 + U_\sigma \,, \tag{6.1}$$

$$S = S_1 + S_2 + S_\sigma \,, \tag{6.2}$$

$$n_j = n_{j1} + n_{j2} + n_{j\sigma} \,. \tag{6.3}$$

The superficial quantities U_σ, S_σ and $n_{j\sigma}$ depend both on the properties of the interfacial region and on the choice of the dividing surface. The specification of the particular dividing surface, which we will use, is given somewhat later.

For the bulk contributions to the thermodynamic quantities, denoted by the subscripts (1) and (2), the common postulates and results of the thermodynamics of homogeneous phases hold (see Sect. 2.2), while the superficial quantities obey a relation similar to the fundamental equation (2.7) (*postulate 2*)

$$dU_\sigma = T_\sigma dS_\sigma + \sum_j \mu_{j\sigma} dn_{j\sigma} + \sigma dA + C_1 dc_1 + C_2 dc_2 \,. \tag{6.4}$$

Here A is the surface or interfacial area, σ the interfacial tension or specific interfacial energy, c_1 and c_2 are the principal curvatures of the considered surface element, while the parameters C_1 and C_2 describe the effect on the variation of the internal energy caused by changes of the curvature of the surface element. If one restricts, as we will do (*assumption 1*), the considerations to spherical interfaces, then Eq. (6.4) is simplified to ($c_1 = c_2 = c$, $C_1 + C_2 = C$)

$$dU_\sigma = T_\sigma dS_\sigma + \sum_j \mu_{j\sigma} dn_{j\sigma} + \sigma dA + C dc \,. \tag{6.5}$$

An integration of this equation results in

$$U_\sigma = T_\sigma S_\sigma + \sum_j \mu_{j\sigma} n_{j\sigma} + \sigma A \; . \tag{6.6}$$

A derivation of Eq. (6.6) and comparison with Eq. (6.5) yields the well-known Gibbs adsorption equation in the general form

$$S_\sigma d\, T_\sigma + A d\sigma + \sum_j n_{j\sigma} d\mu_{j\sigma} = C dc \; . \tag{6.7}$$

It was shown by Gibbs that for a definite choice of the dividing surface the parameter C in Eqs. (6.5) and (6.7) becomes equal to zero. This particular dividing surface is usually denoted as the surface of tension (Gibbs (1928) [249]; Rusanov (1978) [676]; Schmelzer (1985) [689]). Taking the surface of tension as the dividing surface, as we will do (*assumption 2*), Eqs. (6.5) and (6.7) are simplified to

$$dU_\sigma = T_\sigma dS_\sigma + \sum_j \mu_{j\sigma} dn_{j\sigma} + \sigma dA \; , \tag{6.8}$$

$$S_\sigma dT_\sigma + A d\sigma + \sum_j n_{j\sigma} d\mu_{j\sigma} = 0 \; . \tag{6.9}$$

The form of Eq. (6.6) is independent of the particular choice of the dividing surface.

In the subsequent applications it will be assumed (*assumption 3*) that the coexisting phases, e.g., a cluster of the newly formed phase and the ambient phase, are both in a state of an internal thermodynamic equilibrium while the system as a whole is not (e.g., the cluster may grow or shrink). This assumption resembles the preposition of a local thermodynamic equilibrium employed in the thermodynamics of irreversible processes (Haase (1963) [339]). To complete the thermodynamic description of heterogeneous systems a third postulate has to be introduced. Following an argumentation, expressed by Prigogine in the form "*a surface phase has no real autonomy, in general*" (Prigogine and Bellemans (1980) [648]; see also Defay et al. (1966) [161]) or by Rowlinson and Widom as "*we cannot measure or define unambiguously and independently the thermodynamic properties of the surface phase*" ((1982) [672]; see also Rusanov (1978) [676]; Schmelzer (1985) [689]), we assume that the intensive superficial quantities $\mu_{j\sigma}$ and T_σ are equal to the corresponding values of the phase with the higher density (*postulate 3*).

The outlined considerations are strictly applicable for isotropic phases only. However, it has been shown that, at least in a qualitative manner, a reasonable description of the thermodynamic properties of small crystallites embedded in a melt can be attempted using only one scalar quantity. In this case, to σ, some value of the specific interfacial energy has to be assigned, averaged over the different crystallite-melt or crystallite-vapor interfaces (Skripov, Koverda (1984) [771]; Woodruff (1973) [932]; Jackson (1969, 1984) [394, 395]; Mutaftschiev (1993)

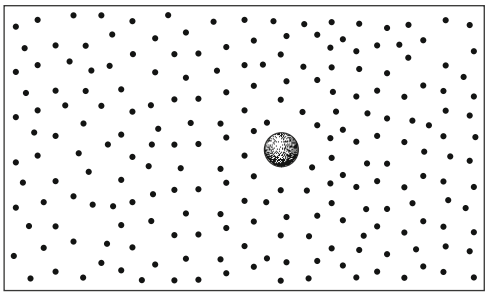

Fig. 6.2 Illustration of the model: formation of a spherical cluster in a solid or liquid quasi-binary solution

[585]). The parameter R has to be considered in these cases as a properly chosen measure of the size of the crystallite. For a more detailed study of the possible ways of describing the properties of small crystallites and, in particular, their equilibrium shapes (Gibbs-Wulff construction) see, e.g., Mutaftschiev (1993) [585].

6.2.2 *The Origin of Metastability: Critical Clusters*

We will now consider the process of formation of a cluster in a solid or liquid solution formed as a result of a segregation process (see Fig. 6.2 for an illustration) and calculate the change of the characteristic thermodynamic potential connected with such a process in dependence on the cluster size expressed by the radius R. Denoting the quantities describing the cluster phase by the subscript α and the matrix characteristics by β, one obtains for the internal energy

$$U_\alpha = T_\alpha S_\alpha - p_\alpha V_\alpha + \sum_j \mu_{j\alpha} n_{j\alpha} \,, \tag{6.10}$$

$$U_\beta = T_\beta S_\beta - p_\beta V_\beta + \sum_j \mu_{j\beta} n_{j\beta} \,, \tag{6.11}$$

$$U_\sigma = T_\sigma S_\sigma + \sigma A + \sum_j \mu_{j\sigma} n_{j\sigma} \,. \tag{6.12}$$

Based on the third of the mentioned postulates of the thermodynamics of surface phenomena (see Sect. 6.2.1) we may write

$$T_\alpha = T_\sigma \,, \tag{6.13}$$

$$\mu_{j\alpha} = \mu_{j\sigma} \,, \tag{6.14}$$

and with the abbreviations

$$n^*_{j\alpha} = n_{j\alpha} + n_{j\sigma} \,, \qquad S^*_\alpha = S_\alpha + S_\sigma \tag{6.15}$$

we obtain

$$U = T_\alpha S_\alpha^* - p_\alpha V_\alpha + \sum_j \mu_{j\alpha} n_{j\alpha}^* + T_\beta S_\beta - p_\beta V_\beta + \sum_j \mu_{j\beta} n_{j\beta} + \sigma A \ , \quad (6.16)$$

$$dU = T_\alpha dS_\alpha^* - p_\alpha dV_\alpha + \sum_j \mu_{j\alpha} dn_{j\alpha}^* + T_\beta dS_\beta - \quad (6.17)$$

$$- p_\beta dV_\beta + \sum_j \mu_{j\beta} dn_{j\beta} + \sigma dA \ .$$

For an isolated system with the boundary condition

$$V = V_\alpha + V_\beta = \text{const.} \quad (6.18)$$

the equilibrium condition reads (compare Eq. (2.33))

$$(\delta U)_{V,S,n} = 0 \ . \quad (6.19)$$

Considering possible variations of the independent variables S_α^*, $n_{j\alpha}^*$ and V_α and taking into account that for a spherical cluster the surface area and the volume of the cluster are dependent quantities Eq. (6.19) yields (see, e.g., Gibbs (1928) [249]; Schmelzer (1985) [689]; Ulbricht, Schmelzer et al. (1988) [874])

$$\mu_{j\alpha} = \mu_{j\beta} \ , \qquad j = 1, 2, \ldots, k \ , \quad (6.20)$$

$$T_\alpha = T_\beta \ , \quad (6.21)$$

$$p_\alpha - p_\beta = \frac{2\sigma}{R} \ , \quad (6.22)$$

where R is the radius of the cluster. While the first two of the equilibrium conditions remain the same as for macroscopic bodies (cf. Eqs. (2.38) and (2.40)), it turns out that in equilibrium the pressure inside a spherical cluster is larger than the pressure in the surrounding phase. This pressure balance equation determines to a large degree the specific properties of small clusters when analyzed from a thermodynamic point of view (see Sect. 6.2.4). It is denoted usually as the Young-Laplace equation.

For processes of cluster formation in glass-forming melts and a large number of further applications, a constant external pressure, p, and temperature, T, can be assumed. For these constraints the process of cluster formation is described thermodynamically by the Gibbs free energy, G. Since the pressure in the ambient phase is equal to the external pressure the total Gibbs free energy of the system consisting of a cluster embedded in the ambient phase is defined by

$$G = U - TS + pV \qquad \text{with} \qquad p = p_\beta \quad (6.23)$$

(for comparison see Eq. (2.19), where p denotes the external pressure). This definition yields with Eq. (6.16) the following expression for the thermodynamic potential of the considered heterogeneous system (cluster in the ambient phase)

$$G = V_\alpha(p_\beta - p_\alpha) + \sigma A + \sum_j \mu_{j\alpha} n_{j\alpha} + \sum_j \mu_{j\beta} n_{j\beta} \; . \tag{6.24}$$

In this and all subsequent equations the superscript $(*)$ is omitted for simplicity of the notations (compare Eq. (6.15)).

The chemical potential of the cluster phase can be considered as a function of the pressure p_α and the independent molar fractions $x_{j\alpha} = n_{j\alpha} / \sum n_{j\alpha}$. Instead of $\mu_\alpha(p_\alpha)$, however, usually the chemical potential of the cluster phase at the external pressure p is applied in the calculations $(\mu_\alpha(p))$. The connection between both quantities can be obtained by a truncated Taylor-expansion as

$$\mu_{j\alpha}(p_\alpha) = \mu_{j\alpha}(p) + \left(\frac{\partial \mu_{j\alpha}}{\partial p_\alpha} \right)_{p_\alpha = p} (p_\alpha - p) \; . \tag{6.25}$$

Since for the bulk part of the cluster phase

$$dG_\alpha = -S_\alpha dT_\alpha + V_\alpha dp_\alpha + \sum_j \mu_{j\alpha} dn_{j\alpha} \tag{6.26}$$

holds, we obtain immediately

$$\frac{\partial \mu_{j\alpha}}{\partial p_\alpha} = \frac{\partial V_\alpha}{\partial n_{j\alpha}} \; . \tag{6.27}$$

Moreover, the sum of the partial molar volumes multiplied by the mole numbers gives the volume of the considered body (Haase (1956) [338]), i.e.,

$$V_\alpha = \sum_j n_{j\alpha} \left(\frac{\partial V_\alpha}{\partial n_{j\alpha}} \right) \; . \tag{6.28}$$

Consequently, Eq. (6.24) may be written also as

$$G = \sum \mu_{j\alpha}(p) n_{j\alpha} + \sum_j \mu_{j\beta}(p) n_{j\beta} + \sigma A \; . \tag{6.29}$$

We calculate, now, the change of the Gibbs free energy, if in a binary system one of the components (say component 1) segregates to form a cluster. The change of the Gibbs free energy, $\Delta G_{(cluster)}$, connected with the formation of a cluster of size, R, in the initially homogeneous system

$$\Delta G_{(cluster)} = G_{het} - G_{hom} \tag{6.30}$$

is obtained then as

$$\Delta G_{(cluster)} = n_\alpha[\mu_\alpha(p) - \mu_{1\beta}(p, x_\beta)] + \sigma A + \sum_j n_j[\mu_{j\beta}(p, x_\beta) - \mu_{j\beta}(p, x)] \,. \tag{6.31}$$

Here $\mu_{1\beta}$ is the chemical potential of the segregating particles in the ambient phase, $\mu_\alpha(p)$ denotes the chemical potential of the segregating particles of the newly evolving phase at a pressure, p. According to the equilibrium conditions at a planar interface $\mu_\alpha(p) = \mu_\beta(p, x_{eq})$ is assumed to be fulfilled, where by x_{eq} the equilibrium value of the molar fraction of the segregating particles in the matrix is denoted. n_α is the number of moles in a cluster of the evolving phase.

In the derivation of Eq. (6.31) the condition $n_\alpha + n_{1\beta} = n_1 = \text{const.}$ was taken into account. Moreover, it was realized that the state of the ambient phase may change as the result of the formation of a cluster, i.e., the molar fraction is changed from x to x_β. These molar fractions x and x_β are determined by

$$x = \frac{n_1}{(n_1 + n_2)} \,, \qquad x_\beta = \frac{n_1 - n_\alpha}{n_1 + n_2 - n_\alpha} \,. \tag{6.32}$$

However, if we restrict the considerations to relatively small clusters and sufficiently large volumes of the matrix then such changes may be neglected and Eq. (6.31) is reduced to

$$\Delta G_{(cluster)} = n_\alpha[\mu_\alpha(p) - \mu_{1\beta}(p)] + \sigma A \,. \tag{6.33}$$

This equation is usually taken as the starting point for the discussion of nucleation phenomena in melts. However, the limits of validity of this expression, evident from the outlined derivation, must always be taken into account. Moreover, the derivation outlined allows one a direct generalization of the results to multi-component systems. The necessary condition for a phase transition to take place consists of $\mu_\alpha(p) < \mu_{1\beta}(p)$ (compare Sect. 2.2.3). Therefore, $\Delta\mu$ can be considered as the thermodynamic driving force of the transformation.

With the notation

$$\Delta\mu = \mu_{1\beta}(p) - \mu_\alpha(p) \tag{6.34}$$

Eq. (6.33) can be rewritten as

$$\Delta G_{(cluster)} = -n_\alpha \Delta\mu + \sigma A \,. \tag{6.35}$$

Since the clusters evolving in the course of the phase transformation consist initially of relatively few particles we will use in their description also the number of particles, j, contained in them. Using this notation Eq. (6.35) may be rewritten as

$$\Delta G_{(cluster)} = -j\Delta\mu + \sigma A \,. \tag{6.36}$$

$\Delta\mu$ in Eq. (6.36) is referred to one particle and not to one mole as in Eq. (6.35). Here and in the following derivations it is also assumed that the cluster has a spherical shape. In this case the volume V_α and the surface area A are given by

$$V_\alpha = \frac{4\pi}{3} R^3 \,, \qquad A = 4\pi R^2 \,. \tag{6.37}$$

For small clusters the term σA dominates, while for larger clusters the bulk term $j\Delta\mu$ determines the behavior of ΔG as a function of R. As the result of these two opposite tendencies an extremum is found determined by

$$\frac{\partial \Delta G_{(cluster)}}{\partial R} = -c_\alpha 4\pi R^2 \Delta\mu + 8\pi R\sigma = 0 \,. \tag{6.38}$$

Here c_α is the volume concentration of particles in the cluster phase. Instead of c_α, the volume per particle v_α is often used, defined by

$$v_\alpha = \frac{1}{c_\alpha} \,. \tag{6.39}$$

The radius of the cluster corresponding to the extremum of $\Delta G_{(cluster)}$ is denoted as critical cluster radius, R_c. It may be obtained from Eq. (6.38) as

$$R_c = \frac{2\sigma}{c_\alpha \Delta\mu} \,. \tag{6.40}$$

Equation (6.40) is usually called Gibbs-Thomson equation.

A second derivation of $\Delta G_{(cluster)}$ with respect to R results in

$$\left(\frac{\partial^2 \Delta G_{(cluster)}}{\partial R^2} \right)_{R=R_c} = -8\pi\sigma \,, \tag{6.41}$$

verifying that the extremum is a maximum. With Eq. (6.40) the expression Eq. (6.36) for $\Delta G_{(cluster)}$ gets the following form

$$\Delta G_{(cluster)} = \frac{1}{3}\sigma A \left(3 - 2\frac{R}{R_c} \right) \,, \qquad A = 4\pi R^2 \,, \tag{6.42}$$

which gives for $R = R_c$ the well-known result

$$\Delta G^{(c)}_{(cluster)} = \frac{1}{3}\sigma A^{(c)} \,, \qquad A^{(c)} = 4\pi R_c^2 \tag{6.43}$$

or

$$\Delta G^{(c)}_{(cluster)} = \frac{16\pi}{3} \frac{\sigma^3}{c_\alpha^2 (\Delta\mu)^2} \,. \tag{6.44}$$

An expression equivalent to Eq. (6.42) is

$$\Delta G_{(cluster)} = \Delta G^{(c)}_{(cluster)} \left[3 \left(\frac{R}{R_c} \right)^2 - 2 \left(\frac{R}{R_c} \right)^3 \right] . \tag{6.45}$$

Equations (6.40), (6.43), and (6.44) were first derived by Gibbs. An alternative derivation of Eq. (6.44) was developed by Volmer (1939) [894]. In his book also a historical survey of alternative attempts in the calculation of $\Delta G^{(c)}_{(cluster)}$ can be found. Its determination for different cases of phase transformation processes is given, for example, in Frenkel's monograph (1946) [233]; for the formulation for crystals see Kaischew (1952 [417], 1957 [421]) and Mutaftschiev (1993) [585].

For further derivations also some additional expressions are needed equivalent to those given above. With

$$j = \frac{V_\alpha}{v_\alpha} , \qquad j = \frac{4\pi}{3} \frac{R^3}{v_\alpha} , \tag{6.46}$$

Eq. (6.45) is transformed into

$$\Delta G_{(cluster)} = \Delta G^{(c)}_{(cluster)} \left[3 \left(\frac{j}{j_c} \right)^{2/3} - 2 \left(\frac{j}{j_c} \right) \right] . \tag{6.47}$$

In terms of j_c and $\Delta\mu$ the work of formation of critical clusters $\Delta G^{(c)}_{(cluster)}$ may be written also as (see Hirth and Pound (1963) [368]; Kashchiev (1982) [436]; Oxtoby and Kashchiev (1994) [619])

$$\Delta G^{(c)}_{(cluster)} = \frac{1}{2} j_c \Delta\mu . \tag{6.48}$$

Finally, we have also to note the following relations

$$\frac{\partial \Delta G_{(cluster)}}{\partial j} = 2 \Delta G^{(c)}_{(cluster)} \left(\frac{j^{-1/3}}{j_c^{2/3}} - \frac{1}{j_c} \right) , \tag{6.49}$$

$$\left(\frac{\partial^2 \Delta G_{(cluster)}}{\partial j^2} \right)_{j=j_c} = -\frac{2}{3} \frac{\Delta G^{(c)}_{(cluster)}}{j_c^2} , \tag{6.50}$$

needed in the subsequent derivations.

Equation (6.43) is valid not only for the case of segregation of a cluster in a binary melt, considered here, but also for any case of iso-concentration nucleation (formation of liquid or crystalline clusters having the same composition as the ambient phase). It is only necessary to define the thermodynamic driving force $\Delta\mu$ in an appropriate way (as will be done in the next section). The result Eq. (6.43) also remains valid if multi-component clusters with a composition different from

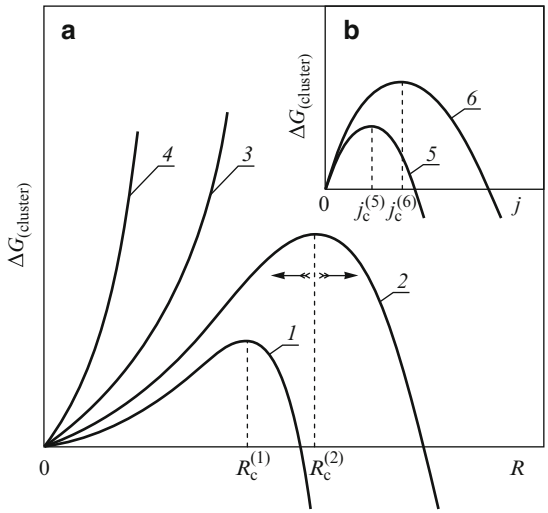

Fig. 6.3 (**a**) Dependence of the change of the Gibbs free energy, $\Delta G_{(cluster)}$, resulting from the formation of a cluster, on its size, R, according to Eq. (6.45). Two curves (*1*) and (*2*) are given calculated for different values of the chemical potential ($\Delta\mu^{(1)} > \Delta\mu^{(2)}$, respectively, $R_c^{(1)} < R_c^{(2)}$). By R_c the critical cluster size is specified corresponding to a maximum of the thermodynamic potential difference. For $\Delta\mu < 0$, $\Delta G_{(cluster)}$ is a monotonically increasing function of R and no maximum exists (curves (*3*) and (*4*); ($|\Delta\mu^{(3)}| < |\Delta\mu^{(4)}|$)). (**b**) The same dependence but this time as a function of the number of particles, j, in the cluster (curves (*5*) and (*6*) with $\Delta\mu^{(5)} > \Delta\mu^{(6)}$)

the ambient phase are formed. Employing Gibbs' theoretical approach, in such a case one has to assume in addition that the composition and density of the clusters are widely the same as for the newly evolving bulk phase.

The function $\Delta G_{(cluster)}$ vs. R, respectively, vs. j is shown in Fig. 6.3. The most probable way of further evolution of the cluster in dependence on its size is indicated by arrows. The direction of evolution follows from the thermodynamic criterion given by Eq. (2.34). According to this criterion a cluster grows spontaneously only after a size $R > R_c$ is reached (deterministic growth of clusters). This property is the reason why a critical cluster is sometimes called a nucleus or, applying a biological analogy, an embryo of the new phase. The formation of critical or supercritical clusters requires the existence of spontaneous fluctuations which are not considered in the framework of classical thermodynamics (fluctuational growth of subcritical clusters).

Systems, which are stable with respect to small but unstable with respect to large fluctuations, are called metastable systems (compare Chap. 2). Processes of cluster formation and growth may proceed in thermodynamically metastable systems. Thus, to initiate a first-order phase transition, a fluctuation of a sufficiently large size is needed to initiate the further growth of the new (thermodynamically favored) phase. This process takes some time and explains the kinetic stability of thermodynamically metastable systems observed experimentally. It also gives,

consequently, the possibility of a kinetic interpretation of glass-formation and the derivation of kinetic criteria for it.

It is known from fluctuation theory (see Landau and Lifshitz (1969) [494]) that the probability, w, of a fluctuation (i.e., of a spontaneous deviation from the equilibrium state) can be expressed by the work W, which is needed to create, in a reversible process, the same change of the state of the system as the considered fluctuation, i.e.

$$w \sim \exp\left(-\frac{W}{k_B T}\right). \tag{6.51}$$

For the considered constraints ($p = \text{const.}$, $T = \text{const.}$) this work is, on the other hand, equal to the change of the Gibbs free energy connected with the considered variation of the state. Thus we obtain

$$w \sim \exp\left(-\frac{\Delta G_{(cluster)}}{k_B T}\right). \tag{6.52}$$

The mentioned relation between W and $\Delta G^{(c)}_{(cluster)}$ is the reason why this quantity is also denoted commonly as the work of formation of a critical cluster. The probability of a phase transformation is determined, consequently, to a large extent by the values of $\Delta G^{(c)}_{(cluster)}(R_c)$ or σ and $\Delta\mu$, respectively, as it is evident from Eq. (6.44).

Equations (6.43)–(6.52) show more precisely, that the probability of formation of critical clusters depends significantly on the surface energy of the critical cluster σA, respectively, on σ^3 and the square of the thermodynamic driving force $(\Delta\mu)^2$. Thus small variations of σ or $\Delta\mu$ may be expected to result in significant variations of the nucleation rate. This expectation is confirmed by experimental results as well as by nucleation theory.

6.2.3 *General Expression for the Thermodynamic Driving Force of First-Order Phase Transformations*

In the special case considered so far in this chapter, only one of the components is assumed to segregate to form a cluster. Qualitatively, the results outlined are not changed if one considers the more realistic situation that the cluster phase is composed of particles of different components with, in general, arbitrary composition. According to the conditions for thermodynamic equilibrium in such more general cases, the thermodynamic driving force of the transformation is determined by the change of the bulk contributions to the thermodynamic potential referred to one mole of the transformed substance. Thus we have to write, in general,

$$\Delta\mu = \frac{[G_{(initial\ state)} - G_{(final\ state)}]}{\sum_j n_{j\alpha}}, \tag{6.53}$$

where $\sum n_{j\alpha}$ is the total number of moles transformed from the initial to the new phase. In Eq. (6.53) only the bulk contributions to the Gibbs's free energies of both phases have to be taken into consideration.

In considering phase transformations in supersaturated solutions or from the gas phase the thermodynamic driving force of the process is expressed usually in terms of the generalized or relative supersaturation χ, defined by

$$\chi = \frac{\Delta\mu}{k_B T} \,. \tag{6.54}$$

More generally this expression can be employed as a measure for the relative deviation from thermodynamic equilibrium. Equation (6.53) allows us to apply the derivations outlined so far for segregation processes in binary and multi-component solutions to another case of phase transformation processes which is directly connected with the conditions of glass-formation: crystallization in glass-forming melts. In these cases the difference in the chemical potentials is determined by the under-cooling.

At a constant pressure, as discussed in Sect. 2.2.3, a definite value of the temperature exists at which an equilibrium coexistence of the melt and the crystalline phase is possible. At this temperature, the melting temperature, the molar values of the Gibbs free energy are the same in the liquid and crystalline phases of the substance considered (compare Sect. 2.2.3). The thermodynamic driving force of the crystallization process, which may take place at temperatures $T < T_m$, is determined, according to Eq. (6.53), by the differences of the Gibbs free energies corresponding to the liquid and crystalline phases, i.e., by

$$\Delta\mu = \frac{G_{(liquid)}(p,T) - G_{(crystal)}(p,T)}{n} \,. \tag{6.55}$$

Here n is the total number of moles of the substance considered. It is assumed, in deriving the above equation, that the compositions of the melt and the crystalline phase are the same. In this way, the thermodynamic functions depend only on pressure p and temperature T.

Taking into account the constancy of the external pressure p and choosing as the reference temperature for the calculation of the Gibbs free energies the melting temperature T_m, Eq. (2.25) reads

$$G(p,T) = G(p,T_m) - S(p,T_m)(T - T_m) - \int_T^{T_m} dT \int_T^{T_m} \frac{C_p}{T}\, dT \,. \tag{6.56}$$

Moreover, since the Gibbs free energies of both phases are equal at the melting point, Eq. (6.55) is transformed to

$$\Delta\mu = -[s^{(liquid)}(T_m) - s^{(crystal)}(T_m)](T - T_m) - \int_T^{T_m} dT \int_T^{T_m} \frac{c_p^{(liquid)} - c_p^{(crystal)}}{T} dT \,. \tag{6.57}$$

Introducing the notations

$$\Delta s = s^{(liquid)} - s^{(crystal)} \,, \qquad \Delta s_m = \Delta s(T_m) \,,$$

where Δs_m is the molar heat of melting and

$$\Delta c_p = c_p^{(liquid)} - c_p^{(crystal)} \,,$$

the differences in the molar entropies and the molar specific heats, respectively, Eq. (6.57) may be rewritten in the form

$$\Delta\mu = \Delta s_m(T_m - T) - \int_T^{T_m} dT \int_T^{T_m} \frac{\Delta c_p}{T} dT \,. \tag{6.58}$$

Taking into account the definition of the specific heats Eq. (2.14) $\Delta c_p / T$ may be replaced by

$$\frac{\Delta c_p}{T} = \left(\frac{d\Delta s}{dT}\right)_p \,. \tag{6.59}$$

In this way, Eq. (6.58) is transformed to

$$\Delta\mu = \int_T^{T_m} \Delta s(T)\, dT \,. \tag{6.60}$$

The same result was obtained in an approximative derivation by Volmer ((1939) [894]; see also Frenkel (1946) [233]; Hoffman (1958, 1964) [375, 376]; Gutzow (1972) [294]). Moreover, a truncated Taylor-expansion of $\Delta s(T)$ in the vicinity of T_m gives

$$\Delta s(T) = \Delta s_m + \left(\frac{\partial \Delta s}{\partial T}\right)_{T_m} (T - T_m) \,, \tag{6.61}$$

resulting after a substitution into Eq. (6.60) in already discussed dependencies (see Eqs. (3.48)–(3.52) and also Gutzow et al. (1975) [297]; Gutzow and Dobreva (1991) [308])

$$\Delta\mu = \Delta s_m(T_m - T)\left[1 - \frac{\Delta c_p(T_m)}{2\Delta s_m}\frac{(T_m - T)}{T_m}\right] \,. \tag{6.62}$$

As mentioned in Sect. 3.3 for typical glass-forming melts the ratio $a_0 = (\Delta c_p/\Delta s_m)$ is of the order

$$\frac{\Delta c_p(T_m)}{\Delta s_m} \approx 1 - 2 \,. \tag{6.63}$$

Taking into account this experimental result, an estimate of the thermodynamic driving force of crystallization can be given. According to Eqs. (6.62) and (6.63) the thermodynamic driving force for crystallization should vary in dependence on temperature in the range from T_m to T_g in the limits

$$\Delta s_m(T_m - T)\frac{T}{T_m} \leq \Delta\mu \leq \Delta s_m(T_m - T)\frac{1}{2}\left(1 + \frac{T}{T_m}\right) \,. \tag{6.64}$$

For small under-coolings $(T/T_m) \approx 1$ holds and, approximately, the often applied expression

$$\Delta\mu = \Delta s_m(T_m - T) \tag{6.65}$$

is obtained (for the cases $a_0 = 1$ and $a_0 = 2$, see Sect. 3.3). The equivalence, with respect to expressions for the thermodynamic driving force of crystallization derived in Chap. 3, gives an additional proof of the validity of the general definition of the driving force of crystallization, introduced with Eq. (6.53). The method outlined here has the advantage that it allows us to calculate the thermodynamic driving force also for the more complicated case when crystallization is accompanied by changes in composition.

The approximations Eq. (6.64) may be applied, strictly speaking, only for moderate under-cooling. More general temperature dependencies for the thermodynamic driving force of the transformation may be derived, as done in Sect. 3.3, when a definite thermodynamic model for the temperature dependence of ΔC_p is introduced. As discussed in application to the particular model employed, it follows from the Third law of thermodynamics that there always exists a value of temperature T_0 below which $\Delta\mu$ remains practically constant (compare Eq. (3.56)). In this way, it is to be expected that below some temperature T_0, a further increase in the undercooling no longer varies the thermodynamic driving force of the phase transformation (Gutzow, Konstantinov, and Kaischew (1972) [325]; Gutzow (1981) [304]).

As also already mentioned in Chap. 3, T_0 generally has values in the range $(T_0 < T_g, T_m/3 \leq T_0 \leq T_m/2)$. Thus, from a theoretical point of view, the upper value of the thermodynamic driving force of crystallization of under-cooled melts is reached at T_0. For practical purposes (as far as $T_g > T_0$ holds) even smaller limiting values are to be expected corresponding to the vitrification temperature T_g. The values of the thermodynamic driving force of crystallization, calculated according to above given equations, are such that only moderate under-cooling can be realized in typical glass-forming melts. This result is an indication that glass-forming systems can be used as convenient model systems for a test of the predictions of the classical

theories of nucleation and crystal growth since their basic premises are fulfilled for these systems to a large extent.

6.2.4 *Size Dependence of the Thermodynamic Properties of Small Clusters*

In the application of Gibbs' original thermodynamic analysis of heterogeneous systems to nucleation processes it is assumed, in general that the bulk thermodynamic properties of small clusters of the newly formed phase are the same as for the corresponding bulk samples.[2] This simplifying assumption was adopted in most of the subsequent derivations of the kinetic equations describing nucleation and growth, though, of course, such an extension of macroscopic properties to small clusters is doubtful from a principal point of view. Indeed, the results of a variety of modern investigations of the properties of clusters of nano-sizes show that their thermodynamic, mechanical, rheological and other properties may significantly deviate from the respective values for the bulk samples (Cahn and Hilliard (1958/59) [119]; Petrov (1982) [633]; Halpern (1967) [344]; Haberland (1994) [340]). Once such assumption is made, then corrections may be introduced into the theoretical description of cluster formation and growth only via the account of a size-dependence of the surface terms in the thermodynamic treatment. By this reason, of particular interest with respect to nucleation theory is the size or curvature dependence of the specific interfacial energy σ, since this quantity determines the nucleation rate in a significant way (compare Eq. (6.44)).[3]

---

[2] This assumption is based on the analysis of Gibbs' equilibrium conditions determining the bulk properties of critical clusters and leading to this consequence.

[3] An alternative approach to the the description of spatially inhomogeneous thermodynamic systems (denoted by us as generalized Gibbs approach) and its application to the determination of the properties of critical clusters was developed by the present authors and coworkers in the last decade starting with a paper published in 2000 (Schmelzer et al. [722]). For an illustration, the method is applied there to phase formation processes in solid and liquid solutions. However, it is applicable quite generally and not restricted to this particularly important but anyway special case. The presented there approach is a generalization of the classical Gibbs' method. It is – like the classical Gibbs method – conceptually simple and directly applicable to real systems, but avoids its shortcomings. Central to this method was originally (later the consequences have been shown to follow directly from the modification of Gibbs classical approach developed by us) the formulation and application of a well-founded principle we denoted as generalized Ostwald's rule in nucleation. The method allows one the determination of the dependence of the bulk properties of the critical clusters and the work of critical cluster formation in dependence on cluster size provided the bulk properties and the macroscopic values of the surface tension (at planar interfaces) for the possible different states of the system under consideration are known. As it turns out, in the framework of the generalized Gibbs approach the bulk properties – and as a consequence also the interfacial properties – of the critical clusters depend significantly on supersaturation (or the size of the critical clusters). Similarly to the van der Waals, Cahn, and Hilliard and density functional calculations in the determination of the work of critical cluster formation, the newly developed

Various methods exist for the theoretical analysis of the specific properties of small clusters. A first attempt in this direction can be made, as we will do, based on a thermodynamic approach. We consider, in the following, the size dependence of the thermodynamic properties of small clusters (droplets, crystallites) from a thermodynamic point of view and compare them with the corresponding properties of the bulk phases. From the very beginning of our analysis we assume a thermal equilibrium to be established in between the cluster and the ambient phase ($T_\alpha = T_\beta = T$). For a one-component system the equilibrium conditions are reduced then to (cf. Eqs. (6.20)–(6.22))

$$\mu_\alpha(p_\alpha, T) = \mu_\beta(p, T) \,, \tag{6.66}$$

$$p_\alpha - p = \frac{2\sigma}{R} \,. \tag{6.67}$$

In the classical Gibbs' thermodynamic approach the deviations of the properties of the cluster phase from the bulk properties of a macroscopic phase in equilibrium with a coexisting second phase, divided from it by a planar interface, are due to the deviations of the pressure as expressed through the Young-Laplace equation, Eq. (6.67). Replacing p_α, used as the independent variable for the determination of the chemical potential μ_α, according to the Young-Laplace equation we get

$$\mu_\alpha(p_\alpha) = \mu_\alpha\left(p + \frac{2\sigma}{R}\right) \,. \tag{6.68}$$

A Taylor-expansion of μ_α and subsequent substitution into Eq. (6.66) yields then

$$\mu_\alpha(p_\alpha, T) = \mu_\alpha(p, T) + v_\alpha(p, T)\left[\frac{2\sigma(p_\alpha, T)}{R}\right] = \mu_\beta(p, T) \,. \tag{6.69}$$

---

method reproduces the results of the classical Gibbs' nucleation theory (involving the capillarity approximation) for small values of the supersaturation. However, in contrast to the classical and in agreement with van der Waals-type methods of descriptions of inhomogeneous systems, for initial states approaching the spinodal curve, the work of critical cluster formation, determined via the newly developed approach, is shown to tend to zero. As an immediate additional consequence, the method gives a more accurate description of the experimental results on nucleation rates also in the intermediate ranges of the initial supersaturation. This method was further developed then in a series of papers and applied also to the determination of the properties of sub- and supercritical clusters (Schmelzer et al. [725]; Schmelzer et al. [3]). The theoretical foundation of the generalized Gibbs approach is given in: Schmelzer et al. [729]. An overview on further developments and the application of this method to the analysis of experimental data is given in: Schmelzer and Abyzov [702]; Abyzov and Schmelzer [3]; Schmelzer [697]; Schmelzer et al. [728]; Abyzov et al. [4]; Schmelzer and Abyzov [703]; Schmelzer and Abyzov [704] (a more detailed overview is given in the Chap. 14). In the present book, however, we employ the classical approach treating the clusters widely as small aggregates with the bulk properties of the newly evolving macroscopic phases and introduce corrections via a curvature dependence of the surface tension.

In the derivation of Eq. (6.69) in addition the relation

$$v_\alpha = \left(\frac{\partial \mu_\alpha}{\partial p}\right)_T \tag{6.70}$$

is used.

In Eq. (6.69) the independent variables are p, T and R. The variable R denotes here those cluster sizes for which the necessary thermodynamic equilibrium conditions are fulfilled. If one changes one of the independent variables, then, in order to retain the equilibrium, a variation of one or both of the other variables is required. Consequently, by a calculation of the total differential of the r.h.s of Eq. (6.69) one obtains with Eq. (2.54) the expression

$$(v_\alpha - v_\beta)dp + d\left(\frac{2\sigma v_\alpha}{R}\right) = (s_\alpha - s_\beta)\, dT\ . \tag{6.71}$$

From this general equation a number of consequences can be derived:

- **Cluster size dependence of the equilibrium pressure of a droplet in the vapor**
  If the temperature is kept constant in the system, Eq. (6.71) is reduced to

  $$(v_\alpha - v_\beta)dp = -d\left(\frac{2\sigma v_\alpha}{R}\right)\ . \tag{6.72}$$

  For a droplet in the vapor $v_\alpha \ll v_\beta$ holds. If in addition the perfect gas law $pv_\beta = k_B T$ is applied, Eq. (6.72) yields (W. Thomson (Lord Kelvin) (1870, 1871)[834])

  $$p_{eq}(R) = p_{eq}(R \to \infty) \exp\left(\frac{2\sigma v_\alpha}{k_B T}\frac{1}{R}\right)\ . \tag{6.73}$$

  Here v_α and v_β are the volumes per particle in the cluster and the ambient phase, respectively. The vapor pressure of a cluster of size R existing in equilibrium in its vapor is, consequently, higher than the respective value for a planar equilibrium coexistence of both phases ($R \to \infty$).
- **Cluster size dependence of the solubility**
  A similar equation can be obtained directly from the Gibbs-Thomson equation, Eq. (6.40), also for the case of segregation in binary melts. If we express in this equation the chemical potential of the segregating particles in the matrix via the perfect solution law

  $$\mu(p, T, x) = \mu_0(p, T) + k_B T \ln x \tag{6.74}$$

  and denote by $x_{eq}(\infty)$ the molar fraction of the segregating component for a stable coexistence at a planar interface, we obtain with the equilibrium condition for coexistence at a planar interface

  $$\mu_\alpha(p, T) = \mu_\beta(p, T, x_{eq}(\infty)) \tag{6.75}$$

the relation

$$x_{eq}(R) = x_{eq}(R \to \infty) \exp\left(\frac{2\sigma}{c_\alpha k_B T}\frac{1}{R}\right) . \tag{6.76}$$

If instead of the molar fraction the volume concentration, c, is used and c_α is replaced by $c_\alpha = (1/v_\alpha)$ the similarity with Eq. (6.73) becomes even more obvious

$$c_{eq}(R) = c_{eq}(T \to \infty) \exp\left(\frac{2\sigma v_\alpha}{k_B T}\frac{1}{R}\right) . \tag{6.77}$$

- **Cluster size dependence of the melting temperature of small crystallites**

  If the pressure is kept constant ($dp = 0$), Eq. (6.71) gives a relation between the (equilibrium) melting temperature of a crystallite and its size, i.e.,

$$(s_\alpha - s_\beta) dT = d\left(\frac{2\sigma v_\alpha}{R}\right) . \tag{6.78}$$

  Here σ is the specific interfacial energy of the crystal-melt interface. Denoting the heat of melting as usual by $q = T(s_\beta - s_\alpha)$ we get with the approximation $q \approx$ constant the expression

$$T_{eq}(R) = T_{eq}(R \to \infty) \exp\left(-\frac{2\sigma v_\alpha}{q}\frac{1}{R}\right) \cong T_{eq}(R \to \infty)\left(1 - \frac{2\sigma v_\alpha}{q}\frac{1}{R}\right) , \tag{6.79}$$

  giving the melting temperature of a crystallite in its melt (compare, e.g., Meiwes-Broer and Lutz (1991) [553]). The same equation also determines the equilibrium of a droplet in the vapor at constant pressure. In this case, q denotes the heat of evaporation and σ the liquid-vapor surface tension. In both cases the equilibrium temperature decreases with a decreasing cluster size. Moreover, from Eq. (6.71) a relation between the equilibrium values of pressure and temperature for fixed values of the cluster radius may be derived, e.g., for a drop in its vapor or a crystallite in the melt. This gives a generalization of the already discussed Clausius-Clapeyron equation, Eq. (2.58).

  Of particular interest in treating problems of formation of liquid and crystalline condensates from vapors is the size dependence of the melting temperature of a crystalline cluster in equilibrium with its own vapor and liquid phases. This problem requires the investigation of the equilibrium of both a droplet and a crystallite of equal masses in a common vapor phase (see Prigogine and Defay (1954) [649]; Hanszen (1960) [347]; Avramov and Gutzow (1988) [24]). The result of such a calculation is

$$T_m(R) = T_m(\infty) - \frac{2\sigma_{cv} v_c}{\Delta s_m R}\left[1 - \frac{\sigma_{fv}}{\sigma_{cv}}\left(\frac{v_f}{v_c}\right)^{2/3}\right] . \tag{6.80}$$

Here the following notations are used: σ_{cv}, σ_{fv} – specific interfacial energies of the crystal/vapor and liquid/vapor interfaces; v_f, v_c – molar volumes of the liquid and the crystal, respectively.

- **Curvature dependence of surface tension**

For a constant temperature and a one-component substance the Gibbs adsorption equation, Eq. (6.9), has the form

$$A d\sigma + n_\sigma d\mu_\alpha = 0 \,. \tag{6.81}$$

From Eq. (6.81) it follows with the Gibbs-Duhem relation Eq. (6.82) written for the cluster phase

$$S_\alpha dT_\alpha - V_\alpha dp_\alpha + \sum_j n_{j\alpha} d\mu_{j\alpha} = 0 \,, \tag{6.82}$$

that σ for isothermal conditions and a one-component system is a function of the pressure p_α (or the density), only. Indeed, according to Eq. (6.82) we have in this special case

$$V_\alpha dp_\alpha = n_\alpha d\mu_\alpha \,, \tag{6.83}$$

verifying above statement.

From the equilibrium conditions and the Gibbs adsorption isotherm Eq. (6.81) the following differential equation for the curvature dependence of σ may be derived (for details see Gibbs (1928) [249]; Tolman (1948, 1949) [842, 843]; Kirkwood, Buff (1949) [455]; Buff, Kirkwood (1950) [110]; Ono, Kondo (1960) [612]):

$$\frac{d\sigma}{\sigma} = -\frac{2\delta}{1 + \dfrac{2\delta}{R}} d\left(\frac{1}{R}\right) \,, \qquad \delta = \frac{\Gamma_0}{c_\alpha - c_\beta} \,. \tag{6.84}$$

The Tolman-parameter, δ, is determined according to Eq. (6.84) by the superficial particle density $\Gamma_0 = (n_\sigma / A)$ and the particle concentrations, c, in both phases. It is a measure of the width of the inhomogeneous region between the coexisting phases. If the Tolman-parameter, δ, is set equal to a constant $\delta(\infty)$, corresponding to its value for a planar interface between both coexisting phases, an expression for the curvature dependence of the surface tension can be obtained by an integration of Eq. (6.84) as

$$\sigma(R) = \frac{\sigma(\infty)}{1 + \dfrac{2\delta(\infty)}{R}} \,. \tag{6.85}$$

This equation is usually denoted as Tolman's equation. The dependence of σ on R as predicted by this equation is shown in Fig. 6.4 (as a function of δ_∞ / R).

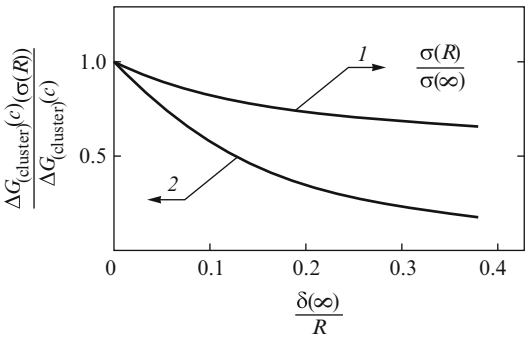

Fig. 6.4 Curvature dependence of the surface tension as predicted by Tolman's equation, Eq. (6.85) (curve (*1*)) and work of formation of critical clusters (curve (*2*)) when a curvature dependence of the surface tension according to Tolman's proposal is used (Toschev-Parlange formula, Eq. (6.90))

On the other hand, since the surface tension σ is also a function of p_α and T, a truncated Taylor-expansion of $\sigma(p_\alpha, T)$ yields

$$\sigma(p_\alpha, T) = \sigma(p, T) + \left(\frac{\partial\sigma}{\partial p}\right)_T \left(\frac{2\sigma(p_\alpha, T)}{R}\right) \tag{6.86}$$

or with $\sigma(p, T) = \sigma(\infty)$ and $\sigma(p_\alpha, T) = \sigma(R)$ we have

$$\sigma(R) = \frac{\sigma(\infty)}{1 - \frac{2}{R}\left(\frac{\partial\sigma}{\partial p}\right)_T} \,. \tag{6.87}$$

A comparison of Eqs. (6.85) and (6.87) shows that the Tolman-parameter $\delta(\infty)$ may be determined as

$$\delta(\infty) = -\left(\frac{\partial\sigma}{\partial p}\right)_T \,. \tag{6.88}$$

Equation (6.88) allows one the determination of $\delta(\infty)$ based on measurements of the pressure dependence of σ (compare Hill (1952) [357]; Gorski (1989) [267]). Since direct measurements of the pressure dependence of σ are not available, estimates may be given through equations connecting the interfacial tension with bulk properties like, e.g., McLeods's equation (see Rowlinson and Widom (1982) [672])

$$\sigma^{1/4} = \text{const}\,(c_\alpha - c_\beta) \,. \tag{6.89}$$

Equation (6.85), introduced into the expressions for the work of formation of the critical cluster and the probability of cluster formation (cf. Eqs. (6.43) and (6.52)) results in a considerable decrease of $\Delta G_{(cluster)}^{(c)}$ and in an increase of

the probability of cluster formation (see, e.g., Toschev (1969 [847], 1973 [848]); Parlange (1970) [625]). The final result in the form obtained first by Toschev reads

$$\Delta G^{(c)}_{(cluster)}(\sigma(R)) = \Delta G^{(c)}_{(cluster)} \frac{1}{4} \left(\frac{\sigma(R)}{\sigma(\infty)} \right)^4 \left(3 - \frac{\sigma(R)}{\sigma(\infty)} \right)^2 . \tag{6.90}$$

Here $\Delta G^{(c)}_{(cluster))}(\sigma(R))$ denotes the work of cluster formation when the size-dependence of σ is accounted for, while $\Delta G^{(c)}_{(cluster)}$ refers to the classical expression obtained by assuming constancy of σ. The above dependence is also illustrated in Fig. 6.4.[4]

It can be seen from Eq. (6.90) that in the range of cluster radii, for which Tolman's equation can be expected to describe more or less correctly the change of $\sigma(R)$ as compared with $\sigma(\infty)$, the deviations in the values of the work of critical cluster formation are smaller than 20 %. Nevertheless, such a decrease in the work of formation of critical clusters may result in a considerable increase of the nucleation rate, as will be discussed in more detail in the subsequent sections.

Following Tolman's derivations a number of different proposals has been developed to account for the most appropriate description of finite size effects in application to nucleation theory. A summary of such attempts is given by Schmelzer and Mahnke (1986) [708] and Schmelzer [690]. It turns out that the majority of such proposals can be obtained from one simple assumption concerning the size-dependence of the Tolman-parameter δ. In most cases, the $\sigma(R)$-curves are quite near to Tolman's prediction. Consequently, similar conclusions can be drawn also with respect to alternative curvature corrections to the work of formation of critical clusters (for a more detailed analysis, see Schmelzer et al. (1995) [690, 708, 719]).

As for the surface tension, similar size dependencies may also be derived for other quantities characterizing a cluster, like the latent heat of evaporation

$$q(R) = q(\infty) - \frac{2\sigma v_\alpha}{R} \tag{6.91}$$

[4]Note as well that independent of the specific expression for the curvature dependence of the surface tension, always the equation

$$\Delta G^{(c)}_{(cluster)}(\sigma(R)) = \Delta G^{(c)}_{(cluster)}(\sigma(R \to \infty)) \left(\frac{\sigma(R)}{\sigma(\infty)} \right)^3$$

holds, if the surface of tension is chosen as the dividing surface (cf. Parlange (1970) [625], Ulbricht, Schmelzer et al. (1988) [874]). Latter result was already well-known to J.W. Gibbs and the effects of a curvature dependence of the surface tension on nucleation have been also already discussed in detail by him [249].

or the specific heat of a cluster

$$c_p(R) = c_p(\infty) - \frac{2\sigma T}{R}\left(\frac{\partial^2 v_\alpha}{\partial T^2}\right) . \tag{6.92}$$

Additional information concerning the properties of small clusters may be found in a number of specialized monographs or conference proceedings (see, e.g., Petrov (1982) [633]; Echt and Recknagel (1991) [182]; Berry et al. (1993) [76]; Jena, Khanna, Rao (1992) [406]; Haberland (1994) [340]).

6.3 Kinetics of Homogeneous Nucleation

6.3.1 Classical Nucleation Theory

Classical nucleation theory was developed in the 1920–1940s by a number of scientists. First of all the names Farkas (1927) [196], Volmer and Weber (1926) [896], Volmer (1939) [894], Kaischew and Stranski (1934) [425], Becker and Döring (1935) [59], Frenkel (1946) [233], and Zeldovich (1942) [949], Turnbull and Fisher (1949) [866] have to be mentioned. As noted by Farkas, the basic kinetic model, underlying classical nucleation theory, was proposed in fact already by L. Szilard. The analysis was initially directed mainly to the case of droplet formation in a one-component vapor (Farkas (1927) [196]; cf. also [197]). Kaischew and Stranski [425] investigated, as early as 1934, the formation of crystals from vapors. The first derivation of nucleation kinetics for the case of crystallization of an undercooled melt was also developed relatively early by Volmer and Weber (1926) [896], while Reiss (1950) [661] was the first to apply the outlined ideas to nucleation in multi-component systems. A summary and thorough discussion of earlier attempts at determining nucleation rates for different systems may be found in Volmer's and Frenkel's monographs (Volmer (1939) [894]; Frenkel (1946) [233]). Further developments are summarized in the monographs by Hirth and Pound (1963) [368] and Zettlemoyer (1969 [954], 1977 [955]) and the review article by Mutaftschiev (1993) [585]. Here we will develop the theory taking as an example precipitation in a quasi-binary solid or liquid solution, when only one of the components segregates to form clusters of the newly evolving phase.

The theory developed by the authors cited above and others, with modifications, is still the most widely applied tool for the interpretation of nucleation processes in many fields. Therefore we will start the discussion of nucleation with an outline of its basic ideas. In classical nucleation theory, a spatially homogeneous system is considered (*assumption 1*), where, in the simplest case, particles of one of the components (atoms, molecules) aggregate to form clusters of the new phase. Moreover, it is supposed that clusters B_j consisting of j ambient phase molecules (also denoted as monomers, building units) grow and decay by addition or evaporation of monomers B_1 only according to the scheme (*assumption 2*)

$$B_1 + B_j \rightleftharpoons B_{j+1} \tag{6.93}$$

as in a binary chemical reaction. Such an assumption is quite reasonable since the number of monomers exceeds, by many orders of magnitude, the concentration of clusters with particle numbers $j > 1$. Monomers have, moreover, the highest mobility. Reactions of other types are excluded in this scheme.

At the advanced stages of cluster formation and for highly mobile clusters, the probability of collisions between clusters of equal or different sizes is, in general, not equal to zero and assumption 2 has to be replaced by a more general scheme involving in addition reactions of the type $B_i + B_j \rightleftharpoons B_{i+j}$. In these cases, relations similar to Smoluchowski's coagulation equations describe the kinetics of the transformation (von Smoluchowski (1916) [898], (1917) [899]; Kashchiev (1984) [437]). In phase transformation processes, proceeding in solids, in general, and glass-forming melts, in particular, the low mobility, respectively, high viscosity of the system excludes such reaction paths to a large extent.

With assumption 2 the change of the number of clusters per unit volume N_j, consisting of j monomers, is connected with two possible reaction channels, with two processes of the form as given with Eq. (6.93) involving (B_{j-1}, B_j, B_1) and (B_j, B_{j+1}, B_1), respectively. The basic equations for the kinetic description of these processes are given by (*assumption 3*)

$$\frac{dN(j,t)}{dt} = J(j-1,t) - J(j,t) \quad \text{for} \quad j \geq 2 \tag{6.94}$$

with

$$J(j,t) = w^{(+)}(j,t)N(j,t) - w^{(-)}(j+1,t)N(j+1,t)\,. \tag{6.95}$$

Here $w^{(+)}(j,t)$ is the average number of monomers which is incorporated into a cluster of size j per unit time, while $w^{(-)}(j,t)$ describes similarly the rate of decay processes. Equation (6.94) is implicitly subject to the assumption that the state of the cluster is determined solely by the number of monomers contained in it (*assumption 4*: equilibrium shape of clusters). This assumption is motivated by the argument that a cluster rapidly goes over into the equilibrium shape and structure corresponding to the respective monomer number contained in it, representing thus the only configuration which has to be taken into account.

An investigation of the kinetics of nucleation, considering non-equilibrium configurations of the clusters and the resulting additional reaction paths, may be found, e.g., in the following references (Ziabicki (1968) [959]; Kaischew and Stoyanov (1969) [424]). The results obtained confirm, in general, the assumption made above. The kinetic coefficients $w^{(+)}$ and $w^{(-)}$ have to be determined based on the analysis of the growth and decay kinetics of the clusters which may differ in dependence on the particular system considered, while the general equations, Eqs. (6.94)–(6.95), remain the same as far as the assumptions 1–4 are fulfilled. Once the kinetic coefficients $w^{(+)}$ and $w^{(-)}$ are known, the evolution of the cluster size distribution and related quantities can be determined numerically (see, e.g.

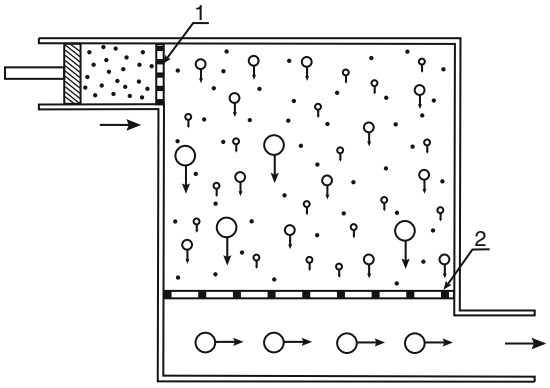

Fig. 6.5 Schematic representation of Szilard's model used in the derivation of the classical expression for the steady-state nucleation rate here shown for the process of vapor condensation. In an isothermal chamber, connected with a reservoir of ambient phase particles, the process of condensation takes place and a population of subcritical and supercritical liquid clusters is formed. The clusters with particles numbers $j \geq g \gg j_c$ are removed from the chamber instantaneously via the semipermeable grate (*2*). It is impenetrable for clusters with sizes $j < g$. Simultaneously an equivalent number of monomers is assumed to enter the system through the membrane (*1*), which is impenetrable for clusters with monomer numbers $j > 1$. In such a way, a constant supersaturation is sustained in the system and a time-independent nucleation rate may be established

Bartels (1991) [39]; Bartels et al. (1991) [43]). However, an analytic approach is also possible and this was the way the theory of nucleation was originally developed. The analytical results are obtained for the case that the state of the system is not changed in the course of nucleation, or in other words, if the supersaturation remains constant during the process (*assumption 5*).[5]

In classical nucleation theory this situation is realized by using the following model proposed by Szilard (see Fig. 6.5; Becker and Dring (1935) [59]; Kaischew (1957) [418]; Becker (1964) [58]). It is assumed that in a certain volume of the initial phase clusters are formed by processes of the type as expressed through equations Eqs. (6.93)–(6.95). Once a cluster reaches an upper limiting size $j = g \gg j_c$ it is removed from the system and g monomers are added to it (*assumption 6*). Consequently, the condition

$$N(j,t) = 0 \qquad \text{for} \qquad j \geq g \gg j_c \tag{6.96}$$

is always fulfilled in the model system. Moreover, since the number of monomers is conserved, in addition, the relation

[5] A complete analytical theoretical description of nucleation-growth processes in solutions accounting for depletion effects – i.e. changes of the state of the ambient phase due to the formation of clusters of the newly evolving phase – is given in Slezov and Schmelzer [776, 778]; and in Slezov [773] as well as in cited there papers.

$$N(1,t) + \sum_{j=2}^{g-1} jN(j,t) \equiv N = \text{ constant} \tag{6.97}$$

holds. Starting with a distribution of monomers only, after a certain time interval, $\tau^{(ns)}$, a time-independent steady-state distribution with respect to cluster sizes is established in the system. In the classical theory, the steady-state is assumed to be established immediately (*assumption 7: steady-state approximation*).

As an intermediate step in the development of the classical theory also the so-called equilibrium distribution of clusters $N^{(e)}(j)$ is determined. This distribution is calculated based on the following additional assumptions (*assumptions 8–10*, see Frenkel (1946) [233]) that

- The ensemble of clusters in the matrix can be considered as a perfect solution (similar to a perfect mixture of gases if vapor condensation is discussed),
- The equilibrium distribution $N^{(e)}(j)$ corresponds to a restricted minimum of the Gibbs free energy G, for which the constraints Eqs. (6.93), (6.96), and (6.97) have to be fulfilled,
- The number of monomers aggregated in clusters with sizes $j \geq 2$ is small as compared with their total number, N.

Based on these assumptions this distribution may be obtained in the form (Frenkel (1946) [233]; Springer (1978) [791]; Demo, Kozicek (1993) [164]; Mutaftschiev (1993) [585])

$$N_j^{(e)} = N \exp\left(-\frac{\Delta G_{(cluster)}(j)}{k_B T}\right), \tag{6.98}$$

which is used as a reference state for the determination of the kinetic coefficients, $w^{(-)}$. In Becker-Döring's approach this equation is introduced as a postulate.

In the assumed steady state, the cluster size distribution in the system is not changed with time. Consequently, $J(j-1) = J(j)$ holds for all values of j in the range $2 \leq j \leq (g-1)$. With this condition from Eq. (6.94) the following set of relations

$$\begin{aligned}
w_1^{(+)} N_1 - w_2^{(-)} N_2 &= J \\
w_2^{(+)} N_2 - w_3^{(-)} N_3 &= J \\
w_3^{(+)} N_3 - w_4^{(-)} N_4 &= J \\
&\cdots \\
w_{g-2}^{(+)} N_{g-2} - w_{g-1}^{(-)} N_{g-1} &= J \\
w_{g-1}^{(+)} N_{g-1} &= 0
\end{aligned} \tag{6.99}$$

is obtained. A multiplication of the second of these equations with $\left(w_2^{(-)}/w_2^{(+)}\right)$, the third with $\left(w_2^{(-)}/w_2^{(+)}\right)(w_3^{(-)}/w_3^{(+)})$ etc. and a subsequent addition of all equations yields (see Becker and Döring (1935) [59]; Volmer (1939) [894]; Kaischew (1957) [418]; Becker (1964) [58])

$$J = \frac{w_1^{(+)} N_1}{\left(1 + \sum_{j=2}^{g-1} \frac{w_2^{(-)}}{w_2^{(+)}} \frac{w_3^{(-)}}{w_3^{(+)}} \cdots \frac{w_j^{(-)}}{w_j^{(+)}}\right)} \,. \tag{6.100}$$

While the attachment rates, $w^{(+)}$, may be determined more or less easily based on a macroscopic approach (see Bartels et al. (1990) [43]; Slezov and Schmelzer (1994) [775]) and the subsequent discussion of growth phenomena) the calculation of the rate of detachment of monomers from the cluster requires, in principle, microscopic considerations.

Though first attempts for a microscopic determination of the detachment rates have been formulated in the last years (Narsimhan, Nowakowski and Ruckenstein (1989, 1991) [593, 608, 674]) the most common approach till now remains the application of the principle of detailed balancing (*assumption 11*, see, e.g., Yourgreau et al. (1966) [939]). In such a line of development in the classical derivation of Becker and Döring the rates of evaporation were determined by the Gibbs-Thomson equation. A similar argumentation was given also by Frenkel (1946) [233]. According to the principle of detailed balancing in an equilibrium state the fluxes in each of the reaction channels are in balance (compare Eqs. (6.93)). This condition yields applying the reference distribution $N_j^{(e)}$ (compare Eq. (6.99))

$$\begin{aligned} w_1^{(+)} N_1^{(e)} - w_2^{(-)} N_2^{(e)} &= 0 \\ w_2^{(+)} N_2^{(e)} - w_3^{(-)} N_3^{(e)} &= 0 \\ w_3^{(+)} N_3^{(e)} - w_4^{(-)} N_4^{(e)} &= 0 \\ &\cdots \\ w_j^{(+)} N_j^{(e)} - w_{j+1}^{(-)} N_{j+1}^{(e)} &= 0 \,. \end{aligned} \tag{6.101}$$

As a first consequence from these equations we obtain with Eq. (6.98)

$$\frac{w_j^{(+)}}{w_{j+1}^{(-)}} = \frac{N_{j+1}^{(e)}}{N_j^{(e)}} = \exp\left\{-\frac{\Delta G_{(cluster)}(j+1) - \Delta G_{(cluster)}(j)}{k_B T}\right\} \,. \tag{6.102}$$

Moreover, a combination of above equations gives (with $N_1^{(e)} \approx N$)

$$\frac{w_2^{(-)}}{w_2^{(+)}}\frac{w_3^{(-)}}{w_3^{(+)}}\cdots\frac{w_j^{(-)}}{w_j^{(+)}} = \frac{N_1^{(e)}w_1^{(+)}}{N_j^{(e)}w_j^{(+)}} \,. \tag{6.103}$$

After a substitution into Eq. (6.100) we obtain with $N_1^{(e)} \approx N_1 \approx N$ the result

$$J = \frac{1}{\sum_{j=1}^{g-1} \frac{1}{[w_j^{(+)}N_j^{(e)}]}} \,. \tag{6.104}$$

For a further evaluation of this expression the monomer number j is considered approximately as a continuous variable (*assumption 12*). With this approximation we get

$$J = \frac{1}{\int_1^{(g-1)} \frac{dj}{[w_j^{(+)}N_j^{(e)}]}} \,. \tag{6.105}$$

Assumption 12 is a good approximation only for systems where the critical cluster sizes are sufficiently large ($j_c \gg 1$). In the opposite case an alternative approach can be developed which is denoted as the atomistic model in the theory of nucleation. It is discussed in one of the subsequent sections.

The distribution, $N_j^{(e)}$, has a sharp minimum at the critical cluster size, j_c. Thus one may replace the attachment rate by its value for the critical cluster size and take it out of the integral. In this way one may write, approximately, taking into account Eq. (6.98)

$$J = \frac{w^{(+)}(j_c)N}{\int_1^{(g-1)} \exp\left(\frac{\Delta G_{(cluster)}(j)}{k_B T}\right) dj} \,. \tag{6.106}$$

A Taylor-expansion of $\Delta G_{(cluster)}(j)$ in Eq. (6.106) in the vicinity of $j = j_c$ (or $R = R_c$), including second order terms, reads

$$\Delta G_{(cluster)}(j) = \Delta G_{(cluster)}(j_c) + \frac{1}{2}\left(\frac{\partial^2 \Delta G_{(cluster)}}{\partial j^2}\right)_{j=j_c}(j-j_c)^2 + \ldots \tag{6.107}$$

Employing Eq. (6.50), Eq. (6.107) may be rewritten in the form

$$\Delta G_{(cluster)}(j) = \Delta G_{(cluster)}^{(c)}\left[1 - \frac{1}{3}\left(\frac{j}{j_c} - 1\right)^2\right] \,. \tag{6.108}$$

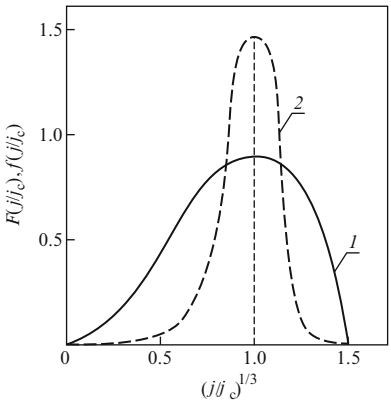

Fig. 6.6 Illustration of the approximations applied in the derivation of the expression for the classical steady-state nucleation rate (After Volmer (1939) [894]). *Full line* (*1*): function in the exponent $f(j) = (\Delta G_{(cluster)}(j)/k_B T)$; *dashed line* (*2*): Integrand $F(j) = \exp[f(j)]$ in Eq. (6.106)

Equation (6.108) is one of the main approximations used throughout the whole theory of nucleation. It was applied by Becker and Döring (1935) [59] instead of Eq. (6.47).

With this expression the basic equation of the classical nucleation theory in the form

$$J = w^{(+)}(j_c)\Gamma_{(z)} N \exp\left(-\frac{\Delta G^{(c)}_{(cluster)}}{k_B T}\right) \tag{6.109}$$

is obtained. Hereby in the determination of the integrals in Eq. (6.106) as a new variable $x = j - j_c$ was introduced and the interval of integration was taken as $(-\infty, +\infty)$ reducing the problem to the calculation of the well-known error function. The quantity $\Gamma_{(z)}$ in Eq. (6.109) is usually denoted as the Zeldovich-factor. It is defined by

$$\Gamma_{(z)} = \left\{-\frac{1}{2\pi k_B T}\left(\frac{\partial^2 \Delta G_{(cluster)}(j)}{\partial j^2}\right)_{j=j_c}\right\}^{1/2} . \tag{6.110}$$

By a calculation of the second-order derivative in Eq. (6.110) one obtains with Eq. (6.50)

$$\Gamma_{(z)} = \frac{1}{2\pi c_\alpha R_c^2}\left(\frac{\sigma}{k_B T}\right)^{1/2} . \tag{6.111}$$

This parameter is typically of the order $\Gamma_{(z)} \approx 10^{-2}$ (for a more full account of possible $\Gamma_{(z)}$ values see Toschev (1973) [848]). An illustration of some of the peculiar properties of the integral in Eq. (6.106) used in the derivation of the steady-state nucleation rate is given in Fig. 6.6.

Historically the first derivation of the classical expression for the steady-state nucleation rate in the form

$$J = \text{const}\, N_1 w^{(+)}(R_c) \exp\left(-\frac{\Delta G_{(cluster)}(R_c)}{k_B T}\right) \tag{6.112}$$

was obtained by Volmer and Weber (see Volmer (1939) [894]) by a simple intuitive argumentation. It was assumed that the concentration of critical clusters in a metastable system is given by Eq. (6.98) and that the nucleation rate, J, is proportional to this concentration multiplied by the probability that a critical cluster passes the maximum of the $\Delta G_{(cluster)}(j)$-potential. This probability was assumed to be proportional to the attachment rate, $w^{(+)}$, of ambient phase molecules to clusters of critical size. To this simple argumentation the further development of theory added in fact the specification of the value of the constant in above equation to const. $= \Gamma_{(z)}$, the Zeldovich-factor.

6.3.2 Analysis of Important Special Cases

The application of Eq. (6.109) requires the knowledge of the attachment rate, $w^{(+)}(j_c)$, for any particular case of phase formation. This quantity can be determined by the analysis of the growth mechanism of a cluster evolving in the ambient phase. This analysis will be performed in Chaps. 8 and 9. However, to allow one estimates for J here $w^{(+)}$ is determined for two important cases, the condensation of droplets from a one-component vapor and the crystallization of a melt, when the initial and the newly formed condensed phases have the same composition.

For the discussion of the first case, we start with the velocity distribution of identical molecules of mass m in a one-component gas, which can be written as (Maxwell's distribution, see, e.g., Becker (1964) [58])

$$dw(v_x, v_y, v_z) = \left(\frac{m}{2\pi k_B T}\right)^{3/2} \exp\left(-\frac{m\mathbf{v}^2}{2k_B T}\right) dv_x dv_y dv_z \,. \tag{6.113}$$

A calculation of the average of the absolute value of the velocity with Eq. (6.113) yields

$$\langle v \rangle = \left(\frac{8k_B T}{\pi m}\right)^{1/2} \,. \tag{6.114}$$

If one considers a unit surface area oriented perpendicular, e.g., to the z-axis, the number of collisions of the molecules of the gas with this surface element per unit time (the impingement rate, Z) can be expressed through the volume density of monomers, N, and the average velocity in z-direction, $\langle v_z \rangle$, as

$$Z = N \langle v_z \rangle \,. \tag{6.115}$$

A determination of $\langle v_z \rangle$ and comparison with Eq. (6.114) yields

$$Z = \frac{1}{4} N \langle v \rangle = \frac{1}{4} N \left(\frac{8 k_B T}{\pi m} \right)^{1/2} . \tag{6.116}$$

By the definition of $w^{(+)}$ this quantity is connected with the impingement rate, Z, by

$$w_j^{(+)} = Z A_j , \qquad A_j = 4\pi R_j^2 . \tag{6.117}$$

Here A_j is the surface area and R_j the radius of a spherical cluster consisting of j monomers. In employing Eq. (6.117) for the determination of the steady-state nucleation rate the quantities A_j have to be identified with the surface area of the critical cluster.

Moreover, if one applies in addition the perfect gas law for the description of the vapor phase ($pV = N k_B T$ with $V = 1$), we obtain, finally,

$$J = \frac{1}{c_\alpha} \left(\frac{p}{k_B T} \right)^2 \left(\frac{2\sigma}{\pi m} \right)^{1/2} \exp \left(- \frac{\Delta G^{(c)}_{(cluster)}}{k_B T} \right) . \tag{6.118}$$

Similarly, for crystallization processes in the melt we get as an estimate for $w^{(+)}(R_c)$ applying the already derived expressions Eqs. (2.106)–(2.110)

$$w_j^{(+)} = Z A_j = \frac{k_B T}{d_0^5 \eta} A_j . \tag{6.119}$$

Taking into account that for melt crystallization $N \equiv c$ holds we obtain from Eq. (6.109)

$$J = \frac{c \varsigma}{d_0^5 \eta c_\alpha} \left(\frac{\sigma}{k_B T} \right)^{1/2} \exp \left(- \frac{\Delta G^{(c)}_{(cluster)}}{k_B T} \right) . \tag{6.120}$$

For melt crystallization the densities of the melt and the crystal are nearly the same and the relation $c \approx c_\alpha$ is fulfilled.

In the above equation, again, the correction factor ς is introduced (compare Sect. 2.4.3), which reflects changes of the probability of attachment of ambient phase particles to the critical nucleus in dependence on its state and the complexity of the ambient phase molecules incorporating into it. For crystalline clusters values of ς of the order 10^{-3}–10^{-5} have to be expected, while for the case of liquid-liquid phase separation, which can be treated similarly, $\varsigma \approx 1$ holds (see Gutzow and Toschev (1968) [318]; Gutzow, Kashchiev, Avramov (1985) [330]). The introduction of the correction factor ς implies that an effective impingement rate is applied. This effective impingement rate is given by $Z^{(eff)} = Z\varsigma$ resulting in

$$w_j^{(+)} = Z^{(eff)} A_j = \varsigma \frac{k_B T}{d_0^5 \eta} A_j . \tag{6.121}$$

For crystallization of melts the thermodynamic driving force of phase formation, $\Delta\mu$, can be expressed through the difference $T - T_m$, for example, by Eq. (6.65). In this case we get assuming, again that nearly spherical clusters are formed

$$J = \frac{\varsigma}{d_0^5}\left(\frac{\sigma}{k_B T}\right)^{1/2}\frac{1}{\eta}\exp\left(-\frac{16\pi}{3}\frac{\sigma^3 v_m^2}{k_B T(\Delta s_m(T_m - T))^2}\right) . \tag{6.122}$$

Here v_m is the molar volume of the crystalline phase.

Similar expressions may be also derived if more complicated relations for the description of the thermodynamic driving force of crystallization have to be employed (compare Sect. 3.3). Generally, it turns out that the term $\exp(-\Delta G^{(c)}_{(cluster)}/k_B T)$ depends strongly on temperature. However, the temperature dependence of the steady-state nucleation rate is determined not only by this term but also by the temperature course of the viscosity, η. If we apply a Frenkel-type equation with a constant activation energy, U_0, for the description of the temperature dependence of the viscosity (compare Eq. (2.78)) Eq. (6.122) obtains the form

$$J = B_1^{(\oplus)}\exp\left(-\frac{U_0}{k_B T}\right)\exp\left(-\frac{B_2^{(\oplus)}}{T(T_m - T)^2}\right) , \tag{6.123}$$

$$B_1^{(\oplus)} = \frac{\varsigma}{d_0^5\eta_0}\left(\frac{\sigma}{k_B T}\right)^{1/2} , \qquad B_2^{(\oplus)} = \frac{16\pi}{3}\frac{\sigma^3 v_m^2}{k_B(\Delta s_m)^2} , \tag{6.124}$$

where the quantities $B_1^{(\oplus)}$ and $B_2^{(\oplus)}$ are relatively slightly varying functions of temperature. The temperature dependence of $B_2^{(\oplus)}$ and, at part also of $B_1^{(\oplus)}$, is connected with the temperature dependence of the specific surface energy. In a first approximation the relation

$$\frac{\sigma(T)}{\sigma(T_m)} \cong (1 - \gamma\Delta\mu(T)) , \qquad \gamma > 0 , \qquad \Delta\mu(T) > 0 \tag{6.125}$$

can be derived (Gutzow, Kashchiev and Avramov (1985) [330]). A consideration of the possible temperature dependence of σ is of importance both for analyzing nucleation but also crystal growth data, when such processes are analyzed in the whole temperature region from T_g to T_m.

The temperature dependence of the steady-state nucleation rate, J, according to Eq. (6.123) is characterized by the following features. The nucleation rate tends to zero both for $T \to T_m$ (the thermodynamic driving force of the transformation becomes equal to zero) and for values of temperature near and below T_g (here the mobility of the ambient phase particles tends to zero). There exists a maximum of this curve at $T = T_{max}^{nucl}$, which can be determined, as calculated first by Frenkel (1946) [233], applying the relation for the temperature dependence of the viscosity, proposed by him, via the relation

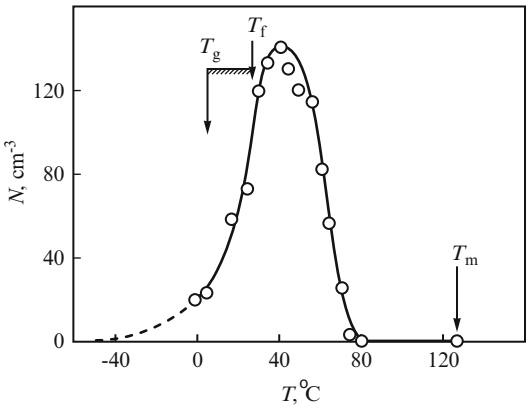

Fig. 6.7 Temperature dependence of the nucleation rate of piperine according to Tammann (1933) [820]. N is the number of crystallization centers observed after heat treatment of the melt and subsequent nucleus development. With T_g and T_f the vitrification temperature and the softening temperature of the substance considered are denoted

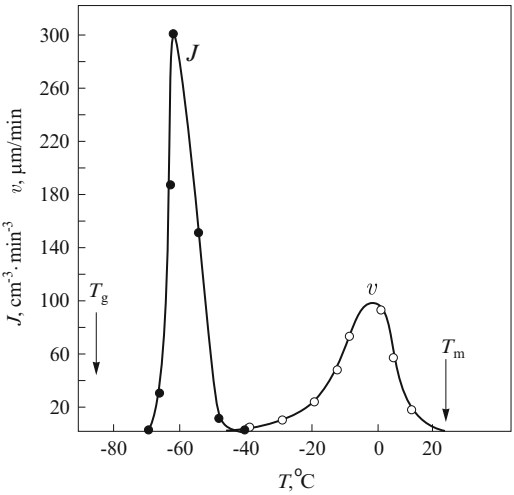

Fig. 6.8 Temperature dependence of the steady-state nucleation rate, J (According to data given by Chernov (1980) [132]) and of the linear rate of crystal growth v (Results of measurements of Volmer and Marder (1931) [895]) for glycerol

$$\frac{T_m - T_{max}^{nucl}}{T_{max}^{nucl}} = \left(\frac{32\pi}{3U_0}\right)^{1/3} \sigma \left(\frac{v_m}{T_m \Delta s_m}\right)^{2/3} . \tag{6.126}$$

Similar estimates for the value of temperature for which $J(T)$ has a maximum based on more realistic $\eta(T)$-dependencies have been made by Filipovich (1963) [206]. In contrast, attempts have also been developed to apply the knowledge of the $J(T)$-course for a specification of the constants employed for the description of the temperature dependence of the viscosity. This was done, for example, by Stoycev et al. (1973) [807] for the VFT-equation applied to simple organic melts.

The first experimental results on the temperature dependence of the nucleation rate in glass-forming melts confirmed the theoretical expectations, at least, qualitatively. One of the first examples in this respect are Tammann's results from 1898 on

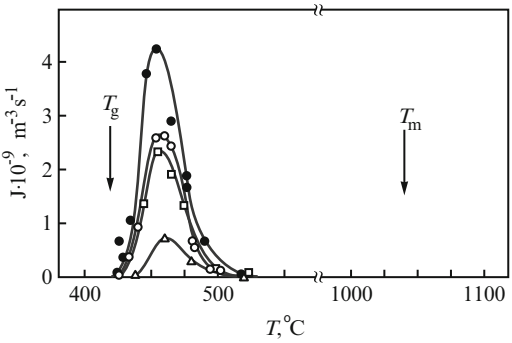

Fig. 6.9 Temperature dependence of the nucleation rate, J, for α-$Li_2O\,2SiO_2$ as obtained by different authors. *Black dots*: James (1974) [400]; *open circles*: Kalinina, Fokin, Filipovich (1976) [427]; *squares*: Zanotto and James (1985) [946]; *triangles*: Matusita and Tashiro (1975) [539]

the temperature dependence of the nucleation rate of piperine (see Tammann (1933) [820]) shown in Fig. 6.7 as well as similar results on glycerol (Fig. 6.8). However, no quantitative comparison between experiment and theory can be made based on these early investigations. This is due to the fact that steady-state nucleation was assumed without any experimental proof.

The experimental results were obtained applying Tammann's method of nucleus development which was accepted and employed by most other investigators of this time. In Tammann's method, the melt is heat-treated first at temperatures corresponding to relatively large values of the nucleation rate, for which, as seen in Fig. 6.8, the growth rates are relatively small. The temperature is increased in a next step and the supercritical clusters formed at lower temperatures (higher supersaturations) are allowed to grow to macroscopically observable sizes. For the higher values of temperature the formation of new nuclei may be excluded practically. The outcome of nucleation is then connected with the experimentally observed number of clusters developed to macroscopic sizes. However, Tammann's method of nucleus development has also some shortcomings as it becomes evident, for example, from Fig. 6.3. Clusters formed at lower values of temperature (higher under-cooling) may be converted to a subcritical size when the system is exposed to higher temperatures (lower supersaturations). In this way, a part of the supercritical clusters formed initially will decay and not grow to macroscopic dimensions.

In Fig. 6.9, results of more recent investigations of the temperature dependence of the nucleation rate as obtained by several authors are given for another glass-forming system (lithium disilicate $Li_2Si_2O_5$). Despite the considerable scattering in the experimental data for the values of the nucleation rate, the position of the maximum is practically the same for all of the different studies shown. The observed scattering is due mainly to the presence of different amounts of insoluble particles in the melt which, as it will be discussed in detail in the next chapter, may considerably increase the rate of nucleation. In systems like lithium disilicate the high number of nucleation dopants may be explained taking into account that even platinum crucibles are corroded during silica and phosphate glass synthesis and may provide

in this way a perceptible population of foreign nucleation cores (see the results of Gutzow, Popov and Streltzina (1968) [323]).

6.3.3 *Problems, Generalizations and Improvements: An Overview*

In application of the basic equations of the classical nucleation theory it is usually assumed that the work of formation of the critical clusters can be expressed in terms of Gibbs' formula, Eq. (6.43), with a value of the specific interfacial energy, σ, determined for a planar interface between both coexisting phases (*assumption 13: capillarity approximation*). As already mentioned this extension of macroscopic concepts to the properties of small clusters, consisting of relatively few particles only, gives rise to serious criticism and originated a number of alternative approaches for the calculation of $\Delta G^{(c)}_{(cluster)}$ (curvature dependent surface tension and the Toschev-Parlange correction; atomistic approach to nucleation). A review of the basic ideas of the atomistic approach to nucleation is given in Sect. 6.3.8. In addition, in our derivations, entropy effects connected with the incorporation of rotational and translational degrees of freedom – with the so-called Lothe-Pound factor (see Kuhrt (1952) [488]; Lothe, Pound (1962) [514], (1966) [515]; Hirth, Pound (1963) [368]) – are not accounted for. A thorough discussion in recent years showed that such a correction factor can be of great importance for vapor condensation but is of little significance for melt crystallization (see Mutaftschiev (1993) [585]).

In the application of nucleation theory to processes of crystallization in the melt, the problem arises of how an independent estimation of the specific interfacial energy between the melt and the evolving small crystallites can be carried out. According to the Skapski-Turnbull rule [764–766, 788, 789]

$$\sigma = \zeta \frac{q_m}{N_A^{1/3} v_m^{2/3}} , \qquad \zeta = 0.4 - 0.6 \tag{6.127}$$

is usually fulfilled.[6] Here q_m is the molar heat of melting, v_m the molar volume of the melt, N_A Avogadro's number. This rule is a particular formulation of a very general dependence proposed many years ago by Stefan ((1886) [796]; see also Moelwyn-Hughes (1972) [567]). According to this rule, the specific interfacial energy for any case of phase equilibrium is determined by the ratio of the molar enthalpy of the transformation (ΔH) divided by the number of molecules at the surface of one mole of the substance $\left(N_A^{1/3} v^{2/3}\right)$. The specific interfacial energy melt-crystal is determined by the heat of melting, while the interfacial tension of the melt-vapor

[6] A derivation of this relation and some additional discussion can be found in Chap. 14.

interface is proportional to the heat of evaporation. Similarly, the specific interfacial energy of the crystal-vapor interface is determined by the enthalpy of sublimation. For interfaces between crystals and aqueous solutions of the respective substance according to a suggestion of Kahlweit (1961) [415] the heat of dissolution can be used for a determination of σ.

For liquid-vapor interfaces the parameter ζ in Eq. (6.127) is usually of the order $\zeta \approx 0.5$. For phase equilibria with crystalline phases ζ depends significantly not only on the substance involved but also on the modification of the crystalline phase. A detailed investigation of these problems was performed by Kaischew and Krastanov (1933) [423]. However, experimental methods for a direct determination of σ for the melt-crystal interface do not exist and the estimates of this quantity are often based on nucleation experiments themselves. With Eq. (6.127) the estimate for T_{max}^{nucl} given by Eq. (6.126) may be rewritten in the form

$$\frac{T_m}{T_{max}^{nucl}} = 1 + \left(\frac{32\pi}{3\epsilon^{\oplus}}\right)^{1/3} \zeta \left(\frac{\Delta S_m}{R}\right)^{1/3}, \qquad \epsilon^{\oplus} = \frac{U_0}{k_B T_m}. \tag{6.128}$$

By substituting typical values of $\epsilon^{\oplus}$ in the range $\epsilon^{\oplus} \cong 20-40$ and $\Delta S_m/R \cong 1-2$ as an estimate $T_{max}^{nucl} \cong (0.5-0.6)T_m$ is found. Similar estimates but carried out with more realistic expressions for the temperature dependence of the viscosity yield $T_{max}^{nucl} \cong (0.6-0.7)T_m$ (Filipovich (1963) [206]).

In the derivation of the classical theory of nucleation, it was assumed that the number of particles in the critical cluster is sufficiently large, so that a continuous description can be used. Such a procedure is questionable taking into account experimental findings that in most cases of nucleation taking place in the formation of thin films, in electro-crystallization, critical clusters constituted of only a few atoms or molecules are to be expected at the high supersaturations involved in such processes. For nucleation processes taking place in glass-forming melts, estimates show (Gutzow (1981) [304]) that here, at least, in processes of homogeneous nucleation and liquid-liquid phase separation, the number of molecules in the critical clusters is sufficiently large even at the highest possible supersaturations (i.e., in the vicinity of T_g). Thus both the capillarity approximation and the transition from a discrete to a continuous description should here to be more acceptable with respect to the validity of the final results. This circumstance can be considered as an additional advantage for using glass-forming systems in order to test the theory of nucleation experimentally and to apply, on the other hand, the classical theory to the interpretation of experimental results in crystallization of glasses.

In the outlined derivations, it was assumed that the ambient phase molecules which have to be incorporated into the growing cluster are of nearly spherical shape resembling billiard balls (cf. Fig. 4.26). However, in most glass-forming melts such a picture has to be modified accounting for the complexity of the basic building units of the new phase. Another limitation of the classical approach consists of the application of the principle of detailed balancing, valid strictly only for equilibrium states, for the determination of the decay rates $w^{(-)}$ for the

non-equilibrium processes under consideration. In this respect, it is of interest to note that recently a new method of determination of these kinetic quantities was developed avoiding the application of the principle of detailed balancing for clusters of supercritical sizes (for the details see Slezov and Schmelzer (1994) [775]), i.e., in the region of cluster sizes for which the application of the above mentioned approach is particularly doubtful. The final results of the classical theory, modified in such a way, remain practically the same, but they have got a sound foundation. In this approach the decay rates are, again, expressed through a function of the type as given by Eq. (6.98), however, this function is to be interpreted, now, as an auxiliary mathematical quantity. In the same paper [775], the generalization of the outlined results to the case of phase formation processes in multi-component solid or liquid solutions is also given for the case that aggregates of a well-defined stoichiometric composition are formed.[7]

Severe restrictions with respect to the applicability of the classical theory are also connected with the assumptions 5 and 7, the supposed constancy of the state of the system in the course of nucleation, i.e., the steady-state character of this process. The intrinsic non-steady character of nucleation arises, in general, from two factors:

- In the model system and also in real situations it takes some induction time, if attainable at all that a stationary cluster size distribution and, consequently, a steady-state nucleation rate, having the same value for clusters of every size, is established via a series of supposed bimolecular reactions (transient nucleation).
- Processes of formation and growth of the clusters change, in general, the supersaturation and the state of the system, where the phase transformation takes place. Consequently, constant nucleation rates cannot be sustained for prolonged periods of time without external interference.

It is evident that this change of the state of the system essentially determines the basic characteristics of the nucleation process as, e.g., the total number of clusters formed in the system in the initial stage of phase formation.

In the case of non-steady state nucleation, problems also arise with respect to the meaning and the definition of the term nucleation rate. For the classical model analyzed so far the nucleation rate J is usually identified with the rate of formation of critical clusters $J(j_c)$ given by Eqs. (6.109), (6.118), and (6.120). In the framework of the considered model, this definition is not restrictive since, due to the assumption of a steady state, the formation rates of clusters of each size are the same. The situation is, however, changed, if nucleation under non-steady state conditions is considered. In both of the mentioned cases the rates of formation of clusters of different sizes differ. This fact requires a more detailed discussion of the meaning of the term nucleation rate and of the consequences arising from the changes of

[7]For a more recent as compared with [775] formulation of these results including further developments, in particular, accounting for depletion effects on the course of first-order phase transitions, see the already cited references Slezov and Schmelzer [776, 778]; Slezov et al. [779]; and Slezov [773] and further cited there papers.

the state of the system with respect to nucleation and the phase transformation as a whole.

In the subsequent sections, first transient nucleation is discussed. Hereby two possibilities exist. The first one is connected with a numerical description of nucleation based on the solution of the set of kinetic equations underlying the classical nucleation theory or equivalent expressions. The second, the classical way, consists of the derivation of approximative analytical solutions. In the subsequent section we proceed in line with the first of the mentioned approaches going over afterwards to a derivation of analytical expressions for the nucleation rate, the time-lag and other characteristics of transient nucleation. The analysis is supplemented by a more detailed discussion of some generalizations and modifications of the classical theory (nucleation of chain-folding polymers, atomistic approach to nucleation, thermal and athermal nucleation) mentioned briefly above.

6.3.4 *General Description of the Time Evolution of the Cluster Size Distribution: The Zeldovich-Frenkel Equation*

The calculation of the steady-state nucleation rate is a major but only a first step in the description of phase transformation processes. A comprehensive characterization of the nucleation process as well as of the whole course of the transition is obtained only if the cluster size distribution is established as a function of time for the whole transformation. In the framework of the numerical approach, the determination of the cluster size distribution can be carried out by a numerical solution of the system of kinetic equations Eqs. (6.94)–(6.97) underlying classical nucleation theory. Here, as examples, the first attempts by Turnbull (1949) [942] and Courtney (1969) [148] are to be mentioned as well as later elaborated calculations by Kelton, Greer et al. (1983) [448]. The numerical calculations are time consuming since the number of equations which have to be solved simultaneously has to exceed the number of particles in the largest cluster evolving in the course of time in the system. For processes of liquid phase separation such calculations could involve a number of equations greater 10^3. Moreover, for an analytical discussion of different stages of the transformation a more compact description is also desirable. It can be obtained in the following way.

First, we rewrite Eqs. (6.94)–(6.95) in the form

$$\frac{\partial N(j,t)}{\partial t} = -[w_j^{(+)} + w_j^{(-)}]N(j,t) + [w_{j-1}^{(+)} N(j-1,t) + w_{j+1}^{(-)} N(j+1,t)] \; . \quad (6.129)$$

Considering j as a continuous variable by a Taylor-expansion of the quantities $w_{j-1}^{(+)} N_{j-1}$ and $w_{j+1}^{(-)} N_{j+1}$, including second order terms, a Fokker-Planck type equation (see, e.g., Röpke (1987) [668]) for the time evolution of the cluster size-distribution function is obtained, i.e.,

$$\frac{\partial N(j,t)}{\partial t} = -\frac{\partial}{\partial j}\left\{[w_j^{(+)} - w_j^{(-)}]N(j,t)\right\} + \frac{1}{2}\frac{\partial^2}{\partial j^2}\left\{[w_j^{(+)} + w_j^{(-)}]N(j,t)\right\} . \tag{6.130}$$

The Fokker-Planck equation was developed originally to describe flow and diffusion processes in real space and later extended to processes in phase space or, as in the present investigation, to a description of the kinetics of cluster formation and growth in cluster size space. At the same level of approximation as inherent in the derivation of Eq. (6.130) this equation may be rewritten also as (see Slezov and Schmelzer (1994) [775])

$$\frac{\partial N(j,t)}{\partial t} = -\frac{\partial}{\partial j}\left\{\left[(w_j^{(+)} - w_{j+1}^{(-)})N(j,t)\right] - \frac{1}{2}\left[(w_j^{(+)} + w_{j+1}^{(-)})\frac{\partial}{\partial j}N(j,t)\right]\right\} . \tag{6.131}$$

This equation has the same structure as the relation describing the macroscopic deterministic flow as well as diffusion processes of particles characterized by a volume concentration c, i.e.,

$$\frac{\partial c}{\partial t} = -\nabla\left\{[c(\mathbf{r},t)\mathbf{v}] - D\nabla c(\mathbf{r},t)\right\} . \tag{6.132}$$

Here $\mathbf{v}$ is the macroscopic (hydrodynamic) velocity of the particles while D is the diffusion coefficient, connected with the diffusive Brownian motion of the considered component in real space.

Similarly, the quantity v_j, defined by

$$v_j = \langle w_j^{(+)} - w_{j+1}^{(-)}\rangle , \tag{6.133}$$

has the meaning of the macroscopic (average) growth velocity of a cluster of size j, while the quantity D_j, given by

$$D_j = \frac{\langle w_j^{(+)} + w_{j+1}^{(-)}\rangle}{2} \tag{6.134}$$

represents the diffusion coefficient for stochastic motions in cluster size space. Since the coefficients $w^{(+)}$ and $w^{(-)}$ describing growth and decay are relatively smooth functions of the number of particles, j, approximately, the relations

$$v_j = \langle w_j^{(+)} - w_j^{(-)}\rangle , \tag{6.135}$$

$$D_j = \frac{\langle w_j^{(+)} + w_j^{(-)}\rangle}{2} , \tag{6.136}$$

may also be used. These relations allow one to give, in addition, also a kinetic definition of the critical cluster size.

In agreement with thermodynamics, the critical cluster is characterized by the property that the macroscopic (deterministic) velocity of growth is equal to zero. Consequently, for the critical cluster the relations

$$w_j^{(+)}(R_c) = w_j^{(-)}(R_c) \,, \qquad D(R_c) = w_j^{(+)}(R_c) \tag{6.137}$$

are fulfilled. With Eq. (6.102) the deterministic rate of growth of clusters of size j may be expressed through the attachment rate $w_j^{(+)}$ and $\Delta G_{(cluster)}(j)$ as

$$v_j = w_j^{(+)} \left\{ 1 - \exp\left[- \frac{\Delta G_{(cluster)}(j+1) - \Delta G_{(cluster)}(j)}{k_B T} \right] \right\} \,. \tag{6.138}$$

For small values of the quantity $[\Delta G(j+1) - \Delta G(j))/k_B T]$ a Taylor-expansion of the exponential function yields, approximately,

$$v_j = -w_j^{(+)} \frac{1}{k_B T} \frac{\partial \Delta G_{(cluster)}}{\partial j} \,. \tag{6.139}$$

Both equations given above will be of particular significance in discussing different mechanisms of cluster growth (see Chaps. 8 and 9).

Neglecting second-order terms in the Taylor-expansion of Eq. (6.133) a continuity equation of the form

$$\frac{\partial N(j,t)}{\partial t} = - \frac{\partial}{\partial j} \left\{ [w_j^{(+)} - w_j^{(-)}] N(j,t) \right\} \tag{6.140}$$

is obtained as a special case from the Fokker-Planck equation. This continuity equation, giving the time dependent change of the concentration of j-meric clusters, can be expressed also in a somewhat different way. Starting with Eq. (6.95)

$$J(j,t) = w_j^{(+)} N(j,t) - w_{j+1}^{(-)} N(j+1.t) \,, \tag{6.141}$$

rewriting it in the form

$$J(j,t) = w_j^{(+)} N_j^{(e)} \left[\frac{N(j,t)}{N_j^{(e)}} - \frac{w_{j+1}^{(-)} N(j+1,t)}{w_j^{(+)} N_j^{(e)}} \right] \tag{6.142}$$

and applying Eq. (6.101)

$$w_{j+1}^{(-)} = w_j^{(+)} \frac{N_j^{(e)}}{N_{j+1}^{(e)}} \,, \tag{6.143}$$

we have

$$J(j,t) = w_j^{(+)} N_j^{(e)} \left[\frac{N(j,t)}{N_j^{(e)}} - \frac{N(j+1,t)}{N_{j+1}^{(e)}} \right] . \tag{6.144}$$

A truncated Taylor-expansion of the second term in the brackets gives

$$J(j,t) = -w_j^{(+)} N_j^{(e)} \frac{\partial}{\partial j} \left(\frac{N(j,t)}{N_j^{(e)}} \right) . \tag{6.145}$$

Moreover, by a Taylor-expansion of $J(j-1,t)$ Eq. (6.94) may be rewritten also as

$$\frac{\partial}{\partial t} N(j,t) = J(j,t) + \frac{\partial J(j,t)}{\partial j}(-1) + \ldots - J(j,t) = -\frac{\partial J}{\partial j} . \tag{6.146}$$

A combination of Eqs. (6.144) and (6.146) yields, finally,

$$\frac{\partial}{\partial t} N(j,t) = \frac{\partial}{\partial j} \left[w_j^{(+)} N_j^{(e)} \frac{\partial}{\partial j} \left(\frac{N(j,t)}{N_j^{(e)}} \right) \right] . \tag{6.147}$$

This relation is usually denoted as Zeldovich-Frenkel equation. It was derived first by Zeldovich (1942) [949] in a discussion of the problem of cavitation (bubble formation in a liquid).

The classical derivation of this equation can be found also in Frenkel's monograph (1946) [233]. Frenkel's approach is somewhat different from the derivation given above. Frenkel started directly with Eqs. (6.94), (6.95), (6.98), and (6.99) and obtained

$$\frac{\partial N(j,t)}{\partial t} = J(j-1,t) - J(j,t) , \tag{6.148}$$

$$J(j-1,t) = w_j^{(+)} N_{j-1}^{(e)} \left(\frac{N(j-1,t)}{N_{j-1}^{(e)}} - \frac{N(j,t)}{N_j^{(e)}} \right) , \tag{6.149}$$

$$J(j,t) = w_{j+1}^{(+)} N_j^{(e)} \left(\frac{N(j,t)}{N_j^{(e)}} - \frac{N(j+1,t)}{N_{j+1}^{(e)}} \right) . \tag{6.150}$$

Applying the relations

$$J(j-1,t) = J(j,t) - \frac{\partial}{\partial j} \left[w_j^{(+)} N_j^{(e)} \left(\frac{N((j,t)}{N_j^{(e)}} - \frac{N(j+1,t)}{N_{j+1}^{(e)}} \right) \right] , \tag{6.151}$$

$$\frac{N(j+1,t)}{N_{j+1}^{(e)}} = \frac{N(j,t)}{N_j^{(e)}} + \frac{\partial}{\partial j} \frac{N(j,t)}{N_j^{(e)}} + \ldots , \tag{6.152}$$

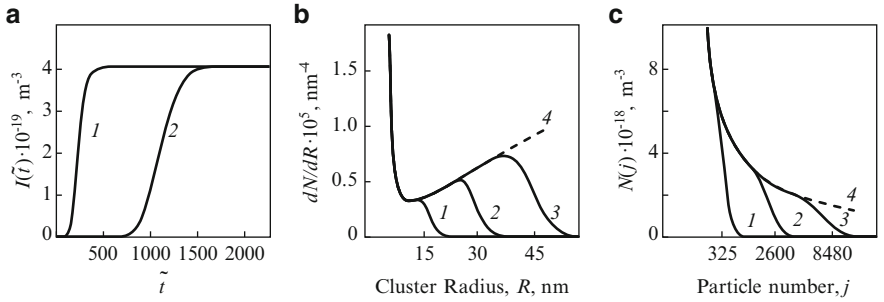

Fig. 6.10 (**a**) Change of the nucleation rate as a function of reduced time, $\tilde{t}$, for clusters of different sizes ($R = 1.08$ nm (curve (*1*)) and $R = 2.76$ nm (curve (*2*)) obtained by the numerical solution of the set of kinetic equations, Eqs. (6.94)–(6.95). In the calculations the supersaturation in the system is kept constant. (**b**) and (**c**) Evolution of the cluster size distribution in nucleation taking place at constant supersaturation expressed through the cluster radius ((dN/dR), (**b**)) and the number of particles, j, contained in it (**c**) for different moments of reduced time $\tilde{t}$: $\tilde{t} = 460$ (*1*); $\tilde{t} = 1,160$ (*2*) and $\tilde{t} = 2,310$ (*3*)

which may be obtained from Taylor-expansions of the respective quantities, the relation, Eq. (6.147), is re-derived, again. With Eq. (6.98) the term in the brackets in Eq. (6.147) can be rearranged to give

$$\frac{\partial}{\partial t}N(j,t) = \frac{\partial}{\partial j}\left[w_j^{(+)}\frac{\partial N(j,t)}{\partial j}\right] + \frac{\partial}{\partial j}\left[w_j^{(+)}N(j,t)\frac{\partial}{\partial j}\left(\frac{\Delta G_{(cluster)}(j)}{k_B T}\right)\right] . \tag{6.153}$$

The flux in cluster size space may be expressed, consequently, as

$$J(j,t) = -w_j^{(+)}\left(\frac{\partial N(j,t)}{\partial j} + N(j,t)\frac{\partial}{\partial j}\frac{\Delta G_{(cluster)}(j)}{k_B T}\right) . \tag{6.154}$$

Equation (6.153) has a similar form as the equation describing diffusion in a force field (see Kramers (1940) [482]; Chandrasekhar (1943) [126]; Hänggi et al. (1990) [346]; Feder et al. (1966) [198]). In this case the generalized thermodynamic "force" is proportional to $(\partial \Delta G_{(cluster)}(j)/\partial j)$. This analogy of the Zeldovich-Frenkel equation to equations describing processes of diffusion in force fields initiated the first attempts of deriving solutions describing the kinetics of transient nucleation as performed by Zeldovich (1942) [949] and Collins (1955) [139].

Results of the solution of the basic set of kinetic equations (Eqs. (6.94) and (6.95)) and of the Fokker-Planck equation, Eq. (6.130), for diffusion limited growth with appropriately chosen rate coefficients $w^{(+)}$ and $w^{(-)}$ (see Bartels et al. (1991) [43]) for the case of segregation of one of the components in a quasi-binary glass-forming melt are shown in Figs. 6.10 and 6.11. The parameter values used refer to the process of segregation of silver chloride clusters in a sodium metaborate

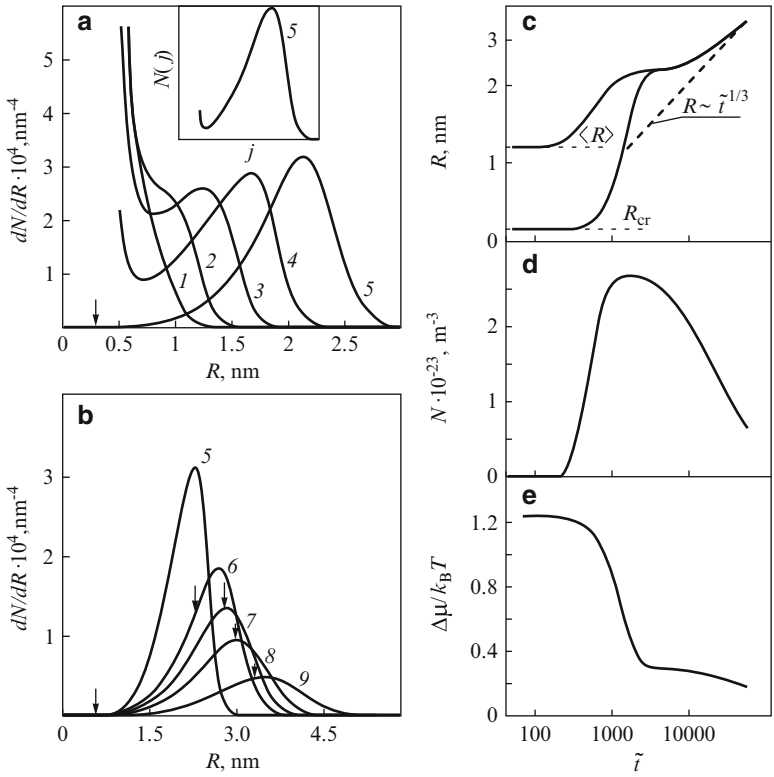

Fig. 6.11 (**a**) Evolution of the cluster size distribution dN/dR in a finite (closed) system, where the total number of particles is conserved. The actual critical cluster size is indicated by *arrows*. For the curves, represented in (**a**), R_c remains practically constant. The different curves correspond to $\tilde{t}$: 116 (*1*); 231 (*2*); 380 (*3*); 588 (*4*); 1,051 (*5*); 7,851 (*6*); 12,330 (*7*); 18,821 (*8*); 37,267 (*9*). (**b**) Average cluster radius, $\langle R \rangle$, total number of clusters, N, and relative supersaturation as functions of time when the total number of particles is conserved. In the calculations only clusters with a radius larger than 0.6 nm are taken into account to allow one a better comparison with experimental results. In experiments, in general, characteristics of the cluster size distribution can be measured only for sizes exceeding a given limit of detectability determined by the experimental method applied

melt also investigated experimentally (see also Fig. 6.12; Specific interfacial energy $\sigma = 0.09\ \mathrm{Jm}^{-2}$; particle concentration in the cluster phase $c_\alpha = 2.3 \cdot 10^{28}\ \mathrm{m}^{-3}$; concentration of segregating particles in the matrix $c = 8.6 \cdot 10^{27}\ \mathrm{m}^{-3}$; equilibrium concentration of segregating particles in the matrix $c_{eq} = 4.2 \cdot 10^{26}\ \mathrm{m}^{-3}$; temperature 458 °C; diameter of matrix building units $d_0 = 6.06 \cdot 10^{-10}$ m. Moreover, a dimensionless time scale $\tilde{t} = tD/d_0^2$ was introduced). It is assumed in the calculations that the segregating phase is distributed initially in the matrix in form of monomeric structural units (atoms or molecules) only. Starting with such an initial state, the rates of formation of clusters of different sizes can be calculated. Hereby

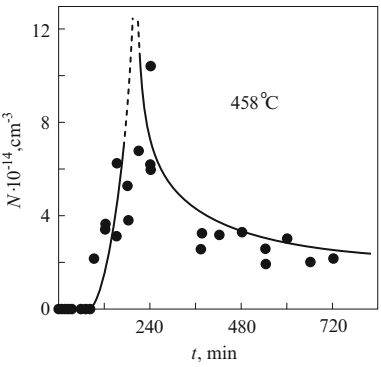

Fig. 6.12 Results of experimental investigations ($N(t)$ vs. t-curves) of the kinetics of formation of silver chloride clusters in a sodium borate glass-forming melt. The process models the process of formation of the photoactive AgCl-phase in photochromic glasses (see Pascova et al. (1990a,b) [627, 628])

it is supposed first that the state of the system is not changed in the course of the transformation (constant supersaturation).

The curves representing the time evolution for the nucleation rate for two different cluster sizes are shown for these conditions in Fig. 6.10a. It can be seen that it takes some time until the steady-state nucleation rate, having the same value for clusters of each size, is established. However, the induction period needed for the establishment of the steady-state nucleation rate is different for different cluster sizes. Figure 6.10b illustrates for the same conditions the time evolution of the cluster size distribution expressed through the variable R (cluster radius) and j (number of particles in the cluster).

If the condition of constant supersaturation is replaced in the numerical calculations by the constraint, which is more natural for segregation processes that the total number of particles of the segregating component (number of monomers) is not changed in the course of the transition

$$\sum_j j\, N(j,t) = \text{ constant}\,, \tag{6.155}$$

a new situation arises. The evolution of the cluster size distributions $f(R,t)$ or $N(j,t)$ and related quantities like the average cluster size

$$\langle R \rangle = \int_0^\infty R f(R,t) dR\,, \tag{6.156}$$

the total number of clusters in the system N, the relative supersaturation depend in this case on time in a form as depicted in Fig. 6.11. Only for a limited interval of time is the supersaturation in the system practically unchanged and, consequently, a constant nucleation rate is observed. In the case discussed, the relative supersaturation χ is defined by the actual concentration of free monomers of the segregating component in the ambient phase. Considering the ambient phase

as a perfect solution, according to the definition of the relative supersaturation (Eq. (6.54)), we obtain

$$\chi = \frac{\Delta\mu}{k_B T} = \ln\left(\frac{c_\beta}{c_{eq}}\right) , \tag{6.157}$$

where c_β and c_{eq} are the actual and the equilibrium concentrations of the monomers in the ambient phase for a stable coexistence of both phases divided by a planar interface. Moreover, in Fig. 6.11a a stage of the transformation with a time dependence of the average cluster size described by the power law $\langle R\rangle^2 \sim t$ can be seen. Via an intermediate interval with a relatively low growth rate of the average cluster size, the growth kinetics is transferred further to an $\langle R\rangle^3 \sim t$ law. An analytical description of these later stages is given in Chap. 9 concerned with diffusion-limited segregation and a process in the transformation denoted commonly as Ostwald ripening.

Results of experimental investigations of the discussed process of formation of silver chloride clusters in a sodium borate melt are shown in Fig. 6.12. It is seen that, at least, qualitatively a coincidence between theoretical predictions and experimental results is found. The results of the numerical calculations modeling phase formation processes in real systems exhibit the complicated character of the changes occurring in the course of the phase transformation and the difficulties attempts of an analytical description of such processes are encountered with.

Going over, now, to a derivation of such analytical results we have to note first that previously obtained expressions for the steady-state nucleation rate may be rederived easily from the Zeldovich-Frenkel equation. Indeed, starting with Eqs. (6.145)–(6.147) and assuming steady-state conditions we may write

$$J(j,t) = J = -w_j^{(+)} N_j^{(e)} \frac{\partial}{\partial j}\left(\frac{N(j)}{N_j^{(e)}}\right) = \text{constant} . \tag{6.158}$$

An integration of this equation with respect to j in the limits from $j = 1$ to $j = \infty$ yields

$$\left(\frac{N(j)}{N_j^{(e)}}\right)\Bigg|_{j=1}^{j=\infty} = -\int_1^\infty \frac{J}{w_j^{(+)} N_j^{(e)}} . \tag{6.159}$$

Taking into account the boundary conditions

$$\frac{N(j)}{N_j^{(e)}} \simeq 1 \qquad \text{for} \qquad j \to 1 , \tag{6.160}$$

$$\frac{N(j)}{N_j^{(e)}} \simeq 0 \qquad \text{for} \qquad j > g \gg j_c \tag{6.161}$$

Eq. (6.105) is re-derived and can be evaluated by the same methods as discussed earlier.

6.3.5 *Transient Nucleation: Time Dependence of the Nucleation Rate and the Number of Supercritical Clusters*

An analytical description of the numerical results, outlined in the previous section, requires a solution of the Zeldovich-Frenkel equation or equivalent expressions. Important problems in this direction are the determination of the time dependence of the nucleation rate in the initial period of the transformation and the evaluation of the induction period. Different approaches have been developed in order to solve this task (for a discussion of classical attempts in this direction see, for example, Mason (1957) [536]; Lyubov and Roitburd (1958) [518]; Kashchiev (1969) [434], Frisch and Carlier (1971) [236]; Toschev (1973) [848] and for more recent developments Binder and Stauffer (1976) [83]; Trinkaus and Yoo (1987) [854]; Shi et al. (1990) [752]; Wu (1992) [933]; Shneidman (1988 [746], 1992 [747], 1994 [748]). Hereby it is commonly assumed that in the initial stage of the transformation the segregating phase consists of monomeric units (atoms, molecules) only, i.e. that

$$N(j,t) = 0 \qquad \text{at} \qquad t = 0 \qquad \text{for} \qquad j > 1 \tag{6.162}$$

holds.

In the initial period of the transformation the supersaturation in the system is practically not changed and the kinetic coefficients $w^{(+)}$ and $w^{(-)}$ can be considered as time-independent quantities. A derivation of Eq. (6.154) with respect to time yields, consequently,

$$\frac{\partial J(j,t)}{\partial t} = -w_j^{(+)} \left(\frac{\partial^2 N(j,t)}{\partial t \partial j} + \frac{\partial N(j,t)}{\partial t} \frac{\partial}{\partial j} \frac{\Delta G_{(cluster)}(j)}{k_B T} \right) . \tag{6.163}$$

Changing the order of the partial derivatives and applying Eq. (6.146) this relation may be rewritten in the form

$$\frac{\partial J(j,t)}{\partial t} = w_j^{(+)} \left(\frac{\partial^2 J(j,t)}{\partial j^2} + \frac{\partial J(j,t)}{\partial j} \frac{\partial}{\partial j} \frac{\Delta G_{(cluster)}(j)}{k_B T} \right) . \tag{6.164}$$

In the vicinity of the critical cluster size $[\partial \Delta G(j)/\partial j] \approx 0$ holds and Eq. (6.164) is reduced to

$$\frac{\partial J(j,t)}{\partial t} = w_j^{(+)} \frac{\partial^2 J(j,t)}{\partial j^2} , \tag{6.165}$$

i.e., to a diffusion equation in cluster size space with a constant value of the diffusion coefficient.

A remarkably simple solution of this equation was proposed first by Zeldovich in 1942 using an analogy to Ornstein's and Uhlenbecks classical analysis of a

mathematically equivalent diffusion problem (see Ornstein and Uhlenbeck (1930) [614]). The expression given by Zeldovich for the time dependence of the rate of formation of critical clusters $J(j_c, t)$ reads

$$J(j_c, t) = J(j_c) \exp\left(-\frac{\tau^{(ns)}}{t}\right) . \tag{6.166}$$

$J(j_c)$ in above equation is the steady-state nucleation rate and $\tau^{(ns)}$ a characteristic time scale of the process, the so-called time-lag in nucleation. It has the meaning of the time determining the approach to the steady-state rate of formation of clusters of critical sizes. The time dependence $J(j_c, t)$ according to Zeldovich's equation has, in agreement with experimental evidence and the numerical calculations, a typical s-shaped form. Moreover, for $t \to 0$ the relation $dJ/dt = 0$ holds.

Both these properties of Zeldovich's solution are absent in another approximative result proposed by Wakeshima (1954) [906] (cf. also Probstein (1951) [651], Kantrowitz (1951) [430])

$$J(j_c, t) = J(j_c)\left[1 - \exp\left(-\frac{t}{\tau^{(ns)}}\right)\right] \tag{6.167}$$

which is given as an example in most standard texts on nucleation kinetics (see Lyubov and Roitburd (1958) [518]; Feder et al. (1966) [198]; Springer (1978) [791]). While Eq. (6.166) resembles a solution of a diffusion type problem, Wakeshima's expression can be considered as the simplest example of a dependence with a relaxation or retardation type behavior. A more exact description of the $J(j_c, t)$ dependence in terms of infinite power series was derived by Collins (1955) [139] and Kashchiev (1969) [434]. Both authors obtained expressions of the form

$$J(j_c, t) = J(j_c)\left[1 + 2\sum_{n=1}^{\infty}(-1)^n \exp\left(-\frac{n^2 t}{\tau^{(ns)}}\right)\right] . \tag{6.168}$$

As mentioned by Shneidman (1988) [746] this expression may be written in a more compact form as

$$J(j_c, t) = J(j_c)\Theta_4\left(0, \exp\left(-\frac{t}{\tau^{(ns)}}\right)\right) \tag{6.169}$$

by introducing the so-called elliptic theta function Θ_4 [652].

Numerical solutions of the set of kinetic equations (6.94) and (6.95), underlying the theoretical description of nucleation processes, and a comparison with analytical expressions were carried out by Kelton et al. (1983) [451]. These authors came to the conclusion that for the applied set of parameter values a quite satisfactory agreement between numerical and theoretical results, expressed by Eq. (6.168), is found when the solution and the value of $\tau^{(ns)}$ as proposed by Kashchiev (1969) [434] is used (see, however, also the critical remarks made in Wu's paper (1992) [933]).

In the further development of the theory Trinkaus and Yoo (1987) [854] as well as Shi et al. (1990) [752] and Shneidman (1988, 1992) [746, 747]), Shneidman and Hänggi (1994) [748] made an important additional step in deriving analytical solutions to the problem of the kinetics of transient nucleation and in reconciling theoretical and experimental results. They take into account that experimentally, in general, not the process of formation of critical clusters is investigated but the rate of formation of clusters of considerably larger sizes determined by the resolution limit of the experimental method employed. Critical cluster sizes (generally of the order 10^{-7}–10^{-9} m) are beyond the possibilities of most microscopic and electron-microscopic techniques.

As it is also evident from the numerical calculations given in the previous section, the induction period both for the nucleation rate, $J(t)$, and the number of clusters, $N(t)$, as functions of time have different values for clusters of different sizes (see also Kelton et al. (1983) [451]). This result is connected with the finite value of time needed for the growth of a critical cluster to experimentally detectable supercritical sizes. In a qualitative way this point was mentioned already by Gutzow and Toschev (1968) [333] who introduced a correction factor for the time-lag, $\tau^{(ns)}$, which was assumed to depend on the growth rate of the supercritical clusters. Shneidman (1988) [746] proposed an expression of the form

$$J(j,t) = J \exp\left\{-\exp\left(\frac{t - t_{(inc)}(j)}{\tau^{(ns)}}\right)\right\} \tag{6.170}$$

for the time dependence of the nucleation rate for clusters of sizes $j \geq j_c$. Here with $t_{(inc)}$ a second characteristic time scale is introduced reflecting the deterministic growth of the clusters. It is defined by

$$t_{(inc)}^{-1} = \left[\frac{\partial}{\partial j}\left(\frac{dj}{dt}\right)\right] , \tag{6.171}$$

where (dj/dt) is the deterministic growth rate of clusters of size j (without considering fluctuations). The size-dependent induction time is given according to Shneidman by

$$t_{(ind)} = t_{(inc)} + \gamma\tau^{(ns)} \qquad \text{with} \qquad \gamma = 0.5772 , \tag{6.172}$$

$\tau^{(ns)}$ being the time-lag for the formation of clusters of critical size. Similar $J(j,t)$-curves were obtained also by Shi and Seinfeld (1990) [752] and Trinkaus and Yoo (1987) [854]. In Fig. 6.13a the time dependence of the nucleation rate is given for clusters of critical sizes ($J(j_c,t)$) as obtained by Zeldovich, Wakeshima, Collins-Kashchiev, and Shi et al. The solution of the latter mentioned authors predicts a somewhat steeper dependence J vs. t than the Collins-Kashchiev and the Zeldovich results.

For practical applications, and in particular if qualitative consequences from the existence of a time-lag in nucleation are discussed, as a first approximation,

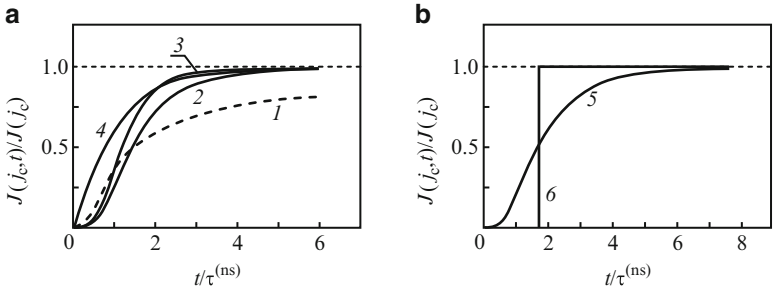

Fig. 6.13 (**a**) Comparison of different expressions for the time-dependence of the rate of formation of critical clusters according to (*1*) Zeldovich; (*2*) Collins-Kashchiev; (*3*) Shi and Seinfeld; (*4*) Wakeshima. (**b**) Step function (*6*) compared with the Collins-Kashchiev result (*5*)

expressions with a relatively simple analytical description, like the Zeldovich's equation, and even the step function

$$J(j_c,t) = \left\{ \begin{array}{lll} 0\ , & \text{for} & 0 \le t \le b\tau^{(ns)} \\ & & \\ J\ , & \text{for} & b\tau^{(ns)} \le t \le \infty \end{array} \right\} \tag{6.173}$$

may be used (see Gutzow and Toschev (1970, 1972) [319, 851]; Gutzow, Kashchiev (1970, 1971) [313]; Shneidman, Weinberg (1993) [749]). This approximation is illustrated in Fig. 6.13b together with the Collins-Kashchiev result.

Once the time-dependence of the nucleation rate is known also the dependencies describing the time evolution of the number of clusters in the system may be calculated. The time dependence of the number of critical clusters can be obtained assuming, as done throughout this section that the state of the system is not changed significantly by cluster formation and growth, i.e., assuming constant supersaturation. With

$$N(j_c,t) = \int_0^t J(j_c,t)\,dt \tag{6.174}$$

we get for the special case $\tau^{(ns)} = 0$ (i.e., when transient effects are neglected) the steady-state solution

$$N(j_c,t) = J(j_c)t\ . \tag{6.175}$$

$N(t)$-curves of this type, going through the origin of the N vs. t coordinate system, are, consequently, an indication that for the considered experimental situation, transient effects are of no importance (see Fig. 6.14b).

Applying Zeldovich's solution for the $J(j_c,t)$-dependence we have instead of Eq. (6.175) (see Gutzow and Toschev (1971) [320])

$$N(j_c,t) = Jt\left[\exp\left(-\frac{\tau^{(ns)}}{t}\right) + t\ \mathrm{Ei}\left(-\frac{\tau^{(ns)}}{t}\right)\right]\ . \tag{6.176}$$

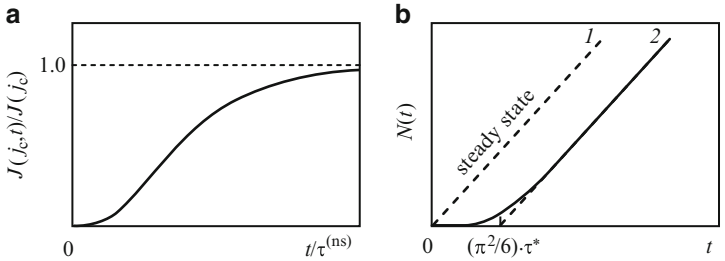

Fig. 6.14 Comparison of (**a**) $J(t)$ and (**b**) $N(t)$-dependencies for steady-state nucleation (*dashed curves*) and transient nucleation (*full curves*). As seen time-lag effects result effectively in a parallel shift of the $N(t)$-curves (compare Eq. (6.178))

Here Ei denotes the integral exponential function. An integration of the Collins-Kashchiev equation, as performed by Kashchiev (1969) [434], yields

$$N(j_c,t) = J\left[t - \frac{\pi^2}{6}\tau^{(ns)} - 2\tau^{(ns)}\sum_{n=1}^{\infty}\frac{(-1)^n}{n^2}\exp\left(-\frac{n^2 t}{\tau^{(ns)}}\right)\right] . \tag{6.177}$$

For large times this and similar solutions are well-approximated by

$$N(j_c,t) = J\left(t - b^*\tau^{(ns)}\right) , \tag{6.178}$$

where for the Kashchiev solution $b^* = \pi^2/6$ holds. Above result implies that the $N(j_c,t)$-curves are shifted by a time interval $\Delta t = \pi^2\tau^{(ns)}/6$ into the positive direction of the t-axis as compared with the dependencies obtained from Eq. (6.175).

$N(j_c,t)$-curves can be determined experimentally only, if Tammann's two-stage cluster development technique is used as done by James (1974) [400] and Kalinina et al. (1976) [427] in investigating the kinetics of nucleation in a lithium disilicate glass. In any isothermal experiment on nucleation, as mentioned, commonly the formation of clusters with sizes j considerably exceeding the critical cluster size $j \gg j_c$ are measured. The $N(j,t)$-curves are shifted along the time-axis compared with the $N(j_c,t)$-dependencies due to the finite time $t_{(inc)}$ the critical clusters need to grow up to detectable sizes. Consequently, an adequate direct interpretation of experimental $N(t)$-curves can be given only applying Shneidman's or equivalent equations.

The solution of Eq. (6.174) with Shneidman's equation (6.170) gives an expression for the time evolution of the number of supercritical clusters with sizes $j \geq j_c$. One obtains

$$N(j,t) = \tau^{(ns)} J\ \mathrm{Ei}\left[\exp\left(-\frac{t - t_{(inc)}(j)}{\tau^{(ns)}}\right)\right] . \tag{6.179}$$

For large times this expression yields

$$N(j,t) = J[t - t_{(inc)}(j)] \; . \tag{6.180}$$

In the first proof of the significance of non-steady state effects in nucleation in glass-forming melts (for crystallization of $NaPO_3$, given by Gutzow et al. (1966) [321] and Gutzow and Toschev (1971) [320]), a similar $N(t)$-dependence as expressed with Eq. (6.180) was also anticipated. The possible value of $t_{(inc)}$ was estimated and found to be much smaller than $\tau^{(ns)}$ by using growth rate data obtained from electron microscopic measurements at the same temperature. By solving the Zeldovich-Frenkel equation expressions for the time evolution of the cluster size distribution function $N(j,t)$ are also obtained. The solution given by Kashchiev (1969) [434] reads

$$\frac{N(j,t)}{N_j^{(e)}} = \frac{1}{2} - (j - j_c)\Gamma_{(z)} - \frac{2}{\pi}\sum_{n=1}^{\infty}\frac{1}{n}\sin[n\pi\Gamma_{(z)})(j - j_c)]\exp(-n^2\pi w^{(+)}(j_c)\Gamma_{(z)}^2 t) \; . \tag{6.181}$$

In the steady state, i.e., for $t \to \infty$ we have for the near-critical region

$$\frac{N(j,t)}{N_j^{(e)}} = \frac{1}{2} - (j - j_c)\Gamma_{(z)} \; . \tag{6.182}$$

It follows that for $j = j_c$ the relation $N(j,t) = N_j^{(e)}/2$ holds and that the slope of the steady-state distribution function is determined by the Zeldovich factor, i.e., by

$$\frac{\partial}{\partial j}\frac{N(j,t)}{N_j^{(e)}} = -\Gamma_{(z)} \; . \tag{6.183}$$

An expression similar to Eq. (6.182) but valid in the whole range of cluster sizes was given by Trinkaus and Yoo (1987) [854]. It reads

$$\frac{N(j,t)}{N_j^{(e)}} = \frac{1}{2}\mathrm{erfc}\left(\frac{\Gamma_{(z)}}{\sqrt{\pi}}(j - j_c)\right) \; . \tag{6.184}$$

A schematic representation of above dependencies as they are formulated in the framework of the classical theory of transient nucleation is given in Fig. 6.15. In addition to the nucleation barrier and the construction of the critical zone of unconstrained diffusive motion the $N(j,t)$-curves are given for different moments of time as well as the $N_j^{(e)}$ and $N(j,t)/N_j^{(e)}$-dependencies. The similarity with the respective curves obtained by computer calculations for constant values of the supersaturation is obvious (see Figs. 6.10–6.11; Bartels et al. (1989–1991) [39–43], cf. also [275, 449]).

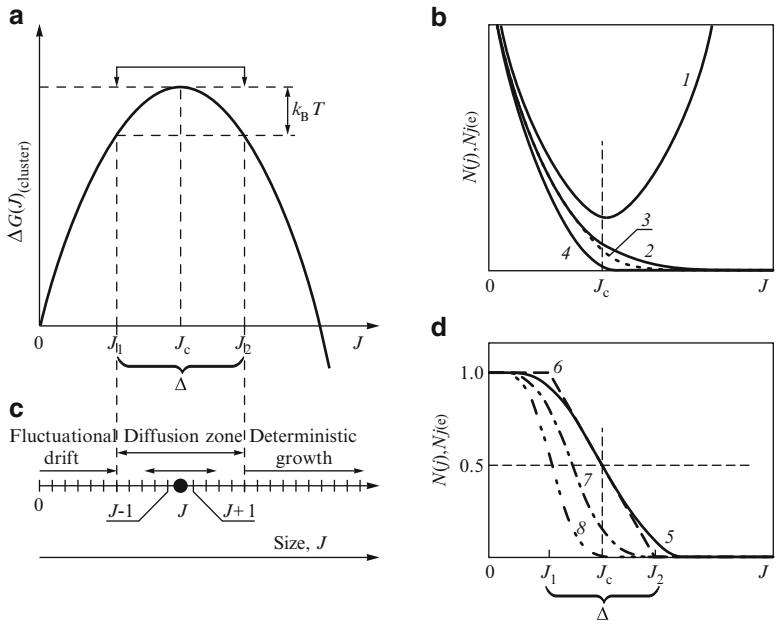

Fig. 6.15 Schematic representation of basic ideas and main results of the theory of transient nucleation: (**a**) nucleation barrier and critical region Δ; (**b**) size distribution in steady-state nucleation (*full curve*) and its time evolution under constant supersaturation (*dashed* and *dotted curves*). By (*1*) the "equilibrium" and by (*2*) the steady-state distribution functions are specified. The numbers (*3*) and (*4*) refer to consecutive stages of the process ($t_3 > t_4$). (**c**) Random walk of a cluster (*black dot*) along the size axis. (**d**) $(N(j)/N^{(e)})$-curve for steady-state conditions and for the approximation given with Eq. (6.182) (*5*). Curves (*7*) and (*8*) refer to consecutive stages corresponding to (*3*) and (*4*) in (**b**)

6.3.6 *The Time-Lag in Transient Nucleation*

As mentioned in the previous section the time-lag in nucleation is a measure of the time-interval required for the establishment of the steady-state nucleation rate for clusters of critical sizes. However, its primary definition, which is connected with above given meaning, was introduced in a different way. In the initial formulation of the theory by Zeldovich (1942) [949], used in all subsequent investigations, the definition of the time-lag is introduced as the time of diffusive motion of an average cluster along the size axis in an appropriately defined region in the vicinity of the critical cluster size. For an illustration let us consider briefly the process of motion of clusters in cluster size space as illustrated in Fig. 6.15.

According to the thermodynamic picture given earlier and in agreement with the Frenkel-Zeldovich equation the random walk of an average cluster is superimposed, in general, by a deterministic flow determined by a driving force proportional to $(-\partial \Delta G/\partial j)$. For $j < j_c$ this term stimulates the decay of the clusters (and growth

may proceed only via stochastic fluctuations) while for $j > j_c$ it supports the further increase of the size of the cluster. Only in the vicinity of the critical size j_c, can the evolution of the clusters be described as an unconstrained random walk along the size axis similar to the Brownian motion of a colloidal particle in a solution. The coefficient of diffusion for this type of motion is given according to Eqs. (6.137) and (6.165) by $D = w^{(+)}$. Approximately, in the near-critical region we may consider $w^{(+)}$ as a constant equal to $w^{(+)}(j_c)$. This unconstrained random walk takes place, according to Zeldovich, in a region of cluster size space for which the inequality

$$\frac{\Delta G^{(c)}_{(cluster)} - \Delta G_{(cluster)}}{k_B T} \leq 1 \tag{6.185}$$

holds. The method of determination of the diffusion zone and of the width of the interval of random walk $\Delta = j_2 - j_1$ is illustrated in Fig. 6.15.

If one employs, in addition, Eq. (6.108) the width of the of the region of unconstrained random walk becomes $\Delta = 2(j_c - j_1)$. With Eqs. (6.185) and (6.107) we arrive at

$$\Delta = \sqrt{\frac{8k_B T}{-\left(\frac{\partial^2 \Delta G}{\partial j^2}\right)_{j=jc}}} \,. \tag{6.186}$$

and with Eq. (6.50) we get the equivalent relation

$$\Delta = \sqrt{\frac{k_B T}{\pi \sigma}} \,. \tag{6.187}$$

Applying Einstein's formula equation (2.103) the average displacement of a colloidal particle in real space is given by $|\Delta \mathbf{r}|^2 = 2Dt$. Consequently, for a cluster starting the random motion at the size axis in the vicinity of $j = j_c$ a relation of the form $(\Delta/2)^2 = 2w^{(+)}(j_c)t^*$ should hold. The average time interval, required for a cluster to pass the critical region from j_1 to j_2, can be approximated, consequently, by $2t^*$. This time interval is identified, as done for the first time by Zeldovich, with $\tau^{(ns)}$. One obtains thus

$$\tau^{(ns)} \cong \frac{\Delta^2}{4w^{(+)}(j_c)} \tag{6.188}$$

or in a more general form with Eq. (6.186)

$$\tau^{(ns)} = \frac{a_0^* k_B T}{w^{(+)}(j_c)} \left| \left(\frac{\partial^2 \Delta G_{(cluster)}(j)}{\partial j^2} \right)_{j=j_c} \right|^{-1} \,. \tag{6.189}$$

A critical analysis of different approaches in determining $\tau^{(ns)}$ is made by Binder and Stauffer (1976) [83]. Adopting the form for $\tau^{(ns)}$ given with Eq. (6.189) these

approaches lead to different values of the constant a_0^* in the range from $a_0^* = 1 - 4$. According to above derivation we have $a_0^* = 2$, Kashchiev's estimate is $a_0^* = \pi^2/6 \cong 1.64$. Equivalent expressions for $\tau^{(ns)}$, which are of use in different applications, are given below. Applying Eq. (6.187) we have

$$\tau^{(ns)} = \frac{k_B T}{4\pi\sigma w^{(+)}(j_c)} \,. \tag{6.190}$$

Similarly, with Eq. (6.50) one obtains from Eq. (6.189)

$$\tau^{(ns)} = \frac{3a_0^*}{2} \frac{k_B T}{\Delta G^{(c)}_{(cluster)}} \frac{j_c}{w^{(+)}(j_c)} \,. \tag{6.191}$$

The time-lag $\tau^{(ns)}$ may be expressed also through the Zeldovich factor $\Gamma_{(z)}$ introduced with Eqs. (6.110)–(6.111) as

$$\tau^{(ns)} = \frac{a_0^*}{2\pi w^{(+)} \Gamma^2_{(z)}} \,. \tag{6.192}$$

Taking into account this relation it follows that the exponent in Eq. (6.181) can be written, again, as a function of $t/\tau^{(ns)}$. Thus $\tau^{(ns)}$ becomes in a third interpretation the time required for a steady-state distribution of clusters to be established.

More generally the meaning of $\tau^{(ns)}$ may be given as the parameter determining the ability of the system to reorganize itself after it was brought into a supersaturated state (Toschev (1973) [848]). In this sense $\tau^{(ns)}$ has the meaning of a time of relaxation or retardation similar to respective parameters introduced in the phenomenological theory of viscoelastic behavior (see Chap. 12). This similarity also explains why most solutions of transient nucleation result in expressions which are more or less complicated functions of $\exp(-t/\tau^{(ns)})$.

Equation (6.192) is usually employed for an evaluation of $\tau^{(ns)}$ in different cases of phase formation (see, e.g., Gutzow and Toschev (1971) [320]). For crystallization in undercooled melts in the above cited paper, the expression

$$\tau^{(ns)} = 2a_0^* d_0^5 \frac{\eta\sigma}{\varsigma(\Delta\mu)^2} \tag{6.193}$$

was given. It follows directly from Eqs. (6.37), (6.40), (6.111), and (6.121). With the same equations one may rewrite above relation also in the form

$$\tau^{(ns)} \cong \frac{a_0^* d_0}{\varsigma\sigma} \eta j_c^{2/3} \,. \tag{6.194}$$

Taking into account the connection between viscosity η and time of molecular relaxation τ_R (see Chap. 2, Eq. (2.110)) it follows from Eq. (6.194) that

$$\tau^{(ns)} \cong \text{constant}\ \tau_R j_c^{2/3} \tag{6.195}$$

holds with

$$\text{constant} = \frac{a_0^* k_B T}{\varsigma \sigma d_0^2} \,. \tag{6.196}$$

Typical values of the constant in Eq. (6.195) are in the range of 10^2–10^3.

Thus it turns out that the time-lag in nucleation $\tau^{(ns)}$ is, in fact, determined by the product of the time of molecular relaxation τ_R of the ambient phase with the number of particles in the surface of the critical cluster ($j_c^{(2/3)}$). Moreover, according to the equations derived above and accounting for the extremely high values of the viscosity of glass-forming melts, in particular, near the vitrification temperature T_g relatively high values of $\tau^{(ns)}$ have also to be expected for such systems. It turns out, consequently that a qualitatively correct description of nucleation in glass-forming melts can be given only if transient effects are taken into account.

The time-lag in nucleation may reach in glass-forming melts values of the order of hours or even days. This is due to the mentioned high values of the viscosity. In most cases $\tau^{(ns)}$ can expected to be of the order $\tau^{(ns)} \cong 10^2 - 10^3$ s. In contrast, for vapor condensation as a rule very small values $\tau^{(ns)} \cong 10^{-5} - 10^{-7}$ s follow from above formulas. For phase formation processes in solutions $\tau^{(ns)} \cong 10^{-1} - 10^1$ s was found (Gindt and Kern (1968) [254]). A summary of estimates for $\tau^{(ns)}$ in different cases of phase formation may be found also in the review article by Toschev and Gutzow (1971) [320].

The possible importance of non-steady state effects for nucleation in glass-forming melts was first mentioned by Zeldovich as early as in 1942 [949], later by Collins (1955) [139] and Hammel (1967) [345]. A more extended analysis in this respect was performed by Gutzow (1981) ([304]; for experimental determinations of $\tau^{(ns)}$ see James (1974) [400]; Fokin et al. (1980) [223]; Gutzow (1980) [328]; Kelton, Greer (1986) [448]). In this way, the classical picture drawn by Tammann according to which the essential parameters determining the kinetic stability of under-cooled melts are the steady-state nucleation rate J and the growth rate v, has to be supplemented by a third essential factor – the non-steady state time-lag $\tau^{(ns)}$. The temperature dependencies of the three quantities $\tau^{(ns)}$, v and J, as they follow from the theoretical predictions, are shown in Fig. 6.16. As already mentioned by Tammann, a necessary requirement for intensive crystallization consists in a sufficiently large degree of overlapping of the $v(T)$- and $J(T)$-curves. However, such an overlapping will be effective – and this is the new point – only, when the time-lag is lower than a given critical value. The schematic representation given in Fig. 6.16 shows also the temperature dependence of the viscosity η of the melt, which determines to a large extent all three characteristics of the nucleation process: $\tau^{(ns)}$, v and J.

It is interesting to note further that though both the steady-state nucleation rate and the time-lag are strongly dependent on the viscosity or the time of molecular relaxation, the product $J\tau^{(ns)}$ is not. Indeed, according to Eqs. (6.109) and (6.192)

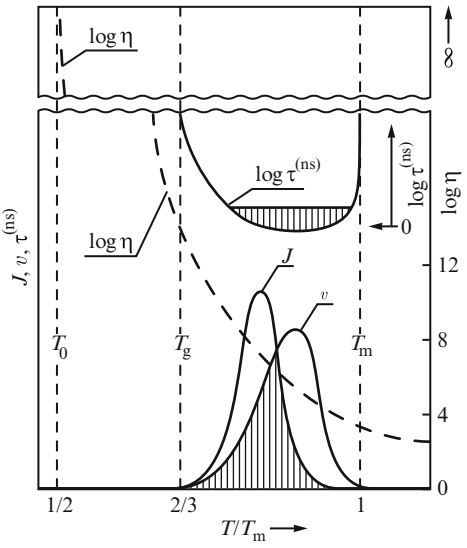

Fig. 6.16 Temperature dependence of steady-state nucleation rate J, growth rate v, time-lag $\tau^{(ns)}$ and viscosity η for a glass-forming melt (schematically)

$$J\tau^{(ns)} = \frac{a_0^* N}{2\pi\Gamma_{(z)}} \exp\left(-\frac{\Delta G^{(c)}_{(cluster)}}{k_B T}\right) \tag{6.197}$$

holds, verifying the above statement. This result is of particular importance taking into consideration that for many glass-forming melts sufficiently accurate viscosity measurements are still lacking. In this way, Eq. (6.197) gives a simple way for a qualitative self-consistent analysis of experimental results on phase formation processes using only nucleation data (see Kashchiev (1984) [437]; Penkov and Gutzow (1984) [632]).

6.3.7 *Nucleation in Processes of Reconstructive Crystallization: Nucleation of Chain-Folding Polymers*

As mentioned in one of the previous sections, modifications of the classical theory of nucleation have to be developed accounting for the possible complexity of the ambient phase molecules forming the new phase. Such a generalization is of particular importance in applying the theory to phase formation in polymer systems. Following a classification introduced by Korshak (1965) [468] we will denote as a polymeric structural unit (or polymeric building unit of the new phase) any complex aggregate in which primary particles are held together by covalent bonds.

In addition to structural units formed in the melt by covalent bonding, the notions "associate" and "aggregate" are also used. As associates in organic melts, usually structural units are denoted formed by hydrogen bonding (Kobeko (1952) [461]).

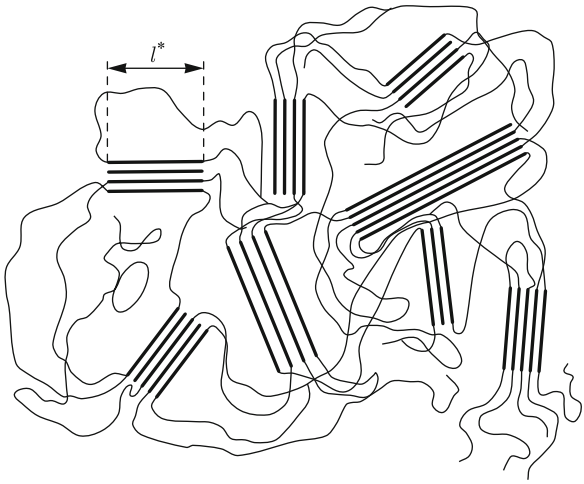

Fig. 6.17 Illustration of the Gerngross model of polymer crystallization (After Price (1969) [646])

With the term aggregate a more general meaning is connected as a structural element with a non-specified type of bonding. In typical cases the C-C covalent bonding is by a factor 10–20 stronger as compared with van der Waals forces acting in between the chain molecules. Thus crystallization in polymer melts proceeds in a way as illustrated in Fig. 4.26d: the polymer chains exist in both the melt and the crystalline phase. Associates as defined above may undergo structural changes. Association processes in the ambient phase reduce, in general, the rate of phase formation when the newly formed phase is constituted of monomeric building units: association processes diminish the concentration of building units which can be incorporated into the growing cluster.

A quantitative determination of the nucleation kinetics when dimer associates are formed in the ambient phase was developed, for example, by Kashchiev (1985) [438]. In any such cases, the actual concentration of the building units has to be determined based on the mass action law. In a first approximation it can be assumed (see, e.g., Knacke and Stranski (1953, 1956) [459, 460]) that in the presence of associates the impingement rate Z has to be multiplied by Arrhenius type exponential factors of the form $\exp(-U_{\oplus}/k_B T)$, where $U_{\oplus}$ is the activation barrier determining the dissolution of complex aggregates into monomeric structural units. In this way the time-lag in nucleation is enlarged and the stationary nucleation rate is reduced as compared with the expressions given in the preceding section.

In the reverse case, when crystallization is connected with the formation of polymer-like modifications from an initially monomeric melt, again, the chemical equilibrium reaction constant for the respective reaction of polymerization has to be known. In the description of the kinetics of nucleation of chain-folding polymer melts the length of the chain molecule may reach such enormous values that one and the same molecule may belong to several crystalline-like configurations.

For a description of such processes of phase formation, two basic models have been developed. One of these models was formulated may years ago by

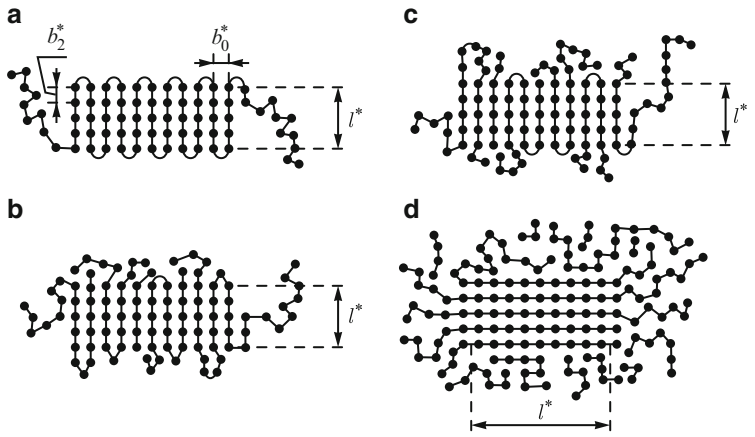

Fig. 6.18 Models of crystalline polymer nucleation (two-dimensional schematic representation): (**a**) Keller's direct reentry chain folding cluster model; (**b**) Fisher's irregular reentry chain folding model; (**c**) Flory's switchboard loose end chain folding polymer crystal growth; (**d**) bundle-like nucleus in a fringed micelle model of polymer melt crystallization (Gerngross' model). l^*: critical thickness; b_0: monomer width (See Gutzow and Dobreva (1992) [309, 310])

Gerngross ([248]; see Price (1969) [646]). In his approach it is assumed that a bundle-like nucleus is formed in a region where several polymeric molecular chains are arranged in a nearly parallel way (fringed micelle model). A schematic representation of the basic idea underlying this model is given in Fig. 6.17. Here the critical size of the chains l_c is determined by a relation similar to the Gibbs-Thomson equation.

However, experimental evidence (X-ray analysis of polymer crystallites) gives a strong support to another model of polymer crystallization and nucleation, the so-called chain-folding crystallization model. A first modification of this type of model (with direct reentry chain folding) was formulated by Keller ((1957) [443], see also Keller (1991) [445]). Different versions of chain folding crystallization, as they are classified by Price (1969) [646], are illustrated in Fig. 6.18.

It is essential to remember that in polymer chain-folding processes, two types of specific interfacial energies are of importance: one of them (the end energy σ_b) corresponding to crystal faces formed of polymer chain bends and another one (the lateral energy σ_s) which is correlated with the faces of the stretched part of the polymer molecules. In this way, the work of formation of clusters in polymer crystallization is usually written as (see Geil (1963) [247]; Price (1969) [646])

$$\Delta G_{(polymer)}(\nu, Y) = \Delta G^{(c)}_{(cluster)} \left[(1 - 2Y) \left(\frac{\nu}{\nu_c} \right)^2 + 2Y \frac{\nu}{\nu_c} \right] , \tag{6.198}$$

$$\Delta G^{(c)}_{(cluster)} = \omega \frac{\sigma_b \sigma_s^2 v_m^2}{(\Delta\mu)^2} . \tag{6.199}$$

Here $Y = l/l^*$ gives the relative length of the chain folds, depending on the supersaturation, (ν/ν_c) is the relative number of chain foldings which form the cluster and ω denotes as usual a steric shape factor (equal to $16\pi/3$ for clusters with spherical shape).

In addition to the modification of the thermodynamic description, the kinetics of polymer crystallization is also varied. In the framework of the latter discussed model, processes of polymer crystallization are connected with the probability of incorporation of chain folds with a length $l > l^*$. These folds are formed as a rule by one molecule constituting even several growing clusters. Thus we have to define, as done by Gutzow and Dobreva (1992) [310], the process of cluster growth on the size axis in a new way: as a process of fluctuational $(\nu < \nu_c)$, diffusional $(\nu \cong \nu_c)$ or deterministic $(\nu > \nu_c)$ incorporation of chain folds. From Eqs. (6.198) and (6.199) and Fig. 6.19 it is evident that for $Y < 0.5$ no stable growth of clusters is possible. Only for $Y \geq 0.5$ does a growth across the nucleation barrier occur.

Figure 6.19 taken from above cited paper shows, moreover that the optimal growth path of crystalline polymeric clusters corresponds to $Y \approx 1$. Inserting this value into Eq. (6.198) one gets

$$\Delta G_{(polymer)}(\nu) = \Delta G^{(c)}_{(cluster)} \left[1 - \left(\frac{\nu}{\nu_c} - 1 \right)^2 \right] . \tag{6.200}$$

This expression is similar to Eq. (6.108) except, however, the additional factor 1/3 resulting there from the Taylor-expansion of the Gibbs free energy for $j \approx j_c$.

The nucleation barrier as given by Eq. (6.200) is illustrated in Fig. 6.20. In addition also the curve given by Eq. (6.108) is shown. In the vicinity of $j = j_c$ the relation resulting from the Taylor-expansion obviously gives the best fit to the $\Delta G(j)$-curve. However, for the whole range of physically meaningful j-values Eq. (6.200) is a more reasonable approximation. Consequently, Eq. (6.200) may be used as an improved version of an inverted parabola model of the thermodynamic barrier of nucleation also for the description of the $\Delta G_{(cluster)}(j)$-dependence in the case of phase formation of low molecular substances instead of Eq. (6.108).

The non-steady state time-lag in polymer crystallization can be determined, again, assuming that the process of formation of supercritical clusters is governed by the diffusive motion of the aggregates in cluster size space. Hereby the evolution is assumed to proceed via the saddle-point as expressed by Eq. (6.200) (see also Fig. 6.19). Similarly to the earlier considered cases we may write (compare Eqs. (6.188) and (6.189))

$$\tau^{(ns)}_{(polymer)} = \frac{\Delta^2}{4D(\nu_c)} = -\frac{a_0^* k_B T}{D(\nu_c) \left(\dfrac{\partial^2 \Delta G_{(polymer)}(\nu)}{\partial \nu^2} \right)_{\nu = \nu_c}} \tag{6.201}$$

and with Eqs. (6.200)

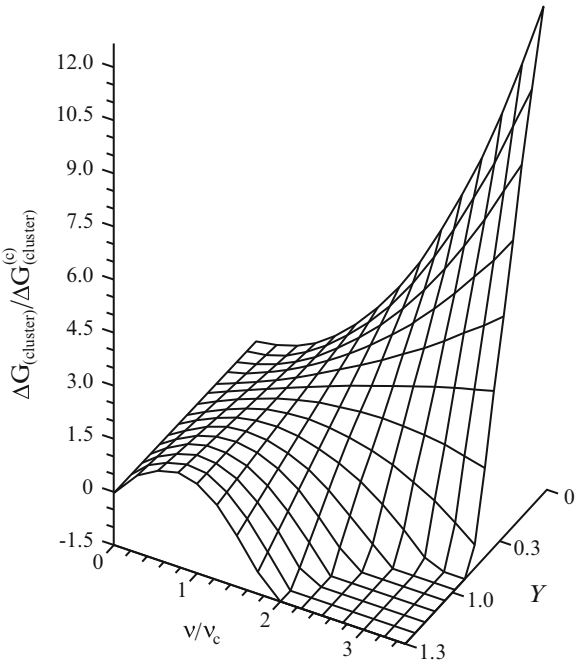

Fig. 6.19 Three-dimensional representation of the potential barrier in polymer nucleation according to Eqs. (6.198)–(6.199). The most effective path of the growing cluster corresponds to $Y = 1$

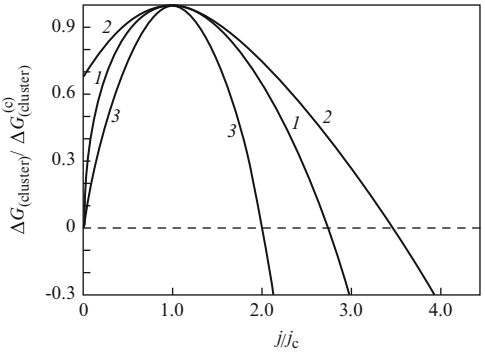

Fig. 6.20 The thermodynamic barrier of nucleation and its different analytical descriptions. Curve (*1*): $(\Delta G_{(cluster)}/\Delta G^{(c)}_{(cluster)})$ according to Eq. (6.47); curve (*2*): the classical Taylor-series approximation Eq. (6.108) as applied, e.g., by Becker and Döring; curve (*3*): inverted parabola approximation for polymer nucleation (Eq. (6.200), Gutzow and Dobreva (1992) [310])

$$\tau^{(ns)}_{(polymer)} = \frac{3a_0^* \sigma_s^2 \sigma_b \xi}{(\Delta\mu)^2}\eta \,. \tag{6.202}$$

The nucleation rate (primary nucleation in the terminology of polymer physics) can be given again in the form of Eq. (6.109), using Eq. (6.199) for $\Delta G^{(c)}_{(cluster)}$ and assuming that N_1 is here proportional to the number of chain folds. The

determination of $w^{(+)}(\nu_c)$ becomes, however, in polymer crystallization a very tricky problem because of possible chain entanglements and strains along the chains produced in the process of crystallization. A discussion of such problems is beyond of the scope of the present book. The interested reader is referred to the already cited and additional specific references on polymer crystallization.

A similar procedure – the construction of $\Delta G_{(cluster)}$-surfaces as functions of several independent parameters and the determination of the most probable way of phase formation determined by the saddle point of this surface – has to be followed also in other cases of phase formation, e.g., in considering nucleation in multi-component systems or cluster formation near and at interfaces (see Schmelzer et al. (1994) [716]). For the first time this method was employed in the calculation of the steady-state nucleation rate for binary nucleation by Neumann and Döring (1940) [602] and later by Reiss (1950) [661]. A non-steady state treatment of nucleation for such cases was given recently by Kozisek and Demo (1993) ([481], see also Kozisek (1991) [480]).

We would like to mention finally an additional similarity between nucleation and chemical reaction kinetics. Both the rates of nucleation and chemical reactions are limited by kinetic barriers. It is the specific feature of nucleation kinetics that the barrier can be constructed based on thermodynamic models. The inverted parabolas, given by Eqs. (6.200) and (6.108), turn out to be a very convenient approximation for determining the barrier to nucleation as this is also known from the general theory of reaction kinetics (see, e.g., the problems of approximating the reaction barrier by an inverted parabola as this is described in Christov's monograph (1980) [136]). It has also to be mentioned in this connection that quite recently Shneidman and Weinberg (1992) [749] showed that the replacement of the classical barrier of nucleation or its approximations by barriers of a different shape does not lead to significant changes in nucleation kinetics.

6.3.8 *Atomistic Approach to Nucleation*

In the preceding derivations the capillary approximation was generally employed. The application of the capillary approximation implies that the clusters considered, in particular, the clusters in the vicinity of the critical cluster size $j = j_c$, are sufficiently large (e.g., $j_c > 20$). Only in this case can the notion of a specific surface energy be applied. Moreover, only for sufficiently large critical clusters is the continuum's approach in deriving the main equations of the theory applicable.

In most cases of crystallization in glass-forming melts the classical capillarity approximation may be used, at least, qualitatively: the expected critical clusters vary in size for homogeneous nucleation from several thousand molecules near the melting temperature to $\sim 10^2$ at $T \to T_g$. However, for vapor condensation, for the process of formation of clusters on active solid substrates, electrolytic deposition of metals and other cases of phase formation clusters consisting of only a few particles

are proven to be capable of further deterministic growth. One way of overcoming problems with the thermodynamic description of clusters of relatively small sizes consists of the application of different expressions for the curvature dependence of surface tension. Such an approach may be extended even to cluster sizes where macroscopic parameters lose any meaning (see, e.g., Schmelzer (1986) [690]). In this case, σ or σA have to be considered as appropriately chosen correction terms allowing us to give a correct description of the thermodynamics of the process, however, without assigning any definite physical meaning to them.[8]

There have also been attempts to develop a theoretical scheme where from the very beginning an atomistic approach is applied for the description of the nucleation process omitting the introduction of a specific surface energy σ. Following Kaischew (1965) [422] in this approach the critical cluster is defined kinetically as the cluster size for which the probabilities of decay and further growth are the same (compare Eq. (6.137)). Such an approach was developed for the first time by Walton (1962) [477] and Rhodin and Walton (1964) [663] in application to vapor condensation on surfaces. In its further development, attempts have been made to reconcile this approach with the classical model of nucleation (see, e.g., Lewis (1967) [506] and, in particular, Stoyanov (1973) [804]; Milchev, Stoyanov, and Kaischew (1974, 1976) [562, 563]). Stoyanov et al. started their analysis with Eq. (6.104). Realizing that for small values of j one of the summands in Eq. (6.104) dominates and, neglecting the others, an alternative expression for the steady-state nucleation rate is derived. In this expression the work of formation of critical clusters is written in the general form

$$\Delta G^{(c)}_{(cluster)} = -j_c \Delta\mu + \Psi_s(j_c) \; . \tag{6.203}$$

The analogy with the classical expression for the work of formation of critical clusters is obvious. For large values of the size of the critical clusters the correction

[8] Indeed, in terms of the classical Gibbs approach, the bulk properties of the cluster phase are determined by Gibbs equilibrium conditions, equality of temperature in the cluster (specified by α) and ambient (β) phases, $T_\alpha = T_\beta$, and equality of chemical potentials, $\mu_{i\alpha} = \mu_{i\beta}$, of all $i = 1, 2, \ldots, k$ components. Provided the cluster is considered to be of spherical shape and the surface of tension is chosen as the dividing surface, then the properties of the critical clusters (W_c work of critical cluster formation; R_c radius of the cluster referred to the surface of tension) are defined via

$$W_c = \frac{1}{3}\sigma A_c \; , \qquad A_c = 4\pi R_c^2 \; , \qquad p_\alpha - p_\beta = \frac{2\sigma}{R_c} \; .$$

Provided W_c is known (for example, from experiment or statistical-mechanical computations) then always R_c and σ can be determined from above set of equations, i.e., one can always construct a spherical cluster – in terms of Gibbs thermodynamic theory – leading to the same value of the work of critical cluster formation as observed in experiment. Of course, in experiment the shape of the critical cluster can be much different as compared to a sphere or the cluster may be too small to allow one a thermodynamic description, anyway, such Gibbs' model cluster can be uniquely defined. Similar considerations hold also in the case that the generalized Gibbs approach is employed in the analysis.

term $\Psi_s(j_c)$ tends to approximate the classical expression σA with $\sigma = \sigma(\infty)$ (or, equivalently, $\Psi_s(j_c) \propto j_c^{2/3}$), corresponding to the already discussed Eqs. (6.36) and (6.48).

It should also be noted that generally the derivative $(d\Delta G^{(c)}_{(cluster)}/d\Delta\mu)$ gives for any model of nucleation the number j_c of building units in the critical cluster (see the corresponding theorem formulated by Kashchiev (1982) [436] and also Oxtoby and Kashchiev (1994) [619][9]). For the considered cases of critical clusters with $j_c \to 1$ the time-lag in non-steady state nucleation is of the order of the time of molecular relaxation as it follows both from the general principles of statistical physics as well as from an extrapolation of the results for $\tau^{(ns)}$ obtained in the previous section (Eq. (6.195)).

While the classical theory allows one an estimate of the surface tension to the power 3 (i.e. σ^3) based on $\{\log J$ vs. $1/[k_B T(\Delta\mu)^2]\}$-plots (compare Eqs. (6.109) and (6.44)) the atomistic theory of nucleation implies another type of analysis of experimental data applying [$\log J$ vs. $\Delta\mu$]-dependencies. In such coordinates, more or less distinct ranges of supersaturation are found with linear [$\log J$ vs. $\Delta\mu$]-behavior and different slopes. In terms of the atomistic model, this result implies that in certain ranges relatively independent of supersaturation, some stable atomic configuration determines the critical cluster size. For lower $\Delta\mu$-values, the slope of the linear parts is increased and a continuous curve is approached corresponding to the classical $\{\log J$ vs. $1/[k_B T(\Delta\mu)^2]\}$ plot.

However, for the most interesting case of small j_c-values the function Ψ_s in Eq. (6.203) is not known, a priori, in contrast to the classical theory, where, at least as a first approximation, the capillarity model may be used. This gap leads to serious difficulties in the application of the atomistic model to the analysis of experimental results as it was demonstrated in a recent attempt by Pascova and Gutzow (1993) [626] to apply the atomistic approach to the description of crystallization of under-cooled glass-forming melts. It is relatively easy to interpret

[9]For a comprehensive discussion of this circle of problems, cf. Schmelzer [693, 694]. In these publications, a detailed analysis of the initial formulation of the nucleation theorem as given by Kashchiev in 1982 [436] is presented. In a next step, a new formulation of the nucleation theorem, mathematically widely equivalent to the form, as derived by Oxtoby and Kashchiev in 1994 [619] employing the classical Gibbs's approach, is developed in above cited publications. This formulation is, however, more easily applicable to the interpretation of experimental results as compared with the original expressions given by Oxtoby and Kashchiev. It can be utilized straightforwardly also in cases where the original version cannot be employed and allows one, in addition, a variety of further theoretical developments. It is shown, moreover, first in the framework of Gibbs's theory of heterogeneous systems that the nucleation theorem holds not only for critical clusters but for clusters of arbitrary sizes as well. The new formulation of the nucleation theorem is applied then to the analysis of different cases of phase formation. It is shown further on that an alternative thermodynamic derivation of the nucleation theorem both for clusters of critical as well as for arbitrary sizes can be given at certain specified conditions based on the van der Waals approach to the description of heterogeneous systems. The limits of validity of the nucleation theorem are analyzed with respect to its applicability to real systems; i.e., the problem is discussed to what extent the nucleation theorem may give an adequate description of properties of the real critical clusters determining the nucleation process in nature.

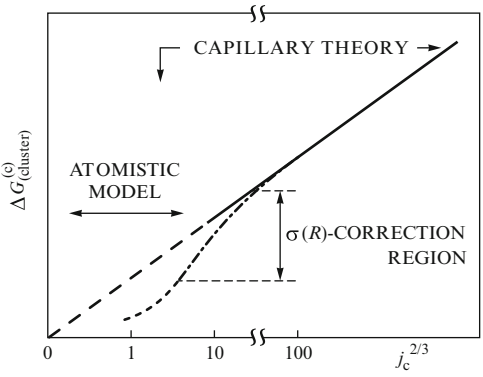

Fig. 6.21 Illustration of the regions of validity of the different approaches in the theory of nucleation (After Mutaftschiev (1993) [585])

experimental results in terms of the atomistic model of nucleation, however, little information is obtained in trying to predict the parameters of nucleation processes in advance. In this respect the classical model is undoubtedly of more use. The regions of applicability of both approaches in the theory of nucleation – of the classical model and the atomistic approach – are illustrated in Fig. 6.21. For sufficiently large cluster sizes a linear dependence $\Delta G^{(c)}_{(cluster)}$ vs. $j_c^{2/3}$ is to be expected according to the capillarity approximation valid only for large cluster sizes. In the other limiting case ($j_c \rightarrow 1$) no definite statement can be made in advance from Eq. (6.203) for the ($\Delta G^{(c)}_{(cluster)}$ vs. j_c)-dependence.

In the intermediate region the approximation $\sigma = \sigma(\infty)$ is unacceptable and corrections as discussed by Gibbs, Tolman, Toschev, Parlange, Schmelzer (see Sect. 6.2.4) and many others have to be introduced into the theory in order to get a quantitatively correct description. It is seen that at present only the classical model gives a definite possibility of predicting the nucleation rate while the atomistic approach merely provides a tool for the theoretical explanation of experimental results. The advantages of the classical theory over the atomistic approach also become evident from the fact that a quantitative description of catalyzed nucleation, as discussed in the next chapter, is based practically totally on the classical theory of nucleation.

6.3.9 Thermal and Athermal Nucleation

As already mentioned, in classical nucleation theory the term nucleation rate is usually identified with the rate of formation of critical clusters. For constant external and internal conditions this rate is at the same time equal to the change of the total number of clusters exceeding the critical size, j_c. However, if the state of the system is changed in the course of the transformation, either due to a variation of the external conditions or internal processes (decrease of supersaturation), then the rate of formation of critical clusters is not equal to the rate of change of the total number of clusters exceeding the critical size. Indeed, if we introduce the notations

$$N(j \geq j_c, t) = \int_{j_c}^{\infty} N(j,t)\, dj \ , \tag{6.204}$$

where $N(j \geq j_c, t)$ is the number of clusters with sizes $j \geq j_c$ at time t in the system, and

$$J(j \geq j_c, t) = \frac{dN(t)}{dt} \tag{6.205}$$

for their rate of formation, then

$$J = \frac{\partial}{\partial t} \int_{j_c}^{\infty} N(j,t)\, dj \tag{6.206}$$

holds. With the continuity equation, Eq. (6.146), one gets for time-independent supersaturations (j_c = constant)

$$J(j \geq j_c, t) = J(j_c, t) \ , \tag{6.207}$$

while for time-dependent situations

$$J(j \geq j_c, t) = J(j_c, t) - N(j_c, t) \frac{\partial j_c}{\partial t} \tag{6.208}$$

is obtained. The first term in Eq. (6.208) describes the stochastic process of formation of supercritical clusters connected with thermal fluctuations in the system. The second term accounts for the process of athermal nucleation which is a consequence of the change in the critical cluster size. However, if the changes in the external or internal conditions proceed too fast, then any analytical approach breaks down and the numerical solution of the system of rate equations, Eqs. (6.94)–(6.95), remains the only tool for the description of nucleation. In the discussion above the process of formation of critical or supercritical clusters is denoted as athermal nucleation due to a change of the state of the system and a resulting variation of the critical cluster size.

In the literature (Avrami (1939, 1940, 1941) [19]) those clusters of supercritical sizes are also denoted as athermal nuclei which are formed in the sample in the course of previous thermal treatments and brought afterwards to a state of higher supersaturation. In these cases, the clusters formed earlier are capable of a further deterministic growth. In terms of nucleation theory, for such populations of athermal supercritical clusters, the nucleation rate is equal to infinity and the time-lag equals zero (see Kashchiev (1969) [434]). In application to glass-forming melts, populations of athermal clusters may be formed in the course of cooling of the melt. In devitrification processes, such clusters serve as centers for devitrification at which an intensive crystallization is observed. Such a possibility always has to be

taken into consideration if the overall crystallization kinetics of different substances and, in particular, of glasses and glass-forming melts is discussed (for the details see Chap. 10).

Finally we have to mention that there is little experimental evidence on the kinetics of homogeneous nucleation in which it is guaranteed that different sources of nucleation catalysis in the melt are excluded. In some cases, as it seems to be for organic polymer melts, it is even impossible to obtain an ambient phase free of active nucleating agents. By this reason experimental evidence on the kinetics of nucleation in glass-forming melts is given in the next chapter only after the possible influence of different catalytic effects on nucleation has been discussed in detail.

6.3.10 General Scenario for the Overall Course of First–Order Phase Transformations in Finite (Closed) Systems: Conclusions from a Thermodynamic Analysis

In the previous sections, the kinetics of nucleation in systems with constant supersaturation was investigated. Only in the case of the computer calculations given in Sect. 6.3 were results also mentioned obtained for closed (or finite) systems, where the supersaturation changes with time in the course of the phase transformation. As already pointed out briefly in Sect. 6.3.3 the change in the state of the system in the course of the transformation can be expected to affect quantitatively nucleation processes and, as will be shown, it determines qualitatively the whole course of the transformation.

In the present section results of a thermodynamic analysis are summarized allowing one, at least, in an approximative form an understanding of the overall course of phase transformations in a finite (closed) system. This analysis is supplemented in Chaps. 8–10 by a kinetic description of growth of the aggregates of the newly evolving phase and of the overall course of the transformation. We assume in the simplified thermodynamic model approach, discussed in the present section that the evolving phase is concentrated in N clusters each of them having the same size and characterized by the same radius R. Comparing the model with a real ensemble of clusters the variable R can be identified with the average cluster size of the real more or less disperse cluster ensemble evolving in the ambient phase. Note, that although this model represents a considerable simplification of the real picture, it allows us to understand both qualitatively and quantitatively a number of results on phase transformation processes observed experimentally (see Schmelzer and Ulbricht (1987) [712]; Schmelzer (1985, 1990) [688, 691]).

The change of the Gibbs free energy $\Delta G_{(N)}$ due to the formation of N identical clusters, all of them having the same size R, depends, in such an approach, on the two parameters N and R. For a given value of N the thermodynamic function $\Delta G_{(N)}$ may be expressed in accordance with Eqs. (6.31) and (6.32) as

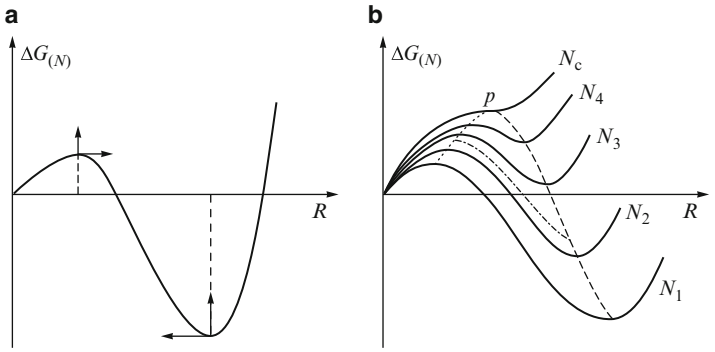

Fig. 6.22 Thermodynamic model for the description of the overall course of a phase transformation (Schmelzer (1985) [689]; Schmelzer, Ulbricht (1987) [712]): (**a**) change of the Gibbs free energy due to the formation of N clusters of a new phase in a segregation process in a solid or liquid solution, each of them having the same size, R. In addition to the maximum a minimum is found caused by the reduction of the monomer concentration of the segregating particles in the ambient phase (decrease of the supersaturation). (**b**) Change of the Gibbs free energy as a function of the cluster size for different values of the number of clusters in the system ($N_1 < N_2 < \ldots < N_c$). Three major stages of the phase transformation may be distinguished according to this simplified model: a stage of dominating nucleation and simultaneous growth of the already formed critical clusters (*dotted curve*), a stage of practically independent growth of the clusters their number being nearly constant (*dashed–dotted curve*) and a third stage of competitive growth (*dashed curve*), where the average size of the clusters is increased and their number decreased

$$\Delta G_{(N)} = N n_\alpha [\mu_{1\beta}(x_{eq}) - \mu_{1\beta}(x_\beta)] + N\sigma A + \sum_{i=1}^{2} [\mu_{i\beta}(x_\beta) - \mu_{i\beta}(x)] n_i \,, \qquad (6.209)$$

where the molar fractions are determined by

$$x = \frac{n_1}{n_1 + n_2} \,, \qquad x_\beta = \frac{n_1 - N n_\alpha}{n_1 + n_2 - N n_\alpha} \,. \qquad (6.210)$$

Qualitatively, the change of the Gibbs free energy as a function of the radius R of the N clusters is shown on Fig. 6.22a.

Changes in the state of the ambient phase due to the decrease of the concentration of the segregating particles result, in general, in a second extremum, a minimum, in addition to the maximum, which is caused by the interplay of bulk and surface contributions. For the case of $N = 1$ the existence of two extrema was mentioned for the first time by Konobejewski (1939) [465] for the model of a drop in finite volume of vapor. The extrema of $\Delta G_{(N)}$ for a fixed value of the number of clusters are determined by

$$\left(\frac{\partial \Delta G}{\partial R} \right)_N = -4\pi R^2 c_\alpha N \left(\mu_{1\beta}(x_\beta) - \mu_{1\beta}(x_{eq}) - \frac{2\sigma}{c_\alpha R} \right) = 0 \,. \qquad (6.211)$$

The type of the extremum is specified by the second derivative of the change of the Gibbs free energy, which can be expressed in the form

$$\left(\frac{\partial^2 \Delta G_{(N)}}{\partial R^2}\right)_N = -8\pi\sigma N(1 + Z^{\oplus}) \tag{6.212}$$

with

$$Z^{\oplus} = -\frac{3c_\alpha R}{2\sigma} \frac{N n_2 n_\alpha}{(n_1 + n_2 - N n_\alpha)^2} \frac{\partial \mu_{1\beta}}{\partial x_\beta} . \tag{6.213}$$

Here $Z^{\oplus}$ is always less than zero. Moreover, for the minima, $1 + Z^{\oplus} < 0$ holds; while for the maxima, the inequality $1 + Z^{\oplus} > 0$ is fulfilled. Both extrema may coincide in a point of inflexion determined by the condition $1 + Z^{\oplus} = 0$.

The position of the extrema, determined by Eq. (6.211), depends on the value of the number of clusters, N, present in the system. Taking into account the existence of such a dependence the variation of the position of the extrema with an increasing number of clusters can be calculated from Eqs. (6.209) and (6.211) as

$$\frac{dR^{(extr)}}{dN} = -\frac{R^{(extr)}}{3N} \frac{Z^{\oplus}}{1 + Z^{\oplus}} , \tag{6.214}$$

$$\frac{d\Delta G_{(N)}^{(extr)}}{dN} = \frac{1}{3}\sigma A^{(extr)} , \qquad A^{(extr)} = 4\pi R_{(extr)}^2 . \tag{6.215}$$

The change of the position of the extrema with an increasing number of clusters in the system is indicated in Fig. 6.22a by arrows. In Fig. 6.22b the curves ($\Delta G_{(N)}$ vs. R) are shown for different values of the number of clusters in the model system. Hereby the inequalities $N_1 < N_2 < \ldots < N_c$ are fulfilled.

Three main different stages of the transition may be distinguished according to this picture: a stage of dominating nucleation with a possible simultaneous growth of the already formed supercritical clusters (dotted curve); a stage of practically independent growth of the supercritical clusters their number being nearly constant (dashed–dotted curve); a stage of competitive growth (dashed curve), where large clusters grow at the expense of smaller ones. This stage, known as Ostwald ripening, is discussed in detail in Chap. 9. From this picture, moreover, an estimate can be derived for the highest possible number of clusters, which can be formed in the system as a result of nucleation. It is determined by the number of clusters N_c, for which both extrema of the curves coincide in a common point of inflexion. The value of R corresponding to the point of inflexion and N_c represent, in addition, the most disperse state for which the process of further deterministic structural reorganization of the system (Ostwald ripening) may start.

In general, the process of nucleation will not proceed along the path indicated by the dotted curve until the point of inflexion is reached, but will go over to the second stage of practically independent growth. The particular point in the model along the dotted curve, for which this transition occurs, may depend only on the initial supersaturation. With an increasing supersaturation the point, where

nucleation is followed by dominating growth, is shifted along the dotted curve into the direction of the point of inflexion marked in the figure by P. According to the above simplified model the number of clusters remains practically unchanged in the second stage of independent growth. In the course of this evolution, a state along the "valley" of the thermodynamic potential is reached. This state along the dashed curve is determined thus also by the initial supersaturation.

Nucleation and independent growth proceed relatively fast as compared with the third stage of the process (Ostwald ripening) depicted in the figure by the dashed curve. It follows that in nucleation experiments usually states are observed corresponding initially to a point in the "valley" (dashed curve) of the thermodynamic potential. This result has, at the same time, the consequence that with an increasing supersaturation the number of clusters observed in nucleation increases but their average size decreases (cf. von Weimarn's law (1926) [900]). It can be shown that the results outlined do not depend on any particular properties of the system under investigation but are consequences only of changes of the state of the system in the course of the transformation. A proof of this statement and a more detailed analysis is given in a series of publications (Schmelzer (1985) [689]; Schmelzer and Ulbricht (1987) [712]; Ulbricht, Schmelzer et al. (1988) [874]; see also Vogelsberger (1982) [890][10]).

[10] A detailed analysis of the peculiarities of nucleation in confined space and the derivation of conclusions concerning the general scenario of first-order phase transitions based on the generalized Gibbs approach was performed recently by one of the authors in cooperation with A. S. Abyzov (Schmelzer and Abyzov [703]). The general conclusions remain widely the same as discussed in the present section and derived here based on the classical Gibbs' approach.

Chapter 7
Catalyzed Crystallization of Glass-Forming Melts

7.1 Introductory Remarks: Ways to Induce Nucleation

Present day theory of nucleation predicts a number of possibilities for increasing the rate of nucleation in processes of phase formation. In science and technology, such possibilities are applied in various methods of induced or catalyzed nucleation. Possible approaches in nucleation catalysis are discussed in the literature beginning with the classical monographs on nucleation theory (see, e.g., Volmer (1939) [894]; Mason (1957) [536]; Hirth, Pound (1963) [368]; Zettlemoyer (1969 [954], 1977 [955])). Here a summary of methods is given in application to crystallization of undercooled melts.

The first possibility of nucleation catalysis was revealed as early as about 140 years ago by Gibbs [249]. Gibbs mentioned the influence of active solid substrates on nucleation resulting from the decrease in the work of formation of critical nuclei. In this way, he succeeded in explaining experimental evidence on crystallization with random dopants and artificial insemination accumulated over more than hundred years. Another case of nucleation catalysis, nucleation caused by charged particles, was employed also relatively early in Wilson's cloud chamber in the first investigations of the nature of radioactivity. Such a possibility of nucleation catalysis was of exceptional importance for atomic and nuclear physics where also a modified device – the bubble chamber – is widely employed. In the bubble chamber not condensation but cavitation is induced by charged particles. In both cases, the enhanced nucleation rate can be explained by a reduction of the work of formation of critical clusters.

It seems that for the first time the term "catalyzed nucleation" was used in 1902 by W. Ostwald (see Volmer and Weber (1926) [896]). Ostwald mentioned that in analogy to chemical reaction kinetics, a lowering of the kinetic barrier of nucleation should catalyze phase transformations. In glass technology, nucleation catalysis – or induced crystallization as it is termed in technology – is used in order to produce crystalline or semicrystalline materials from glass-forming melts. The first such application was reported as early as 1739 by Reaumure [159], who produced the first

I.S. Gutzow and J.W.P. Schmelzer, *The Vitreous State*,
DOI 10.1007/978-3-642-34633-0_7, © Springer-Verlag Berlin Heidelberg 2013

glass-ceramic material – the so-called Reaumure porcelain – by surface catalyzed nucleation. Modern attempts in this direction – in what is termed heterogeneous nucleation – have been developed beginning with the 1950s by Lungu and Popescu (1954) [523], Stookey (1959) [803] and many others.

In the modern technology of synthesis of glass-ceramics, foreign nucleation cores are introduced or formed in the melt for nucleation catalysis. However, as will be shown in the subsequent sections of this chapter, a number of alternative methods of homogeneous nucleation catalysis can also be used. An interesting turn in the purpose of the studies on crystallization and crystal growth took place in connection with such developments. While in the 1920s and 1930s these processes were analyzed mainly from the point of view of preventing crystallization and obtaining defect-free glasses, in the 1950s and 1960s, the opposite goal became of importance: the development of the most effective methods of nucleation catalysis.

It will be seen in the further analysis that despite the variety of possible mechanisms underlying nucleation catalysis, the theory of heterogeneous nucleation is, as in the first discussed examples, guided by the basic idea that nucleation activity is determined entirely or at least to a large extent by the decrease in the work of formation of critical clusters. Based on this idea, the experimental results are interpreted in terms of the classical approach to homogeneous nucleation. In the subsequent discussion of nucleation catalysis in glass-forming melts, we follow this approach, having, however, in mind the limitations of the classical theory mentioned in the previous chapter.

7.2 Heterogeneous Nucleation: Basic Thermodynamic Relationships

From the very beginning of the study of precipitation and crystallization it was established experimentally that foreign substrates – i.e., the walls of a vessel containing the solution or the melt, foreign insoluble particles – as a rule enhance nucleation. An account of the history of these studies can be traced in great detail in Volmer's monograph (1939) [894]. The basic model allowing one an understanding of nucleation on foreign substances is the following. Let us assume that a liquid condenses on a solid (see Fig. 7.1; Volmer (1939) [894]; Hirth, Pound (1963) [368]). The liquid forms a spherical cap with the radius, R, and a contact (or wetting) angle, θ.

The interfacial tensions or specific surface energies between the different phases are denoted here as σ_{lv} (liquid-vapor interface), σ_{ls} (liquid-solid interface) and σ_{sv} (solid-vapor interface), respectively. The change of the Gibbs free energy due to the formation of such a cap-shaped cluster of the liquid phase is given by

$$\Delta G^{(*)}_{(cluster)} = -j\Delta\mu + \sigma_{lv}A_{lv} + (\sigma_{ls} - \sigma_{sv})A_{sv} \ . \tag{7.1}$$

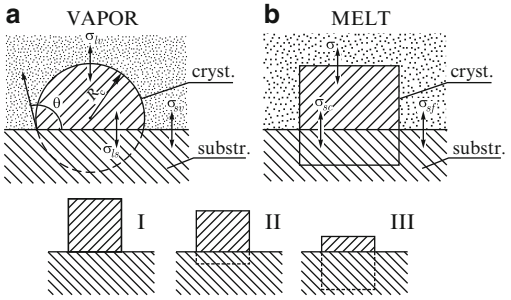

Fig. 7.1 Illustration of the simplest models of heterogeneous nucleation: (**a**) Formation of *cap-shaped* clusters on a solid planar surface; θ is the wetting angle. (**b**) Kaischew's cubic crystal cluster model for nucleation on a planar solid. With decreasing Φ-values the shape and size of the initially cubic critical cluster change as indicated by *I*, *II* and *III*

Here A denotes the area of the interface between liquid and vapor (A_{lv}), respectively, solid and vapor (A_{sv}). The quantities referring to heterogeneous nucleation are specified here and in the following by an asterisk (*).

Since the interfacial tension can also be defined as the force acting on a unit element of the line of coexistence of the three considered phases, from the condition of mechanical equilibrium one obtains

$$\sigma_{sv} = \sigma_{ls} + \sigma_{lv} \cos\theta \ . \tag{7.2}$$

Equations (7.1) and (7.2) allow us to express the work of formation of a critical cluster for a given value of the wetting angle, θ (Volmer (1939) [894]). One obtains

$$\Delta G^{(c*)}_{(cluster)} = \Delta G^{(c)}_{(cluster)} \Phi \tag{7.3}$$

with

$$\Phi = \frac{1}{2} - \frac{3}{4}\cos\theta + \frac{1}{4}\cos^3\theta \ , \tag{7.4}$$

where $\Delta G^{(c)}_{(cluster)}$ is the work of formation of a critical cluster in the absence of foreign substrates for the same value of the supersaturation (see Eq. (6.44)).

The parameter Φ, introduced with Eqs. (7.3) and (7.4), is a measure of the activity of the substrate with respect to nucleation catalysis. By definition and physical meaning it should have, in general, values between zero and one, i.e.,

$$0 \le \Phi \le 1 \ . \tag{7.5}$$

It can be seen from Eq. (7.4) and Fig. 7.2 that for $\theta = 0$ (complete wetting) the work of formation of the critical cluster tends to zero, while for $\theta = \pi$ (complete non-wetting) homogeneous nucleation occurs. For intermediate values of the contact angle the work of formation of the clusters is more or less decreased dependent on the values of the respective interfacial energies.

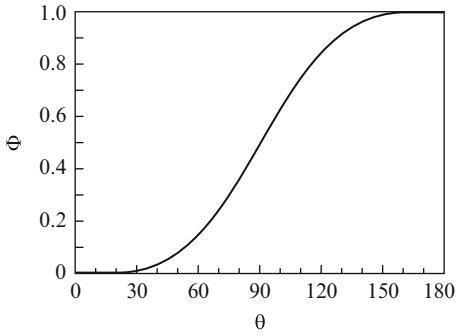

Fig. 7.2 Nucleation activity, Φ, of a planar interface in dependence on the wetting angle, θ, according to Eq. (7.4)

The relation between nucleation activity, Φ, and contact angle, θ, allows one a characterization of the nucleation activity to be made in terms of the degree of wetting. For condensation of liquids on solids the measured macroscopic contact angle gives, consequently, an indication of the nucleation activity of a given substrate with respect to the overgrowing crystal. As seen from Fig. 7.2 contact angles below 30° guaranty effective nucleation catalysis. This connection between nucleation activity and wetting angle is sometimes also used for a characterization of nucleation of a solid phase on a solid surface. In a more or less formal way it is done by introducing the radius of the sphere enclosing the crystalline nucleus. A more realistic model for a crystalline nucleus having a cubic shape at $\Phi = 1$ is also shown on Fig. 7.1.

According to Kaischew (1952) ([417]; see also Mutaftschiev (1993) [585]) as a general measure of the nucleating activity applicable to any case of phase transformation, the ratio of the volumes of the critical clusters formed by heterogeneous (V_c^*) respectively homogeneous (V_c) nucleation may be used, i.e.,

$$\Phi = \frac{V_c^*}{V_c} \,. \tag{7.6}$$

This formula turned out to be a very fruitful guide in the determination of the nucleation activity Φ in different cases of heterogeneous nucleation. It is, of course, also fulfilled for the case of melt crystallization considered so far.

The model of a cap-shaped nucleus on a planar surface discussed above can be generalized, applying Eq. (7.6) to the case where the substrate is comparable in size to the critical cluster (see Fig. 7.3), i.e., to phase formation on foreign dopants or nucleation cores of a finite size (described by a radius of the core R_s), when $(R_c/R_s) \to 1$ or even $R_c/R_s < 1$ holds. The activity of such nucleation cores and, in particular, size effects in nucleation catalysis were analyzed first by Krastanov (1957) [483], Fletcher (1958 [213], 1962 [214]), Kaischew and Mutaftschiev (1959) ([422]; see also Mutaftschiev (1993) [585]).

The general conclusion, obtained as the result of these investigations, is that the nucleating activity of foreign substrates is significantly reduced if the size of the substrate, R_s, is comparable with the critical cluster size, R_c. Size effects are

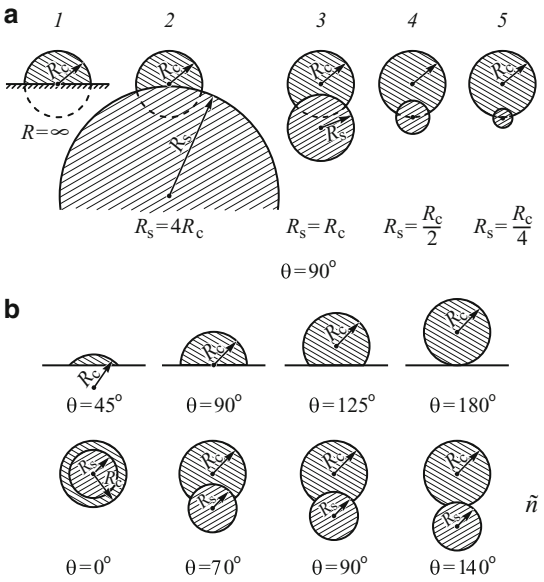

Fig. 7.3 Size effects in heterogeneous nucleation. (**a**) Influence of substrate curvature at constant contact angle ($\theta = 90°$): (*1*) Homogeneous *cap-shaped* nucleus with critical radius R_c on a flat surface ($R_s \rightarrow \infty$); On substrates with an increasing (R_c/R_s)-ratio the volume of the heterogeneously formed nucleus increases continuously from (*2*) to (*5*) and according to Eq. (7.6) lower nucleation activities are to be expected. (**b**) Influence of different contact angles on the volume (and thus on the activity Φ) of *cap-shaped* nuclei formed on a flat surface. (**c**) Influence of contact angles on volume (and activity) of nuclei formed on crystallization cores with $(R_c/R_s = 1.45)$. It is seen that for slightly active nuclei (e.g., for $\theta = 140°$) their volume is practically equal to that of homogeneously formed critical clusters

more pronounced the lower the activity of the substrate at planar interfaces is. The details of the respective derivations made in the framework of the capillarity theory of nucleation can be found in the cited papers. In Fig. 7.3, a summary of results is given illustrating the effect of both the change in the (R_c/R_s)-ratio (for constant values of the contact angle θ) and in the wetting angle, θ. In any case, Kaischew's formula Eq. (7.6) gives the possibility of determining, on the basis of simple geometrical considerations, possible Φ-values. Usually, sub-microscopic foreign seed crystals with dimensions comparable with the crystalline nuclei to be formed act as nucleation catalysts in glass-forming melts. Thus the discussed size effects in nucleation are of particular importance for processes of induced devitrification of glasses as recognized first by Stookey (1959) [803] and Maurer (1958) [540]. A direct proof of size effects in catalyzed nucleation is described by Gutzow (1980) [303] (in an investigation of the activity of gold particles of different size on the crystallization of $NaPO_3$-glasses). A discussion of further applications of Kaischew's model to substrates with a rough surface structure (on edges, corners etc.) is given in Mutaftschiev's review article [585] in line with results previously obtained by Kaischew. Another generalization of the model discussed

above consists in its application to liquid phase formation at the liquid-gas or liquid-liquid interface (Gibbs's lenses). A summary of results in this respect can be found, again, in Volmer's monograph [894].

In studying processes of heterogeneous nucleation in application to solids, the model of a cubic nucleus formed on a planar surface also proved to be of particular use (Fig. 7.1; Kaischew (1952) [417]). In this model the activity, Φ, is expressed employing another thermodynamic characteristic of the interface, the work of adhesion β. Denoting the specific interfacial energy of the crystal-melt interface by σ, according to Kaischew we have to write

$$\Phi = \left(1 - \frac{\beta}{2\sigma}\right) . \tag{7.7}$$

With such an approach, new possibilities are opened for quantitative predictions of the nucleation activity, at least, for substrates with similar structures. At $\Phi = 0$, the volume of the critical nucleus tends to zero. This result means that, in the process of condensation on such a planar interface, practically any particle condensed is capable of further deterministic growth. The rate of phase formation is determined in these cases only by the impingement rate of the ambient phase molecules.

A more detailed thermodynamic analysis performed by Bauer (1958) [52], Toschev et al. (1968) [852], and Markov and Kaischew (1973) [532] shows that the limiting case $\Phi = 0$ corresponds also to the process of formation of a layer of molecules on its own substrate via two-dimensional nucleation. Layer formation and subsequent growth by two-dimensional nucleation is one of the possible mechanisms of crystal growth as discussed in detail in Chap. 8. In the above mentioned papers, it was also shown that even negative values of Φ may correspond to physically relevant situations. This case may be realized in the process of formation of two-dimensional nuclei on foreign substrates when the forces of adhesion between substrate and overgrowing crystal exceed the forces of cohesion between the monolayer and its own crystalline bulk phase. In processes of formation of three-dimensional nuclei at or near planar interfaces between two solids with different values of Young's modulus an inhibition of nucleation may take place (see Sect. 7.7). This situation corresponds to values of Φ larger than one.

7.3 The Kinetics of Heterogeneous Nucleation: Basic Equations

Following the basic ideas of classical nucleation theory the steady-state nucleation rate for heterogeneous nucleation may be written similarly to Eq. (6.109) in the form

$$J^* = N^*_{(cores)} \Gamma^*_{(z)} w^{(+*)}(j^*_c) \exp\left(-\frac{\Delta G^{(c)}_{(cluster)}}{k_B T} \Phi\right) . \tag{7.8}$$

Here $N^*_{(cores)}$ denotes either the actual concentration of active centers for nucleation at the surface of a substrate or the volume concentration of crystallization cores in the bulk of the ambient phase. For $w^{(+*)}$ we have to write, again, (compare Eq. (6.121))

$$w^{(+*)} = Z^{(eff)} A_c^* \,, \tag{7.9}$$

where by A_c^* the interfacial area between ambient phase and critical cluster and by $Z^{(eff)}$ the effective impingement rate of ambient phase molecules are denoted.

Introducing with $N^*_{(tot)}$ the total number of foreign active nucleation sites initially present in the system and taking into account that the actual number of active centers for nucleation decreases in the course of the transformation we obtain the following expression for the rate of formation of critical clusters $N^*(t)$ in the system

$$\frac{dN^*(t)}{dt} = \left(\frac{N^*_{(tot)} - N^*(t)}{N^*_{(tot)}} \right) J^*_{(init)} \,. \tag{7.10}$$

Here $J^*_{(init)}$ is the initial nucleation rate for heterogeneous nucleation in the system. According to Eq. (7.8) it is given by

$$J^*_{(init)} = N^*_{(tot)} \Gamma^*_{(z)} w^{(+*)} (j_c^*) \exp\left(-\frac{\Delta G^{(c)}_{(cluster)}}{k_B T} \Phi \right) \,. \tag{7.11}$$

The solution of Eq. (7.10) can be written as

$$N^*(t) = N^*_{(tot)} \left[1 - \exp\left(-\frac{J^*_{(init)}}{N^*_{(tot)}} t \right) \right] \,. \tag{7.12}$$

For the time-dependence of the nucleation rate we obtain by a derivation of this expression

$$J^*(t) = J^*_{(init)} \exp\left(-\frac{J^*_{(init)}}{N^*_{(tot)}} t \right) \,, \tag{7.13}$$

i.e., the nucleation rate tends exponentially to zero with time, since all available nucleation cores become exhausted (see Fig. 7.4). In an experimental investigation performed by Gutzow et al. (1971) [317] it was shown in fact that the number of crystallites formed in the process of devitrification of a $NaPO_3$-glass is directly determined by the number of crystallization cores (platinum micro-crystals) introduced into the bulk of the melt.

Non-steady state effects in the kinetics of heterogeneous nucleation were treated for the first time by Toschev and Gutzow (1967) [849]. Defining τ^*, again, similarly to Eq. (6.189) as

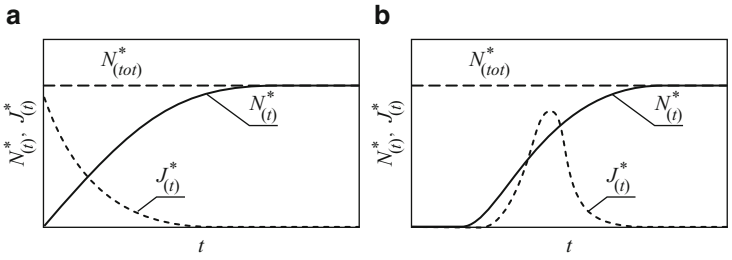

Fig. 7.4 Time dependence of the number of clusters, $N^*(t)$ (*solid lines*), and of the nucleation rate, $J^*(t)$ (*broken lines*), in heterogeneous nucleation on a limited number of active sites, $N^*(t)$, for (**a**) steady-state nucleation and (**b**) transient nucleation kinetics (schematically)

$$\tau^* = \frac{a_0 k_B T}{w^{(+*)}(j_c^*)} \left| \left(\frac{\partial^2 \Delta G^{(*)}_{(cluster)}(j)}{\partial j^2} \right)_{j=j_c^*} \right|^{-1} \tag{7.14}$$

the ratio $\tau^*/\tau^{(ns)}$ can be written first as

$$\frac{\tau^*}{\tau^{(ns)}} = \frac{w^{(+)}(j_c) \left(\frac{\partial^2 \Delta G_{(cluster)}(j)}{\partial j^2} \right)_{j=j_c}}{w^{(+*)}(j_c^*) \left(\frac{\partial^2 \Delta G^{(*)}_{(cluster)}(j)}{\partial j^2} \right)_{j=j_c^*}} . \tag{7.15}$$

Taking into account Eq. (7.9) we obtain further

$$\tau^* = \tau^{(ns)} \Psi(\Phi) , \qquad \Psi(\Phi) = \frac{A_c \left(\frac{\partial^2 \Delta G_{(cluster)}(j)}{\partial j^2} \right)_{j=j_c}}{A_c^* \left(\frac{\partial^2 \Delta G^{(*)}_{(cluster)}(j)}{\partial j^2} \right)_{j=j_c^*}} . \tag{7.16}$$

The function $\Psi(\Phi)$ has to be equal to unity for $\Phi = 1$.

Using as an estimate Eqs. (6.43) and (6.50) both for homogeneous and heterogeneous nucleation Eq. (7.16) yields with Eq. (7.3)

$$\tau^* = \tau^{(ns)} \left(\frac{j_c^*}{j_c} \right)^{4/3} \frac{1}{\Phi} . \tag{7.17}$$

With Kaischew's formula Eq. (7.6), which is equivalent to $\Phi = j_c^*/j_c$, we have, finally,

$$\tau^* = \tau^{(ns)} \Phi^{1/3} . \tag{7.18}$$

In this way, a simple method for determining the activity of foreign substrates by measuring the time-lag of nucleation is obtained. It was used in a number of subsequent experimental investigations (see Sect. 7.8).

Taking into account transient effects, more complicated time dependencies for the number of critical clusters, $N^*(t)$, formed in the course of heterogeneous nucleation and for the nucleation rate, $J^*(t)$, are found. Applying, for example, Zeldovich's equation, Eq. (6.166), we have

$$\frac{dN^*(t)}{dt} = \left(\frac{N^*_{(tot)} - N^*(t)}{N^*_{(tot)}} \right) J^*_{(init)} \exp\left(-\frac{\tau^*}{t} \right) \tag{7.19}$$

with the solution (see Toschev and Gutzow (1967) [850]; Gutzow, Toschev (1971) [320])

$$N^*(t) = N^*_{(tot)} \left\{ 1 - \exp\left[-\frac{J^*_{(init)}}{N^*_{(tot)}} t \exp\left(-\frac{\tau^*}{t} \right) \right] + \frac{\tau^*}{t} \mathrm{Ei}\left(-\frac{\tau^*}{t} \right) \right\} . \tag{7.20}$$

Here, again, Ei denotes the integral exponential function. The respective $N^*(t)$-curves are illustrated on Fig. 7.4. It is seen that non-steady state effects result in a shift of the $N^*(t)$-curves along the t-axis, thus giving a simple way for an estimation of the value of τ^*.

A more extended analysis of nucleation kinetics on active nucleation sites can be found in a paper by Markov and Kashchiev (1972) [531]. A particular case consists of heterogeneous nucleation on point defects. A treatment of this topic in the framework of the outlined general theory is given in a paper by Stoyanov (1974) [805].

7.4 Activity of Foreign Substrates in Induced Crystallization

First attempts at the theoretical determination of the nucleating activity of foreign solid substrates were focused mainly on crystallographic criteria, i.e., by analyzing the effects of structural matching or misfit between the crystallographic parameters of the substrate and the overgrowing crystal. Typical examples in this respect are the investigations of Turnbull and Vonnegut (1952) [867] or the epitaxy rule of Dankov. According to such criteria, nucleation catalysis by foreign insoluble dopants takes place only if the relative linear misfit parameter δ_l, defined by

$$\delta_l = \frac{(d_{crystal} - d_{substrate})}{d_{substrate}} , \tag{7.21}$$

is lower than 15 %. Here d_i are the lattice parameters of the overgrowing crystal and the substrate.

In order to derive more general expressions for the nucleating activity of solid substrates we may start with Eq. (7.7). The adhesion energy, β, in between the two crystalline phases – the substrate (specified in the following derivations by a subscript (s)) and the overgrowing crystal (specified by (c)) – can be calculated by using Dupre's equation. If the lattice parameters of both crystalline phases are equal ($d_{substrate} = d_{crystal}$) and denoting by β^0 the value of the adhesion energy for this case this equation reads

$$\beta^0 = \sigma_{cf} + \sigma_{sf} - \sigma_{sc} \ . \tag{7.22}$$

Here σ_{cf}, σ_{sf} and σ_{sc} are the specific interfacial energies for the crystal-melt (cf), substrate-melt (sf) and substrate-crystal (sc) interfaces.

If lattice parameter differences have to be taken into account (i.e., for $\delta_l \neq 0$) then following van der Merwe (1973) ([878]; see also Markov and Stoyanov (1987) [533]) an additional elastic energy, E_d, is stored in the interface. This energy is released later in form of misfit dislocations. Consequently, in the general case ($\delta_l \neq 0$) we have to write

$$\beta = \beta^0 - E_d \ . \tag{7.23}$$

The adhesion energy β^0 is proportional to the forces of molecular interaction between the s and c faces. In order to give a quantitative estimate of β^0 a classical approximation, introduced into the physical chemistry of solid solutions by van Laar (1936) [877] and London (1930) [513], may be used.

Supposing that both the substrate and the overgrowing solid layer are ionic crystals, i.e. that only Coulomb forces are acting between the respective building units, the energy of cohesive interactions ϕ in both solids and in between them are determined by dependencies of the form

$$\phi_{cc} \sim \frac{q_c^2}{d_0} \ , \qquad \phi_{ss} \sim \frac{q_s^2}{d_0} \ , \qquad \phi_{sc} \sim \frac{q_s q_c}{d_0} \ . \tag{7.24}$$

Here q_c and q_s are the respective electric charges of the ions under consideration and d_0 an intermediate reference lattice parameter defined by

$$d_0 = \frac{2 d_s d_c}{d_s + d_c} \ . \tag{7.25}$$

It follows from the above equations that the energy of adhesion, ϕ_{sc}, can be expressed as

$$\phi_{sc} = (\phi_{ss} \phi_{cc})^{1/2} \ . \tag{7.26}$$

This latter equation is known in literature as the van Laar-London formula. Though it was initially derived for ionic and van der Waals crystals only, it was shown to be applicable, at least qualitatively, also to non-ionic crystals (Staverman (1937) [795]).

With Eq. (7.26) the specific interfacial energies σ_{sc}, σ_{cf} and σ_{sf} in Eq. (7.22) may be written in the form (see Gutzow (1980) [303]; Dobreva, Gutzow (1993) [175])

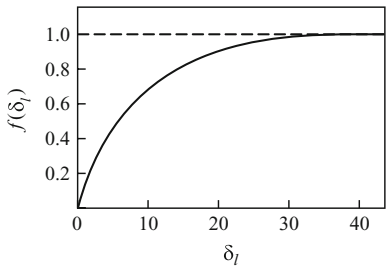

Fig. 7.5 Illustration of the course of van der Merwe's misfit function (see text)

$$\sigma_{sc} = \frac{1}{2d_0^2}\left(\sqrt{\phi_{ss}} - \sqrt{\phi_{cc}}\right)^2 , \qquad \sigma_{sf} = \frac{1}{2d_0^2}\left(\sqrt{\phi_{ss}} - \sqrt{\phi_{ff}}\right)^2 ,$$

$$\sigma_{cf} = \frac{1}{2d_0^2}\left(\sqrt{\phi_{cc}} - \sqrt{\phi_{ff}}\right)^2 , \tag{7.27}$$

which allows one a determination of β^0 and β from the forces of cohesion. The cohesion (or the bond energies) occurring in Eqs. (7.27) can be approximated by the respective heats of sublimation or evaporation of both the substrate and the overgrowing crystal. Latter quantities are proportional to the heats of melting or to the melting temperatures of substrate $T_m^{(s)}$ and overgrowing crystal $T_m^{(c)}$.

As derived in detail by Dobreva and Gutzow (1993) [175] the parameter E_d can be also expressed in terms of ϕ_{cc} and ϕ_{ss} in the form

$$E_d = b_0\left(\phi_{ss} + \frac{x}{1-x}\phi_{cc}\right) f(\delta_l) . \tag{7.28}$$

In this equation, $f(\delta_l)$ is the van der Merve misfit function having a course as shown in Fig. 7.5. For $\delta_l = 0$ this function equals zero while for $\delta_l > 15\,\%$ it is practically equal to unity. x in Eq. (7.28) is a dimensionless adjustable parameter of the order 0.5 and b_0 a constant.

Above given equations result in a parabolic dependence of the nucleating activity Φ on the quantity $\sqrt{\phi_{ss}/\phi_{cc}}$ in the form

$$\Phi = A^{(\ominus)} - B^{(\ominus)}\sqrt{\frac{\phi_{ss}}{\phi_{cc}}} + C^{(\ominus)}\left(\sqrt{\frac{\phi_{ss}}{\phi_{cc}}}\right)^2 . \tag{7.29}$$

For systems with zero lattice misfit $C^{(\ominus)} = 0$ holds and Eq. (7.29) is reduced to

$$\Phi = A^{(\ominus)} - B^{(\ominus)}\sqrt{\frac{\phi_{ss}}{\phi_{cc}}} . \tag{7.30}$$

In general, $A^{(\ominus)}$, $B^{(\ominus)}$ and $C^{(\ominus)}$ are constants, which do not depend on ϕ.

Replacing the ratio (ϕ_{ss}/ϕ_{cc}), approximately, by the ratio of the melting temperatures of the substrate, $T_m^{(s)}$, and the overgrowing crystal, $T_m^{(c)}$, experimental evidence concerning the nucleation activity of different substances can be correlated and new effective crystallization cores may be proposed. For the case of one and the same overgrowing crystal (i.e., at $\phi_{cc} = \text{constant}$) a simple dependence of Φ on ϕ_{cc} (or the heat of melting, respectively, the melting temperature) is to be expected. It follows that the activity of a substrate changes with its melting temperature (cf. also Gutzow et al. (1978) [329]).

The formalism sketched in the present section was developed in two papers by Dobreva and Gutzow (1993) [175] where the details of the derivations are given. It is seen that by using Eqs. (7.29) and (7.30) it is possible to determine the change of Φ in a series of substrates, having equal (or at least similar) lattice parameters but different melting temperatures, i.e., different values of the cohesive energies.

7.5 Homogeneous Nucleation Catalysis: The Influence of Surfactants

With Eqs. (6.122), (6.193), (7.8) and (7.18) we may write the following expressions for the steady-state nucleation rate, J^*, and the time-lag, τ^*, in heterogeneous nucleation

$$J^* = \frac{B_1}{\eta} \exp\left(-B_2 \frac{\sigma^3}{(\Delta\mu)^2} \Phi\right) , \tag{7.31}$$

$$\tau^* = B_3 \frac{\eta}{\varsigma} \frac{\sigma}{(\Delta\mu)^2} \Phi^{1/3} , \tag{7.32}$$

$$B_1 = \frac{\varsigma}{d_0^5} \left(\frac{\sigma}{k_B T}\right)^{1/2} , \qquad B_2 = \frac{16\pi}{3} \frac{v_m^2}{k_B T} , \qquad B_3 = 2a_0 d_0^5 .$$

An inspection of above equations shows that for a given value of the supersaturation there exist, in principle, three possibilities to induce nucleation in under-cooled glass-forming melts (i.e., to increase the nucleation rate and to decrease the time-lag) by

- A lowering of the viscosity of the melt, i.e., by lowering of the kinetic barrier of crystallization,
- The introduction of crystallization cores with $\Phi < 1$ and by
- A lowering of the specific interfacial energy at the crystal-melt interface.

The first of the mentioned ways of nucleation catalysis can be applied in the technology of organic polymers by introduction of monomeric plastifiers. Another extreme possibility in this respect consists of the dissolution of the glass in an appropriate solvent. Such a process has been observed by Grantcharova and Gutzow (1986) [268] in the dissolution of phenolphthalein glass in water. This possibility is,

however, of no technological significance. The other two methods of enhancing the rate of nucleation are aimed at decreasing the thermodynamic barrier of the process. The second of the mentioned methods, the introduction of insoluble nucleation cores, has already been discussed in the previous section. The third of the possible methods, consisting of lowering the specific interfacial energy σ, may be realized by the introduction of surface active dopants into the system. Thus homogeneous nucleation catalysis can be achieved.

The possibilities of modifying σ by the addition of surfactants have been described by Bliznakov (1958) [84], Kaischew and Mutaftschiev (1959) [422], applying classical nucleation theory. It seems that Hillig (1964) [360] was the first to mention the possible application of this method to processes of formation of silicate-glass ceramic materials. For the considered case in the expression for the work of formation of critical clusters, Eq. (6.44), the specific interfacial energy, σ, has to be replaced by $\sigma \Rightarrow (\sigma - \Delta\sigma)$, where $\Delta\sigma$ is the change of the specific interfacial energy caused by the addition of surfactants to the system. We get

$$\Delta G^{(c*)}_{(cluster)} = \Delta G^{(c)}_{(cluster)} \left(1 - \frac{\Delta\sigma}{\sigma}\right)^3 . \tag{7.33}$$

Consequently, Eqs. (6.122), (7.31) and (7.32) yield (with $\Phi = 1$)

$$J^* = J \left(1 - \frac{\Delta\sigma}{\sigma}\right) \exp\left\{-\frac{B_2\sigma^3}{(\Delta\mu)^2}\left[\left(1 - \frac{\Delta\sigma}{\sigma}\right)^3 - 1\right]\right\} , \tag{7.34}$$

$$\tau^* = \tau^{(ns)} \left(1 - \frac{\Delta\sigma}{\sigma}\right) . \tag{7.35}$$

Since the nucleation rate depends exponentially on σ^3 this method may lead to a dramatic increase in the rate of phase formation.

In general, if insoluble active dopants are also present in the system the introduction of surfactants may result in a variation of the specific interfacial energy melt-substrate. In this case, the energy of adhesion β, determining Φ via Eq. (7.7), may be decreased more drastically than σ. As the result the inequality

$$\frac{\beta_{(surf)}}{2\sigma_{(surf)}} > \frac{\beta}{2\sigma} \tag{7.36}$$

may be fulfilled resulting in an increase in Φ and a relative deactivation of the crystallization cores. By the subscript (surf) the respective values of the quantities β and σ after the introduction of surfactants are specified.

If nucleation proceeds at insoluble crystallization cores in the presence of soluble dopants we have to write, taking into account the results outlined in the present and the previous sections, instead of Eqs. (7.33) and (7.35)

$$\Delta G^{(c*)}_{(cluster/surf)} = \Delta G^{(c)}_{(cluster)} \left(1 - \frac{\Delta\sigma}{\sigma}\right)^3 \Phi_{(surf)} \,, \tag{7.37}$$

$$\tau^*_{(surf)} = \tau^{(ns)} \left(1 - \frac{\Delta\sigma}{\sigma}\right) \Phi^{1/3}_{(surf)} \,, \qquad \Phi_{(surf)} = 1 - \frac{\beta_{(surf)}}{2\sigma_{(surf)}} \,. \tag{7.38}$$

In the above given equations, σ denotes as usual the specific interfacial energy melt-crystal. However, in most cases not σ but only the value of the interfacial energy σ_{fv} at the melt/vapor or melt/air interface is known. The change of σ_{fv} due to the addition of surfactants can be measured relatively easily, e.g., by contact angle determinations. In this connection it is of interest to have the possibility of making predictions with respect to the variations of σ knowing the change of σ_{fv}.

In a paper devoted to problems of surfactant-induced nucleation (Gutzow and Penkov (1989) [316]) a formalism was developed connecting the interfacial concentration of surfactant molecules, n_s, with the change of the specific interfacial energy. It was shown that in general a relation of the form

$$\frac{\Delta\sigma}{\sigma} \cong \text{const.} \frac{\Delta\sigma_{fv}}{\sigma_{fv}} \tag{7.39}$$

holds. This relation gives a simple theoretically founded rule for choosing the most appropriate surfactants for melt crystallization. According to this rule substances resulting after addition to the melt in a significant relative decrease in σ_{fv} are also expected to be most effective for a lowering of σ and for homogeneous crystallization catalysis. In the already cited and a previous paper (Penkov and Gutzow (1984) [632]) it was shown that MoO_3 – the universal oxide dopant, lowering surface energies in silicate technology – is also the most powerful nucleator in homogeneous nucleation catalysis of silicate glass-forming melts. Other promising oxides in this respect are V_2O_3 and Cr_2O_3.

In order to correlate $\Delta\sigma$ or $\Delta\sigma_{fv}$ with the volume concentration, n_s, of dopants Sziszkowski's equation

$$\frac{\Delta\sigma}{\sigma} = b_s \ln\left(1 + \frac{n_s}{a_s}\right) \tag{7.40}$$

may be used, a_s and b_s are two constants. For relatively low values of the ratio (n_s/a_s) this equation yields

$$\frac{\Delta\sigma}{\sigma} \sim n_s \,. \tag{7.41}$$

In most cases of melt crystallization the possible influence of surfactants on the pre-exponential factors in Eq. (7.31) and particularly on the viscosity may be neglected. However, there is also the possibility that the adsorption of surfactants at the interface of the clusters inhibits the process of cluster growth. Thus, an optimal concentration of the dopants has to be chosen.

Both mechanisms of nucleation catalysis discussed above have their merits and disadvantages. The main advantage of heterogeneous nucleation catalysis consists

of the possibility of determining, by introducing nucleation cores with $\Phi \approx 0$, in advance the number of active nucleation sites and thus of crystallites formed in the system in the course of the transformation. Moreover, a wide variety of active substances may be employed (in silicate glass-forming melts: noble metals like Pt, Au, Ag etc., oxides like TiO_2, CeO_2 etc.; in polymers TiO_2 and other fillers) in order to find the most appropriate dopant. To some extent it is possible to predict in advance the nucleating activity Φ applying theoretical methods as discussed above.

An obvious shortcoming of heterogeneous nucleation catalysis consists of the two-stage character inherent in it (formation of crystallization cores in the first stage of heat pretreatment and crystallization in the second stage). In addition, each of the crystallites formed by heterogeneous nucleation contains the foreign crystallization core, which may have a negative effect on the properties of the material produced.

Homogeneous nucleation catalysis by surfactants proved to be in a number of cases a more efficient method of initiating crystallization than the heterogeneous process. It provides uniformly distributed crystallization centers free of foreign nucleation cores. However, the dispersity of the size distribution of crystallites is larger and determined by nucleation and growth mechanisms. The most obvious shortcoming of nucleation catalysis by surfactants is due to the fact that the number of active substances is very limited. In the case of silicate melts it is restricted to the three or four substances mentioned above.

In the previous sections, the nucleating effect of insoluble substrates (or crystallization cores) and of completely soluble dopants was discussed. In some applications, the nucleating effect of soluble or slightly soluble nucleation cores may be of significance (e.g., nucleating activity of hygroscopic condensation cores in atmospheric processes of nucleation: condensation of water on NaCl-substrates). It can be shown that in such cases the thermodynamic potential (or the vapor pressure) of the nucleus formed on the soluble substrate is diminished (because the substrate is partially dissolved in the nucleus) when compared with the homogeneous case or with the case of condensation on an absolutely insoluble particle. The detailed thermodynamics of this interesting form of nucleation catalysis is discussed in detail in the literature concerned with atmospheric condensation (see, e.g., Mason (1957) [536]; Boucher (1969) [95]).

Nucleation of silicate melts on oxide substrates, as frequently employed, may also be in fact a case of this type: solubility of oxide or silicate crystals overgrowing an oxide substrate can never be excluded. This fact may explain some of the results of extraordinarily high activity of certain oxide crystallization cores. It has also to be mentioned that the activity of substrates with distorted lattices or even of amorphisized crystallization cores may be much higher than the activity of defect free crystalline solids. A thorough discussion of these topics and the necessary formalism for the calculation of the change of Φ upon amorphization of a solid may be found in the already cited paper by Gutzow (1980) [303], where a number of relevant experimental results are given. Those of most significance seem to be the increased activity of mixed oxide substrates ($Cr_2O_3VO_5$) or the influence of radiation damage on the activity of condensation cores.

7.6 Nucleation on Charged Particles and in Electromagnetic Fields

Condensation on electrically charged particles, or more general, phase formation processes under the influence of electric and magnetic fields are of exceptional physical significance. A first discussion of this topic was given by J.J. Thomson (see Thomson (1906) [835]; Thomfor and Volmer (1936) [833]) and is reviewed in a number of monographs (e.g., Volmer (1939) [894]; Frenkel (1946) [233]; Leontovich (1953) [504]; Mason (1957) [536]; Hirth and Pound (1963) [368]). Taking into account the change of the energy of the electric field in the process of formation of a cluster (characterized by a dielectric constant $\epsilon_{(cluster)}$) around an ion with a charge q and a radius $R_{(ion)}$ in an ambient phase (with a dielectric constant $\epsilon_{(matrix)}$) we may write the following modified expression for the change of the Gibbs free energy of cluster formation (compare Eq. (6.36))

$$\Delta G_{(cluster)}(j) = -j\Delta\mu + \sigma A + \frac{q^2}{8\pi}\left(\frac{1}{\epsilon_{(cluster)}} - \frac{1}{\epsilon_{(matrix)}}\right)\left(\frac{1}{R_{ion}} - \frac{1}{R}\right) . \quad (7.42)$$

The dependence of $\Delta G_{(cluster)}$ on the cluster radius R for $\epsilon_{(cluster)} > \epsilon_{(matrix)}$ according to above equation is shown in Fig. 7.6a. For comparison the same function is presented also for $q = 0$. The respective vapor pressure curves are given in Fig. 7.6b.

The existence of the electrically charged particles influences nucleation in two ways. First, as can be seen in Fig. 7.6, the existence of the charge results in the formation of an additional extremum (a minimum) for small cluster sizes. In accordance with the thermodynamic equation given above it is to be expected that around each charged particle the condensation of ambient phase molecules takes place spontaneously until the cluster size corresponding to the minimum of $\Delta G_{(cluster)}$ is reached. The further growth of the cluster is hindered by a nucleation barrier equal to the difference between the values of $\Delta G_{(cluster)}(j)$ for the maximum and the minimum, respectively. This nucleation barrier is lower than in the case of homogeneous nucleation. Moreover, for sufficiently large supersaturations the nucleation barrier may completely disappear.

By a derivation of Eq. (7.42) with respect to R a modified Gibbs-Thomson equation of the form

$$\Delta\mu - \frac{2\sigma}{c_\alpha R} - \frac{1}{2c_\alpha}\left(\frac{q}{4\pi R}\right)^2\left(\frac{1}{\epsilon_{(cluster)}} - \frac{1}{\epsilon_{(matrix)}}\right) = 0 \quad (7.43)$$

is obtained. For vapor condensation on charged ions – the classical situation encountered in Wilson's cloud chamber – we have (considering the vapor as a perfect gas (compare Eq. (6.34)))

$$\Delta\mu = \mu_\beta(p) - \mu_\alpha(p) = \mu_\beta(p) - \mu_\beta(p_{eq}(\infty)) \cong k_B T \ln\left(\frac{p}{p_{eq}(\infty)}\right) , \quad (7.44)$$

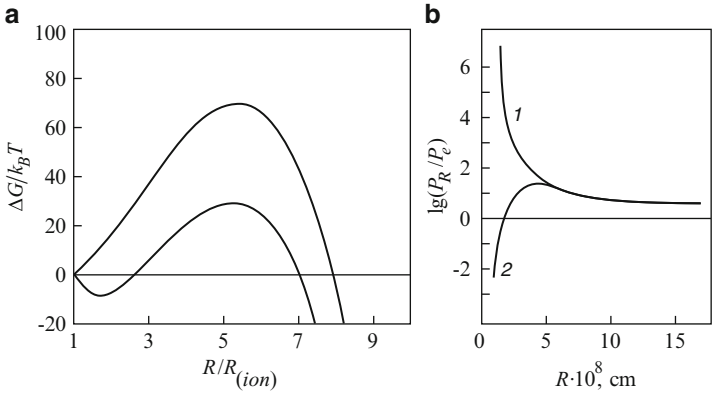

Fig. 7.6 Change of the Gibbs free energy and of the vapor pressure of clusters with radius R in condensation on charged particles of a radius R_{ion}. Simultaneously also the respective dependencies are given for the case $q = 0$ (homogeneous nucleation). (**a**) Gibbs free energy $\Delta G_{(cluster)}$ vs $R/R_{(ion)}$; (**b**) vapor pressure $\ln(p/p_{(eq)})$ vs. R. In both cases the curve (*1*) refers to homogeneous nucleation ($q = 0$) while curve (*2*) illustrates heterogeneous nucleation on a charge q with a radius $R_{(ion)}$

resulting with Eq. (7.43) in

$$\ln\left(\frac{p_{eq}(R)}{p_{eq}(\infty)}\right) = \frac{1}{c_\alpha k_B T}\left[\frac{2\sigma}{R} + \frac{1}{2}\left(\frac{q}{4\pi R}\right)^2\left(\frac{1}{\epsilon_{(drop)}} - \frac{1}{\epsilon_{(vapor)}}\right)\right]. \tag{7.45}$$

Here $p_{eq}(R)$ is the equilibrium vapor pressure of a drop of size R, while $p_{eq}(\infty)$ is the respective value for a planar interface (see also Eq. (6.73) and Fig. 7.6b). Similarly, we have for segregation processes around ions in quasi-binary melts (see Eqs. (6.74)–(6.77))

$$\ln\left(\frac{c_{eq}(R)}{c_{eq}(\infty)}\right) = \frac{1}{c_\alpha k_B T}\left[\frac{2\sigma}{R} + \frac{1}{2}\left(\frac{q}{4\pi R}\right)^2\left(\frac{1}{\epsilon_{(cluster)}} - \frac{1}{\epsilon_{(melt)}}\right)\right]. \tag{7.46}$$

The work of formation of critical clusters in condensation processes on charged particles was calculated first by Volmer (1939) [894]. From the above given formalism one obtains in a good approximation

$$\Delta G^{(c*)}_{(cluster)} = \frac{4\pi}{3}\sigma(R_c^2 - R_{ion}^2) + \frac{q^2}{8\pi}\left(\frac{1}{\epsilon_{(cluster)}} - \frac{1}{\epsilon_{(matrix)}}\right)\left(\frac{1}{R_{ion}} - \frac{1}{R_c}\right). \tag{7.47}$$

This result can be rewritten as

$$\Delta G^{(c*)}_{(cluster)} = \Delta G^{(c)}_{(cluster)}\left\{\left[1 - \left(\frac{R_{ion}}{R_c}\right)^2\right] + \right. \tag{7.48}$$

$$+\frac{3q^2}{32\pi^2\sigma R_c^2}\left(\frac{1}{\epsilon_{(cluster)}}-\frac{1}{\epsilon_{(matrix)}}\right)\left(\frac{1}{R_{ion}}-\frac{1}{R_c}\right)\Bigg\}\ ,$$

which gives in the limit $R_c \gg R_{ion}$

$$\Delta G^{(c*)}_{(cluster)} \cong \Delta G^{(c)}_{(cluster)}\left\{1+\frac{3q^2}{32\pi^2\sigma R_c^2}\left(\frac{1}{\epsilon_{(cluster)}}-\frac{1}{\epsilon_{(matrix)}}\right)\frac{1}{R_{ion}}\right\}\ . \quad (7.49)$$

For $q = 0$, Eq. (6.44) is obtained, again, as a special case.

Up to now, induced crystallization of glass-forming melts by electrically charged particles has hardly been studied. Only some relatively early investigations exist of the effect of radium radiation on crystallization of a number of simple model melts (for sulfur by Frischauer (1909) [238]; Kuznetsov (1925) [490]; for piperin by Kondogoury (1926, 1928, 1930) [466]). An overview on these investigations and the respective literature can be found in Kuznetsov's monograph (1954) [489]. In the cited investigations, an increased nucleation rate was observed for irradiated samples. It remains, however, unclear whether this effect is due to ion formation in the matrix and thus to a charged induced initiation of nucleation or to more complex mechanisms.

Another possibility of influencing the kinetics of phase formation consists of the application of electric or magnetic fields generated externally. Two different effects may be of importance here:

- The applied fields may cause an orientation of the ambient phase particles. This will be the case, in particular, when the basic units are of non-symmetric shape and exhibit a significant permanent or induced polarization or magnetization. Such effects should be of importance with respect to the value of the impingement rate of ambient phase molecules. The theoretical estimation of the possible magnitude of the influence of electromagnetic fields on steady-state nucleation rate and time-lag is, however, associated with difficulties since it depends strongly on the specific properties of both the initial and the newly evolving phases. An account of possible approaches with respect to the kinetics of this process is given by Gattef and Dimitriev (1979, 1981, 1987) [243–245].
- The ambient and the newly evolving phases are, in general, characterized by different values of the dielectric constants which are again denoted by $\epsilon_{(matrix)}$ and $\epsilon_{(cluster)}$. Similarly to the already considered situation of cluster formation around ions, phase formation under the influence of an external electric field is connected with additional thermodynamic contributions to the free energy of cluster formation.

It seems that the first time the described thermodynamic mechanism of influence of electric and magnetic fields on phase formation processes was recognized by Sirota (1967 [762], 1968 [763]; cf. also Koslovski et al. (1976) [470]). However, his contributions were published in little known conference proceedings.

In 1972, Kashchiev [435] and later Izard (1974 [389], 1977 [390]) developed the general thermodynamic formalism for nucleation in an ambient phase subjected

to external electromagnetic fields evidently without being aware of Sirota's results. Kashchiev carried out his investigation within the framework of the more general non-steady state formulation of the theory of nucleation discussed in the previous sections. The final results obtained by Sirota, Kashchiev and Izard on the thermodynamic barrier of nucleation may be rewritten in the form

$$\Delta G_{(cluster)}^{(c/field)} = \Delta G_{(cluster)}^{(c)} \left(1 - \frac{\kappa^{(E)} E^2}{\Delta\mu}\right)^{-2} , \tag{7.50}$$

$$R_c^{(field)} = \frac{2\sigma v_m}{(\Delta\mu - \kappa^{(E)} E^2)} ,$$

$$\kappa^{(E)} = \frac{v_m \epsilon_{(matrix)} \left(1 - \frac{\epsilon_{(cluster)}}{\epsilon_{(matrix)}}\right)}{8\pi \left(2 + \frac{\epsilon_{(cluster)}}{\epsilon_{(matrix)}}\right)} . \tag{7.51}$$

Here $\Delta\mu$ denotes the thermodynamic driving force of the transformation in the absence of electric fields, **E** is the electric field applied externally.

In considering the influence of electric fields on processes of phase formation in under-cooled melts it has to be taken into account that typically $\epsilon_{(melt)} > \epsilon_{(crystal)}$ holds. It can be recognized easily that in dependence on the sign of $\kappa^{(E)}$ the polarization work $\kappa^{(E)} E^2$ either increases (the steady-state nucleation rate J decreases) or decreases (J increases) the work of formation of the critical clusters. For the time-lag, Kashchiev obtained a result which may be rewritten in the form

$$\tau^{(field)} = \tau^{(ns)} \left(1 - \frac{\kappa^{(E)} E^2}{\Delta\mu}\right)^2 . \tag{7.52}$$

For nucleation in magnetic fields the equations remain the same but **E**, $\epsilon_{(matrix)}$ and $\epsilon_{(cluster)}$ have to be replaced by the magnetic field vector, **H**, and the magnetic permeabilities of the ambient ($\mu_{(matrix)}$) and the newly evolving ($\mu_{(cluster)}$) phases (Sirota (1968) [763]; Kashchiev (1972) [435]). It should be noted that Kashchiev's and Izard's results are equivalent except for the definition of $\kappa^{(E)}$, which in the articles of both authors differs by a minus sign. A possible resolution of the mentioned discrepancy and a criticism of Kashchiev's result can be found in Izard's publication.

There exist a number of experimental investigations on nucleation and crystal growth in under-cooled melts taking place under the influence of external electric and magnetic fields. A summary of results in this respect may be also found in Kuznetsov's monograph as well as in subsequent literature (Koslovski et al. (1976) [469]). The only evidence known to the authors, where such effects are investigated in application to crystallization of silicate glass-forming melts is a paper by Hülsenberg (1993) [384]. An exceptionally interesting example are processes of the mentioned type taking place in so-called *Ovonics*-devices, i.e., in the processes

of crystallization of thin amorphous semiconducting layers and their subsequent melting and vitrification. For these systems by cycles of crystallization and melting under applied external fields information may be stored or erased again.

A detailed analysis of such processes was performed by Gattef and Dimitriev (1979, 1981, 1987) [243–245] by using the formalism given with Eqs. (7.50) and (7.51). It was assumed that by electro-induced crystallization in line with the above given theoretical considerations a conducting state was generated while melting and subsequent vitrification led to a non-conducting state. Electro-induced nucleation on charged particles (trapped electron sites in solid solutions) was analyzed in two papers by Stoyanov et al. (1970) [806] in application to photographic processes. This theoretical investigation also opens possibilities for applications still not employed in solid-state nucleation kinetics.

7.7 Surface Induced Crystallization of Glasses

7.7.1 Inhibition of Bulk Crystallization by Elastic Strains

The experimental fact that glasses crystallize preferentially from internal and external surfaces was mentioned already by Tammann in his monograph "Der Glaszustand" in 1933 [820]. A bit earlier, a detailed discussion of this topic was given by Tabata (1927) [816]. In addition to an experimental overview, Tabata drew attention to the possible catalytic role of "sharp edges" and "cicatrices" on the glass surface in crystallization.

Crystallization processes in glasses initiated by surface-induced nucleation in application to glass technology were analyzed first by Sack in 1959 [678]. According to Sack, surface-induced nucleation can be more effective than any other method of nucleation catalysis. Sack worked with samples which were sinter-crystallized in order to produce a glass-ceramic material. Similar glass-ceramic materials later found applications in architecture under the name "Neoparies" (see Tashiro (1985) [827], Karamanov et al. (1994) [334, 431]). In subsequent years the investigation of the kinetics of surface induced crystallization was continued mainly by Zanotto et al. (1983) [945], Zanotto (1991) [947], Müller (1989 [582], 1990 [584]), Müller, Hübert, and Kirsch (1986, 1988) [383,583] and Yuritsyn, Fokin et al. (1992) ([940]; see also Köster (1988) [474] for metallic glasses).

Different hypotheses have been developed to explain the ability of the free glass surface to act as a catalyst for crystallization. Tabata connected it with "the surface contraction ... caused by the surface tension of the glass". According to Blumberg (1939) [85] the chemical corrosion of the free glass surfaces and the formation of silica rich gels may facilitate surface crystallization of silica glasses. The existence of dust particles and contaminations (Neely and Ernsberger (1966) [594]; Matox (1967) [538]; Burnett, Douglas (1971) [112] or powdered glass of the same composition at the surface (Gutzow and Slavtschev (1971) [317] were also

proposed as possible sources of preferential surface crystallization. Other theoretical approaches associate surface crystallization with the concentration differences in the bulk and at the surface of the sample, with a decrease in the total surface energy or an easier stress relaxation by viscous flow near or at the surface.

Omitting a detailed discussion of these various attempts, we would like to draw the attention to a relatively new hypothesis connecting the nucleating activity of the free glass surface or of small glass particles with reduced values of the energy of elastic deformations evolving in the course of the transformation from the glass to the crystalline phase near or at interfaces or in small particles compared with the same processes in the bulk (for the details see Schmelzer et al. (1993 [715], 1995 [716])). This approach starts with the following considerations. According to existing rheological data and the concepts of phenomenological rheology (see Chap. 12) glass-forming liquids have to be treated as viscoelastic bodies, i.e., as viscous bodies with an elastic response. The relative significance of the elastic properties of the melts is determined by the value of the viscosity. Near and below the temperature of vitrification, T_g, corresponding to viscosities of the order $10^{13} - 10^{14}$ dPas, glass-forming liquids behave as isotropic elastic bodies. With an increase in temperature, elastic properties become less important and viscous properties dominate. In the subsequent analysis we neglect possible viscous relaxation processes due to viscous properties of the matrix in order to demonstrate

- That elastic strains significantly diminish the thermodynamic driving force for bulk devitrification and
- That this decrease is sufficiently less for devitrification near and at free surfaces and in samples with linear dimensions of the order of the critical cluster size ($\ll 10 R_c$).

As it is discussed in detail in the mentioned papers [715, 716] viscous stress relaxation proceeds more easily for devitrification near surfaces as compared with the bulk. Consequently, it even amplifies the analyzed effect.[1]

The basic idea of the argumentation is the following: Since crystallization is connected, in general, with a change of the molar volume of the crystallizing substance, this process results in a volume dilation of both the matrix and the crystallite and, consequently, in the evolution of elastic strains. The strength of this effect is determined by the relative volume dilatation, δ_0, in the transformation defined as

$$\delta_0 = \frac{v_{glass} - v_{crystal}}{v_{crystal}} , \tag{7.53}$$

where v_{glass} and $v_{crystal}$ are the molar volumes of the substance as a glass and a crystal, respectively. Calculations show that the total energy of elastic defor-

[1] A detailed analysis of the interplay between stress development and stress relaxation and its effect on crystal nucleation and growth processes in highly viscous glass-forming melts is given in Möller et al. [571]; Schmelzer et al. [723]; Schmelzer et al. [724]; Schmelzer et al. [727] (see also the Chap. 14 for further details).

mations connected with the evolution of a cluster of volume, V_α, in an isotropic homogeneous elastic solid can be expressed as (Nabarro (1940) [588]; Gutzow (1973) [295]; Ulbricht, Schmelzer et al. (1988) [874])

$$\Psi^{(\varepsilon)} = \varepsilon_0 V_\alpha = \epsilon_0^* \delta_0^2 V_\alpha . \tag{7.54}$$

Here ϵ_0^* is, in general, some combination of elastic constants of the matrix and the newly evolving crystalline phase.

Taking into account the possible evolution of elastic strains in crystallization, the change of the Gibbs free energy in cluster formation now obtains the form (compare Eq. (6.36))

$$\Delta G_{(cluster)}(j) = -j\Delta\mu + \sigma A + \Psi^{(\varepsilon)} . \tag{7.55}$$

Denoting by c_α, as usual, the density of particles in the crystalline (cluster) phase Eqs. (7.54) and (7.55) yield

$$\Delta G = -j\,[\Delta\mu - \Delta\mu_0^{(\varepsilon)}] + \sigma A\ , \qquad \Delta\mu_0^{(\varepsilon)} = \frac{\varepsilon_0}{c_\alpha} . \tag{7.56}$$

It follows that elastic strains of the considered type evolving in crystallization processes of glasses or, more generally, in recrystallization processes of solids lead to a decrease in the thermodynamic driving force of the transformation by a constant amount, $\Delta\mu_0^{(\varepsilon)}$, and, consequently, to an inhibition of crystallization. The magnitude of this effect is determined by the value of the ratio

$$\alpha_0 = \frac{\Delta\mu_0^{(\varepsilon)}}{\Delta\mu} . \tag{7.57}$$

Obviously, all equations describing phase formation in the presence of elastic strains have the same form as discussed earlier with the only difference being that the thermodynamic driving force, $\Delta\mu$, has to be replaced by $\Delta\mu \Rightarrow [\Delta\mu - \Delta\mu_0^{(\varepsilon)}]$. The parameter α_0 can be determined based on Eq. (6.62) and the knowledge of the elastic constants of both phases. Estimates of the values of δ_0, α_0 and other relevant quantities are given in Table 7.1 (for the details of the calculations and further information see Schmelzer et al. (1993) [715]).

Neglecting possible variations in the viscosity and the specific interfacial energy due to elastic strains the ratio of the steady-state nucleation rate affected by elastic strains $J^{(\varepsilon)}$ to J may be written as (compare Eq. (6.120))

$$J^{(\varepsilon)} = J\left[\exp\left(-\frac{\Delta G^{(c)}_{(cluster)}}{k_B T}\right)\right]^{\beta-1} , \qquad \beta = (1-\alpha_0)^{-2} . \tag{7.58}$$

For the respective ratios of the time-lags we have further (compare Eq. (6.193)), within the same approximation,

Table 7.1 Summary of experimental data and theoretical estimates concerning the influence of elastic strains on crystallization in the bulk of highly viscous glass-forming melts for different classes of glass-forming substances near the temperature of vitrification, T_g. δ_0: relative volume dilatation, $\alpha_0 = \Delta\mu^{(\varepsilon)}/\Delta\mu$, J ($J^{(\varepsilon)}$): Steady-state nucleation rates without (and with) an account of elastic strains, $\tau^{(\varepsilon)}$ ($\tau^{(ns)}$): time-lag for the rate of formation of critical clusters with (and without) the influence of elastic strains

	Inorganic glass-forming oxides	Organic glass-forming polymers	Metallic glass-forming alloys
δ_0	$10^{-1} - 2 \cdot 10^{-1}$	$\sim 10^{-1}$	$\sim 5 \cdot 10^{-2}$
α_0	$0.56 - 2.7$	$0.6 - 0.68$	$0.08 - 0.1$
$\log(J^{(\varepsilon)}/J)$	< -300	< -130	-2.6
$\tau^{(\varepsilon)}/\tau^{(ns)}$	$10 - \infty$	$6.3 - 10$	1.2

$$\frac{\tau^{(\varepsilon)}}{\tau^{(ns)}} = (1 - \alpha_0)^{-2}. \tag{7.59}$$

Applying the Zeldovich equation, Eq. (6.166), for the description of transient nucleation we may write for nucleation under the influence of elastic strains the similar relation

$$J^{(\varepsilon)}(j_c, t) = J^{(\varepsilon)}(j_c) \exp\left(-\frac{\tau^{(\varepsilon)}}{t}\right) . \tag{7.60}$$

With Eqs. (7.58) and (7.59) we have, finally,

$$J^{(\varepsilon)}(j_c, t) = J(j_c, t) \left[\exp\left(-\frac{\Delta G^{(c)}_{(cluster)}}{k_B T}\right) \exp\left(-\frac{\tau^{(ns)}}{t}\right)\right]^{\beta - 1} , \tag{7.61}$$

showing in a compact form the effect of elastic strains on the nucleation rate for clusters of critical sizes.

It can be seen from the estimates of the values of the nucleation rate and the time-lag that at and below the temperature of vitrification, elastic strains inhibit strongly crystallization, in particular, for inorganic glass-forming oxides and organic glass-forming polymers. This effect is less important for metallic glass-forming alloys. In this way, we arrive at the conclusion that in addition to the rapid decrease in the mobility (or increase in the viscosity) of the building units of the glass-forming melts at and below the temperature of vitrification, discussed in Sect. 2.4, also a thermodynamic inhibition of crystallization occurs in the vicinity of T_g connected with the evolution of elastic strains. As seen from the results presented in the table the inhibiting term may even exceed ($\alpha_0 > 1$) the thermodynamic driving force of crystallization.

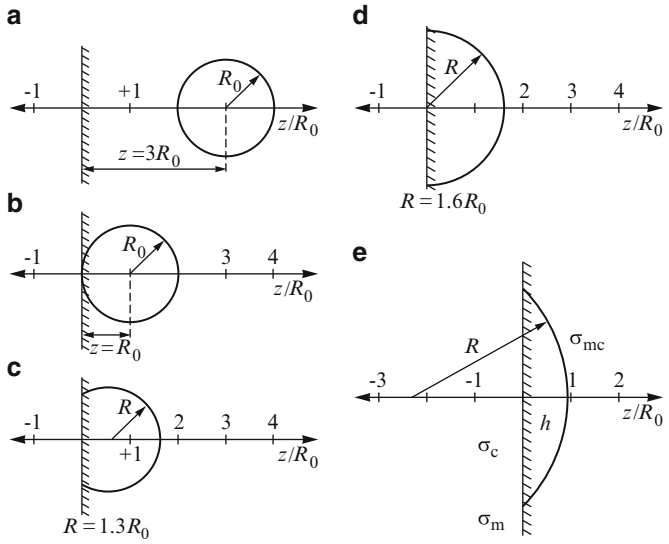

Fig. 7.7 Illustration of the model investigated. (**a**)–(**d**) A cluster is formed at the surface ($z/R_0 \leq 1$) or in the bulk ($z/R_0 > 1$) of a solid matrix. The shape of the cluster is determined by the radius of curvature R (or R_0) and the distance z of the center of the sphere to the surface of the ambient phase. (**e**) Notations used in the calculation of the free energy of cluster formation at planar interfaces. σ_c is the specific free energy of the surface between crystal and air, σ_m the corresponding value for the matrix, while σ_{mc} refers to the crystallite-matrix interface. For the description of the shape of clusters formed at the interface instead of z (compare Fig. 7.7**a**–**d**) also the parameter h is used, connected with z by the relation $h = z + R$

7.7.2 *Elastic Strains and the Catalytic Effect of Planar Interfaces*

We consider now the problem of how the energy of elastic deformations, generated by the process of formation of a solid cluster having a spherical shape or the form of a segment of a sphere, depends on the distance of the cluster from a planar surface as well as of the geometry of the newly evolving phase. Both solid phases are assumed, again, to be homogeneous and isotropic. The problem analyzed is illustrated in Fig. 7.7 for two possible situations. Denoting by z the distance between the center of the spherical cluster and the planar surface and by R its radius, the situation depicted in Fig. 7.7a,b corresponds to $z/R > 1$, while Fig. 7.7c–e refer to $-1 < z/R < 1$. Alternatively to the variable z also the parameter h may be used for a description of the shape of the evolving phase connected with R by the relation $h = z + R$.

A detailed analysis shows (Möller et al. (1993a,b) [569,570]) that for finite values of the ratio z/R, in particular, in the range $-1 < z/R < 2$ for the same amount of crystallizing substance the energy of elastic deformations $\Psi^{(\varepsilon)}$ is significantly reduced as compared with the case of crystallization in the bulk ($z/R \to \infty$). The

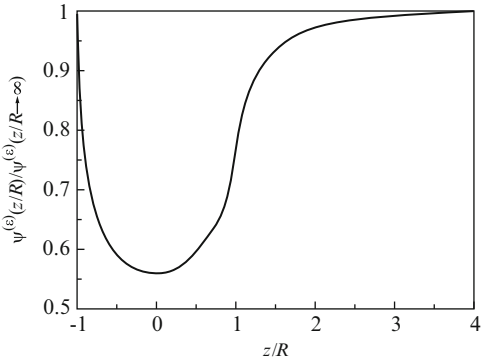

Fig. 7.8 Ratio of the energy of elastic deformations $\psi(z/R) = \Psi^{(\varepsilon)}(z/R)/\Psi^{(\varepsilon)}(z/R \to \infty)$ for crystallization of one and the same amount of the substance near or at a planar surface of a solid matrix to the corresponding value for bulk crystallization. The curve shown corresponds to a value of Poisson's ratio $\gamma = 0.3$

ratio $\psi(z/R) = \Psi^{(\varepsilon)}(z/R)/\Psi^{(\varepsilon)}(z/R \to \infty)$ is shown in Fig. 7.8 for the case of equal elastic constants of both solid phases and a value of Poisson's number $\gamma = 0.3$. It turns out in this way that the energy of elastic deformations connected with the formation of a cluster of shapes as depicted in Fig. 7.7 can be written similarly to Eq. (7.54) as

$$\Psi^{(\varepsilon)}\left(\frac{z}{R}\right) = \varepsilon\left(\frac{z}{R}\right) V_\alpha \,, \qquad \varepsilon\left(\frac{z}{R}\right) = \varepsilon_0 \psi\left(\frac{z}{R}\right) \,. \tag{7.62}$$

Taking into account only configurations as represented in Fig. 7.7a, b (i.e., clusters of spherical shape located totally inside the solid matrix) the work of formation of critical clusters formed at a distance z from the interface may be expressed in the form (compare Eqs. (6.45), (7.56) and (7.62))

$$\Delta G^{(c)}_{(cluster)}(z) = \frac{16\pi}{3} \frac{\sigma^3}{c_\alpha^2 [\Delta\mu - \Delta\mu^{(\varepsilon)}]^2} \,, \qquad \Delta\mu^{(\varepsilon)} = \frac{1}{c_\alpha} \varepsilon\left(\frac{z}{R}\right) \,. \tag{7.63}$$

With the notation $\alpha = (\Delta\mu^{(\varepsilon)}/\Delta\mu)$ (compare Eq. (7.57)) we may write also

$$\Delta G^{(c)}_{(cluster)}(z) = \Delta G^{(c)}_{(cluster)}(z \to \infty) \Phi \,, \qquad \Phi = \frac{(1-\alpha_0)^2}{(1-\alpha)^2} \,. \tag{7.64}$$

Generally, the inequalities $\alpha < \alpha_0$ and $\Phi < 1$ hold (the inhibition of nucleation by elastic strains is less expressed near interfaces compared with the bulk).

The reduction of the energy of elastic deformations has, for the considered cases illustrated in Fig. 7.7a, b, a maximum for critical clusters formed tangentially to the planar interface of the ambient solid. This reduction of the energy of elastic deformations, compared with crystallization in the bulk, leads to a considerable decrease in the critical cluster size, the work of formation of critical clusters and, consequently, to a decrease in the inhibiting effect of elastic strains in crystallization of glasses. However, according to the dependence shown on Fig. 7.8 the minimum

of the value of the specific energy of elastic deformations refers to $(z/R) = 0$, i.e., to the formation of hemispherical clusters (Fig. 7.7d).

At a first glance, deviations from such a shape surprisingly result in higher values of the energy of elastic deformations referred to the same amount of the crystallizing substance. Qualitatively such a minimum can be explained if one takes into account that for the same amount of the crystallizing substance the volume of the solid matrix affected by elastic strains has a minimum compared with all other considered geometrical configurations. Taking into account only the influence of elastic strains, it seems therefore probable that critical clusters with a hemispherical shape are formed with the highest probability and determine the rate of formation of the newly evolving phase. On the other hand, interfacial contributions also play an important role in cluster formation. Therefore, in considering the problem of what the most probable shape of a critical cluster will be, both elastic energy and interfacial contributions have to be taken into account.

The analysis of the problem, which of the both mentioned factors dominates, can be carried out in the following way. Assume an aggregate of the new phase at the surface of a solid is formed in the range of z/R-values given by $(-1 \leq z/R \leq +1)$. The shape of the newly evolving solid phase will be characterized then by two parameters, the radius of curvature R and h (see Fig. 7.7e). In terms of h, the considered range of (z/R)-values corresponds to $0 \leq h \leq 2R$. Note that the case of crystallization on surfaces of a solid, considered here, differs from processes of phase formation at the interface of two liquids, respectively, a liquid and a gas. In the latter cases, the new phase commonly has the form of a lens (see Volmer (1939) [894]). For solids, as in the considered example, the surface forces are not large enough to result in considerable changes of the shape of the newly evolving phase as compared with the initial one.

Denoting the specific values of the interfacial energies by σ_c (newly evolving phase – surrounding air), σ_m (ambient phase – air) and σ_{mc} (ambient phase – newly evolving solid), the change of the Gibbs free energy, ΔG, connected with the formation of a segment of a sphere at the interface is given by

$$\Delta G_{(cluster)} = -j\Delta\mu + (\sigma_c - \sigma_m)A_c + \sigma_{mc}A_{mc} + \varepsilon V_\alpha \ . \tag{7.65}$$

Applying well-known expressions for the volume and the surface area of a segment of a sphere (see, e.g., Korn and Korn (1968) [467]) we get

$$\begin{aligned}\Delta G_{(cluster)}(h, R) = &- c_\alpha \left(\frac{\pi h^2}{3}(3R - h)\right)\left(\Delta\mu - \frac{\varepsilon}{c_\alpha}\right) \\ &+ (\sigma_c - \sigma_m)\pi[R^2 - (R - h)^2] + \sigma_{mc}2\pi Rh \ .\end{aligned} \tag{7.66}$$

For $h = 2R$ the case of a spherical cluster formed in the bulk of the matrix tangent to the interface is obtained as a special case (compare Fig. 7.7b). It is evident from Eq. (7.66) that ΔG is uniquely determined by two parameters R and h. Critical

clusters which are formed with the highest probability, correspond, consequently, to the saddle-point of the $\Delta G_{(cluster)} = \Delta G(R, h)$ surface.

For an analytical determination of the values of R and h, corresponding to the saddle-point (and denoted as R_c and h_c), the partial derivatives of ΔG with respect to R and h have to be calculated and set equal to zero. After some straightforward calculations we obtain (see Schmelzer et al. (1995) [716])

$$h_c = \frac{2\sigma_{mc}}{c_\alpha \left(\Delta\mu - \dfrac{\varepsilon}{c_\alpha} \right)} (1 + \Xi) \; , \qquad \Xi = \frac{\sigma_c - \sigma_m}{\sigma_{mc}} \; , \tag{7.67}$$

$$R_c = \frac{2\sigma_{mc}}{c_\alpha \left(\Delta\mu - \dfrac{\varepsilon}{c_\alpha} \right)} \; . \tag{7.68}$$

It follows from Eqs. (7.67) and (7.68) that the shape of the critical cluster, corresponding to the saddle-point of the $\Delta G(R, h)$-surface, is determined to a large extent by the ratio $\Xi = (\sigma_c - \sigma_m)/\sigma_{mc}$. Indeed, Eq. (7.68) may be rewritten in the form

$$\frac{h_c}{R_c} = 1 + \frac{\sigma_c - \sigma_m}{\sigma_{mc}} = 1 + \Xi \; , \tag{7.69}$$

verifying above statement. A substitution of the parameters of the critical clusters into Eq. (7.66) gives, after some straightforward transformations, the following expression for the work of formation of a critical cluster for phase formation at the interface

$$\Delta G^{(c)}_{(cluster/surface)} = \frac{4\pi}{3} R_c^2 \sigma_{mc} \, g(\Xi) \; , \qquad g(\Xi) = \frac{1}{4}(1 + \Xi)^2 (2 - \Xi) \; . \tag{7.70}$$

The function $g(\Xi)$ describes the influence of shape effects on the work of formation of the critical clusters. Its value is determined by the parameter Ξ only. It is independent of the degree of inhibition of the phase formation by elastic strains. Elastic strains affect the work of formation of the critical clusters only via modifications of the critical cluster size R_c. Physically reasonable values of Ξ are those in the range $-1 \le \Xi \le +1$ (compare Eq. (7.69)). In this range $g(\Xi)$ changes monotonically from zero (for $\Xi = -1$) to one (for $\Xi = +1$) (see also [716]).

Denoting by $R_c(z \to \infty)$ the critical cluster radius for nucleation in the bulk of the sample ($\varepsilon = \varepsilon_0$) Eq. (7.70) may also be written in the form

$$\Delta G^{(c)}_{(cluster/surface)} = \Delta G^{(c)}_{(cluster)} (z \to \infty) \Phi \; , \quad \Phi = \phi(\alpha, \alpha_0) g(\Xi) \; , \tag{7.71}$$

$$\phi(\alpha, \alpha_0) = \frac{(1 - \alpha)^2}{(1 - \alpha_0)^2} \; .$$

Since the relation $\alpha \le \alpha_0$ always holds (the influence of elastic strains on crystallization is less near the surface than in the bulk) in addition to $g(\Xi) \le 1$ the relation $\phi(\alpha, \alpha_0) \le 1$ is always fulfilled. The parameter Φ describes here the nucleating

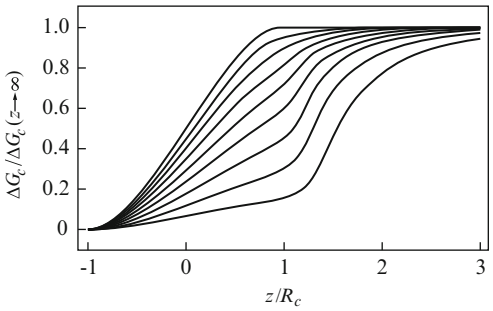

Fig. 7.9 Work of formation of critical clusters in dependence on the distance z of the center of the cluster from the planar interface (in coordinates z/R_c). Poisson's number γ was chosen equal to $\gamma = 0.3$. The *upper curve* corresponds to $\alpha_0 = (\Delta\mu_0^{(\varepsilon)}/)(\Delta\mu) = 0$, when the inhibiting effect of elastic strains on bulk nucleation is negligible. With an increasing value of this parameter (α_0 =0.1, 0.2,. . .,0.9) a shift of the curves occurs represented in the figure by the dependencies below the upper one. As it is to be expected the activity of the interface with respect to nucleation catalysis increases with increasing values of the parameter α_0, i.e., with an increasing degree of inhibition of bulk crystallization by elastic strains

activity of the surface similarly to nucleation catalysis by insoluble dopants. The value $\Phi = 1$ in the considered case corresponds to bulk nucleation while $\Phi < 1$ yields a decrease in the work of formation of critical clusters, hence, a catalysis of nucleation.

The function $(\Delta G^{(c)}_{(cluster/surface)}/\Delta G^{(c)}_{(cluster)}(z \to \infty))$ is shown in dependence on (z/R_c) for the whole range of possible z-values in Fig. 7.9. It turns out that for all possible values of Ξ the work of formation of critical clusters at the surface of the solid is always less than in the case of cluster formation near the surface or in the bulk. From the possible Ξ-values, of particular interest in application to crystallization processes of glasses is the case $\Xi = +1$. Indeed, for a one-component system of the same composition of glass and crystal the difference $(\sigma_c - \sigma_m)$ is relatively small. However, taking into account that according to Stefan's law (Stefan (1886) [796]) the specific surface energy σ is proportional to the heat of the phase transition, q, we obtain with $q_s = q_{ev} + q_m$ (q_s: heat of sublimation; q_{ev}: heat of evaporation; q_m: heat of melting) the relation σ_{mc}=$\sigma_c - \sigma_m$. Consequently, for systems for which these estimates hold, at least, in a good approximation $\Xi \approx +1$ should be fulfilled. The case of formation of a cluster tangent to the interface, as already discussed in detail previously, thus, turns out to be a very important special case. This special case is also realized for $\Xi > +1$. In these cases, the reduction of the work of formation of the critical clusters is due only to the decrease in the energy of elastic deformations for cluster formation near interfaces. However, for all values of Ξ different from this limiting value, in general, considerably lower values for the work of formation of the critical cluster are obtained (see, again, Fig. 7.9). In this way, an explanation is given for preferential surface crystallization of glasses, in particular for those having relatively high δ_0-values.

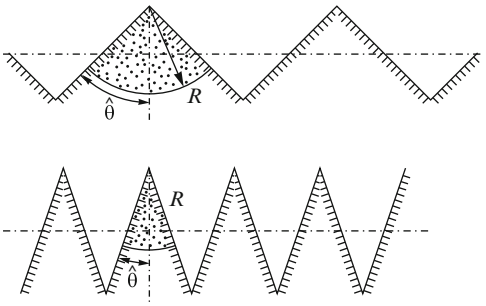

Fig. 7.10 Illustration of the model applied for the analysis of the effect of the degree of smoothness of the surface of a solid on the work of formation of critical clusters in crystallization processes at the surface. The parameters of the newly evolving phase are the radius of curvature, R, and the angle, $\hat{\theta}$. $\hat{\theta} \to \pi/2$ corresponds to a planar surface. Low values of $\hat{\theta}$ model surfaces with a rough structure (i.e., cones on the surface) while values of $\hat{\theta}$ in the range $\pi/2 \leq \hat{\theta} \leq \pi$ refer to *conically shaped* holes in the surface of the solid sample

7.7.3 *The Influence of Surface Roughness on Crystallization of Glasses*

The influence of surface roughness on crystallization processes of solids, in general, and glasses, in particular, can be studied by a simplified model as illustrated in Fig. 7.10. The surface roughness is described by the existence of cones or edges of different types. The analysis is carried out here for the case of cones located on the surface as shown in the figure. Edges and their influence on the catalytic activity of surfaces can be treated similarly with qualitatively equivalent results. In dependence on the angle $\hat{\theta}$ (see Fig. 7.10) the degree of smoothness of the surface can be changed in the model. Values of $\hat{\theta}$ near $\pi/2$ correspond to a nearly planar surface, while $\hat{\theta} \to 0$ refers to the opposite situation of a very rough surface structure. Values of $\hat{\theta} > \pi/2$ model conically shaped holes in the surface.

We assume, again that the new phase is formed as a sector of a sphere characterized by a radius of curvature R and an angle $\hat{\theta}$, as shown in Fig. 7.10. The critical cluster radius and the work of formation of a critical cluster for such a situation may be calculated in the same way as done in the preceding sections. From Eq. (7.65) we get

$$\Delta G_{(cluster)} = -j\left(\Delta\mu - \frac{\varepsilon}{c_\alpha}\right) + \sigma_{mc}(A_{mc} + \Xi A_c)\ . \tag{7.72}$$

Taking into account the geometrical relations (see Korn and Korn (1968) [467]) determining the volume and the interfacial area of the newly evolving solid phase, we obtain with Eq. (7.72)

$$\Delta G_{(cluster)} = -c_\alpha \left(\Delta\mu - \frac{\varepsilon}{c_\alpha} \right) \frac{2\pi}{3} R^3 (1 - \cos\hat{\theta}) + \tag{7.73}$$

$$+\sigma_{mc} [2\pi R^2 (1 - \cos\hat{\theta}) + \Xi \pi R^2 \sin\hat{\theta}] \, .$$

By a derivation of Eq. (7.73) with respect to R expressions for the critical cluster radius and the work of formation of critical clusters are found as

$$R_c = \frac{2\sigma_{mc}}{c_\alpha \left(\Delta\mu - \frac{\epsilon}{c_\alpha} \right)} \left(\frac{1 - \cos\hat{\theta} + \frac{1}{2}\Xi \sin\hat{\theta}}{(1 - \cos\hat{\theta})} \right) \, , \tag{7.74}$$

$$\Delta G^{(c)}_{(cluster/cone)} = \frac{2\pi}{3} \sigma_{mc} R_c^2 \left(1 - \cos\hat{\theta} + \frac{1}{2}\Xi \sin\hat{\theta} \right) \, , \tag{7.75}$$

which may be written also in the form

$$\frac{R_c}{R_c(z \to \infty)} = \left[\frac{(1 - \alpha_0)}{(1 - \alpha)} \right] \left[\frac{(1 - \cos\hat{\theta} + \frac{1}{2}\Xi \sin\hat{\theta})}{(1 - \cos\hat{\theta})} \right] \, , \tag{7.76}$$

$$\Delta G^{(c)}_{(cluster/cone)} = \Delta G^{(c)}_{(cluster)} (z \to \infty) \Phi(\hat{\theta}, \Xi, \alpha, \alpha_0) \, , \tag{7.77}$$

$$\Phi = \left[\frac{(1 - \alpha_0)^2}{(1 - \alpha)^2} \right] \left[\frac{\left(1 - \cos\hat{\theta} + \frac{1}{2}\Xi \sin\hat{\theta} \right)^3}{2(1 - \cos\hat{\theta})^2} \right] \, . \tag{7.78}$$

It turns out that the nucleating activity of surface inhomogeneities is determined by the product of two terms, again, expressed by the functions $\phi(\alpha, \alpha_0)$ and $f(\hat{\theta}, \Xi)$ (compare Eq. (7.71)), i.e.,

$$\Phi = \phi(\alpha, \alpha_0) f(\hat{\theta}, \Xi) \, , \qquad f = \frac{\left(1 - \cos\hat{\theta} + \frac{1}{2}\Xi \sin\hat{\theta} \right)^3}{2(1 - \cos\hat{\theta})^2} \, . \tag{7.79}$$

Here $\phi(\alpha, \alpha_0)$ describes the influence of the decrease in the energy of the elastic strains on phase formation.

As already mentioned, in general, the relation $\alpha < \alpha_0$ holds for the considered cases. The value of α depends on the shape and the location of the new phase in the sample. For our model we may expect

$$\lim_{\hat{\theta} \to 0} \alpha = 0 \, , \qquad \lim_{\hat{\theta} \to 0} \phi(\alpha) = (1 - \alpha_0)^2 \, , \tag{7.80}$$

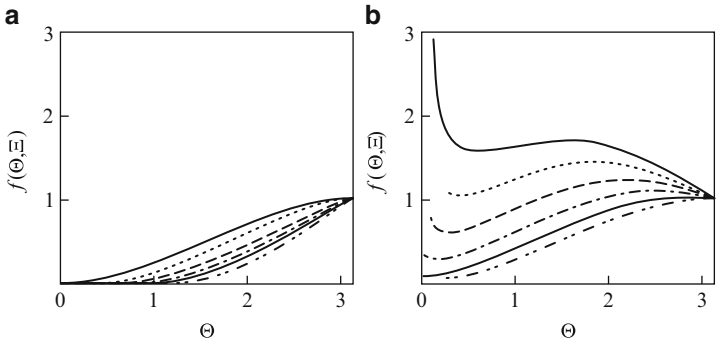

Fig. 7.11 Course of the function $f(\hat{\theta}, \Xi)$ for different values of Ξ (see text). The *curves on the left hand side* of the figure refer to the following values of the parameter Ξ (from the top down): $\Xi = 0$, -0.2, -0.4, -0.6, -0.8, -1. Similarly the *curves on the right hand side* of the figure are drawn for the following parameter values (again, from the top down): $\Xi = 1$, 0.8, 0.6, 0.4, 0.2, 0.0

since for such a limiting case practically all the strains may relax easily. In other words, the part of the volume of the matrix which is affected by the elastic deformation tends to zero.

The function $f(\hat{\theta}, \Xi)$ reflects properties of the surfaces of the different phases (via the ratio of the specific interfacial energies Ξ) and the mechanical structure of the surface (via the parameter $\hat{\theta}$). A particularly simple case consists of $\Xi = 0$. In this case, the function f is reduced to

$$f(\Xi = 0, \hat{\theta}) = \frac{1 - \cos\hat{\theta}}{2} \tag{7.81}$$

and for $\hat{\theta} \to 0$ the relations $f \to 0$ and $\Phi \to 0$ hold.

The course of the function $f(\hat{\theta}, \Xi)$ is shown in dependence on $\hat{\theta}$ $(0 \leq \hat{\theta} \leq \pi)$ for different values of Ξ $(-1 \leq \Xi \leq +1)$ in Fig. 7.11. It turns out that independent of the value of the function $\phi(\alpha, \alpha_0)$, describing the influence of elastic terms, for $(\Xi \leq 0)$ there is always a finite value of $\hat{\theta} = \hat{\theta}_0$ for which the work of formation of critical clusters becomes equal to zero. Consequently, in this range of Ξ-values surface effects alone stimulate crystallization on rough surface structures (for $\hat{\theta} \leq \hat{\theta}_0$ the nucleation barrier ΔG_c vanishes or the transformation is even favored thermodynamically). This is the range of parameter values for which Tabata's explanation of preferred surface crystallization would be of some relevance.

For the opposite case $(0 < \Xi < +1)$ till $\Xi \approx 0.8$, there are always values for the angle $\hat{\theta}$ in the range $(0 < \hat{\theta} < \pi/4)$ for which $f < 1$ holds, i.e., for which crystallization is catalyzed for cones of the respective geometry compared with nucleation in the bulk. However, for glasses in the particularly relevant parameter region $\Xi \approx 1$, surface energy effects do not favor crystallization. A nucleation catalysis can be connected for these cases only with a decrease in the elastic strains

for small (but not zero) values of $\hat{\theta}$ as expressed with Eq. (7.80). This effect is expected to be of importance, in particular for cases when the inhibiting term due to elastic strains for bulk crystallization $\Delta\mu_0^{(\varepsilon)}$ is comparable in magnitude with the thermodynamic driving force of crystallization.

Finally, in this subsection we would like to mention the following interesting fact: Taking into account the relations describing the volume and the surface area of the crystalline phase, the work of formation of critical clusters Eq. (7.75) may be expressed also through the volume of the critical cluster V_c as

$$\Delta G^{(c)}_{(cluster/cone)} = \frac{V_c \sigma_{mc}}{R_c} \left(\frac{1 - \cos\hat{\theta} + \frac{1}{2}\Xi \sin\hat{\theta}}{1 - \cos\hat{\theta}} \right) . \tag{7.82}$$

Similarly, for cluster formation in the bulk of the matrix we may write

$$\Delta G^{(c)}_{(cluster)}(z \to \infty) = \frac{4\pi\sigma_{mc}(R_c(z \to \infty))^2}{3} = \frac{V_c(z \to \infty)\sigma_{mc}}{R_c(z \to \infty)} . \tag{7.83}$$

A comparison of Eqs. (7.82) and (7.83) yields with Eq. (7.76)

$$\frac{\Delta G^{(c)}_{(cluster/cone)}}{\Delta G^{(c)}_{(cluster)}(z \to \infty)} = \frac{V_c}{V_c(z \to \infty)} \left(\frac{1 - \alpha}{1 - \alpha_0} \right) . \tag{7.84}$$

Neglecting the influence of elastic strains on the value of the critical cluster radius Eq. (7.84) leads to

$$\frac{\Delta G^{(c)}_{(cluster/cone)}}{\Delta G^{(c)}_{(cluster)}(z \to \infty)} \cong \frac{V_c}{V_c(z \to \infty)} . \tag{7.85}$$

It turns out that for the considered approximation, the nucleating activity of "cones" on the surface can be expressed through the ratio of the volumes of the critical clusters at the surface and in the bulk similarly to the theorem formulated first by Kaischew (see Eq. (7.6)) for nucleation processes on surfaces or on foreign particles.

Note that this theorem also holds for the cases considered here, however, modified, in general, by a term specifying the ratio of degrees of inhibition of the transformation by elastic strains in the bulk and at the interface. The conclusions of the theoretical analysis are illustrated in Fig. 7.12. In the upper part of Fig. 7.12 various possible shapes of a droplet formed in vapor condensation on solid surfaces for two values of the contact angle θ are given. Following from Eq. (7.2), the contact angle is determined by the values of the different specific interfacial energies in the same way as Ξ in the analysis performed in the present section. Due to surface effects, the work of formation of critical clusters corresponding to shapes specified by (b) and (d) is smaller than in the cases (a) and (b). An interpretation can be given directly by applying Kaischew's equation (7.6). In the lower part of the figure for

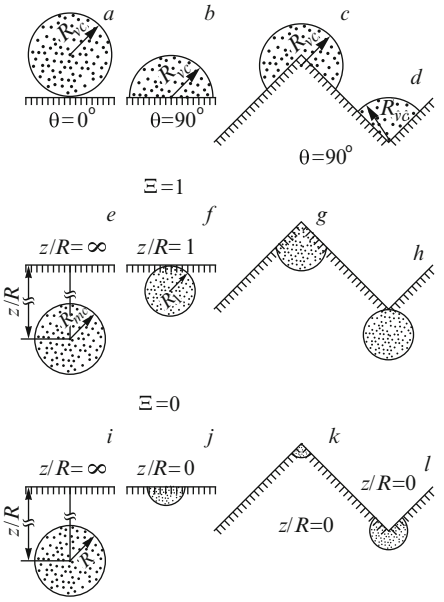

Fig. 7.12 Different possibilities for a formation of clusters of a new phase in solid-solid phase transformations for planar and rough interfaces (see text). For comparison also the case of vapor condensation is depicted schematically in figures (**a**)–(**d**)

two values of Ξ, possible shapes of the critical clusters both for planar and rough surface structures are shown. For planar surfaces the shapes specified by (f) and (j) refer to the critical clusters formed with the highest probability at $\Xi = 1$ and $\Xi = 0$, respectively. Due to a lower value of the work of formation of critical clusters for rough surface structures they are formed preferably at the tips of the cones (see Fig. 7.12g, k) and not in positions specified by (h) and (i). Consequently, preferential surface crystallization is to be expected along scratches or on surfaces seeded with cones with characteristic angles $\hat{\theta} < \pi/2$ (see also Schmelzer et al. (1994) [716]). As a heuristic rule, it can be stated that crystallization of the solid matrix occurs preferably at positions where the volume of the solid matrix deformed elastically has a minimum.

The discussion above is restricted to cases where the shape of the cluster of the new phase can be characterized by only one parameter, the radius of curvature, R. Even for this particular case it could be shown that free surfaces of solid samples catalyze nucleation. However, it is probable that there are geometrical configurations which are even more active with respect to nucleation catalysis than the considered ones. Generally, from the assumed isotropy of both phases – the ambient and the newly evolving phase – it follows that the critical cluster – corresponding to the saddle point of the ΔG-surface – should have, near planar interfaces, a shape with cylindrical symmetry. The detailed analysis of the most probable shapes of the critical clusters in dependence on the particular properties of the phases involved in the transformation requires a more detailed separate analysis (cf. Nabarro (1940) [588]). First estimates show (Möller (1994) [568]) that near free planar surfaces, the formation of clusters having an ellipsoidal form with the axis of symmetry

perpendicular to the interface should be favored. Moreover, if the vitreous matrix is in contact with a solid having a higher value of Young's modulus than the matrix, a catalysis of nucleation is not found but a further depression of phase formation. This inhibition of phase formation would correspond to $\Phi > 1$.

In addition, the shape of the critical clusters, formed with the highest probability (corresponding to the saddle-point configuration), is changed to disc-like structures. In this way, the consideration of the influence of elastic strains on phase formation may give not only a key to the understanding of preferred surface crystallization of glasses and small glass particles but also for orientational effects in phase formation.

7.7.4 Crystallization of Glass Powders and Elastic Strains

For a qualitative explanation of the decrease in the inhibiting effect of elastic strains in crystallization at and near interfaces of a solid it was proposed above that this effect is proportional to the deformed part of the volume of the solid matrix. Following such an idea, it has to be expected that the inhibiting effect of elastic strains is also diminished for crystallization in small solid particles comparable in size with the critical cluster size in nucleation.

For a verification of this consequence we will consider the following simplified model. Suppose in the center of a spherical sample of a solid with the radius R_2, a cluster with the radius R_1 is formed. Due to the misfit between both phases elastic strains occur which in the case of equal elastic constants (E – Young's modulus, γ – Poisson's number) of matrix and cluster may be expressed in the form (see Möller et al. (1993a,b) [569, 570], Heinrich and Ulbricht (1981) [353])

$$\Psi^{(\varepsilon)} = \frac{E\delta_0^2}{9(1-\gamma)}\left(1 - \frac{R_1^3}{R_2^3}\right)V \ , \qquad V = \frac{4\pi}{3}R_1^3 \ . \tag{7.86}$$

Within the limit ($R_2 \to \infty$) the case of formation of a spherical cluster in the bulk of a solid matrix is obtained as a special case. This special case is reached in a good approximation already when the inequality $R_2 > 5R_1$ is fulfilled. Even more, significant variations of the energy of elastic deformations due to finite size effects are found only for $R_2 < 2R_1$. However, if this condition is fulfilled, a significant dependence of the total energy of elastic deformations on the radius of the cluster R_1 (at a fixed size of the matrix R_2) has to be expected. $\Psi^{(\varepsilon)}$ is equal to zero for $R_1 = R_2$ and $R_1 = 0$, it has a maximum at $R_1 = R_2/\sqrt[3]{2}$. Moreover, the quantity $\Psi^{(\varepsilon)}(R_1)/R_1^3$ is a monotonically decreasing function of R_1.

In application to nucleation catalysis, we may conclude from these results that glass powders with characteristic dimensions of the particles less than 5 R_c should exhibit a catalytic activity similar to "cones" on the surface of a glass sample. Moreover, elastic strains may even stimulate the crystallization since, as shown, the crystallization of small samples may be accompanied by a decrease in the total energy of elastic deformations. The discussed effect of nucleating activity of small

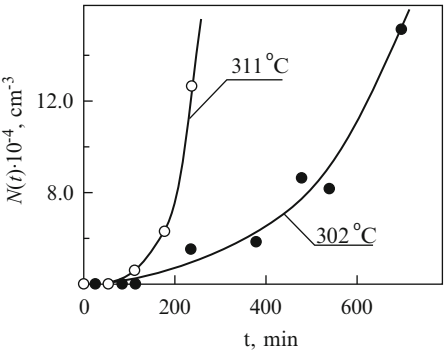

Fig. 7.13 Kinetics of induced nucleation of $NaPO_3$-melts catalyzed by Ir-microcrystals at two different temperatures indicated in the figure (Gutzow and Toschev (1971) [320])

glass particles should be even larger if the new phase is formed not in the center but near the boundaries of the sample or if the sample is not spherical but irregular having "sharp edges" and "cicatrices" as denoted by Tabata [816].

7.8 Kinetics of Nucleation and Induced Crystallization of Glass-Forming Melts: Experimental Evidence

In the first investigations on the temperature dependence of the rate of nucleation, mentioned in Chap. 6, no special analysis was performed concerning the character of the process investigated. As a rule only the number of detectable crystallization centers was counted under the assumption that steady-state nucleation takes place so that the course of the $N(t)$-curves is given by Eq. (6.175). The first experimental evidence on the non-steady state character of the nucleation process in glass-forming melts was given in an investigation of heterogeneous crystallization in $NaPO_3$-melts on submicroscopic crystallization cores of the noble metals (Ir, Rh, Pd, Pt, Au and Ag) (see Gutzow et al. (1966) [322]; Gutzow, Toschev (1971) [320]; Gutzow (1980) [303]). The initial part of the $N(t)$-curves obtained in this study clearly manifests the non-steady state character of nucleation in glass-forming melts (Figs 7.13 and 7.14).

These results were obtained for temperatures below the maximum of the nucleation rate, in the vicinity of the temperature of vitrification. When the activity of substrates is taken into account Eqs. (7.8) and (7.14) can be combined to give similarly to Eq. (6.197) the result

$$\tau^* J^* = \frac{a_0 N^*_{(cores)}}{2\pi \Gamma^{(*)}_{(z)}} \exp\left(-\frac{\Delta G^{(c)}_{(cluster)} \Phi}{k_B T}\right) . \tag{7.87}$$

If one defines t_1^* as the average time interval when a cluster is formed under steady-state conditions (i.e., $t_1^* \sim (J^*)^{-1}$) one obtains with Eqs. (6.65) and (6.44)

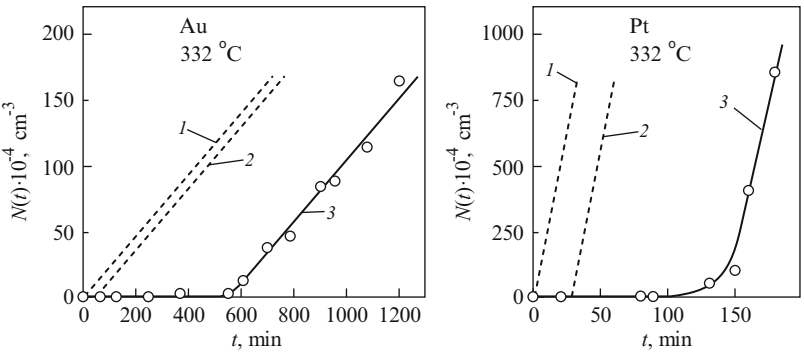

Fig. 7.14 Kinetics of nucleation in $NaPO_3$-melts induced by gold and platinum crystallization cores. Curve (*1*): Expected $N(t)$-curve when no transient effects are involved; curve (*2*): Possible shift of the $N(t)$-curves accounting for the growth of the crystalline clusters to visible dimensions; curve (*3*): Experimentally observed $N(t)$-curves

$$\frac{\tau^*}{t_1^*} = \frac{a_0 N^*_{(cores)}}{2\pi \Gamma^{(*)}_{(z)}} \exp\left(-\frac{16\pi}{3} \frac{\sigma^3 v_m^2}{k_B T_m [\Delta s_m (T_m - T)]^2} \Phi\right) . \tag{7.88}$$

An inspection of this equation shows that $\tau^* \gg t_1^*$ holds most probably for low temperatures, i.e., in the vicinity of T_g and for active substrates ($\Phi < 0.5$). Under these conditions it is always to be expected that the non-steady state time-lag is considerably greater than the time, t_1^*, to form the first nuclei (or a given number of nuclei, N). These conditions were in fact chosen in the above cited investigation to give in 1966 the first proof of the non-steady state nucleation kinetics in glass-forming melts.

The growth rate of spherulites in $NaPO_3$-melts was also investigated in the framework of the same study (Gutzow (1980) [303]) and it was shown that the induction periods, $t_{(ind)}$, exceed considerably the expected shift of the $N(t)$-curves along the t-axis due to growth effects (see Fig. 7.14). A further proof of the non-steady state character of the nucleation process in a $NaPO_3$-glass was made by analyzing the size distribution curves of $NaPO_3$-crystallites in the heat-treated partly crystallized samples: It turned out that they correspond to the theoretical prediction for a non-steady state process of nucleation (Toschev and Gutzow (1967) [927, 929]). In a number of subsequent papers, the same shape of the $N(t)$-curves, initially found for $NaPO_3$ glass, was confirmed by several authors for crystallization in the vicinity of T_g for other model systems (Fig. 7.15). Here the paper by James (1974) [400] is of particular importance.

As already mentioned in a previous section, this author used Tammann's two-stage method of crystallization development of the initially formed crystalline nuclei. In this way, an influence of growth effects on the induction period was omitted. James showed also that the experimentally determined $N(t)$-curves for the crystallization of lithium disilicate glass may be satisfactorily described in coordinates corresponding to the solution of the Zeldovich-Frenkel equation given

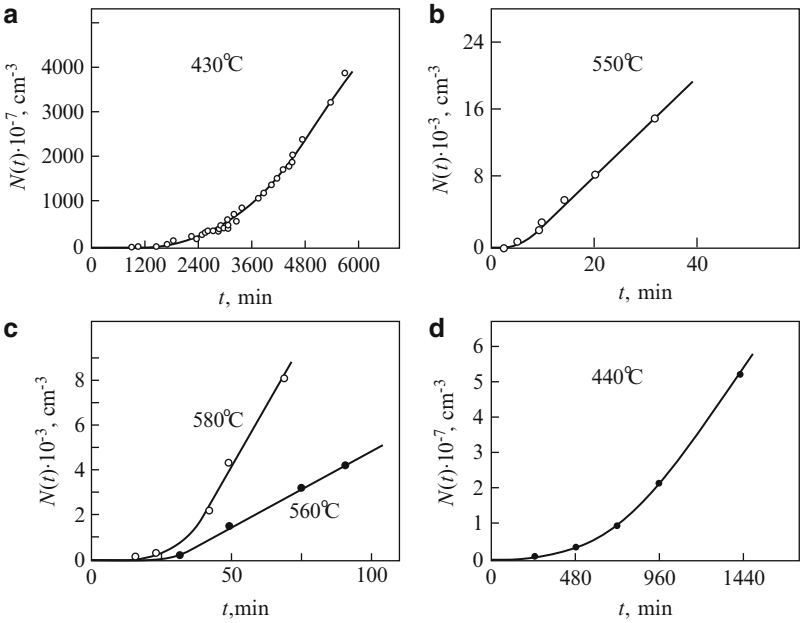

Fig. 7.15 Non-steady state $N(t)$-curves obtained upon crystallization of various glass-forming melts. (**a**) $Li_2O \cdot 2SiO_2$ (Kalinina et al. (1976) [427]); (**b**) Glass with a composition 16.7 % Na_2O 16.7 % BaO 66.6 % SiO_2 (Burnett and Douglas (1971) [112]); (**c**) Glass with a composition 21.2 % Na_2O_3 21.2 % CaO 57.5 % SiO_2 at two different temperatures (Strnad (1986) [812]); (**d**) $Li_2O \cdot 2SiO_2$ (James (1974) [400])

by Collins and Kashchiev. The nucleation kinetics in the same glass ($Li_2O_2SiO_2$) was also very thoroughly investigated by Kalinina, Fokin, and Filipovich (1974) [427] for different conditions of crystallization.

Further results in the study of crystallization of glass-forming systems made by Gutzow et al. (1977) [328] and by Penkov and Gutzow (1984) [632] showed that the non-steady state nature of the nucleation process can be confirmed also in the crystallization of multi-component glass-forming systems used as precursors in the formation of glass-ceramics and glass-ceramic enamels. The nuclei number vs. time curves obtained in these two cases correspond to the $N(t)$-dependencies with a typical saturation plateau (see Fig. 7.4). The high spherulitic density normally reached in the crystallization of technical glass-ceramic precursor melts greatly hampers the quantitative study of the crystallization process. In order to overcome this difficulty the nucleation kinetics in the mentioned technical glass-forming melts was examined in thin films blown from the initial glass in the same way as soap bubbles.

According to Eqs. (6.193) and (7.18) the value of τ^* in the region of large undercoolings (in the vicinity of T_g) is determined mainly by the temperature dependence of Z, i.e., from the temperature dependence of the viscosity η. Figures 7.16 and 7.17 show the temperature dependence (plotted in coordinates $\log \tau$ vs. $1/T$) of the non-

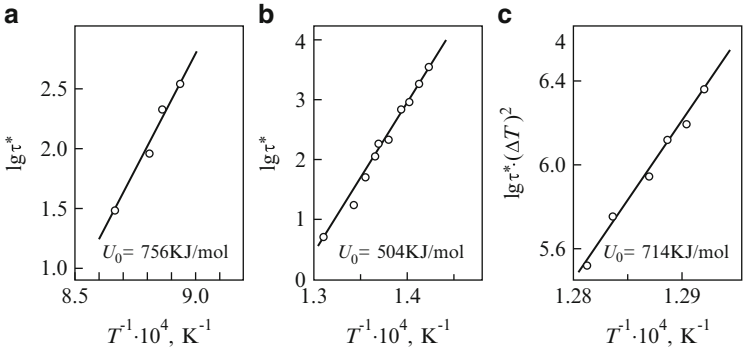

Fig. 7.16 Plot of $\log \tau^*$ vs. $1/T$ for different cases of nucleation in glass-forming melts (After Gutzow et al. (1977) [327]; Fokin, Kalinina et al. (1977) [222]; Scott and Ramachandrao (1977) [742]; analyzed by Gutzow (1980) [303]). (**a**) Crystallization of anosovite in an enstatite-type glass-ceramic material; (**b**) Devitrification of $Li_2O \cdot 2SiO_2$-glass ($N(t)$-data after Kalinina et al. (1977) [222]); (**c**) Crystallization of $Fe_{0.8}P_{0.13}C_{0.07}$-glass (Scott and Ramachandrao (1977) [742])

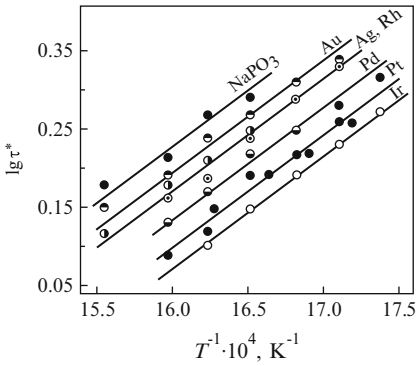

Fig. 7.17 Experimental results for induced crystallization of $NaPO_3$ on various metal cores presented as a $\log \tau^*$ vs. $1/T$ plot. The data for different nucleants are shifted with respect to pure $NaPO_3$ by $\log \Phi$ into parallel straight lines and determine the activation energy as $U_0 = 270\,\mathrm{kJmol}^{-1}$. The mean activation energy for viscous flow of $NaPO_3$ in the same temperature range is $U_0(\mathrm{j}) = 334\,\mathrm{kJmol}^{-1}$ (Gutzow and Toschev (1971) [320])

steady state induction period in the crystallization of several glass-forming melts. The activation energies determined in these coordinates are close to the activation energy for the viscous flow in the corresponding melts as it is to be expected in fact according to the mentioned equations. The $\log \tau^*$ vs. $1/T$-curves for the case of heterogeneous nucleation in the $NaPO_3$-melts are shifted along the ordinate axis by the value $\log \Phi$, as it is to be expected from the formula Eq. (7.18) derived by Toschev and Gutzow for the time-lag in heterogeneous nucleation. In Fig. 7.18, the final results of the experimental determinations of induction periods in a $NaPO_3$-glass are given together with the theoretical curve describing the temperature dependence of τ^* multiplied by a factor $\varsigma = 10^{-5}$.

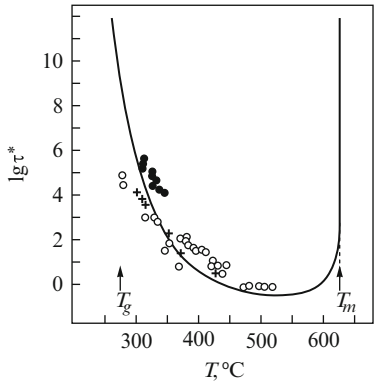

Fig. 7.18 Plot of $\log \tau^*$ vs. T for crystallization of pure $NaPO_3$-glass (Gutzow and Toschev (1968) [318]): experimental induction periods τ^* calculated from $N(t)$-curves (*black dots*) and growth measurements (*open circles*) and the overall crystallization kinetics (*crosses*)

Table 7.2 Lattice misfit, δl, and nucleation activity, Φ, in the catalyzed nucleation of $NaPO_3$ and poly(ethylenetherephtalate) (PET) on noble metal crystallization cores. Lattice parameters: $NaPO_3$ (orthorhombic): a = 7.93 Å, b = 13.14 Å, c = 7.75 Å. PET (triclinic): a = 4.56 Å, b = 5.94 Å, c = 10.74 Å. The percentage misalignment, δ_l, is in both cases given as the optimum value calculated assuming $\delta_{NaPO_3} = 100(1 - 2d/c)$ and $\delta_{PET} = 100(1 - d/a)$

Metal substrate	Activity Φ	Contact angle θ °	Lattice misalignment δ_l [%]	Lattice parameter d [Å]
			$NaPO_3$	
Ir	0.007	15	+1.17	3.83
Pt	0.009	18	−1.15	3.92
Pd	0.022	29	−0.13	3.88
Rh	0.058	37	+1.94	3.80
Ag	0.058	37	−5.29	4.08
Cu	0.05–0.06	34–38	+6.84	3.61
Au	0.125	30	−4.97	4.07
			PET	
Au	0.670	103	10.75	4.07
Pt	0.86	122	14.03	3.92
Ir	1.00	180	16.00	3.83

$N(t)$-curves obtained in the crystallization of amorphous silicon layers (Köster (1978) [472]) confirmed the transient character of the nucleation process in another interesting class of glass-forming systems, amorphous semiconductors. In recent times Köster ((1984) [473]; Köster and Herold (1981) [475]) and Spassov and Budurov (1988) [790] supplied a number of results on the kinetics of nucleation in the devitrification of metallic alloy glasses. Non-steady effects in the nucleation of polymer systems were also proven in the devitrification of glass-forming polymer systems. The results of these investigations obtained in studying the kinetics of overall crystallization of the respective melts, performed by Dobreva and Gutzow (1993) [174], are given in Chap 10.

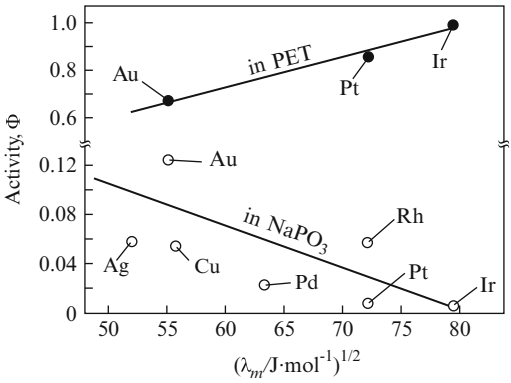

Fig. 7.19 Activity Φ of metallic crystallization cores in the case of induced crystallization of $NaPO_3$ (○) and polyethyleneterephthalate (PET) (●) melts in coordinates Φ vs. $(\lambda_m)^{1/2}$. Here λ_m is the heat of melting of the respective f.c.c. metals

Considerable evidence was collected in the earlier literature on the efficiency of different nucleants in the induced nucleation of glass-forming melts and especially in silicate melts. A typical example in this respect is the paper of Rabinovich (1963) [654] where connections between crystallographic matching and activity of substrates were the primary object of investigation (cf. also [86]). A thorough investigation was performed on the heterogenously induced crystallization of sodium metaphosphate glasses and organic polymer melts (Gutzow (1980) [303]; Dobreva, Gutzow (1993) [175]). As initiators the noble metal cores mentioned were used. It was shown that the principle of lattice disregistry and matching cannot explain the considerable differences existing between the activities of these crystallographically very similar nucleants (see Table 7.2 and Fig. 7.19). Moreover, it was proven by Dobreva and Gutzow (1993) [175] that the activity of nucleants employed obeys the predictions of the formalism developed in Sect. 7.4. Further experimental evidence in this respect may be traced in the cited papers where it is shown, in particular that Φ vs. $\sqrt{T_m^{(s)}}$ or Φ vs. $\sqrt{\lambda_m}$-plots may be used in order to correlate and predict activities of different substrates in the induced heterogeneous nucleation of glass-forming melts (see Fig. 7.19).

Size effects in the activity of substrates can be directly demonstrated to be of importance in the nucleation of glass-forming systems. The first pioneering results in this direction were obtained by Maurer (1958) [540] who found a difference in the activities of differently sized crystallization cores in the formation of technical glass-ceramic materials. In papers by Gutzow and Toschev (1968) [318] and Gutzow (1980) [291] a similar effect is described for the crystallization of $NaPO_3$-melts initiated by gold crystallization cores.

In Fig. 7.20, an experimental example for surface catalyzed devitrification is shown. For a rod of sodium metaphosphate glass, in the vicinity of T_g surface crystallization is observed in the form of thousands of $\alpha - NaPO_3$-needles, growing from the surface into the bulk of the glass matrix. Also of interest is the observation (see Fig. 7.21) that newly formed surfaces are less active with respect to crystallization than surfaces exposed for prolonged times to a laboratory

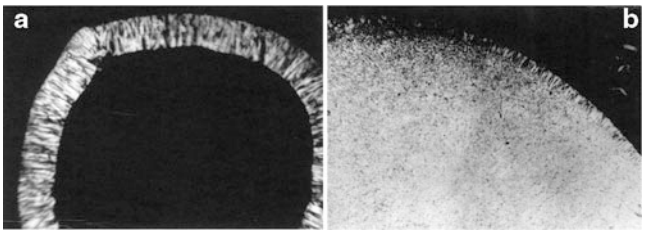

Fig. 7.20 Surface and bulk devitrification of $NaPO_3$-glass rods heat treated for 150 min at 320 °C. (*left side*) Crystalline layer at the surface of a $NaPO_3$-sample. (*right side*) Crystallization of a sample in which bulk devitrification is initiated by the addition of $5{\cdot}10^{-3}$ wt % platinum forming a population of platinum crystallization cores. Despite the addition of the bulk initiator of crystallization, surface nucleation is clearly visible (micrograph of thin slides at 50 magnification, crossed nicols)

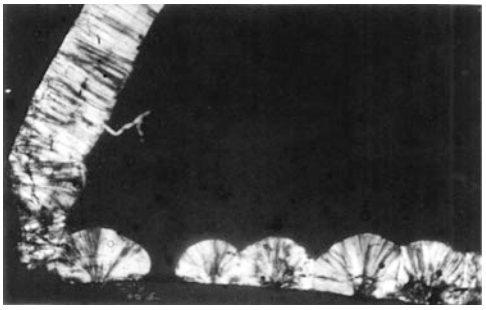

Fig. 7.21 Surface devitrification of a corroded and a newly formed $NaPO_3$-glass surface. A glass rod was broken in vacuum immediately before the heat treatment. In this way, in addition to the corroded surface (*upper left corner*) a new surface was generated (*bottom part*). While at the newly formed surface only a few spherulites are detected, the corroded surface is covered by thousands of crystalline needles growing perpendicular to the surface

atmosphere. This observation can be connected with an additional decrease in the work of formation of critical clusters due to a roughening of the surface by corrosion processes. Numerous results in this respect were also collected by Zanotto and James (1985) [946].

Devitrification of some glasses is facilitated if glass powders of the same composition are deposited on the surface (Gutzow and Slavtschev (1971) [317]; Schmelzer et al. (1993 [716], 1995 [717])). This effect can be explained in the framework of the outlined theory taking into account the catalytic activity of small glass particles. Other examples are discussed by Avramov et al. (1981) [29] in analyzing crystallization of glass semolina samples.

A strong indication that elastic strains are responsible for the inhibition of bulk devitrification consists of the experimental finding that B_2O_3-glasses do not crystallize even after long heat treatments in the vicinity of T_g. For B_2O_3, the misfit parameter δ_0 is of the order $\delta_0 \approx 0.37$, which results in very large values of the energy of elastic deformations in crystallization. Other examples in this respect are

given by Gutzow and Slavtschev (1971) [317], Zanotto and Müller (1991) [948]. Zanotto and Müller showed that out of approximately 20 glass-forming substances, bulk devitrification was observed only when the misfit parameter δ_0 was less than 0.04. In the other cases, only surface crystallization was found. In line with the discussed theoretical concept a second observation of Zanotto and Müller is also of interest: surface induced nucleation occurs preferably in substances where the maximum of the nucleation rate is located in temperature regions below T_g. In such cases, bulk nucleation is most effectively suppressed by elastic strains. Further experimental examples giving a verification of the outlined theoretical results were given by Schmelzer et al. (1993 [716], 1995 [717]).

Summarizing the results concerning surface induced nucleation we may conclude that in addition to the possible existence of foreign nucleation cores preferential surface crystallization of glasses is due, on one hand, to the decrease in the work of formation of critical clusters connected with the decrease in the energy of elastic deformations for crystallization near or at interfaces or in small particles. On the other hand, as an additional factor stimulating crystallization at the interface, the reduction of the surface of the newly formed critical clusters may play also an important role. However, for isoconcentration crystallization of glasses, the decrease in elastic strains for crystal formation near or at glass interfaces dominates in nucleation catalysis. Both effects are significantly enhanced for rough surface structures. In this way, a key is given also for understanding the effects of mechanical treatments of glass surfaces on the intensity of devitrification processes occurring on them.

In analyzing the literature on the kinetics of nucleation in glass-forming melts and on the possibilities of inducing crystallization in order to obtain glass-ceramic materials, the following conclusions can be drawn:

- Quantitative results on the temperature dependence of the rate of nucleation and on the activity of substrates in the induced nucleation of glasses can only be obtained if the transient character of the process involved is accounted for.
- The general theory of nucleation in its classical formulation can be used to predict criteria for nucleation catalysis in agreement with experimental findings. Up to now, heterogeneous nucleation and surface energy modifications have been mainly employed. The theory indicates, however that there are still alternative possibilities (effect of strained and unstrained nucleation, influence of surfaces and surface structure, electric fields and charged particles), which are still either not or insufficiently employed in producing high-tech materials.

We would like to mention as well that it was mainly the application of the theory of crystal nucleation and growth which changed the character of production of glasses and of glass-ceramic materials from an art to a modern theoretically based technology. However, the demands of the technology of glass-ceramics also opened a new development in the theory and in the field of experimental investigation of catalyzed nucleation.

The history and details of the technological developments connected with the production of glass-ceramic materials cannot be given here. The interested reader

is referred for detailed information to a number of exceptional books on this subject. Among them we would like to mention the monographs of Buckley (1951) [106], McMillan (1964) [549], Filipovich (1965) [207], Vogel (1969, 1971) [888], Pavlushkin (1970) [631], Bereshnoi (1981) [67], Strnad (1986) [812] and the review articles of Stookey (1957 [802], 1959 [803]), James (1982) [402] and Hülsenberg (1993) [384]. Details concerning the significance of surface induced crystallization in the production of glass ceramic materials can be found in the papers of Tashiro (1985) [827] and Karamanov et al. (1994) [431] and the respective parts of Strnad's monograph.[2]

[2]Some recent new developments are briefly reviewed also in the Chap. 14.

Chapter 8
Theory of Crystal Growth and Dissolution in Under-cooled Melts: Basic Approaches

8.1 Introduction

The theoretical considerations concerning the description of crystal growth are based on three very general models, i.e.,

- Normal (or continuous) growth,
- Growth determined by processes of formation of two-dimensional nuclei and their subsequent enlargement and
- Growth mediated by screw dislocations.

According to the theory of normal growth, initially proposed by Wilson at the beginning of the last century (see Cahn et al. (1964) [120]) and reformulated later by Frenkel (1934) [185] and Volmer (1939) [894], it is assumed that the interface between the growing crystal and the surrounding medium displays a sufficiently high concentration of growth sites. On these growth sites the incorporation of ambient phase molecules takes place in a continuous way. As growth sites in the theory of crystal growth, such configurations on the interface are denoted where an impinging ambient phase molecule is bound to the evolving phase at least as strongly as being in the so-called half-crystal position (see Fig. 8.1). In this half-crystal position, an ambient phase molecule has equal values of the probability either to remain in this position or to evaporate (dissolve).

A first theoretical analysis of the energetics of different sites on the crystal face and their significance with respect to the process of crystal growth was performed by Stranski (1928) [809] and Kossel (1929) [471] who introduced into the theory of crystal growth the fruitful concept of the half-crystal position. The particular importance of this position is, on one hand, due to its property that aggregation of a building unit onto such a position is a repeatable step in crystal growth. On the other hand, a building unit at this particular position on the interface has a value of the work of separation equal to one half of the energy of evaporation of the same crystal building unit for the bulk of the crystal. In this sense, the energetic properties of the half-crystal position also determine the thermodynamic potential of the infinitely large crystal.

I.S. Gutzow and J.W.P. Schmelzer, *The Vitreous State*,
DOI 10.1007/978-3-642-34633-0_8, © Springer-Verlag Berlin Heidelberg 2013

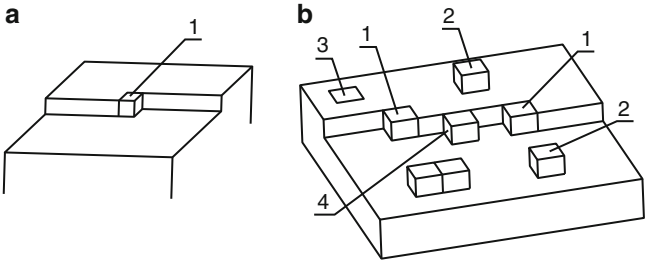

Fig. 8.1 Typical possible positions of building units of the evolving phase on a crystal plane: *(1)*: half-crystal position; *(2)*: adsorbed atoms; *(3)*: a hole at the interface; *(4)*: adsorption at a step on the interface

In the simplest of the possible growth modes mentioned – the normal growth – the crystal face advances continuously (hence its second name) into the direction of its normal with a velocity proportional to the impingement rate of ambient phase molecules. For this case, it is assumed that a sufficiently large surface concentration of growth sites is sustained in the course of growth. Such a high concentration of growth sites is found only at crystal faces which are rough on an atomic or molecular scale. According to the classical theory, only defective or non-equilibrium crystal faces have this property. However, more recent theoretical approaches, introduced by Jackson (1958) [393], Jackson et al. (1967) [398], Cahn (1960) [115], Cahn et al. (1964) [120], Temkin (1962) [828] into the theory of melt crystallization, subsequent computer simulations and experimental results show that an equilibrium form crystal face in contact with its own melt may also become atomically rough and thus growth may proceed on it via the normal mode.

The specification of the thermodynamic and structural conditions for the development of a roughened diffusive melt-crystal interface growing according to the normal growth mode was the subject of prolonged discussions (see Jackson et al. (1967) [398]). It turned out that normal growth is possible for equilibrium crystal faces only if melt and crystal possess basic building units with a similar structure. This is the reason why, for the discussion of phase transformations in glass-forming systems, this problem is of particular interest in connection with the kinetics of reconstructive and non-reconstructive crystallization. As already mentioned (compare Sect. 4.10), in glass-forming melts, considerable differences in the structure of the basic building units may occur between crystal and melt. This result has to be taken into account when the normal growth mode for equilibrium shaped crystal faces is discussed in the following sections.

In contrast to normal growth, the other two mentioned mechanisms of crystallization are characterized by processes of growth of layers originating from permanently existing (screw dislocation-mediated) or fluctuationally appearing (surface nucleation-mediated) growth sites. In the latter case, the growth proceeds via a lateral aggregation of ambient phase building units to permanent or stochastically appearing edges. In this way, the dislocational and the surface nucleation mediated growth proceed more or less periodically in the sense that a new crystal layer starts to evolve, in general, only after the growth of the foregoing layer is completed.

This periodicity of growth in the direction normal to the interface is the main characteristic feature of the layer by layer growth model proposed by Kaischew and Stranski (1934 [425]; see also Kaischew (1957) [418]). In this classical model, it is assumed that the rate of lateral growth surpasses by many orders of magnitude the frequency of formation of two-dimensional nuclei. Also further developments are given where the mentioned restriction is replaced by more general assumptions. The idea of a possible formation of two-dimensional nuclei on ideally smooth growing crystal faces was expressed originally by Gibbs (see the frequently quoted footnote in his work on the thermodynamics of heterogeneous substances [249]). The kinetic formulation of this idea in attempts to describe crystal growth was developed by Volmer at the end of the 1920s (see also Volmer (1939) [894]) and by Kaischew and Stranski (1934) [425]. The connection between screw dislocations and crystal growth was established by F. C. Frank in 1949 [227].

An overview on the historical development of ideas concerning possible models of crystal growth can be found in the monographs of Volmer (1939) [894], Frenkel (1946) [233] and Buckley (1951) [106] as well as in a number of more recent books and review articles (see, e.g., Honigman (1958) [378]; Pamplin (1975) [622]; Stricland-Constable (1968) [813]) and conference proceedings (Discussions of the Faraday Chemical Society No. 5 (1949): Crystal Growth and Perfection of Crystals). In Buckley's book a number of more or less intuitively formulated ancient ideas on crystal growth modes are also given, most of them rejected by the further development of the theory of crystal growth. An account of the development of the theory of crystal growth as seen by one of the main participants can be found in one of Kaischew's articles (Kaischew (1981) [420]).

In the following sections, the three basic growth modes mentioned will be discussed in detail in application to melt crystallization. Hereby, the discussion is not restricted, as done in most of the literature on crystal growth, to the consideration of growth of planar crystal faces (i.e., of infinitely large crystals) but includes also the analysis of size effects in crystal growth, i.e., the growth of small crystallites (Chap. 9). Only by taking into account such size effects, can a quantitatively correct description of the kinetics of nucleation (remember that the application of Eqs. (6.94) and (6.95) and also of the set of kinetic equations, Eqs. (6.129), requires the knowledge of the rates of attachment $w^{(+)}$ in dependence on cluster size) and of overall crystallization be given as well as that of the late stages of the transformation (Ostwald ripening).

8.2 The Normal or Continuous Mode of Growth and Dissolution: The Transition Frequency

We consider in the following discussion a crystal, characterized by a value, g_c, of the Gibbs free energy per particle, in contact with a supersaturated ambient phase, e.g., a melt (with a Gibbs free energy, g_f, per particle in the melt) at a planar interface. If we denote, moreover, the number of nucleation or growth sites per unit surface area of the interface by n_{gs} and the total number of building units of the melt in

the vicinity of this part of the interface by n_f, then the relative number, $\gamma_0^{(f/c)}$, of growth sites on the crystal face may be introduced defining it by

$$\gamma_0^{(f/c)} = \frac{n_{gs}}{n_f} \,. \tag{8.1}$$

In addition to the relative number of growth sites the kinetics of the growth or dissolution process is determined by energetic properties of the interface.

Following the basic ideas of the absolute rate theory (see Glasstone, Laidler and Eyring (1941) [255]) it is usually assumed that in order to determine the frequency of interface exchanges of molecular building units an activated state of the molecules has to be assumed. In this activated state the Gibbs free energy equals $g^{(*)}$. The activation energies we denote by $u_{f\to *}$ for the transformation of a particle from the melt into the activated state and by $u_{c\to *}$ for the respective process from the crystalline state. These quantities are determined as

$$u_{f\to *} = g^{(*)} - g_f \,, \qquad u_{c\to *} = g^{(*)} - g_c \,. \tag{8.2}$$

According to Eyring's theory (see Glasstone et al. (1941) [255]) the frequency of transformation of ambient phase molecules from the melt into the activated state is given by

$$\omega_{f\to *} = \left(\frac{k_B T}{h}\right) \exp\left(-\frac{u_{f\to *}}{k_B T}\right) \,, \tag{8.3}$$

while for the transformation from the crystalline into the activated state

$$\omega_{c\to *} = \left(\frac{k_B T}{h}\right) \exp\left(-\frac{u_{c\to *}}{k_B T}\right) \tag{8.4}$$

holds. Here h is Planck's constant. The two possible situations with respect to the energetics of the two-phase system melt-crystal are depicted in Fig. 8.2. The activated state of the complex corresponds to the maximum of the potential barrier separating the crystal from the liquid.

Let us assume first that the Gibbs free energy per particle is higher in the liquid than in the crystalline state of the same substance (undercooled melt in contact with its own crystal). The net frequency of transitions from the melt to the crystalline state is given in this case by

$$\omega^{(f/c)} = \omega_{f\to *} - \omega_{c\to *} = \omega_{f\to *}\left[1 - \exp\left(-\frac{u_{c\to *} - u_{f\to *}}{k_B T}\right)\right] \tag{8.5}$$

or taking into account Eq. (8.2) as

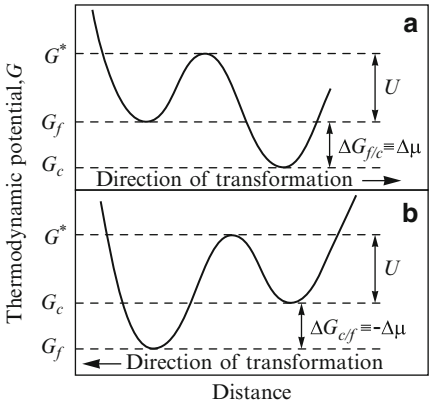

Fig. 8.2 Diagram illustrating the energetic conditions at the interface melt-crystal for (**a**) the case of crystal growth and (**b**) the case of crystal dissolution (schematically)

$$\omega^{(f/c)} = \omega_{f\to *}\left[1 - \exp\left(-\frac{\Delta\mu^{(f/c)}_{(particle)}}{k_B T}\right)\right], \qquad \Delta\mu^{(f/c)}_{(particle)} = g_f - g_c > 0\,. \tag{8.6}$$

It turns out that the frequency of incorporation of ambient phase building units at a given crystalline growth site is completely determined by $\omega_{f\to *}$ and the thermodynamic driving force of crystallization, $\Delta\mu^{(f/c)}$ (compare Eqs. (6.53), (6.55) and (6.64)).

Based on the equations outlined above the rate of crystal growth, $v_n^{(f/c)}$, into the direction normal to the interface can be written as

$$v_n^{(f/c)} = \gamma_0^{(f/c)}\omega^{(f/c)} d_{cr}\,, \tag{8.7}$$

where by d_{cr} the width of the crystal lattice spacings in the direction of growth is denoted. Equations (8.6) and (8.7) yield

$$v_n^{(f/c)} = \gamma_0^{(f/c)} d_{cr}\omega_{f\to *}\left[1 - \exp\left(-\frac{\Delta\mu^{(f/c)}_{(particle)}}{k_B T}\right)\right]. \tag{8.8}$$

Note the similarity between this expression and Eq. (6.138) derived earlier in a quite different way.

If one assumes that the frequency $\omega_{f\to *}$ is determined by the mobility of the ambient phase particles of the melt above equation can be simplified. Using the earlier applied notations, $\omega_{f\to *}$ can be expressed through the flux of particles to a nucleation site, i.e., as

$$\omega_{f\to *} \cong Z^{(eff)} d_0^2\,, \tag{8.9}$$

where $Z^{(eff)}$ is the effective impingement rate (compare Eqs. (2.106)–(2.110) and (6.121)). Here d_0^2 is the area of an active nucleation site, with d_0 the mean

intermolecular distance in the ambient phase is denoted. Equations (8.8) and (8.9) yield

$$v_n^{(f/c)} = \gamma_0^{(f/c)} Z^{(eff)} d_0^3 \left[1 - \exp\left(-\frac{\Delta\mu_{(particle)}^{(f/c)}}{k_B T} \right) \right] . \tag{8.10}$$

In the derivation of this expression the approximation $d_0^3 \cong d_0^2 d_{cr}$ was used realizing as in the derivation of Eq. (8.9) that the average intermolecular distances and the average sizes of the ambient phase particles in the melt differ only by a few percent from the respective values for the crystal (see, e.g., Frenkel (1946) [233] and experimental evidence summarized by Ubbelohde (1965) [871]).

A substitution of Eq. (6.121) for the effective impingement rate into Eq. (8.10) finally gives

$$v_n^{(f/c)} = \frac{\varsigma \gamma_0^{(f/c)} k_B T}{d_0^2 \eta} \left[1 - \exp\left(-\frac{\Delta\mu_{(particle)}^{(f/c)}}{k_B T} \right) \right] . \tag{8.11}$$

For small values of the under-cooling (of the ratio $\Delta\mu_{(particle)}^{(f/c)} / k_B T$) we obtain instead of Eqs. (8.10) and (8.11)

$$v_n^{(f/c)} \cong \frac{\gamma_0^{(f/c)} Z^{(eff)} d_0^3}{k_B T} \Delta\mu_{(particle)}^{(f/c)} , \tag{8.12}$$

$$v_n^{(f/c)} \cong \frac{\varsigma \gamma_0^{(f/c)}}{d_0^2 \eta} \Delta\mu_{(particle)}^{(f/c)} . \tag{8.13}$$

Moreover, at small under-cooling the thermodynamic driving force of the transformation referred to one mole may be expressed through the difference $(T_m - T)$ via Eq. (6.65). A substitution into Eqs. (8.12) and (8.13) yields

$$v_n^{(f/c)} \cong \frac{\gamma_0^{(f/c)} Z^{(eff)} d_0^3 \Delta s_m}{R_g} \left(\frac{T_m - T}{T_m} \right) \tag{8.14}$$

or

$$v_n^{(f/c)} \cong \frac{\varsigma \gamma_0^{(f/c)} T_m \Delta s_m}{d_0^2 \eta N_A} \left(\frac{T_m - T}{T_m} \right) . \tag{8.15}$$

In above equations, R_g and N_A are the universal gas constant and Avogadro's number, respectively.

For the considered case it is assumed that the temperature dependence of $\omega_{f\to *}$ is determined by the temperature dependence of the viscosity of the melt. If, however, more complicated processes proceed at the interface as a precondition for the incorporation of ambient phase molecules to the crystal, then also a more complicated temperature dependence of the pre-exponential factors are to be expected. In the opposite case that the Gibbs free energy of the particles in the

crystalline state, g_c, is higher than the respective value for the melt (e.g., superheated crystal), the transition frequency per growth (or dissolution) site, $\omega^{(c/f)}$, is given by

$$\omega^{(c/f)} = \omega_{c\to *} - \omega_{f\to *} = \omega_{c\to *}\left[1 - \exp\left(-\frac{u_{f\to *} - u_{c\to *}}{k_B T}\right)\right] . \tag{8.16}$$

If we define $\Delta\mu^{(c/f)}_{(particle)}$, again, as a positive quantity then similarly to Eq. (8.6) we arrive at

$$\omega^{(c/f)} = \omega_{c\to *}\left[1 - \exp\left(-\frac{\Delta\mu^{(c/f)}_{(particle)}}{k_B T}\right)\right] , \qquad \Delta\mu^{(c/f)}_{(particle)} = g_c - g_f . \tag{8.17}$$

The rate of dissolution, $v_n^{(c/f)}$, of the crystal can be expressed then as

$$v_n^{(c/f)} = \gamma_0^{(c/f)}\omega^{(c/f)} d_{cr} \tag{8.18}$$

or

$$v_n^{(c/f)} = \gamma_0^{(c/f)}\omega_{c\to *} d_{cr}\left[1 - \exp\left(-\frac{\Delta\mu^{(c/f)}_{(particle)}}{k_B T}\right)\right] . \tag{8.19}$$

It is usually assumed and confirmed by experiment (see Fig. 8.17 and the subsequent discussion) that the ratio of growth sites, $\gamma_0^{(f/c)}$, is nearly equal to the ratio of dissolution sites, $\gamma_0^{(c/f)}$.

The determination of $\omega_{c\to *}$ is connected with difficulties. Therefore, another way to express the rate of dissolution is used. Starting with Eq. (8.16) we may write

$$\omega^{(c/f)} = \omega_{f\to *}\left(\frac{\omega_{c\to *}}{\omega_{f\to *}} - 1\right) \tag{8.20}$$

resulting in

$$\omega^{(c/f)} = \omega_{f\to *}\left[\exp\left(-\frac{\Delta\mu^{(f/c)}_{(particle)}}{k_B T}\right) - 1\right] \tag{8.21}$$

and

$$v_n^{(c/f)} = \gamma_0^{(c/f)} d_{cr}\omega_{f\to *}\left[\exp\left(-\frac{\Delta\mu^{(f/c)}_{(particle)}}{k_B T}\right) - 1\right] . \tag{8.22}$$

If it is assumed, again that the frequency $\omega_{f\to *}$ is determined by the mobility of the ambient phase molecules in the bulk of the liquid, we arrive similarly to Eqs. (8.11)–(8.15) at

$$v_n^{(c/f)} = \frac{\varsigma\gamma_0^{(c/f)} k_B T}{d_0^2\eta}\left[\exp\left(-\frac{\Delta\mu^{(f/c)}_{(particle)}}{k_B T}\right) - 1\right] , \tag{8.23}$$

$$v_n^{(c/f)} \cong -\frac{\gamma_0^{(c/f)} Z^{(eff)} d_0^3}{k_B T} \Delta\mu_{(particle)}^{(f/c)} , \tag{8.24}$$

$$v_n^{(c/f)} \cong -\frac{\varsigma \gamma_0^{(c/f)}}{d_0^2 \eta} \Delta\mu_{(particle)}^{(f/c)} , \tag{8.25}$$

and, finally, for $T_m \to T$ at

$$v_n^{(c/f)} \cong -\frac{\gamma_0^{(c/f)} Z^{(eff)} d_0^3 \Delta s_m}{R_g} \left(\frac{T_m - T}{T_m} \right) , \tag{8.26}$$

$$v_n^{(c/f)} \cong -\frac{\varsigma \gamma_0^{(c/f)} T_m \Delta s_m}{d_0^2 \eta N_A} \left(\frac{T_m - T}{T_m} \right) . \tag{8.27}$$

Taking into account the relation $\gamma_0^{(f/c)} \approx \gamma_0^{(c/f)}$ we come to the conclusion that for the considered case of small supersaturations the absolute values of the rates of growth and dissolution coincide and depend linearly on the thermodynamic driving force of the transformation, $\Delta\mu$. In the opposite case of relatively large absolute values of the supersaturation the growth or dissolution rate, v_n, becomes independent of the thermodynamic driving force of the transformation and is determined by kinetic factors only. For this case we obtain, e.g., from Eq. (8.10)

$$v \cong \gamma_0 Z^{(eff)} d_0^3 . \tag{8.28}$$

These simple model considerations were carried out for the first time by Volmer (1939) [894] and reformulated later by Turnbull (1965) [861].

8.3 Crystal Growth Determined by Two-Dimensional Nucleation

According to the theory of normal growth outlined in the previous section, the rate of growth is strongly dependent on the concentration of growth sites which are provided at a sufficiently large concentration only by atomically rough crystal/melt interfaces. The growth of a perfect atomically smooth crystal requires the formation of two-dimensional nuclei on the interface (see Fig. 8.3). In this case, the rate of growth is determined by processes of formation of such nuclei. Consequently, for a calculation of the growth rate, knowledge of the kinetics of formation of two-dimensional nuclei is required.

The thermodynamics and kinetics of two-dimensional nucleation on smooth crystal faces can be developed similarly as for the case of formation of three-dimensional clusters (see Sect. 6.3) as was done first by Brandes (1927) [100]; in

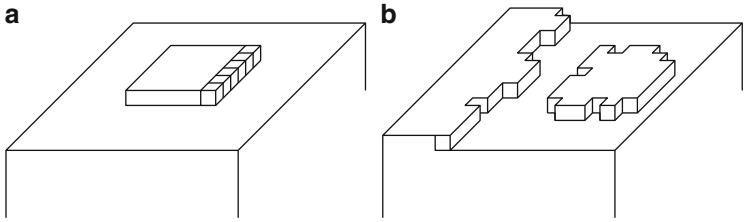

Fig. 8.3 Quadratic two-dimensional nuclei on a perfect crystal face. (**a**) Two-dimensional nucleus with a row of newly added atoms just attached to it in lateral direction according to the Kaischew-Stranski model; (**b**) two-dimensional nucleus with a kinked edge (see Hillig (1966) [361]) formed in the vicinity of a kinked step

his classical derivation (see also Volmer (1939) [894]). Instead of Eq. (6.36) we have to write

$$\Delta G^{(2)}_{(cluster)} = -j\Delta\mu + \kappa_l L \ . \tag{8.29}$$

Here κ_l is the so-called specific edge energy (or line tension) which plays the same role in two-dimensional nucleation as the specific interfacial energy (surface tension) in the three-dimensional case, while the surface area, A, of a three-dimensional cluster is replaced now by the length, L, of the perimeter of the edge of the two-dimensional nucleus. Let us assume that the nucleus is of nearly spherical shape with a radius, R, and a surface density of building units, $c^{(2)}_\alpha$, equal to

$$c^{(2)}_\alpha = \frac{j}{A^{(2)}_{(cluster)}} \qquad \text{with} \qquad A^{(2)}_{(cluster)} = \pi R^2 \ , \quad L = 2\pi R \ . \tag{8.30}$$

The critical cluster size in two-dimensional nucleation and the work of formation of two-dimensional critical clusters are, consequently, given by

$$R^{(2)}_c = \frac{\kappa_l}{c^{(2)}_\alpha \Delta\mu} \ , \tag{8.31}$$

$$\Delta G^{(2/c)}_{(cluster)} = \frac{1}{2}\kappa_l L_c \ . \tag{8.32}$$

If one assumes, in addition that

$$\frac{c_\alpha}{c^{(2)}_\alpha} = \frac{1}{d_{cr}} \ , \qquad \frac{\sigma}{\kappa_l} = \frac{1}{d_{cr}} \tag{8.33}$$

holds then for the same value of the supersaturation as an estimate for the critical cluster radius in two-dimensional nucleation

$$R_c^{(2)} = \frac{R_c}{2} \tag{8.34}$$

is found.

The second of Eq. (8.33) follows directly if one takes into account that both σ and κ_l can be determined through the mean work of separation, ϕ_1, of one particle from the crystal lattices as (Kaischew and Stranski (1934) [425])

$$\sigma = \frac{\phi_1}{d_{cr}^2}\,, \qquad \kappa_l = \frac{\phi_1}{d_{cr}}\,. \tag{8.35}$$

Taking into account above given considerations we may also write

$$\Delta G_{(cluster)}^{(2/c)} = \frac{\pi \kappa_l^2}{c_\alpha d_{cr} \Delta\mu} = \frac{\pi \sigma^2 d_{cr}}{c_\alpha \Delta\mu} \tag{8.36}$$

and (compare Eq. (6.44))

$$\frac{\Delta G_{(cluster)}^{(2/c)}}{\Delta G_{(cluster)}^{(c)}} = \frac{3}{16} \frac{\Delta\mu}{\sigma d_{cr}^2 N_A}\,. \tag{8.37}$$

As discussed in detail by Kaischew (1957, 1965) [418, 419] and by Hirth (1959) [367] the steady-state nucleation rate for two-dimensional nucleation can be written similarly to the three-dimensional result as (compare Eqs. (6.109) and (6.110))

$$J_{(2)} = w_{(2)}^{(+)}(R_c^{(2)}) \Gamma_{(z)}^{(2)} N_s \exp\left(-\frac{\Delta G_{(cluster)}^{(2/c)}}{k_B T}\right)\,, \tag{8.38}$$

$$\Gamma_{(z)}^{(2)} = \left\{-\frac{1}{2\pi k_B T}\left(\frac{\partial^2 \Delta G_{(cluster)}^{(2)}}{\partial j^2}\right)_{j=j_{(2/c)}}\right\}^{1/2} = \left(\frac{\Delta G_{(cluster)}^{(2/c)}}{4\pi k_B T j_{(2/c)}^2}\right)^{1/2}\,. \tag{8.39}$$

Here N_s denotes the number of ambient phase molecules adsorbed per unit surface area of the crystal face and $j_{(2/c)}$ is the number of particles in a two-dimensional critical cluster.

The attachment rate $w_{(2)}^{(+)}(R_c^{(2)})$ is defined for two-dimensional nucleation as the rate at which ambient phase particles are incorporated to the edge of the critical cluster (compare Eqs. (6.119) and (6.121)). Denoting the effective impingement rate for two-dimensional nucleation by $Z_{(2)}^{(eff)}$ we obtain

$$w_{(2)}^{(+)}(R_c^{(2)}) = Z_{(2)}^{(eff)} L_c \tag{8.40}$$

or introducing a two-dimensional sticking coefficient $\varsigma^{(2)}$

$$w_{(2)}^{(+)}(R_c^{(2)}) = Z^{(2)} \varsigma^{(2)} L_c \ . \tag{8.41}$$

$Z^{(2)}$ is the lateral impingement rate of ambient phase molecules to the edges of the two-dimensional critical cluster. Assuming, again, a nearly spherical shape of the critical cluster, L_c can be replaced through the number of building units in it, which gives, finally

$$w_{(2)}^{(+)}(R_c^{(2)}) \cong Z^{(2)} \varsigma^{(2)} d_{cr}^2 j_{(2/c)}^{1/2} \ . \tag{8.42}$$

In considering melt crystallization it can be assumed in a first approximation that N_s is given by the number of ambient phase molecules in a layer of thickness, d_0, adhering to the growing crystal face. In this case, $Z^{(2)}$ can be determined directly via Eqs. (2.106)–(2.110). Two different models have been developed in this respect:

- According to the classical model, a row of molecules of a critical length has to be formed at an edge of a two-dimensional nucleus before a further deterministic growth is possible (see Fig. 8.3a; Kaischew and Stranski (1934) [425]). In some respects, such a model represents a repetition of two-dimensional nucleation at the next uni-dimensional level.
- In an alternative approach it is assumed (as done by Hillig (1966) [361]) that the peripheral edges of the two-dimensional nucleus are kinked in such a way as to provide a roughening on an atomistic scale (compare Fig. 8.3b) and thus to guarantee a sufficiently large concentration of growth sites. In this model, $\varsigma^{(2)}$ is connected with the density of growth sites (kinks) at the edges of the two-dimensional cluster. In this respect the second model is connected with a modification of one of the already discussed mechanisms of normal growth.

Simple considerations concerning the energy of kink formation, the energetics of adsorption and desorption of building units at the edges of two-dimensional crystalline layers as well as arguments for the possible formation of diffusive interfaces between crystal and melt give a distinct preference for the second of the discussed models.

For a calculation of the growth rate determined by two-dimensional formation of growth sites, a connection has to be established between the nucleation rate, $J^{(2)}$, and the rate, v_n, of crystal growth normally to the interface. Again, two basic models have been developed in this direction. Suppose that $\tau_{(av)}^{(2d)}$ is the average time interval elapsing between the formation of two successive layers on the growing crystal. Then v_n can be expressed as

$$v_n = \frac{d_{cr}}{\tau_{(av)}^{(2d)}} \ . \tag{8.43}$$

The two models mentioned correspond to two limiting cases in the determination of $\tau_{(av)}^{(2d)}$:

- At high tangential growth rates v_t, when the inequality $\tau_{(av)}^{(2d)} \gg L_f / v_t$ holds for a crystal face with a characteristic size parameter L_f, then $\tau_{(av)}^{(2d)}$ is simply the

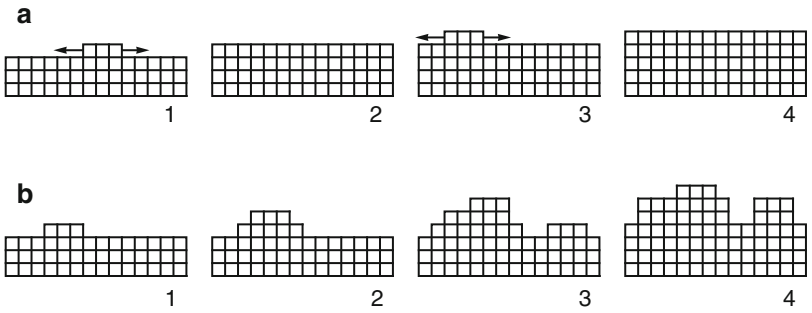

Fig. 8.4 Consecutive stages of growth mediated by two-dimensional nucleation. The cross sections through the growing crystal illustrate schematically (**a**) layer by layer growth and (**b**) polynucleus mode of growth. The numbers *(1)*, *(2)*, *(3)* and *(4)* refer to different moments of time after the process has started

average time interval between two subsequent nucleation events. In the steady state $\tau_{(av)}^{(2d)} = 1/(J^{(2)} L_f^2)$ holds and Eq. (8.43) gives

$$v_n \cong J^{(2)} L_f^2 d_{cr} \ . \tag{8.44}$$

This model is the layer by layer growth mechanism developed by Kaischew and Stranski (1934) ([425]; see also the derivation given by Kaischew (1957) [418]; Fig. 8.3a). The respective mode of growth results in perfectly smooth surface structures (Fig. 8.4).

- If in contrast $\tau_{(av)}^{(2d)} \ll L_f / v_t$ holds we have to expect the appearance of new two-dimensional nuclei before the growth of the first layers are completed (see Fig. 8.3b). For this poly-nucleus growth model the time $\tau_{(av)}^{(2d)}$ can be calculated according to Nielsen (1964) [603] and Hillig (1966) ([361]; see also Chernov (1980) [132]) from the condition

$$\int_0^{\tau_{(av)}^{(2d)}} J^{(2)} \pi (v_t t)^2 \, dt = 1 \ . \tag{8.45}$$

It determines the average time interval after which on the upper surface of the growing layer, having a surface area $\pi (v_t t)^2$, a new two-dimensional nucleus appears. For steady-state nucleation we obtain from this relation

$$\tau_{(av)}^{(2d)} = \left(\frac{3}{J^{(2)} \pi v_t^2} \right)^{1/3} \tag{8.46}$$

and

$$v_n = d_{cr}\left(\frac{J^{(2)}\pi v_t^2}{3}\right)^{1/3} . \tag{8.47}$$

In contrast to the layer by layer mechanism for poly-nucleus growth a rough interface profile develops in time which is preserved during the further growth (see Fig. 8.4).

A more elaborate analysis of the second of the models discussed was given by Vetter (1967) [886] as well as in the papers by Bertocci (1969) [77], Borovinski and Zindergosen (1969) [92]. Equations (8.38), (8.41), (8.44) and (8.47) yield

$$v_n \propto Z^{(2)} \exp\left(-\frac{\Delta G^{(2/c)}_{(cluster)}}{k_B T}\right) , \tag{8.48}$$

for layer by layer growth and

$$v_n \propto (Z^{(2)})^{1/3} \exp\left(-\frac{\Delta G^{(2/c)}_{(cluster)}}{3k_B T}\right) \tag{8.49}$$

for multi-nucleus growth. If $Z^{(2)}$ is determined mainly by the viscosity of the melt according to Eq. (6.119) and the thermodynamic driving force of the transformation by Eq. (6.65) then we have with Eqs. (8.31) and (8.32)

$$v_n \propto \frac{1}{\eta} \exp\left(-\frac{B_2}{T_m - T}\right) , \tag{8.50}$$

for layer by layer growth

$$v_n \propto \left(\frac{1}{\eta}\right)^{1/3} \exp\left(-\frac{B_2}{3(T_m - T)}\right) \tag{8.51}$$

for multi-nucleus growth. For both cases

$$B_2 = \frac{\pi\sigma^2 d_{cr} N_A}{k_B T_m c_\alpha \Delta s_m} \tag{8.52}$$

holds.

According to the classical concepts given in this section, processes of dissolution of perfect crystal faces proceed via the formation of negative two-dimensional nuclei (holes) in the smooth crystal surface. In this way, a dependence of dissolution rate $v_n^{(-)}$ vs. $\Delta\mu$ similar to the one obtained for growth processes can be derived. From the above equations governing crystal growth via two-dimensional nucleation, it becomes evident that at small under-cooling ($T \rightarrow T_m$) a threshold in the (v_n vs. ΔT)-curves is to be expected. Only by exceeding this threshold should perceptible growth occur.

Quantitative estimates, made by introducing reasonable values for the respective materials constants into above equations, prove that this threshold is reached for values of the relative supersaturation, χ, of the order $\approx 20\,\%$ (compare Eq. (6.54)). However, experimental evidence showed that perceptible crystal growth rates are observed at considerably lower values of the supersaturation (of the order $\chi < 5\,\%$ and even lower). In this way, at the end of the 1940s the experimental evidence on crystal growth began more and more to contradict the theoretical predictions as outlined in the present section. The differences between theoretical predictions and experimental results concerning the growth rate reached an order of magnitude of exp(100) (see Kittel (1969) [458]). A way out of this discrepancy and an explanation of the possibility of perceptible growth even at low supersaturations was found in a remarkable idea formulated by Frank (1949) [227]. According to Frank lattice defects, known as screw dislocations, emerging at a growing crystal face lead to surface structures at the interface providing a constant source of growth sites (cf. also [230]). Frank's ideas of crystal growth mediated by screw dislocations are discussed in the subsequent section.

8.4 Screw Dislocations and Crystal Growth

A screw dislocation emerging on a crystal face is schematically shown in Fig. 8.5. It serves as the origin for the development of crystallization fronts as indicated also in Fig. 8.6. In an isotropic approximation the crystal fronts developed have the form of Archimedean spirals. Archimedean spirals have been frequently observed in optical and electron-microscopic investigations of crystal faces (see Verma (1953) [884] for first observations; Wunderlich (1973–1980) [935] and Geil (1963) [247] for examples in organic polymers; Kaischew, Budevski and Malinovski (1955) [426], Nanev and Kaischew (1979) [590] for growth spirals in electrolyte deposition). These investigations gave the first proof of the validity of Frank's idea. Further evidence giving support to this mechanism may be found in the monographs of Stricland-Constable (1968) [813], Pamplin (1975) [622] and Chernov (1980) [132].

Simple considerations show (Burton, Cabrera and Frank (1951) [114]) that the spiral growth edge developed on the crystal face is stable, when

- The distance δ_s between the spiral coils is larger than the radius of the corresponding two-dimensional nucleus (see Fig. 8.5) and
- The edge of the growth spiral is kinked guaranteeing the existence of a sufficiently large number of growth sites.

In this way there is no need to form a two-dimensional nucleus on the growing interface. The energetic barrier for crystal growth is considerably diminished and growth is observed for supersaturations significantly lower than one would expect it according to the mechanism of two-dimensional nucleation.

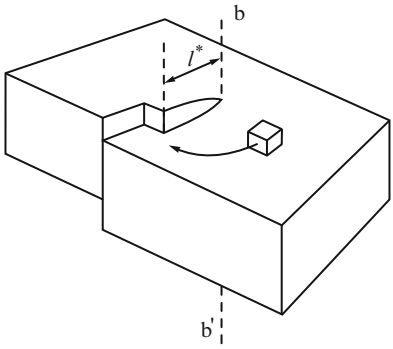

Fig. 8.5 Screw dislocation on a crystal face and mono-atomic growth step formed by it. With *(bb′)* the so-called Burgers vector of the dislocation is indicated

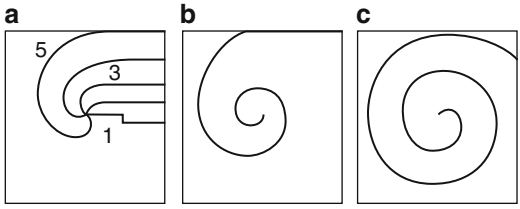

Fig. 8.6 Screw dislocations and crystal growth. The snapshots *(1)–(5)* in (**a**), (**b**) and (**c**) refer to consecutive stages of development of a spiral growth front on the crystal face (After Verma (1953) [884])

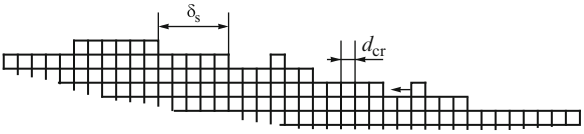

Fig. 8.7 Illustration of the determination of $\gamma_0^{\oplus}$ for growth mediated by screw dislocations. In the figure a perpendicular cut through the growing crystal face is given with a growth spiral formed on it

Following Turnbull and Cohen (1958) [864] the relative number $\gamma_0^{\oplus}$ of growth sites on a crystal face, where a growth spiral has been developed, is given by (see Fig. 8.7)

$$\gamma_0^{\oplus} = \frac{d_{cr}}{\delta_s} \,. \tag{8.53}$$

As an estimate for δ_s for Archimedean spirals, Burton, Cabrera and Frank (1951) [114] found

$$\delta_s = 2\pi R_c^{(2)} = \frac{4\pi\sigma}{c_\alpha^{(2)} \Delta\mu} \,. \tag{8.54}$$

A similar relation for the case of polygonized spirals was given by Kaischew, Budewski and Malinovski (1955) [426]. Considering the special case of relatively low under-cooling Eq. (8.12) yields

$$v_n^{(f/c)} \cong \text{const.}^{(1)} \gamma_0^{\oplus} Z^{(eff)} \Delta\mu \,, \qquad \text{const.}^{(1)} = \frac{d_0^3}{k_B T} \tag{8.55}$$

and a substitution of Eq. (8.54) into this relation gives

$$v_n^{(f/c)} \propto (T_m - T)^2 \qquad \text{for moderate undercoolings .} \tag{8.56}$$

We may conclude that for relatively small undercoolings the growth rate referring to the spiral growth mechanism is proportional to $(\Delta T)^2$.

For large under-cooling (compare Eq. (8.28)) the velocity of normal growth is independent of supersaturation. However, since for dislocational crystal growth $\gamma_0^{\oplus}$ is proportional to $\Delta\mu$ we arrive this time at a linear dependence (v_n vs. ΔT), i.e., at

$$v_n^{(f/c)} \propto (T_m - T) \qquad \text{for large undercoolings .} \tag{8.57}$$

Applying the Skapski-Turnbull rule in the determination of σ from Eqs. (8.53) and (8.54) both parameters δ_s and $\gamma_0^{\oplus}$ can be calculated. An estimate shows that for $T \to T_g$ values of $\gamma_0^{\oplus}$ in the range from 0.05 to 0.1 are found, which guarantees relatively high growth rates. The temperature dependence of the rate of dissolution of crystals containing screw dislocations can be determined in the same way, provided the spiral front is not destroyed in the process of dissolution. Consequently, also for dissolution processes a relation $v_n \propto (\Delta T)^2$ has to be expected for medium supersaturations.

8.5 Further Developments of the Basic Models: Diffusive Melt-Crystal Interfaces, Transient Effects in Two-Dimensional Nucleation and Crystal Growth

In the theory of crystal face structures a distinction is made between singular and non-singular equilibrium crystal faces (see Landau, Lifshitz (1969) [494]). Singular faces have low crystallographic indices and they are atomically smooth. Non-singular (or vicinal faces) are highly indexed, they are atomically rough.

Burton and Cabrera (1949) ([113]; see also Burton, Cabrera and Frank (1951) [114]) demonstrated the possibility of a singular – non-singular transition for a crystal face in contact with its own vapor by applying a simple mean-field model. According to their derivations a critical temperature, the roughening temperature $T_{(rough)}$, should exist where the atomically smooth singular equilibrium face is transformed into an atomically rough non-singular face. This idea was also connected with the problem of surface melting (for further results see Nenov (1984) [599]; Nenov and Trayanov (1989) [600]) and widely discussed subsequently. Transformations of facetted crystal shapes into skeleton or dendritic forms and problems of the stability of crystal faces are also discussed in Nanev's review (1994) [591].

For our analysis, the most significant aspect of this development is that the theory predicts criteria for the existence of thermodynamically stable but atomically rough surface structures, allowing growth via the normal growth mode. In this way,

new dimensions for the classical continuous growth models are opened. From a morphological point of view, the transition singular – non-singular face is connected with a transformation from a polygonized equilibrium shape of the crystal to non-faceted crystal forms (in the limiting case, to a sphere). It was Jackson (1958) ([393]; see also Jackson, Uhlmann and Hunt (1967) [398]) who developed the first simple but realistic mean-field model of the melt-crystal boundary predicting a roughening transition at the melt-crystal interface.

A more elaborate model was soon developed by Cahn (1960) ([115]; see, in addition, Cahn, Hillig and Sears (1964) [120] but also the critical remarks of Jackson et al. (1967) [398]). An atomistic model derived by Temkin (1962) ([828]; see also Chernov (1980) [132]) followed as well as numerous computer simulations of this phenomenon. According to Cahn's theory it is to be expected that a diffusive layer is developed at the crystal-melt interface. The thickness of this layer is determined thermodynamically, it depends on the value of the parameter $\Delta S_m/R$ and on the undercooling. The macroscopically observable morphological instability (non-singular crystal faces, rounded crystal shapes) is connected with the formation of the diffusive interfacial layer (see the experimental evidence in this respect summarized by Jackson et al. (1967) [398]). For $\Delta S_m/R < 2$ a diffusive atomically rough interface develops with rounded crystal faces. In this case, a continuous mode of growth should be expected to occur for any temperature T below T_m.

Surface nucleation and screw dislocation mediated growth dominate for substances with high values of the molar entropy of melting ($\Delta S_m/R > 4$). For substances having values of this ratio in the range ($2 \leq \Delta S_m/R \leq 4$) an intermediate type of behavior is found. For low values of the under-cooling the crystal faces remain atomistically smooth. Only after a certain critical under-cooling is reached is a transition from smooth to rough surface structures found. This transition is accompanied by a transition from dominating lateral (mediated by two-dimensional nucleation or screw dislocations) to normal growth. The value of the critical undercooling is determined hereby mainly by the parameter $\Delta S_m/R$. Below the transition temperature $T_{(rough)}$ the thickness of the diffusive layer changes dependent on the undercooling. As a result the parameter γ_0 also varies.

The decisive role of the parameter $\Delta S_m/R$ for growth and dissolution can be understood taking into account that this parameter represents a measure of the similarity respectively dissimilarity of the structures of melt and crystal. For melts iso-structural with their own crystal, as it is the case for most metals, $\Delta S_m/R \approx 1$ holds (see Ubbelohde (1965) [871], [125] and Chap. 3) and continuous growth modes are, in fact, observed. If melting is accompanied by more significant structural changes, higher values of this ratio are found. Thus for substances going over from the melt into the solid phase by reconstructive crystallization (cf. Sect. 4.10) significantly higher values of $\Delta S_m/R$ are found and, as a rule, lateral crystal growth modes are observed experimentally.

Another generalization of the theoretical considerations outlined above consists of the incorporation of non-steady state effects into the model of two-dimensional nucleation and the determination of its importance for nucleation-mediated crystal growth. For the first time this problem was formulated by Lyubov (1966) [517].

A detailed analysis was given somewhat later by Gutzow and Toschev (1970) [319] for the classical layer by layer growth model and by Stoyanov (1973) [804] for the multi-layer growth mode. If the time-lag in two-dimensional nucleation is defined similarly to Eqs. (6.189) and (6.110) as

$$\tau^{(2/ns)} = \frac{a_0 k_B T}{w^{(+)}(j_{(2/c)})} \left| \left(\frac{\partial^2 \Delta G^{(2)}_{(cluster)}}{\partial j^2} \right)_{j=j_{(2/c)}} \right|^{-1} = \frac{a_0}{2\pi w^{(+)}_{(2)}(j_{(2/c)}) \Gamma^2_{(2/z)}} \tag{8.58}$$

then, e.g., for the layer by layer growth mode the average time interval between two successive nucleation events $\tau^{(2d)}_{(av)}$ (cf. Eq. (8.43)) may be approximated in analogy to the three-dimensional case by

$$\tau^{(2d)}_{(av)} \cong \tau^{(2/ns)} + \frac{1}{J^{(2)} L^2_f} \,. \tag{8.59}$$

A substitution into Eq. (8.44) yields

$$v_n \cong J^{(2)} L^2_f d_{cr} \left(\frac{1}{1 + J^{(2)} L^2_f \tau^{(2/ns)}} \right) \,. \tag{8.60}$$

It turns out that for relatively small under-cooling ($1 \gg J^{(2)} L^2_f \tau^{(2/ns)}$) the classical expression, Eq. (8.44), derived by Kaischew holds. In the opposite case of large under-cooling in the vicinity of T_g, in contrast,

$$v_n \cong \frac{d_{cr}}{\tau^{(2/ns)}} \tag{8.61}$$

is obtained. In this limiting case, the growth rate is determined mainly by the time-lag for two-dimensional nucleation. A substitution of Eq. (8.58) into the above expression and a comparison with the derivations, outlined in Sect. 8.2, shows that in this case growth proceeds via the normal growth mechanism. Thus, it becomes evident that, in general, non-steady state effects in two-dimensional growth modify the growth mechanism (Gutzow and Toschev (1970) [319]). However, in contrast to nucleation theory, time does not enter the equations explicitly. The same conclusion can be also drawn with respect to the multi-layer growth mode analyzed by Stoyanov.

Another point of further development and discussion is connected with the determination of the temperature dependence of the impingement rate, Z. In classical approximations, applied at part also in above given derivations, a relation of the form $Z \sim 1/\eta$ is assumed. From a more detailed analysis of layer growth it has, however, to be expected that the incorporation of ambient phase particles into a given growth site is determined not only by the direct impingement from the bulk (the mobility of the ambient phase particles) but also could involve drift processes

of the particle adsorbed at the interface. As a consequence, in the calculation of the effective transition frequency melt-crystal the particular properties of such adsorbed ambient phase molecules also become important (see e.g. Chernov (1980) [132]; Avramov, Grantcharova, and Gutzow (1981, 1988) [28, 30]).

Avramov et al. (1988) assumed that the activation energy for diffusion of the ambient phase molecules at the melt-crystal interface U_i can be expressed as

$$U_i \cong (1 - x)U_{bulk} + xU_{surf} \,, \tag{8.62}$$

where by U_{bulk}, the activation energy for viscous flow in the bulk, and by U_{surf}, the activation energy for diffusion at the interface are denoted. x in above equation is an adjustable parameter. According to current concepts (see Burton, Cabrera, and Frank (1951) [114]; Chernov (1980) [132]) it is commonly assumed that

$$U_{surf} = \left(\frac{1}{5} - \frac{1}{6}\right) U_{des} \tag{8.63}$$

holds. U_{des} is the energy of desorption, it has a value of the order of the energy of sublimation. In application of this estimate to crystallization phenomena in metallic melts or to ionic structures, where the activation energy for surface diffusion is always lower than U_{des}, effective values of U_i lower than the value of U_{bulk} are found.

However, for many systems like As_2O_3, sulfides and oxides it turned out in contrast that $U_{surf} > U_{des}$ holds. In these cases a motion of the adsorbed particles on the crystal face would result in higher effective activation energies (cf. Knacke and Stranski (1952) [459]). Such considerations may give an explanation of the experimental finding that in many cases the activation energy for crystal growth of glass-forming melts determined experimentally is considerably lower than the activation energy for viscous flow in the bulk in the same temperature range. This result is also an indication that the analysis of crystal growth data in coordinates, where the activation energy of viscous flow is introduced as a decisive characteristic, may be quite misleading.

8.6 Modes of Crystal Growth in Chain-Folding Polymer Melts

The structure and mechanisms of nucleation of chain-folding polymers have been discussed already in Sects. 4.6, 4.9 and 6.3.8 with particular attention directed to organic chain-folding polymers. The same physical models as employed for the description of nucleation of chain-folding polymers have been applied also to a study of the further growth of the lamellae forming the spherulites which are the typical morphological elements of organic polymer melt crystallization (see Fig. 8.8). The lamellae in spherulitic growth as well as the plate-like single

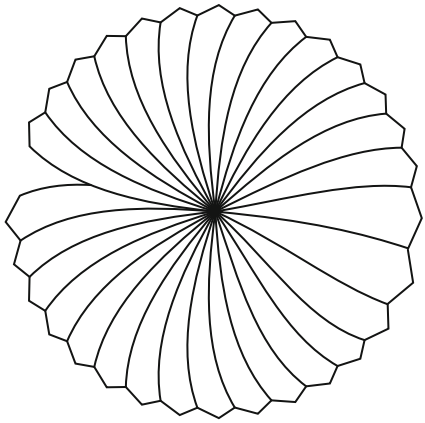

Fig. 8.8 Morphology of a spherulite formed in an organic high polymer melt. The spherulite is constituted by lamellae growing in a radial direction from a common center, formed initially by nucleation processes as discussed, for example, in Sect. 6.3.8

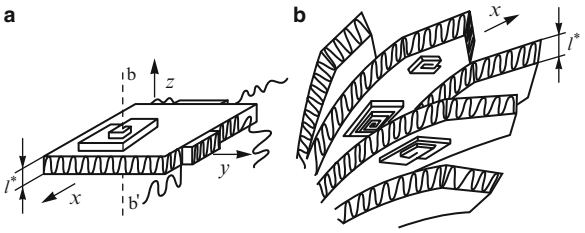

Fig. 8.9 Illustration of possible modes of polymer crystal growth. (**a**) A plate-like polymer crystal of thickness, l^*, growing in the $x - y$-plane via the formation of two-dimensional regular reentry nuclei. With *(bb′)* the position of the Burgers vector of a screw dislocation is indicated around which a growth front could have been developed. Screw dislocation growth fronts can be formed only on flat non-growing surfaces of the lamellae. (**b**) Polymeric lamellae growing from a common spherulitic center

crystallites growing preferably from dilute polymer solutions consist of folded polymer chains of thickness, l^*, which is determined by the actual supersaturation in the system (see Figs. 6.18 and 8.9).

A detailed discussion of spherulitic growth and of other morphological elements of polymer crystallization may be found in the literature (Geil (1963) [247]; Mandelkern (1964) [528]; Price (1969) [646]; Wunderlich (1973–1980) [935]). In the physics of polymer melt crystallization it is usually assumed that formation of two-dimensional polymeric nuclei at the growing crystal faces is the typical (or even the only) mode of growth of polymer crystals. Lauritzen and Hoffman ((1959 [498], 1960 [499]); see also Frank and Tosi (1961) [229]) developed a theory of formation of two-dimensional polymer nuclei (see Fig. 8.9a) being a prerequisite of the growth of the polymer crystal. This model resembles, to some extent, the already discussed mode of growth by two-dimensional nucleation developed for low molecular substances. However, in comparing the previously discussed models with growth in polymer melts, one has to take into account that

- Two different specific interfacial energies, the specific end energy σ_b and the lateral energy σ_s (cf. Sect. 6.2.2), have to be accounted for in considering polymer nucleation and growth,
- The tangential spreading of two-dimensional nuclei is possible only into two directions normal to the chain-folding (Fig. 8.9a),
- The growth of the crystallites via two-dimensional nucleation is possible only into the directions indicated in Fig. 8.9a by x and y. A thickening of the crystallite proceeds through complicated mechanisms, it is a very slow process and requires separate considerations,
- The same molecule may form many two-dimensional nuclei. Entanglements between the coils of one and the same molecule or in between different molecules play a major role in the determination of the essential factors governing two-dimensional nucleation.
- The thermodynamic barrier of two-dimensional nucleation is given in analogy to Eq. (8.36) by

$$\Delta G^{(2/c)}_{(cluster)} = \frac{\omega \sigma_b \sigma_s}{(\Delta\mu)^2} \,. \tag{8.64}$$

  Together with Eq. (6.199) for the three-dimensional case it allows one the determination of σ_b and σ_s, provided both $\Delta G^{(2/c)}_{(cluster)}$ and $\Delta G^{(c)}_{(cluster)}$ are known from experiments on polymer nucleation and growth.

These conclusions can be verified from the following considerations.

Suppose that a screw dislocation emerges on a polymer crystal plane as shown in Fig. 8.9a or b. In order to allow a growth the height of the spiral coils should be approximately equal to l^*: only in this way a growth into the z-direction, i.e., a thickening of the crystals could take place. However, the directions of rapid growth are located in the $x-y$-plane. On these rapidly growing lateral planes the formation of screw dislocational growth fronts is excluded, even if screw dislocations occur. As outlined in Sect. 8.4 there is some limitation on the distance between the coils of a stable crystal growing by spiral growth. As the thickness of the crystal plate is of the order of l^* growth spirals should be either larger than the growth front (see Fig. 8.10) or they should violate the theoretical requirements for stable growth. Both conditions are unacceptable from a physical point of view. For the description of the process of formation of two-dimensional nuclei all three models of chain-folding are applied as already mentioned in Sect. 6.3.8 (Keller's direct reentry chains, Fisher's irregular reentry model and Flory's switchboard model (see Fig. 6.18)).

8.7 Experimental Investigations on the Mechanisms of Crystal Growth in Glass-Forming Melts

Going over to a comparison between the outlined theoretical approaches in the description of crystal growth from melts and the experimental observations it can be noted that it was, again, Tammann (1903 [817], 1922 [818]) who made the

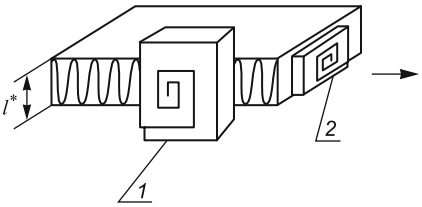

Fig. 8.10 Illustration of the conclusion that dislocational spirals cannot develop on the growth front of a polymer chain-folding crystal. The number *(1)* indicates a growth spiral having the necessary inter-coil distance allowing a further growth. The number *(2)* shows a growth spiral with a size adjusted to the growing crystal front, it has inter-coil distances lower than required for a stable growth

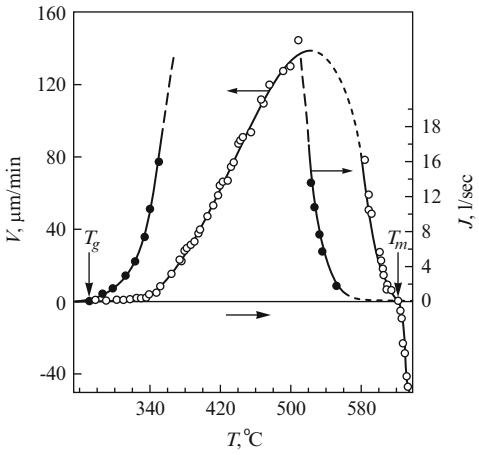

Fig. 8.11 Temperature dependence of the rates of nucleation, J, and crystal growth, v, in under-cooled $(NaPO_3)_x$-melts. *Open circles*: crystal growth and (above the melting point) dissolution rates of $\alpha - NaPO_3$ from its own melt (according to Gutzow and Konstantinov (1970) [314]); *black dots*: nucleation frequency in undercooled $NaPO_3$-droplets (Grantcharova and Gutzow (1990) [269])

first steps in this direction. Tammann used a number of low melting model organic glass-forming substances to determine the temperature dependencies of the rates of nucleation and linear growth v. An example in this respect is given in Fig. 6.8.

The well-expressed maximum in the $v(T)$-curves, as it is to be expected from the theoretical considerations given above, was the most essential feature of these early results. As discussed in detail above, the maximum occurs as the result of two opposite tendencies, the increase in the thermodynamic driving force of the transformation on one hand and the decrease in the mobility (increase in the viscosity of the melt) on the other. Figure 8.11 gives an example of a thorough investigation of the temperature dependence of the rates of crystal growth and dissolution of a simple and convenient for experimental studies glass-forming model substance $(NaPO_3)_x$ (Graham's glass). Measurements of the nucleation frequency for the same substance are also shown.

Experiments for a determination of the particular mechanisms of crystal growth were carried out as a further step after the basic ideas concerning possible crystal growth modes were formulated. Based on their investigations of the temperature

dependence of the growth rates of glycerol, Volmer and Marder (1931) [895] concluded that the growth of this substance may be described as being mediated by two-dimensional nucleation. However, subsequent analysis showed that, at least for lower under-cooling, growth by screw dislocations prevails in this case (see Turnbull and Cohen (1960) [865]).

The first experimental example where growth mediated by two-dimensional nucleation was comparatively unambiguously established experimentally – characterized by a threshold in the supersaturation which has to be surpassed to initiate growth – was described by Danilov and Malkin (1934) [151]. In these investigations, salol was used as a model substance. A series of further experimental investigations on crystal growth mechanisms was initiated by the formulation of the theory of spiral growth. Typical experimental work of this period was summarized by Hillig and Turnbull (1956) [362]. Similarly considerable efforts have also been directed to the investigation of the mechanism of normal growth after its theoretical reformulation by Jackson (1958) [393], Cahn et al. (1964) [120] and Temkin (1962) [828].

The kinetics of crystallization of more complicated (mainly silicate) multi-component glass-forming systems was studied simultaneously with the investigation of the simple model one-component organic melts. From the first investigations in this direction performed by Zschimmer and Dietzel (1926) [961] (although they have been more of a technological orientation) the temperature dependence of the growth rate of silicate glasses and their dependence on composition were deduced for the first time.

Of particular importance in this respect are also the papers by Preston (1940) [645] and Swift (1947) [814]. In Swift's article for the first time in addition to growth modes also processes of dissolution of crystals in the melt were analyzed based on experimental results. Crystal dissolution experiments are of considerable importance for the determination of the mode of growth respectively dissolution at small under-cooling. Moreover, such investigations allow one a precise determination of the melting or liquidus temperatures. The main experimental problem which has to be solved in performing crystallization experiments in under-cooled melts is to maintain the interface melt-crystal at a temperature, at least, nearly equal to the temperature of the melt. In this direction, capillary techniques have proven to be very useful.

In classical modifications of the capillary technique crystallization in thin-bored capillary tubes or in between two parallel glass slides ("two-dimensional capillary") is investigated. A detailed analysis of experimental techniques employed, methodological problems and possible solutions can be found in a review article by Gutzow ((1977a) [299]; see also Gutzow (1977b) [300]). In metallic or metal-like under-cooled glass-forming melts with rapidly growing crystal fronts, the heat of crystallization cannot be dissipated at sufficiently high rates and instead of the well-expressed maximum of the $v(T)$-curves a temperature region is observed where the growth of the crystal front is determined not by the actual value of the under-cooling but by the latent heat and by the rate of the processes of heat conduction (see Tammann's saturation plateau curves given on Fig. 8.12). In typical glass-forming

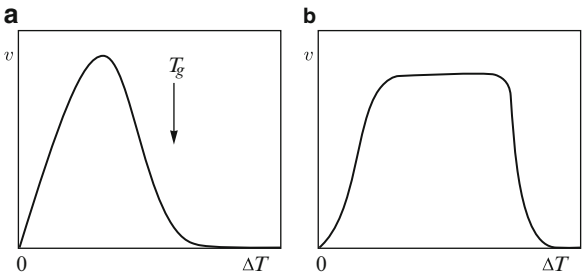

Fig. 8.12 Rates of linear growth, v, for the crystallization of under-cooled melts (schematically). (**a**) Normal type of temperature dependence when the temperature of the melt-crystal interface is the same as in the bulk of the melt. (**b**) Tammann's saturation plateau type curve for rapidly crystallizing substances. In the range corresponding to the plateau the growth rate is dominated by the latent heat of crystallization and processes of heat conduction and not by the under-cooling

melts, crystal growth rates are so low that, as a rule, the normal Tammann $v(T)$-curves with a well-expressed maximum determined by the degree of under-cooling are found.

In interpreting experimental $v(T)$-curves, one has to take into account, however that although the analysis of these curves allows us to draw certain conclusions concerning the type of possible modes of growth the results are, in general, mostly far from being fully convincing. This conclusion is connected from a theoretical point of view with the different possibilities how the impingement rate Z varies with temperature (see Sect. 8.5). Moreover, also for the temperature dependence of the thermodynamic driving force, $\Delta\mu$, of the transformation different dependencies can be expected depending on the structure of the melt and the ratio $a_0 = \Delta C_p(T_m)/\Delta S_m$ (cf. Sects. 3.7 and 6.2.3).

In most cases, especially when the complex structures of silicate, borate and phosphate glasses are to be considered, the determination of the structural unit taking part in flow and restructuring processes at the interface, the definition and the choice of ΔS_m and, thus, of the relevant temperature dependence of $\Delta\mu$ can be more than arbitrary. These circumstances have been completely ignored by many authors and are also not accounted for in the $v(T)$-analysis performed by Jackson, Uhlmann and Hunt (1967) [398]. The same difficulties arise when molar values of the melting entropy are used to estimate, in accordance with the $\Delta S_m/R$-criterion proposed by Jackson, Cahn and others, the conditions for the appearance of a diffusive crystal-melt interface and morphological instabilities.

These considerations are the reason why in under-cooled melts the specification of the type of growth modes should rely mostly on the analysis of the $v(T)$-curves at small under-cooling and especially on a comparison of the growth and dissolution rates (see Gutzow (1977) [299, 300]). If growth and dissolution proceed in a symmetric way with respect to $\Delta\mu$ for the three growth mechanisms discussed above a dependence of the growth rate v on $\Delta\mu$ is to be expected as shown in Fig. 8.13. For processes of growth on substrates by condensation from

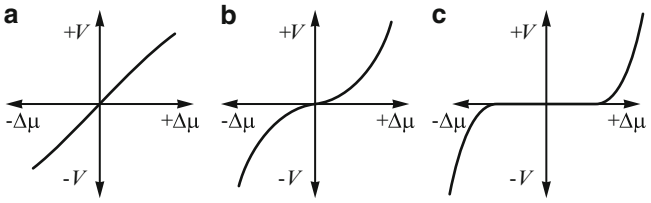

Fig. 8.13 Symmetrical with respect to the value of the chemical potential difference curves for the rates of growth and dissolution of crystals for the different growth mechanisms discussed above. $+v$: rate of growth; $-v$: rate of dissolution; (**a**) normal growth, (**b**) spiral growth, (**c**) two-dimensional nucleation. As far as the process of direct incorporation and dissolution of particles proceeds on the same sites for normal growth the same linear dependence is to be expected for growth and dissolution. Spiral growth or dissolution starts with relatively low absolute values of $\Delta\mu$, while for growth mediated by two-dimensional nucleation a threshold has to be reached, before perceptible growth takes place. Such symmetric curves are found experimentally only for small supersaturations

the vapor phase such a symmetry is, indeed, observed (see Stricland-Constable (1968) [813]). The same conclusion is valid with respect to melt crystallization and dissolution experiments with relatively large crystals. As an example in this direction the results of Gutzow and Pancheva (1976) [315] can be mentioned where the growth of superheated gallium crystals in two-dimensional capillaries was analyzed experimentally and a symmetric growth-dissolution behavior was found. However, the dissolution of initially faceted crystals begins at corners or edges where a weaker bonding of the molecules to the crystal is to be expected. Therefore, a rounded crystal shape and atomically rough melt-crystal interfaces develop and a dissolution law corresponding to that of normal growth is found even at low superheatings (see Fig. 8.14). In such a case, for spiral growth, a parabola (for growth) is replaced for negative values of $\Delta\mu$ by a straight line representing normal mode dissolution.

The same result is obtained also in growth and dissolution experiments with glass-forming substances. The thin needle-like crystallites typically observed in devitrified glasses rapidly develop a rounded non-equilibrium crystal-melt interface and the normal mode of dissolution is observed (see Fig. 8.14a, b). For such cases, the dissolution proceeds always via the normal mode independent of the mode of growth (see Fig. 8.14c). The first experimental investigations concerning the mechanism of growth and dissolution of crystals in typical silicate and oxide glass-forming melts seemed to indicate a normal mode as exemplified on Fig. 8.15. Further investigations confirmed the normal growth and dissolution mode also for a number of other glass-forming substances with low values of the molar entropy of melting. In Fig. 8.16, rates of growth and dissolution of two such cases for temperatures in the vicinity of the melting temperature T_m are shown. Most of the substances for which continuous growth was observed have values of the molar entropy of the order $\Delta S_m/R < 2$. Gutzow and Pancheva (1976) [315] showed that

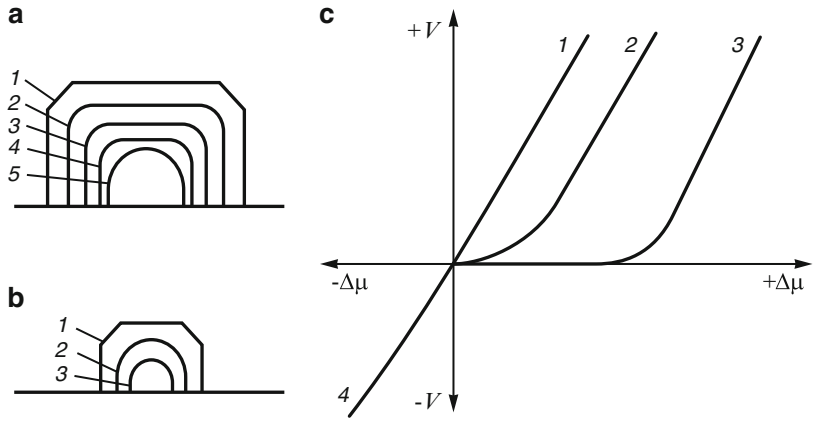

Fig. 8.14 Dissolution morphology of a large crystal front (**a**) and of small crystallites (**b**): the formation of a rounded melt-crystal interface and consecutive stages of dissolution are shown by the numbers *(1)*, *(2)*, ... *(5)*. (**c**): $v(T)$-curves corresponding to normal *(1)*, dislocational *(2)* and to growth mediated by two-dimensional nucleation *(3)*, while dissolution proceeds via the normal mode *(4)*

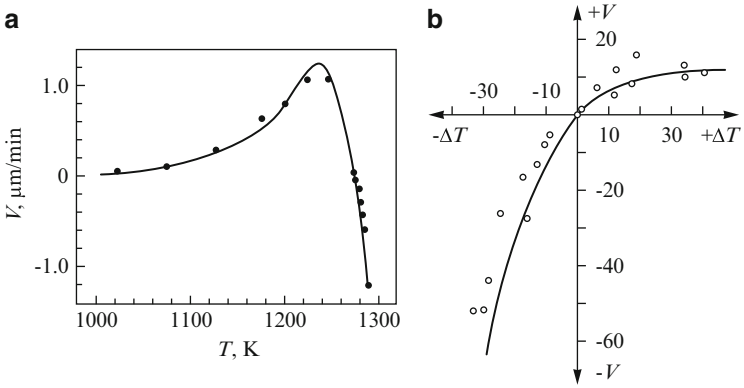

Fig. 8.15 Results of the first investigations of the temperature dependence of growth and dissolution rates in typical glass-forming melts. (**a**) Rates of crystal growth and dissolution in a $Na_2O-CaO-SiO_2$ melt (Swift (1947) [814]); (**b**) Crystallization of tetragonal P_2O_5 from its own melt according to Cormia et al. (1963) [147] (See also Rawson (1967) [657])

even in growth and dissolution of CBr_4 (with $\Delta S_m/R = 1.2$) absolutely spherical crystals are formed developing according to the normal growth mode.

From a structural point of view the SiO_2-crystal phase cristobalite can be considered as being formed of a rigid three-dimensional network, going through the melt-crystal interface. This is the reason why, for SiO_2, a continuous growth mechanism has also been predicted from a purely structural point of view (see Cooper (1971, 1977) [142–144]). Applying Jackson's criteria for normal growth,

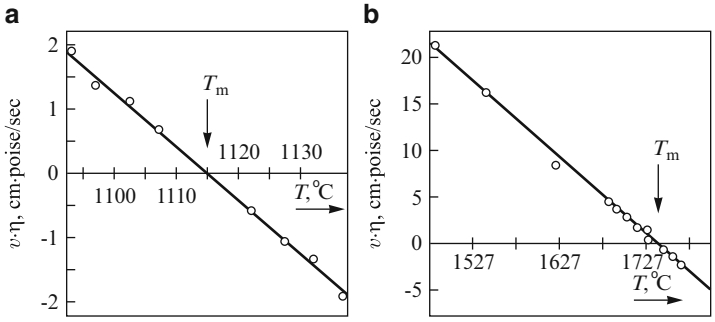

Fig. 8.16 Continuous growth and dissolution kinetics of simple glass-forming melts: results of detailed measurements in the vicinity of T_m. (**a**) Crystallization of GeO_2 according to Vergano and Uhlmann (1970) [885]; (**b**) Growth and dissolution of cristobalite ($\Delta S_m = 0.6\,\mathrm{R}$) from a SiO_2-melt (Wagstaff (1969) [905])

some of the considered examples (SiO_2, GeO_2) should belong to substances where a diffusive crystal-melt interface is to be expected. However, in some cases, e.g., for P_2O_3 and $Na_2B_4O_7$, the respective criterion is not fulfilled since values of the molar entropy of $\Delta S_m/R = 3.4$ (for P_2O_5) and $\Delta S_m/R = 8.6$ are found.

An explanation of this discrepancy in the theory can be given taking into account that the structural unit determining the process of crystallization must not be identical with the molar composition. In crystallization of sodium borate melts, for example, the structural unit determining diffusion and transport through the crystal-melt interface is much smaller than $Na_2B_4O_7$ (see also Gutzow (1977b) [300]). It turns out that the Jackson criterion has to be applied to glass-forming melts with caution. Only in cases when the real structural units involved in the transformation are described by the gross formula of the substance under consideration (noble gases, metals, oxides) is the molar value of ΔS_m a real criterion for the determination of the growth mode. The first case where reliable experimental evidence on spiral growth in a typical glass-forming melt was reported seems to be the paper by Meiling and Uhlmann (1967) [551] on crystallization of $Na_2O \cdot 2SiO_2$. The results of Meiling and Uhlmann and additional evidence for this mode of growth are shown on Fig. 8.17.

In each of the cases given in Fig. 8.17, a parabolic temperature dependence of the growth rate in coordinates v vs. ΔT and a linear dependence for dissolution is observed. Consequently, in $\sqrt{v}$ vs. ΔT coordinates straight lines for the temperature dependence of the crystal growth rate are found (see Fig. 8.18). Spiral growth is generally observed for substances with high values of the molar entropy of melting, characterized, in addition, by considerable differences in the structure of the melt and the crystalline phase. Clearly faceted interfaces are always observed in cases when such lateral growth modes are obtained (reconstructive crystallization).

It turns out, consequently that the growth of real crystals in typical glass-forming melts proceeds in two ways:

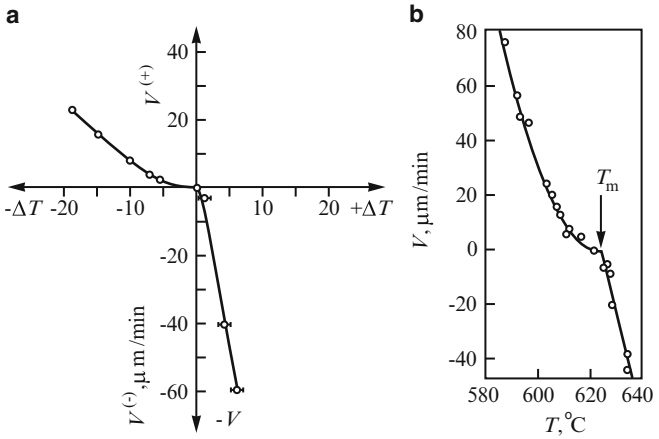

Fig. 8.17 Typical examples for growth by screw dislocations: Parabolic dislocational growth and linear dissolution according to the normal mode. (**a**) Data of Meiling and Uhlmann (1967) [551] on $Na_2O \cdot 2SiO_2$; (**b**) Dislocational growth and continuous dissolution of the anionic chain-polymer glass ($LiPO_3$) according to Avramov, Pascova et al. (1979) [27]

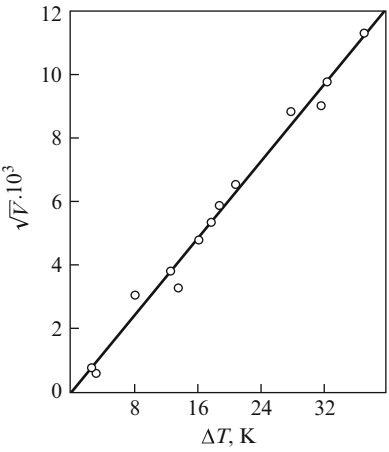

Fig. 8.18 Experimental verification of the dislocational mechanism of growth (data on spiral growth in $NaPO_3$-melts). In accordance with Eq. (8.56) in coordinates $v^{1/2}$ vs. ΔT a straight line is observed for the temperature dependence of the growth rate of $\alpha - NaPO_3$ from its own melt at small under-cooling

- For cases when crystal and melt have a similar structure and the formation of a diffusive melt-crystal interface becomes possible, continuous growth prevails;
- When crystallization is connected with structural changes (as it is found for inorganic anionic chain polymers like $NaPO_3$, $LiPO_3$, $Na_2Si_2O_5$ etc. (see also Sect. 4.10)) as a rule, dislocational growth is observed.

The third of the discussed theoretically possible growth mechanisms – via the formation of two-dimensional nuclei – can be obtained only if precautions are undertaken to prepare really perfect crystals free of dislocations. Thus, it seems

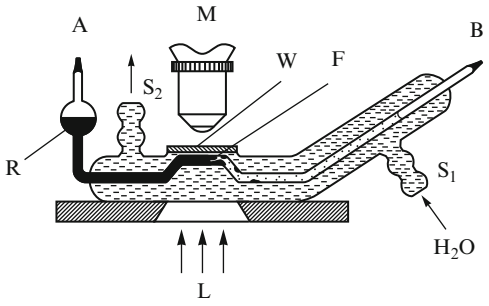

Fig. 8.19 Crystallization cell with glass capillary in which the mode of growth mediated by two-dimensional nucleation was demonstrated for $Na_2S_2O_3 \cdot 5H_2O$: *A, B* – sealed glass capillary; *W* – optical window; S_1, S_2 – input and output for thermostat water; *F* – advancing crystal front. A seed crystal was initially introduced at *R* (According to Gutzow, Razpopov, and Kaischew (1970) [324])

as if many of the initial claims made for a verification of this growth mechanism have to be rejected.

Experiments with simple molecular organic melts (the already mentioned case of salol or the results obtained by Gutzow et al. (1972) [326] for thymol) showed that only in melts purified by multi-fold vacuum distillation in which possible lattice defects have been eliminated by prolonged heat treatments can a threshold in the $(v(T)$ vs. $\Delta T)$-dependence be found, being the most typical characteristic feature of surface nucleation mediated growth. Also the opposite conclusion is obviously true: If growth proceeds by two-dimensional nucleation then the crystal has a perfect lattice structure.

A detailed analysis of the possibility of verification of the surface nucleation of growth in melt crystallization was performed by Gutzow, Razpopov and Kaischew (1970) [324]. A simple low-melting glass-forming system ($Na_2S_2O_3 \cdot 5H_2O$ with a melting temperature of about 48 °C) was chosen as the model substance. Growth and dissolution were analyzed by applying the already mentioned capillary technique. An important advantage of this technique consists of the possibility of producing dislocation-free mono-crystals as was demonstrated by Budewski et al. (1966) ([107]; see also Kaischew and Budewski (1967) [421]) in an investigation of electrolytic growth of silver single crystals in glass capillaries. In these investigations for the first time a direct experimental verification of the mode of growth mediated by two-dimensional nucleation was given. The capillary technique in this new version – as a method for producing dislocation-free crystals – was applied by Gutzow et al. (1970) [324] by means of an apparatus shown in Fig. 8.19 (for the details see the original paper). The experimental results obtained are presented in Fig. 8.20.

At the beginning of each of the series of measurements on initially defect crystal faces the growth velocity of the $Na_2S_2O_3 \cdot 5H_2O$-front depends on under-cooling according to a parabolic relationship as given with curve 2 on Fig. 8.20a. However, after a prolonged growth in the capillary tube at small under-cooling, the crystallization velocity decreases as a rule, reaching with time immeasurably

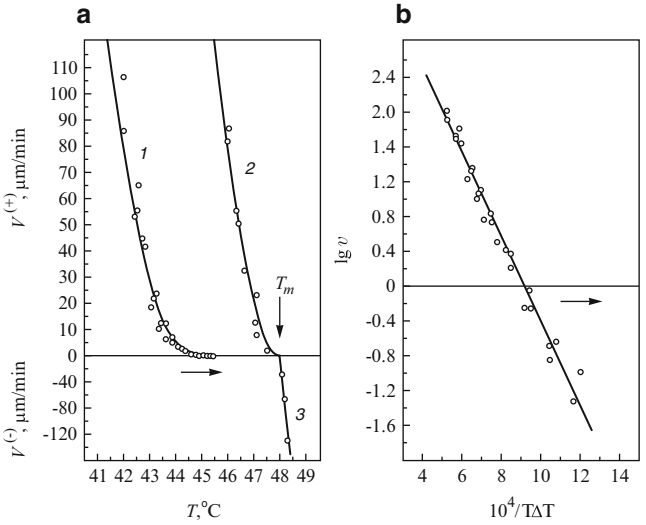

Fig. 8.20 (**a**) Growth and dissolution rates as functions of temperature for α-$Na_2S_2O_3 \cdot 5H_2O$ crystals: *(1)* Perfect crystal with a growth mode mediated by two-dimensional nucleation; *(2)* Mechanically damaged crystal growing via spiral growth; *(3)* Dissolution of rounded crystals by normal growth. The experimental data are taken from Gutzow et al. (1970) [324]. (**b**) Temperature dependence of the growth rate mediated by surface nucleation (curve *(1)* from (**a**)) in coordinates ($\log v$ vs. $1/T\Delta T$)

low values. Single crystals treated in such a way exhibit perceptible growth only at higher under-cooling as it is seen from curve 1 in the same figure. This shape of the $v(T)$-curve is typical for growth mediated by two-dimensional nucleation. Thus, similarly to the results of Budewski et al. [107] the possibility of such a growth mode was demonstrated also for crystallization of glass-forming melts.

A mechanical damage of the dislocation free crystal faces inside the capillary leads almost immediately to a growth behavior as represented by curve 2 in Fig. 8.20, i.e., to growth mediated by screw dislocations. It could not be decided finally whether the growth of the $Na_2S_2O_3 \cdot 5H_2O$-crystals proceeds by layer for layer or by multi-nucleus modes of growth, though it seems as if some preference should be given to Hillig's polynucleus model (see Gutzow et al. (1970) [324]). It should be mentioned also that Wunderlich (1980) [935] obtained results for growth and dissolution of organic polymers giving a direct proof for the two-dimensional nucleation model of growth.

Summarizing, the investigations mentioned have shown that

- Continuous growth mechanisms prevail in crystallization of glass-forming melts when melt and crystal have a similar structure;
- In all other cases, dislocational growth modes dominate as the rule;
- Two-dimensional nucleation in undercooled melts can be observed only when measures are undertaken to eliminate dislocations, i.e., to obtain perfect crystals.

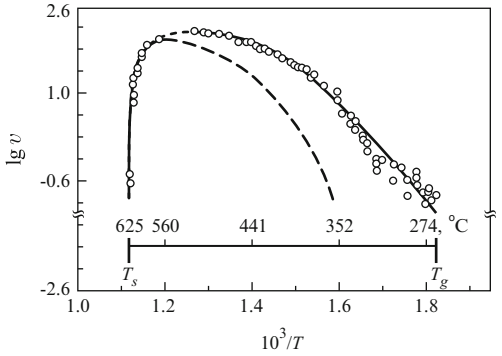

Fig. 8.21 Temperature dependence of the rate of linear growth of $\alpha - NaPO_3$ from its own melt in coordinates $\log v$ vs. $1/T$. The growth rate determined experimentally is given by a *full line*. The theoretical prediction obtained according to the dislocational growth mechanism when viscosity data are used for the determination of the impingement rate Z is shown by a *dashed curve*

On the other hand, the occurrence of growth mediated by two-dimensional nucleation is an indication that a perfect crystal grows.

The analysis of the mechanism of crystal growth for higher values of the supersaturation has to be carried out with caution. As an example, in Fig. 8.21, the linear rate of crystal growth of $\alpha - NaPO_3$ is shown in coordinates ($\log v$ vs. $1/T$).

As shown in Figs. 8.11, 8.17 and 8.18 for small under-cooling dislocational growth dominates for this substance. This implies that according to Eq. (8.56) we should expect a dependence of the type

$$v \propto \frac{(T_m - T)^2}{\eta} \,. \tag{8.65}$$

If this dependence is extrapolated to lower values of temperature the temperature dependence of the growth rate should be determined mainly by the steep increase in the viscosity. However, comparing the results of the temperature dependence of the growth rate with the respective dependence of the viscosity of the same substance it turns out that the rate of growth of $NaPO_3$ cannot be described by applying the relation $Z \propto 1/\eta$ (see Avramov et al. (1987) [29]). In contrast,

- Much smaller values for v are obtained applying Eq. (8.65) (dashed line in Fig. 8.21) as compared with the experimental data;
- Much smaller activation energies are found experimentally for the growth rate as compared with the data for the viscosity vs. $1/T$-dependence.

The observed deviations between experimental curves and theoretical predictions can be interpreted in terms of the considerations given by Avramov et al. (1988) [30] and discussed in Sect. 8.5.

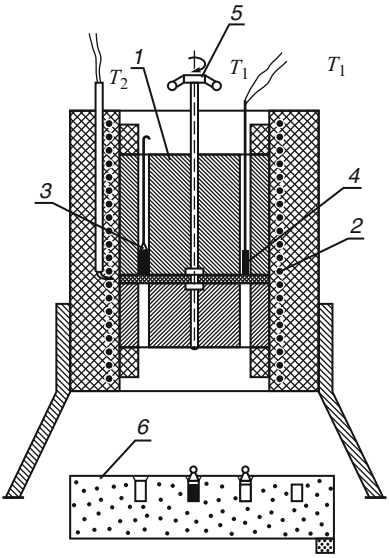

Fig. 8.22 Revolver-type crystallization furnace. *(1)*: metallic block with eight sample holding tubes; *(2)*: revolving metallic bottom disc with aperture; *(3)*: platinum crucibles with glass samples; *(4)*: thermocouple with platinum shoe; *(5)*: handle for bottom disc; *(6)*: water-cooled copper quenching block (After Gutzow (1977) [298])

From a technical point of view experiments on crystal growth of low-melting substances are possible by direct microscopic observations (see, e.g., Fig. 8.19). For a number of glass-forming substances with higher values of the melting point only samples obtained by quenching can be investigated. In such experiments the so-called revolver quenching furnace proved to be useful. It allows one to perform the simultaneous heat treatment of 12 samples (see Fig. 8.22).

The linear growth velocity, v, is usually determined from $(L-t)$-measurements. Hereby L denotes the size of the crystal at time t (see Fig. 8.23). The linearity of the L vs. t dependence is an indication that the latent heat of the transformation does not significantly influence the growth or dissolution. In Fig. 8.23, an example is given for growth at relatively small under-cooling. At high under-cooling non-steady state induction periods in nucleation have also to be accounted for. As shown, for example, in Fig. 8.24 a considerable induction time is observed in the $L(t)$-curve, which may be interconnected with the time-lag in nucleation.

Additional information on experimental techniques and results on crystal growth may be found in the literature (e.g., Zschimmer and Dietzel (1926) [528]; Eitel (1954) [185]; Mandelkern (1964) [528]; Gutzow (1977) [298]; Chernov (1980 [132], 1988 [133])). Also of particular interest in the last decades have been problems connected with instabilities of the melt-crystal interface and the resulting pattern selection in fingered growth phenomena and growth of fractal aggregates. For a detailed overview on results and directions of research on these topics see, e.g., the review articles by Kessler et al. (1988) [452], Meakin (1988) [550], Botet and Jullien (1988) [93] as well as the monograph by Feder (1988) [199].

Generally, in studying crystal growth and, in particular, the growth of a single crystal in a capillary tube, when it is observed how vividly it responds to mechanical

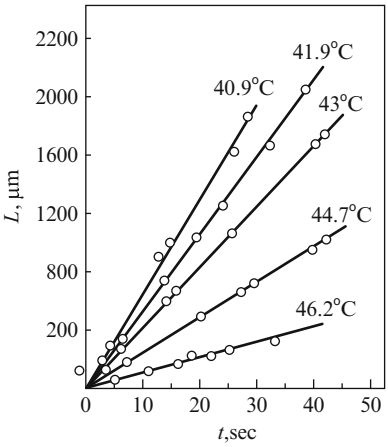

Fig. 8.23 L vs. t-curves for small under-cooling. Growth of a thymol single crystal in the capillary tube at different values of temperature indicated at each line (Gutzow et al. (1972) [326])

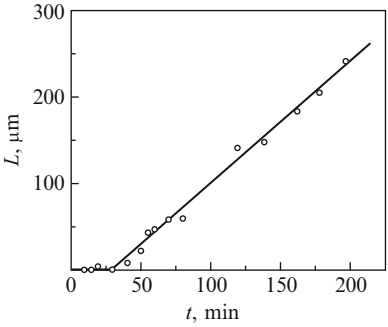

Fig. 8.24 L vs. t-curves for large values of the undercooling. Growth of $NaPO_3$ crystallites at 319.5 °C. The measurements are performed by electron and by optical microscopy. The induction period is due to time-lag effects in nucleation and the finite time a critical cluster needs on average to grow to a measurable size

damage, how it reacts upon any external influence (change of temperature, addition of impurities), one is almost involuntarily reminded of Goethe's words written in "Grundzüge einer allgemeinen Naturbetrachtung" (1823): "... *we must ... regard the process of crystallization arising out of the basic principles of nature as a form of life, but life petrifies in the dead structure of the crystal; so the crystal is the relic, the caput mortuum of life.*". Similarly Haeckel wrote in his booklet "The souls of crystals: Studies in inorganic life" (1917) [342]: "... *the process of crystallization is to be regarded as a true manifestation of life ... Growth is typical for both living organisms and crystals and growth determines the nature of every individual organism and the properties of every individual crystal*".

Chapter 9
Growth of Clusters and of Ensembles of Clusters: Ostwald Ripening and Ostwald's Rule of Stages

9.1 Introductory Remarks: General Observations

In the foregoing chapter, the basic mechanisms of growth were analyzed for the case when the ambient phase-crystal interface has a radius of curvature $R \to \infty$, i.e., we discussed the growth of infinitely extended crystals. However, when processes of phase formation in the bulk of the ambient system are considered we have to take into account pecularities connected with the growth of small clusters. Here we have to consider clusters with sizes beginning with radii of an order of $10^{-8} - 10^{-7}$ cm. Typically Gibbs-Thomson radii in the initial stages of growth are found in a range from 10^{-6} up to 10^{-4} cm. For such cluster dimensions, it can be expected that the classical capillary theory and its consequences, e.g., the Gibbs-Thomson equation Eq. (6.40), are directly applicable. For larger clusters Gibbs-Thomson corrections in the thermodynamic description are frequently negligible. However, in general, Gibbs-Thomson corrections have also to be considered in the growth kinetics in establishing the kinetics of overall-crystallization and in considering the further structure formation in a system undergoing phase transformations. A particular important example in this respect is the competitive growth of ensembles of clusters, the so-called Ostwald ripening process.

Such corrections of the growth equations are also of importance in analyzing the problem which of the possible different modifications of a substance is formed preferably and what the sequence of their transformations from one to the other is. An attempt of solving the latter problem is given with the so-called Ostwald rule of stages outlined in one of the subsequent sections. For ultra-small clusters with sizes less than 10^{-7} cm, not only the applicability of the capillarity theory is more than doubtful but it is even difficult to make definite conclusions in what state of aggregation of matter the substance forming the cluster is: e.g., liquid or crystalline in vapor condensation processes (see Halpern (1967) [344]; Avramov and Gutzow (1980) [23]). Sometimes it is even necessary to consider some particular non-defined cluster like states of matter (Petrov (1986) [633]) which are observed in computer modelling experiments.

I.S. Gutzow and J.W.P. Schmelzer, *The Vitreous State*,
DOI 10.1007/978-3-642-34633-0_9, © Springer-Verlag Berlin Heidelberg 2013

Of particular significance for the mechanism of growth of clusters is also the state of the respective interface. In most cases a roughened interface boundary crystal-melt and thus a normal-like growth mode in the sense as discussed in Sect. 8.2 should be expected. Hereby, it is probable that the degree of roughening of the interface increases with diminishing sizes. In most cases of the theoretical description of the growth of small clusters it is assumed that direct impingement of ambient phase molecules dominates the growth of clusters, i.e. that every molecule reaching the cluster ambient phase interface adheres to the growing center. In processes of vapor condensation this mode of growth is called the ballistic growth model.

In the growth of clusters three regions have to be distinguished as already discussed in Sect. 6.3. Fluctuational growth of subcritical clusters (for $j < j_c$), diffusion-like growth in the near-critical region ($j = j_c$) and deterministic growth for $j > j_c$. The deterministic growth range is of particular interest in the present chapter. In a first approximation it is usually assumed (see Lifshitz and Slezov (1958, 1959, 1961) [508–511]; Shneidman and Weinberg (1993) [750]) that the size dependence of deterministic growth rates of clusters with a radius R may be expressed (at least, for small deviations from R_c) as

$$v_R \cong v_R^{(\infty)} \left(1 - \frac{R_c}{R}\right) , \tag{9.1}$$

where $v_R^{(\infty)}$ denotes the growth rate of the infinitely large crystal. This type of dependence is obtained immediately if one assumes that the growth rate is proportional to the difference of the chemical potentials of a particle in the ambient phase and the cluster, i.e., $v_R \propto \Delta\mu = (\mu_\beta(p,T) - \mu_\alpha(p_\alpha,T))$. By a Taylor-expansion of μ_α (compare Eqs. (6.66)–(6.78)) we get

$$v_R \propto \mu_\beta(p,T) - \left[\mu_\alpha(p,T) + \left(\frac{2\sigma v_m}{R}\right)\right] = \Delta\mu(p,T)\left(1 - \frac{2\sigma v_m}{\Delta\mu(p,T)R}\right) , \tag{9.2}$$

resulting with Eq. (6.40) directly in Eq. (9.1). More exact dependencies for v_R, valid for the whole region $R_c < R < \infty$, may be traced in the above mentioned paper by Shneidman and Weinberg (1993) [750].

In the development of the classical theory of phase transformations other possibilities for the description of cluster growth have also been utilized. Thus in the classical derivation of the Kolmogorov-Avrami kinetics of overall-crystallization it is assumed that the clusters formed initially are so large (crystallization centers) that they grow with a constant time-independent rate, $v_R^{(\infty)}$. From a purely thermodynamic argumentation it is to be expected that new phase clusters retain their equilibrium shape at any dimension (a sphere if the cluster is a liquid; an equilibrium shaped crystal if it is a crystalline nucleus). This assumption is inherent in the classical formulation of the theory of nucleation (assumption 4, Sect. 6.3.1).

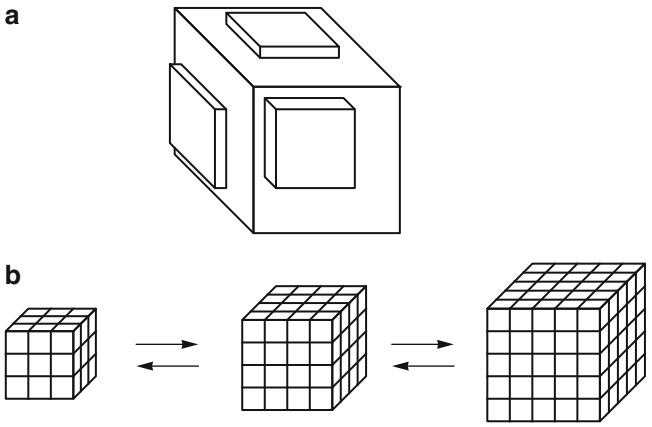

Fig. 9.1 Kaischew-Stranski model for surface mediated growth of equilibrium shaped crystalline clusters. (**a**): Formation of three two-dimensional nuclei on three opposite faces of the cubic cluster guarantees growth leading from one equilibrium shaped cluster (having n building units per edge) to the next one having $n + 1$ building units per edge. (**b**): Three successive stages of growth

In the classical model of crystal nucleation proposed in 1934 by Kaischew and Stranski, the equilibrium shape of crystalline clusters is assumed from the very beginning of the process. Supposing that the crystal has a cubic shape (see Fig. 9.1) the mentioned authors argued that the equilibrium form is preserved only if on the three opposite faces of the cluster three two-dimensional clusters are formed simultaneously (when two-dimensional nucleation determines the growth of the crystalline nucleus). The probability, w, of such an event is proportional to ν^3 where ν is the frequency of nucleus formation per unit area of one of the crystal faces. Consequently, the assumption of growth via equilibrium shaped crystals mediated by two-dimensional nucleation implies a considerable inhibition of the growth of small crystallites when compared with the growth of liquid droplets or the mechanism of growth of crystalline-like clusters via the normal mode.

The model of Kaischew and Stranski was adopted in a paper by Gutzow and Toschev (1968) [318]. It was shown that it leads to probabilities of the order of $w \approx 10^{-3}$ to 10^{-5}. Knowing the rate of growth of crystallites with $R \to \infty$ and the ambient phase impingement rate Z then in a first approximation, assuming the Kaischew-Stranski model, we have to expect

$$w = \frac{v_R^{(\infty)}}{Z} \,. \tag{9.3}$$

In most cases of segregation (and particularly when crystallization or, more generally, segregation from a multi-component ambient phase is considered) nucleation and growth is governed by diffusion fluxes towards the segregating particles. In these cases, diffusion-limited growth has to be considered taking in account, in

addition, size effects in cluster formation, decay and growth described by the Gibbs-Thomson equation. Such an analysis is given in the next section.

9.2 Diffusion-Limited Segregation

We consider a cluster developing in an ambient phase by a process of precipitation as shown in Fig. 6.2. Once a cluster of supercritical size is formed, its further growth is determined by diffusion fluxes of the condensing particles to it from relatively distant parts of the matrix. The determination of the growth rate for such a mechanism of growth is usually based on the following simplified model (see also Crank (1975) [150]). It is assumed that at some distance $r = R$ from a center of spherical symmetry and at large distances ($r \to \infty$) the concentrations of the segregating particles are fixed, i.e. that the relations

$$c(r = R) = c_R \,, \qquad c(r \to \infty) = c \,. \tag{9.4}$$

hold. The density of fluxes of particles j_i of the different components are determined by the diffusion equation

$$\mathbf{j}_i = -\frac{D_i c_i}{k_B T} \text{grad}\, \mu_i \,. \tag{9.5}$$

Here D_i is the partial diffusion coefficient of the i-th component and c_i its volume density in the system.

We consider for simplicity of the notations, again, a quasi-binary system, where only one of the components segregates to form a cluster of the new phase. In this case the expression Eq. (9.5) is simplified to

$$\mathbf{j} = -\frac{D c}{k_B T} \text{grad}\, \mu \,. \tag{9.6}$$

For a perfect solution, the relation

$$\mu(p, T, x) = \mu_0(p, T) + k_B T \ln x \tag{9.7}$$

holds and Eq. (9.6) can be written in the well-known form of the first Fick's law

$$\mathbf{j} = -D \text{grad}\, c \,. \tag{9.8}$$

In this expression D is the partial diffusion coefficient of the segregating particles and c (respectively x) their volume concentration (molar fraction). With the continuity equation, Eq. (9.9)

$$\frac{\partial c}{\partial t} + \text{div}\, \mathbf{j} = 0 \,, \tag{9.9}$$

which reflects the conservation of the number of segregating particles, the diffusion equation is obtained (for the spherically symmetric case) as

$$\frac{\partial c}{\partial t} = \frac{\partial}{\partial r}\left(r^2 D \frac{\partial c}{\partial r}\right) . \tag{9.10}$$

By applying the boundary conditions, Eq. (9.4), for large times ($t \rightarrow \infty$), a stationary concentration field is established. This concentration field is found, from the stationary solution of Eq. (9.10), to be

$$c(r) = -\frac{c - c_R}{r} R + c . \tag{9.11}$$

The density of fluxes through the surface with the radius R is given in this case by

$$j_R = -D\left(\frac{\partial c}{\partial r}\right)_{r=R} \tag{9.12}$$

or

$$j_R = -D\frac{c - c_R}{R} . \tag{9.13}$$

If one assumes that in the vicinity of a growing cluster at each moment of time a practically stationary concentration profile is established as given by Eq. (9.11) (steady-state approximation for cluster growth (compare Zener (1949) [952])), the change of the cluster radius with time may be described by

$$\frac{dR}{dt} = -\frac{1}{c_\alpha} j_R \tag{9.14}$$

or by

$$\frac{dR}{dt} = \frac{1}{c_\alpha}\frac{c - c_R}{R} . \tag{9.15}$$

Hereby it is assumed, in addition that in the immediate vicinity of the clusters in the matrix a local equilibrium concentration is established. Thus c_R may be expressed as (compare Eq. (6.77))

$$c_R = c_{eq}(\infty) \exp\left(\frac{2\sigma v_\alpha}{k_B T}\frac{1}{R}\right) . \tag{9.16}$$

The concentration c in the undisturbed matrix corresponds, on the other hand, to a critical cluster size R_c, determined by

$$c = c_{eq}(\infty) \exp\left(\frac{2\sigma v_\alpha}{k_B T}\frac{1}{R_c}\right) . \tag{9.17}$$

A substitution of Eqs. (9.16) and (9.17) into Eq. (9.15) and a subsequent Taylor-expansion of the exponential functions yields

$$\frac{dR}{dt} = \frac{2\sigma D c_{eq}(\infty)}{c_\alpha^2 k_B T} \frac{1}{R} \left(\frac{1}{R_c} - \frac{1}{R} \right) . \tag{9.18}$$

Equation (9.18) is the basic relation for the description of diffusion-limited segregation processes. It can be generalized to describe other mechanisms of growth as well.

The result of such an extension can be written in the general form (see Slezov and Sagalovich (1987) [774])

$$\frac{dR}{dt} = \frac{2\sigma D c_{eq}(\infty)}{c_\alpha^2 k_B T} \frac{a^{n-1}}{R^n} \left(\frac{1}{R_c} - \frac{1}{R} \right) , \tag{9.19}$$

where a is a length parameter reflecting specific properties of the considered growth mechanism. Different growth mechanisms are described by this equation for different values of n ($n = 0$: ballistic or interface kinetic limited growth; $n = 1$: diffusion-limited growth; $n = 2$: diffusion along grain boundaries; $n = 3$: diffusion in a dislocation network (Slezov and Sagalovich (1987) [774]). Equation (9.18) serves, moreover, as one of the basic equations for the development of the theoretical description of Ostwald ripening, the competitive growth of an ensemble of clusters in the late stages of the phase transformation, which we are going to discuss in the next section.

9.3 Growth of Ensembles of Clusters: The Lifshitz-Slezov-Wagner Theory

If the state of the system is not changed significantly by nucleation and growth processes of the already formed supercritical clusters, the critical cluster size is nearly constant, the supercritical clusters grow at the expense of primary building units in the ambient phase and (for $R \gg R_c$) from Eq. (9.18) a time dependence of the average cluster radius as $\langle R \rangle^2 \sim t$ is to be expected for diffusion-limited growth (compare Fig. 6.11). The situation becomes different if due to the growth of the ensembles of clusters the number of segregating particles is decreased to a value near the equilibrium concentration in the matrix and the critical cluster radius is increased to a size comparable with the dimensions of the majority of clusters formed (Fig. 6.11). In this stage, according to Eq. (9.18) and the results of the thermodynamic analysis, clusters with radii $R < R_c$ shrink and are dissolved supplying in this way the larger clusters with monomers for a further growth. The critical cluster radius cannot be considered any more as a constant but has to be determined in a self-consistent way.

From a kinetic point of view this mechanism is determined by the cluster size dependence of the equilibrium solubility, c_{eq} (compare Eq. (6.77)). Small clusters are characterized by higher values of c_{eq}, thus, for a given value, c, of the average concentration of the segregating particles in the melt clusters with equilibrium solubilities larger this value ($R < R_c$) shrink, while clusters with a lower value of the solubility ($R > R_c$) are capable to a further growth. The thermodynamic driving force of dissolution, respectively, growth is hereby proportional to the differences $(c - c_{eq})$ or $(\mu(c) - \mu(c_{eq}(R)))$. The dissolution of the smaller clusters provides the monomeric building units for the growth of the supercritical ones. From a macroscopic thermodynamic point of view the evolution of the ensemble of clusters is governed by the general thermodynamic evolution criteria, the decrease in the respective thermodynamic potential due to the decrease in the interfacial contributions to it (compare Sect. 6.3.10). The process is completed, in general, only after one super-large cluster has won the competition process. However, the situation may be different, if additional factors – like elastic strains – influence the coarsening process (see Sect. 9.4).

Though the process of competitive growth considered here has been a well-known experimental fact since the first detailed investigation by W. Ostwald (see Ostwald (1901) [617]), a satisfactory theory was developed first in the 1950s by Lifshitz and Slezov (1958, 1959, 1961) [508–511] and repeated for kinetically limited growth by Wagner (1961) [904]. The Lifshitz-Slezov theory was formulated initially for diffusion-limited growth, described by Eq. (9.18). Here the main assumptions and results are summarized briefly.

If we denote by R^*_{co} the critical cluster radius for the homogeneous metastable initial state, as a first step a dimensionless time scale may be introduced by

$$t^* = \frac{2\sigma D c_{eq}(\infty)}{c_\alpha^2 k_B T R^{*3}_{co}} t \tag{9.20}$$

and Eq. (9.18) can be rewritten in the simpler form

$$\frac{dR}{dt^*} = \frac{R^{*3}_{co}}{R}\left(\frac{1}{R_c} - \frac{1}{R}\right) . \tag{9.21}$$

As a next step the dimensionless variables u, x and $\tilde{\theta}$ are introduced via

$$u = \frac{R}{R_c} , \qquad x = \frac{R_c}{R^*_{co}} , \qquad \tilde{\theta} = 3\ln[x(t^*)] . \tag{9.22}$$

In these reduced variables the growth equation, Eq. (9.21), reads

$$\frac{du^3}{d\tilde{\theta}} = \gamma(\tilde{\theta})[u - 1] - u^3 \qquad \text{with} \qquad \gamma(\tilde{\theta}) = \frac{1}{x^2 \dfrac{dx}{dt^*}} . \tag{9.23}$$

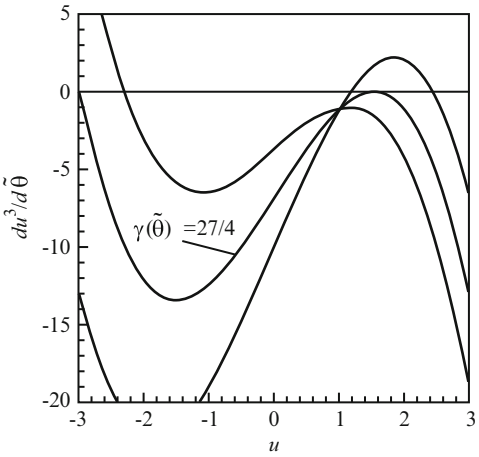

Fig. 9.2 Possible types of curves (v_u vs. u). For the late stage of coarsening only the situation corresponding to $\gamma = (27/4)$ is relevant

Possible curves for the growth rate, v_u, in reduced variables

$$\frac{du}{d\tilde{\theta}} = v_u = \frac{\gamma(\tilde{\theta})[u-1] - u^3}{(3u^2)} \tag{9.24}$$

are shown in Fig. 9.2.

From a physical point of view for large times only the situation corresponding to a value of γ equal to $\gamma = (27/4)$ in Fig. 9.2 is of relevance (only one cluster size exists for which the growth rate is equal to zero). This particular value of γ is found taking into account that in the asymptotic region $\gamma(\tilde{\theta})$ is determined by

$$v_u = \frac{\partial v_u}{\partial u} = 0\,. \tag{9.25}$$

With these conditions Eqs. (9.24) and (9.25) yield

$$\gamma = \frac{27}{4}\,, \qquad u = \frac{3}{2}\,. \tag{9.26}$$

In this way with Eq. (9.23)

$$\frac{dx^3}{dt^*} = \frac{4}{9} \qquad \text{or} \qquad R_c^3(t^*) = R_{co}^{*3}(1 + t^*) \tag{9.27}$$

is obtained. Thus, for diffusion-limited growth the critical cluster radius grows as

$$R_c(t) \sim t^{1/3} \tag{9.28}$$

in agreement with the numerical results, shown in Fig. 6.11.

In the Lifshitz-Slezov theory in addition to the cluster size distribution, $f(R,t)$, describing the cluster ensemble in absolute variables, also the cluster size distribution function, $\varphi(u,\tilde{\theta})$, in reduced variables is introduced. It is connected with $f(R,t)$ by

$$f(R,t)dR = f(R,t)R_c(t)d\left(\frac{R}{R_c(t)}\right) = \varphi(u,\tilde{\theta})du \tag{9.29}$$

or

$$\varphi(u,\tilde{\theta}) = f(R,t)R_c(t)\ . \tag{9.30}$$

For the determination of $\varphi(u,\tilde{\theta})$ only the condition of conservation of the number of monomers is used.

The derivation is somewhat lengthy and cannot be given here. The main results are the following (see Lifshitz and Slezov (1958, 1959, 1961) [508–511]):

- The cluster size distribution function $\varphi(u,\tilde{\theta})$ can be expressed in the form

$$\varphi(u,\tilde{\theta}) = A\exp(-\tilde{\theta})P(u)\ , \qquad A - \text{constant}\ . \tag{9.31}$$

- The time-independent part of the cluster-size distribution function, $P(u)$, obeys the normalization condition

$$\int_0^\infty P(u)\,du = 1\ . \tag{9.32}$$

For diffusion-limited growth in addition the relations

$$P(u) = \frac{3^4 e u^2 \exp\left\{-\dfrac{3}{2[(3/2)-u]}\right\}}{2^{5/3}(u+3)^{7/3}[(3/2)-u]^{11/3}} \tag{9.33}$$

$$\int_0^\infty uP(u)du = 1 \tag{9.34}$$

hold, resulting in

$$\langle R\rangle = R_c(t)\ . \tag{9.35}$$

- According to Eqs. (9.31) and (9.32) the evolution of the number of clusters is determined by the pre-factor $A\exp(-\tilde{\theta})$ only, which gives

$$\frac{N(t)}{N(0)} \sim \exp(-\tilde{\theta}) = \left(\frac{R_{co}}{R_c}\right)^3 \sim \frac{1}{t}\ . \tag{9.36}$$

In this way, the whole process of structural reorganization considered is characterized by two equations giving the time-dependence of the average cluster size and the number of clusters in the system. Both the average cluster size and the critical Gibbs-Thomson cluster radius behave for diffusion-limited growth as $\sim t^3$. For $t \to \infty$, only one very large cluster will survive this process of competitive growth.

9.4 Modifications and Generalizations

Equations (9.28)–(9.36) form the basic content of the theoretical description of Ostwald ripening as developed first by Lifshitz and Slezov (1958, 1959, 1961) [508–511]. This theory was modified and extended subsequently, the main results remained, however, unchanged (see also Voorhees (1985) [901]; Slezov, Schmelzer, Möller (1993) [777]). The series of extensions of the theory to different growth mechanisms, e.g., of the type given by Eq. (9.19), was opened by Wagner (1961) [904], who applied the outlined ideas to the case of kinetically limited growth (for other results in this direction see the overview given by Slezov and Sagalovich (1987) [774]).

A second line of generalizations of the theory is connected with the incorporation of direct diffusion interactions of the clusters into the kinetic description of Ostwald ripening (Voorhees and Glicksman (1983, 1984) [902]; Marqusee and Ross (1984) [535]; Tokuyama and Kawasaki (1984) [841]; Marder (1987) [530]). The analysis shows, however that the asymptotic power laws remain unchanged, only some additional pre-factors in the expressions for R_c and $\langle R \rangle$ occur, which are functions of the volume fraction of the segregating phase. In the case of diffusion interactions, a time-independent cluster size distribution is also established in the course of time, however, the curves are more symmetric than those of the Lifshitz-Slezov distribution. As another factor, which may diminish the gap between experiment and theory the influence of thermal (stochastic thermal fluctuations) or externally generated noise has recently found to be of importance (Ludwig, Schmelzer, and Bartels (1994) [521]; Möller (1994) [568]). An extended discussion of further factors which may account for a deviation from the Lifshitz-Slezov distribution is given by Jayanth and Nash (1989) [405].

Other generalizations of the Lifshitz-Slezov theory deal with an alternative approach to the theory of Ostwald ripening, allowing the description of the first non-asymptotic stage of coarsening (Schmelzer (1985) [689]; Schmelzer and Ulbricht (1987) [712]) and a thermodynamic interpretation of this process. This approach is based on the thermodynamic analysis outlined in Sect. 6.3.10. A further problem of intensive research is connected with the influence of elastic strains on the process of Ostwald ripening, in particular, its asymptotic behavior (Schmelzer (1985) [689]; Schmelzer, Gutzow (1988) [705]; Kawasaki, Enomoto (1988) [441]; Pascova et al. (1990a,b) [627, 628]; Schmelzer et al. (1990a,b) [713, 714]). For the case that only elastic matrix-cluster interactions have to be taken into account it can be shown that qualitatively the growth kinetics is modified as compared with the results obtained

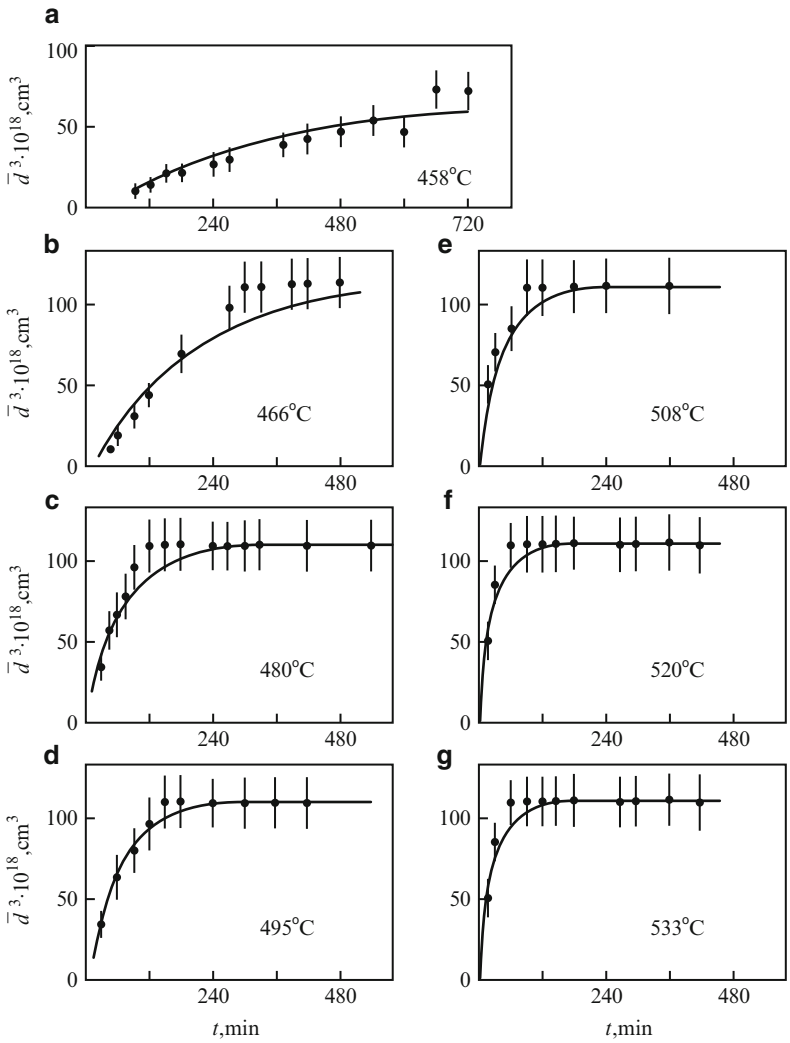

Fig. 9.3 Time dependence of the average size of AgCl-clusters segregating in a model sodium metaborate glass-forming melt. The temperature of the system, at which segregation takes place, is indicated at each curve. Note that a finite stationary value of the average cluster size is established in the system asymptotically in contrast to the type of behavior as one would have to expect it from the classical LSW-theory of coarsening (After Pascova et al. (1990a,b) [627, 628]). Precipitation of silver halides in glass-forming melts is the first step in the technology of formation of so-called photochromic glasses (See Arayo (1980) [17]; Fanderlik and Prodhomme (1973) [195])

first by Lifshitz and Slezov, if the total energy of elastic deformations due to the formation and growth of one cluster increases more rapidly than linear with the volume of the cluster.

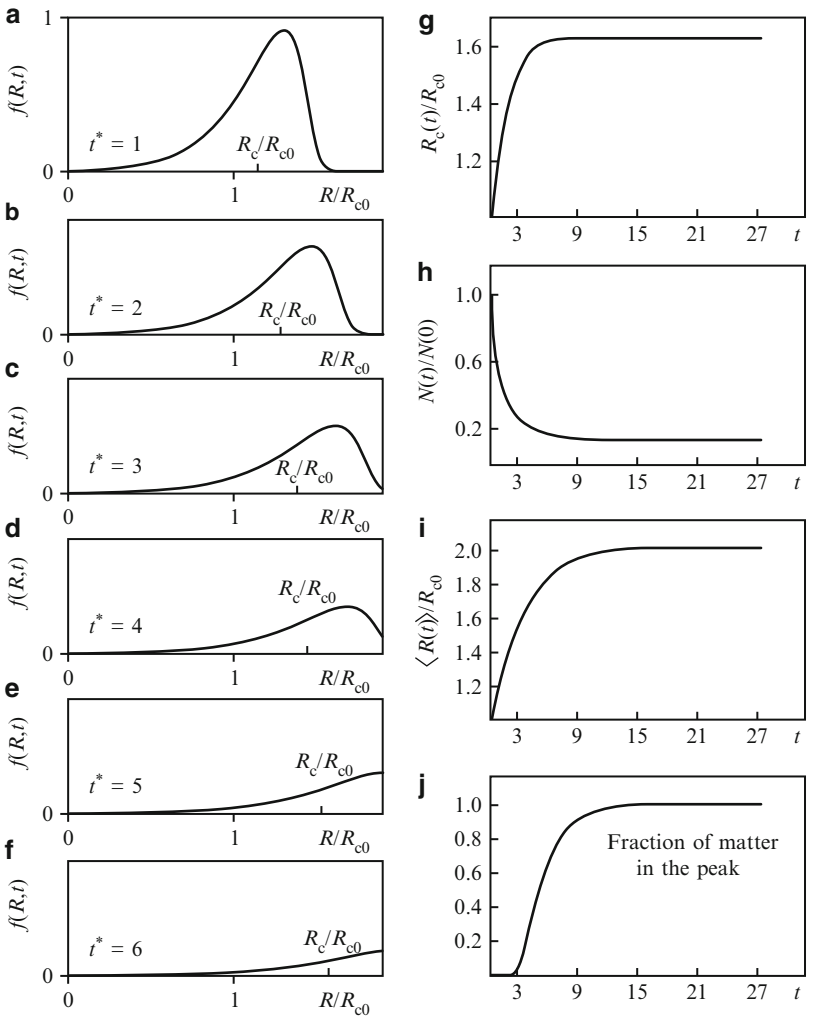

Fig. 9.4 Time evolution of the cluster size distribution, $f(R,t)$, and related quantities like the critical cluster radius $R_c(t)$, the number of clusters in the system $N(t)$, the average cluster radius $\langle R(t)\rangle$ and the fraction of matter in the peak for the process of Ostwald ripening in a system of rigid pores of equal size. On the left hand side the cluster size distribution is shown for different moments of time. R_{co} and $N(0)$ are the critical cluster size and the number of clusters in the initial state of coarsening

One experimental example, when elastic strains in coarsening modify the growth kinetics qualitatively, is shown in Fig. 9.3. In this figure the time dependence of the average size of an ensemble of clusters, segregating in a sodium metaborate glass-forming melt, is shown for the stage of coarsening. In the course of evolution a relatively mono-disperse distribution is established consisting of a large number

of clusters. This distribution remains practically unchanged for prolonged times (Pascova et al. (1990a) [627]). A thorough analysis of the experimental results shows (Pascova et al. (1990b) [628]; Schmelzer et al. (1990a,b) [713, 714]) that in the considered case the process of Ostwald ripening is inhibited by the interaction of the growing clusters with the matrix, which behaves as a viscoelastic Kelvin's body (cf. Chap. 12). In the considered experimental example each AgCl-cluster is growing in a viscoelastic cage in the matrix formed by the segregation process itself. Qualitative changes of the ripening kinetics as shown in Fig. 9.3 may occur generally if the diffusion coefficient of the segregating particles is considerably higher as compared with the self-diffusion coefficient of the matrix building units.

A theoretical interpretation of the experimental results, discussed here briefly, can be given based on the following simplified model (which is also of interest in a different aspect, for the consideration of coarsening in porous materials). It is assumed in the model that clusters are formed and grow exclusively inside the pores of a solid matrix. Hereby in a first approximation a mono-disperse pore size distribution is assumed here. The evolution of the cluster size distribution and related quantities for Ostwald ripening in a solid with a mono-disperse pore size distribution are illustrated in Fig. 9.4. It exhibits typical features which are found also in the experimental investigations of AgCl-segregation discussed above. For the details of both analytical and numerical methods in the description of coarsening processes in elastic and viscoelastic solids as well as in porous materials see the original papers (Slezov, Schmelzer, and Möller (1993) [777], Schmelzer, Möller, and Slezov (1994) [717]; Schmelzer and Möller (1992) [710].[1]

9.5 Growth of Clusters with Different Structures and Ostwald's Rule of Stages

9.5.1 Introduction

In 1897, W. Ostwald [615] formulated a rule, denoted today as Ostwald's rule of stages, which according to his belief was the manifestation of a very general principle applicable to any process in nature (including chemical reactions). However, Ostwald's rule of stages is in fact only the generalization of a relatively small number of experimental results on the sequence of appearance of different crystalline modifications in precipitation in supersaturated solutions or in crystallization from undercooled melts. According to Ostwald's experience in such processes as a rule not the thermodynamically most stable modifications are formed

[1] An more detailed overview on the theoretical description of coarsening including results obtained by one of the present authors together with him can be found in the monograph of one of the authors of the theory of coarsening, V.V. Slezov (2009) [773] (see also Chap. 14).

initially; in Ostwald's words: "... *in the course of transformation of an unstable (or metastable) state into a stable one the system does not go directly to the most stable conformation (corresponding to the modification with the lowest free energy) but prefers to reach intermediate stages (corresponding to other possible metastable modifications) having the closest free energy difference to the initial state*". As a particular case, applying Ostwald's rule, one has to expect that the first stage of vapor condensation should always consist of the formation of a liquid phase, which can be transformed in a next step into crystalline condensates. Such an idea was, in fact, adopted also by Semenov ((1930) [744]; see also Palatnik and Papirov (1964) [620]) and formulated by him as a general requirement for any case of condensation of supersaturated systems. Semenov's argumentation in favor of such a rule was based on a two-dimensional modification of a van der Waals type equation of state.

Experimental findings as the preferential formation of liquid-like precipitates in crystallization of a number of organic substances from solution (see also Feenstra et al. (1981) [200, 201] for amorphous Ca-phosphate precipitates from aqueous solutions) seem to support the general validity of this rule. Abundant evidence in this respect was also accumulated on crystallization of metastable modifications from vapors, melts and solutions. The most striking example of an application of Ostwald's rule of stages seemed to consist of the synthesis of the metastable modification of carbon, of diamonds, under conditions, where graphite is the thermodynamically stable carbon modification (see Meisel (1972) [552]; Deryaguin and Fedosseev (1973) [165]; Novikov, Fedosseev et al. (1987) [606]). However, similarly as in other cases of empirically formulated rules, in the course of time many exceptions from Ostwald's rule have been found. One of the most well-known examples in this respect is the direct formation of crystalline condensates from the vapor phase.

As a method to reconcile such exceptions to his rule, Ostwald himself discussed the possible existence of very short-living intermediate metastable modifications (see also Palatnik and Papirov (1964) [620] for a discussion of the existence of intermediate liquid condensates in vapor quenching). However, such an explanation is not applicable to each of the observed exceptions. The existence of exceptions to Ostwald's rule of stages shows that it cannot be considered as a general thermodynamically founded law. In contrast, experience has demonstrated that both the origin for its validity and the explanation of possible deviations have to be interconnected with kinetic factors.

The first step in a kinetic argumentation of the region of applicability and the limits of validity of Ostwald's rule of stages was made by Stranski and Totomanov ((1933) [810]; see also Volmer (1939) [894]). According to Stranski and Totomanov the type of the phases formed from a supersaturated ambient phase is determined by the magnitude of the activation energy, $\Delta G^{(c)}$, required for the formation of the corresponding phases: in this way, the competition of the rates of formation of clusters of different modifications or of different phases, which can be formed under the given thermodynamic conditions, determines the dominant appearance of one of them.

The original ideas of Stranski and Totomanov in the kinetic interpretation of Ostwald's rule of stages were developed subsequently in three directions[2]:

- A more exact formulation of the problem in the framework of the classical capillary theory of nucleation considering the dependence of the height of the barriers to nucleation on the thermodynamic parameters of the process (e.g., on supersaturation, cf. Palatnik and Zorin (1959) [621]; Defay, Prigogine et al. (1966) [161]; on the activity of substrates, cf. Gutzow and Avramov (1974) [306]);
- Introduction of the more general non-steady state formulation of nucleation theory (Gutzow and Toschev (1968) [318]);
- Account of the possibility of transformations between two or more fluxes of different new phase clusters (e.g., of the possibility of melting of crystalline clusters and of crystallization of liquid clusters (Avramov and Gutzow (1980)[23]; Gutzow, Avramov (1981) [307])) and thus of introducing cluster transformations into the consideration.

According to Ostwald's original formulation the process of formation of different phases is determined by the magnitude of the free-energy differences for the formation of the different clusters. The Stranski-Totomanov treatment and its above mentioned further developments reflect, as it will become evident from the considerations outlined in the two subsequent sections, consecutive stages of development of a very general idea: The preferential formation of the thermodynamically less stable phases is, in fact, the result of predominant formation of the kinetically favored states. Thus, it turns out that Ostwald's rule of stages is the consequence of the general premise that the activation energy of a process and not the affinity of the possible reactions determines its rate. This governing idea can (and has to be) explained in terms of the existing kinetic models of formation, growth and possible transformations of clusters of different structures from one modification to another one.

9.5.2 The Classical Kinetic Treatment of Ostwald's Rule of Stages

In the framework of the classical capillary formulation of the theory of nucleation, as given in Chap. 6, the dominant formation of one of two possible phases or modifications, specified by the subscripts c (e.g., crystallites) and f (e.g., liquid

[2] As already mentioned, a generalization of Ostwald's rule of stages was employed originally by us in the development of the generalized Gibbs approach in application to nucleation and growth processes (Schmelzer et al. (2000) [722]; Schmelzer et al. (2010) [728]). This approach implies the possibility and necessity of changes of the bulk properties of the clusters in dependence on cluster size and state of the ambient phase. The realization of Ostwald's rule of stages in connection with elastic stresses and variations of external pressure is discussed in detail in Möller et al. (1988) [572].

droplets), is determined by the respective values of the steady-state nucleation rates J or by the value of the ratio

$$\Upsilon = \ln\left(\frac{J_f}{J_c}\right) . \tag{9.37}$$

Here J_f and J_c are the steady-state rates of formation of the two phases or modifications, both of which are assumed to be more stable from a thermodynamic point of view as compared with the initial state (specified by a subscript v, e.g., for vapor condensation). This is the case, when the thermodynamic driving forces for the formation of clusters of both considered phases $\Delta\mu_{(v\to f)}$ and $\Delta\mu_{(v\to c)}$ are greater than zero. Moreover, let us assume, in addition that the phase, specified by the subscript c is, for the considered thermodynamic boundary conditions, more stable from a thermodynamic point of view, i.e., that the inequality

$$\frac{\Delta\mu_{(v\to c)}}{\Delta\mu_{(v\to f)}} \geq 1 \tag{9.38}$$

holds.

In the framework of the classical theory of nucleation the steady-state nucleation rate for homogeneous nucleation is given by Eq. (6.109) and for heterogeneous nucleation by Eq. (7.8). The thermodynamically less stable phase (specified by the subscript f) is, according to the classical approach, formed predominantly if the inequality $\Upsilon > 0$ holds or, equivalently,

$$\Upsilon = \ln\left[\left(\frac{J_0^f}{J_0^c}\right)\frac{\exp\left(-\dfrac{\Delta G^f_{(cluster)}}{k_B T}\Phi_f\right)}{\exp\left(-\dfrac{\Delta G^c_{(cluster)}}{k_B T}\Phi_c\right)}\right] > 0 . \tag{9.39}$$

If we assume, in addition that the pre-exponential factors J_0, which are determined according to the cited equations by the attachment rate, the Zeldovich factor, the density of monomeric building units, respectively, foreign nucleation cores, are the same for the process of formation of both of the considered phases then Eq. (9.39) is reduced to

$$\Upsilon = \frac{\Delta G^c_{(cluster)}}{k_B T}\Phi_c\left(1 - \frac{\Delta G^f_{(cluster)}\Phi_f}{\Delta G^c_{(cluster)}\Phi_c}\right) > 0 \tag{9.40}$$

or to

$$\left(1 - \frac{\Delta G^f_{(cluster)}\Phi_f}{\Delta G^c_{(cluster)}\Phi_c}\right) > 0 . \tag{9.41}$$

Remember, however that for liquid phase formation the sticking coefficient, ς, is nearly equal to unity, while for the process of formation of crystallites $\varsigma \ll 1$ holds.

In the particular case of competition between the formation of liquid and crystalline clusters this difference has also to be accounted for (see Sects. 9.5.5 and 11.3).

A substitution of the expressions for the work of formation of the critical clusters, Eq. (6.43), and the critical cluster radius, Eq. (6.44), yields, finally, the following expression as the condition for validity of Ostwald's rule of stages (preferential formation of the f-phase)

$$\left(\frac{\Phi_c}{\Phi_f}\right)\left(\frac{\sigma_c}{\sigma_f}\right)^3\left(\frac{v_c}{v_f}\right)^2 > \left(\frac{\Delta\mu_{(v\to c)}}{\Delta\mu_{(v\to f)}}\right)^2 \tag{9.42}$$

and with Eq. (9.38)

$$\left(\frac{\Phi_c}{\Phi_f}\right)\left(\frac{\sigma_c}{\sigma_f}\right)^3\left(\frac{v_c}{v_f}\right)^2 > \left(\frac{\Delta\mu_{(v\to c)}}{\Delta\mu_{(v\to f)}}\right)^2 > 1\,. \tag{9.43}$$

Equation (9.43) was derived first by Gutzow and Avramov (1974) [306] assuming that the specific volumes of both phases v_c and v_f are nearly the same ($v_c \cong v_f$). Such an assumption is quite permissible in cases like the formation of amorphous condensates (compare Sect. 7.7.1), in other applications, e.g., for metastable diamond synthesis from the vapor phase, such density differences may have to be accounted for.

If one assumes, in addition to $v_c \cong v_f$ that the nucleation activities, Φ, of the possible nucleation cores are also of the same order of magnitude for the process of formation of both types of clusters considered and that, moreover, $\Delta\mu_{(v\to c)} \cong \Delta\mu_{(v\to f)}$ holds, then the inequality Eq. (9.43) is reduced to

$$\left(\frac{\sigma_c}{\sigma_f}\right)^3 > 1\,. \tag{9.44}$$

This is the relation originally derived by Stranski and Totomanov (1933) [810]. It turns out, provided the mentioned conditions are fulfilled that Ostwald's rule of stages is obeyed if the specific interfacial energy between the ambient phase and phase (c) (the more stable phase) is higher than the respective value for the interface between ambient phase and phase (f) (the less stable phase). Taking into account Stefan's rule (cf. Eq. (6.127)) it is to be expected that for cases, when (f) and (c) denote the liquid, respectively, crystalline state of a substance, this rule is always fulfilled (as far as the heat of sublimation always exceeds the heat of melting). Equation (9.44), as evident from the derivation, can be considered, however, only as a first estimate compared with the more general condition Eq. (9.43).

The conditions for fulfilment of Ostwald's rule of stages may be formulated also in a somewhat different form. Taking into account that the thermodynamic driving forces of the $v \to f$, $v \to c$ and $f \to c$ transformations are connected by an equation of the form

$$\Delta\mu_{(v\to c)} = \Delta\mu_{(v\to f)} + \Delta\mu_{(f\to c)} \tag{9.45}$$

Eq. (9.42) may be rewritten as

$$\left(\frac{\Phi_c}{\Phi_f}\right)^{1/2}\left(\frac{\sigma_c}{\sigma_f}\right)^{3/2}\left(\frac{v_c}{v_f}\right)-1>\frac{\Delta\mu_{(f\to c)}}{\Delta\mu_{(v\to f)}}>0 \tag{9.46}$$

or as

$$C_0 \geq \frac{\Delta\mu_{(f\to c)}}{\Delta\mu_{(v\to f)}} \geq 0\,, \tag{9.47}$$

where C_0 is defined as

$$C_0 = 1-\left[\frac{v_c}{v_f}\left(\frac{\sigma_c}{\sigma_f}\right)^{3/2}\left(\frac{\Phi_c}{\Phi_f}\right)^{1/2}\right]^{-1}\,. \tag{9.48}$$

By introducing the respective Gibbs-Thomson radii $R_c(v\to c)$ and $R_c(v\to f)$ above given general condition can be written also in the form

$$0 \leq R_c(v\to c) \leq mR_c(v\to f)\,, \qquad m = C_0\frac{\sigma_c}{\sigma_f}\,. \tag{9.49}$$

This inequality shows that Ostwald's rule is fulfilled, when the thermodynamically less stable modification is characterized by smaller values of the critical cluster radius or, when the subscript (f) and (c) refer to different modifications of the same substance, it is constituted of a smaller number of building units. The equations, derived above, have been applied by Gutzow and Avramov (Gutzow and Avramov (1974) [306, 307]; Avramov and Gutzow (1980) [23]) in order to analyze in detail the formation of amorphous (liquid or vitreous) condensates. This process will be discussed in more detail in Sect. 9.5.5.

9.5.3 *Influence of Non-Steady State Effects and Sticking Coefficient Differences*

The present section is devoted to the analysis of the problem, to what extent the conclusions outlined in the previous section are modified, if non-steady state effects in nucleation and sticking coefficient differences are taken into account. For the description of non-steady state effects in nucleation we will apply Zeldovich's solution of the Frenkel-Zeldovich equation as given by Eq. (6.166). Thus, the condition that clusters of the less stable phase (f) are formed preferentially at any moment of time may be written in the form

$$\Upsilon = \ln\left(\frac{J_f(j_c,t)}{J_c(j_c,t)}\right) > 0 \tag{9.50}$$

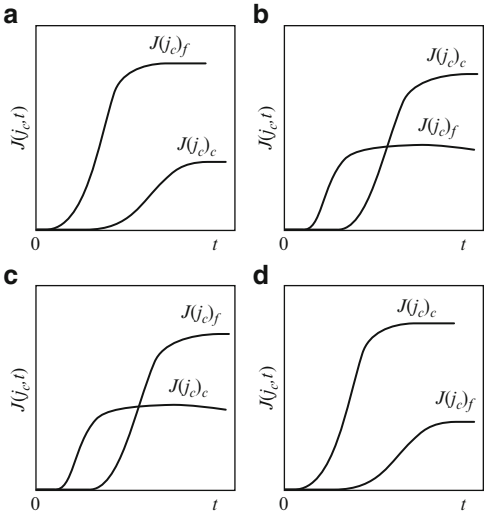

Fig. 9.5 Ostwald's rule of stages in terms of the non-steady state nucleation kinetics (see text)

or

$$\Upsilon = \ln\left(\frac{J_0^f}{J_0^c}\right) + \frac{\Delta G^c_{(cluster)}}{k_B T}\Phi_c\left(1 - \frac{\Delta G^f_{(cluster)}\Phi_f}{\Delta G^c_{(cluster)}\Phi_c}\right) + \frac{\tau_c^{(ns)}}{t}\left(1 - \frac{\tau_f^{(ns)}}{\tau_c^{(ns)}}\right) > 0\,. \tag{9.51}$$

If in the pre-exponential factors J_0 of the steady-state nucleation rate only the sticking coefficients ς significantly differ (for example $\varsigma_f \gg \varsigma_c$ for the formation of droplets (f) or crystallites (c)) then Eq. (9.51) may be reformulated to give

$$\Upsilon = \ln\left(\frac{\varsigma_f}{\varsigma_c}\right) + \frac{\Delta G^c_{(cluster)}}{k_B T}\Phi_c\left(1 - \frac{\Delta G^f_{(cluster)}\Phi_f}{\Delta G^c_{(cluster)}\Phi_c}\right) + \frac{\tau_c^{(ns)}}{t}\left(1 - \frac{\tau_f^{(ns)}}{\tau_c^{(ns)}}\right) > 0\,. \tag{9.52}$$

For larger times ($t \to \infty$) Eq. (9.52) is reduced to Eq. (9.40), again, but modified by the additional term $\ln(\varsigma_f/\varsigma_c)$. Accounting for the mentioned ς-values this term may reach a value of the order 10.

It is evident that the formation of the metastable modification (f) is guarantied when Eq. (9.52) is fulfilled for any moment of time (see Fig. 9.5a). The account of non-steady state effects enlarges the number of possibilities of formation of the metastable phase. If $\tau_c^{(ns)} \geq \tau_f^{(ns)}$ holds, then the formation of (f)-phase clusters may dominate initially even when in the steady state preferably (c)-phase clusters are formed ($J_c(j_c) > J_f(j_c)$) (see Fig. 9.5b). If, in contrast, the relation $\tau_c^{(ns)} \leq \tau_f^{(ns)}$ holds, then initially preferably (c)-phase clusters are formed (see Fig. 9.5c). The exclusive formation of the thermodynamically more stable phase

is to be expected only when both inequalities $J_c(j_c) > J_f(j_c)$ and $\tau_c^{(ns)} \leq \tau_f^{(ns)}$ hold simultaneously (see Fig. 9.5d). A detailed quantitative evaluation and discussion of above conditions for the case of amorphous thin film formation may be found in the already cited paper by Gutzow and Toschev (1968) [307] (see also Sect. 9.5.5).

9.5.4 Further Developments and Applications

The kinetic treatment of Ostwald's rule of stages, as given in the preceding two sections, is based on the analysis of two independent fluxes in cluster size space: one flux representing the formation of c-clusters and one for f-clusters (cf. Fig. 9.6a: applying the notation introduced above). In terms of vacuum condensation experiments, for example, an independent formation both of liquid and crystalline clusters have been assumed so far. Transformations between these two types of clusters were excluded from the considerations. However, in general, transformations of liquid into crystalline clusters ($f \rightarrow c$) and vice versa ($c \rightarrow f$) are possible and have to be accounted for. The thermodynamic driving force of such transformations in the case of vacuum deposition is determined by the melting respectively crystallization temperatures of both types of clusters embedded in the vapor phase and, in particular, by the size dependence of these quantities (compare Sect. 6.2.4). To account for such transformations in the structure of the clusters probabilities ω for a ($f \rightarrow c$)-transformation (crystallization of droplets: $\omega_{(f \rightarrow c)}$) as well as for the ($c \rightarrow f$)-change (melting of crystallites: $\omega_{(f \rightarrow c)}$) have to be introduced into the theoretical description. The particular expressions for these transformation probabilities depend on the process considered. Moreover, in general, these quantities are cluster size dependent.

Taking into consideration such transformations in the structure of the clusters of different types the classical Becker-Döring scheme of nucleation (Sect. 6.3.1), underlying the estimates made in the previous sections, has to be generalized. The respective generalization, proposed by Gutzow and Avramov (1981) [307], is illustrated in Fig. 9.6b. Let us introduce with w_c^* the overall probability that a complex of type c (e.g., a crystalline cluster) grows starting from a size, j_1, to some sufficiently large size, j^*, without being transformed into an f-complex (without melting). The probability that such a transformation occurs, is given, consequently, by $(1 - w_c^*)$. Similarly, w_f^* is the probability that a complex consisting of j_1 particles with an f-structure reaches a size, j^*, without undergoing the $f \rightarrow c$-transformation (without crystallization). The probability that such a process takes place is, again, given by $(1 - w_f^*)$.

In above definitions by j_1 the number of ambient phase particles in the smallest cluster is denoted for which a distinction between f- or c-clusters is meaningful. It is evident that such a lowest limit has to exist since below some cluster size the division between different macroscopic states of matter loses any meaning. The

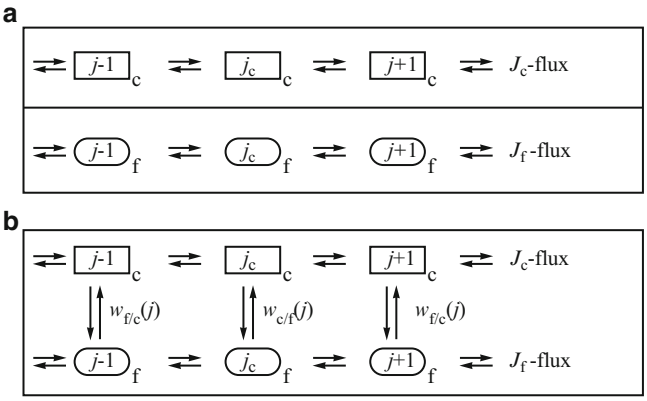

Fig. 9.6 Nucleation fluxes in the process of formation of two possible phases from the same initial phase: (**a**): Classical Becker-Döring nucleation model where transformations between clusters of different types are excluded. (**b**) Generalization of the classical model: The clusters of a given size may be transformed into the alternative structure with size-dependent probabilities $\omega_{(c\to f)}$, respectively, $\omega_{(f\to c)}$

quantities w_c^* and w_f^* can be determined from the transition probabilities $\omega_{(c\to f)}(j)$ and $\omega_{(f\to c)}(j)$ as

$$w_c^*(j^*) = \prod_{j=j_1}^{j^*} (1 - \omega_{(c\to f)}(j)), \tag{9.53}$$

$$w_f^*(j^*) = \prod_{j=j_1}^{j^*} (1 - \omega_{(f\to c)}(j)). \tag{9.54}$$

It was shown by Gutzow and Avramov (1981) [307] that for the considered case of two fluxes (crystalline and liquid clusters) the classical expressions for the steady-state nucleation rates for clusters of critical sizes have to be modified to

$$J_c^{(mod)}(j_c) = J_c w_c^*(j_c)\ , \tag{9.55}$$

$$J_f^{(mod)}(j_c) = J_f + J_c(1 - w_c^*(j_c))\ , \tag{9.56}$$

when the possibility of transformations between the clusters of different types is taken into account. The condition for fulfillment of Ostwald's rule, Eq. (9.37), gets thus the form (Gutzow and Avramov (1981) [307])

$$\Upsilon = \ln\left[\frac{\{[J_f + J_c(1 - w_c^*(j_c))]w_f^*(j_c)\}}{\{J_c w_c^*(j_c) + [J_f + J_c(1 - w_c^*(j_c))](1 - w_f^*(j_c))\}}\right]\ . \tag{9.57}$$

The classical Stranski-Totomanov result is retained for the special case $w_c^* = w_f^* = 1$. Of particular interest is also the case $J_c \cong J_f$. In such a situation, not the values of the nucleation rate but the overall transition probabilities determine the phase which will be formed preferentially. Additional special cases are discussed in the already cited paper (Avramov and Gutzow (1981) [307]).

The kinetic interpretation of Ostwald's rule of stages, even in its simplest formulation as given with Eq. (9.39), gives a large number of possibilities for an explanation of the sequence of appearance of different phases in undercooled melts. The understanding of the kinetic origin of Ostwald's rule of stages also gives the possibility of manipulating the process of the transformation in the desired direction, e.g., by introducing active substrates having different activities with respect to the desired and undesired phases (for example, by introducing crystallization cores with $\Phi_f = 0$ or $\Phi_c = 0$; see Gutzow and Avramov (1974) [306]). One of the simplest methods in this direction consists of the introduction of microcrystallites of the desired phase itself (metastable synthesis of diamonds). Ostwald's rule of stages allows one also to give a kinetic interpretation of the sequence of appearance of different crystalline modifications of one and the same substance (e.g., of cristobalite, tridymite and quartz) in under-cooled melts.

Möller (1994) [568] recently directed the attention to the fact that in processes of solid-to-solid phase transformations the energy of elastic deformations, resulting from cluster formation, may be of major significance for the sequence of formation of different phases. According to Möller's suggestion in such processes those phases are formed preferably for which the difference in the molar volumes, compared with the ambient phase, is the lowest one. For systems, for which elastic effects determine the sequence of formation of different phases, according to this proposal, the degree of stability or metastability is correlated with the molar volume of the respective phases (compare Sect. 7.7.1).

9.5.5 *Ostwald's Rule of Stages and the Formation of Vitreous Condensates*

The interest in thin amorphous films produced by vapor condensation has considerably increased in the last decades. According to this technique vapors of a given substance are brought into contact with a substrate cooled to temperatures below the melting point, T_m (or the vitrification temperature T_g) of the vaporized substance. The vapor quenching method turned out to be both a simple and very effective method of vitrification for an unexpectedly large variety of substances (oxides, metals, metal alloys, halides, chalcogenides, organic substances; see Behrnd (1970) [60]; Secrist, Mackenzie (1964) [743]; Novick (1970) [605]; Gutzow et al. (1976) [327]; Palatnik, Papirov (1964) [620]; Chopra (1962) [134]; Grudeva, Kanev (1986) [279]). The first experiments in this fields were carried out, again, by Tammann (see Tammann and Starinkewitsch (1913) [823]; Tammann (1922) [818]). Tammann

succeeded in obtaining a number of glassy layers by simple vacuum quenching experiments. Tammann and Starinkewitsch also described a number of different experimental realizations of vacuum quenching techniques (for modern versions of such experimental techniques see Gutzow and Avramov (1981) [307] (static vacuum experiments); Secrist and Mackenzie (1964) [743]; Gutzow et al. (1976) [327]; Grudeva and Kanev (1986) [279] (dynamic vacuum quenching techniques)).

In ascertaining the possibilities of vacuum quenching firstly the thermodynamic conditions for the stability of the considered condensate on the substrate have to be formulated. In order to do this, imagine that in a vacuum cell maintained at a temperature $T_{(ev)}$ a sufficiently large quantity of the respective crystalline substance to be evaporated is placed. Its vapors, having an equilibrium vapor pressure $p(T_{ev})$, are in contact with a substrate, sustained at a temperature $T_{(sub)} < T_{(ev)}$. The thermodynamic condition for a condensate (either crystalline *(c)*, liquid *(f)* or vitreous *(g)*) to exist on the substrate is that its vapor pressure at the given temperature $T_{(sub)}$ is lower than the respective value for the crystalline substance which is evaporated, i.e.,

$$p_c(T_{(sub)}) \leq p_c(T_{(ev)}) \quad \text{or} \quad \Delta\mu_{(v\to c)} \geq 0\,, \tag{9.58}$$

$$p_f(T_{(sub)}) \leq p_f(T_{(ev)}) \quad \text{or} \quad \Delta\mu_{(v\to f)} = \Delta\mu_{(v\to c)} - \Delta\mu_{(f\to c)} \geq 0\,, \tag{9.59}$$

$$p_g(T_{(sub)}) \leq p_g(T_{(ev)}) \quad \text{or} \quad \Delta\mu_{(v\to g)} = \Delta\mu_{(v\to c)} - \Delta\mu_{(g\to c)} \geq 0. \tag{9.60}$$

In order to construct a temperature diagram corresponding to above given thermodynamic stability conditions an expression for the $p(T)$-dependence, e.g., in the traditional form

$$\ln[p(T)] \cong -\frac{\Delta H_{(evap)}}{k_B T} + \text{const.} \tag{9.61}$$

has to be used to determine in accordance with the relation

$$\Delta\mu_{(v\to c)} \cong k_B T_{(sub)} \ln\left[\frac{p_c(T_{(ev)})}{p_c(T_{(sub)})}\right] \tag{9.62}$$

the $\Delta\mu$-values, appearing in Eqs. (9.58)–(9.60).

For $\Delta\mu_{(f\to c)}$ the expressions discussed in Sect. 6.2.3 can be used, while for a calculation of the vapor pressure of the vitreous condensate the argumentation outlined in Sect. 3.12 has to be applied. In this way, as done first by Avramov and Gutzow (1980) [23], the regions of thermodynamic stability of crystalline, liquid and glassy condensates may be established in form of a diagram schematically shown in Fig. 9.7a in coordinates $Y = T_{(ev)}/T_m$ vs. $X = T_{(sub)}/T_m$ for a substance having the melting temperature, T_m. In constructing the diagram it was assumed that the thermodynamic potential difference ΔG, determining $\Delta\mu_{(f\to c)}$ of the substance in the temperature range from zero to T_m, is given with Eqs. (3.56) and (3.58) with $T_0 = T_m/2$ and that the glassy condensate has a vitrification temperature $T_g \cong 2/3\ T_m$.

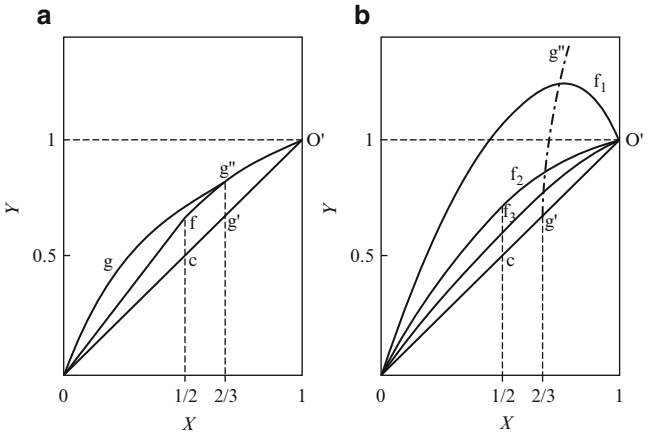

Fig. 9.7 (**a**) The thermodynamic limits of the existence of crystalline, liquid and glassy condensates; (**b**) The kinetic boundaries for formation of liquid and crystalline condensates according to the kinetic treatment of Ostwald's rule of stages based on classical nucleation theory. The respective C_0-values are given as a parameter to each curve (see text)

According to the general thermodynamic requirements, outlined above, in the part of the figure located on the right hand side of the straight line in Fig. 9.7a no condensate is stable. On the left of this dividing line, crystalline condensates may be formed for any values of X and Y. On the left hand side of the curve (Ofg'0') liquid condensates are also stable; however, liquid condensates are thermodynamically unstable in the shaded area (0fg'0'c0), which is reserved for crystals, only. On the left of the line (0gg"0) besides liquid and crystalline condensates also vitreous thin films with the mentioned T_g-value may exist for substrate temperatures corresponding to $T_g/T_m \leq 2/3$.

The kinetic treatment of Ostwald's rule of stages, outlined in Sect. 9.5.2, gives, dependent on the value of the parameter C_0 (defined by Eq. (9.49)), the analytical expressions for the kinetically determined boundaries of the regions for primary formation of liquid, respectively, crystalline condensates. The results are shown in Fig. 9.7b. In this figure, the lines $(0 f_i 0')$ are determined by

$$\frac{1}{Y} = \frac{1}{X} - \frac{1}{C_0}(1 - X) \qquad \text{for} \qquad 0.5 < X < 1, \tag{9.63}$$

$$\frac{1}{Y} = \frac{1}{X}\left(1 - \frac{1}{4C_0}\right) \qquad \text{for} \qquad 0 < X < 0.5. \tag{9.64}$$

To the left of any of the $(0 f_i 0)$-lines (with $i = 1, 2, 3$) the formation of liquid condensates is to be expected; crystalline condensates can be formed only in the area in between the $(0 f_i 0')$-lines. It is seen that with increasing C_0-values (compare Eq. (9.48)) the area of primary formation of crystalline condensates is decreased,

while the area of possible (X, Y)-values, for which Ostwald's rule of stages is fulfilled (i.e., where liquid condensates are primarily formed) is increased.

The comparison with Fig. 9.7a shows the dramatic change when one compares the predictions based on a thermodynamic analysis from one side and on kinetic considerations from the other side: In the kinetic interpretation only for a relatively small region in parameter space, is the primary formation of crystalline condensates allowed, though the crystalline phase is stable from a thermodynamic point of view in the whole region where condensation may occur. The argumentation outlined above as well as the figures are taken from two papers by Avramov and Gutzow ((1980) [23]; Gutzow, Avramov (1981) [307]). In these papers also a more detailed analysis of conditions for the formation of vitreous condensates can be found. The results can be summarized as follows.

As outlined already in Sect. 3.6, vitrification takes place when the time of molecular relaxation, τ_R, of the system becomes larger than the characteristic times of change of external parameters (e.g., temperature variations in cooling processes). In application to vacuum deposition experiments this condition implies that a vitreous condensate will be obtained, when the inequality

$$\tau_R(condensate/surface) \geq \tau_{(vapor\ deposition)} \tag{9.65}$$

holds, i.e., when the time of molecular rearrangements of the surface layer of the amorphous condensate becomes equal or larger than the average time for vapor deposition $\tau_{(vd)}$ at which a monolayer covers the surface of the condensate thus burying-in its initial disorder. Defining $\tau_{(vd)}$ through the vapor deposition rate Z_v (expressed in numbers of mono-layers per unit time) as

$$\tau_{(vapor\ deposition)} = \frac{1}{Z_v} \tag{9.66}$$

and assuming that $\tau_R(condensate/surface)$ may be expressed via a simple Frenkel-type temperature dependence with a constant activation energy U_0 (cf. Eq. (3.78)) it follows that the critical temperature for vitrification, T_c, of a liquid condensate will be (see Avramov et al. (1990) [32])

$$\frac{1}{T_c} \geq \frac{k_B}{U_0}\left[\ln\left(\frac{1}{\tau_0}\right) - \ln\left(Z_v\right)\right] . \tag{9.67}$$

The analogy of above given expressions with Eq. (3.73) and the Bartenev-Ritland equation Eq. (3.85) is obvious. Defining Z_v in Eq. (9.67) through the $(T_{(sub)}/T_{(ev)})$-differences a line is obtained in the $(Y$ vs. $X)$-diagram schematically indicated in Fig. 9.7b by a dashed-dotted line (gg'). In Fig. 9.7a in the same way the T_g-value is indicated corresponding to $X = 2/3$.

From the foregoing analysis it is evident that the full set of requirements determining the possibility of formation of vitreous condensates should consist of

- The thermodynamic conditions for the possibility of the formation of condensed phases (Eqs. (9.58)–(9.60)),
- The kinetic conditions providing the possibility of the primary formation of a liquid condensate (here expressed via Eq. (9.47)),
- The conditions guaranteeing vitrification (i.e., sufficiently low temperatures and/or sufficiently high condensation rates).

In a qualitative way, conditions for the formation of solid amorphous thin films have been formulated already years ago by Hirth and Pound (1963) [368] as well as by Chopra (1969) [134]. The mentioned authors argued that vitreous films are obtained when the temperature of the substrate is so low that the deposited atoms become immobile. Dependencies similar to the expressions, Eq. (9.67), derived here have been proposed and verified experimentally by Krikorian and Sneed (1966) [485] and Sloope and Tiller (1965) [781]. Additional effects due to the latent heat of condensation and a more detailed analysis of vitrification in the process of formation of thin films may be traced in a recent paper by Avramov et al. (1990) [32].

9.5.6 Discussion

As it became evident from the analysis given in the preceding section, the prerequisite in obtaining an amorphous thin film – either liquid or glassy – is the fulfilment of Ostwald's rule of stages. The analysis summarized here and given in more detail in the cited literature shows that in most cases the kinetic requirements for the validity of this rule are indeed fulfilled. The direct formation of crystalline condensates, although possible from a thermodynamic point of view, is to be regarded as an exception under normal experimental conditions (i.e., for typical C_0-values). Thus the vapor-liquid-solid (VLS) mechanism of condensation should be the normal mode in the formation of crystalline films: they are obtained in the process of secondary crystallization of initially formed amorphous layers. It was Palatnik (see Palatnik and Papirov (1964) [620]), who gave the first convincing experimental evidence for a prevailing of the VLS-mechanism in most cases, even in the formation of metallic thin films.

It is interesting to note that the VLS-mechanism of condensation was anticipated many years ago by one of the greatest exponents of natural philosophy, by J.W. Goethe [258]. In the foreword to Caruz's mineralogy, Goethe argued that a state of partial order and of softness – that of the liquid – has always to precede the change from the state of absolute disorder – the vapor – to that of the absolute order – the crystal. Similar statements can be found also in Hegel's Naturphilosophie (1817): a jump from a state of disorder to an absolutely ordered state has to proceed through an intermediate state – that of a liquid. Such statements can be considered as more or less definitely formulated precursors of Ostwald's rule of stages.

The results outlined in this section may be used as a starting point also in the consideration of the conditions of formation of glassy layers from solutions

or by electrodeposition. By this type of process, presumably the natural glassy mineral hyalite (amorphous SiO_2) is formed by precipitation from hydrothermal geological solutions. In application to electrolytic deposition (i.e., under galvanostatic conditions) the electric current determining the deposition rate has to exceed some upper value. In this way, a simple formulation of the conditions for formation of amorphous alloys in electrodeposition processes may be derived.

Chapter 10
Kinetics of Overall Crystallization: Kinetic Criteria for Glass-Formation

10.1 Introduction

As mentioned in Sect. 2.4.1, it was Tammann who divided the process of overall melt crystallization into two consecutive stages: the formation of crystallization centers and their further growth. This division allows us to investigate separately various specific features of the process of phase transformation. However, such a division is in some respect artificial since it separates into different parts one process which in fact involves both nucleation and growth of clusters generally taking place simultaneously in the same volume of the melt. In such a way we have to solve the problem of how the knowledge obtained in exploring separately nucleation and growth can be interconnected in a subsequent step to give a satisfactory description of the process of overall crystallization or of the overall course of phase transformations, in general. This reverse problem – the synthesis of the knowledge concerning nucleation and growth into a unique description of the kinetics of the overall process of phase transformation – is a complicated and interesting task and a beautiful mathematical problem. Its solution was achieved initially in two independent and different approaches by two authors, by the outstanding Russian mathematician Kolmogorov (1937) [464], the American metallurgist Avrami (1939, 1940) [19] and simultaneously by Johnson and Mehl (1939) [412]. By this reason, the respective resulting in the theory final equation is widely also denoted as Johnson-Mehl-Avrami-Kolmogorov (JMAK) equation (cf. also [135]).

The main difficulty in solving the problem of overall crystallization kinetics in the finite volume of an under-cooled melt is to account adequately for the possibility of contact of different crystallites and the resulting inhibition of growth when two or more growing crystallites meet. Another point is the decrease of the ratio of the volume in the course of the transformation where further nucleation may take place. Such a depletion of the volume open to nucleation has also to be taken into account in the analysis of overall crystallization. Kolmogorov used a very elegant derivation: He determined the probability that at time, t, elapsed from the beginning of the crystallization process there is still a volume, $V_0 - V(t)$, accessible

I.S. Gutzow and J.W.P. Schmelzer, *The Vitreous State*,
DOI 10.1007/978-3-642-34633-0_10,

to nucleation. Here $V(t)$ is the actual volume of the newly evolving phase and V_0 the initial volume of the melt. The details of Kolmogorov's calculations may be traced in his original publication (Kolmogorov (1937) [464] or in the textbook of Umanski et al. (1955) [875]).

It has to be mentioned, however that a similar mathematical formalism was used by another famous mathematician (Poisson; see his book on the theory of probability (1837) [637]) a 100 years earlier in order to solve a more idyllic problem: It rains and every rain drop forms a concentric wave on the surface of a pond. What is the probability for the existence of an area on the pond not affected by such a concentric wave at time, t? The answer to this question similarly requires the consideration of generation of waves (i.e., of "wave" clusters formed by sporadic nucleation) and its further motion in space (growth); it leads immediately to Kolmogorov's solution for the kinetics of overall crystallization.

Parallel derivations of the theory of overall crystallization were also obtained in the framework of solid state reaction kinetics. Here in most cases the problem is considered of how to find an appropriate description of the kinetics of overall transformation in an ensemble of equal spheres assuming that the crystallization (or reaction) of every sphere starts from the surface. For a solution to this problem, more or less complicated expressions have been derived employing in part methods of physico-chemical similarity or scaling. These attempts will also be mentioned in the following sections so far as they are connected with the general problem under investigation and the problem of kinetic stability of undercooled melts and glasses.

The adequate theoretical description of the overall course of phase transformations is of great importance per se. However, in connection with the discussion of criteria of vitrification it has an additional merit. It was Uhlmann (1972 [872], 1977 [873], cf. also Turnbull (1969) [862]) who succeeded in demonstrating that the simplest and most appropriate way to formulate kinetic criteria for glass-formation from a physical point of view is to use as the starting point the equations describing the overall kinetics of crystallization. The derivation of kinetic criteria for vitrification will be given in this chapter after a discussion of the overall crystallization kinetics where in addition to classical results also effects resulting from the non-steady state character of the nucleation process are incorporated.

10.2 The Kolmogorov-Avrami Equation

While Kolmogorov used the theory of probability to derive the basic equations describing the process of overall crystallization, Avrami preferred another more formalistic way of analysis of this process. Avrami's approach starts with a determination of the so-called extended volume Y_n, given, in general, by

$$Y_n(t) = \omega_n \int_0^t J(t')dt' \left(\int_{t'}^t v(t'')dt'' \right)^n . \tag{10.1}$$

Table 10.1 Values of the Avrami coefficient, $m = n + 1$, for different dimensions of growth and morphology of the clusters of the newly evolving phase. With h the thickness of the discs or the radius of the needles is denoted; J and N^* refer to the density of nuclei per cubic centimeter formed sporadically or athermally. With J_2 and N_2^* the respective quantities for two-dimensional transformations (on surfaces) are denoted

Mechanism of nucleation	Growth morphology	Formula for k_n	$m = n + 1$	Author
Sporadic	Spherical	$\frac{\omega_n}{(n+1)} v^3 J$	4	Avrami [19]
Athermal	Spherical	$\frac{\omega_n}{(n+1)} v^3 N^*$	3	Avrami [19]
Sporadic	Disc-like	$\frac{\omega_n}{(n+1)} v^2 h J$	3	Avrami [19]
Athermal	Disc-like	$\frac{\omega_n}{(n+1)} v^2 h N^*$	2	Avrami [19]
Sporadic	Needle-like	$\frac{\omega_n}{(n+1)} v h^2 J$	2	Avrami [19]
Athermal	Needle-like	$\frac{\omega_n}{(n+1)} v h^2 N^*$	1	Avrami [19]
Surface sporadic	Surface growth	$\frac{\omega_n}{(n+1)} v^2 J_2$	3	Vetter [886]
Surface athermal	Surface radial growth	$\frac{\omega_n}{(n+1)} v^2 N_2^*$	2	Vetter [886]
Sporadic	Sheaf-like bundle-like		5, 6	Morgan [575]

Here Y_n is the volume of the newly evolving phase formed till time, t, when the interaction of the growing crystallites and its effects on the transformation kinetics are neglected. J is the nucleation rate, v the linear growth velocity and ω_n a geometrical shape factor equal to $(4\pi/3)$ for spheres. The parameter n has different values for different nucleation and growth mechanisms and dimensions of space (see Table 10.1), where the transformation takes place.

For constant (time and cluster-size independent) values of the growth velocity, v, Eq. (10.1) gets the form

$$Y_n(t) = \omega_n v^n \int_0^t J(t')(t - t')^n dt' \,, \tag{10.2}$$

The degree of overall crystallization, $\alpha_n(t)$, at time, t, is defined as the ratio

$$\alpha_n(t) = \frac{V_n(t)}{V_0} \,, \tag{10.3}$$

where $V_n(t)$ is, as mentioned, the volume crystallized at time t, V_0 is the initial volume of the melt. The value of α_n can be determined experimentally using any property of the crystallizing system, depending monotonically on α_n.

In the derivation made by Avrami it is assumed that the change of the degree of crystallization with time depends on the ratio of still non-crystallized volume in the form

$$d\alpha_n(t) = (1 - \alpha_n(t))dY_n(t) \,. \tag{10.4}$$

This equation may be integrated to give

$$\alpha_n(t) = 1 - \exp[-Y_n(t)] \,. \tag{10.5}$$

Kolmogorov and Avrami supposed that both the rates of nucleation and of growth in Eq. (10.1) can be considered as time-independent quantities ($J(t) = J = \text{const.}$; $v(t) = v = \text{const.}$). Under such an assumption the extended volume becomes equal to

$$Y_n(t) = \omega_n J v^n \int_0^t (t - t')^n dt' \,, \tag{10.6}$$

leading after integration to the well-known classical result

$$\alpha_n(t) = 1 - \exp\left(-\frac{\omega_n}{(n+1)} J v^n t^{n+1}\right) \,. \tag{10.7}$$

The dependence of α_n on t for $(n + 1) > 1$ has the typical sigmoidal course given in Fig. 10.1; for $n + 1 = 1$ an inverted radioactive decay type dependence follows, which is also shown in the figure.

In Eq. (10.7) instead of n usually the coefficient $m = (n + 1)$ is introduced. The parameter m is denoted as the Avrami coefficient of the transformation. It is an integer number with a value depending on the dimensionality and on the morphology of growth. A derivation of Eq. (10.7) with respect to time gives the rate of overall crystallization in the form

$$\frac{d\alpha_n(t)}{dt} = k_n(n+1)t^n \exp\left(-k_n t^{n+1}\right) \qquad \text{with} \qquad k_n = \frac{\omega_n}{(n+1)} J v^n \,. \tag{10.8}$$

The parameter k_n is the so-called Avrami kinetic coefficient. Equation (10.8) may be rewritten in the form

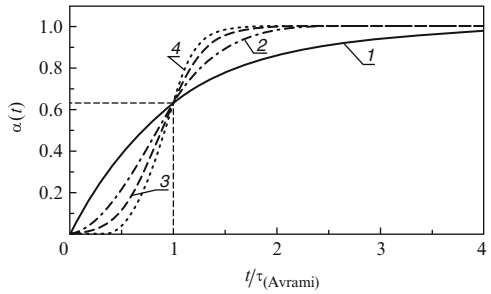

Fig. 10.1 $\alpha_n(t)$-course for $m = (n + 1) = 1$ and $n + 1 \geq 1$ according to Avrami's equation, Eq. (10.7), in reduced coordinates. Curve (*1*): $(n + 1) = 1$; curve (*2*): $(n + 1) = 2$; curve (*3*): $(n + 1) = 3$; curve (*4*): $(n + 1) = 4$. Note that at $(t/\tau_{(Avrami)}) = 1$, α_n equals 0.632 independent of the value of n

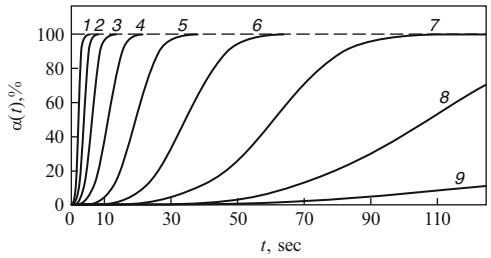

Fig. 10.2 $\alpha_n(t)$-course for $n = 3$ and different values of the kinetic Avrami coefficient, k_n (in seconds) according to Umanski et al. (1955) [875]. The different curves are drawn with the following k_n-values: (*1*): $k_n = 5 \cdot 10^0$; (*2*): $k_n = 5 \cdot 10^1$; (*3*): $k_n = 5 \cdot 10^4$; (*4*): $k_n = 5 \cdot 10^5$; (*5*): $k_n = 5 \cdot 10^6$; (*6*): $k_n = 5 \cdot 10^7$; (*7*): $k_n = 5 \cdot 10^8$; (*8*): $k_n = 5 \cdot 10^9$ and (*9*): $k_n = 5 \cdot 10^{10}$

$$\frac{d\alpha_n(t)}{dt} = (n + 1)k_n^{1/(n+1)} f(\alpha) \,, \tag{10.9}$$

$$f(\alpha_n) = (1 - \alpha_n)[-\ln(1 - \alpha_n)]^{n/(n+1)} \,. \tag{10.10}$$

The rate of change of the degree of overall crystallization, $d\alpha_n(t)/dt$, has a maximum (for $n > 1$) at a definite value of α_n, it corresponds to the point of inflexion in the $\alpha_n(t)$-curves.

For a given value of n the value of the other parameters, for example, the value of ω_n affects only the time scale of the process as illustrated in Fig. 10.2. The dependence of n on the shape and the spatial dimensionality of growing crystalline centers (rod-like: $n = 1$; disc-like: $n = 2$; spheres: $n = 3$) was analyzed first by Avrami. It was discussed in detail by Hollomon and Turnbull (1953) [377] and in a number of monographs (e.g., Mandelkern (1964) [528]; Young (1966) [938]; Barret (1973) [38] etc.). In these discussions also the values of n for more complicated morphologies of growth (bundle-like, sheaf-like crystallites, with $n = 5, 6$) were established (see Morgan (1954) [575]). A summary of results in this respect is given

in Table 10.1. In present-day terminology the result given by Eq. (10.7) corresponds to a system where sporadic steady-state nucleation takes place with constantly growing clusters at constant temperature (thus processes of phase formation with an insufficient degree of thermal dissipation are not considered).

As shown by Avrami, above formalism also describes cases when in the course of the thermal prehistory of the samples (e.g., during an initial cooling run in order to vitrify the melt) a population, N^*, of supercritical clusters of the new phase is formed and frozen-in in the melt. In the process of a subsequent secondary heat treatment (in our case in the process of isothermal devitrification above T_g) such clusters behave like crystallization cores with an activity $\Phi = 0$. Avrami called them athermal nuclei. Avrami's analysis showed that when a population of athermal nuclei (or other insoluble crystallization cores with $\Phi \ll 1$) exists in the melt for a given value of n the term t^{n+1} in Eq. (10.7) has to be replaced by t^{n-1} and J by $N^*_{(tot)}$, where $N^*_{(tot)}$ is the total number of athermal nuclei in the system per unit volume. Thus, instead of Eq. (10.7) we have

$$\alpha_n(t) = 1 - \exp\left(-\frac{\omega_n}{(n+1)} N^*_{(tot)} v^n t^{n-1}\right) . \tag{10.11}$$

In this way, when the morphology and thus the dimensionality of growth is known from additional experiments, the analysis of experimentally observed $\alpha_n(t)$ dependencies allows us to draw conclusions concerning the mechanism of nucleation (homogeneous or heterogeneous) taking place in the system.

The analysis of experimental data on the overall crystallization kinetics is, according to Eqs. (10.7) and (10.11), usually performed in coordinates $\{\ln[-\ln(1-\alpha_n)]$ vs. $\log t\}$. In such coordinates we get

$$\ln[-\ln \alpha_n(t)] = \ln\left(\frac{\omega_n}{(n+1)} J v^n\right) + (n+1)\ln t . \tag{10.12}$$

The slope of the curve gives the value of n; thus, if the type of growth is established by independent experiments, the mechanism of nucleation involved in the considered phase transformation can be determined.

Equation (10.12) may be reformulated also in a somewhat different form introducing a characteristic time scale, $\tau_{(Avrami)}$, of the process of overall crystallization. We may write

$$\ln[-\ln(1-\alpha_n(t))] = \ln\left(\frac{t}{\tau_{(Avrami)}}\right)^{(n+1)} , \tag{10.13}$$

$$\tau_{(Avrami)} = \left(\sqrt[n+1]{\frac{\omega_n}{(n+1)} J v^n}\right)^{-1} .$$

This characteristic time interval $\tau_{(Avrami)}$ can be determined thus simply from experimental $\alpha_n(t)$-curves as the value of t for which $\alpha_n(t)$ equals 0.632 (see Fig. 10.1).

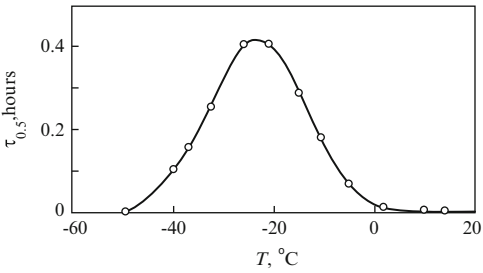

Fig. 10.3 Half-crystallization time $t(\alpha_n = 0.5)$ vs. temperature T for undercooled rubber melts according to the investigations by Bekkedahl (1935) [61]

More generally, the time interval $t(\alpha_n)$ after which a particular ratio α_n of the newly evolving phase has developed in the system, can be written according to Eq. (10.13) as

$$t(\alpha_n) = \tau_{(Avrami)} \left[-\ln(1-\alpha_n)\right]^{1/(n+1)} . \tag{10.14}$$

For small values of α_n this equation may be approximated by

$$t(\alpha_n) = \tau_{(Avrami)} \alpha_n^{1/(n+1)} \qquad \text{for} \qquad \alpha_n \to 0 . \tag{10.15}$$

Experimental determinations of $\alpha_n(t)$ are most precise in the vicinity of $\alpha_n \cong 0.5$. By this reason, for an investigation of the dependence of isothermal overall crystallization processes on temperature curves $[\ln t(\alpha_n = 0.5)]$ vs. temperature T are often determined (see Fig. 10.3). This time interval $t(\alpha_n = 0.5)$ is denoted as half-crystallization time.

Equation (10.15) was employed as the starting point in the derivation of kinetic criteria for vitrification (Uhlmann (1972) [872]). In such an approach it is assumed that the system can be considered as a glass if the time interval the system is heat treated is less than that to reach a very low, just perceptible, degree of overall crystallization, which for microscopic optical observation methods equals $\alpha_n \approx 10^{-6}$.

The formalism developed by Avrami has been applied to a number of problems of crystallization of thin amorphous films (two-dimensional Avrami kinetics, see Vetter (1967) [886]), surface induced crystallization of dispersed systems, solid state reaction kinetics (Young (1966) [938]; Erofeev (1956) [190]; Belkevich (1956) [62]; Jacobs and Tompkins (1955) [397]). With respect to crystallization of glasses the second of the mentioned applications is of particular interest in the crystallization of grained glass samples (glass powders, glass semolina, grained glass frits) (see Müller et al. (1986 [583], 1989 [582]); Fokin et al. (1977) [222]; Gutzow (1979) [302]; Zanotto (1991) [947]; Gutzow et al. (1994) [336]).

The kinetics of overall crystallization taking place in dispersed systems (ensembles of equal spheres of molten droplets, grained glass samples, dust particles etc.) can be described in terms of the theoretical models proposed first by Mampel (1940) [527] and Todes (1940) [840] (see also the generalizations given by Young (1966) [938] and Barret (1973) [38]). In these models it is assumed that on the surfaces of the particles either sporadic two-dimensional nucleation takes place or

that a definite concentration of athermal nuclei exists. The further deterministic growth of the supercritical clusters is directed to the bulk of the particles. Closed analytical solutions to this problem in its general form, however, do not exist; for the application of scaling methods of analysis see Kaseev (1956) [433].

This problem is also of interest from another more general point of view. It is a particular case of a topochemical reaction, i.e., of a reaction where the transformation rate is determined by the interface between newly formed aggregates and the initial phase and not by the bulk concentration of the reactants. Analytical solutions of this problem, however, are also not found. In a first approximation, the kinetics of surface induced crystallization of dispersed systems can be described, again, in terms of Eqs. (10.7) and (10.8) as (see Gutzow (1979) [302])

$$\alpha_n(t) = 1 - \exp\left(-k_n t^{n+1}\right) \ . \tag{10.16}$$

However, the constants k_n and n lose their original meaning and become, as it was established in a recent investigation by Gutzow et al. (1994) [336], functions of the ratio, v/R_0, of the rate of growth, v, and the average size of the particles, R_0, in the disperse system. Equations of the considered type, in particular, Eqs. (10.7), (10.8) and (10.10) are also applied as the starting point for a theoretical interpretation of overall crystallization in non-isothermal crystallization (Yinnon and Uhlmann (1983) [936]; Henderson (1979) [354]; see also Dobreva and Gutzow (1991) [174]).

Methods of analysis of non-isothermal crystallization kinetics are of particular significance when differential scanning calometry (DSC) is applied in investigating crystallization processes in glass-forming systems. In heating run DSC-experiments usually the formalism developed by Henderson (1979) [354] is applied; cooling run DSC-methods, as proven by Dobreva et al. (1993) [175], give, however, a more direct possibility of determining the activity of substances and of other parameters of importance for nucleation.

10.3 Generalization Accounting for Non-steady State Nucleation Kinetics

The derivations given in the preceding section did not account for the time-lag in nucleation. Consequently, they can be valid strictly speaking only if the time-lag in nucleation can be neglected for the experimental situation considered. First attempts to include time-lag effects into the description of overall crystallization were made by Gutzow and Kashchiev (1971, 1972) [313] (see also Gutzow, Kashchiev, and Avramov (1985) [330]). In their calculations the growth rate was further considered as a constant but a time dependent nucleation rate was used in the form as proposed by Collins (1959) [139] and Kashchiev (1969) [434]. The time-dependence of $\alpha_n(t)$ was obtained, thus, in the form

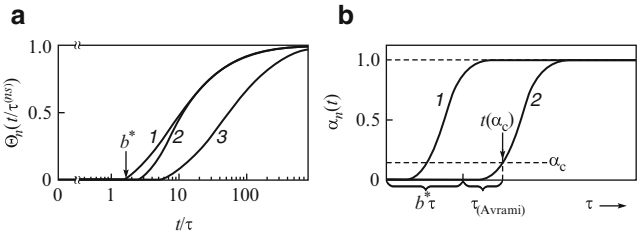

Fig. 10.4 Influence of non-steady state effects in nucleation on the kinetics of overall crystallization. (**a**) Possible $\Theta(t/\tau^{(ns)})$-dependencies (for $n = 3$): (*1*) The exact Gutzow-Kashchiev solution accounting only for transient nucleation effects; (*2*) the approximative solution (Eq. (10.18)) obtained with the step function approach (Eq. (6.173)); (*3*) the Shneidman-Weinberg correction accounting for both steady-state effects and size-dependent growth rates (for $\Delta G_{(cluster)}/k_B T = 20$). (**b**) $\alpha_n(t)$-dependencies: (*1*) the steady-state solution; (*2*) the Gutzow-Kashchiev result with a shift of the curves along the time-axis according to Eqs. (10.17) and (10.18). With α_c a just detectable degree of crystallization is indicated, which in the case of transient nucleation is reached after a time interval $t(\alpha_c) = b^*\tau^{(ns)} + \tau_{(Avrami)}$

$$\alpha_n(t) = 1 - \exp\left[-\frac{\omega_n}{(n+1)} J v^n t^{n+1} \Theta_n\left(\frac{t}{\tau^{(ns)}}\right)\right] . \tag{10.17}$$

In the above equation, Θ_n is a well-defined but relatively complicated function of $(t/\tau^{(ns)})$. Its course for different values of n is given in the paper by Gutzow and Kashchiev (1971) [313].

If one applies in the simplest possible approach a step function for the description of time-lag effects as introduced in Sect. 6.3.6 (Eq. (6.173)), an approximative solution of the form

$$\Theta_n \cong \begin{cases} 0 & \text{for} \quad 0 \le t \le b^*\tau^{(ns)} \\ \left(1 - \dfrac{b^*\tau^{(ns)}}{t}\right)^{n+1} & \text{for} \quad b^*\tau^{(ns)} \le t \le \infty \end{cases} \tag{10.18}$$

is found. With Kashchiev's definition of the time-lag we have $b^* = \pi^2/6$. As seen from Fig. 10.4, Eq. (10.18) is a quite acceptable approximation for the Θ_n-function, it gives even exact results in both limiting cases $t \to 0$ and $t \to \infty$. As manifested by Eq. (10.18) within such an approximation the $\alpha_n(t)$-curves are simply shifted along the t-axis by an interval $b^*\tau^{(ns)}$ (see Fig. 10.4).

The solutions of the problem of non-steady state nucleation kinetics, described here and proposed by Gutzow and Kashchiev (1971) [313], have, however, a limitation: no evaluation is made for a possible size dependence of the rate of growth of the supercritical clusters (compare Chap. 9, Eqs. (9.1) and (9.2)). Two possibilities of avoiding such a limitation exist:

- We can assume that J describes the rate not of the formation of critical clusters but of supercritical clusters with sizes $j \gg j_c$. In such a case the growth rate can be considered as being approximately constant. This method is in fact used in the original Kolmogorov-Avrami approach for the calculation of Y_n, where a steady state nucleation rate is assumed to be established in the system independent of the cluster size. In non-steady state nucleation kinetics, however, the nucleation frequency is size and time-dependent as shown both by numerical calculations and the more recent analytical solutions of the Zeldovich equation by Shneidman (1988 [746], 1992 [747]), Shi, Seinfeld, and Okuyama (1990) [752] and others (see Sect. 6.3.5). In this way, considering the rate of formation of sufficiently large clusters the assumption $v_R = v_R^{(\infty)}$ can be retained, however, more sophisticated time-dependencies for $J(t)$ than the Collins-Kashchiev function have to be used. This was done in a recent paper by Shi and Seinfeld (1991) [751].
- In an alternative approach, appropriate expressions for the rate of formation of critical clusters can be used simultaneously with size-dependent growth rates for the supercritical clusters. This method was applied by Shneidman and Weinberg (1993) [750], who employed Shneidman's $J(j_c, t)$-dependence and a size dependent growth rate v_R of the form given by Eq. (9.1).

The results obtained in these two alternative but equivalent ways were also expressed by the authors in the form given by Gutzow and Kashchiev (see Eq. (10.17)). For comparison, the Shneidman-Weinberg result is shown in Fig. 10.4a. In general, again, a typical sigmoid-shaped form of the $\Theta_n(t)$-course is found shifted along the t-axis. In the $\alpha(t)$-curve, again, a shift by an induction period is observed determined by the time-lag in nucleation and by growth effects.

Both solutions, mentioned above, can be considered as representing a new step in the right direction. However, the advantages in the interpretation of experimental results are till now (from an experimental point of view) relatively insignificant, taking into account the limitations of the different techniques employed in present-day investigations of the overall course of crystallization and the possibilities of computer analysis of non-linear dependencies. It turns out that for practical purposes it is usually sufficient to interpret experimental results by $\alpha(t)$-curves of the Gutzow-Kashchiev form as given by Eq. (10.17), i.e., by

$$\alpha_n(t) = 1 - \exp\left[-k_n(t - t_{(ind)})^{n+1}\right]. \tag{10.19}$$

Here, however, $t_{(ind)}$ accounts both for time-lag effects in nucleation and growth (Dobreva and Gutzow (1994) [177]).

10.4 The Kinetics of Overall Crystallization: Experimental Results

Different experimental methods have been employed in order to investigate overall crystallization in glass-forming melts (quantitative X-ray or IR-analysis (Gutzow (1979) [302]); pycnometric measurements). For polymeric systems different versions of dilatometric and DSC measurements have proven to be useful. In the first experimental investigations of overall crystallization kinetics in devitrification of an inorganic glass ($NaPO_3$; see Gutzow (1959 [287], 1979 [302])) IR-spectroscopy and direct chemical determinations of the fraction of the cyclic $Na_3P_3O_9$ formed in the melt were used (see Fig. 10.5 and Sect. 4.6). In the mentioned and similar experiments (with Na-silicate glasses, with metaphosphates of bivalent metals – $ZnPO_3$, $Cd\,PO_3$ etc.) glass semolina samples were used and a thermally activated surface induced crystallization was observed as a rule (Gutzow (1965) [291]). The experimental results were analyzed in $\log[\log(1-\alpha_n(t))]$-coordinates and straight lines with a slope between 2 and 3 have been found. Such n-values are typically obtained in crystallization of medium sized glass semolina samples; for very large sample fractions (i.e., for low (v/R_0)-values) $n = 1$ is observed as a rule (Gutzow et al. (1994) [336]).

According to the topo-chemical nature of the devitrification process taking place in such samples and the mentioned generalized Mampel-Todes analysis the Avrami coefficient, n, increases with increasing dispersity reaching values of the order $n = 3$ for glass-powder like specimens guaranteeing the existence of a high concentration of athermal surface nuclei and surface induced crystallization. Quite different results are obtained (Westman and Krishnamurthy (1962) [918]; see also Gutzow (1979) [291]) when the crystallization of relatively large glass samples (glass beads) with an intact fire-polished surface is analyzed. In this case, well-expressed induction periods are found resulting from a sporadic thermal surface nucleation and further bulk growth (see Fig. 10.5b).

Volumetric determinations of the overall crystallization in glass-forming melts reveal also another typical feature of the crystallization process (see Fig. 10.6): Stabilization of the glass to higher densities (indicated in the figure by a broken line) preceeds surface induced crystallization of the samples. Non-steady state effects in the overall crystallization were demonstrated to be of importance also in crystallization of metallic glass-forming alloys (Budurov et al. (1987) [108]) and of organic polymers (see Fig. 10.7; Gutzow and Dobreva (1993) [175]). $\alpha_n(t)$-curves obtained with polymer melts at temperatures near the melting temperature, T_m, show no measurable induction period while in the vicinity of the temperature of vitrification, T_g, a significant shift of the curves along the time-axis is observed as it is to be expected from Eqs. (10.17) and (10.18). The change of the length of the induction time $\tau_{(ind)}$ follows the predictions of the Gutzow-Kashchiev analysis taking into account time-lag in nucleation.

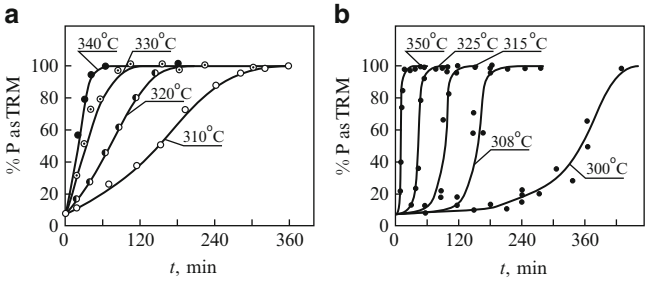

Fig. 10.5 Kinetics of devitrification of $NaPO_3$-glass samples heat treated at different temperatures above T_g (the temperatures are given as a parameter to each curve in °C). (**a**) Typical example of surface induced crystallization by athermal nuclei: Surface induced devitrification of glass semolina (with average diameters of glass particles of the order $\overline{d} = 0.75 - 1.00$ mm) investigated by quantitative IR-analysis (Gutzow (1964, 1966) [291, 322]). (**b**) Devitrification of glass beads with an intact surface (thermally activated nucleation with a typical induction period (Westman and Krishnamurthy (1962) [918])) examined by quantitative paper chromatography. T_g for $NaPO_3$-glass is 275 °C

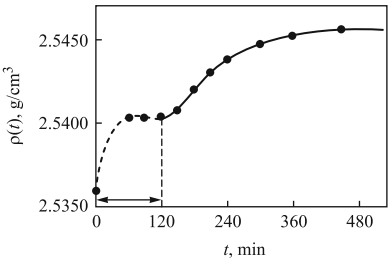

Fig. 10.6 Pycnometric determination of surface crystallization of a Na-silicate glass at 520 °C (glass semolina sample with $\overline{d} = 0.75 - 1.0$ mm). Note the initial stabilization process *(broken line)* preceding crystallization

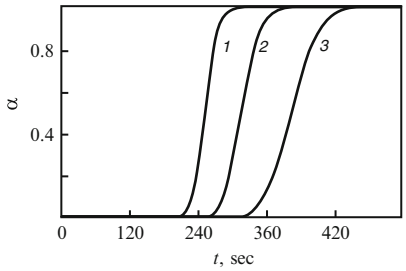

Fig. 10.7 $\alpha_n(t)$-curves for polymers: Crystallization kinetics of (poly)ethylene terephthalate with a typical non-steady-state shift for temperatures in the vicinity of T_g (equal to $T_g = 340$ K). The different curves refer to (*1*): 371 K; (*2*): 369 K; (*3*): 367 K (Gutzow and Dobreva (1992) [310]; Dobreva (1992) [173])

10.5 Kinetic Criteria for Glass-Formation: Time-Temperature-Transformation (TTT) Diagrams

There are three independent possibilities of estimating the ability of a given substance to form a glass. The first one, which involves purely structural or geometric ideas, has already been discussed in Chap. 4. Most well-known examples in this direction are Goldschmidt's ratio criterion and Zachariasen's rules. However, definite geometric rules have been developed and can be applied only to a given class of substances (oxides, halides etc.). More generally, often intuitively formulated statements, e.g. that glass-forming liquids should possess structures allowing the formation of various complexes or groupings (Hägg's rule) that they have to be formed of complexes permitting "mixed" types of bonding (Smekal's criterion (cf. Rawson's monograph [657])), Stanworth's electronegativity model (1946) [792] or the "p-electron" criterion of Winter (1957) [928], although of considerable historical interest, give only qualitative indications. They cannot be considered as quantitatively correct approaches in formulating criteria for glass-formation. A summary of the above mentioned and similar ideas is given in the already cited literature (Rawson (1967) [657]; Scholze (1965, 1977) [732]).

A second approach in formulating criteria for glass-formation is based upon bond strength considerations. In this approach, it is supposed that the stronger the bonds in the melts the more sluggish will be the process of rearrangement of the ambient phase particles connected with crystallization (see again Rawson's monograph [657]). As a realistic parameter in such a line of argumentation the ratio between bond strength and average kinetic energy of the ambient phase particles (e.g., at the melting point T_m) may be introduced. In this way, a classification of substances can be carried out into potential glass-formers and easily crystallizable substances. This second approach, as well as argumentations based on purely geometric criteria, do not take into account the conditions, in particular, the value of the cooling rate q, at which vitrification takes place.

In both approaches it is assumed from the very beginning that substances can be divided into two classes – 'vitroids' and 'crystalloids' (if an older classification already mentioned in Chap. 2 is applied) – and that a more or less sharp distinction between both classes of substances can be made. The necessary generalization can be obtained only in the third, kinetic group of approaches by linking the glass-forming ability of a substance with the kinetics of crystallization of the respective under-cooled melts or with its kinetic stability. The first author to follow this line of argumentation, although in a qualitative way, was one of the founders of glass-science, G. Tammann. According to Tammann's suggestion glass-formation is to be expected when the curves representing the temperature dependencies of nucleation and growth rates do not overlap (compare Fig. 2.12). In the reverse case crystallization of the melt will probably occur. In a subsequent step in this direction, the qualitative statement concerning the connection between glass-forming ability and crystallization parameters had to be reformulated in a quantitative way. Here a

number of different possibilities exist because, as it is evident from Chaps. 6 and 8, any crystallization process is determined by three main parameters

- The steady-state nucleation rate J,
- The rate of growth of crystalline clusters v and
- The non-steady state time-lag in nucleation $\tau^{(ns)}$.

The temperature course of these three parameters, as it is to be expected theoretically, is schematically shown in Fig. 6.16.

In the pioneering works dealing with a derivation of kinetic criteria of glass-formation, the glass-forming ability of substances was connected with only one of the mentioned characteristics of the crystallization process. Dietzel and Wiekert (1956) [172] supposed that the glass-forming ability, E_g, is inversely proportional to the growth rate v ($E_g \sim 1/v$). Turnbull and Cohen (1960) [865] connected E_g with the steady-state nucleation rate as $E_g \sim 1/J$ while Gutzow and Kashchiev (1970 [312], 1971 [313]) took E_g proportional to the time-lag in non-steady state nucleation ($E_g \sim \tau^{(ns)}$). In choosing, intuitively, only one of the three characteristics of the crystallization process as the dominant one, the other two were disregarded in the above-mentioned early studies as insignificant. Thus Turnbull and Cohen (1960) [865] assumed an infinitely fast rate of growth of the crystalline nucleus after its formation (which is in fact approximately true only for low-viscosity liquids near to the melting temperature, T_m). Dietzel and Wiekert (1956) [172] started from the preposition that devitrification (i.e., crystallization in the process of reheating the glass) takes place on already existing nucleation cores formed during the quench of the melt. In this way, devitrification was considered by the mentioned authors as a process of crystal growth on athermal nuclei (see also Gutzow (1959) [287], in particular, the experimental evidence given there).

In the approximation made by Gutzow and Kashchiev (1970 [312], 1971 [313]) it was supposed that in the crystallization of an undercooled melt, the time needed to reach a very low just detectable percentage of crystallization, α_c, by nucleation and growth can be neglected as compared with the non-steady state time-lag, $\tau^{(ns)}$. In 1972, Uhlmann ([872]; see also his paper from 1977 [873]) formulated a kinetic criterion for vitrification based on the Kolmogorov-Avrami synthesis of nucleation and growth via the kinetics of the overall crystallization process. However, in Uhlmann's analysis of the kinetic stability of under-cooled melts the time-lag in nucleation, $\tau^{(ns)}$, was not taken into account. The necessary generalization of Uhlmann's criterion, based on the extended non-steady-state formulation of the process of overall crystallization as it is given in the preceding sections, was carried out in a paper by Gutzow, Kashchiev and Avramov (1985) [330]. In this way, a criterion for glass-formation was obtained dependent on the three parameters of the crystallization process (J, v and $\tau^{(ns)}$) listed above.

The connection of the process of glass-formation with the kinetics of vitrification, as described above, gives general criteria for glass-formation, valid for all substances, and general rules for glass-formation which are independent of the particular structure and the type of bonding of the considered substance. Moreover, the kinetic approach allows us to calculate the minimal cooling rate required to

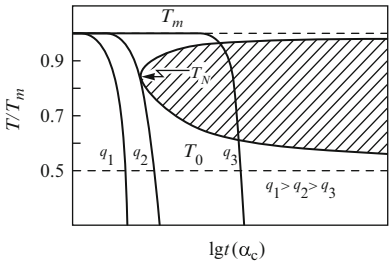

Fig. 10.8 TTT-curve, 'nose'-temperature, T_N, and cooling rate, q, in coordinates (T/T_m) vs. $\log t(\alpha_c)$ (assuming $q \approx$ constant). The *shaded area* corresponds to $\alpha > \alpha_c$, in this region pronounced crystallization is to be expected

obtain a given substance as a glass. Such estimates are of considerable technological and practical interest. However, the theoretical significance of such calculations is even greater. They give as a result that a sharp distinction between so-called 'vitroids' and 'crystalloids' has no meaning and that any substance can be vitrified provided the required cooling rate can be attained experimentally.

The kinetic criterion for vitrification as developed first by Uhlmann is most easily formulated in terms of the so-called TTT-diagrams. These diagrams describe the **T**emperature dependence of the **T**ime interval, $t(\alpha_c)$, at which a given degree, α_c, of the melt-crystal **T**ransformation is reached. The value of α_c is determined by the lower limit of detection of crystallization. According to Uhlmann (1972) [872] the lowest value of detectable crystallization corresponds (considering typical optical microscopic methods of investigation) to $\alpha \cong 10^{-6} - 10^{-5}$. In some cases (depending on the method of detection and the required degree of amorphousness) to α_c much smaller values have to be assigned to (e.g., in glasses designed for application in fiber optics). In contrast, in employing other methods of structural investigations like differential scanning microscopy (DSC) or X-ray analysis α_c may have considerably higher values (of the order of 10^{-3}).

It follows from the general theory outlined in Sect. 10.2 that the temperature dependence of $t(\alpha_c)$ is determined, in general, by J, v and $\tau^{(ns)}$ and thus by the temperature course of the viscosity, η, and the thermodynamic driving force of the transformation $\Delta\mu$, respectively, the undercooling ΔT (compare Eqs. (10.13) and (10.15)). The natural asymptotic lines of the TTT-curves, where $t(\alpha_c)$ tends to infinity, are found in this way at the melting temperature T_m, where $\Delta\mu$ equals zero and at $T = T_0$, where the viscosity tends to infinity. In both limiting cases $\tau_{(Avrami)}$ approaches zero and a finite volume fraction of the crystalline phase can evolve only after very large time intervals tending to infinity (see Fig. 10.8).

The shaded area on the right hand side of the figure corresponds to the region in the parameter space where pronounced crystallization occurs, the non-shaded area refers to amorphous samples. In Fig. 10.8, three different cooling curves are indicated corresponding to different constant cooling rates, $q = -dT/dt$. In TTT-diagrams T vs. $\log t(\alpha_c)$ coordinates are used and thus, at $q =$ constant, the linear T vs. t dependencies are transformed into curves of a form as shown in the figure. The curve, corresponding to the cooling rate q_3, intersects the region of the crystalline phase. In such cases, the cooling rate is too low to prevent crystallization while for a

quench with a rate q_1 no detectable crystallization is found. The curve q_2, which is tangent to the $t(\alpha_c)$-curve at the 'nose' temperature, T_N, corresponds to the critical or minimal cooling rate, q_c, for which the formation of a glass is still possible. TTT-curves have been used in experimental metallography for many years in order to determine the conditions for formation of metastable or unstable phases. In glass science, following Uhlmann's suggestion, they are utilized to determine q_c.

Carrying out a critical quench with a constant cooling rate the temperature T_N is reached after a time $t_N(\alpha_c)$, i.e.,

$$T_N = q_c t_N(\alpha_c) \; . \tag{10.20}$$

The time interval $t_N(\alpha_c)$ can also be determined as the time for which, at a constant temperature T_N, a critical ratio of the crystalline phase has evolved in the system (compare Fig. 10.8). Moreover, approximating T_N by

$$T_N \approx \frac{1}{2}(T_m + T_0) \tag{10.21}$$

we get

$$q_c \cong \frac{1}{2}\left(\frac{T_m + T_0}{t_N(\alpha_c)}\right) \; . \tag{10.22}$$

The above considerations have to be generalized if non-steady state effects (time-lag in nucleation) are taken into account.

As mentioned in the previous sections non-steady state effects are of particular importance for the understanding of nucleation in glass-forming systems and also of the overall course of melt crystallization. Consequently, such a generalization is necessary if critical cooling rates for glass-forming melts are estimated. The desired generalization may be based on Eqs. (10.17) and (10.18) instead of Eqs. (10.13) and (10.15). According to Eq. (10.17) we have to write

$$\left(-\frac{\ln(1-\alpha)}{\frac{\omega}{n+1} J v^n}\right)^{1/(n+1)} \approx \frac{\alpha^{1/(n+1)}}{\left(\frac{\omega}{n+1} J v^n\right)^{1/(n+1)}} = t \sqrt[n+1]{\Theta_n} \; . \tag{10.23}$$

It turns out that, in general, a complicated dependence has to be expected between the classical expression for $t(\alpha_c)$ and the modified version taking into account non-steady state effects in nucleation. However, with the approximative expression Eq. (10.18) a simple linear relationship of the form

$$t(\alpha_c) = b^* \tau^{(ns)} + \frac{\alpha_c^{1/(n+1)}}{\left(\frac{\omega}{n+1} J v^n\right)^{1/(n+1)}} = b^* \tau^{(ns)} + \tau_{(Avrami)} \tag{10.24}$$

is obtained (see also Gutzow, Kashchiev, and Avramov (1985) [330], Fig. 10.4). It allows one a simple analysis of the influence of non-steady state effects on processes of glass-formation as done by Gutzow, Avramov and Kästner (1990) [331]. Rewriting Eq. (10.24) in the form

$$t(\alpha_c) \cong b^* \tau^{(ns)} \left[1 + \frac{\alpha_c^{1/(n+1)}}{(J v^n)^{1/(n+1)} b^* \tau^{(ns)}} \right] = b^* \tau^{(ns)} \left(1 + \frac{\tau_{(Avrami)}}{b^* \tau^{(ns)}} \right) \quad (10.25)$$

it becomes evident that in dependence on the value of the ratio $\tau_{(Avrami)}/\tau^{(ns)}$ the time interval $t(\alpha_c)$ is entirely determined either by the time-lag $\tau^{(ns)}$ (for $\tau_{(Avrami)}/\tau^{(ns)} \ll 1$) or by $\tau_{(Avrami)}$ (for $\tau_{(Avrami)}/\tau^{(ns)} \gg 1$). In the latter case, time-lag effects may be neglected as done by Uhlmann.

The temperature dependence of $\tau_{(Avrami)}$ is determined both through kinetic (the viscosity, η) and thermodynamic factors (supersaturation, $\Delta\mu$). However, according to Eqs. (6.122), (6.194), (8.11), (8.50) and (8.55) the quantities J, v and $\tau^{(ns)}$ depend on viscosity, η, as $J \sim \eta^{-1}$, $v \sim \eta^{-1}$ and $\tau^{(ns)} \sim \eta$. Consequently, the combination of these quantities $(J v^n)^{1/(n+1)} \tau^{(ns)}$ is independent of η and the temperature dependence of $\tau_{(Avrami)}$ is determined exclusively by the temperature dependence of the thermodynamic driving force of the transformation.

A more detailed analysis given in above cited paper allows us to conclude that for homogeneous nucleation $\tau_{(Avrami)} \gg \tau^{(ns)}$ holds, in general, and we may rewrite Eq. (10.25) as

$$t(\alpha_c) \cong \tau_{(Avrami)} \qquad \text{for homogeneous nucleation .} \quad (10.26)$$

Considering catalyzed nucleation, in addition, the activity Φ (cf. Eqs. (7.8) and (7.18)) and the dependence of nucleation rate and time-lag on the concentration of surfactants (cf. Eqs. (7.34) and (7.35)) have to be taken into account in determining the ratio $\tau_{(Avrami)}/\tau^{(ns)}$. However, the dependence of the nucleation rate on these factors is much steeper (of exponential form) and, consequently,

$$t(\alpha_c) \cong b^* \tau^* \qquad \text{for catalyzed nucleation} \quad (10.27)$$

has to be expected as supposed years ago by Gutzow and Kashchiev (1970 [312], 1971 [313]). Thus, two different estimates for $t(\alpha_c)$ may be made, one for the case if vitrification in a pure substance is considered and the other when nucleation in glass-forming melts under more realistic conditions is analyzed, i.e., in the presence of surface-active contaminants and crystallization cores.

After some straightforward computations, taking into account realistic values of the parameters (e.g., the number of nucleation cores $N^*_{(cores)}$ has a value of $10^7 - 10^8$ cm^{-3} for natural and $10^{12} - 10^{13}$ cm^{-3} for artificially doped melts) and applying the Skapski-Turnbull rule, Eq. (6.127), we arrive at

$$t(\alpha_c) \cong \alpha_c^{1/4} c_1 c_2 \tau(T_N) \exp\left(-\frac{32\pi\zeta^3 \Delta S_m (1-\theta_0^*)\theta_0^*}{3R}\right), \tag{10.28}$$

for homogeneous nucleation,

$$t(\alpha_c) \cong c_2 \frac{R}{\Delta S_m} \tau(T_N) \sqrt[3]{\Phi} \left(1 - \frac{\Delta\sigma}{\sigma}\right), \tag{10.29}$$

for catalyzed nucleation.

In writing Eq. (10.29) it was assumed that in the presence of both surface active substances and foreign nucleation cores an additive catalytic effect on the time-lag has to be expected (cf. Eqs. (7.18) and (7.35)). The possible combined effect of both mentioned factors on $\Delta G_c^{(cluster)}$ and, in particular, on the steady-state nucleation rate J, has been investigated in detail by Kaischew and Mutaftschiev (1959) [422]. In the above equations, c_1 and c_2 are numerical constants having values of the order $c_1 \approx 0.1$, $c_2 \approx 0.25$, respectively, and θ_0^* is defined by $\theta_0^* = (1 + T_0/T_m)/2$.

In order to calculate $t(\alpha_c)$ we have to specify the temperature dependence of the time of molecular relaxation, $\tau(T_N)$, in above equations. A thorough analysis (cf. Gutzow, Avramov, and Kästner (1990) [331]) leads to $\tau(T_N) \cong \exp(U(T_m)/RT_m)$ as an optimal estimate for $\tau(T_N)$. Introducing this estimate into above equations, Eqs. (10.28) and (10.29), we arrive, finally, at

$$\log q_c \cong 20 - \frac{U(T_m)}{RT_m} - \frac{2\Delta S_m}{R} \tag{10.30}$$

for homogeneous nucleation,

$$\log q_c \cong 17 - \frac{U(T_m)}{RT_m} \tag{10.31}$$

for catalyzed nucleation.

In deriving these relations the value of the parameter ζ in the Skapski-Turnbull rule was set equal to $\zeta = 0.45$. Moreover, it has been assumed that the ratio T_0/T_m varies within the limits 0.2–0.5 that T_m varies in between 200 and 2,000 K and that $(1 - \Delta\sigma/\sigma)\sqrt[3]{\Phi} = 0.1$ holds. In this way estimates of q_c may be obtained out exclusively by knowing the molar entropy of melting ΔS_m and the value of the activation energy U at the melting temperature T_m.

In Fig. 10.9, a summary of data for halides collected from the respective reference literature is given. In the case when $U(T_m)$-values were not known precisely, the values were estimated by a procedure described by Gutzow, Avramov and Kästner (1990) [331]. By a substitution of these data the q_c-values were calculated with Eqs. (10.30) and (10.31) and plotted as a function of the cation to anion ratio R_C/R_A. Based on the value of the critical cooling rate required to obtain a glass in the process of cooling of the melt, again, a classification of substances may be introduced into 'vitroids' (substances which may be easily transformed into a glass) and 'crystalloids'. In Fig. 10.9, for example, this division was performed

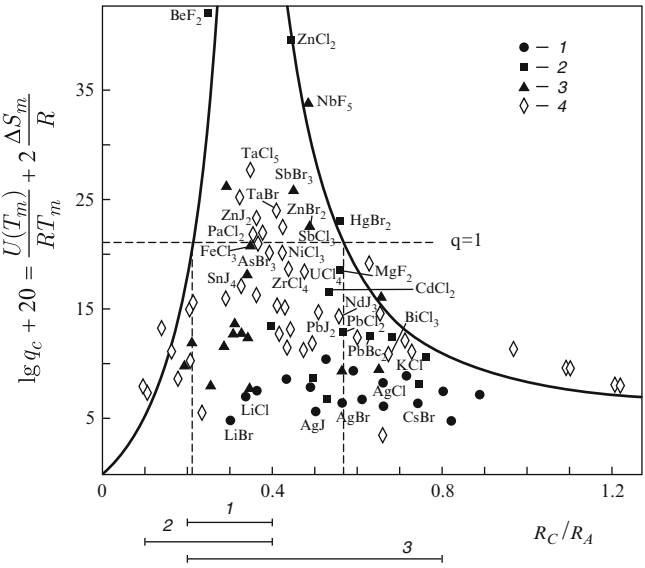

Fig. 10.9 Halide substances in coordinates $U(T_m)/RT_m + 2\Delta S_m/R = 20 - \log q_c$ according to Eq. (10.30) (homogeneous nucleation). (*1*): Monovalent metal halides; (*2*): divalent metal halides; (*3*): metal halides with a valency higher than 2. The data for the cases (*1*)–(*3*) were calculated based on experimental $\eta(T)$-dependencies and ΔS_m-values while the set of values (*4*) is calculated from the enthalpy of evaporation ΔH_{ev} (Gutzow, Avramov, and Kästner (1990) [331])

by assigning to the boundary between both classes of substances the value $q_c = 1\,\mathrm{Ks}^{-1}$. Such an obviously more or less artificial division allows one to establish relationships between kinetic and structural criteria of glass-formation as discussed in the next section.

10.6 Kinetic, Bond Energy and Structural Criteria for Vitrification: A Comparison

When the value of the activation energy for viscous flow $U(T_m)$, appearing in Eqs. (10.30) and (10.31), is calculated according to existing model theories (see Chap. 12 and the already cited paper by Gutzow, Avramov and Kästner (1990) [331]) it turns out that because of $U(T_m) \cong \Delta H_{ev}$, the critical cooling rate, q_c, may be written in the form

$$\log q_c \cong \text{constant} - \frac{\Delta H_{subl}}{RT_m}\,, \qquad \Delta H_{subl} = \Delta H_{ev} + T_m \Delta S_m\,. \tag{10.32}$$

Here ΔH_{subl} and ΔH_{ev} are the molar enthalpies of sublimation and evaporation of the melt, respectively,

Suppose, now, we introduced, as discussed in the previous section, the value $q_c = 1\,\mathrm{Ks}^{-1}$ of the cooling rate as the criterion for a division of the substances into 'vitroids' and 'crystalloids', then 'vitroids' are substances for which the inequality

$$\frac{\Delta H_{subl}}{RT_m} \geq \text{constant} \tag{10.33}$$

holds (cf. Eq. (10.32)). Taking into account that the enthalpy of sublimation of a substance is proportional to its bond energy it is evident that Eq. (10.33) reflects in fact Sun's and Rawson's 'bond-strength' criterion for glass-formation already mentioned at the beginning of Sect. 10.5. With Eq. (10.32), the enthalpy of evaporation can be expressed through the entropy of evaporation as $\Delta H_{ev} = T_b \Delta S_{ev}$, where T_b denotes the boiling temperature of the melt. Taking into account the relation $T_b \approx (5/2)T_m$ (cf. Eq. (2.74)) we obtain from Eq. (10.31)

$$\frac{\Delta S_{ev} + \Delta S_m}{R} \geq \text{constant}\,. \tag{10.34}$$

The inequality Eq. (10.34) indicates that as 'vitroids' substances may be considered for which the sum of the entropies of evaporation and melting is a sufficiently large quantity. This condition is fulfilled, as a rule, for associating liquids, i.e., for systems with a tendency of formation of complex or mixed type structural units in the melt. In this way, a connection may be established with the criteria formulated by Smekal and Hägg.

In Fig. 10.9, the values of q_c for about 100 binary halides are represented. It is seen that typical halide glass-formers (BeF_2, $ZnCl_2$, $ZnBr_2$) as well as substances like SbF_5, forming highly viscous melts, or halides acting as glass promoters in multi-component glass-forming halide systems ($CdCl_2$, $PbCl_2$) are located within the range of (R_C/R_A)-values suggested by Goldschmidt's radius ratio criterion (cf. Eq. (4.1)) if $q_c = 1$ (or equivalently $\log q_c = 0$) is taken as the boundary between 'vitroids' and 'crystalloids'. Indeed, the points of intersection of the curves drawn as an envelope of the experimental data in $[U(T_m) + 2T_m \Delta S_m]/(RT_m)$ vs. (R_C/R_A) coordinates (full curves in Fig. 10.9) with the straight line $q_c = 1\mathrm{Ks}^{-1}$ show that the glass-forming halides are located inside the limits

$$0.2 \leq \frac{R_C}{R_A} \leq 0.5\,. \tag{10.35}$$

This result may be regarded as a direct confirmation of Goldschmidt's original statement (Eq. (4.1)) and similar developments such as Poulain's structural criterion for halide substances.

However, not all halides which fall within the limits given by Eq. (10.35) are, indeed, glass-formers. In contrast, below the $\log q_c = 0$ line a great number of substances are found, for which Eq. (10.30) determines such enormous q_c-values that glass-formation is practically excluded for them. This result is a verification of the conclusion that Eq. (10.35) (like Goldschmidt's and similar criteria) is a necessary but not a sufficient criterion for glass-formation. A closer inspection of the data summarized in Fig. 10.9 reveals that only halides (for which Eq. (10.35) is fulfilled) with valencies higher than two are potential glass-formers. Moreover, only those halides have sufficiently large $U(T_m)$-values for which a well-expressed tendency of polymerization of the primary building units is found. Structural data, available for the known or prospective glass-formers, verify, in fact that halides like $ZnCl_2$, $ZnBr_2$, BeF_2, $PdCl_2$, VF_5, $SbBr_3$ etc. form polymer-like associative structural elements in the melt and can be termed thus as polymeric halides. For halides both these additional requirements, which have to be fulfilled together with Eq. (10.35), guaranty a high glass-forming ability. In this sense they are supplementary to Eq. (10.35) similarly as Zachariasen's or Hägg's criteria had to be combined with Goldschmidt's original statement.

The analysis carried out in the present section shows that, in fact, structural or bond energy criteria for vitrification can be, at least, in principle, derived from the more general physical picture of kinetic stability of under-cooled melts and from the kinetic criteria for glass-formation outlined in the previous section.

Chapter 11
Liquid Phase Separation in Glass-Forming Melts

11.1 Introduction

Up to now in considering in our derivations possible phase transformations in undercooled glass-forming melts mainly segregation and crystallization processes were considered proceeding via nucleation and growth and independently from each other. However, in most multi-component systems crystallization may be accompanied by processes of liquid phase separation and vice versa.[1] In addition, another mechanism of phase separation may be also of importance denoted as spinodal decomposition.

Let us consider, for simplicity, an idealized two-component glass-forming system, in which both liquid phase separation and crystallization may take place. The phase diagram is shown on Fig. 11.1. Inside the binodal curve (acb) the homogeneous system is thermodynamically unstable with respect to decomposition

[1]For a recent analysis of phase separation in solutions including finite-size effects in terms of the generalized Gibbs' approach, cf. Schmelzer et al. (2000, 2004, 2007) [702, 722, 725, 726], Abyzov and Schmelzer (2007) [3], Abyzov et al. (2010) [4] and Schmelzer and Abyzov (2011) [703]. In this analysis, basic features of spinodal decomposition, on one side, and nucleation, on the other side, and the transition between both mechanisms are analyzed within the framework of a generalized thermodynamic cluster model based on the generalized Gibbs approach. Hereby the clusters, representing the density or composition variations in the system, may change with time both in size and in their intensive state parameters (density and composition, for example). In the first part of the analysis, we consider there phase separation processes in dependence on the initial state of the system for the case when changes of the state parameters of the ambient system due to the evolution of the clusters can be neglected as this is the case for cluster formation in an infinite system. As a next step, the effect of changes of the state parameters on cluster evolution is analyzed. Such depletion effects are of importance both for the analysis of phase formation in confined systems and for the understanding of the evolution of ensembles of clusters in large (in the limit infinite) systems. The results of the thermodynamic analysis are employed in both cases to exhibit the effect of thermodynamic constraints on the dynamics of phase separation processes as it has been performed briefly in the present book, employing the classical Gibbs'S approach in Sect. 6.3.10.

I.S. Gutzow and J.W.P. Schmelzer, *The Vitreous State*,
DOI 10.1007/978-3-642-34633-0_11, © Springer-Verlag Berlin Heidelberg 2013

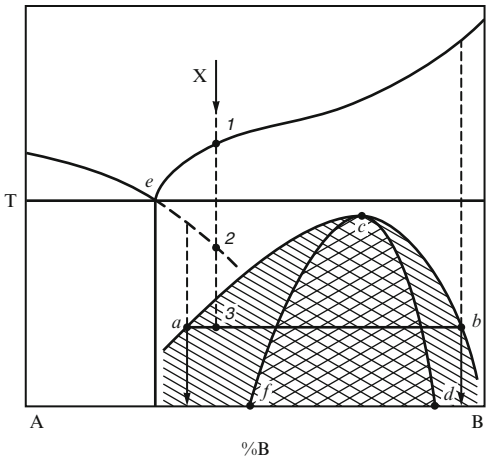

Fig. 11.1 Schematic binary phase diagram of a glass-forming system with eutectic point (*e*) and entirely subsolidus liquid-liquid immiscibility cupola with the binodal *(acb)* and spinodal *(fcd)* curves

processes and may separate into a two-phase system either by nucleation and growth (approximately in the region bounded by the binodal and spinodal curves) or by spinodal decomposition (inside the spinodal curve (fcd)) (see, e.g., van der Waals (1899) [880]; Cahn and Hilliard (1958, 1959) [119]; Cook (1970) [141]; Langer, Bar-on, and Miller (1975) [497]; Binder (1992) [82]; James (1975) [401]; Andreev, Mazurin et al. (1974) [14]). If a sample is cooled from the liquidus temperature T_1 to some temperature T_3 (we assume that $T_3 > T_g$ is fulfilled) at a composition x, indicated in the figure by an arrow, then, in addition to liquid phase separation, the component A may crystallize. The driving force for the crystallization process is determined by the under-cooling, $\Delta T = T_2 - T_3$.

11.2 Kinetics of Spinodal Decomposition

Following van der Waals ((1893) [880]; see also Rowlinson (1979) [670]; Cahn and Hilliard (1958, 1959) [119]) in a first approximation the Gibbs free energy of a binary solution at constant pressure and temperature may be expressed as

$$G = \int \left[g(c) + \kappa_\Sigma (\nabla c)^2 \right] dV \, . \tag{11.1}$$

Here $c(\mathbf{r}, t)$ is the volume density of one of the components of the solution, $g(c)$ the volume density of the Gibbs free energy and $\kappa_\Sigma > 0$ a coefficient describing the contributions to the thermodynamic potential due to inhomogeneities in the system (interfacial contributions). Provided the deviations from the initial concentration c_0 are relatively small, then a Taylor expansion of g results in the following expression for the change of the Gibbs free energy ΔG connected with the evolution of the concentration field $c(\mathbf{r}, t)$

$$\Delta G = \int \left[\frac{1}{2} g''(c_0, T)(c - c_0)^2 + \kappa_\Sigma (\nabla c)^2 \right] dV \ , \qquad g''(c_0, T) = \left(\frac{\partial^2 g}{\partial c^2} \right)_{C_0, T} . \tag{11.2}$$

In agreement with the thermodynamic stability conditions a spontaneous growth of the density fluctuations takes place only for $g''(c_0, T) < 0$, since only in this case is the amplification of the density profile accompanied by a decrease of the free enthalpy of the system. Here g'' denotes the second partial derivative of the volume density of the Gibbs free energy, g, with respect to concentration, c.

In the framework of the Cahn-Hilliard-Cook theory the kinetics of spinodal decomposition is described by a generalized diffusion equation interconnecting the variations of the thermodynamic potential G with the kinetics of the decomposition process. This generalized diffusion equation follows from the set of equations, Eqs. (11.3)–(11.5)

$$\frac{\partial c}{\partial t} + \mathrm{div}\mathbf{j} = 0 \ , \tag{11.3}$$

$$\mathbf{j} = \mathbf{j}_D + \mathbf{j}_B \ , \tag{11.4}$$

$$\mathbf{j}_D = -M \nabla \frac{\delta G}{\delta c} \ , \qquad \mathbf{j}_B = -\nabla B(\mathbf{r}, t) \tag{11.5}$$

and has the form

$$\frac{\partial c(\mathbf{r}, t)}{\partial t} = M g''(c_0, T) \nabla^2 c(\mathbf{r}, t) - 2M \kappa_\Sigma \nabla^4 c(\mathbf{r}, t) + \nabla^2 B(\mathbf{r}, t) \ . \tag{11.6}$$

Here $\mathbf{j}_D$ has the meaning of a deterministically determined density of fluxes of particles, while $\mathbf{j}_B$ describes the flow connected with the fluctuating scalar field $B(\mathbf{r}, t)$, superimposed on the deterministic flow. M is a mobility coefficient. The $c(\mathbf{r}, t)$ and $B(\mathbf{r}, t)$ fields can be expressed through Fourier expansions via

$$c(\mathbf{r}, t) = c_0 + \sum_{-\infty}^{+\infty} S(k_n, t) \exp(i \mathbf{k}_n \mathbf{r}) \ , \tag{11.7}$$

$$S(\mathbf{k}_n, t) = \frac{1}{V} \int [c(\mathbf{r}, t) - c_0] \exp(-i \mathbf{k}_n \mathbf{r}) d\mathbf{r} \ , \tag{11.8}$$

$$B(\mathbf{r}, t) = \sum_{-\infty}^{+\infty} L(k_n, t) \exp(i \mathbf{k}_n \mathbf{r}) \ , \tag{11.9}$$

$$L(\mathbf{k}_n, t) = \frac{1}{V} \int B(\mathbf{r}, t) \exp(-i \mathbf{k}_n \mathbf{r}) d\mathbf{r} \ . \tag{11.10}$$

V is the volume of the system.

From above equations the following differential equation for a description of the time dependence of the spectral function, $S(\mathbf{k}_n, t)$, can be obtained

$$\frac{\partial S(\mathbf{k},t)}{\partial t} = R(\mathbf{k},t)S(\mathbf{k},t) - \mathbf{k}^2 L(\mathbf{k},t) \ , \tag{11.11}$$

where the amplification factor, $R(\mathbf{k},t)$, is determined by

$$R(\mathbf{k},t) = -M\mathbf{k}^2 \left[\left(\frac{\partial^2 g}{\partial c^2} \right)_{C_0,T} \right] . \tag{11.12}$$

The subscript n in $\mathbf{k}_n$ is omitted here and further-on for simplicity of the notations. The value of the wave number k, for which the derivative $(\partial S/\partial t)$ is equal to zero, is commonly denoted as critical wave number.

From an experimental point of view processes of spinodal decomposition are studied usually by X-ray measurements. In these and similar investigations not the spectral function, S, itself but a quantity proportional to the average of the square of the spectral function $\langle SS^* \rangle$ is measured. The time-dependence of this quantity can be shown to be governed by an equation of a form similar to Eq. (11.11), i.e.,

$$\frac{\partial \langle S^2(\mathbf{k},t) \rangle}{\partial t} = 2R(\mathbf{k},t)\langle S^2(\mathbf{k},t) \rangle + \mathbf{k}^4 Q(\mathbf{k}) \tag{11.13}$$

with (see, e.g., Ludwig, Schmelzer, and Milchev (1994) [522])

$$Q(\mathbf{k}) = \frac{2Mk_BT}{V} \frac{1}{\mathbf{k}^2} \ . \tag{11.14}$$

The theory outlined so far is applicable strictly only for relatively small deviations from the initial state. For a description of the later stages of the transformation additional non-linear terms have to be included in the basic equations (see, e.g., Langer, Bar-on, and Miller (1975) [497]; Binder (1992) [82]).

However, an impression of the overall scenario of spinodal decomposition one may also obtain by solving the above given equations but assuming that the system where the transformation occurs is adiabatically isolated from the environment. In such a case, the latent heat of the transformation results in a change of temperature, which is equivalent to a decrease of the thermodynamic driving force of the transformation. Similarly to segregation processes proceeding via nucleation and growth one may expect that such changes of the state of the system determine qualitatively the whole course of the transformation also for processes starting from unstable initial states.

In Fig. 11.2a–c results of the numerical solution of the set of equations, given above, are shown. Figure 11.2a shows the time dependence of the critical wave vector (in reduced coordinates) as a function of time. After an initial period, where the critical wave vector is practically not changed, a stage of rapid decrease in k_c follows going over continuously into a third state of reorganization of the concentration field connected with the elimination of the contributions in the Fourier expansion with higher wave numbers in favor of the smaller ones.

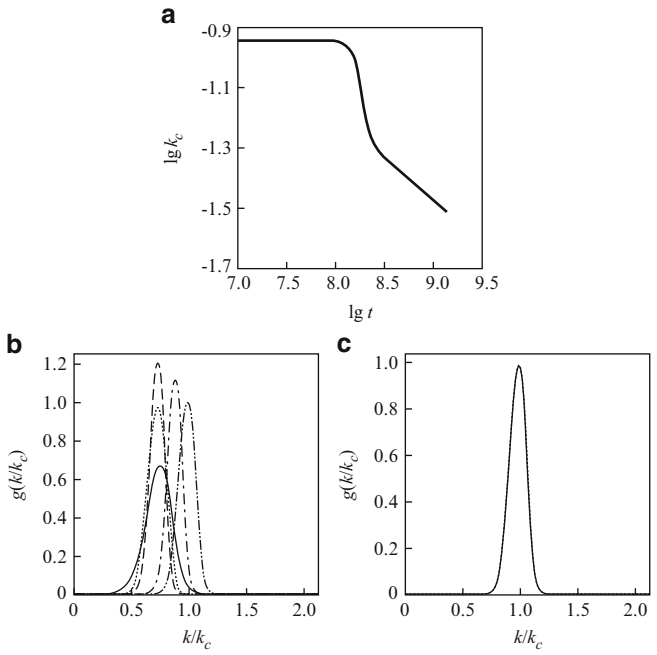

Fig. 11.2 (**a**): Critical wave number, k_c, versus time, t, in reduced units and a logarithmic plot. The linear part of the curve in the third stage of the decomposition process indicates the existence of a power law for the critical wave number, k_c, being proportional to $t^{-\alpha}$. As the result of a linear regression $\alpha = 0.245$ is found. (**b/c**): The wave number dependent part of the structure factor $g(k/k_c)$ for different moments of time (in reduced units). The different curves correspond to $t = 1{,}000$ *(full curve)*, $t = 2{,}000$ *(dotted curve)*, $t = 3{,}000$ *(dashed curve)*, $t = 4{,}000$ *(dashed-dotted curve)*, $t = 5{,}000$ *(double dashed curve)*. In the course of the evolution a time independent distribution in reduced variables is approached as shown in figure (**c**). The normalized curves obtained for $t = 5{,}000$ *(full curve)* and $t = 9{,}000$ *(dotted curve)* coincide practically

This process resembles the stage of competitive growth of ensembles of clusters corresponding to Ostwald ripening. It is characterized by power laws $k_c \sim t^{-1/4}$ and a time-independence of the structure function in reduced variables (k/k_c) (see Fig. 11.2b, c). Hereby the square of the structure function is written in the form

$$\langle S^2(\mathbf{k}, t)\rangle = f(t)g\left(\frac{k}{k_c}\right) \tag{11.15}$$

with

$$\int g\left(\frac{k}{k_c}\right) d\left(\frac{k}{k_c}\right) = 1\ . \tag{11.16}$$

The results, shown in Fig. 11.2, can be verified both analytically, by so-called Cell Dynamical Systems- (CDS; see Oono and Puri (1989) [613]) and by Monte-Carlo simulations (for the details see Schmelzer and Milchev (1991) [709]; Ludwig

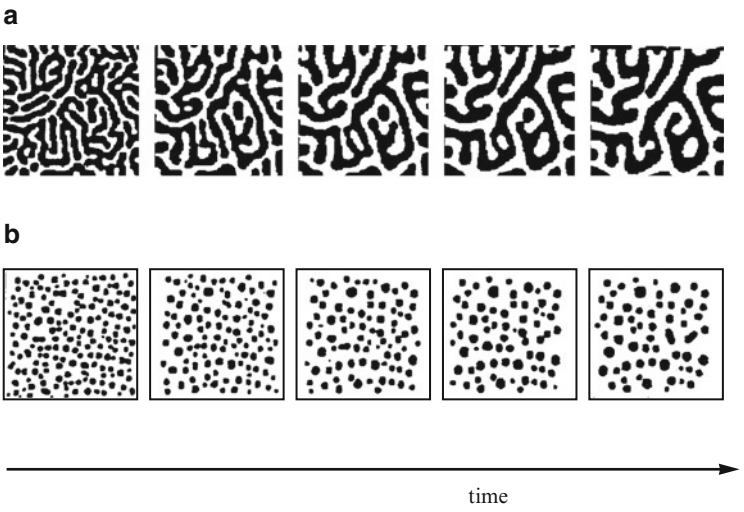

Fig. 11.3 Different stages of a phase transformation as obtained, as a rule, by (**a**) spinodal decomposition and (**b**) nucleation and growth

et al. (1994) [522]; Milchev et al. (1994) [564]; Schmelzer et al. (1995) [718]). Schematically the basic difference between the two types of transformations discussed – nucleation and growth, respectively, spinodal decomposition – is illustrated in Fig. 11.3. The pictures are obtained based on CDS-simulation methods (for the details see Ludwig (1993) [520]). It is to be noted, however that sometimes nucleation and growth processes may also lead to interconnected structures typical of spinodal decomposition and, vice versa, spinodal decomposition to localized clusters distributed randomly in the matrix.

11.3 Liquid-Phase Separation Versus Crystallization

Whether liquid phase separation or crystallization takes place in the system depends on the interrelation between the rates of formation of the two phases (cf. the discussion of Ostwald's rule of stages in Sect. 9.5). Inside the spinodal curve there is no barrier to nucleation. Therefore, from such initial states liquid phase separation commonly takes place well before the crystalline phase starts to develop. In considering binodal liquid phase separation, starting from initial states as indicated in Fig. 11.1, the process has to be described as a non-steady state nucleation process with a time-dependent nucleation rate.

An experimental proof of the intrinsic non-steady state character of liquid phase separation processes was given first by Ohlberg and Hammel (1965) ([610]; see also Hammel (1967) [345]). One of the $N(t)$-curves obtained by these authors is shown on Fig. 11.4. The curve corresponds to the $N(t)$-dependencies given in Fig. 7.4.

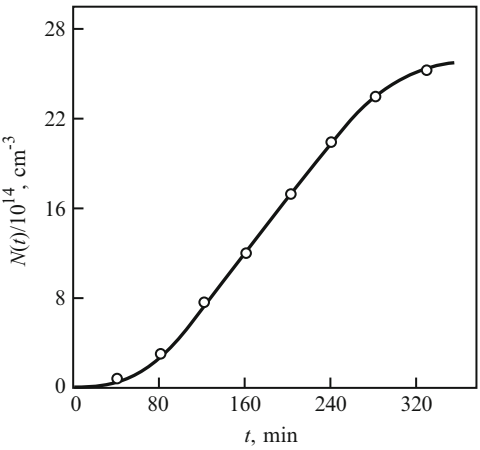

Fig. 11.4 Kinetics of nucleation in liquid-phase separation of a soda-lime-silica glass (After Ohlberg and Hammel (1965) [610])

Here, however, the saturation plateau is determined by exhausting the volume of the melt accessible for phase formation. It is particularly important to note that the experimental data of Ohlberg and Hammel give (taking into account the respective viscosity data and Eq. (6.194)) a value of the sticking coefficient ς of the order $\varsigma \approx 1$. Such a value has to be expected having in mind the considerations made in Sect. 6.3.2 concerning the values of ς in the case of formation of isotropic phases.

This result implies that at approximately equal values of the viscosities the time-lags for the formation of the crystalline (τ_c), respectively, the fluid phases (τ_f) behave as $\tau_c \gg \tau_f$. Moreover, it has to be expected that the value of the specific surface energy for the liquid-liquid interface is lower than the corresponding value for the liquid-crystal surface. Consequently, the work of formation of critical clusters for liquid-liquid phase separation processes may be expected, in general, to be considerably lower as compared with the respective value for crystal formation. Thus, also $J_f(j_c) \gg J_c(j_c)$ holds, in general, and a situation as shown in Fig. 9.4a is to be expected.

From the above considerations it follows that in both cases of binodal and spinodal liquid phase separation the liquid phase will be formed before the formation of the crystalline phase takes place. This result is of considerable technological interest for the kinetics of formation of glass-ceramic materials. It can be considered as a special case of fulfilment of Ostwald's rule of stages (see also Gutzow and Toschev (1968) [318] and the discussion in Sect. 9.5).

11.4 On the Effect of Primary Liquid-Phase Separation on Crystallization

The separation of the initially homogeneous phase into two or more different liquid phases may substantially affect the course of the subsequent crystallization process since

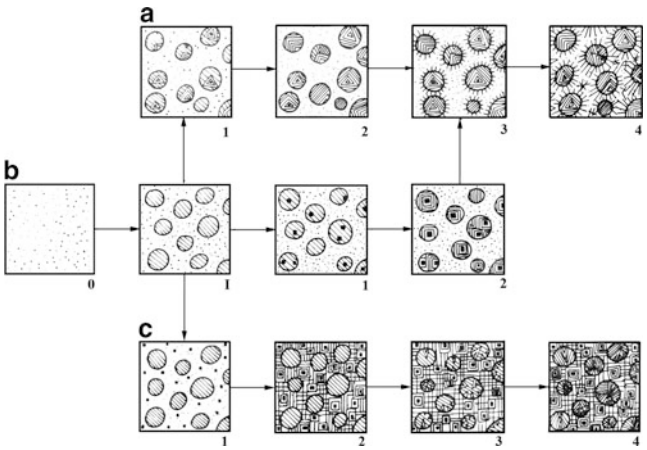

Fig. 11.5 Schematic diagram illustrating possible effects of liquid-liquid phase separation on crystallization phenomena. The initially homogeneous melt *(0)* is phase separated after heat treatment *(I)*. *(A)*: Crystallization of the droplet phase is facilitated; (A_1, A_2): Crystallized drops serve as seeds for the subsequent crystallization of the matrix phase (A_3); Partial or even complete crystallization of the matrix follows; *(B)*: Formation of active crystallization cores is possible in the droplet phase (B_1); Active cores cause complete crystallization of the droplet phase (B_2) followed eventually by states (A_3) and (A_4); *(C)*: Crystallization of the matrix phase facilitated, e.g., through the formation of insoluble seed crystals (C_1); complete crystallization of the matrix phase is achieved (C_2) and the crystallization of the droplet phase is induced via the droplet-matrix interface (C_3). The result is a completed crystallization of both matrix and droplet phases (C_4)

- The supersaturation with respect to crystallization in the different liquid phases may be quite different than the initial homogeneous phase;
- The viscosity in the evolving new phases may differ;
- In the bulk of the melt new interfaces are created which may favor nucleation;
- Nucleation cores may be distributed differently in the newly formed phases.

The possible interdependence between liquation and crystallization phenomena is schematically illustrated in Fig. 11.5. The different stages of the phase separation process shown in this diagram are confirmed by well-known electron microscopic observations made by Vogel (see, for example his monograph from (1979) [888]) and by experimental evidence reported by Tashiro (1969) [826]. Further evidence concerning the kinetics and thermodynamics of liquid phase separation and on the particular mode denoted as spinodal decomposition may be found in the cited literature. The particular problems of liquid phase separation in glass-forming melts are treated in details in James's review article (1975) [401], in the monographs of Andreev, Mazurin et al. (1974) [14] and Vogel (1965 [888], 1979 [889]).

Chapter 12
Rheology of Glass-Forming Melts

12.1 Introduction

Rheology, as indicated by its very name (*rheos*: to flow) is in its classical sense the science describing flow processes of matter, i.e., the displacement of the building units of a substance as a whole or parts of it under the influence of an applied force. The modern interpretation of rheology includes both the meaning as given above as well as the description of relaxation kinetics, i.e., the response of a system after an initially applied stress (or, more general, an external influence) has ceased to operate. An instructive and technically important example of the latter process is relaxation of strains (strain birefringence) in glass-annealing. In the terminology used in Chap. 3, annealing and relaxation of glasses may be considered as particular examples of stabilization processes, i.e., the evolution of an initially frozen-in system of increased disordered to the state of metastable equilibrium characterized by a lower degree of disorder.

Two approaches have been developed in the rheology of glass-forming melts:

- A *phenomenological approach*, based on considerations following from a number of phenomenological models and their combinations;
- A *microscopic approach* involving more or less well-defined molecular model considerations concerning the mechanism of flow.

In the phenomenological approach, the flow and relaxation of condensed matter is described with model dependencies derived from the behavior of different idealized systems. The two basic models, which are used in different combinations, are Hooke's absolutely rigid elastic body and Newton's viscous liquid.

The classical phenomenological models of flow and relaxation of viscoelastic bodies, due to Maxwell, Kelvin, Voigt, Zener and others, can also be obtained as combinations of elementary mechanical elements reflecting the properties of Hookean bodies (elastic spring) and Newtonian fluids (dashpot). An overview on the classical phenomenological model approaches and of their significance in the development in the theory of flow and relaxation for different systems can be

I.S. Gutzow and J.W.P. Schmelzer, *The Vitreous State*,
DOI 10.1007/978-3-642-34633-0_12, © Springer-Verlag Berlin Heidelberg 2013

found in the respective literature (see, e.g., Reiner (1956) [659]; Freudenthal (1956) [235]; Wilkinson (1960) [922]; Sobotka (1984) [785] for a general description of rheological models; Treloar (1949) [853]; Stanworth (1953) [793]; Morey (1954) [574]; Alfrey (1955) [7] for the application to glasses and polymer systems). Of exceptional importance was the finding (due mainly to Meixner (1953, 1954) [555, 556]; see also Zener's model described by Dehlinger (1955) [162]) that the most important of the classical rheological models can be derived based on the thermodynamics of irreversible processes in its linear formulation. Zener's model, giving a very general description of viscoelastic bodies, turned out to be a consequence of one of the basic relationships of the thermodynamics of irreversible processes – the so-called dynamic equation of state (for the derivation of Zener's model from this fundamental equation see Meixner's original paper [555] or Haase (1963) [339]). In this sense the phenomenological rheology has no longer to be considered as a random collection of more or less intuitively formulated models of flow and relaxation but as a consequence of another more general phenomenological theoretical approach – the thermodynamic one.

One of the most fruitful and general directions in the microscopic approach to the description of flow turned out to be the Prandtl-Eyring model of flow under shear stress (see Prandtl (1928) [644]; Glasstone, Laidler, and Eyring (1941) [255] and generalizations of this model by Beaver (1986) [56]; Gutzow, Dobreva, and Schmelzer (1993) [332]). From a more general point of view the Prandtl-Eyring model can be interpreted as an activated complex approach in terms of the absolute rate theory. Other important molecular concepts are connected with free volume and hole theories of liquids, with the "thermodynamic" approach in deriving the temperature dependence of the viscosity (developed by Adam and Gibbs (1965) [5]), energetic level models (bond lattice models; Rao and Angell (1972) [656]) with entangled or free draining coil models of polymer solutions (Bueche (1962) [109]) etc. Molecular models of relaxation of glass-forming melts, formulated in terms of two-, three- or multi-dimensional energetic level models were derived by Volkenstein and Ptizyn (1956) [892] (see also Volkenstein (1959) [891]; Mazurin (1986) [543]; Avramov and Milchev (1984 [25], 1988 [26], 1991 [21])). The latter mentioned authors also succeeded in giving a molecular model of vitrification and relaxation of glasses capable of describing memory effects.

A summary of classical attempts in the molecular theory of rheology may by found in the monographs by Frenkel (1946) [233], Glasstone et al. (1941) [255], Bartenev, Frenkel, Sanditov (1982, 1986, 1990) [47, 48, 683], and Melvin-Hughes (1972) [567]; more recent developments in application to polymer systems ("tube-flow" models) are discussed by Doi (1980) [178]. In Frischat's monograph (1975) [237] a summary of model approaches and experimental data can be found concerning diffusion and self-diffusion in inorganic glass-forming systems. A thorough discussion of the different microscopic approaches to viscous flow and molecular models of diffusion including disordered systems is given by Manning (1968) [529]; this problem is also treated in detail by Milchev and Avramov (1983) [559] (cf. also [121]). It turns out that in terms of different molecular models of flow the viscosity and self-diffusion in glass-forming melts can even be described

quantitatively. However, all efforts to interpret relaxation in simple and polymer glass-forming melts, using either linear combinations of Newtonian and Hookean elements or existing molecular models, failed or allowed one only a qualitative description.

An example in this respect is the failure to describe processes of glass annealing by using Maxwell's equation, i.e., a linear combination of elements reflecting Hookean elastic bodies and Newtonian viscous flow. A summary concerning this problem is given by Morey (1954) [574]. In order to overcome the difficulties connected with the description of relaxation in real systems three different attempts have been developed:

- More than one relaxation time is introduced into the description using a set of linear relaxation equations of Maxwellian type with more or less arbitrarily chosen relaxation times. Hereby up to 6–10 Maxwellian exponents are employed in order to reach a quantitatively correct description of the process. This method, described in detail by Mazurin (1986) [543], has been widely employed by Kovacs (cf. Kovacs et al. (1979) [479] and for earlier investigations Treloar (1949) [853]).
- More complicated non-linear empirical dependencies are used, in particular, relations with a time-dependent relaxation time. A classical example in this respect is Kohlrausch's fractional exponent formula which he first proposed in 1876 [462]. It was introduced into the rheology of silicate glass-forming melts by Rekhson and Mazurin (1974, 1977) [542, 662]. Similar time-dependencies were used by Jenckel (1955) [407] in order to model relaxation in organic glass-forming melts and by Williams and Watts for a description of dielectric relaxation (see Mazurin (1986) [543]). Another classical non-linear dependence of this type is the Adams-Williamson annealing equation, employed for many years in the technology of glass annealing [6], (see also Morey (1954) [574]). In a more formalistic but more general way such generalizations can be introduced by the method employed for the description of stabilization in Sect. 3.9 by introducing an effective relaxation time depending on the prehistory of the system.
- A third method in the description of relaxation kinetics consists in the introduction of real Non-Newtonian flow dependencies into the corresponding kinetic equations. In this way, the specific rheological behavior of the relaxing system is directly accounted for. This method was indicated for the first time by Eyring et al. (1948) [839], it was extended by using existing or appropriately modified models of flow by Gutzow et al. (1993) [332]. It can be shown that, in this way, existing empirical dependencies used in the description of the kinetics of relaxation (including Kohlrausch's formula and similar relations capable of describing quantitatively relaxation in real glass-forming systems) can be obtained, which are determined by the particular flow mechanism of the system under investigation.

In analyzing the rheological properties of viscoelastic bodies, the elastic component can be considered as the direct response of the system to external disturbances, while the viscosity reflects its dissipative reaction. Viscoelastic bodies thus represent, with

respect to their rheological behavior, a bridge between matter in different states of aggregation, indicating their similarities despite their qualitative differences (or in the words of Hegel (1817) [351] "water, like air, is fluid but its fluidity is elastic").

The elastic component in the rheological behavior of liquids and glass-forming melts is of importance not only for flow and relaxation but also in processes of crystallization and segregation taking place in them. Consequently, in the description of the kinetics of such processes modifications have to be introduced as compared with phase formation in Newtonian liquids (cf. Chap. 6) or crystallization of Hookean elastic solids (cf., e.g., Sect. 7.7.1). One example, where elastic strains in segregation processes in viscoelastic melts modify the kinetics qualitatively, was given in Fig. 9.3 in Sect. 9.4 (segregation in photo-chromic glasses). In this way, it turned out that a quantitatively correct description of crystallization and phase formation in glass-forming melts, especially in the vicinity of T_g, has to be developed in terms of a theory of phase transformations in viscoelastic bodies.

12.2 Phenomenological Rheology of Glass-Forming Melts in its Linear Approximation

The basic rheological characteristics of a liquid or plastic solid body are given by the dependence of rate of shear flow, $d\gamma/dt$, on shear stress, Π. For Newtonian or ideal liquids the relation

$$\frac{d\gamma}{dt} = \frac{\Pi}{\eta} \tag{12.1}$$

holds, where η is the Newtonian shear viscosity of the melt. It depends on temperature but not on the applied stress. In the practice of rheological investigations it turns out, however that Eq. (12.1) is usually fulfilled only in the limiting case of very small applied stresses ($\Pi \to 0$). Real liquids deviate from Newtonian liquids in two ways: $d\gamma/dt$ increases either faster or slower than the linear dependence as described by the above equation allowing one to develop a classification of Non-Newtonian liquids into two classes discussed in the following section.

The second classical idealization used in rheology is the model of a Hookean absolutely elastic body. The relation between stress and deformation can be written for this case in the form

$$\gamma = \frac{1}{G^*}\Pi \ , \tag{12.2}$$

where G^* is the modulus of elasticity for the particular type of deformation. In a solid body without viscous flow, the relation $\Pi = G^*\gamma$ is fulfilled at any time, moreover, the relation

$$\frac{d\gamma}{dt} = \frac{1}{G^*}\frac{d\Pi}{dt} \tag{12.3}$$

holds. In the presence of viscous flow strains will disappear with time at a rate depending on the actual value of Π.

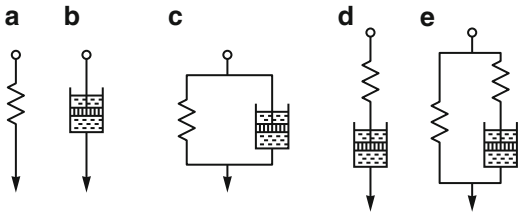

Fig. 12.1 Mechanical models, combinations of springs and dashpots, reflecting the properties of viscoelastic bodies according to several classical models. It is assumed that the reaction of the spring (**a**) is described by Hooke's law, while the dashpot (**b**) has the properties of a Newtonian viscous liquid. The different combinations refer to (**c**) Kelvin's, (**d**) Maxwell's and (**e**) Zener's bodies

If we make the simplest possible assumption, that the rate of change of the strain is proportional to the strain itself, then we get, by a combination of above equations,

$$\frac{d\Pi}{dt} = G^* \frac{d\gamma}{dt} - \frac{\Pi}{\tau_R} \,, \tag{12.4}$$

where

$$\tau_R = \frac{\eta}{G^*} \tag{12.5}$$

is the already discussed characteristic time scale of the process – Maxwell's time of relaxation (cf. Sect. 2.4.3). Note that above given equations, Eqs. (12.1) and (12.2), are obtained from Eq. (12.4) as special cases (for $d\Pi/dt = 0$, respectively, $d\gamma/dt = 0$). Equation (12.4) may be rewritten in the form

$$\frac{d\gamma}{dt} = \frac{\Pi}{\eta} + \frac{1}{G^*}\frac{d\Pi}{dt} \,, \tag{12.6}$$

which is the equation of the so-called Maxwell body.

Another well-known classical relation, the Kelvin-Voigt equation, follows if, in the second term on the right hand side of Eq. (12.6), Π is replaced by $\Pi = G^*\gamma$ and afterwards $d\gamma/dt$, again, by a linear dependence of the form $d\gamma/dt = -\gamma/\tau_R$. One gets

$$\frac{d\gamma}{dt} = \frac{\Pi}{\eta} - \frac{1}{\tau_R}\gamma \,. \tag{12.7}$$

It follows that Maxwell's and Kelvin-Voigt's equations are linear combinations of Eqs. (12.1) and (12.3). A mechanical interpretation of these and of a further rheological dependence (Zener's equation) in terms of combinations of the basic models is given in Fig. 12.1.

The classical rheological models – Hooke's, Newton's, Maxwell's and Kelvin-Voigt's bodies – can be considered as particular cases of a more general rheological equation – Zener's equation. This equation can be derived, as mentioned in the preceding section, by the methods of the linear thermodynamics of irreversible

processes. It is equivalent to the dynamic equation of state. Zener's equation may be written in the form (see Meixner (1953) [555]; Haase (1963) [339])

$$\frac{d\gamma}{dt} = \frac{G^*}{\kappa\eta}\Pi + \frac{\eta}{\zeta^* G^*}\frac{d\Pi}{dt} - \frac{1}{\tau_R}\gamma \,, \tag{12.8}$$

where κ is the modulus of bulk elasticity (compressibility) and ζ^* Stokes's bulk viscosity (cf. Haase (1963) [339]).

According to existing theoretical estimates (see Tobolsky (1960) [838]; Landau and Lifshitz (1953 [492], 1957 [495])) the relations

$$\frac{\zeta^*}{\eta} = \alpha_1 \cong 3 \,, \tag{12.9}$$

$$\frac{\kappa}{G^*} = \alpha_2 \cong 2 \tag{12.10}$$

hold and we obtain in a good approximation

$$\frac{d\gamma}{dt} = \frac{1}{2\eta}\Pi + \frac{1}{3G^*}\frac{d\Pi}{dt} - \frac{1}{\tau_R}\gamma \,. \tag{12.11}$$

It is evident that

- At small γ-values, i.e., at

  $$\Pi/2\eta \gg (1/3G^*)d\Pi/dt - \gamma/\tau_R \,,$$

  Newton's equation, Eq. (12.1), follows;
- At high γ-values , i.e., at

  $$\Pi/2\eta - \gamma/\tau_R \gg (1/3G^*)d\Pi/dt \,,$$

  the Kelvin-Voigt equation, Eq. (12.7), is obtained;
- At high $(d\Pi/dt)$- and small γ-values both Hooke's equation, Eq. (12.3), for

  $$(1/3G^*)d\Pi/dt \gg \Pi/2\eta - \gamma/\tau_R \,,$$

  and Maxwell's relation, Eq. (12.6), for

  $$\Pi/2\eta + (1/3G^*)d\Pi/dt \gg \gamma/\tau_R$$

  are found.

In the subsequent analysis of special cases we omit the numerical factors 2 and 3 for simplicity of the notations.

The above equations may be also applied to the description of flow in systems consisting of two or more building units. Following Arrhenius and Eyring

(see Hirschfelder et al. (1954) [366]) the viscosity of a two-component system with the molar fractions of the two components x, respectively, $(1-x)$ may be written in the form

$$\ln \eta = x \ln \eta_1 + (1-x) \ln \eta_2 \,, \tag{12.12}$$

where η_1 and η_2 are the viscosities of the pure components for the same thermodynamic conditions. Since the modulus of elasticity, G^*, changes only slightly from one substance to another, a similar expression for the relaxation time, τ_R, may be obtained in the form

$$\ln \tau_R = x \ln \tau_{R1} + (1-x) \ln \tau_{R2} \,. \tag{12.13}$$

12.3 Analysis of Special Cases

The solutions of Eqs. (12.1), (12.3), (12.6) and (12.7) give the degree of deformation as a function of time for the different models considered. With the boundary and initial conditions ($\Pi = \Pi_0 = \text{const.}$) and ($\gamma(t=0) = 0$) we have, for example,

$$\gamma(t) = \frac{\Pi_0}{\eta} t \tag{12.14}$$

for Newton's liquid and

$$\gamma(t) = \frac{\Pi_0}{G^*} \left[1 - \exp\left(-\frac{t}{\tau_R} \right) \right] \tag{12.15}$$

for Kelvin-Voigt's model. A derivation of Eq. (12.15) with respect to time yields

$$\frac{d\gamma(t)}{dt} = \frac{\Pi_0}{G^* \tau_R} \exp\left(-\frac{t}{\tau_R} \right) \,. \tag{12.16}$$

It follows that the rate of deformation in a viscoelastic body, described by Kelvin-Voigt's equation, is smaller by a factor $\exp(-t/\tau_R)$ than for the same process taking place in a Newtonian liquid.

Another important special case is the relaxation of a system after an applied external strain becomes suddenly equal to zero. In this case, Zener's as well as Kelvin-Voigt's equations, are reduced to

$$\frac{d\gamma(t)}{dt} = -\frac{1}{\tau_R} \gamma(t) \tag{12.17}$$

with the solution (for $\gamma(t=0) = \gamma_0$)

$$\gamma(t) = \gamma_0 \exp\left(-\frac{t}{\tau_R} \right) \,. \tag{12.18}$$

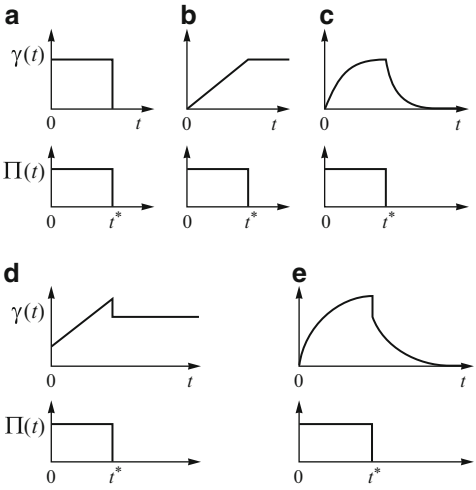

Fig. 12.2 Deformation behavior of different bodies. The letters (**a**) – (**e**) refer to the same models as depicted in Fig. 12.1

In application to the description of the reaction of a system, when an external strain is suddenly applied, the characteristic time, τ_R, is usually denoted as retardation time and the respective process as a process of retardation. For the considered simple models relaxation and retardation times coincide.

Another type of reaction of a system, which is of interest in applications, consists of the kinetics of relaxation of stress at constant deformation (i.e., at $\gamma = \gamma_0 = \text{const.}$). From Eqs. (12.1) and (12.7) it becomes obvious that Newton's and Kelvin-Voigt's equations lead to quite unrealistic time-dependencies of $\Pi(t)$ for this case ($\Pi = 0$, $\Pi = \gamma_0/G^* = \text{const.}$). In contrast, Zener's and Maxwell's models provide the possibility of stress relaxation, the first one in the form

$$\frac{1}{G^*}\frac{d\Pi}{dt} = -\frac{1}{\tau_r}\left(\frac{\Pi}{G^*} - \gamma_0\right) \tag{12.19}$$

with the solution

$$\Pi(t) = G^*\left[\gamma_0 + \left(\frac{\Pi(0)}{G^*} - \gamma_0\right)\exp\left(-\frac{t}{\tau_R}\right)\right] . \tag{12.20}$$

The problem of relaxation, as described by Maxwell's model, is analyzed in more detail in Sect. 12.5. The deformation behavior of a system described by different rheological equations at constant values of Π is illustrated in Fig. 12.2.

Summarizing we may conclude that in the derivation of the classical rheological models

- Flow is described as in an ideal Newtonian liquid;
- Elastic and flow reactions are connected by linear additive combinations;
- Elastic deformation is assumed to be proportional to the stress (i.e., validity of Hooke's law is assumed).

Only a comparison with experimental flow and relaxation curves can show how far the above assumptions are realistic approximations.

In application to glass-forming systems, such comparisons lead to the conclusion that the first assumption is practically never fulfilled for the highly viscous glass-forming melts. Flow of real glass-forming liquids turns out to be, in general, Non-Newtonian; particularly strong Non-Newtonian behavior is found in polymer melts. This result also implies that the kinetics of relaxation of stresses in glasses does not follow the simple Maxwellian kinetics. As far as only relatively small stresses are required to initiate a flow of liquids, Hooke's behavior (assumption 3) is valid in most cases. Thus, in particular, assumptions 1 and 2 require a reconsideration in discussing the rheological properties of glass-forming melts.

12.4 Non-Newtonian Flow Models

In order to retain the classical form of Eq. (12.1) even for Non-Newtonian liquids an apparent (or effective) value of the shear viscosity, $\eta_{(app)}$, is usually introduced, so that the relation

$$\frac{d\gamma}{dt} = \frac{\Pi}{\eta_{(app)}} \tag{12.21}$$

holds. When $\eta_{(app)}$ is a decreasing function of Π the liquid is called pseudo-plastic (or, in polymer literature, shear thinning). In the opposite case, when $\eta_{(app)}$ increases with an increasing value of Π, the liquid is denoted as dilatant (or shear thickening in polymer technology). The pseudo-plasticity or dilatancy of liquids is illustrated in Figs. 12.3a, b. In addition, also the $d\gamma/dt$-dependence corresponding to Bingham's plastic body is given in the same figure as a limiting case of pseudo-plasticity (Fig. 12.3c). It has the form

$$\frac{d\gamma}{dt} = \frac{1}{\eta}(\Pi - \Pi_0) \tag{12.22}$$

In experimental rheology the flow behavior of Non-Newtonian liquids is usually described by a number of empirical relations. Of these equations particularly often employed is the de Waele-Ostwald formula (Ostwald (1925, 1929) [618]; Houwink (1957) [381]):

$$\frac{d\gamma}{dt} = A_0 \frac{\Pi^n}{\eta} \,. \tag{12.23}$$

It describes the flow kinetics of pseudo-plastic liquids.

Another often used equation is Darcy's relation

$$\frac{d\gamma}{dt} = A_0 \frac{\Pi^{(1/2)}}{\eta} \tag{12.24}$$

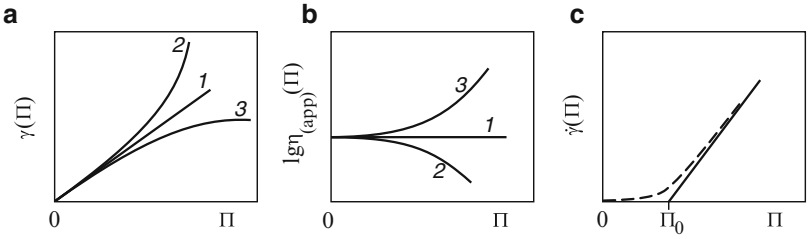

Fig. 12.3 Possible types of flow behavior of liquids (shear-rate vs shear-stress dependencies, schematically). (**a**): Newtonian fluid *(1)*, pseudo-plastic melt *(2)*, dilatant liquid *(3)*. (**b**): Dependence of the apparent shear viscosity on stress: Newtonian liquid *(1)*, pseudo-plastic *(2)* and dilatant *(3)* fluids. (**c**): Shear rate vs shear stress dependence for pseudo-plastic liquids *(dashed curve)* and for Bingham's body approximation *(full curve)*

applied for dilatant liquids. Both equations can be reformulated in terms of Eq. (12.21) with apparent viscosities of the form

$$\eta_{(app)} = \eta \frac{1}{A_0 \Pi^{(n-1)}} \tag{12.25}$$

for the de Waele-Ostwald liquid and

$$\eta_{(app)} = \eta \frac{\Pi^{(1/2)}}{A_0} \tag{12.26}$$

for Darcy's body. It is seen from above dependencies and from Fig. 12.3, that for pseudo-plastic bodies $\eta_{(app)}$ is a decreasing and for dilatant liquids an increasing function of Π.

It can be shown by using well-known expressions for expansion of the sinh-function (Gutzow et al. (1993) [333]) that the de Waele-Ostwald formula, as well as a number of similar dependencies, used for a description of pseudo-plastic bodies, e.g., of the form

$$\eta_{(app)} = \frac{\eta}{(1 + B_0 \Pi^{n-1})} \tag{12.27}$$

can be obtained as particular cases of a very general formula, known as Prandtl-Eyring's equation

$$\frac{d\gamma}{dt} = \frac{A_0}{\eta} \sinh\left(a_0^{\odot} \Pi\right) , \tag{12.28}$$

which yields values of the apparent viscosity of the form

$$\eta_{(app)} = \frac{\eta a_0^{\odot} \Pi}{\sinh\left(a_0^{\odot} \Pi\right)} . \tag{12.29}$$

Typical glass-forming melts are, as a rule, pseudo-plastic liquids. In terms of de Waele-Ostwald's formula, widely employed in experimental polymer rheology,

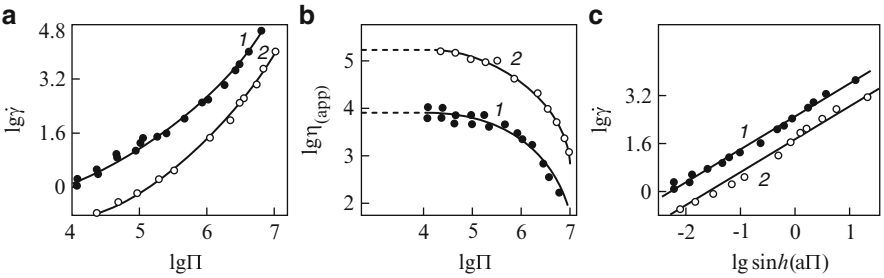

Fig. 12.4 Stress-induced flow of poly(methyl metacrylate) melts as an example of a pseudo-plastic Non-Newtonian liquid. Experimental data are reported by Gul and Kulesnev (1966) [282]: (**a**) $\log(d\gamma/dt)$ vs $\log(\Pi)$ data for two temperatures interpolated by applying the de Waele-Ostwald equation. (**b**) Stress dependence of the apparent viscosity. (**c**) Experimental $(d\gamma/dt)$ vs Π data in coordinates according to the Prandlt-Eyring model; *(black dots)*: data for 523 K; *(circles)* data for 473 K

values of the coefficient n in this equation of the order $n = 1.5$ are usually found. However, the application of the Prandtl-Eyring equation should be preferred: not only does it give a more correct description (cf. Fig. 12.4) but has also the advantage of a molecular foundation, discussed in the next section. It is seen also on Fig. 12.4 that at low Π-values $\eta_{(app)}$ approaches constant values (zero-stress approach to Newtonian liquids). This behavior gives a simple method for determining the Newtonian viscosity of glass-forming liquids by extrapolating the $\eta_{(app)}$-curves to zero stress.

12.5 Linear (Maxwellian) and Non-Maxwellian Kinetics of Relaxation

Maxwell's equation, Eq. (12.6), describes the kinetics of relaxation of stresses, Π, in a body at a constant deformation, γ, in the form

$$\frac{d\Pi}{dt} = -\frac{1}{\tau_R}\Pi \tag{12.30}$$

with the well-known solution

$$\Pi = \Pi_0 \exp\left(-\frac{t}{\tau_R}\right) . \tag{12.31}$$

The above equations also give the kinetics of relaxation of the deformation (for $\Pi = 0$) in an initially stressed body when it is described by the Kelvin-Voigt equation.

From a more general point of view the relaxation of strains in a Maxwell body, the relaxation of deformations in a Kelvin-Voigt body or relaxation processes in real systems – relaxation of strains in glasses or the retarded response of glass-forming melts to external disturbances – can be treated either as an evolution of the frozen-in system towards equilibrium (relaxation as a process of glass stabilization) or as the response of a dissipative system to a time-limited external influence. Thus the rheology of glass-forming melts, which determines the kinetics of the most significant processes in under-cooled melts (their vitrification and crystallization), gives also an illustration of the behavior of dissipative systems, in general. This similarity becomes also evident from a comparison of Eqs. (12.15), (12.17) and (12.30) with the derivations given in Sect. 3.9.

From Eqs. (12.5) and (12.6) it is obvious that in Maxwell's kinetics of relaxation the assumption of a Newtonian flow behavior (with constant values of η and τ_R) of the systems under consideration is inherent. A straightforward generalization of the Maxwellian relaxation kinetics can be given, consequently, by introducing for real systems an apparent relaxation time, $\tau_R^{(app)}$, as

$$\tau_R^{(app)} = \frac{\eta_{(app)}}{G^*} \,. \tag{12.32}$$

By this procedure, determining, in analogy to Eq. (12.30), relaxation via the relation

$$\frac{d\Pi}{dt} = -\frac{\Pi}{\eta_{(app)}} \tag{12.33}$$

a large variety of possible solutions, accounting for the real flow behavior of viscoelastic bodies, may be achieved by using $\eta_{(app)}$-dependencies as discussed in the previous section. In this way, in the already mentioned paper by Gutzow et al. (1993) [333] a detailed analysis of different solutions is given for possible models of dilatant and pseudo-plastic behavior of real liquids.

As an example, the de Waele-Ostwald equation gives for $n = 2$ a dependence of the form

$$\frac{1}{\Pi(t)} - \frac{1}{\Pi(0)} = A_1 \frac{t}{\tau_0} \tag{12.34}$$

corresponding to the empirically established formula by Adams and Williamson [6, 925]. The differential equation, giving a relaxation kinetics as described by Eq. (12.34), is of the form

$$\frac{d\Pi}{dt} = -\frac{1}{\tau_0}\Pi^2 \,. \tag{12.35}$$

It follows that the Maxwellian type of relaxation kinetics, according to which the rate of stress relaxation is proportional to the stress itself, can be considered only as the simplest possible assumption. Moreover, while in the original Maxwellian relaxation kinetics (Eq. (12.30)) the relaxation time, τ_R, is considered as a constant, in the generalized dependencies this is not the case. According to Eq. (12.33), $\tau_R^{(app)}$ depends, in general, on the stress, Π. But since the stress is a function of time, $\tau_R^{(app)}$

also becomes time dependent. This argumentation allows us to rewrite $\tau_R^{(app)}$ in the form $\tau_R^{(app)} = \tau_R \tau^*(t)$ and with Eq. (12.33) the result

$$\frac{d\Pi}{dt} = -\frac{A_2}{\tau_R \tau^*(t)} \Pi \tag{12.36}$$

is obtained, where A_2 and τ_R are constants and $\tau^*(t)$ is a function of time, determined by the kind of rheological behavior of the considered liquid. In the case where

$$\tau^*(t) = t^p \tag{12.37}$$

holds (the effective relaxation time increases with time by a power law), p being a real number smaller than one, an equation for the relaxation behavior proposed first by Kohlrausch (1876) [462] is obtained as a special case. It reads

$$\Pi = \Pi(0) \exp\left[-\left(\frac{t}{\tau_k}\right)^b\right], \qquad b = 1 - p\,, \qquad \tau_k = \left(\frac{\tau_R b}{A_2}\right)^{1/b}. \tag{12.38}$$

The equation given above is usually denoted as the fractional (or stretched) exponent relaxation function. It is used with success for a description of relaxation of glass-forming melts.

According to the experimental evidence collected by Mazurin (1986) [543] values of b of the order $b = (0.5 - 0.75)$ (i.e., $p = (0.5 - 0.25)$) have to be expected for glass-forming liquids; for polymers, lower b-values are found in the range $b = (0.3 - 0.35)$ (i.e., $p = (0.7 - 0.65)$). As shown by Gutzow et al. (1993) [332] such values of the b-parameter are equivalent to respective n-values in the de Waele-Ostwald equation ($n \cong p + 1$). Recalling that for relaxation in glass-forming liquids $n = 1.5$ for the de Waele-Ostwald equation gives the best fit to experimental results, therefore the above mentioned b-values are easily explained.

12.6 Molecular Models of Viscous Flow

In the discussion of molecular models of viscous flow and molecular relaxation of glass-forming liquids it is usually assumed (see Sanditov and Bartenev (1982) [683]) that two independent steps are involved in this process, described by two different probabilities:

- The probability of activation of a molecule to break the bonds with the neighboring molecules and
- The probability that in the vicinity of an activated molecule, a sufficiently large void is formed, so that N_f building units responsible for the flow may enter it.

In accordance with earlier models by Eyring (see Glasstone et al. (1941) [255]) for the probability of activation of a molecule a constant activation energy, U_0, is supposed proportional to the enthalpy of evaporation, $\Delta H_{(ev)}$, of the liquid.

The second step in molecular models of viscous flow is connected with the determination of the probability of formation of a sufficiently large void in the liquid, equal or larger than the volume of N_f molecules, in the vicinity of the activated unit. Such calculations were performed in two variants by Cohen and Turnbull (1959) [137] and by Bueche (see Bueche (1962) [109]). It turns out that this probability depends exponentially on the reciprocal of the relative free volume $1/\xi(T)$ as assumed, for example, in Doolittle's empirical equation, Eq. (2.90). In this way, equations of such a type reflect mainly the process of hole formation as essential in the determination of the viscosity. The generalized molecular description of flow processes in glass-forming melts, taking into account both above mentioned steps in the description of flow, results in temperature dependencies of the viscosity which may be written in a form similar to the Macedo-Litovitz equation, Eq. (2.96), as

$$\eta(T) = \eta_0 \exp\left(\frac{U_0}{k_B T}\right) \exp\left(\frac{B}{\xi(T)}\right) , \tag{12.39}$$

where B depends on the number of molecules forming an average flow unit. According to an analysis made by Gutzow et al. (1985) [330] B varies, in general, from 1 (noble gas melts, liquid metals) to 6 (liquids formed by associating organic compounds).

The Vogel-Fulcher-Tammann equation, Eq. (2.84), follows from the above equation, if ξ is of the form $\xi \propto (T - T_\infty)$. Such a dependence has been discussed, in fact, already in one of the previous sections (cf. Eq. (3.32)). Replacing ξ according to Eq. (5.78) by the configurational entropy of the liquid Eq. (12.34) may be rewritten in the form

$$\eta(T) = \eta_0 \exp\left(\frac{U_0}{k_B T}\right) \exp\left(2.5 \frac{\Delta S_m}{\Delta S(T)}\right) . \tag{12.40}$$

For simple liquids $\Delta S_m \cong R$ holds. The second part of Eq. (12.40) is equivalent to a relation derived by Adam and Gibbs (1965) [5]. The above combination was proposed and discussed in detail by Gutzow et al. (1985) [330].

Summarizing, we may conclude that, as already mentioned in Chap. 2, temperature dependencies of the viscosity, involving only one activation energy and one exponential term reflect only one side of the mechanism of viscous flow (like Frenkel's original equation Eq. (2.78) derived in the framework of free volume and hole theories of liquids). Additional processes which have to be taken also into account lead to additional exponential terms as described above. Other mechanisms of viscous flow in glass-forming liquids lead to temperature dependencies of the form as given with Eqs. (2.92) and (2.95). Such models are essentially based on Anderson's idea (1958) [10] of treating structural disorder in terms of an ensemble of energetic barriers of different heights (while an ordered system is characterized by only one energetic barrier). By such an approach, developed in a series of papers by Avramov and Milchev [20, 22, 26, 559], the process of self-diffusion in both ordered and disordered structures may be treated in a straightforward way; in disordered

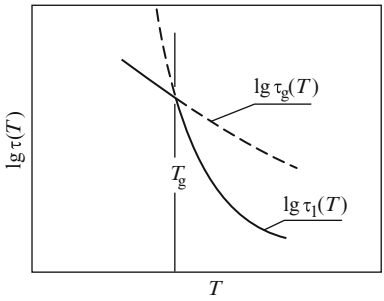

Fig. 12.5 Temperature dependence of the time of molecular relaxation in the vicinity of the glass transition temperature, T_g

structures the activated complex may use different diffusion channels for an escape while in an ordered state only one reaction possibility exists.

Also some additional conclusions can be drawn from the above-given derivations. Upon vitrification $\Delta S(T)$ (in Eq. (12.40)) or $\xi(T)$ (in Eq. (12.39)) are frozen in. Consequently, below the temperature of vitrification, we have to expect

$$\left(\frac{d\eta(T)}{d(1/T)}\right)_{T<T_g} = \frac{U_0}{k_B} = \text{const.} \tag{12.41}$$

in agreement with experimental findings (cf. Figs. 2.14, 2.16 and 12.5) and with more general considerations. It is essential to note that the freezing-in process also implies constant values of the activation energy below T_g (see Gutzow, Dobreva, and Pye (1994) [335]). The salient point of the $\log \eta$ vs $(1/T)$-curve gives an additional kinetic method of determination of the temperature of vitrification (see Mazurin (1986) [543]). The ratio

$$\Theta = \frac{\left(\frac{d \log \eta}{d \frac{1}{T}}\right)_{T \leq T_g}}{\left(\frac{d \log \eta}{d \frac{1}{T}}\right)_{T \to T_g}} \tag{12.42}$$

determines the so-called Narayanaswami coefficient. Methods of determination of this coefficient are discussed by Avramov et al. (1987 [29], 1988 [31]). It has values of the order of 0.5.

12.7 Molecular Models of Flow of Liquids Under Stress

The flow of a liquid under stress can be analyzed in terms of a molecular model developed by Prandtl (1928) [644] in the framework of the absolute rate theory (Glasstone et al. (1941) [255]). It gives an instructive explanation of Non-Newtonian behavior of pseudoplastic materials. Both Prandtl and Eyring assumed that in a

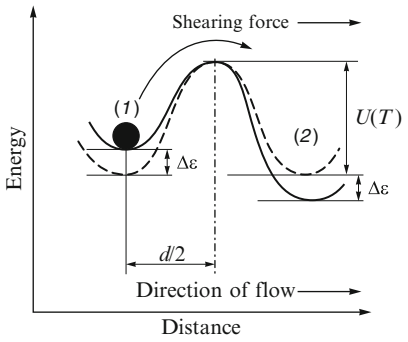

Fig. 12.6 The Prandtl-Eyring model for the change of the activation energy in a pseudo-plastic liquid under applied stress. For zero stresses *(dashed curve)* the probability of motion of a particle of the liquid is the same for both considered possible directions, while under stresses *(full curve)* a preferred direction of flow exists

liquid subjected to tangential stresses the activation energy, $U(T)$, for self-diffusion decreases in the direction of the applied stresses, Π, by a quantity $\Delta\varepsilon$ proportional to the stress. In the opposite direction $U(T)$ increases by the same value (see Fig. 12.6). Thus, the rate of net flow in the direction of the applied stress becomes equal to

$$\frac{d\gamma}{dt} = \frac{2D}{d^2} \sinh\left(\frac{d^3}{2k_B T}\Pi\right) , \tag{12.43}$$

where D is the self-diffusion coefficient of the ambient phase building units realizing the flow and having a volume of the order d^3 (the so-called "viscous" volume). The "viscous" volume can be expected to be proportional to the volume d_0^3 of the building units of the liquid. In the paper by Gutzow et al. (1993) [332], a generalization of the above model is given accounting in addition to energetic considerations also for entropy effects in viscous flow. This approach also allows us a description of the flow of dilatant liquids in terms of the same activated complex model.

Additional, more or less complicated, molecular models describing flow processes in polymer liquid solutions under various conditions can be traced mainly in literature on polymers. Here of particular importance are models describing the flow of polymer molecule coils through "tubes" formed by surrounding solute molecules (tube and coil models, see Doi (1980) [178]). The Prandtl-Eyring model, although leading to considerable difficulties in application to polymer liquid flow (where entropy effects are dominating), gives a safe basis in correlating experimental evidence on Non-Newtonian flow of inorganic and metallic glass-forming melts (see the evidence collected in a paper by Gutzow et al. (1993) [332]; the results of Li and Uhlmann (1970) [508] on silicate glasses, of Wäsche and Brückner (1986) [912] for phosphate melts and of Russev et al. (1990) [677] on metallic glass-forming alloys).

12.8 Kinetics of Nucleation and Growth in Viscoelastic Media

The incorporation of specific rheological viscoelastic properties of the matrix into the description of the segregation kinetics in glass-forming melts was carried out in a series of papers by Pascova et al. and Schmelzer et al. (see [627,628,710,713,714]). It was shown, in particular that the rate of growth of clusters in segregation processes of silver chloride particles in a highly viscous melt can be described by an equation of the form

$$\frac{dV}{dt} = \left(\frac{dV}{dt}\right)_N \exp\left(-\frac{t}{\tau_{(eff)}}\right) , \tag{12.44}$$

where $(dV/dt)_N$ is the rate of growth of a cluster in a perfect Newtonian liquid and $\tau_{(eff)}$ a parameter depending on the properties of the liquid. The integration of this equation results in a Kelvin-Voigt type behavior of the growth kinetics and also in a qualitative change of the coarsening behavior as shown in Fig. 9.3. Moreover, peculiarities in the time evolution of the cluster size distribution of segregating particles can be interpreted based on the same theoretical considerations (cf. Bartels et al. (1991) [43]).

This approach gives a new, more general way of interpreting crystallization and segregation phenomena in glass-forming liquids, in particular, in the vicinity of T_g. The mentioned effects become essential in the determination of the growth kinetics for segregation processes when the self-diffusion coefficient of the segregating particles is considerably higher than the respective coefficient for the matrix building units [713,714]. For nucleation processes themselves the effect is of less importance since the velocity of deterministic growth of clusters of near-critical sizes is practically equal to zero. These problems are discussed in detail in the cited papers.

Chapter 13
Concluding Remarks

Wrong are all those, dear friend Shuvalov, who value glass below minerals.
I am singing a song of admiration on the merits not of rubies, not of gold but of glass ...
Mikhail V. Lomonosov
In: Poetic Letter on the Merits of Glass addressed to Ivan I. Shuvalov (1752)

In this book, we have tried to give an outline of the historical development, of the past and the present state of understanding of a particular kind of condensed matter, i.e., matter in the vitreous state. We have endeavored to collect all the evidence showing that glasses, as known for many hundredth of years, represent only particular examples of a broad class of thermodynamically non-equilibrium systems with an or even non-amorphous structure, where an increased degree of disorder is kinetically frozen in, corresponding to a higher temperature equilibrium configuration.

A description has been given of the change of the properties of substances upon vitrification and of the kinetic characteristics of such processes both by the methods of phenomenological and statistical thermodynamics. It was demonstrated that this process has to be considered as an example not of an equilibrium phase transition but of a dynamic transformation, i.e., of a freezing-in process. Moreover, it has been shown that, in principle, each substance can be transferred into the vitreous state provided the necessary sufficiently high cooling rates or other methods of vitrification (e.g., vapor condensation on under-cooled substrates) can be realized experimentally. We have tried to demonstrate that vitrification as a process and glasses as a physical state have been and can be analyzed and understood both from macroscopic and microscopic points of view. Therefore, there is no excuse except ignorance when authors considering the vitreous state of matter characterize it as something unknown or unexplored.

In describing the structure of glasses we have tried to give a general outline of principles applicable, more or less, to all vitrified substances. It has been shown that, in fact, there are as many different structures as there are different glasses. Nevertheless, as discussed in detail in the respective chapter, general criteria allowing us to classify the seemingly innumerable structures of glasses do exist.

I.S. Gutzow and J.W.P. Schmelzer, *The Vitreous State*,
DOI 10.1007/978-3-642-34633-0_13, © Springer-Verlag Berlin Heidelberg 2013

We have tried to reestablish, in the analysis, the historical course and the inner logics of development of molecular physics from perfect gases to real liquids, on one side, and from perfect to real crystals and their melts on the other, and from both sides – from absolute disorder and total order – to the wide field of partially disordered, amorphous structures and their properties, which in their multitude of possible realizations are *"limited only by our imagination"*. Such an evolution of ideas is similar to the way the thermodynamics of macroscopic systems has evolved: from systems in an internal thermodynamic equilibrium to non-equilibrium systems and, in particular, to frozen-in non-equilibrium systems, i.e., to glasses.

A classification was developed further of possible kinds of disorder, respectively, order, frozen-in into the vitreous state. Moreover, evidence was given that materials having a non-amorphous crystalline structure with respect to the atomic or molecular configuration, may also have the properties of a vitrified system. In such cases, the frozen-in disorder is related to properties not connected with the topological ordering (orientational glasses, spin glasses, etc.). Adopting the enlarged definition of the vitreous state given in this book, it has also been shown that even life may be frozen-in to a glass.

A comprehensive analysis was devoted to problems of nucleation and crystal growth in glass-forming melts. This was done taking into account that nucleation and cluster growth are the main factors limiting the possibilities of transforming a given substance into the vitreous state. The understanding of the mechanisms of crystallization is also of significant importance for obtaining defect free glasses. It opens up the wide field of nucleation catalysis for induced crystallization of glass-forming melts in order to produce new materials with a broad spectrum of technological applications: glass-ceramics, semicrystalline solids and thin amorphous films including semiconductors and even high-temperature superconductors. Moreover, no other systems exist in nature where non-steady state effects in nucleation are of similar importance for the kinetics of phase transformation processes as for glass-forming melts. A detailed analysis of non-steady state effects is, therefore, a prerequisite for the formulation of quantitatively correct kinetic criteria for vitrification. On the other hand, the analysis of such effects for glass-forming melts also allows us to gain a deeper understanding of processes of phase formation, in general. This statement is also true with respect to the understanding of possible growth mechanisms. The three basic mechanisms of crystal growth analyzed above have been confirmed for the first time in experiments with glass-forming melts.

The outline of basic ideas and results concerning the rheological properties of glass-forming melts concludes the present book. Technological aspects, possible applications and the specific properties of particular glasses have been discussed, as mentioned in the introduction, only in connection with the development and verification of the general ideas and approaches to understand the vitreous state. This gap is supposed to be closed in a subsequent specialized monograph in

preparation which can be considered in some respect as a necessary supplement to the present book.[1]

In characterizing the main features and the state of the field which is called glass science we have tried to do our best in order to distinguish the most important lines of evolution, the most important ideas and theories in their past and present-day significance and possible importance for further development. Being convinced that in the evolution of science it is also true what A. Wellesley, Duke of Wellington (1769–1852) mentioned in another connection (*"All the business of ... life is to endeavor to find out what you don't know by what you do; that's what I called 'guessing what was the other side of the hill'."*) we hope that with the present volume in hand it will be easier for the reader to make his own predictions concerning "*what is of the other side of the hill*". Its our belief that there are not many problems of physics, chemistry and biology which have such a striking perspective and rapid future development as those connected with the vitreous state.

[1] A considerable extension of the scope of problems outlined in the present book including the new major developments of the last decades – sketched here only briefly in the footnotes and partly in some more detail in Chap. 14 – can be found in the following monographs: Schmelzer (2005, 2014) [695, 701]; Schmelzer and Gutzow (2011) [707]; Gutzow et al. (2014) [337].

Chapter 14
Brief Overview on Some New Developments

The present monograph is, as mentioned, widely identical to the first edition of our book [1] removing several printing mistakes and indicating in footnotes briefly some new developments (in this respect, referring to this book, we have in mind both the first and the widely identical presented here second edition). In Chap. 14, we are attempting to give a more extended but necessarily also brief overview on new developments, trying to summarize problems, scientific ideas and results, as they have been developed mainly in the fields of the theory of vitrification, in the understanding of the nature of vitreous states and in treating nucleation, phase separation and crystallization in glass-forming systems in the years after the first edition of this book [1] has been published. In deriving these ideas and results and bringing them to the attention of our readers, we have followed mainly the route of development, as it appeared in the framework of our own understanding and interests and as far as they could be considered as a continuation of the analysis of problems and ideas, developed in the first edition of this book. As far as these ideas are to a great extent in line with the general main tendencies in the present international literature, they give also an impression of general trends and developments in glass science literature. We have tried to supplement this presentation with additional literature, given at the end of this chapter in a separate bibliography, which is a supplement to the initial bibliography of the first 1995 edition of our book. In order to be self-consistent in this respect, some of the references contained in the initial bibliography are included here as well once again.

The first edition of the present monograph was written in the years before 1995 in the framework of two well established theoretical concepts, which both can be considered as two remarkable approximations, two outstanding thermodynamic models. One of them gives the possibility to treat thermodynamically – in the framework of classical equilibrium thermodynamics – glasses, which are non-equilibrium systems, and are thus out of the "normal" scope of classical equilibrium thermodynamics. This is Simon's model treating vitrification as the transition – at some given discrete temperature, T_g – of a (metastable) thermodynamic equilibrium state into a frozen-in thermodynamic non-equilibrium state, the glass [2]. For both these states, reversible processes can be performed and classical thermodynamics,

I.S. Gutzow and J.W.P. Schmelzer, *The Vitreous State*,
DOI 10.1007/978-3-642-34633-0_14, © Springer-Verlag Berlin Heidelberg 2013

at least, as far as the first and second laws are concerned, is fully applicable. The second of the mentioned thermodynamic models is concerned with the ways in which processes of nucleation and growth can be treated thermodynamically although the processes considered require the consideration of nano-sized systems, with new-phase clusters, which are, in general, also out of the scope of thermodynamics in its classical formulations. The present chapter begins with the discussion of developments, which are concerned with the first circle of problems: those, connected with the description of glasses as a particular physical state, the second section is devoted to the thermodynamic analysis of nano-systems and the kinetic description of cluster formation and growth processes, in particular, in glass-forming melts.

14.1 Glasses and the Glass Transition

14.1.1 Generic Phenomenology of the Glass Transition and the Thermodynamic Properties of Glasses

We start the analysis of glasses and the glass transition by showing the ways in which in the last 10–15 years the approximate classical approach based on Simon's approximation was replaced by an analysis in the framework of the thermodynamics of irreversible processes: i.e. by a non-equilibrium thermodynamic phenomenological treatment.

In our analysis of the properties of glasses and of the process of glass transition, of the kinetics of vitrification and glass stabilization as we described them in Chaps. 2 and 3 of the present book, we employed the classical thermodynamic approaches in the form as they followed from the mentioned approximation first proposed by F. Simon at the end of the 1920s [2] and used then by many researchers throughout the following 90 years. Chapter 2 in our book thus begins and ends with this fruitful approximation. However, already Simon himself mentioned that the transition to a glass does not proceed at some fixed temperature but in some temperature interval with a reference to Gustav Tammann [3] who already elaborated this idea in detail. Simon even discussed qualitatively a possible dependence of glass transition temperature and properties on cooling rate but considered these effects as small.

Anyway, it became evident already at that times, since the first developments of one of the variants of the thermodynamic treatment of non-equilibrium systems, that thermodynamics of irreversible processes, as it has been developed by scientists like Th. De Donder, I. Prigogine, S. R. De Groot and many others, will be and is the phenomenological approach, opening new horizons in treating non-equilibrium systems with frozen-in structure and thermodynamic properties, i.e., glasses, glass relaxation and the glass transition. This is the reason why in Chap. 3 of our book a number of problems like the process of relaxation, the definition of specific heats

of liquids as being separated into two additive parts (a liquid-like configurational one and a crystalline-like phonon contribution) are described theoretically already in terms of non-equilibrium thermodynamic ideas, developed by the mentioned authors and applied to glass science in general first mainly by Davies and Jones, Cooper, Moynihan and also by one of the present authors (I.S.G.) to several specific problems of glass thermodynamics: to vapor pressure and solubility of glasses, the jump in specific heats, $\Delta C_p(T)$, at glass transition temperature, the definition of T_g and many other details as this is outlined here in the introduction of Chap. 3 of our book. However in treating such essential problems like the dependence of the properties of glasses on cooling rate as performed by Gutzow and Dobreva-Veleva [4, 5], again, the simpler way of Simon's approximation was initially employed as shown here in Sect. 3.7. It led to results of considerable significance, as it was confirmed and then extended in subsequent developments given in a series of recent publications by Schmelzer, Tropin, and Schick [6, 7] and performed now already fully in the framework of the thermodynamics of irreversible processes. Simon's approximation was also a useful initial approach in analyzing vapor pressure, solubility and chemical reaction activity of glasses as they are treated here in Sects. 3.9, 3.10, 3.12, and 3.13.

In 1934 in investigating the possibility of solidification of the structure of metastable metallic alloy systems, Bragg and Williams [8] introduced for the first time and in an ad-hoc manner a simple equation which we shall write here as

$$\frac{d\xi}{dT} = -\frac{1}{q\tau(T)}\left(\xi - \xi_{eq}(T)\right) , \qquad q = \frac{dT}{dt} . \tag{14.1}$$

It describes, according to Bragg and Williams, the freezing-in of a given alloy structure as a non-isothermal relaxation process. The freezing-in process is characterized in our presentation by the internal structural order parameter ξ.

In the present book, we have introduced in Sect. 3.9 the notion of ξ as a generalized structural order-parameter, characterizing the structure of a glass-forming liquid. The deviation from its equilibrium value, $\xi_{eq}(T)$, describes in terms of the difference $(\xi - \xi_{eq}(T))$ the driving force for the approach to equilibrium. In the thermodynamics of irreversible processes this driving force is the affinity, $A = -(dG(T,\xi)/d\xi)$. By a truncated Taylor expansion of $G(T,\xi)$ in the vicinity of $\xi = \xi_{eq}$ we obtain the well-known approximate expression for the thermodynamic driving force and the formalism in treating relaxation processes, given in Sect. 3.9 of the present monograph in terms of the dependence

$$\frac{d\xi}{dt} = -\frac{1}{\tau(T,\xi)}\left(\xi - \xi_{eq}(T)\right) . \tag{14.2}$$

Equation (14.1) follows from the isothermal relaxation law, Eq. (14.2) by replacing dt in above dependence or in Eq. (3.122) of the book via $(dT/dt) = q$.

Bragg and Williams have in fact written in 1934 Eq. (14.1) using the concept of fictive temperature, $\tilde{T}$, of the system and constructing the kinetics of isothermal

relaxation of the investigated alloy systems in terms of a process in which the actual temperature, T, is changed in accordance with the second term in Eq. (14.1) and the driving process of relaxation is assumed to be proportional to the difference $(\tilde{T} - T_{eq})$. Such an approach was used frequently in glass science in the 1930s and later in the analysis relaxation phenomena especially in the publications of Tool [9, 10], Narayanaswamy [11] and a variety of other colleagues. In particular, in 1956/1957 Vol'kenstein and Ptizyn [12,13] and then also Filipovich and Kalinina (in 1971 [14]) employed again Eq. (14.1) as an empirical *ansatz* to the development of a kinetic treatment of vitrification, which in the Russian literature of those times was termed "the kinetic theory of glass transition" [15]. In this series of investigations – which found also a continuation in several well-known papers by Moynihan, Kovacs et al. – these authors also retained the ad-hoc nature of the assumption, on which Eq. (14.1) was based in 1934 by Bragg and Williams [8]. In the first Vol'kenstein – Ptizyn paper [12] even the possibility of an additional semi-quadratic dependence of $(d\xi/dT)$ on $(\xi - \xi_{eq})$ is discussed. The temperature course of the enthalpy $\Delta H(T)$ or the volume $\Delta V(T)$-differences upon cooling and heating runs was given in these publications, using Eq. (14.1) and its solutions, employing the direct proportionality between ξ and ΔH or ΔV, as it follows from the linear formulations of the thermodynamics of irreversible processes and assuming the simplest possible temperature dependence ($U(T) = U_0 = \text{const.}$) in the classical expression for the relaxation time

$$\tau(T) = \tau_0 \exp\left(\frac{U(T)}{RT}\right) \tag{14.3}$$

for the activation energy, $U(T)$, determining the time, τ, of molecular relaxation of the vitrifying melt.

By constructing the course of $\xi(T)$ for various cooling rates, q, and with the mentioned assumption that volume, ΔV, or enthalpy, ΔH, differences are connected via direct proportionality with the structural order parameter, ξ, and its equilibrium value $\xi_{eq}(T)$, the first dependencies of the change of thermodynamic functions upon temperature at vitrification, taking place at different cooling rates, were constructed in a semi-quantitative approximation (see Filipovich and Kalinina [14], and Moynihan et al. [16]). Moreover, it was also proposed in these series of publications to determine in the framework of the theoretical approach developed the vitrification temperature, T_g, from the course of the $\xi(T)$-curves obtained: it was in fact proposed to identify them with the extremal values of the respective $(d\xi^2/dT^2)$-curves, as indicated many years earlier already by Tammann in his analysis of experimental $\Delta C_p(T)$-curves (see [3]). These results showed in their generality that the simple kinetic approach to glass transition as it is given with Eq. (14.1), can be taken as the basic starting point in deriving a thermodynamically well founded theory and thus to develop the description of the whole process of vitrification in an unambiguous way starting from the very foundations of the thermodynamics of irreversible processes.

This program was initiated by one of the present authors in a lecture course an account of which is published in [17, 18]. The following development was to be realized according to this program and was in fact performed in an initial series of publications by Gutzow et al. [19–22] and then by Gutzow and Schmelzer [23, 24] in the following years:

1. It was obvious that Eq. (14.1), ad-hoc assumed at various occasions by several authors could be *derived*, as a non-isothermal continuation of Eq. (14.2) (as given in the derivation of Eq. (3.122)), from one of the basic principles of the thermodynamics of irreversible processes: the so called Phenomenological Law. It was, however, also evident that for glass-forming systems the linear dependencies, given with Eqs. (14.1) and (14.2), could lead only to trivial results, non-consistent with the experimentally known peculiarities of relaxation in typical glass-forming systems. The necessary formalism, as it was employed by Gutzow and Schmelzer, in writing this law in a non-linear form is evident from the derivation summarized here and in the first edition of our book with Eqs. (3.110)–(3.114). In doing so it was assumed that the coefficients L in dependencies like the one, given with Eq. (3.115), were not constants, but have to be functions of the deviation of the vitrifying system from equilibrium. It seems that for the first time a similar assumption for the possibility of the non-constant character of the coefficients L in equations like the one given, with Eqs. (14.1) and (14.2), was suggested by Callen [25].
2. The deviation of L from its constant value, as supposed in the classical linear formulations of the thermodynamics of irreversible processes, was assumed (see e.g. in [19]) to depend exponentially, via the value of the activation energy $U(T, \xi)$, on the deviation from equilibrium. This assumption led us [23], following a proposal by Prigogine [26], instead of Eq. (14.3) to

$$\tau \cong \tau_0 \exp\left[\frac{U(T)}{R}\right] \exp\left[\frac{(\xi - \xi_{eq})}{\xi_{eq}}\right] \tag{14.4}$$

for the coefficient τ in Eq. (14.1). The relaxation time, τ, becomes dependent in this way on the current structural properties, i.e., the formation of the density- and/or compositional fluctuations is thus dependent (i.e. via the activation energy $U(T, \xi)$) on the structure of the system out of equilibrium. Thus, it is a process to be governed by the fluctuation-dissipation theorem [25, 27].

Considering pressure to be constant, and in expanding the exponent $U(T, \xi)$ into a Taylor series with respect to the two independent variables (T and ξ) the derivation was truncated at the first linear term in ξ in order to preserve the linear character of the adopted linear formulation of the thermodynamics of irreversible processes. For the value of $U(T)$ in Eq. (14.3) as the simplest assumption follows $U(T) = U_0 - b_0 T$, thus satisfying the condition of Kanai and Satoh ($dU(T)/dT < 0$) discussed in Sect. 2.4.1 with Eqs. (2.80) and (2.81). As the result, for the rate of non-isothermal relaxation governing glass transition, an

expression with a semi-linear dependence on $(\xi - \xi_{eq}(T))$ was derived (Gutzow et al. [23]) of the form

$$\frac{d\xi}{dT} = -\frac{(\xi - \xi_{eq})}{q\tau_0} \exp\left(-\frac{U(T)}{RT}\right) \exp\left(-\frac{\xi - \xi_{eq}}{\xi_{eq}}\right) . \tag{14.5}$$

It can be shown, as done by the present authors in [23] that Eq. (14.5) corresponds in fact to the most general form of the dependence describing first-order reaction kinetics in terms of the De Donder-Marcelin equation (see [28] and literature, given there). From Eq. (14.5) (written for the isothermal case, i.e. in terms of $(d\xi/dt)$) the first-order reaction kinetics, as it is written usually in its approximated form, introduced by van't Hoff into physico-chemical literature, follows directly.

3. The value of the internal structural parameter, ξ, usually considered in the thermodynamics of irreversible processes as a generalized De Donder reaction coordinate was defined in our series of investigations in such a way as to be equal to $\xi = 0$ for the crystalline state of absolute order and as approaching $\xi = 1$ in the respective gas phase. In order to have at our disposal a suitable model for the description of the vitrifying melt, a MFA-lattice-hole model earlier developed by Milchev and Gutzow [29, 30] was utilized. In this way a distinct course of the $\xi_{eq}(T)$-function was guaranteed and the artificial second-order phase transition point at the Kauzmann temperature T_k, introduced in glass science with the MFA-lattice-hole polymeric chain model of Gibbs and Di Marzio [31] was avoided, as shown by Milchev and Gutzow in the cited papers and as summarized in Sect. 5.4.3 of the monograph. A generalization of this model to polymer glasses was also attempted in a computer model approach, developed later on by Petroff, Milchev, and Gutzow in 1997 [32].
4. All the considerations on the kinetics and thermodynamics of vitrification performed in terms of Eq. (14.1) by authors like Bragg and Williams, Vol'kenstein and Ptizyn, Kalinina and Filipovich, and Moynihan et al. and also the first series of publications of the present authors (e.g. in [19]) were developed without accounting for the possibility (and, in general, the necessity!) of introducing entropy production terms into the analysis of the process of glass transition. This effect was also not considered in the first edition of the present monograph. In general, the inclusion of such effect is, however, a necessity, accounting for the circumstance that according to the basic laws of thermodynamics, expressed in the De Donder – Prigogine equation via

$$\frac{dS}{dt} = \frac{d_e S}{dt} + \frac{d_i S}{dt} , \tag{14.6}$$

entropy has to be generated in any non-equilibrium process $(d_i S > 0)$ and thus also in passing the glass transition region in both directions: in heating and in cooling runs. Starting with the general definition for $d_i S/dt$ and expressing it in a similar form as we have written it for the variation of the structural

order parameter for the non-equilibrium process of non-isothermal relaxation, we arrive at [24, 37]

$$\frac{d_i S}{dT} = \frac{A}{T}\frac{d\xi}{dT} = \frac{R}{q\tau(T,\xi)}\frac{(\xi - \xi_{eq}(T))^2}{\xi_{eq}(T)} \tag{14.7}$$

for the expression governing entropy production in the glass transition region. Results of numerical computations of the entropy production in dependence on cooling and heating rates are given here later (cf. Fig. 14.7).

The respective first quantitative analysis of entropy production in the glass transition region was performed by the present authors in collaboration with J. Möller [37]. This analysis on the respective values of the total entropy, $\Delta_i S$, produced in the glass transition, shows that the entropy values generated at "normal" cooling rates through the glass transition region, $T_g^{(-)} \leq T \leq T_g^{(+)}$ with

$$T_g^{(+)}: \quad \text{upper value of the glass transition range ,}$$
$$T_g^{(-)}: \quad \text{lower value of the glass transition range ,}$$

are only a relatively small percentage of the entropy values, ΔS_g, frozen-in at vitrification. Assuming a "classical" process of glass transition in the framework of Simon's approximation, according to which the glass transition interval is degenerated to the glass-transition temperature itself, to a salient point in the $\Delta S(T)$ curve and to a sharp "jump" at $T = T_g$, as this is assumed also according to the "classical" model of vitrification (see here Sect. 3.2), no entropy production at vitrification has to be expected, as mentioned already also by Simon himself [2] and later on also by Davies and Jones [38]. Entropy production is to be considered if the realistic course of glass-transition in a glass transition interval is accounted for but this effect may be, and as it turns out, it is small in the overwhelming majority of cases analyzed so far. Some numerical computations illustrating these statements will be given here later.

By this reason, even when entropy production in the glass transition interval is accounted for, it turns out that the entropy produced has values, which in most applications can be neglected: even in constructing the course of the thermodynamic functions and potentials upon vitrification, as done by Gutzow et al. e.g. in [19]. The results of such construction is seen on Fig. 14.1 which is in fact the first construction of the thermodynamics of vitrification done in terms of the generic phenomenological approach based on the application of the Bragg-Williams equation, Eq. (14.1), and its further development in a series of investigations (cf. [24]) and now here. A comparison with experimental data is given in Fig. 14.2.

5. On Fig. 14.3 is given the temperature course of the first, the second and the third order temperature derivatives of the structural order parameter ξ in the process of vitrification described in terms of Eqs. (14.1) and (14.2), as it was for the first

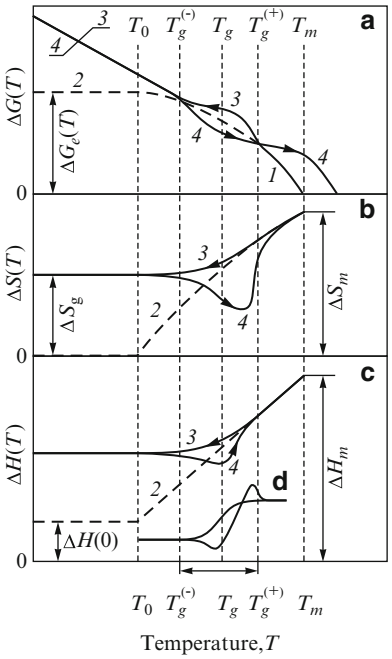

Fig. 14.1 Thermodynamics of the glass transition in terms of the generic theory of vitrification (see text and Fig. 3.10 in [24]): (**a**) temperature dependence of the configurational part of Gibbs' thermodynamic potential difference, $\Delta G(T)$, in terms of the differences liquid/crystal or glass/crystal: (*1*) equilibrium course, $\Delta G_e(T)$, in cooling in the range from $T = T_m$ to temperatures tending to zero; (*2*) $\Delta G(T)$, course upon vitrification in a cooling run; (*3*) $\Delta G(T)$, course in heating from zero temperatures to temperatures near T_g; (*4*) $\Delta G(T, \xi)$ of the vitrified melt representing the tangent to $\Delta G_e(T)$ of the under-cooled melt. T_m, T_g and T_0 are melting, glass transition and Kauzmann temperatures, respectively. The glass transition interval is determined by the steep change of the specific heat, ΔC_p, and is bounded to the range $T_g^{(-)} \leq T \leq T_g^{(+)}$. With $\Delta G(0)$ the extrapolated zero-point potential difference of the metastable liquid is specified; (**b**) temperature dependence of the entropy difference, $\Delta S(T)$ liquid/crystal (*2*) and of glass/crystal in cooling (*3*) and heating (*4*). ΔS_m is the entropy of melting and ΔS_g is the frozen-in entropy of the glass; (**c**) change of the enthalpy difference, $\Delta H(T)$, liquid/crystal (*3*, *4*). $\Delta H(0)$ is the zero-point enthalpy corresponding to the metastable under-cooled liquid; (**d**) liquid/crystal or glass/crystal specific heat differences. In cooling, ΔC_p decreases monotonically with decreasing temperature, and in heating a minimum and a maximum is observed

time depicted in our paper [19]. It defines $d\xi/dT$ (which thermodynamically corresponds to $\Delta C_p(T)$) as a sigmoidal curve with an inflection point at the temperature of glass transition, $T = T_g$. This temperature course gives a new unambiguous way of defining glass transition first adopted by Gutzow et al. in 2000 in [19]: as being determined by

$$\frac{d^2 \Delta C_p(T)}{dT^2} = 0 \tag{14.8}$$

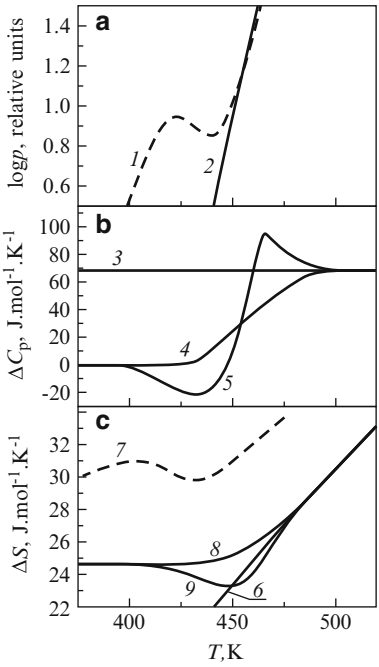

Fig. 14.2 Coincidence of theory and experiment in the determination of $\Delta G(T,\xi)$ and $\Delta S(T,\xi)$ as shown in Fig. 14.1 and employing vapor pressure, $p(T,\xi)$, and specific heat, $\Delta C_p(T,\xi)$-data reported by Kinoshita [33] and Schnaus et al. [34] for As_2Se_3 for the liquid, glassy and crystalline forms of this substance (predicted according to [35, 36]): (**a**) temperature dependence of the vapor pressure of As_2Se_3 at heating (curve *1*) and very slow cooling (curve *2*) of the melt. (**b**) Temperature dependence of the specific heat difference, ΔC_p, of As_2Se_3 for liquid/crystal at equilibrium (curve *3*), for cooling (*4*) and heating (*5*) of the under-cooled liquid/crystal or the glass. (**c**) Computed values of the entropy difference, $\Delta S(T)$: under-cooled liquid/crystal (curve *6* obtained from curve *3*); glass-liquid/crystal (curve *7* obtained from the experimental $p = p(T)$ curve (*1*)); curve *8* obtained from curve *4* and curve *9* from curve *5* (from calorimetric data). Note the similar $\Delta S(T)$ course of curve *7* obtained from tensimetric measurements and of curve *9* following from calorimetric measurements on samples with similar thermal history

from the inflection point of the $\Delta C_p(T)$-curve i.e. from the course of the respective $(d\xi/dT)$-curve as $(d\xi^3/dT^3) = 0$. The already mentioned maximum $(d\xi^2/dT^2)$-definition of T_g, earlier proposed by Vol'kenstein and Ptizyn [12, 13] and by Kalinina and Filipovich [14], gives *not*, as it is seen from Fig. 14.3, an unambiguous way of defining T_g: there are two, or even three extremal values on the $(d\xi^2/dT^2)$-curve (or on the respective $(d\Delta C_p(T)/dT)$-curves) to be expected in heating run experimentation, usually experimentally employed for T_g-determinations.

6. The condition, Eq. (14.8), for the course of the derivative $(d^2\Delta C_p(T)/dT^2)$ gives, moreover, as shown by Gutzow et al. [19], a direct *thermodynamic* way

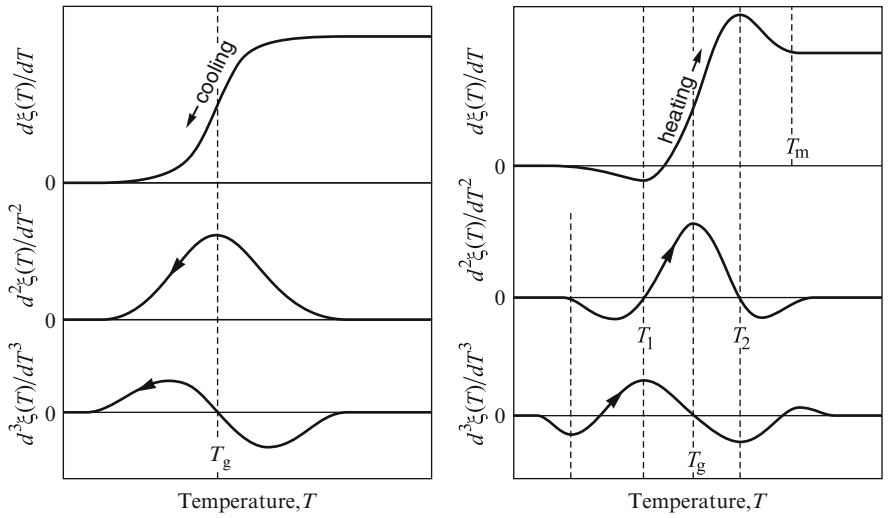

Fig. 14.3 Dependence of the derivatives of the structural order parameter, ξ, with respect to temperature, T, for the cooling (*left*) and heating (*right*) runs. At $T = T_g$, the third order derivative of $\xi(T)$ is by definition nullified which corresponds to an inflexion point in the configurational contributions to the specific heats (see Gutzow et al. [19–22])

to define and *to derive* without further assumptions also the general equation of the glass transition kinetics

$$q_0 \tau(T, \xi) \cong C_1 \ , \tag{14.9}$$

which we have already discussed in our present book in Sect. 3.6 as the Frenkel-Kobeko postulate. The course of the respective mathematical derivations can be followed in [19]. This derivation gives for the constant in Eq. (14.8) the value

$$C_1 \approx x_0 \frac{R T_g^2}{U_0} \cong x_0 \left(\frac{1}{30} \div \frac{1}{40} \right) T_g \cong 1 \div 5 \tag{14.10}$$

for values of the ratio $(R T_g / U_0)$ changing in the limits as seen from above written dependence. Thus for substances with medium values of T_g the usually observed value of the Frenkel-Kobeko constant (approximately equal from 1 to 5 K according to Bartenev [39]) is to be expected. The factor x_0 has values $x_0 = 1.62$ at cooling and $x_0 = 0.62$ at heating run experimentation according to the derivation, given in [19]. Thus, according to above formalism it also follows that between the glass transition temperatures at cooling and heating run experimentation the temperature difference

$$T_g^{heating} - T_g^{cooling} \approx 0.012 T_g^{mean} \tag{14.11}$$

has to exist, where T_g^{mean} specifies the mean value of the glass transition temperature at the given experimental conditions. In this way, with increasing glass transition temperatures the difference between the T_g-values in heating up ($T_g^{heating}$) and cooling down ($T_g^{cooling}$) experimentation has to increase, as this was in fact observed in experiment. In this way, this derivation gives (as really observed in experiment) also the a difference in the values of T_g as they are observed upon cooling or upon heating run experimentation.

7. Simple purely *kinetic* definitions of T_g and derivations of the Frenkel-Kobeko dependence, as proposed e.g. by Reiner (or, more exactly by Stevels, see Sect. 3.6 in this book) or as also discussed below, lead to the same value of the constant in Eq. (14.8). According to Stevels' and Cooper's kinetic approach, described in Sect. 3.6 of the present monograph, it is *assumed* that the condition for glass formation can be formulated as (see also Gutzow and Dobreva [18]) that at $T \approx T_g$ the time of molecular relaxation of the vitrifying system becomes equal to the time of observation, $\Delta t = (t - t_0)$, i.e. that there the relation

$$\tau_R(T, \xi) \cong \Delta t = (t - t_0) \tag{14.12}$$

holds. In a recent publication [40] one of the present authors has generalized this kinetic approach eliminating the concepts of Deborah number and time of observation from the description by introducing with

$$\tau_T = \left(\frac{T}{|q|}\right) \tag{14.13}$$

a characteristic time scale of the cooling and heating process. The condition for vitrification can be now written, following Schmelzer [40], in the form that the characteristic time of molecular relaxation has to be approximately equal to the characteristic time of change of temperature, i.e.,

$$\tau_R(T, \xi) \cong \tau_T \ . \tag{14.14}$$

Note as well that, since τ_R depends both on temperature and the structural order parameter, Eq. (14.14) yields different values of T_g for cooling and heating since τ_R is different for cooling and heating runs. Straightforward modifications of this relation have been employed by Schmelzer and Tropin, in addition, in order to determine the upper and lower boundaries and the width of the glass transition interval in dependence on cooling and heating rates [41].

A differentiation of the combination of Eqs. (14.13) and (14.14) with respect to T gives the same result as the Reiner and Stevels approach, i.e.,

$$\frac{d\tau_R(T, \xi)}{dT}\left(\frac{dT}{dt}\right) \cong 1 \ . \tag{14.15}$$

As far as $\tau_R(T, \xi)$ is an exponential function of the type given with Eqs. (14.3) or (14.4), with the additional assumption $U(T, \xi) = U_0$ follows directly the result already given with Eqs. (3.79) and (3.82) in the present book and here in Chap. 14 repeated with Eqs. (14.8) and (14.9). In this respect it is to be mentioned, that this circumstance shows that vitrification is a consequence of the *exponential* character of the dependence of intensity of flow, of the relaxation properties of the system on reciprocal temperature. This fact can be proven also by computer experiments as an inherent for the glass transition necessity.

The description of vitrification in terms of the characteristic time τ_T of change of the external parameter gives advantages also in treating more complicated changes of the temperature (or of other parameters causing vitrification), for example, when the cooling rate is not a constant but a function of the time, t (e.g. with $q \cong at^n$) or even a periodic function of the time, in describing so-called dynamic glass transitions. Dynamic glass transitions may proceed at the change of the state of the system with a given characteristic frequency, ν, or angular frequency, $\omega = 2\pi\nu$, by varying the frequency of external perturbations. For such cases, the equilibrium value of the structural order parameter, ξ_{eq}, is varied as

$$\xi_{eq} \propto \exp(i\omega t) \tag{14.16}$$

The characteristic time, τ_D, of change of the respective equilibrium state, ξ_{eq}, can be determined in the framework of above theoretical formalism [40] then via the set of equations

$$\frac{d\xi_e}{dt} = i\omega\xi_e \ , \qquad \frac{d\xi_e}{dt} = -\frac{1}{\tau_D}\xi_e \ , \qquad i\omega = -\frac{1}{\tau_D} \ . \tag{14.17}$$

Taking the absolute value in the latter two dependencies we arrive at the result

$$\tau_D\omega \cong 1 \ . \tag{14.18}$$

The criterion for glass formation at dynamic glass transitions can be written consequently as

$$\tau_R \cong \tau_D \qquad \Rightarrow \qquad \omega\tau_R \cong 1 \ . \tag{14.19}$$

In other words, in above relation for the kinetic criterion of glass formation in cooling and heating processes, $(|q|/T)$ has to be replaced by ω. A first formulation of latter equation has been given by Bartenev in 1949 [42] by analyzing some particular model of viscoelastic behavior. The sketched here derivation due to Schmelzer [40] is more general i.e. model-independent.

8. In analyzing the formation of glassy thin layers at processes of vapor quenching or at electrolytic deposition of metallic alloy glasses, analogs of Eq. (14.19) have been used by Avramov et al. [43] and by Jordanov et al. [44] to derive an appropriate description of the kinetics of vitrification processes. In both latter mentioned processes, the formation of amorphous thin layers, the deposition of ad-atoms on them and their subsequent burial under the following ad-layers

resemble periodic processes of an interesting class of dynamic glass transition which were described using Bartenev's equation Eq. (14.19) to derive the necessary quantitative formalism. Another interesting case of the formation of glassy layers in vapor quenching on super-cooled substrates (like the formation of Ar-glass at substrates, cooled with liquid helium) is described in Sect. 3.12 of the present book.

9. One of the main results following from the development of a phenomenological model capable of describing, at least, in a semi-quantitative way glass transition, is the possibility it gives to analyze the ways to form glasses with desired properties. Of particular interest is also the possibility to derive expressions for the prediction of dependencies leading to glasses with extreme properties (for the details see e.g. [6, 7, 24]).

In this way, with a series of results, published in a steadily increasing sequence of papers, recently also summarized in our second monograph [24], the present authors hope to have succeeded in generically deriving a fundamentally safe and sufficiently correct phenomenological picture in describing glass transitions in the general framework of the thermodynamics of irreversible processes. It is of essence to point out that this picture has been drawn in this series of publications in a generic way out of the thermodynamics of irreversible processes in its linear formulation, without introducing any particular new assumptions or "glassy" models and using the thermodynamic model of this generalized thermodynamic description in a form as it was derived in the already cited developments given mainly by authors like De Donder [45] and Prigogine and Defay [46] in their classical publications. Our approach has opened also, so we hope, the possibility of developing simple, but nevertheless direct ways in solving a variety of additional problems connected with the kinetics and the thermodynamics of vitrification and, moreover, with the properties of different glasses obtained at different conditions of glass transition. In the subsequent part, we would like to review some important consequences and applications.

14.1.2 Glasses and the Third Law of Thermodynamics

In a comprehensive effort of the present authors and partly in cooperation with Möller and Petroff [23, 24, 47], the behavior of glass-forming systems (and more generally: of matter with frozen-in disorder) at temperatures approaching the absolute zero-point was analyzed. Here the general conclusions obtained from this analysis are summarized (for the details see above given references).

The glass transition temperature can be considered in a generalized approach as the temperature at which the vitrifying system changes from Boltzmann's statistics to quantum statistics. In this respect the glass transition temperature, T_g, shows some analogy with the gas-degeneration temperature, T_d, the temperature, at which any gas changes its behavior from the one, corresponding to a system

described by Boltzmann's statistics, to a system following quantum statistics. In this way, as predicted by Nernst even before appearance of quantum statistics as a science, gases fulfill at absolute temperatures $0 \leq T \leq T_d$ the requirements of the Third Principle of thermodynamics and, in particular, its consequence that specific heats of all forms of matter have to be equal to zero at zero temperature, i.e. that, at $T \to 0$, not only $C_p^{cryst}(T) \to 0$ and $C_p(T)^{amorph} \to 0$ hold, but also $C_p^{gas}(T) \to 0$ is fulfilled. In writing the latter relation, we should say more generally that we know now that, in order to fulfill the requirements of the Third Principle, even the behavior of gases is changed at $T \leq T_d$ in such a way as to fulfill the Third Principle in this its form, according to which any system in any possible state cannot reach the absolute zero of temperatures.

In the same way, at temperatures below the glass transition region, the specific heats of glasses, $C_p(T)$, and the specific heat differences glass and crystal, $\Delta C_p(T)$, approach at temperatures, $T \to 0$, values $\Delta C_p(T) \to 0$. This is so, because below T_g in both glass and crystal the value of $C_p(T)$ is determined only by the oscillations of their building units, which can be considered as an ensemble of quantum oscillators. Thus they follow the predictions of quantum statistics and their $C_p(T)$-course is entirely determined by the well-known Einstein or Debye (or Tarassov) formalism (see Chap. 4 of the present book), predicting temperature dependencies, leading at $T \to 0$ to $C_p(T) \to 0$ both for the crystal and the glass. At temperatures approaching zero, thus for any equilibrium crystalline substance remains valid the classical formulation of M. Planck, according to which we have to expect $S_{cryst}(T)_{T\to 0} = 0$, now also following from the results of quantum statistics. However, in any body with frozen-in non equilibrium (and especially in a glass!), despite above quantum statistical expectation, confirmed by numerous experiments showing that $C_p^{glass}(T)\,|_{T\to 0} = 0$ both classical and quantum mechanics confirm also another prediction of Planck: that any non-equilibrium system with frozen-in disorder (and thus especially any glass) approaches $T = 0$ with a residual entropy $\Delta S(T)\,|_{T\to 0} = \Delta S_g = \text{const.} > 0$. The value of this residual entropy (frozen-in in the glasses at $T \approx T_g$) can be *considered* and calculated (or at least estimated!) according to Planck in terms of Boltzmann's statistics as an entropy of mixing (of thermodynamically distinct *real* or *virtual* structural elements). A classical example in this respect gives the possibility of free volume calculation of the value of ΔS_g of simple and polymer glasses, as it was performed by one of the present authors years ago [48] and as it is summarized in Sect. 5.6 of the present monograph.

In Chap. 5 of our second monograph [24] also other systems with frozen-in disorder – crystalline alloys, defect crystals (with structural defects, frozen-in at the melting point, $T = T_m$), so-called "glassy" crystals, amorphisized crystals, so-called spin-glasses etc. – are discussed. In all these systems above mentioned remarkable duality, first observed in common model laboratory glasses is followed: their specific heats $C_p(T)$ are nullified at temperatures approaching zero point, their zero point entropy, however, remains a positive constant. Any substance, in equilibrium or not because in both cases $C_p(T)_{T\to 0} = 0$, follows the requirements of the Third Principle, if we formulate it as a principle of the non-attainability of the absolute zero of temperatures. With no device or process, even with the use

of non-equilibrium systems, could we thus reach the absolute zero of temperature. However, in approaching this temperature with a system in non-equilibrium, we will approach it in a way different from the route, observed with a system in equilibrium (i.e. with a crystal or with *liquid* helium, the only system, remaining liquid even at $T \to 0$). These differences are discussed here in Sect. 2.52 and in greater details in the cited publications of the present authors.

In these publications also a detailed discussion may be found concerning claims of some authors [49] that vitrification processes are accompanied by an approach to zero of the residual entropy values. In three recent our papers [50–52], a special critical analysis of the consequences of such an approach are performed and it is found that they contradict both in their derivation and in the final results the Second Principle of thermodynamics. This conclusion concerns properties which are described above $T = T_g$ with Boltzmann statistics. For properties like the electric conductivity of metallic alloy glasses or the thermoelectric properties of glass/crystal contacts the respective systems follow quantum statistics and the temperature dependencies it determines. Thus in metallic alloy glasses the thermoelectric driving force glass/crystal, $\Delta\alpha(T)\,|_{T\to 0} = 0$, as we have shown using both theoretical and experimental evidence, despite the circumstance that this property is determined by an entropy analog: the drift entropy of the respective electricity carriers (for the details see [47, 51]). Thus it turns out that while in "normal" molecular "laboratory" glasses the configurational entropy of the structural units of the glass is frozen-in below T_g, the drift entropy of the electric carriers in the metallic glass (i.e. the nearly fully degenerated electronic gas there) follows both above and below T_g the requirements of Fermi's quantum statistics and determines at $T \to 0$ *both* specific heat and entropy dependencies, leading to $C_p(T) \to 0$ and to $S(T) \to 0$.

14.1.3 The Prigogine-Defay Ratio

14.1.3.1 Second-Order Equilibrium Phase Transitions: Ehrenfest's Relations and Ehrenfest's Ratio

Following Ehrenfest, second-order equilibrium phase transitions are characterized by equality of Gibbs' free energies of the different phases,

$$G^{(1)}(p,T) = G^{(2)}(p,T)\,, \tag{14.20}$$

and, in addition, by equality of the first-order derivatives,

$$\left(\frac{\partial G^{(1)}}{\partial p}\right)_T = \left(\frac{\partial G^{(2)}}{\partial p}\right)_T\,, \qquad \left(\frac{\partial G^{(1)}}{\partial T}\right)_p = \left(\frac{\partial G^{(2)}}{\partial T}\right)_p \quad \Longrightarrow \quad p = p(T) \tag{14.21}$$

or equality of volume, v, and entropy, s,

$$v^{(1)} = v^{(2)} \,, \qquad s^{(1)} = s^{(2)} \,, \tag{14.22}$$

but inequality of the second-order derivatives,

$$\left(\frac{\partial^2 G^{(2)}}{\partial p^2}\right)_T \neq \left(\frac{\partial^2 G^{(1)}}{\partial p^2}\right)_T \,, \qquad \left(\frac{\partial^2 G^{(1)}}{\partial T^2}\right)_p \neq \left(\frac{\partial^2 G^{(2)}}{\partial T^2}\right)_p \,, \tag{14.23}$$

$$\left(\frac{\partial^2 G^{(1)}}{\partial T \partial p}\right) \neq \left(\frac{\partial^2 G^{(2)}}{\partial T \partial p}\right) \,.$$

With

$$S = -\left(\frac{\partial G}{\partial T}\right)_p \,, \qquad V = \left(\frac{\partial G}{\partial p}\right)_T \,, \tag{14.24}$$

and the definitions of the specific heat at constant pressure, C_p, the isothermal expansion coefficient, α, and the compressibility, κ,

$$C_p = T\left(\frac{\partial S}{\partial T}\right)_p \,, \qquad \alpha = \frac{1}{V}\left(\frac{\partial V}{\partial T}\right)_p \,, \qquad \kappa = -\frac{1}{V}\left(\frac{\partial V}{\partial p}\right)_T \,, \tag{14.25}$$

we obtain, consequently,

$$C_p^{(1)} \neq C_p^{(2)} \,, \qquad \alpha^{(1)} \neq \alpha^{(2)} \,, \qquad \kappa^{(1)} \neq \kappa^{(2)} \,. \tag{14.26}$$

As indicated in Eq. (14.21), each of the considered identities defines the dependence of pressure on temperature (or vice versa) for the states where a second-order equilibrium phase transition may occur. These two relations can be expressed in the form

$$\frac{dp}{dT} = \frac{1}{VT}\left(\frac{C_p^{(1)} - C_p^{(2)}}{\alpha^{(1)} - \alpha^{(2)}}\right) \,, \qquad \frac{dp}{dT} = \frac{\alpha^{(1)} - \alpha^{(2)}}{\kappa^{(1)} - \kappa^{(2)}} \,. \tag{14.27}$$

They are denoted as Ehrenfest's relations. Since both equations have to be equivalent, we arrive from them at a relation denoted as Ehrenfest's ratio, Π_E, i.e.,

$$\Pi_E = \frac{1}{VT}\frac{\Delta C_p \Delta \kappa}{(\Delta \alpha)^2} \,, \qquad \Pi_E = 1 \,. \tag{14.28}$$

For second-order equilibrium phase transitions, the combination of jumps of the thermodynamic coefficients as expressed via Ehrenfest's ratio, Eq. (14.28), has to be equal to one.

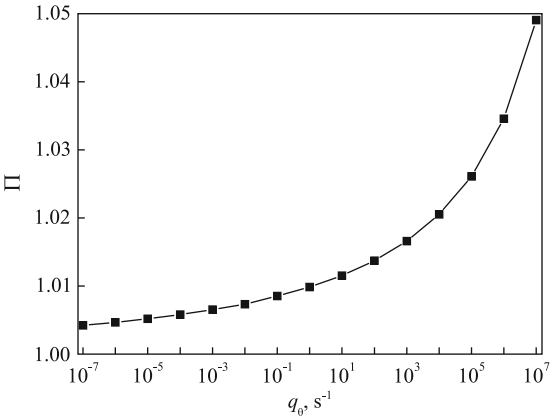

Fig. 14.4 Dependence of the Prigogine-Defay ratio of the given model system on cooling rates. Here the cooling rate is defined via Eq. (14.36)

14.1.3.2 The Prigogine-Defay Ratio: Beyond Simon's Model

Treating the glass transition in terms of Simon's model, Prigogine and Defay [46] and Davies and Jones [38,53] arrived at similar to Eqs. (14.27) and (14.28) relations for the description of the glass transition employing different methods. In the simplest version, the respective results can be obtained as follows: Assuming that at the glass transition the relations

$$\Delta V = V_{liquid} - V_{glass} = 0\,, \qquad \Delta S = S_{liquid} - S_{glass} = 0 \tag{14.29}$$

hold, immediately the relations

$$\frac{dT_g}{dp} = \frac{\Delta\beta}{\Delta\alpha}\,, \tag{14.30}$$

$$\frac{\Delta\beta}{\Delta\alpha} = TV\frac{\Delta\alpha}{\Delta C_p}\,, \tag{14.31}$$

$$\frac{1}{VT}\frac{\Delta\kappa\Delta C_p}{(\Delta\alpha)^2}\bigg|_{T=T_g} = 1 \tag{14.32}$$

are obtained, provided the system under consideration is described by one structural order parameter. Such relations and the corresponding value of the Prigogine-Defay ratio are widely discussed and employed later by different authors. Based on these results in addition the conclusion was drawn that glasses have to be described in general by more than one structural order parameters since in experiment usually

$$\Pi(T_g) > 1\,, \qquad \frac{dT_g}{dp} = TV\frac{\Delta\alpha}{\Delta C_p} < \frac{\Delta\beta}{\Delta\alpha} \tag{14.33}$$

is found (Goldstein [54]).

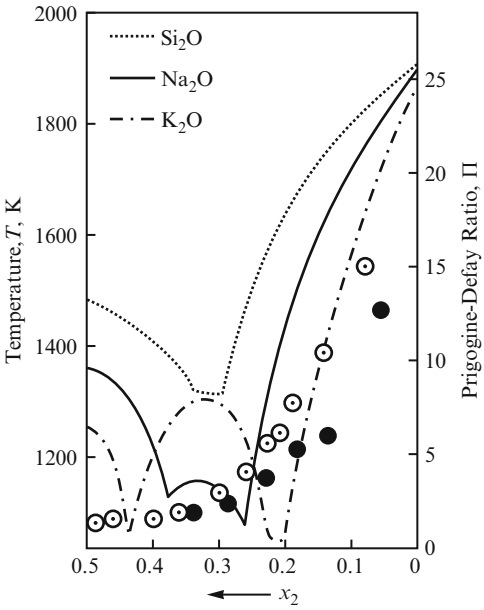

Fig. 14.5 Results of measurements of the Prigogine-Defay ratio on two alkali-silicate glasses with different compositions [55,56] (*circles* refer to $SiO_2 - Na_2O$; *full points* to $SiO_2 - K_2O$). The *full*, *dotted* and *dashed-dotted curves* represent the phase diagrams, x_2 is the content of the alkali component. Note that in agreement with Eq. (14.35) a decrease of Π is found with increasing entropy of melting

However, as elaborated by us in [1, 55] and later re-derived in more detail in [6,7,24], employing the method of Prigogine and Defay and utilizing one structural order parameter, the Prigogine-Defay ratio can be in a good approximation written as

$$\Pi(T_g) = \frac{h_{p,T}}{A + h_{p,T}} \left. \frac{\left[1 + \frac{1}{v_{p,T}} \left(\frac{\partial A}{\partial p}\right)_T\right]}{\left[1 - \frac{T}{A + h_{p,T}} \left(\frac{\partial A}{\partial T}\right)_p\right]} \right|_{T=T_g} \cong \left. \frac{h_{p,T}}{A + h_{p,T}} \right|_{T=T_g} . \tag{14.34}$$

Equation (14.34) holds for any given state of the system under consideration. As shown first in [55], in order to apply these relations to the interpretation of experimental results, the value of the affinity, A, for cooling has to be substituted into Eq. (14.34). Here the affinity has negative values. Consequently, if the glass transition is assumed to proceed in some temperature interval (and not at some discrete value of temperature, T_g, as assumed if Simon's model is employed), then the affinity at the glass transition is not equal to zero and $\Pi(T_g) > 1$ holds (for more details cf. also [6,7,24]). Since the state of the glass depends on cooling rate, also the Prigogine-Defay ratio depends, in general, not only on the properties of the system under consideration but also on cooling rate. An example for such dependence is shown in Fig. 14.4. Based on this approach, an approximate expression for the dependence of the value of the Prigogine-Defay ratio on composition can be

theoretically developed given

$$\Pi \propto \frac{30R}{\Delta S_m}\,, \tag{14.35}$$

where ΔS_m is the melting entropy. Experimental data in this respect are shown in Fig. 14.5 (for the details see [55]).

In a second alternative approach [24, 57], directly the experimentally measured values of the Prigogine-Defay ratio were determined by us theoretically avoiding the application of the concepts of affinity etc. by computing directly the differences of the thermodynamic coefficients of the liquid and the glass. It is shown for a model system that this approach also leads to values of the Prigogine-Defay ratio larger than one. In a third independent approach to the solution of this problem, it was shown in [40] how the glass transition temperature depends on pressure. The resulting relations are different from Eqs. (14.27) and only in limiting cases show some similarity. This approach gives in this way a third independent proof that the Prigogine-Defay ratio is not necessarily equal to one from a theoretical point of view even if only one structural order parameter is employed for the description as it was believed widely for several decades following the classical suggestions of Prigogine and Defay and Davies and Jones.

14.1.4 Kinetics of Vitrification at Variable Rates of Change of Control Parameters

The first task which was solved in analyzing the dependence of vitrification kinetics on the rates of change of the external control parameters was the analysis of the kinetics of formation of glasses with different properties when temperature, pressure or electric field strength are changed with a different rate. It was first performed in the framework of the already mentioned approximation of Simon by Gutzow in collaboration with A. Dobreva and C. Rüssel [4, 5, 58–60]. In Sect. 3.7 of this book, results are given in which it is seen how the frozen-in entropy, ΔS_g, the enthalpy, ΔH_g and the frozen-in free enthalpy, ΔG_g, of glasses are changed when vitrification is performed with different cooling rates: the analysis being, as mentioned, performed in the framework of Simon's approximation. Of considerable significance in the results thus obtained is the fan-like increase of the array of $\Delta G_g(T)$-curves, as it is depicted on Fig. 3.8 of the present book. It opens a new insight into widely unexplored so far possibilities of the application of glasses with increased thermodynamic potential which could be used in various technical applications. A detailed analysis of the geometry of this fan-like construction may be found in two publications by Gutzow et al. [61,62]. A survey of such possibilities thus opened in reaction kinetics, in galvanic batteries or even in the application to natural phenomena is given in a recent paper by Gutzow and Todorova [63].

In continuation of these first efforts by Gutzow, Dobreva, and Rüssel, a series of papers was published by the same authors [59, 60] in which the effect of change of pressure and electric field strength was investigated: leading to a change of glass transition temperature and thus also to a corresponding change of properties. In a recent publication [40] Schmelzer enlarged and generalized this task, calculating directly, via the above discussed kinetic approach, the effect of pressure on the glass transition temperature. In a further development, based upon the thermodynamic approach outlined in the referred publications of the present authors and employing an MFA lattice-hole model it was shown by Garden, Wondraczek et al. [64] that an appropriate variant of the generic phenomenological approach, developed here, is capable of representing, at least in a semi-quantitative manner, with sufficient accuracy the change of properties (especially the temperature induced change) of the configurational specific heats in a concrete example – an organic polymer glass-forming melt.

14.1.5 On the Dependence of the Properties of Glasses on Cooling and Heating Rates: Some Results of Numerical Computations

14.1.5.1 Structural Order Parameter

In recent analysis [6, 7, 37, 40, 41], the behavior of a variety of thermodynamic properties of glass-forming melts and glasses has been analyzed by one of the present authors (J.W.P.S.) in cooperation with T. Tropin and C. Schick in dependence on cooling and heating rates varying its absolute value in a wide range. This renewed interest is partly caused by the fact that such experiments are feasible, now, allowing one to analyzing glass-forming melts for cooling and heating rates in the range between 10^{-4} K/s up to 10^5 K/s [65, 66]. In this theoretical analysis, we concentrated the attention on the computation of several quantities which are of particular interest in a variety of applications and for the general understanding of the nature of the glass transition. In the computations, we employed Eqs. (14.1) and (14.4) latter one in a form as also used in [37].

In Fig. 14.6a, the $\xi = \xi(T)$-curves are shown in a wide range of rates of change of temperature. The temperature is given here as $\theta = T/T_m$ and the rate of change of temperature as

$$q_\theta = \frac{d}{dt}\left(\frac{T}{T_m}\right) = \frac{d\theta}{dt}\,, \qquad \theta = \frac{T}{T_m}\,. \tag{14.36}$$

As seen from the figure, with a decrease of the rate of change of temperature the cooling-heating hysteresis loops become less expressed and the process of glass transition approaches more and more the simplified model as suggested by Simon,

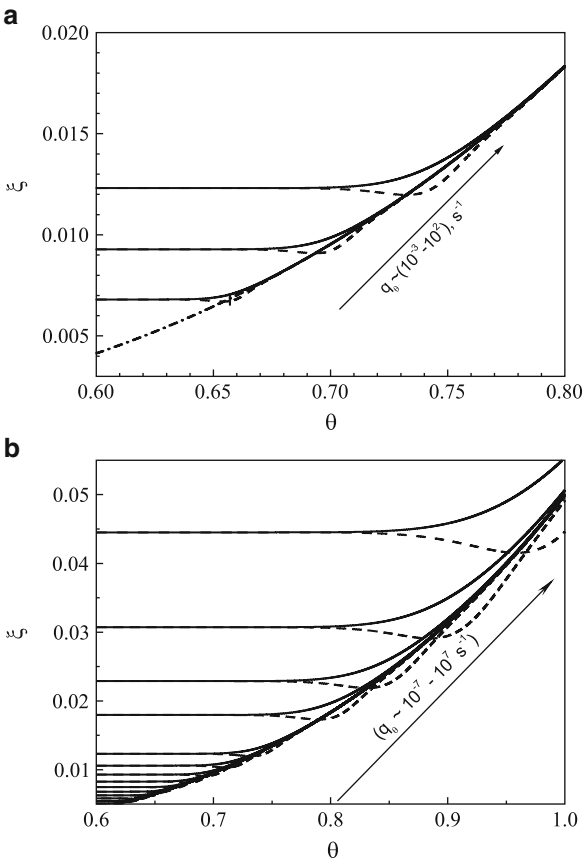

Fig. 14.6 Dependence of the structural order parameter $\xi = \xi(\theta)$ (with $\theta = (T/T_m)$) on cooling and heating rates defined by Eq. (14.36) (**a**) in the range $10^{-3}\text{s}^{-1} \leq q_\theta = (d\theta/dt) \leq 10^{2}\text{s}^{-1}$ (more or less easily accessible experimentally); (**b**) in the whole range of q_θ-values ($10^{-7}\text{s}^{-1} \leq q_\theta \leq 10^{8}\text{s}^{-1}$) exceeding partly the ranges of cooling and heating rates accessible, at least, at present, The *dashed curves* refer to cooling, the *full curves* to heating runs (q_θ is given here in s^{-1}, see also text and [6,7])

i.e., the system goes over to the glass suddenly at a certain temperature, T_g. Vice versa, with increasing rate of change of the control parameters the glass transition temperature and also the width of the glass transition region increases [41] and, as a consequence, also the difference between glass transition temperatures in heating and cooling as expected according to Eq. (14.11). Two questions arise in this respect: Will such kind of behavior continue also down to even lower values of cooling-heating rates which can be analyzed within reasonable computer times? What will be the behavior if we similarly further increase cooling and heating rates? Or to be more precise, provided we can reach such cooling rates that the characteristic times of relaxation and cooling are comparable already at or even above the melting temperature T_m, will there occur certain peculiarities or not?

The answers to these questions are illustrated in Fig. 14.6b. Here the results are shown for the $\xi(T)$-dependencies for the cooling and heating rates in the range of q_θ-values (in units of s^{-1}) given by $10^{-7} \leq q_\theta \leq 10^{8}$ and for reduced temperatures in the range $0.5 \leq \theta \leq 1.3$. It is obvious that the already mentioned tendency – approach of a behavior as reflected by the Simon model – is retained also for

the much larger range of cooling and heating rates in the limit of cooling and heating rates tending to zero. And, in the alternative limiting case of very high cooling and heating rates, the curves show no peculiarity when the glass transition temperature approaches the melting temperature, T_m, or even becomes larger than T_m. So, provided such very high rates of change of temperature could be reached, the transition to a glass proceeds in a qualitatively similar way independent on whether we go over to a glass from a metastable or a stable equilibrium state of the liquid.

14.1.5.2 Entropy Production and Frozen-In Entropy

Once the dependence of the structural order parameter on time and/or temperature is established, one can directly compute the structural contributions to the thermodynamic and kinetic parameters of the system, provided the general dependence of these properties on the structural order parameter is known. We will start the respective computations with the determination of the entropy production following the respective advice of Prigogine and Defay ([46], page xviii): *The fundamental problem of the thermodynamics of irreversible processes is the explicit evaluation of the entropy production*.

The hysteresis effects, shown in Fig. 14.6a and b, are deeply connected with entropy production in cooling and heating due to irreversible relaxation processes of the structural order parameter to the respective equilibrium value. This interrelation is illustrated in Fig. 14.7. Here the entropy production terms are shown, again, in dependence on the rate of cooling and heating processes. The curves are computed via Eq. (14.37) [24, 37]

$$\frac{d_i S}{d\theta} = \frac{G_e^{(2)}}{T_m \theta q_\theta \tau}(\xi - \xi_e)^2 \ . \tag{14.37}$$

Again, similar to the $\xi(T)$-curves, with increasing rates of change of temperature the effect of entropy production becomes more expressed reconfirming the theoretical prediction given by us in [24, 37]. From a general point of view, this effect can be interpreted as follows: With an increase of the rate of change of external parameters, the deviations from equilibrium, as a rule, become larger. As a result, the rate of entropy production becomes higher.

Having at one's disposal the dependencies of the structural order parameter on temperature for different cooling and heating rates, one can immediately reproduce the respective dependencies for the configurational entropy, S_{conf}/R. They coincide in its qualitative shape with the curves of the temperature dependence of the structural order parameter (cf. [24, 37] and Fig. 3.7a of the present monograph). For any given value of cooling and heating rate, a definite non-zero value of the configurational entropy is frozen-in, the respective value increases with increasing absolute value of the cooling rate. The dependence of this frozen-in value of entropy on cooling rates is shown in Fig. 14.8.

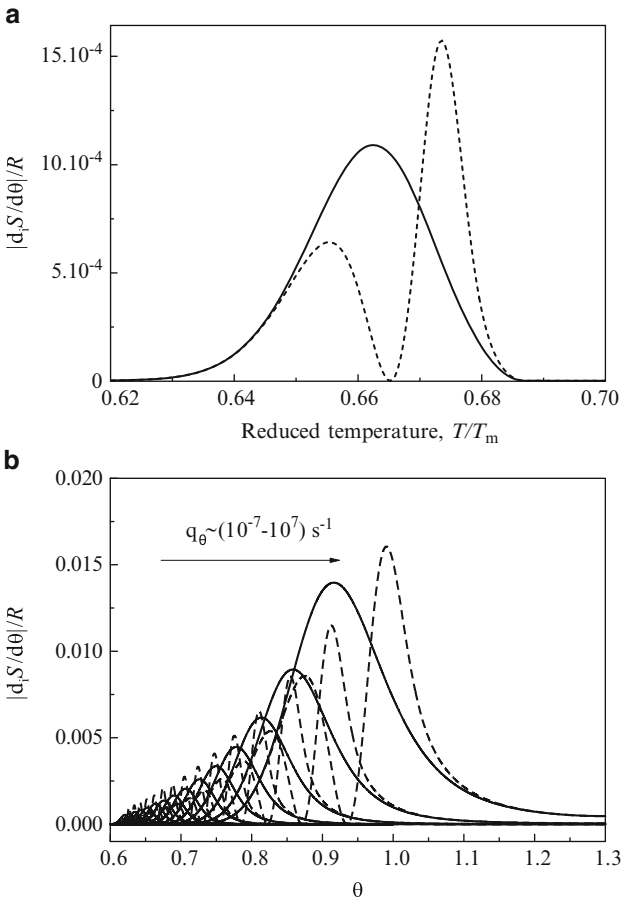

Fig. 14.7 Entropy production (Eq. (14.37)) in vitrification and devitrification in a cyclic cooling-heating run experiment [6, 7]. *Top*: the entropy production has one maximum for cooling (*full curve*) and two maxima in heating processes (*dashed curve*). *Bottom*: similar curves for different cooling and heating rates: the cooling and heating rates are changed in the range $10^{-7} \leq q_\theta \leq 10^{7}$ (q_θ is given here in s^{-1}, see also text). With an increase of the rate of change of temperature, the effect of entropy production increases

A comparison of the total entropy production in a cyclic cooling and heating experiment, being in the order of magnitude equal to

$$\frac{\Delta_i S}{R} \cong 10^{-4} - 10^{-5} , \tag{14.38}$$

with the configurational contributions, being in the order of magnitude equal to

$$\frac{S_{conf}}{R} \cong 10^{-2} , \tag{14.39}$$

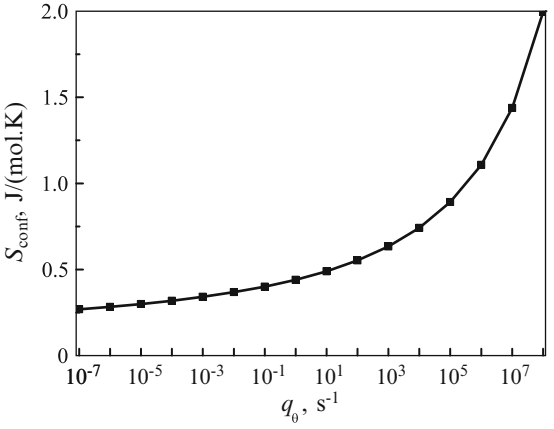

Fig. 14.8 Dependence of the frozen-in values of the configurational entropy, S_{conf}, of the given model system on cooling rates [6, 7]

shows that entropy production terms are negligible as compared with the configurational contributions to the entropy. This fact is established also by a more detailed thermodynamic analysis [24, 52] reconfirming previous qualitative predictions e.g. by Davies and Jones [38]. Davies and Jones noted as a result of their analysis of this problem: ... *we conclude that the neglect of the irreversible production of entropy leads to no significant error in determining the residual entropy* ... and, at another place, to glasses *the Nernst heat theorem is not applicable*. Consequently, the thermodynamic determination of the zero-point entropy of glasses – as discussed in detail in [1, 24] – leading to non-zero values at $T \rightarrow 0$ is fully correct. In general and as it follows also from the analysis of the model system employed here, while the metastable liquid fulfils the third law of thermodynamics in the formulation assigned commonly to Planck (cf. [24]), the frozen-in glass does not obey this formulation.

At another place in their papers, Davies and Jones especially analyzed the applicability of thermodynamics to glass transition. Accounting for that the effect of entropy production is small, they concluded that thermodynamics in its classical form is applicable to glass formation. Even more, as evident from the analysis performed here and outlined in previous sections, the results for the model system as derived here are obtained by non-equilibrium thermodynamic methods fully accounting for the non-equilibrium character of the glass transition. They give as well – and in contrast to alternative statements as summarized recently in [49] – an additional proof of the validity of the "conventional point of view" that glasses have a non-zero residual entropy depending on cooling rates. A detailed discussion of a variety of additional arguments in favor of this point of view can be found in [1, 24, 51, 52, 67, 68].

14.1.5.3 On the Value of the Viscosity at the Glass Transition Temperature

Gustav Tammann [3] connected in his well-known books the glass transition temperature with a value of the viscosity equal to 10^{13} Poise. However, having

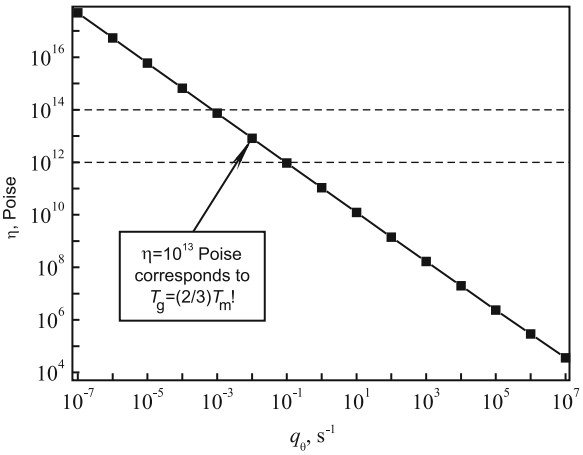

Fig. 14.9 Dependence of the viscosity at glass transition temperature on cooling rates. Since according to the Bartenev-Ritland equation (when the VFT-equation is employed for the description of the viscosity [1,6,7,24]), the ratio $(1/(T_g - T_0))$ is a linear function of the logarithm of the cooling rate, according to $\eta = \eta_0 \exp(U_a^*/(R(T - T_0)))$ a linear dependence of $\log \eta$ on $\log q_\theta$ has to be expected. This result is confirmed by the numerical computations [6,7]

in mind the dependence of the glass transition temperature on cooling rate as expressed, for example, by the Bartenev-Ritland equation, this identification cannot be general. For example, Mazurin [69] noted that "*the widespread opinion that the glass transition temperatures for glasses of any compositions are close to temperatures corresponding to viscosities of* 10^{13} *Poise does not hold true. However, the glass transition temperatures determined under conditions similar to the standard conditions for the majority of the glasses studied up to now correspond to temperatures at which the viscosities vary in the range from* 10^{12} *to* 10^{14} *Poise*". However, allowing the rate of change of temperature to vary in broad intervals, these limits can be widely enhanced. Indeed, performing the computations described here and identifying the viscosity at $T \cong (2/3)T_m$ with the conventionally assumed for T_g value equal to 10^{13} Poise, we can determine the viscosity at the glass transition temperature in dependence on cooling rate. The results are shown in Fig. 14.9. It is evident that, at least, in terms of the model analysis where the cooling rates may be changed in a very large interval the viscosity at T_g may considerably deviate from the standard value and by far exceed even the commonly found experimentally range as reported by Mazurin (10^{12} to 10^{14} Poise).

Finally, we have to mention that even such large cooling rates may be considered in the model system that the transition to a glass proceeds not from the metastable continuation of the equation of state of the liquid but directly by freezing-in the equilibrium liquid. It is interesting to note here that the possibility of glass transition above the normal melting or freezing point was realized already very early e.g. by Jones [70] with reference to experimental work performed by Smekal [71]. However, in some contradiction to such insight the viscosity at glass transition

was identified by them also [53, 70] – following Tammann [3] – to be equal to 10^{13} Poise. Jones [70] already stated as well that a melting temperature may even have no meaning since *many organic substances form glasses on cooling because no crystalline structure can form on account of the length or complicated nature of the molecules*, a situation, which is frequently found in polymer physics.

14.1.6 The Viscosity of Glass-Forming Systems Described in Terms of the Generic Phenomenological Approach: The Activated State Model of Viscous Flow

In Sects. 2.4 and 12.6 of our book [1] we have given an empirical description of several of the most popular approaches in describing viscosity. They are based on empirical models leading to a more or less convenient and sufficiently satisfactory description of the viscosity of glass-forming liquids and especially of its steep temperature dependence. Flow in glass-forming liquids is based on the frequency, ω, of density or structure fluctuations. According to basic assumption of statistical thermodynamics [27], this frequency is determined by the expression

$$\omega = \omega_0 \exp\left[\frac{\Delta S^*}{R}\right] . \tag{14.40}$$

Here ΔS^* indicates the entropy difference between two different states in the small volume of the system connected with the fluctuation via some known (or assumed) mechanism. For a sufficiently large system in thermodynamic equilibrium (provided also that T = const. and p = const. holds) in which the fluctuation is formed, the well known relation [27]

$$\Delta S^* = \left(-\frac{W_{\min}}{T}\right) = -\left(\frac{\Delta G^*(T)}{T}\right) \tag{14.41}$$

can be then employed, where W_{min} is the minimal thermodynamic work required to form (in our case) the flow determining fluctuation. With $\Delta G^*(T)$ is denoted (at p = const.) the corresponding Gibbs free potential difference.

The value of $\Delta G^*(T)$ in Eq. (14.41) can be calculated for any appropriate thermodynamic model system. In a very general formal way this can be done in the framework of the *Activated* (or *Transient) State Model* of the so called *Absolute Rate Theory* (see [72]). In some respect any of the existing molecular models of viscous flow can be derived (at least, in principle) as particular cases of this thermodynamic model, formulated many years ago as a general approach for the description of chemical reaction kinetics. It is due mostly to the efforts of Wigner, Eyring, Laidler and many other well-known scientists of the middle 1930/1940s. In applying this concept it is essential to note that according to the *Activated State Approach* it is assumed that there exists some non-specified activated molecular

configuration (the *Activated State Complex*), enabling the transport process. It is further on assumed that this complex has the properties of a thermodynamic system (i.e. that it is sufficiently large!) and exists for the time τ_0, also sufficiently large, so that thermodynamic equilibrium can be established. Then and only then, this imaginary activated complex could be characterized thermodynamically by the above written Gibbs free energy excess, $\Delta G^*(T)$.

From elementary considerations it is obvious that both above mentioned conditions can only approximately be fulfilled for the "activated" molecular complex, constituted of not more than several molecules in the liquid and existing, most probably, not longer than the time, elapsed between several eigen-frequency molecular oscillations ($\tau_0 \cong 10^{-12} \div 10^{-13}$ s). Nevertheless these two approximations (at least, implicitly assumed in fact also in any more or less elaborated "molecular viscosity models" based on the existence of fluctuations) seem somehow to describe sufficiently correctly the very essence of the decisive step of the process in both chemical reaction kinetics (where the *Activated State Approach* is usually applied in the form of the so called *Absolute Reaction Rate Theory*) and in self-diffusion and molecular flow in liquids. We employed the notions of the *Activated Complex Approach* in [23, 73, 74] mainly because of its disarming simplicity, demonstrating possible error sources, remaining hidden in more sophisticated molecular models and because of the easiness with which necessary estimates of changes in terms of both classical and non-equilibrium thermodynamics can be performed. This is the model we used in assessing especially the influence of non-equilibrium conditions: this we have done in terms of Prigogine's Taylor expansion of the activation energy, $U(T, \xi)$, as already discussed in connection with the derivation of Eq. (14.4) also in the present chapter.

Note that, in terms of the Eq. (14.4) and similar ones, formulated in our generic phenomenological approach, it is possible, together with constructing the course of change of thermodynamic functions, also to describe the change of $\tau(T, \xi)$ with temperature and deviation from equilibrium (e.g. [19]). Results in this respect we obtained in several of our recent investigations, as they are demonstrated here on Fig. 14.10. On this picture the peculiar delay in the change of the $\tau(T, \xi)$-curve with changing temperature is seen, the $\tau(T, \xi)$-course remains somehow "out of schedule" with the initial change of temperature: in this manner then follows, however, a peculiar "break-down" of the frozen-in non-equilibrium structure of the initial glass. This was a somewhat unexpected result on the influence of non-equilibrium on relaxation in typical heating-up regimes of glassy systems. It gives rise to several interesting phenomena when connected with crystallization in heating-up of glasses, as discussed in details in several of our respective publications [73].

Of particular interest here is the possibility of flare-up of density fluctuations in heating-up of an initially quenched glass, following from this $\tau(T, \xi)$ vs. time, t, regime: in heating-up a glass especially in an appropriate "optimal" heating regime and bringing-up the frozen – in system to higher temperatures. This flare-up of fluctuations causes optical turbidity effects observed years ago, mainly by the Russian glass structure school in St. Petersburg: by E. A. Porai-Koshits and his team of scientists. In our paper [73] an account of these fluctuation determined flare-up

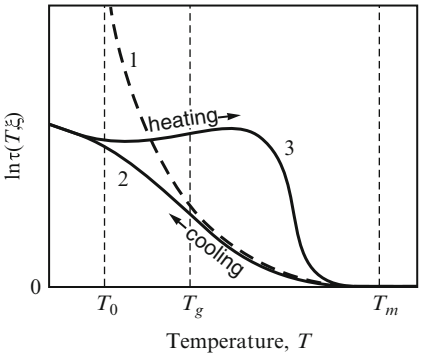

Fig. 14.10 Results of theoretical computations of the time of molecular relaxation, $\tau(T, \xi)$, on temperature: (*1*) temperature course of $\tau_e(T)$ determined employing a temperature dependence of the activation energy as in the Vogel-Fulcher-Tammann equation (i.e., $U(T) = \text{const}/(T - T_0)$); (*2*) normal cooling; (*3*) heating run [19, 73]

effects near T_g is given. In some respect they can be juxtaposed (or confronted!) with the classical flare-up of fluctuations in the vicinity of second-order phase transition temperatures, at $T \approx T_2$, as they have been theoretically analyzed e.g. by Landau and Ginzburg (see e.g. [27]). In both cases fluctuations are promoted because both at $T \to T_g$ and at $T \to T_2$, the non-equilibrium glass (in approaching T_g) or the system, undergoing a second-order phase transition (at T_2) become particularly and even catastrophically unstable. An interesting difference between these two cases of fluctuational flare-up is that, while in second-order phase transitions fluctuations are easily generated by approaching the temperature T_2 *from both sides* (i.e. both upon heating up or cooling down sequences), an "easy-fluctuation state" of the initially frozen-in system is achieved and experimentally observed only in heating-up experimentation.

Concluding the discussion of relaxation, we would like to note that accounting for the dependence of relaxation time on the structural order parameter, also a variety of relaxation laws can be described [24, 75] commonly treated in terms of several structural order parameters. Our approach predicts that, in addition to the exponential decay near to equilibrium, relaxation may be governed in intermediate stages by laws of the form $\xi(t) = (\xi^k(0) - (k/a_k)t)^{1/k}$. Such kind of relaxation behavior (with k = 2) was already distinguished by Kauzmann [76] and recently reconfirmed to dominate the dielectric α process in viscous organic liquids [77]. In addition, it allows one to understand the origin of stretched exponential type relaxation processes, it gives estimates of the coefficient β in agreement with experimental findings ($0.3 \leq \beta \leq 0.75$). Consequently, also from such considerations the possibility of an adequate description of glass-forming systems by employing only one structural order parameter gets an additional support. However, this statement does not mean that, in general, not more than one structural order parameters may be required to appropriately describe the system under consideration. In particular, an analysis performed in [78] shows that for the explanation of the dependence of

viscosity on pressure and temperature, the account of the dependence of viscosity on several structural order parameters is essential. However, as shown, this statement does not refer to the explanation of laws of the form $\xi(t) = (\xi^k(0) - (k/a_k)t)^{1/k}$ and of stretched exponential relaxation as shown in [24, 75] and discussed here. Such kind of relaxation behavior can be understood employing only one structural order parameter.

14.1.7 Thermodynamic and Kinetic Fragility of Glass-Forming Systems: Thermodynamic and Kinetic Structural Coefficients

Following a proposal by Angell [79–81] and the results of his attempts to connect glass dynamics and glass thermodynamics, as *fragile* are classified glass-forming systems in which the change of viscosity, $\eta(T)$ (or more, generally, the time of molecular relaxation, $\tau(T)$) with temperature, T, is steeply (non-Arrhenius-like) changing in approaching T_g (cf. Fig. 14.11). As *strong* on the contrary are classified glass-forming systems in which the temperature dependence, $\eta(T)$, in approaching $T = T_g$ remains nearly linear (in a logarithmic scale) as corresponding to the classical Arrhenius temperature dependence. In the German technical glass-science nomenclature of the 1930s, glasses with the respective above mentioned two types of temperature behavior were termed (maybe more appropriately!) as "long" and "short" glasses.

In order to introduce a measure to quantify the *kinetic fragility* (or steepness in the temperature course of the viscosity), the *dynamic* steepness index

$$m = \left.\frac{d\log_{10}[\tau(T)]}{T_g d\left(\frac{1}{T}\right)}\right|_{T=T_g} \tag{14.42}$$

is usually employed in recent literature. In the same sense, also the character of change of structurally determined thermodynamic properties (i.e. of the configurational entropy, $\Delta S(T) \cong S_{liq}(T) - S_{cryst}(T)$) can be described by the term *thermodynamical fragility*. For that purpose, we could use in a way analogous to above definition here the derivative

$$\left.\frac{d\Delta S(T)}{\Delta S_m d(T/T_m)}\right|_{T=T_m} = \frac{\Delta C_p(T_m)}{\Delta S_m} \tag{14.43}$$

to define a *thermodynamic* steepness index of fragility; either at melting temperature, T_m, or also, as above, at $T = T_g$. It can be and has been shown that both these indices are connected with (or better: through) the ratio

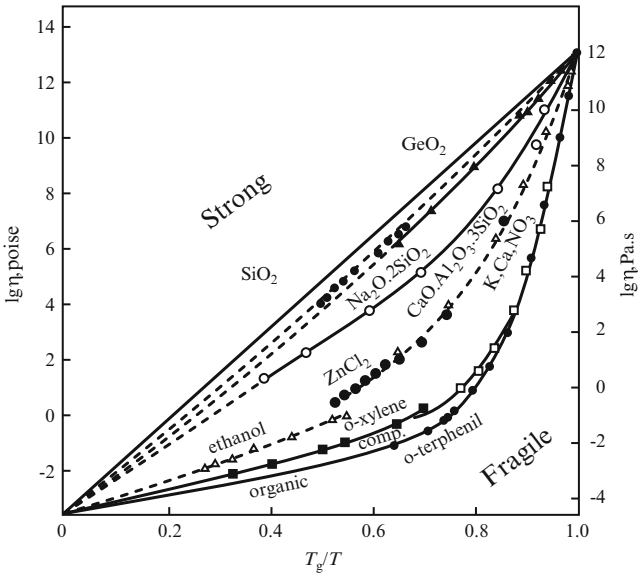

Fig. 14.11 Viscosity of several glass-forming melts in Angell's coordinates $\log \eta(T)$ vs. (T_g/T) [79–81]. Note the "strong"-type rheological behavior of SiO_2, GeO_2 and BeF_2 and the "fragile"-type change of the viscosity in systems with temperature dependent structures and activation energies of viscous flow, $U(T)$, depending on reduced temperature, T/T_g. It is, however, interesting to note [82] (Johari, 2010, personal communication) that similar coordinates have been employed much earlier and partly in a much more detailed description by Oldekop [83] and Laughlin and Uhlmann [84]

$$a_0 = \frac{\Delta C_p(T_m)}{\Delta S_m} \,. \tag{14.44}$$

Here, the difference $\Delta C_p(T) \approx C_p^{glass}(T) - C_p^{cryst}(T)$ (with the index *glass* referring to both glass *or* liquid) indicates the configurational specific heats of the system and ΔS_m is the respective melting entropy (cf. also Fig. 14.12).

The significance of this ratio in describing both the thermodynamics and the kinetics of glass-forming systems, as acknowledged by Angell and others (see e.g. [81]), was elaborated by one of the present authors many years ago (see Gutzow [86] and Gutzow and Dobreva [4, 5]). Its extraordinary significance follows from the following considerations:

- From a general point of view it is obvious that this ratio quantifies the change of the possible numbers of configurations or structural arrangements, $\Omega(T)$, of the system (e.g. via $S(T) \cong \mathrm{R} \ln \Omega(T)$) with the easiness, with which its temperature, T, is changed, when an amount of energy in form of heat, Q, is introduced into it (determined by the value of $C_p(T)$).

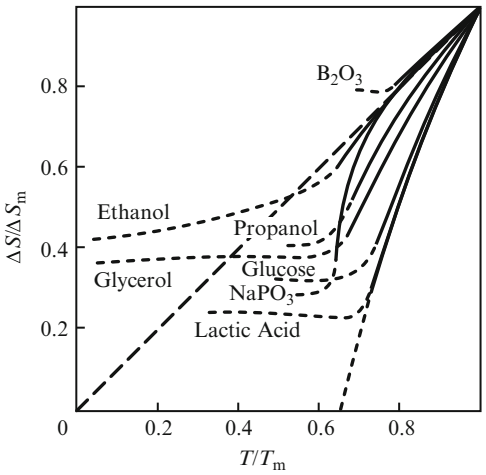

Fig. 14.12 Temperature dependence of the configurational entropy for several glass-forming substances, $\Delta S(T) = S_{liquid}(T) - S_{crystal}(T)$ and $\Delta S(T) = S_{glass}(T) - S_{crystal}(T)$ (for $T \leq T_g$), in Kauzmann's coordinates $(\Delta S(T)/\Delta S_m)$ vs. (T/T_m) [76]. Note the fan-like divergence in the temperature dependence, the similarity in the break-points near $T = T_g$ and the negative values of the extrapolated ΔS-values below T_0. Additionally, data for $NaPO_3$ are introduced into Kauzmann's diagram (according to the measurements of Grantscharova et al. [85]) in order to illustrate the "fragile" behavior of a typical inorganic glass-former

- Any structural or phase-transitional thermodynamic change in the glass-forming system is predestined by driving forces, governed (at $p = \text{const.}$) by the configurational part of the thermodynamic potential difference, $\Delta G(T)$, between liquid and crystal. As already discussed in Sect. 3.3, a Taylor expansion of $\Delta G(T)$ in the vicinity of T_m, truncated at the second term, can be written as

$$\Delta G(T) \cong T_m \Delta S_m \left[1 - \frac{\Delta C_p(T_m)}{2\Delta S_m}(1-\theta)\right](1-\theta)\,, \tag{14.45}$$

where

$$\theta = \left(\frac{T}{T_m}\right) \tag{14.46}$$

is the reduced with respect to T_m temperature. In deriving above dependence two well-known thermodynamic relations have been employed

$$\left(\frac{d\Delta G(T)}{dT}\right)_p = -\Delta S(T)\,, \qquad \left(\frac{d\Delta S(T)}{dT}\right)_p = \frac{\Delta C_p(T)}{T}\,. \tag{14.47}$$

As discussed in detail in Sect. 3.3 of the present monograph here and already in the first edition, all the known dependencies, governing the driving force for crystallization of under-cooled glass-forming melts, can be directly derived from Eq. (14.45) by assigning different values to the ratio

$$a_0 = \frac{\Delta C_p(T_m)}{\Delta S_m} \ . \tag{14.48}$$

The values of the parameter a_0 may vary according to experimental findings in the range

$$1 \leq a_0 \leq 2 \tag{14.49}$$

in dependence on the types of structures of the systems under consideration (see also Chap. 8 of our monograph [24]). As far as it can be assumed that in the temperature interval (T_0, T_m) (with $T_0 \leq T_g$) the approximation $a_0 =$ constant holds, the temperature dependence of the configurational part of the entropy of the under-cooled melt can be written with above equations as

$$\Delta S(T) = \Delta S_m \, (1 + a_0 \ln \theta) \ . \tag{14.50}$$

In this way with above dependence also the Kauzmann temperature $T_K = T_0$, defined by the condition $\Delta S(T) = 0$, is determined by the same parameter a_0 as

$$\theta_0 = \left(\frac{T_0}{T_m} \right) = \exp \left(-\frac{1}{a_0} \right) \ . \tag{14.51}$$

Consequently, the thermodynamic properties, the configurational structure, and even the crystallization of glass-forming melts are (in the framework of the adopted approximation) unambiguously determined by the value of the ratio a_0. By this reason, this parameter can be justly denoted as the thermodynamic structural factor. This conclusion is supported also by additional considerations as summarized below:

- In the framework of generalized versions of the *Activated State* model, expressions can be derived showing that again the ratio

$$a_0 = \left(\frac{\Delta C_p(T_m)}{\Delta S_m} \right) \ , \tag{14.52}$$

multiplied with the factor B^*, determines viscous flow, and more generally, the dynamic behavior of the system under consideration. The factor B^* depends on the complexity of the system (and especially on configurational factors like degree of association, polymerization and the like). The value and the frequency of the flow determining fluctuations are determined now according to Eqs. (14.40) and (14.41) by the thermodynamic potential difference

$$\Delta G^*(T) = G(T)_{activated\,state} - G(T)_{ground\,state} \ . \tag{14.53}$$

The activation energy of the flow process becomes dependent again on the ratio a_0 e.g. via

$$\frac{d\log_{10}\tau(T)}{d\left(\frac{1}{T}\right)} = \frac{d}{d\left(\frac{1}{T}\right)}\left(\frac{[G^*(T)_{act.\,state} - G_{cryst}(T)] - \Delta G(T)}{RT}\right) \tag{14.54}$$

and on appropriately truncated Taylor expansions of the Planck potential function difference $(\Delta G(T)/RT)$ written for different possible models, e.g. in terms of the VFT-viscosity function or as the Adam-Gibbs viscosity model. This latter mentioned case supplies us with a very instructive example of how a_0 has to enter the dependencies, governing the temperature dependence of viscosity of glass-forming liquids. Equation (14.54) can be easily derived in terms of the activated state model.

- It can be shown further-on, as we demonstrated recently [73, 74] that from above written dependence can be obtained (after appropriate transformations, at least, in an approximative form) as particular cases most of the viscosity formulas, discussed in Sect. 2.4.1, including the VFT-dependence and even the viscosity formula, referred to already in Sect. 12.6, the Adam-Gibbs formula (cf. also [685]). According to this relatively new and theoretically initially somewhat unexpected dependence the temperature course of viscosity or, more directly, of the time of molecular relaxation can be given as

$$\ln\tau(T) = \ln\tau_0 + \left(\frac{B^{\#}}{T\Delta S(T)}\right), \tag{14.55}$$

where $\Delta S(T)$ is the already discussed temperature dependence of the configurational entropy of the glass-forming melts. Taking the derivative employing Eq. (14.42) gives for the coefficient m, Angell's dynamic kinetic fragility coefficient, the desired connection with our thermodynamic structural factor, the ratio a_0, defined here in terms of above mentioned Adam-Gibbs dependence in the form

$$m = B^{\#}\left(\frac{1 + \frac{\Delta C_p(T)}{\Delta S(T)}}{\Delta S(T)}\right)_{T=T_g} \approx b_0(1 + 3a_0)\,. \tag{14.56}$$

In writing the right hand side of above dependence, we have used one of the invariants of glass transition (see [1, 24]) according to which

$$\Delta S(T_g) \cong (1/3)\Delta S_m \tag{14.57}$$

and have employed further the notation

$$b_0 = \left(\frac{3B^{\#}}{\Delta S_m}\right). \tag{14.58}$$

In this way, in analogy with previous results obtained by Gutzow and Dobreva [4, 5] we have connected the kinetic fragility factor, m, with the thermodynamic

structural ratio, a_0, introducing the coefficient b_0, which, according to its above introduced definition, depends in a reciprocal way (via ΔS_m) on the complexity of the melt considered: the entropy of melting of a more complex liquid has higher values.

In using one of above given dependencies (see [52]), for the value of $\Delta S(T)$ a somewhat more elaborated dependence, connecting m with a_0, can be written employing above derived formula, but accounting for the scatter of existing experimental data, we think that Eq. (14.58) can be used with sufficient accuracy. From above derivations it becomes evident that the right way to generalize Fig. 14.11 is to introduce there "θ" as a thermodynamic quantity indicating the temperature reduced with respect to the melting point "T_m" and not to "T_g" which is in fact a kinetic quantity depending on the conditions of vitrification.

14.2 Phase Formation Processes in Glass-Forming Systems

14.2.1 Generalized Gibbs' Approach to the Thermodynamics of Heterogeneous Systems and the Kinetics of First-Order Phase Transitions

14.2.1.1 Introduction

The description of nucleation in both its thermodynamic and kinetic aspects as it is outlined in detail in the present book follows widely the thermodynamic model of heterogeneous systems and of the process of nucleation as developed by J.W. Gibbs in his series of papers 1875–1878 [87]. This theory is the basis of classical nucleation theory as outlined in the book.

In addition, we had introduced into our book in 1995 a very substantial idea, new and still unproven at these times: the notion that phase transitions in glass-forming systems are substantially determined by non-steady state effects in their nucleation kinetics. This idea was developed in 1940s by the great Russian scientist Ya. B. Zel'dovich, as this is described in detail here in Chap. 6 and in a newer publication [88]. In this chapter is summarized also both theoretical expectation and experimental finding, the whole existing evidence, that the Zeldovich's model of non-steady-state kinetics of nucleation has to determine any process of phase transition in glasses, and to a great extent also the kinetic stability of under-cooled melts and glasses. In combination of transient effects with classical developments and notions in nucleation theory, already proposed or firmly accepted, the present authors succeeded in developing a new theoretical picture of the crystallization in glass-forming systems, which found its experimental verification in numerous experiments on both homogenous and heterogenous crystallization, many of them initiated and performed by one of the present authors and his colleagues at the

Institute of Physical Chemistry in Sofia, employing mainly simple model glasses as described in Chaps. 6 and 7 and additionally employed in later publications discussed below. Similar model glasses, both organic polymers and inorganic relatively low melting glasses like $NaPO_3$ were used also to model even technically important processes, the synthesis of glass-ceramics, the dissolution of glasses, and their rheological behavior. In this way a new theoretically well-founded development of the classical theory gave a possibility to develop new ideas, to ask, search and really bring experimental verification to a new development in phase transition and crystallization in glasses. This development was accepted and further expanded in several laboratories and by prominent representatives of the glass science community and even brought with it technical developments in different applications of new materials synthesis, in application of glasses, and even in extra-terrestrial experiments, as they are described below.

However, as already mentioned, according to Gibbs' theory, the bulk properties of new phase nuclei are widely identical to the macroscopic properties of the newly evolving bulk phase. Such an extrapolation allows one to arrive at simple and straightforward estimates of parameters determining nucleation but, as already indicated in the 1995 edition (see e.g. Sects. 6.2, 6.3.1, and 6.3.8), leads partly to great difficulties of a very general nature: it opens the discussion down to which dimensions, to complexes of how many building units can thermodynamic terms be applied and thermodynamic calculus performed. Where to place here the interphase layer, how to justify the assumption, that the properties of such nano-sized complexes can be described in terms of macroscopic phases and their extrapolated properties?

One way out of these difficulties was given by the so called atomistic model of nucleation, initially formulated by Walton and Rhodin (see Sect. 6.3.8 of the present book) and generalized further on by Stoyanov, Milchev, and Kaischew ([424], for a recent overview in application to electro-crystallization see [89]). The latter mentioned authors also clarified the general connections of the original Walton-Rhodin ad hoc formulated atomistic approach with the classical thermodynamic Gibbs model and the classical kinetic models of Volmer, Kaischew-Stranski, Becker-Döring, and Zeldovich describing the nucleation-growth course. There have been also proposed different variants of theoretical approaches to improve or generalize the initial model of Gibbs, introducing into it new features, bringing it nearer both to real experimental evidence and to newly developed theoretical concepts. At the same time authors of such approaches have to try to change the initial model in such an order as not to disturb the peculiar, but fine balance existing in the original picture, drawn by Gibbs, in which several obvious flaws seem to lead to a mutual compensation of the original in direction of an acceptable semi-quantitative first approximation of the thermodynamics of the nucleation process. Here we would like briefly to sketch a new approach to the description of heterogeneous systems – we denoted as generalized Gibbs approach – allowing one to retain the advantages of Gibbs theory but avoiding its shortcomings.

As already mentioned, in the interpretation of experimental results on the dynamics of first-order phase transitions starting from metastable (stable with

respect to small and unstable with respect to sufficiently large fluctuations exceeding some critical sizes, the so-called critical cluster sizes) initial states, up to now predominantly the classical nucleation theory is employed treating the respective processes in terms of cluster formation and growth [1, 90–103]. This theoretical approach is discussed in detail also in the present book. In the specification of the cluster properties, thermodynamic methods are intensively utilized based in the majority of cases on the thermodynamic description of heterogeneous systems developed by Gibbs [87]. As one additional simplifying assumption it is assumed hereby frequently that the bulk properties of the clusters are widely similar to the properties of the newly evolving macroscopic phases. This or similar assumptions, underlying the classical approach to the description of cluster formation and growth, are supported by the results of Gibbs' classical theory of heterogeneous systems applied to processes of critical cluster formation. Indeed, following Gibbs thermodynamic treatment one comes to the conclusion that the critical clusters have to have properties widely similar to the properties of the newly evolving macroscopic phases. Treating clusters of arbitrary sizes as small particles with bulk properties of the macroscopic phase, the process of cluster growth and dissolution is considered then to proceed basically via addition or emission of single units (atoms, molecules) retaining the bulk state of the clusters unchanged [90, 92, 97, 98].

As a second additional thermodynamic assumption employed widely in classical theory of nucleation and growth processes (the so-called capillarity approximation), the interfacial specific energy of critical clusters is supposed in a first approximation to be equal to the respective value for an equilibrium coexistence of both phases at planar interfaces. In order to come to an agreement between experimental and theoretical results on nucleation-growth processes, this second assumption often has to be released by introducing a curvature dependence of the surface tension (or a temperature dependence of the specific interfacial energy which is, from a theoretical point of view, widely equivalent). However, such an assumption leads to other internal contradictions in the theory which cannot be resolved remaining inside the concepts of Gibbs' thermodynamic treatment of cluster properties [87, 104, 105]. This way, Gibbs' classical treatment of surface phenomena is confronted with serious principal difficulties in application to nucleation. Gibbs employed in his approach a simplified but fully correct model considering the cluster as a homogeneous body divided from the otherwise homogeneous ambient phase by a sharp interface of zero thickness. The thermodynamic properties of the system under consideration are described in this approach by the contributions of the both homogeneous phases, known from classical thermodynamics, and correction terms connected with the existence of the interface. The main problem in such approach is then how correctly to determine these interface correction terms.

The alternative to Gibbs' model continuum's concept of a thermodynamic description of heterogeneous systems was originally developed by van der Waals [106]. It has been applied for the first time to an analysis of nucleation by Cahn and Hilliard [107, 108]. In application to nucleation-growth processes, Cahn and Hilliard came to the conclusion that the bulk state parameters of the critical clusters may deviate considerably from the respective values of the evolving

macroscopic phases and, consequently, from the predictions of Gibbs' theory. Such deviations occur, in particular, in the vicinity of the classical spinodal curve dividing thermodynamically metastable and thermodynamically unstable initial states of the systems under consideration. These results of the van der Waals' approach were reconfirmed later-on by more advanced density functional computations [109].

Moreover, Cahn and Hilliard developed also the alternative to the nucleation-growth model theoretical description of spinodal decomposition (see also [110]). According to the common believe (having again its origin in the classical analysis of Gibbs [87]), the nucleation-growth model works well for the description of phase formation starting from metastable initial states, while thermodynamically unstable states are believed to decay via spinodal decomposition. As one consequence, the problem arises how one kinetic mode of transition (nucleation-growth) goes over into the alternative one (spinodal decomposition) if the state of the ambient phase is changed continuously from metastable to unstable states, i.e., how the transition proceeds in the vicinity of the classical spinodal curve. The classical Gibbs' approach predicts here some kind of singular behavior, which is, however, not confirmed by the Cahn-Hilliard description, statistical-mechanical model analysis [111–113] and experiment [114]. From a more general point of view, we are confronted here with an internal contradiction in the predictions of two well-established theories which has to be, hopefully, and can be resolved as shown for the first time by the present authors [115, 116].

In a first approach to the resolution of these problems, we started our analysis with a generalization of Ostwald's *Rule of Stages* to nucleation. According to Ostwald's experience [117] in processes, where different macroscopic phases can be formed, as a rule not the thermodynamically most stable modifications but intermediate ones are formed initially. In Ostwald's words, "*... in the course of transformation of an unstable (or metastable) state into a stable one the system does not go directly to the most stable conformation (corresponding to the modification with the lowest free energy) but prefers to reach intermediate stages (corresponding to other possible metastable modifications) having the closest free energy difference to the initial state.*" Ostwald's rule of stages in his original formulation – as discussed above and in more detail in Sect. 9.5.5 of the present book – gives a selection rule for the sequence of formation of different stable or metastable phases. But – as we will see – in a generalized interpretation, it can also be quite useful for a theoretical understanding of processes of nucleation, when only one macroscopic phase can be formed in the system.

According to the classical Gibbs approach, the critical clusters of the newly evolving phase have essentially the same properties as the newly evolving macroscopic phases. Quantitatively, the properties are modified to some extent due to the higher pressure in the critical cluster (Young–Laplace equation), however, this effect is as a rule small. In the generalization both of Gibbs classical approach and of Ostwald's rule of stages, we abandoned this highly questionable assumption of the classical approach and replaced it by a prescription we denoted as the generalized Ostwald's rule of stages. This generalization of Ostwald's rule of stages we formulated as follows: *"In phase transformation processes, the structure*

and properties of the critical nucleus may differ qualitatively from the properties both of the ambient and the newly evolving macroscopic phases. Those classes of critical clusters determine the process of the transformation, which correspond to a minimum of the work of critical cluster formation (as compared with all other possible alternative structures and compositions, which may be formed at the given thermodynamic constraints)". By this approach, bulk parameters of the critical clusters are obtained which are in agreement with the van der Waals approach and more advanced density functional computations. However, the predictions of our approach are now in contrast to Gibbs classical approach.[1]

The resolution of above mentioned circle of problems was shown by us to be possible in the framework of a generalization of Gibbs' classical thermodynamic method developed by us in recent years. In this generalization, we were confronted with the serious problem that most people are fully convinced that Gibbs "is always right". As it seems, meanwhile we could overcome this resistance and the early observations and theoretical developments of W. Gerlach [121], E. Scheil [118], and G. Masing [122] and others give additional support to our strong believe in the necessity of generalizing Gibbs's classical approach.

[1]In discussing our approach at a conference in Cherkassy, Ukraine, in June 2012, organized by Andriy Gusak and coworkers, one of the participants (E. Rabkin, Haifa, Israel) noted that eventually similar ideas have been anticipated earlier by E. Scheil [118] and J. N. Hobstetter [119] in application to nucleation-growth processes in metal physics, where this approach is denoted as Scheil-Hobstetter model [120]. As it turned out this suggestion was fully correct. Indeed, Scheil started his paper of 1950 with the observation of W. Gerlach [121] that in segregation of nickel-gold particles from a solid solution as a rule particles are formed which do not have the equilibrium composition. He cited also the observation of G. Masing [122] in his book on metal physics that such effect – the difference of the composition of the clusters from the composition of the macroscopic phases – is not an exception but the rule in metal physics. Employing similarly to our analysis in [115] Becker's equation [123] for the description of the interfacial energy in dependence on composition, he demanded similarly to our approach that the critical cluster composition is, in general, different from the equilibrium composition of macroscopic samples and determined by the condition of the minimum of the work of critical cluster formation, i.e., he had really expressed the same idea as advanced by us 50 years later by us not being aware then of this earlier work. However, Scheil presumably did not recognize that this approach is in deep conflict to Gibbs classical theory which leads – if correctly employed – to different results. Consequently, in the analysis of Scheil the question remains unanswered how one can employ on one side Gibbs theory but replace one of the inherent consequences by a different assumption contradicting the conclusions of Gibbs' classical approach. By the way, as mentioned by Scheil as well, Becker, developing and employing the relation for the description of the surface tension in dependence on composition, employed in the analysis Gibbs' classical theory, i.e., identified the composition of the newly evolving critical clusters with the composition of the newly forming macroscopic phase. In addition, Scheil supposed that eventually the state of the critical cluster may refer to some metastable phase which under certain conditions may be formed macroscopically remaining in this way to some extent at the level of the classical Ostwald's rule of stages (but leaving open also the possibility that such metastable states may not exist). According to our treatment formulated in the generalized Ostwald's rule of stages, the composition of the critical clusters is from the very beginning supposed to refer to transient states (composition, density, structure etc.) having no macroscopic analogon.

In this task, while Gibbs' thermodynamic theory is restricted in its applicability to equilibrium states exclusively (by this reason, it is without the introduction of partly grave additional assumptions strictly not applicable to the description of clusters of sub- and supercritical sizes), the generalized Gibbs' approach is aimed from the very beginning at a description of thermodynamic non-equilibrium states consisting of clusters of arbitrary sizes and composition in the otherwise homogeneous ambient phase [124–128]. It was demonstrated by us that, by developing such generalization of Gibbs' thermodynamic approach, Gibbs' and van der Waals' methods of description of critical cluster formation in nucleation can be reconciled. The consequences with respect to the properties of the critical clusters are the same as in the case when the generalized Ostwald's rule of stages (minimization of the work of critical cluster formation) is employed, but they follow now directly as special cases from the thermodynamic theory. The generalized Gibbs' approach was shown to lead for model systems to qualitatively and partly even quantitatively similar results as compared with density functional approaches. In particular, it leads to a significant dependence of the bulk and surface properties of the critical clusters on supersaturation and – in contrast to the classical Gibbs' approach when the capillarity approximation is employed – to a vanishing of the work of critical cluster formation for initial states in the vicinity of the spinodal curve.

The generalized Gibbs' approach has also one additional advantage as compared with existing alternative approaches to the description of cluster formation. Similarly to the classical Gibbs' approach, the van der Waals' method as well as modern density functional analysis of the description of heterogeneous systems have the same common limitation: they are restricted in their applicability to thermodynamic equilibrium states exclusively. As a consequence, the mentioned theories can supply us with information on the properties of critical clusters, governing nucleation. However, they cannot supply us with any theoretically founded description of the properties of single clusters or ensembles of clusters (required for a description of their further evolution) being not in equilibrium with the ambient phase. By this reason, in order to describe the evolution of ensembles of clusters in first-order phase transitions, evolving either as the result of nucleation or of spinodal decomposition, additional assumptions have to be made concerning their properties and the evolution of their properties with the changes in cluster size and supersaturation in the system. However, as far as one remains inside the mentioned approaches, one has no theoretical tool to check the degree of validity of these assumptions.

As will be demonstrated here, the generalized Gibbs' approach supplies us – in addition to its advantages in the specification of the properties of critical clusters – with the basis for determining the change of the composition of the clusters in dependence on their sizes and supersaturation allowing us in this way a detailed description not only of nucleation but also of growth and dissolution processes [129–131]. In addition, a variety of additional general conclusions can be derived employing it for the interpretation of experimental results (cf. also [104, 105, 128, 129, 132–134]). In particular, it turns out that the classical picture of nucleation does not give, in general, a correct description of the initial stages of cluster formation and growth. In contrast, nucleation proceeds via a scenario

widely similar to spinodal decomposition. Vice versa, even in unstable initial states, not spinodal decomposition but ridge-crossing nucleation (in a generalized interpretation) may represent the basic mechanism of evolution of the new phase. The generalized Gibbs approach allows one also the understanding of some other typical features of spinodal decomposition. These and further consequences of the generalized Gibbs approach will be discussed in detail briefly below.

14.2.1.2 Thermodynamics and Nucleation Phenomena

In his fundamental papers [87], published first in the period of 1875–1878, J. W. Gibbs extended classical thermodynamics to the description of heterogeneous systems consisting of several macroscopic phases in thermodynamic equilibrium and gave first a theoretical interpretation of the physical origin of metastability and instability. As one of the applications, he analyzed thermodynamic aspects of nucleation phenomena and the dependence of the properties of critical clusters – aggregates being in unstable equilibrium with the otherwise homogeneous ambient phase (corresponding, in general, to saddle points of the appropriate thermodynamic potential) – on supersaturation. Such critical clusters have to be formed by fluctuations in nucleation processes in order to allow their subsequent deterministic growth to macroscopic sizes.

Regardless of existing impressive advances of computer simulation techniques and density functional computations [109,111,112], the method developed by Gibbs is predominantly employed till now in the theoretical interpretation of experimental data on nucleation phenomena. It is utilized either in order to estimate the so-called work of critical cluster formation, or, in cases when this quantity is determined by density functional computations or other methods, to determine the properties of the critical clusters employing Gibbs' model assumptions. Hereby it is often supposed that the properties of Gibbs' model clusters give a correct description of the real critical clusters evolving in the systems under consideration. The thermodynamic state parameters – size and composition – of the critical clusters (being of essential significance for the determination of the nucleation rate) are determined in Gibbs' classical approach via a subset of the well-known thermodynamic equilibrium conditions (equality of temperature and chemical potentials of the different components) identical to those obtained for the description of phase equilibria of macroscopic systems. Employing these relations, the bulk properties of the critical clusters turn out to be widely the same as those of the newly evolving macroscopic phases. However, the above mentioned result of Gibbs' theory is in contradiction to predictions of molecular dynamics and density functional computations of the respective parameters as demonstrated first by Cahn and Hilliard [107,108]. In such alternative approaches it is shown that the properties of critical clusters deviate, in general, considerably from the properties of the newly evolving macroscopic phases the deviations being particularly significant for large supersaturation, i.e., states in the vicinity of the classical spinodal curve. This way, the question arises what the origin of such discrepancies is and how they can be resolved eventually.

In order to arrive at a solution of this problem, we have to remember first that Gibbs restricted his analysis from the very beginning to "equilibrium states of heterogeneous substances" (the title of his analysis), exclusively. He never even posed the problem to determine thermodynamic potentials for heterogeneous systems in non-equilibrium states. In application to the analysis of phase equilibria of macroscopic systems, Gibbs' theory served so well that it is considered frequently as being equivalent to the basic laws of thermodynamics or even as being a consequence of them. Such point of view is not correct as can be traced easily following Gibbs' derivations. In addition, such interpretation contradicts Gibbs' own point of view considering his theory merely as one of the possible methods of description of heterogeneous systems but, of course, a good one. He wrote (cf. [135]): *Although my results were in a large measure such as had been previously obtained by other methods, yet, as I readily obtained those which were to me before unknown or vaguely known, I was confirmed in the suitableness of the method adopted*. Mentioned point of view about the equivalence of Gibbs' approach to the basic laws of thermodynamics is also in contrast to different attempts to modify or replace Gibbs' treatment as developed, for example, by Guggenheim, Prigogine, Defay et al. or Hill (cf. also [125–127, 129, 130, 136, 137]). However, these alternative approaches have their own limitations as mentioned partly by the authors themselves or as it became evident in their further discussion in the scientific community. In most cases, these and further alternative approaches (if correct) turned out to be widely equivalent in their consequences to the results of Gibbs' theory.

However, Gibbs' theory has – in application to the description of cluster formation – one grave limitation which has not been noticed or, at least, not further elaborated so far. Restricting the analysis to equilibrium states, Gibbs considers exclusively variations of the state of heterogeneous systems proceeding via sequences of equilibrium states. For such quasi-stationary reversible changes of the states of a heterogeneous system, Gibbs' theory leads to the consequence that the surface tension depends on the state parameters of one of the coexisting phases merely. This limitation is not restrictive with respect to the analysis of macroscopic equilibrium states and quasi-stationary processes proceeding in between them. For such cases, the properties of one of the phases are uniquely determined via the equilibrium conditions by the properties of the alternative coexisting phase. However, the situation is very different if Gibbs' theory is applied to the description of cluster nucleation and growth.

Critical clusters, determining the rate of nucleation processes, correspond to a saddle point of the appropriate thermodynamic potential. In order to search for saddle or other singular points of any potential surface, we have to know the values of the potential function first for any possible states of the system. In application to cluster formation and growth, we have to know also the thermodynamic functions of a cluster or an ensemble of clusters not being, in general, in equilibrium with the otherwise homogeneous ambient phase. Only having this information, we can search for singular points by well-established rules. Since Gibbs restricts his analysis from the very beginning to equilibrium states, his theory does not allow us – strictly speaking – to apply the common methods of search for saddle points.

And here we come to the basic limitation of Gibbs' theory in application to cluster formation and growth processes: In the search for the critical cluster we have to compare not different equilibrium states but different non-equilibrium states of the heterogeneous system under consideration. For the different non-equilibrium states considered, the surface tension has to depend, in general, on the state parameters of both coexisting phases. Gibbs' classical approach does not allow us, in principle, to account for such dependence and has to be generalized to open the possibility to incorporate this essential new ingredient into the thermodynamic description.

An extension of Gibbs' thermodynamic treatment of heterogeneous systems to include non-equilibrium states along the lines as discussed above was initiated by the authors of the present book [115,133] (by formulating the generalized Ostwald's rule of stages) and then further advanced into a comprehensive thermodynamic theory in cooperation with Vladimir G. Baidakov and Grey Sh. Boltachev (both Yekaterinburg, Russia [116, 124, 126–128, 138]), Alexander S. Abyzov (Kharkov, Ukraine) [130, 131, 133, 134, 139–142] and applied to the interpretation of nucleation-growth processes in glass-forming melts in cooperation with Vladimir M. Fokin and Edgar D. Zanotto [104, 105, 129, 143–145]. This – as we denote it – generalized Gibbs' approach employs Gibbs' model as well. However, Gibbs' fundamental equation for the superficial or surface quantities is generalized (extending previous approaches of one of the authors [146], assuming certain well-defined constraints to prevent irreversible flow processes) allowing one to introduce into the description the essential dependence of the surface state parameters (including the surface tension) on the bulk state parameters of both coexisting phases. Then the thermodynamic potentials for the respective non-equilibrium states are formulated. After this task is performed, the equilibrium conditions are derived. Similarly to Gibbs' classical theory, the critical cluster corresponds to a saddle point of the characteristic thermodynamic potential (a maximum with respect to variations of the cluster size at fixed intensive state parameters of both cluster and ambient phase and a minimum with respect to variations of the intensive bulk state parameters of the cluster).

The equilibrium conditions, derived via the generalized Gibbs' approach, coincide with Gibbs' expressions for the limiting case of phase coexistence at planar interfaces; they are, however, of a different form when applied to the determination of the properties of finite size critical clusters, the properties coincide with the parameters determined via the generalized Ostwald's rule of stages. These different equilibrium conditions lead, consequently, also to different results for the work of critical cluster formation as compared to the Gibbs' classical treatment. In the absolute majority of cases, the generalized Gibbs' approach leads to lower values of the work of critical cluster formation as compared with the classical treatment utilizing the capillarity approximation [128]. In more detail, in application to nucleation, the generalized Gibbs' approach leads to the following new set of equilibrium conditions for the determination of the properties of the critical clusters [127, 128],

$$\left(T_\alpha - T_\beta\right) s_\alpha + \left(p_\beta - p_\alpha\right) + \sigma \frac{dA}{dV_\alpha} + \sum_{j=1}^{k} \rho_{j\alpha} \left(\mu_{j\alpha} - \mu_{j\beta}\right) = 0 \,, \tag{14.59}$$

$$\left(\mu_{j\beta} - \mu_{j\alpha}\right) = \frac{3}{R} \left(\frac{\partial \sigma}{\partial \rho_{j\alpha}}\right)_{\{\rho_{i\beta}\}, T_\beta} \,, \tag{14.60}$$

$$\left(T_\beta - T_\alpha\right) = \frac{3}{R} \left(\frac{\partial \sigma}{\partial s_\alpha}\right)_{\{\rho_{i\beta}\}, T_\beta} \,. \tag{14.61}$$

Here T is the temperature, p the pressure, σ the surface tension, A the surface area, V the volume, s is the entropy density, ρ_i are the particle densities and μ_i the chemical potentials of the different components, R is the radius of the critical cluster referred to the surface of tension. The subscripts α specify the parameters of the cluster phase, while β denotes the state parameters of the ambient phase. In the limit of large critical cluster sizes or, alternatively, if one assumes that for given parameters of the ambient phase the surface tension is uniquely determined (as supposed in the classical Gibbs' approach [87]) then the conventional Gibbs' equilibrium conditions

$$\left(p_\beta - p_\alpha\right) + \sigma \frac{dA}{dV_\alpha} = 0 \,, \tag{14.62}$$

$$\left(\mu_{j\beta} - \mu_{j\alpha}\right) = 0 \,, \qquad \left(T_\beta - T_\alpha\right) = 0 \tag{14.63}$$

are obtained as special cases. The general expressions for the work of critical cluster formation, W_c, remain in the generalization of Gibbs' approach [127, 128] the same as in the classical Gibbs' method [87] of description of heterogeneous systems

$$W_c = \frac{1}{3} \sigma A \,, \tag{14.64}$$

provided in both approaches the surface of tension is chosen as the dividing surface. However, since the properties of the critical clusters are different as compared to the properties determined via the classical Gibbs approach, the respective values of the work of critical cluster formation are different. As already mentioned, the generalized Gibbs approach leads as a rule to higher values of the work of critical cluster formation as compared to the generalized Gibbs approach, in this way, the classical Gibbs approach allows us to determine an upper limit the real value of the work of critical cluster formation will not exceed as a rule.

Some examples of the resulting differences between the predictions of the classical and generalized Gibbs' approaches and their relation to density functional studies are given in Fig. 14.13. In Fig. 14.13, parameters of the critical clusters are shown in dependence on supersaturation (here, as an example, boiling in helium-nitrogen solutions is considered [126]). For the chosen temperature, the density $\rho_{liq} = 24.7\,\mathrm{kmol/m^3}$ corresponds to the binodal curve (representing the boundary between thermodynamically stable and metastable homogeneous states of

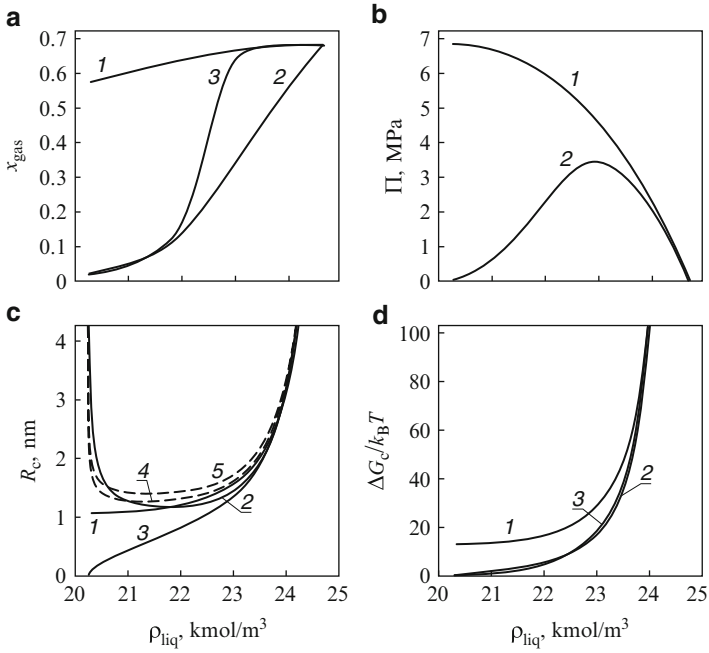

Fig. 14.13 Composition of the critical cluster x_{gas} (here a bubble of critical size), thermodynamic driving force of nucleation Π, the radius, R_c, of the critical cluster for different definitions of this parameter (*full curves* refer to the surface of tension while the *dashed curves* refer to the equimolecular dividing surfaces in Gibbs' classical approach) and the work of critical cluster formation, ΔG_c, for bubble formation in a binary liquid-gas solution [126] (see text)

the system), while the density $\rho_{liq} = 22.48\,\text{kmol/m}^3$ refers to the spinodal curve. In Fig. 14.13, x is the molar fraction of helium in the critical bubble, Π is a measure of the thermodynamic driving force of critical bubble formation, R_c is a well-defined measure (surface of tension (full curves) and equimolecular dividing surfaces for both components (dashed curves *4* and *5*, correspondingly)) of the size of the critical bubble, ΔG_c is the work of critical bubble formation. The dependencies, obtained via Gibbs' classical approach employing the capillarity approximation, are given by curves *1*, the results obtained via the generalised Gibbs' approach by curves *2* and the results of density-functional computations are given by curves *3* (for more details see [126]).

It is evident that the generalized Gibbs' approach leads to different values of the work of critical cluster formation as compared to the classical Gibbs' approach employing the capillarity approximation and – similarly to density functional computations – to vanishing values of the work of critical cluster formation for initial states near the spinodal curve. Note as well that, according to the generalized Gibbs' approach, the driving force of nucleation is not a monotonously increasing function of supersaturation. Moreover, the radius of the surface of tension in the

generalized Gibbs approach behaves similarly as the characteristic size parameters of the critical clusters obtained via density functional computations [107, 108]. It diverges for initial states both near to the binodal and spinodal curves. In the intermediate range of moderate supersaturation, where nucleation processes may occur, its size is of the same order of magnitude as the respective parameter obtained via Gibbs' classical method employing the capillarity approximation. Moreover, in this range of moderate supersaturation this size parameter varies only slightly. It turns out that, for moderate supersaturation where nucleation phenomena can be observed commonly, the size of the critical clusters is widely independent on supersaturation. Qualitatively similar results have been also obtained already for segregation processes in solid or liquid solutions [116] and condensation and boiling in one-component van der Waals' fluids [124].

The results of above given analysis show that the generalized Gibbs' approach allows us to describe the parameters of the critical clusters both in one- and multi-component systems in a way which is qualitatively in agreement with density functional computations. As compared to the latter ones, it has the advantage that only the thermodynamic properties of both bulk phases and the dependence of the surface tension on the state parameters of both coexisting phases for planar interfaces have to be known. Methods to determine such dependencies are discussed in [126–128].

14.2.1.3 Trajectories of Cluster Evolution

Since – in the classical Gibbs' approach – the bulk properties of the critical clusters turn out to be widely identical to the properties of the newly evolving macroscopic phases, one can assume then with some sound foundation that sub- and supercritical clusters have similar properties as well. This assumption is commonly employed so far in the theoretical description of growth and dissolution processes [93, 98, 147]. However, the above performed analysis – based on the generalized Gibbs' approach – leads to the consequence that clusters of critical sizes have properties which are different, in general, from the properties of the newly evolving macroscopic phases. By this reason, also the properties of sub- and supercritical clusters have to depend, as a rule, both on supersaturation and cluster size. In order to develop an appropriate description of the course of the phase transition, one has to establish, consequently, the dependence of the composition of arbitrarily sized clusters on mentioned parameters.

In order to solve this task, we proposed recently as a first approximation that the preferred path of cluster evolution is defined by some well-defined valley of the thermodynamic potential surface [129]. This proposal was then generalized to account in addition to thermodynamics also for the effect of the kinetics. In such more general approach, the preferred path of evolution is identified with the trajectory determined by the deterministic equations of cluster growth and dissolution starting with initial states slightly above and below the critical cluster size [129, 130]. In other words, we identify the deterministic trajectory with the

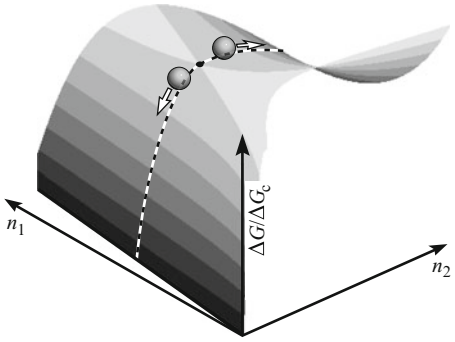

Fig. 14.14 Illustration of the method of determination of the preferred trajectory for cluster growth and dissolution processes. The trajectory is determined by the solution of the deterministic growth equations – representing generally the most probable course of evolution of a stochastic process – starting with initial states slightly above or below the critical point corresponding to the saddle point of the thermodynamic potential surface

most probable trajectory in the stochastic realization of the respective processes. The behavior of the system in the space of cluster variables resembles then in the simplest cases the motion of a body in a viscous fluid in some force field determined by the shape of the thermodynamic potential surface. This method of determination of the most probable evolution path is illustrated in Fig. 14.14. It is applicable regardless of the particular kind of phase transformation considered. In application to segregation in binary solutions, the change of the state of the clusters in dependence on their sizes (both for sub- and supercritical cluster sizes) is illustrated in Fig. 14.15 for a metastable initial state and different values of the ratio of the diffusion coefficients, D_1 and D_2, of both components (for details see [130, 131, 134]).

The change of the composition of the clusters in dependence on their sizes leads to a size-dependence of almost all thermodynamic (in particular, driving force of cluster growth and surface tension) and kinetic (diffusion coefficients and growth rates) parameters determining the dynamics of the phase transition [129, 130]. Some first results of an experimental analysis confirming these theoretical predictions are given in [87, 104, 129, 148, 149] (see also Fig. 14.16). Taking into account such size dependence, it can be also easily explained, in particular, why thermodynamic and kinetic parameters obtained from nucleation experiments may not be appropriate for the description of growth or dissolution and vice versa (cf. [150]).

14.2.1.4 Nucleation Versus Spinodal Decomposition

Following the analysis given above, we come to the conclusion that the kinetics of nucleation and growth in solutions exhibits features typical for spinodal decomposi-

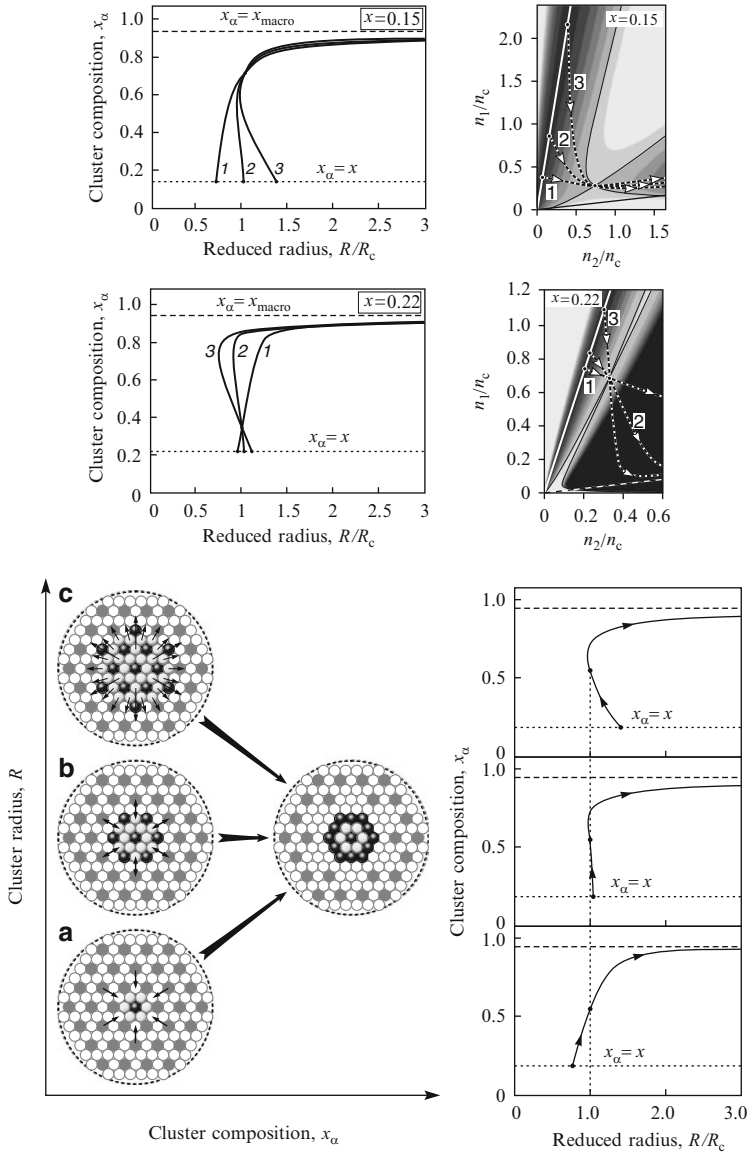

Fig. 14.15 Change of composition, x_α, of the cluster in dependence on its size in reduced units, R/R_c (*left*), and path of evolution in the space of particle numbers in the clusters, n_1 and n_2 (*right*), for metastable initial states. The state of the ambient phase is assumed to be unchanged by cluster formation processes and determined by the molar fraction, x, of one of the components of the solution. Here R_c and n_c are the radius (referred to the generalized surface of tension) and the total number of particles in the critical cluster. The computations are performed for segregation in a regular solution for different values of the ratio of the diffusion coefficients of both components: (*1*) $D_1/D_2 = 0.1$, (*2*) $D_1/D_2 = 1$, (*3*) $D_1/D_2 = 10$ (*upper part*). In the *lower part*, the mechanism of growth and the resulting dependencies of the concentration on cluster size are shown for the different possible cases [130, 131]

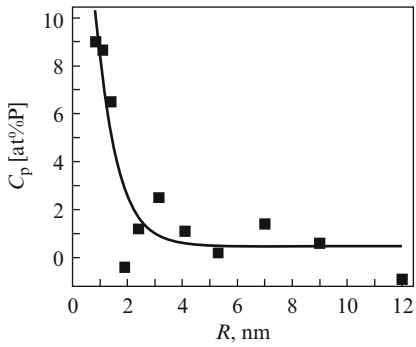

Fig. 14.16 Size-dependence of the cluster composition (C_p is here the content of phosphorus) for the case of primary crystallization of Ni(P) particles in a hypoeutectic Ni-P amorphous alloy as obtained via small-angle scattering of polarized neutrons as performed by Tatchev et al. [148, 149]

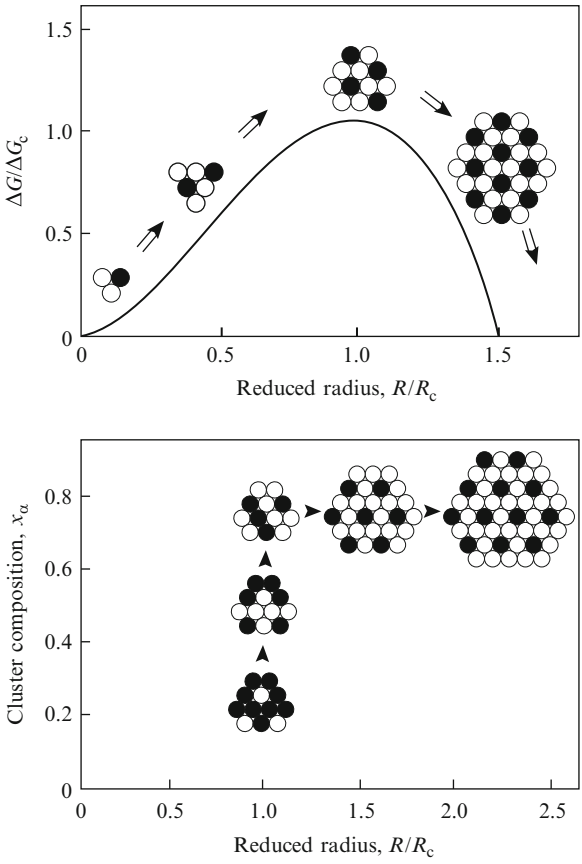

Fig. 14.17 Comparison of the classical model of phase separation in multi-component solutions (*top*) with the scenario as developed based on the generalized Gibbs' approach (*bottom*)

tion [129–131]. Indeed, according to the results illustrated in Fig. 14.15, nucleation proceeds as follows (cf. also Fig. 14.17): in a certain part of the ambient phase with a radius close to the critical one, the composition is changed until the properties of the newly evolving macroscopic phase are nearly reached. Only afterwards, the

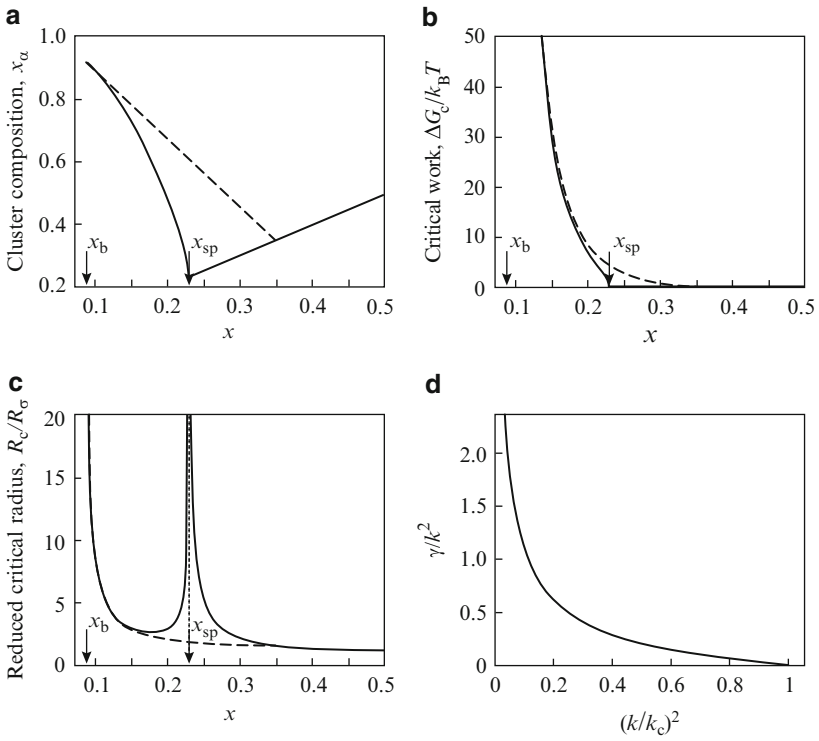

Fig. 14.18 Composition (**a**), work of formation (**b**) and size (**c**) of critical clusters obtained via the generalized Gibbs' approach (*full curves*) for segregation in solutions in a wider range of the initial supersaturation [130]. For the considered system and temperature, the *left side* value of the binodal curve corresponds to $x = 0.086$ while the respective branch of the spinodal curve is located at $x = 0.226$. By *dashed curves*, size, composition and work of formation of a particular ridge cluster are shown having the same size as the critical cluster (referred to the surface of tension) in Gibbs' original method employing the capillarity approximation. In Fig. 14.18d, the dependence of the rate of composition amplification on the wave number for $x = 0.4$ is shown [131]

classical picture – change in size of aggregates with nearly constant composition – reflects the situation correctly. The classical model does not supply us, consequently, with a correct description of nucleation. Note that this result is reconfirmed by statistical mechanical analysis of model systems [111,112] giving thus an additional confirmation of the validity of the generalized Gibbs' approach.

So far we have restricted the analysis to thermodynamically metastable states located between classical binodal and spinodal curves. The generalized Gibbs' approach allows us to get also some insight into the kinetics of phase formation processes in solutions starting from thermodynamically unstable initial states. Indeed, in Fig. 14.18 the composition and the size of the critical clusters are shown for a broader range of initial supersaturation including both metastable and unstable initial states. For initial states in the unstable region, the generalized Gibbs approach

predicts (full curves on Fig. 14.18a–c): (a) values of the composition of the critical cluster equal to the composition of the ambient phase; (b) a value of the work of critical cluster formation equal to zero; (c) a dependence of the critical cluster size on supersaturation similar to the characteristic sizes of the spatial regions of highest composition amplification [130] as obtained in the classical Cahn-Hilliard theory of spinodal decomposition [107, 108]; and (d) a dependence of the rate of composition amplification on the wave number similar to the growth increment as derived in the classical Cahn-Hilliard theory of spinodal decomposition [131]. This way, the generalized Gibbs approach allows us to assign a definite meaning – in terms of critical cluster parameters – to some of the well-known features of spinodal decomposition.

Summarizing the results, we conclude that nucleation and spinodal decomposition are not qualitatively different but very similar in their nature modes of first-order phase transitions. The only qualitative difference consists in the existence (for nucleation) or absence (for spinodal decomposition) of an activation barrier for the evolution to the new phase.

14.2.1.5 Saddle Point Versus Ridge Crossing

Another important question is whether the system will always select the thermodynamically favored evolution path through the saddle-point of the landscape of the thermodynamic potential or pass via the ridge of the potential well (cf. Fig. 14.14). As demonstrated, for example, in Fig. 14.18a–c by full curves, for states in the vicinity of the classical spinodal curve, saddle-point crossing requires the formation of very large in size aggregates. Although being favorable from an energetic point of view, such path a of transition is unfavorable by kinetic reasons and alternative trajectories of evolution gain in importance. Indeed, as shown in Fig. 14.18a–c with dashed curves [130], in the vicinity of the spinodal curve both for metastable and unstable initial states ridge crossing is a possible path of evolution to the new phase with relatively low values of the activation energy and characteristic sizes of the ridge clusters comparable in size to the critical clusters as determined via Gibbs' classical approach employing the capillarity approximation. Consequently, ridge-crossing nucleation (overcoming a finite potential barrier) may be the dominating mechanism of formation of viable units of the newly evolving phase not only for metastable but also for unstable initial states in the vicinity of the spinodal curve. Provided the system follows such ridge crossing channels of evolution to the new phase, no peculiarities have to be expected in the kinetics of the transformation in the vicinity of the spinodal curve as it is exemplified also both by computer simulations of model systems [111, 112], by numerical computations [139] and by direct experimental analysis [114].

14.2.1.6 Conclusions

In the present chapter we have outlined several deep controversies, connected with the very essence of Gibbs's thermodynamic theory underlying the classical nucleation theory. Here are also summarized ideas and ways, which give possibilities to overcome these difficulties. New, and as we hope, fruitful new notions in it can and have to be introduced into nucleation theory in general, and especially in its applications to vapor condensation, to phase transitions in thermodynamically unstable systems, or at conditions of heterogenous nucleation, when the new-phase embryo has degenerated to one or two building units only. This latter mentioned case is of significance in the crystallization of glass-forming systems, of course, with not as dramatic consequences as in other cases of phase formation, but nevertheless, as discussed in Sect. 6.3.8 of the present book: it is also of great significance in treating catalyzed nucleation of glass-forming melts. And there is also another question: how to apply nucleation theory, developed for more or less idealized models, to experiments, performed with and in the complicated structures of polymer melts, of multi-component solutions, in the difficult structures of ionic or metallic glasses. Are we here always on the right track with the most correct theoretical model? These problems are partly still open to discussion, and they are in some respect more difficult in comparing theory and experiment than in considering glass transition and thermodynamics of frozen-in states: the thermodynamics of non-equilibrium, especially in its present-day development in terms of even the linear formulations of the thermodynamics of irreversible processes seems to give a sufficiently sound fundament for both theory and experiment in application to glass-forming systems. In some respects, Simon's approximation in glass thermodynamics and the developments, we and our colleagues had to perform, to overcome and to go beyond it, are in many respects an easier task, than the difficulties, the problems and the wide horizons, connected with the nucleation model that J. W. Gibbs, one of the greatest scientists of the nineteenth century, has given us with his remarkable approximations. There, in nucleation theory, it seems is still more urban land remaining, and maybe there are more fields to be ploughed: there is also a higher theoretical and experimental yield to be expected if the ground is thoroughly upturned!

As it is evident from the outlined analysis, the correct account of changes of thermodynamic bulk state parameters of the clusters evolving in nucleation-growth processes in dependence on size and state of the ambient phase are, as a rule, of outstanding significance for the correct determination, in particular, of the value of the work of critical cluster formation in the expression for the steady-state nucleation rates. Classical theory of nucleation and growth ignores widely such effects. It follows as a consequence that the commonly employed equations for the determination of the thermodynamic driving force for nucleation-growth processes, Eqs. (6.62)–(6.65), represent – not accounting for deviation of the cluster bulk properties from the values of the respective macroscopic phases – an approximation, which may be or may be not fulfilled. This neglect leads generally to a significant overestimation of the work of critical cluster formation and an underestimation of

the steady-state nucleation rates and to deviations between theory and experiment in the description of nucleation and of growth and dissolution processes of the clusters. The effect of variation of cluster properties in their evolution can be treated consistently in the framework of the generalized Gibbs approach giving a new generally applicable tool for the treatment of nucleation-growth processes and the theoretical interpretation of experimental results retaining the advantages of the classical approach and avoiding its shortcomings.

Of course, in order to proceed in this direction one has to have at one's disposal the knowledge about the thermodynamic bulk properties of the respective phases in dependence on the state parameters and the surface properties for planar interfaces. However, even without such detailed knowledge one can interpret also in the generalized Gibbs's approach qualitatively a variety of effects in nucleation starting with the classical relation for the work of critical cluster formation, $W_c = (1/3)\sigma A$. This expression is shown to be of the same form both in the classical and the generalized Gibbs's approaches. Moreover, beyond the near vicinity of a spinodal curve the critical cluster sizes obtained via the classical and generalized Gibbs's approaches do not differ significantly. By this reason, in order to interpret nucleation data, one can further use, as a good approximation, the commonly employed expression

$$W_c \cong \Omega \frac{\sigma^3}{(\rho \Delta\mu)^2} \Phi \ , \tag{14.65}$$

Ω being a numerical shape factor. Effects of heterogeneous nucleation cores (via the specification of the parameter Φ) and nucleation catalysis by dopants via changes of the surface energy (see Chap. 7) can be treated similarly as in the classical theory. However, in the analysis one has also to take into account that the driving force for critical cluster formation may be different as compared with the macroscopic value. Consequently, the generalized Gibbs's approach – allowing one to incorporate into the description of nucleation-growth processes changes of the cluster properties with their sizes – opens a new perspective in the interpretation of these phenomena retaining on the other side the advantages of the classical approach. Such approach can be of considerable use in applications in the sketched above highly complex systems.

The fascination of a growing science lies in the work of the pioneers at the very borderland of the unknown, but to reach this frontier one must pass over well-traveled roads; of these one of the safest and surest is the broad highway of thermodynamics. These words, written about a century ago by Lewis and Randall in their well-known book on chemical thermodynamics [151], retain their validity till now. Nonetheless, even the highway of thermodynamics is shown here to be in need of improvement when applied to the description of processes of self-structuring of matter at nanoscale dimensions. Performing these corrections, the generalized Gibbs' approach leads, in addition to the already discussed conclusions, to a variety of further new insights into the course of first-order phase transformations and to the interpretation of experimental data which have not found a satisfactory solution so far. It allows us, for example, a new interpretation of the problem of existence or non-existence of metastable phases in crystallization of different

glass-forming melts – considering them not as metastable but as transient phases of cluster evolution – and the formation of bimodal cluster size distributions for intermediate stages of segregation processes in solutions (cf. [129]). Moreover, a detailed analysis allows us to suggest that the temperature of the critical clusters is, in general, different from the temperature of the ambient phase [125–128, 138, 152]. In addition, the generalized Gibbs' approach supplies us with a sound basis for the description of cluster growth and dissolution processes.

This way, we believe that the further development of the generalized Gibbs' approach may serve in future – combining the simplicity of the classical Gibbs' approach in nucleation with the accuracy of density functional approaches and computer simulation methods – as a quite powerful new and generally applicable tool in order to resolve problems in the comparison of experimental results on processes of self-structuring of matter.

14.2.2 Some Comments on the Skapski-Turnbull Rule

The estimation of the value of the specific surface energy is a major problem in the application of nucleation theory to crystallization in glass-forming melts both in the classical and generalized Gibbs's approaches. By this reason, we discuss the Skapski-Turnbull rule giving a widely employed tool for the determination of the specific surface energy here in somewhat more detail.

The origin of the Skapski-Turnbull relation and the values of the parameter ζ ($\zeta = 0.4 - 0.6$) in Eq. (6.127) in the present book as observed experimentally can be understood as follows: Let us denote by n_1 the number of particles on the surface of a cluster consisting of $n = N_A$ (N_A is Avogadro's number) particles. The volume, V, of the cluster and its surface area, A, is equal to $V = (4\pi/3)R^3$ and $A = 4\pi R^2$, where R is the radius of the cluster. If we denote by v_1 and r_1 the volume and the radius of one particle, respectively, then we can write similarly for the volume, v_1, and the surface area, a_1, occupied by one particle $v_1 = (4\pi/3)r_1^3$ and $a_1 = 4\pi r_1^2$. The number of particles in the cluster is given then via $n = (V/v_1) = (4\pi/3)(R^3/v_1)$ while the number of particles on the surface of the cluster, n_1, is determined by

$$n_1 = k\frac{4\pi R^2}{4\pi r_1^2} = k\left(\frac{R}{r_1}\right)^2 = k\left(\frac{\frac{3}{4\pi}(nv_1)}{\frac{3}{4\pi}v_1}\right)^{2/3} = n^{2/3}k\ . \tag{14.66}$$

Here k is the thickness of the surface layer (that is number of monolayers which determines the thickness of the surface layer (cf. also [153, 154]))

Now, we make the basic assumption (which may be denoted as Stefan's rule [155] who first formulated such an idea) that the specific surface energy, σ, is proportional to the enthalpy required to remove a part of the surface layer divided

by the surface area, i.e.,

$$\sigma \propto \frac{n_1 q_1}{A} = \frac{n_1 q_1 N_A}{A N_A} = \frac{n^{2/3} k q_m}{N_A 4\pi \left(\frac{3n}{4\pi}\frac{v_m}{N_A}\right)^{2/3}} = k(36\pi)^{-1/3}\frac{q_m}{N_A^{1/3} v_m^{2/3}} , \quad (14.67)$$

where q_m is the molar heat of melting and v_m is the molar volume, i.e., $q_m = q_1 N_A$ and $v_m = v_1 N_A$ and q_1 being the latent heat of melting per particle. As the result we get the Skapski-Turnbull rule in the form

$$\sigma = \zeta \frac{q_m}{N_A^{1/3} v_m^{2/3}} , \qquad \zeta = k(36\pi)^{-1/3} = 0.4 - 0.6 \qquad \text{for} \qquad k = 2 - 3 . \quad (14.68)$$

In this way, the Skapski-Turnbull relation is obtained and immediately also some tentative explanation of the values of the parameter $\zeta = 0.4 - 0.6$ as found from experiment is given.

Note, however, that Skripov and Faizullin [100] showed for 25 different liquids that the surface tension liquid-vapor, σ_{LV}, can be nearly perfectly described via the dependence

$$\sigma_{LV} \cong A \left(\frac{\Delta H_{LV}}{V_L}\right)^m , \qquad m = 2.15 , \quad (14.69)$$

where ΔH_{LV} is the change of the enthalpy, when the volume V_L of the liquid is transferred into the gas phase. The parameter A can be expressed hereby via the respective parameters for an appropriately chosen reference state. Although Eq. (14.69) refers to liquid-vapor coexistence, it nevertheless shows that the linear proportionality of the specific interfacial energy and the enthalpy of transformation is eventually not as obvious as widely assumed and a further detailed investigation may be of importance.

Note as well that σ in Eq. (6.127) has to be identified originally with the value of the specific interfacial energy at the melting point. It can be and has eventually to be modified accounting for a possible temperature dependence of this quantity, for example, according to Eq. (6.125). Latter relation predicts a decrease of the specific surface energy with increasing temperature similar to liquid-vapor coexistence. However, fitting the nucleation rate data by assigning appropriate values to the specific interfacial energy, a $\sigma(T)$-dependence is found exhibiting a slight increase of the specific interfacial energy. Fokin and Zanotto [156] tried to reconcile this result with relations like Eq. (6.125), leading to an opposite conclusion, by accounting for a size-dependence of the specific interfacial energy. As stated by these authors in the abstract of their paper, *the fitted $\sigma(T)$-dependence arises from two different factors: the temperature dependence of $\sigma(T)$ for a planar interface (σ_∞) and its size dependence. This paper focuses on the temperature dependence of the macroscopic value of surface energy, decoupling it from the size dependent part. Tolman's equation was used to eliminate the size dependence of surface energy from published nucleation data for two stoichiometric silicate glasses (*$Li_2O \cdot 2SiO_2$

and $Na_2O \cdot 2CaO \cdot 3SiO_2$*). It is shown that the Tolman parameter may be chosen so that surface tension decreases with temperature;* $(d\sigma_\infty/dT) < 0$. *The value of* $(d\sigma_\infty/dT)$ *obtained in this way is close to theoretical predictions*. In an alternative analysis, in their cited here already monograph, Skripov and Faizullin [100] gave examples of both an increase and a decrease of the specific interfacial energy melt-crystal for different substances. In a recent study, based on molecular dynamics investigations of crystal nucleation in Lennard-Jones liquids, V. G. Baidakov [157] and coworkers found an increase of the specific surface energy of a planar interface with increasing temperature while curvature corrections are found in this analysis to be of minor significance. Consequently, also in this respect, a further detailed investigation is expected to be of significant importance.[2]

14.2.3 Cluster Growth and Coarsening in Segregation Processes, Crystallization of Glasses and Elastic Stresses

Continuing the analysis of the effect of elastic stress on phase formation processes, in general, of segregation in multi-component solid solutions and crystallization processes, in particular, as reviewed in Chaps. 7 and 9 of the present book, some further investigations in this respect have been performed. They are reflected in [158–178]. The following problems have been treated:

- Elastic stresses in surface crystallization of glasses, in particular, in phase transformations at spike tips [158]: In this analysis, the elastic energy, evolving in the crystallization of the tip of a spike located at a planar interface of a solid, is determined by finite element method calculations. The energy per volume of the newly evolving phase is shown to depend significantly on the geometry of the spike. In agreement with expectations expressed earlier, it tends to zero for thin needles. The results give additional support to the theoretical concept that differences in the degree of evolution of elastic stesses in crystallization in the bulk and near interfaces may be the origin for the preferential surface crystallization of solids in general, and glasses as a special case (cf. Chap. 7). In particular, the results explain why sharp comers, edges etc. on the surface of the glass may act as catalysts for crystallization but not all of them are indeed active.
- Elastic stress effects on critical cluster shapes [159]: In this analysis, the shape and size of clusters of the newly evolving phase are determined which correspond to the minimal work of cluster formation in nucleation. Both elastic field and surface energy terms are taken into consideration. This work is not restricted to the consideration of spherical interfaces in between cluster and ambient solid

[2]This section has benefitted highly from discussions with Alexander S. Abyzov which are gratefully acknowledged.

phase but allows the consideration of the more general case of arbitrary shapes of the new phase. In application to crystallization of glass-forming melts it gives additional support to the idea that differences in the degree of evolution of elastic stresses in crystallization in the bulk and near external or internal surfaces of highly viscous glass-forming melts in the vicinity of the temperature of vitrification T_g may be the origin for the preferential surface crystallization of glasses extending the results as given here in Chap. 7.

- Specification of the optimum growth shapes of clusters near planar interfaces [160]: The results on the optimal shape of critical clusters accounting for both surface and elastic energy terms are extended here – employing the same model assumptions – to the determination of the shapes of sub- and super-critical clusters forming as the result of nucleation and subsequent growth. The optimum shape of the newly evolving phase is again determined by the requirement that the work of cluster formation for a given volume of the cluster has to be minimal. It is shown that for homogeneous and isotropic solids the optimum growth shapes of sufficiently large aggregates of the newly evolving solid phase are hemispheres due to the dominance for macroscopic samples of elastic energy as compared to surface energy terms.
- Effect of elastic stresses and external pressure on Ostwald's Rule of Stages [161]: The effect of elastic stresses on the applicability of Ostwald's rule of stages in solid to solid phase transformation processes (recrystallization) is analyzed in this paper based on the classical Stranski-Totomanov kinetic interpretation of this rule. It is shown that elastic strains favor a sequence of formation of different solid phases characterized by a gradual decrease of the density of the solid modifications developing subsequently. However, if a sufficiently large external hydrostatic pressure is applied onto the system, then, as shown as well, the kinetic interpretation of Ostwald's rule of stages leads to the conclusion that, in accordance with the principle of Le Chatelier-Braun, such a tendency may be reversed and, on the contrary, phases with higher values of the differences in the molar volumes develop preferentially. Experimental results are summarized giving support to the conclusions derived theoretically.
- Ostwald ripening in elastic, viscoelastic and in porous materials (cf. Chap. 9 and [102, 162, 171, 172, 174, 175]): In 1984/1985, Schmelzer and Gutzow developed a theory of cluster growth and coarsening under the influence of elastic stresses due to cluster-matrix interactions interpreting coarsening as the evolution along some appropriately defined valley of the thermodynamic potential describing the system [171, 172]. It results in two differential equations describing the evolution in time of the average cluster size, $\langle R\rangle$, and the number of clusters, N. The respective equations read for diffusion limited growth

$$\frac{d\langle R\rangle}{dt} = \frac{8Dc}{27c_\alpha^2 k_B T}\frac{1}{\langle R\rangle^2}\left\{\sigma + \frac{3}{4\pi\langle R\rangle^2}\left[\Phi^{(\varepsilon)} - V\frac{\partial\Phi^{(\varepsilon)}}{\partial V}\right]\right\} \times \frac{1}{\Gamma}\left\{1 + \Gamma - \frac{\langle R\rangle^2}{2\sigma}\frac{\partial^2\Phi^{(\varepsilon)}}{\partial\langle R\rangle\partial V}\right\}, \tag{14.70}$$

$$\frac{d\ln N}{dt} = -\frac{1}{\Gamma}\left\{\left[1 - \frac{\langle R\rangle^2}{2\sigma}\frac{\partial^2 \Phi^{(\varepsilon)}}{\partial\langle R\rangle \partial V}\right]\right\}\frac{d}{dt}\left[\ln\langle R\rangle\right] . \tag{14.71}$$

Here c is the actual concentration of segregating particles in the ambient phase, D their diffusion coefficient, k_B the Boltzmann constant and T the absolute temperature. The quantity Γ reflects specific properties of the system under consideration. In general, the relation $\Gamma \leq 1$ holds and the absolute value of this quantity increases with increasing average cluster size. In this limit of large $|\Gamma|$ (and in the absence of stresses), the asymptotic solutions obtained by Lifshitz and Slezov are included in this theoretical approach as a limiting case.

Above theory allows one to describe the whole coarsening process including its initial stages. It allows one to describe in a relatively simple and straightforward way the effect of elastic stresses on coarsening and was employed for an interpretation of experimental results obtained by Pascova and Gutzow ([173–175], cf. also Fig. 14.19 and Chap. 9). From above equations, the following consequences can be drawn:

- If the energy of elastic deformations, due to the evolution of a cluster, is equal to zero, $\Phi^{(\varepsilon)} = 0$ (absence of elastic stresses) or in the case that the energy of elastic deformations increases linearly with the volume of the cluster $\Phi^{(\varepsilon)} = \varepsilon V$, then elastic strains do not modify the coarsening process qualitatively. The Lifshitz-Slezov results are obtained asymptotically as limiting cases.
- If elastic stresses result in energies of elastic deformations growing more rapidly than linear with the volume of the clusters (i.e., $\Phi^{(\varepsilon)} \propto \varepsilon(V/V_0)^{\beta}$ with $\beta > 1$), then elastic strains will lead to an inhibition of coarsening.

These investigations have been further developed in cooperation with Möller and Jacob [162,163] and one of the founders of the theory of coarsening, V. V. Slezov (cf. Chap. 9 and [177, 178]). A comprehensive overview on the results of our common efforts with V. V. Slezov in this respect is given in the monograph of V. V. Slezov (2009) [102] edited by one of the authors of the present book. Examples demonstrating some of the possible effects of elastic stresses on coarsening are shown in Figs. 14.19–14.22.

- Interplay of elastic stress development and stress relaxation on crystallization analyzed both for nucleation and growth processes [165–169]: In [165], a theory of nucleation in viscoelastic bodies is developed. The theory is applicable generally if phase formation processes are accompanied both by stress evolution and relaxation. As a particularly important application, crystallization processes in glass forming melts in the vicinity of the temperature of vitrification, T_g, are analyzed here as an example. The theoretical approach developed shows that the degree of inhibition of crystallization by elastic stresses depends basically on the ratio of two characteristic time scales, the time-lag or time of non-steady state nucleation, τ_{ns}, versus the time of molecular relaxation, τ_{rel}, of the system. A general method is outlined allowing one the determination of this functional

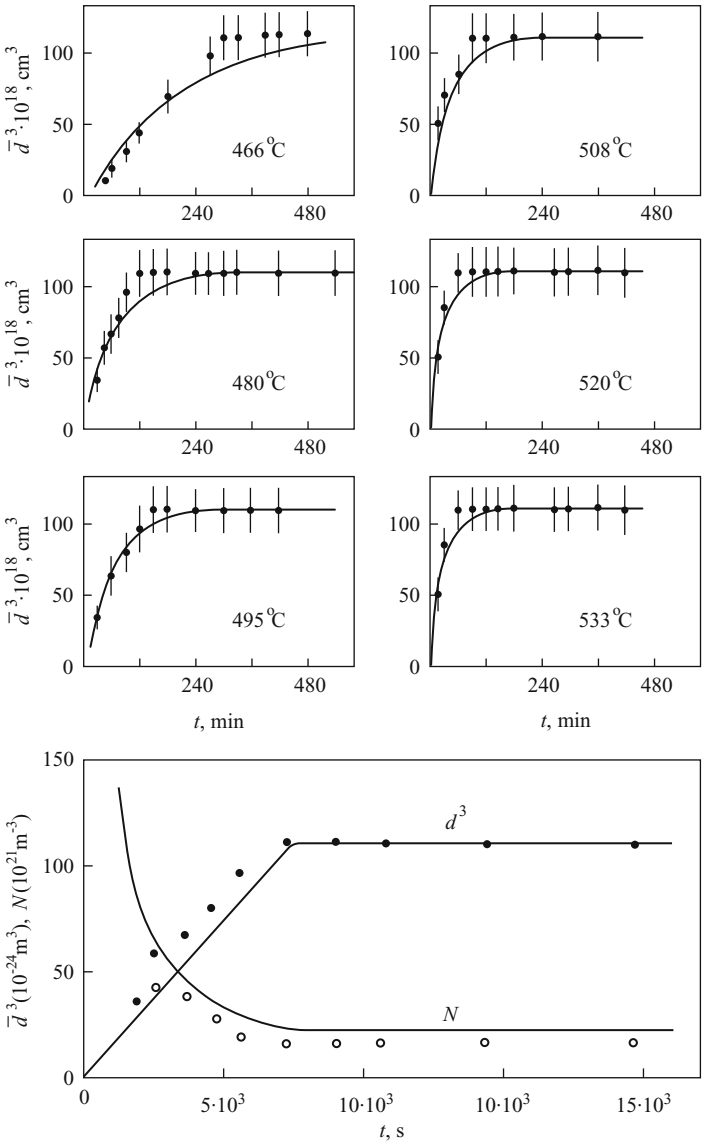

Fig. 14.19 *Top*: time-dependence of the average size of AgCl-clusters segregating in a sodium metaborate glass-forming melt [173]. The temperature of the system, at which segregation processes take place, is indicated at each *curve*. While in the first stage of the process the coarsening kinetics is described by the L(ifshitz)S(lezov)W(agner) asymptotic power laws $\langle R \rangle^3 \propto t$, $N \propto t^{-1}$, a finite stationary value of the average cluster size and a constant number of clusters are established asymptotically in the system corresponding to a monodisperse cluster size distribution ([172], cf. also Chap. 9). *Bottom*: comparison of experimental data (*dots* for the average cluster size and *open circles* of numbers of clusters in the system) and theoretical predictions for the process of Ostwald ripening of AgCl clusters in a sodium borate melt [174, 175]

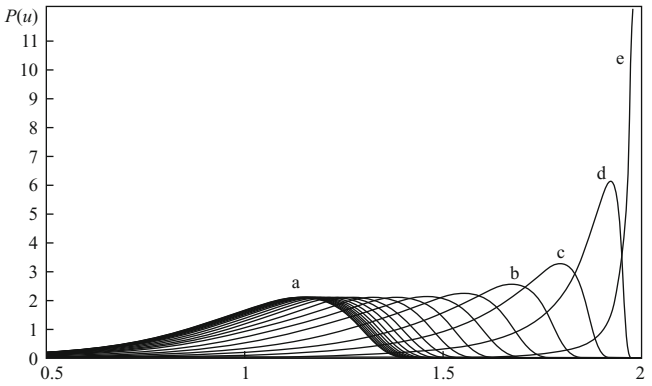

Fig. 14.20 Cluster size distribution functions $P(u)$ for different values of time. The numbers refer to the following reduced times: (*a*) small times, (*b*) $t' = 6.6 \cdot 10^5$, (*c*) $t' = 9.8 \cdot 10^5$, (*d*) $t' = 1.47 \cdot 10^6$, (*e*) $t' = 2.2 \cdot 10^6$ (for further details see [176–178] and the recent overview on these common results in the monograph of V. V. Slezov (2009) [102])

dependence. This method is applied then to two particularly important cases of viscous relaxation described by Maxwell's and Kohlrausch's laws, respectively. Further on, a proper definition of the work of critical cluster formation for nucleation in viscoelastic media is advanced. The general theory developed here contains the well-known expressions for the steady state nucleation rates in Hookean solids (for $T \ll T_g$) as well as in Newtonian liquids (for $T \gg T_g$) as limiting cases. Most importantly it allows an adequate description of nucleation also in the intermediate range, for temperatures in the vicinity of T_g giving the bridge between the mentioned limiting cases. In this way an adequate description of the influence of viscoelastic properties of the matrix on the nucleation stage in crystallization of glass forming melts is developed here to our knowledge for the first time. An extended discussion of the relevance of the theory developed in application to the interpretation of crystallization processes in glass forming melts is given in the accompanying paper [166] and applied to particular systems in [167]. It is shown that decoupling of diffusion and relaxation is required in order that elastic stresses may have a significant influence on nucleation. The situation is here similar to coarsening in multi-component solutions, when differences in the mobility (and, consequently, the characteristic times of motion) of segregating and ambient phase building units are the origin of evolution of elastic stresses in cluster growth and coarsening [174, 175]. As a limiting case, in the consideration of Ostwald ripening in porous materials, the mobility of the ambient phase particles is equal to zero (cf. also Chap. 9).

In [168, 169], these ideas were applied to the description of growth processes accounting for the possibility of evolution of elastic stresses with similar conclusions as obtained for the case of nucleation.

- Inhibition of cluster formation, cluster growth and coarsening by process-induced changes of viscosity [170]: In [170], an alternative mechanism of stabilization

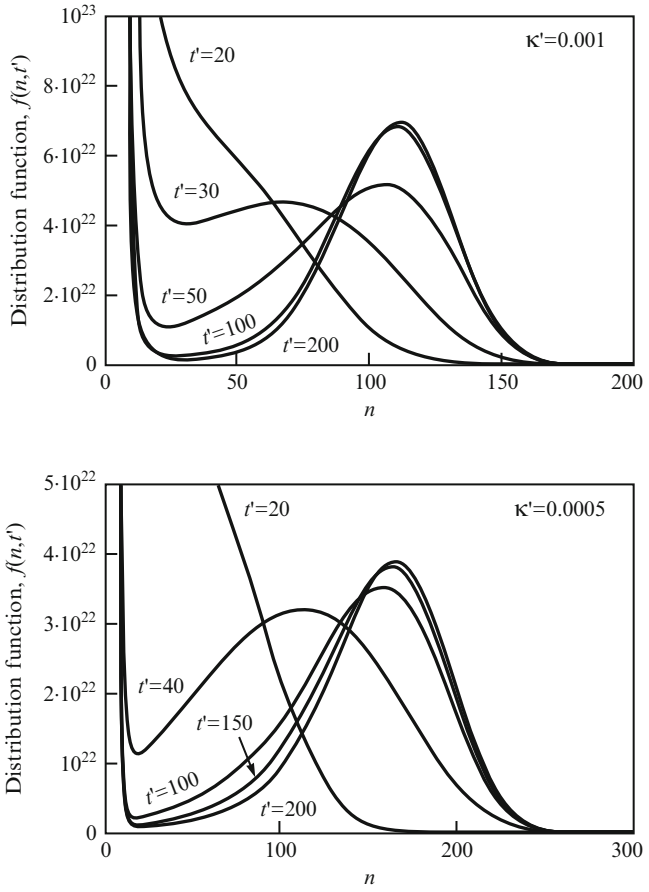

Fig. 14.21 Evolution of the cluster size distribution function for the case of nonlinear inhibition of cluster growth. In the course of time, a mono-disperse cluster size distribution is established. Such kind of behavior is always to be expected if the inequality $\beta > 1$ is fulfilled. Note also the peculiarities in the approach to the final distribution (for the details see [102, 178])

of the evolving cluster size distributions and the change of the coarsening behavior was studied by us connected with technological problems of formation of polymeric foams (styropor, styrodur) as employed by BASF. In polymer-gas solutions, bubbles may be formed at appropriate conditions. This process of bubble formation leads to a decrease of the concentration of gas in the solution and may be accompanied by a considerable increase in the viscosity. This increase of the viscosity may partly or fully inhibit the further process of formation and growth of bubbles, so here we have a process the evolution of which is terminated mainly by the considerable increase of viscosity of the ambient phase in the course of cluster formation and growth.

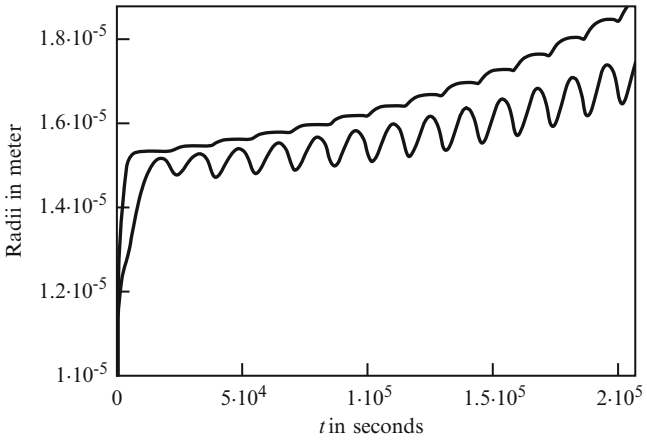

Fig. 14.22 Time development of the critical radius (*lower curve*) along with the mean cluster radius (*upper curve*) (for the details see [162, 163]). Such oscillatory approach to conventional coarsening has been experimentally observed earlier by Morozova [164]. These experimental data were originally not known to us at the time when the theory was developed

In addition, possible mechanisms of evolution and the effect of elastic stresses on crystallization processes of solid particles of finite size, in particular, on phase selection and the initiation of pore formation have been analyzed in recent years in [142, 179–182]. As a model of the theoretical analysis, crystallization processes in finite spherical domains were analyzed. Two cases were considered reflecting two possible scenarios of crystallization in particles of finite size: (i) crystallization of the internal part of a finite domain and (ii) crystallization from the boundaries. In order to account for the different types of response of the matrix to crystal formation, first, the computations were performed for the case that both the ambient and newly formed phases can be considered as Hooke's elastic solids. In a second alternative approach, the effect of viscous relaxation of the matrix on the magnitude of the evolving stresses is estimated for the different situations analyzed. The results of the analysis were applied to stress induced pore formation and phase selection in a crystallizing stretched diopside glass, respectively, in the corresponding glass-forming melt (Fig. 14.23).

The formation of the surface crystalline layer starts with nucleation and growth of highly dense diopside crystals (1). At the moment of impingement of these crystals on the sample surface, the crystallization pathway switches from diopside to a wollastonite-like phase (2) (in (a) and (b)). This crystal phase produces less elastic stress energy than diopside due to its lower density, which is closer to the liquid density. Such switching effects have been comprehensively treated earlier by us in connection with the discussion of Ostwald's rule of stages [161]. The relative content of the two crystalline phases can be changed by varying the sample size. Due to the density misfit, the growth of the wollastonite-like crystalline layer leads to uniform stretching of the encapsulated liquid and finally to formation of

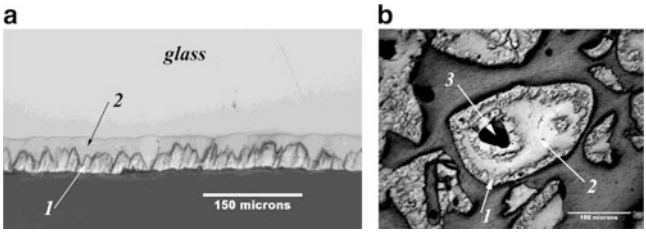

Fig. 14.23 Illustration of the possible effects of elastic stresses in the crystallization of semolina glass samples (see text and [179–182])

one pore (marked by (3) in (b)), which rapidly grows up to a size that almost eliminates the elastic stress and, therefore, dramatically reduces the driving force for pore nucleation. This nucleation process occurs in a very narrow range of negative pressures indicating that it proceeds via homogeneous nucleation. This result was corroborated by theoretical calculations of the elastic stress fields and their effect on nucleation. Qualitative and quantitative agreement between experiment and theory is found. The results of this analysis are quite general because the densities of most glasses significantly differ from those of their iso-chemical crystals, and are thus of high technological significance for glass-ceramic development and sinter-crystallization processes. The subject area is, consequently, of general relevance in the field of crystallization of amorphous materials, and more specifically in crystallization processes occurring in glass ceramics produced via the powder route.

The described above analysis can be considered as a continuation and an extension of the work performed 1998 by the authors [183] in cooperation with R. Pascova and A. Karamanov. In this paper, the combined kinetics of surface induced crystallization of glass semolina or glass powders was considered in connecting sintering and crystallization. In this combined analysis a proposal, first expressed by R. Müller, was employed and further developed: that surface crystallization inhibits sintering to an extent proportional to the surface area crystallized. These investigations have been further developed simultaneously and independently by Karamanov et al. In particular, the observation was made by Karamanov et al. [184, 185] that in systems with considerable differences in the molar volume ratio crystal-glass, a porous volume formation has to been expected as it was also in fact observed. In [186], also attempts have been developed to connect these effects with elastic stresses.

In [187] it was shown in an experimental analysis of the glass semolina samples under consideration that the Avrami parameter may vary in the range from one to three as was predicted in a theoretical analysis performed in the already mentioned paper [183]. Such changes were connected theoretically in [183] with peculiarities of surface controlled nucleation. The analysis of the overall kinetics of surface induced crystallization in all the above cited cases of surface induced crystallization of disperse sintering glassy systems showed an effect already discussed in Sects. 10.2 and 10.3 of the present book, i.e., that the Avrami coefficient

in Eq. (10.11) may have a physical background strongly differing from the original ideas as developed by Avrami and Kolmogorov. These authors and most of the investigators to follow them considered in fact the overall crystallization process taking place in a volume $V_0 \gg V_R$ where V_R is the mean diameter of the crystallites formed. In the crystallization kinetics of glass semolina of any dispersed sintering material, as first observed by Gutzow [188] many years ago, the Avrami coefficient m in Eq. 10.11 changes from $m = 1$ to $m = 3$, not because of changing mechanism and interplay of nucleation and growth, but because of the changing mean diameter of the crystallizing dispersed initial material. This change analyzed in the above cited paper by Gutzow et al. [183] is observed in both isothermal and, as shown now, also non-isothermal crystallization kinetics.

In a further development [189] the process of surface crystallization of dispersed glass samples was activated by an appropriate pre-treatment process of the initial batch constituents. In the cited investigation, the crystallization of cristobalite was initiated in such a way that the formation and stabilization of the highly desirable high temperature β-cristobalite modification (which shows nearly a zero value coefficient of thermal expansion) was obtained. The stabilization of β-cristobalite is in applications a necessity, because the $\beta - \alpha$-cristobalite transition taking place as a first-order phase transition at temperatures in the range 250–300 °C is connected with a considerable volume dilatation (of ∼5 %) and stress development. In the activated sinter-crystallization process, described in [189], the stabilization of β-cristobalite was achieved by the introduction of a relatively small amount of both Al_2O_3 and CaO, which stabilize the fully cross-linked three dimensional SiO_2 network of the initial glass into the high-temperature β-cristobalite structure which is metastable below 250–300 °C. From a more general point of view, in the cited investigation the switch of a first-order phase transition into a second-order phase transition was achieved by the introduction of chemical toughening agents (the mentioned CaO and Al_2O_3), stress induction and relaxation, leading to an appropriate immobilization of the SiO_2 network. As it is well-known, first-order phase transitions require a mobility of the structural units forming the system. In the discussed case the introduction of Al_2O_3 and CaO stabilized in so far the three dimensional SiO_2 structure, that only a second-order-like change remained possible and was observed in the temperature region of 250–300 °C. Landau's theory of continuous phase changes [27] predicts such first-order to second-order changes, e.g., for the case, when additional, stress inducing mobility and inducing elements are introduced into a structure.

14.2.4 Catalyzed Crystallization of Glass-Forming Melts: Activity of Nucleants

The results, obtained in the induced sinter-crystallization of dispersed, grained or even powdered glass samples are, it turns out, of considerable technical importance,

especially with glasses, in which ecologically important waste products are immobilized to useful glass-ceramic materials. As mentioned above, the initiation of the crystallization process depends on the glass-air interface. The classical method of inducing desired crystallization in glass forming melts, is, however, still the introduction of active crystallization cores into the glass.

For many years the nucleation activity of foreign insoluble crystallization cores in under-cooled liquids and especially in glass-forming melts has been expressed only in terms of crystal lattice disregistry nucleant-overgrowing crystal, thus totally neglecting the energetics of the process of heterogenous nucleation. In 1992/1993 and in the following several years by Dobreva, Gutzow et al. [190–198] was formulated a new, thermodynamically founded theoretical approach, in which the value of the nucleating activity coefficient, Φ, was determined from the adhesion energy nucleant-overgrowing crystal, calculated via London's adhesion-cohesion formula from the respective molecular cohesion. In this calculation, lattice disregistry plays a secondary, correcting role, only. The respective results obtained in this way are summarized in Sect. 7.5 of our book.

In the following years this adhesion-based nucleation activity approach was applied (initially in 1997 [192, 193]) by Gutzow et al. to correlate for the first time in a unique way practically all the existing experimental evidence for the crystallization of aqueous aerosols, in which ice formation is initiated by natural or artificial insoluble crystallization cores (analyzed were results for more than 80 different ecologically or meteorologically significant dopants). Further experimental evidence, this time on the catalyzed crystallization of glass-forming systems, was obtained in a detailed investigation, performed in the Otto-Schott-Institute on Glass Chemistry in Jena (see [197, 198]) in which the activity of metallic crystallization cores (of all the platinum metals, Cu, Ag and Au, carefully crystallographically characterized) and of several other ionic and oxide crystalline nucleants was investigated in three different model phosphate glasses (based on $Ca[PO_3]_2$ and $NaPO_3$) with the same result: the thermodynamic cohesion approach gave a unique possibility not only to correlate but also to predict in advance nucleating activity in induced crystallization of different crystallization cores, thus enabling formation of glass-ceramic materials with distinct properties. In international literature in the last years have been reported more than 100 cases, in which the crystallization of nucleation filled organic polymers, glasses and aqueous systems were correlated in terms of this thermodynamic approach.

It is of considerable interest, to analyze also crystallization of glass-forming melts and devitrification of glasses at the conditions of micro-gravity, as they exist in space. It was to be expected that the absence of convection and the thus decreased thermal conductivity in the crystallizing sample could substantially change the mechanism of crystallization and thus change the condition e.g. for the synthesis of glass-ceramic materials in micro-gravity. In the framework of a joint German-Bulgarian-Russian Project, supported by the Deutsche Agentur für Raumfahrt-Angelegenheiten (DARA), a decisive experiment in this sense was performed at the end of the 1990s on board of the Russian Space Station MIR. It was decided to use for this experiment the crystallization in a one-component

model phosphate glass ($NaPO_3$), the crystallization in which is induced by Pd–micro-crystals. The properties of this glass, its crystallization behavior, the course of the heterogeneous nucleation process initiated by the Pd–micro-crystalline cores, their structure and activities were studied in a series of preliminary investigations in both the Institute of Physical Chemistry (IPC) of the Bulgarian Academy of Sciences (BAS) in Sofia and in the Otto-Schott-Institut für Glaschemie at the Friedrich-Schiller University in Jena. A part of the results of these measurements, as they are described in details in [196], are also given in a summary in Sect. 7.8 of the present book. Thus to the micro-gravity crystallization experiments were subjected samples of a relatively low melting glass, forming with its Pd nucleant an exceptionally carefully examined system, characterized in both its thermodynamic, rheological and crystallographic characteristics. The Pd-initiated glass samples were filled in Pt-ampoules, vacuum-sealed at earth conditions, and a greater number of the prepared twin-samples was simultaneously heat-treated on board of the MIR-station at micro-gravity and (in the identical TITUS-oven) at the German MUSC Space Center Laboratory in Cologne at terrestrial conditions. The simultaneous heat-treatment of the samples at the MIR station and in Cologne at terrestrial and at space conditions was performed in an integrated DTA-like arrangement, giving the possibility for a direct electronic comparison of the kinetics of the crystallization process at micro-gravity and at terrestrial conditions (to each of the evacuated platinum sample holders were sealed three Pt/Rh thermo-couples). After the flight mission was completed, both series of samples crystallized were additionally examined at terrestrial conditions using different techniques. It was found that, as expected, micro-gravity conditions considerably enhanced the rate of the Pd-micro-crystal-catalyzed devitrification of the $NaPO_3$-glass: the nucleation rate was increased at cosmic conditions approximately by a factor of 10^3 (at temperatures close above T_g). This effect, as it turned out, is determined in the vicinity of T_g mainly by the temperature rise in the devitrifying glass samples at micro-gravity conditions, where crystallization heat transfer is drastically decreased by diminished convection. However, at crystallization runs close below T_m, where temperature rise even diminishes crystallization rates, no micro-gravity effect on the crystallization behavior was, as expected, observed.

14.2.5 Some Further New Results in the Kinetic Description of Phase Formation Processes

14.2.5.1 Analytical Description of Phase Formation Kinetics: Finite-Size and Depletion Effects

In Sect. 6.3.10 of the present book, the general scenario of first-order phase transitions is described when depletion effects, i.e., the change of the state of the ambient phase due to consumption of some of the components by cluster

formation and growth is described. An analytical description of the first stages of first-order phase transitions according to this scenario has been developed by one of the authors in cooperation with Vitali V. Slezov. The analytical results are illustrated by numerical computations covering also the effect of elastic stresses on coarsening. These investigations have been published first in [178, 199, 200] and recently reproduced in a comprehensive form in the monograph of V. V. Slezov (2009) [102] (cf. also [139]). Combining these results with the theory of coarsening developed by Lifshitz, Slezov and Wagner, this work allows one to get a complete description of nucleation growth processes.

Depletion effects result not only in a definite scenario of the phase transition process but affect also considerably nucleation processes in systems of finite size (cf. Chap. 6). An overview on these problems can be found in our recent papers [131, 134, 140, 141], where earlier obtained results are generalized employing in the description the generalized Gibbs approach.

14.2.5.2 Decoupling of Diffusion and Viscosity

As discussed in detail in Sects. 2.4.3 and 6.3.2, primarily the kinetic pre-factor J_0 in the expression for the steady-state nucleation rate is determined by the diffusion coefficient of the basic units in the melt undergoing crystallization. For one-component systems, we may write

$$J = \sqrt{\frac{\sigma}{k_B T}} \left(\frac{D}{d_0^4} \right) \exp\left(-\frac{W_c}{k_B T} \right) . \tag{14.72}$$

Replacing the diffusion coefficient, D, by the viscosity, η, via the Stokes-Einstein equation,

$$D = \frac{k_B T}{d_0 \eta} , \tag{14.73}$$

we get the commonly employed relation

$$J = \frac{\sqrt{\sigma k_B T}}{d_0^5 \eta} \exp\left(-\frac{W_c}{k_B T} \right) . \tag{14.74}$$

However, the replacement of the diffusion coefficient by viscosity is already questionable for one-component systems (due to the possible decoupling of diffusion and relaxation), it becomes even more questionable for crystallization processes in multi-component systems, where an effective diffusion coefficient, D_{eff}, determines primarily the nucleation-growth process, being a function of the partial diffusion coefficients, D_i, of the independently diffusing components in the melt and their molar fractions, x_i, both in the melt and in the evolving crystal phase (see [178, 199, 200] for more details).

The effective diffusion coefficient is given by the following relation:

$$\frac{1}{D_{eff}} = \sum_{i=1}^{k} \frac{\nu_{i\alpha}^2 \left[1 + \left(\frac{D_i^*}{D_i}\right)\left(\frac{d_\alpha}{d_\beta}\right) n^{1/3}\right]}{D_1^* x_{i\beta}} \,. \tag{14.75}$$

Here d_α and d_β are parameters describing the average size of the independently moving particles in the melt and the crystal cluster phase, D_i and D_i^* are the partial diffusion coefficients of the respective components in the bulk of the melt and near to the interface melt-crystal, $x_{i\beta}$ are the molar fractions of the different components in the ambient melt and $\nu_{i\alpha}^2$ is given by $\nu_{i\alpha}^2 = x_{i\alpha} + n(dx_{i\alpha}/dn)$, where n is the total number of particles in a crystal cluster. D_{eff} is the effective diffusion coefficient which plays the role of D in Eq. (14.74) for multi-component crystal nucleation. A detailed estimate of the magnitude of the error one introduces by the replacement of the effective diffusion coefficient via viscosity is believed to represent a highly interesting problem (for first results in this respect see [201]), however, as it seems it is probably hardly possible to realize such analysis for a wide class of systems due to the limited knowledge of the respective parameters.

14.2.5.3 Size of the Structural Unit

In Eqs. (14.72) and (14.74), the size parameter d_0 enters having for one-component systems the meaning of the size of the structural unit moving independently in the liquid and being responsible for crystallization. The question arises in this respect how such size parameter has to be defined in the cases that crystallization proceeds in a multi-component system. In [202] this problem has been analyzed in detail. Provided the process of crystallization is realized via an independent motion of several components, then this parameter has to be defined as the average size of the independently moving components. This result holds true both for the description of nucleation and the description of growth processes. An earlier discussion in this direction may be also found in [203].

14.2.5.4 Alternative Mechanisms of Crystallization

In the book by Skripov and Faizullin [100] one can find the following statement: *the transition from the liquid to the fcc-crystal and back cannot be accomplished by just small (of atomic size) shifts in the positions of single atoms: for such transitions a significant part of atoms should be moved by a distance of about one atomic spacing.* It follows that these processes cannot be interpreted via above sketched kinetic mechanisms of crystal nucleation and growth being based on the consideration of the more or less independent motion of the single particles of the different components of the glass-forming melt. Similarly, Leko [204] connects in his comprehensive analysis of crystallization of quartz glass the respective processes

with bond switching. As it seems, a detailed specification of the kinetic pre-factor J_0 for both these mechanisms of crystallization is not performed so far.

14.2.5.5 Dependence of the Properties of Glass-Forming Melts on Prehistory and Its Effect on Nucleation Processes

The proper account of the circle of problems sketched above is already a hard task. However, the situation may become even more complex taking into account the possible dependence of the properties of glass-forming melts on prehistory.

Since the structural order parameter is a function of pressure and temperature and of the prehistory of the melt, also the thermodynamic properties of the melt depend on the same set of parameters. It follows as a consequence that the thermodynamic state parameters of the crystal cluster in the ambient phase are, as a rule, dependent on prehistory as well. Once the bulk properties depend on prehistory, also the surface properties have to depend on prehistory. Consequently, the kinetics of crystal nucleation and growth is affected, in general, by prehistory and may proceed, in particular, in a different way for cooling and heating processes.

In above considerations, the order parameter is assumed to have the same value in the whole system. However, the intensity of fluctuations in the glass transition range is as a rule higher as compared to systems in thermodynamic equilibrium. In the glass transition range, local fluctuations are not damped out since the system is in a non-equilibrium state. A particular experimental realization of such effects consists in the already discussed here briefly "fluctuation flashes" in glass heating experiments as they are described here in brief in Sect. 14.1.6 and in [73]. Since the thermodynamic state parameters are dependent on the structural order parameter, the kinetic parameters have to depend, in general, on the structural order parameter(s) as well. For the case discussed here, the dependence is demonstrated in Fig. 14.10. Employing in this way the order parameter concept for the description of glass-forming melts, the discussion of the dependence of the crystal nucleation and growth processes on the structure of the glass-forming melts (see e.g. [205] for more details) can be given a quantitative basis.

14.3 Concluding Remarks

In 1995, when the first edition of the present book was published by Springer, P. W. Anderson [206] noted in an answer on possible frontiers in the future of science: *The deepest and most interesting unsolved problem in solid state theory is probably the theory of the nature of glass and the glass transition. This could be the next breakthrough in the coming decade*. We are quite satisfied to have been involved intensively in these processes but, as it seems, the task is far from being finally solved. So, we are looking forward to new may be even unexpected developments.

References to Chapter 14

1. Gutzow, I., Schmelzer, J.: The Vitreous State: Thermodynamics, Structure, Rheology, and Crystallization. Springer, Berlin (1995)
2. Simon, F.: Über den Zustand der unterkühlten Flüssigkeiten und Gläser. Z. Anorg. u. Allg. Chemie **203**, 219 (1931)
3. Tammann, G.: Aggregatzustände; Der Glaszustand. Leopold Voss Verlag, Leipzig, 1923; 1933
4. Gutzow, I., Dobreva, A.: Structure, thermodynamic properties and cooling rate of glasses. J. Non-Cryst. Solids **129**, 266 (1991)
5. Gutzow, I., Dobreva, A.: Thermodynamic functions of glass-forming systems and their dependence on cooling rate. Polymer **33**, 451 (1992)
6. Tropin, T.V., Schmelzer, J.W.P., Schick, C.: On the dependence of the properties of glasses on cooling and heating rates: I. entropy, entropy production, and glass transition temperature. J. Non-Cryst. Solids **357**, 1291 (2011)
7. Tropin, T.V., Schmelzer, J.W.P., Schick, C.: On the dependence of the properties of glasses on cooling and heating rates: II. Prigogine-Defay ratio, fictive temperature and fictive pressure. J. Non-Cryst. Solids **357**, 1303 (2011)
8. Bragg, W.L., Williams, E.J.: The effect of thermal agitation on atomic arrangements in alloys. Proc. R. Soc. Lond. **145 A**, 699 (1934)
9. Tool, A.Q., Eichlin, C.G., Variations caused in the heating curves of glass by heat-treatment. J. Am. Ceram. Soc. **14**, 276 (1931)
10. Tool, A.Q.: Relation between inelastic deformability and thermal expansion of glass in its annealing range. J. Am. Ceram. Soc. **29**, 240 (1946)
11. Narayanaswamy, O.S.: A model of structural relaxation. J. Am. Ceram. Soc. **54**, 491 (1971)
12. Volkenstein, M.V., Ptizyn, O.B.: Relaxation theory of glass transition. Dokl. Akad. Nauk USSR **103**, 795 (1955) (in Russian)
13. Volkenstein, M.V., Ptizyn, O.B.: Relaxation theory of glass transition: solution of the basic equation and its analyis. Zh. Tekhnicheskoi Fiziki **26**, 2204 (1956) (in Russian)
14. Filipovich, V.N., Kalinina, A.M.: On the nature of change of properties of glasses at vitrification. In: Porai-Koshits, E.A. (ed.) Determination of the Nucleation Rate of New Phases in Glasses at the Initial Stages of Phase Conversion. The Vitreous State. Proceedings of the 5th All Union Conference, Leningrad, 1969, p. 28. Nauka, Leningrad (1971) (in Russian)
15. Mazurin, O.V.: Vitrification. Nauka, Leningrad (1986) (in Russian)
16. Moynihan, C.T., Easteal, A.J., Wilder, J., Tucker, J.: Dependence of the glass transition temperature on cooling and heating rate. J. Phys. Chem. **78**, 2673 (1974)
17. Gutzow, I.: The generic phenomenology of glass formation. In: Boolchand, P. (ed.) Insulating and Semiconducting Glasses. Series on Directions in Condensed Matter Physics, vol. 17, pp. 65–93. World Scientific, Singapore/London (2000)
18. Gutzow, I., Dobreva, A.: Kinetics of glass formation. In: Thorpe, M., Mitkova, M. (eds.) Amorphous Insulators and Semiconductors, pp. 21–45. Kluwer Academic Publisher, Boston (1997)
19. Gutzow, I., Ilieva, D., Babalievski, F., Yamakov, V.: Thermodynamics and kinetics of the glass transition: a generic geometric approach. J. Chem. Phys. **112**, 10941 (2000)
20. Gutzow, I., Yamakov, V., Ilieva, D., Babalevski, F., Pye, L.D.: Generic phenomenological theory of vitrification. Glass Phys. Chem. **27**, 228 (2001)
21. Gutzow, I., Ilieva, D., Yamakov, V., Babalievski, F., Pye, L.D.: Glass transition: an analysis in terms of a differential geometry approach. In: Schmelzer, J.W.P., Röpke, G., Priezzhev, V.B. (eds.) Nucleation Theory and Applications, pp. 368–418. Joint Institute for Nuclear Research Publishing Department, Dubna (1999)
22. Gutzow, I., Babalievski, F.: A geometric formulation and a derivation of the kinetic condition for vitrification. Comptes Rend. Bulg. Acad. Sci. **52**, 61 (1999)

23. Gutzow, I., Schmelzer, J.W.P., Petroff, B.: The phenomenology of metastable liquids and the glass transition. J. Eng. Thermophys. **16**, 205 (2007)
24. Schmelzer, J.W.P., Gutzow, I.S.: Glasses and the Glass Transition. Wiley, Berlin/Weinheim (2011)
25. Callen, H.B.: Thermodynamics. Wiley, New York (1963)
26. Prigogine, I.: Introduction to Thermodynamics of Irreversible Processes. Thomas, Springfield (1955)
27. Landau, L.D., Lifschitz, E.M.: Statistische Physik. Akademie-Verlag, Berlin (1969); Statistical Physics. Pergamon, New York (1980)
28. Dyakonov, T.K., Problems of the Theory of Similarity in Physico – Chemical Processes. Publishing House of the Soviet Academy of Sciences, Moscow (1956)
29. Milchev, A., Gutzow, I.: Temperature dependence of the configurational entropy of undercooled melts and the nature of the glass transition. J. Macromol. Sci. Phys. **B 21**, 583 (1982)
30. Gutzow, I., Milchev, A.: Thermodynamic behavior of a simple liquid – MFA with nonadditive lateral interactions. Phys. Chem. Liq. **11**, 25 (1981)
31. Gibbs, J.H., Di Marzio, E.A.: Nature of the glass transition and the glassy state. J. Chem. Phys. **28**, 373 (1958)
32. Petroff, B., Milchev, A., Gutzow, I.: Thermodynamic functions of both simple (monomeric) and polymeric melts: MFA approach and Monte Carlo simulation. J. Macromol. Sci. Phys. **B 35**, 763 (1996)
33. Kinoshita, A.: Characterization of glass transition in $\alpha - As - 2Se_3$ by heat of vaporization. J. Non-Cryst. Solids **42**, 447 (1980)
34. Schnaus, U.E., Moynihan, C.T., Gammon, R.W., Macedo, P.B.: The relation of the glass transition temperature to vibrational characteristics of network glasses. Phys. Chem. Glasses **11**, 213 (1970)
35. Grantscharova, E., Gutzow, I.: Vapor pressure, solubility and affinity of under-cooled melts and glasses. J. Non-Cryst. Solids **81**, 99 (1986)
36. Gutzow, I.: Über den Dampfdruck und die Löslichkeit unterkühlter Schmelzen und Gläser. Z. Phys. Chem. (Neue Folge) **81**, 195 (1972)
37. Möller, J., Gutzow, I., Schmelzer, J.W.P.: Freezing-in and production of entropy in vitrification. J. Chem. Phys. **125**, 094505/1-13 (2006)
38. Davies, R.O., Jones, G.O.: The irreversible approach to equilibrium in glasses. Proc. R. Soc. (Lond.) **A 217**, 26 (1953)
39. Bartenev, G.M.: On the relation between the glass transition temperature of silicate glass and rate of cooling or heating. Dokl. Akad. Nauk SSSR **76**, 227 (1951) (in Russian); Structure and Mechanical Properties of Inorganic Glasses. Building Materials Press, Moscow (1966) (in Russian)
40. Schmelzer, J.W.P.: Kinetic criteria of glass-formation and the pressure dependence of the glass transition temperature. J. Chem. Phys. **136**, 074512 (2012)
41. Schmelzer, J.W.P., Tropin, T.V.: Dependence of the width of the glass transition interval on cooling and heating rates. J. Chem. Phys. **138**, 034507 (2013)
42. Bartenev, G.M.: On the vitrification of high-polymer materials at periodic deformation. Dokl. Akad. Nauk USSR **69**, 373 (1949) (in Russian)
43. Avramov I., Gutzow, I., Alyakov, S.: The formation of amorphous and crystalline condensates from the vapour phase. Thin Solid Films **34**, 35 (1976)
44. Jordanov, N., Wondraczek, L., Gutzow, I.: Thermodynamic properties of amorphous solids: the electrochemical approach. J. Non-Cryst. Solids **358**, 1239 (2012)
45. De Donder, Th., van Rysselberghe, P.: Thermodynamic Theory of Affinity. Stanford University Press, Stanford (1936)
46. Prigogine, I., Defay, R.: Chemical Thermodynamics. Longmans, London (1954)
47. Gutzow, I., Petroff, B., Möller, J., Schmelzer, J.W.P.: Glass transition and the third principle of thermodynamics: reconsideration of a classical problem. Phys. Chem. Glasses **B 48**, 168 (2007)
48. Gutzow, I.: Über die Nullpunktsentropie des Glaszustandes. Z. Phys. Chem. (Leipzig) **221**, 153 (1962)

49. Mauro, J.C., Loucks, R.J., Sabyasachi, S.: Heat capacity, enthalpy fluctuations, and configurational entropy in broken ergodic systems. J. Chem. Phys. **133**, 164503 (2010)
50. Schmelzer, J.W.P., Gutzow, I.: Structural order parameters, the Prigogine-Defay ratio and the behavior of the entropy in vitrification. J. Non-Cryst. Solids **355**, 653–662 (2009)
51. Gutzow, I., Schmelzer, J.W.P.: The third principle of thermodynamics and the zero-point entropy of glasses: history and new developments. J. Non-Cryst. Solids **355**, 653 (2009)
52. Gutzow, I., Pascova, R., Schmelzer, J.W.P.: Glass transition behavior: a generic phenomenological approach. Int. J. Appl. Glass Sci. **1**, 221 (2010)
53. Davies, R.O., Jones, G.O.: Thermodynamic and kinetic properties of glasses. Adv. Phys. **2**, 370 (1953)
54. Goldstein, M.: Viscous liquids and the glass transition. IV. Thermodynamic equations and the transition. J. Phys. Chem. **77**, 667 (1973)
55. Schmelzer, J.W.P., Gutzow, I.: The Prigogine-Defay ratio revisited. J. Chem. Phys. **125**, 184511/1–11 (2006)
56. Nemilov, S.V.: Thermodynamic and Kinetic Aspects of the Vitreous State. CRC, Boca Raton/London (1995)
57. Tropin, T.V., Schmelzer, J.W.P., Gutzow, I., Schick, C.: On the theoretical determination of the Prigogine-Defay ratio in glass transition. J. Chem. Phys. **136**, 124502 (2012)
58. Dobreva, A., Gutzow, I.: Kinetics of vitrification under changing external parameters,. Bulg. Chem. Commun. **28**, 808 (1995)
59. Dobreva, A., Gutzow, I.: Kinetics of vitrification under electric fields. J. Non-Cryst. Solids **220**, 235 (1997)
60. Gutzow, I., Dobreva, A., Rüssel, C., Durschang, B.: Kinetics of vitrification under hydrostatic pressure and under tangential stress. J. Non-Cryst. Solids **215**, 313 (1997)
61. Gutzow, I., Pye, L.D., Dobreva, A.: A geometric and analytic approach to the process of melt vitrification. Part I: thermodynamic treatment. J. Non-Cryst. Solids **180**, 107 (1995)
62. Gutzow I., Dobreva, A., Pye, L.D.: A geometric and analytic approach to the process of melt vitrification. Part II: kinetic treatment. J. Non-Cryst. Solids **180**, 117 (1995)
63. Gutzow, I., Todorova, S.: Glasses as systems with increased solubility, high chemical reactivity and as sources of accumulated energy. Phys. Chem. Glasses Eur. J. Glass **B 51**, 83 (2010)
64. Garden, J.-L., Guillou, H., Richard, J., Wondraczek, L.: Affinity and its derivatives in the glass transition process. J. Chem. Phys. **137**, 024505 (2012)
65. Minakov, A.A., Schick, C.: Ultrafast thermal processing and nanocalorimetry at heating and cooling rates up to 1 MK/s. Rev. Sci. Instrum. **78**, 073902 (2007)
66. Zhuravlev, E., Schick, C.: Fast scanning power compensated differential scanning nanocalorimeter: 1. The device. Thermochim. Acta **50**, 1 (2010)
67. Johari, G.P., Khouri, J.: Entropy change on the cooling and heating paths between liquid and glass and the residual entropy. J. Chem. Phys. **134**, 034515 (2011)
68. Johari, G.P., Aji, D.P.B.: Time-dependent paths, fictive temperatures and residual entropy of glass. Philos. Mag. **90**, 4377 (2010)
69. Mazurin, O.V.: Problems of compatibility of the values of glass transition temperatures published in the world literature. Glass Phys. Chem. **33**, 22 (2007)
70. Jones, G.O.: Viscosity and related properties in glass. Rep. Prog. Phys. **12**, 133 (1949)
71. Smekal, A., Über die Natur der glasbildenden Stoffe, Glast. Berichte **22**, 278 (1949)
72. Glasstone, S., Laidler, H.J., Eyring, H.: The Theory of Rate Processes. Princeton University, New York/London (1941)
73. Gutzow, I., Schmelzer, J.W.P., Todorova, S.: Frozen-in fluctuations, immiscibility and crystallization in oxide melts and the structural and thermodynamic nature of glasses. Phys. Chem. Glasses Eur. J. Glass Sci. Technol. **B 49**, 136 (2008)
74. Gutzow,I., Grigorova, Ts., Avramov, I., Schmelzer, J.W.P.: Generic phenomenology of vitrification and relaxation and the Kohlrausch and Maxwell equations. In: Proceedings XIX International Congress on Glass, Edinburgh, 1–6 July 2001; Phys. Chem. Glasses **43C**, 477 (2002)

75. Schmelzer, J.W.P., Schick, C.: Dependence of crystallization processes of glass-forming melts on melt history: a theoretical approach to a quantitative treatment. Phys. Chem. Glasses Eur. J. Glass Sci. Technol. **B 53**, 99 (2012)
76. Kauzmann, W.: The nature of the glassy state and the behavior of liquids at low temperatures. Chem. Rev. **43**, 219 (1948)
77. Nielsen, A.I., Christensen, T., Jakobson, B., Niss, K., Olsen, N.B., Richert, R., Dyre, J.C.: Prevalence of approximate $\sqrt{t}$-relaxation for the dielectric α-process in viscous organic liquids. J. Chem. Phys. **130**, 154508 (2009)
78. Schmelzer, J.W.P., Zanotto, E.D., Fokin, V.M.: On the pressure dependence of viscosity. J. Chem. Phys. **122**, 074511 (2005)
79. Angell, C.A.: Strong and fragile liquids: glass transition and polyamorphous transitions. In: Thorpe, M.F., Mitkova M.I. (eds.) Amorphous Insulators and Semiconductors. NATO-ASI-Series, High Technology, vol. 23, p. 1. Kluwer Academic Publishers, Dordrecht, London (1977)
80. Martinez, L.-M., Angell, C.A.: A thermodynamic connection to the fragility of glass-forming liquids. Nature **410**, 663 (2001)
81. Wang, L.-M., Angell, C.A., Richet, R.: Fragility and thermodynamics in non-polymeric glass-forming liquids. J. Chem. Phys. **125**, 074505 (2006)
82. Johari, G.P.: On Poisson's ratio of glass and liquid vitrification characteristics. Philos. Mag. **86**, 1567 (2006)
83. Oldekop, W.: Theoretische Betrachtungen über die Zähigkeit von Gläsern. Glastechnische Berichte **30**, 8 (1957)
84. Laughlin, W.T., Uhlmann, D.R.: Viscous flow in simple organic liquids. J. Phys. Chem. **76**, 2317 (1972)
85. Grantscharova, E., Avramov, I., Gutzow, I.: Calorimetric study of vitreous and crystalline sodium meta-phosphate $NaPO_3$. Naturwissenschaften **73**, 95 (1986)
86. Gutzow, I.: On the electrochemical behaviour of undercooled melts and glasses. J. Non-Cryst. Solids **45**, 301 (1981)
87. Gibbs, J.W.: On the equilibrium of heterogeneous substances. Trans. Conn. Acad. Sci. **3**, 108, 343 (1875–1878); Thermodynamics. The Collected Works, vol. 1. Longmans & Green, New York (1928)
88. Gutzow, I., Schmelzer, J., Dobreva, A.: Kinetics of transient nucleation in glass-forming liquids: a retrospective and recent results. J. Non-Cryst. Solids **219**, 1 (1997)
89. Milchev, A.: Electro-crystallization: nucleation and growth of nano-clusters on solid surfaces. Russ. J. Electrochem. **44**, 619 (2008); Published in Russian in Elektrokhimiya **44**, 669 (2008); Electrochemical phase formation: some fundamental concepts. J. Solid State Electrochem. **15**, 1401 (2011)
90. Volmer, M.: Kinetik der Phasenbildung, Th. Steinkopff, Dresden/Leipzig (1939)
91. Hirth, J.P., Pound, G.M.: Condensation and Evaporation. Pergamon, London (1963)
92. Skripov, V.P.: Metastable Liquids. Wiley, New York (1974)
93. Nielsen, A.E.: Kinetics of Precipitation. Pergamon, Oxford (1964)
94. Christian, J.W.: The Theory of Transformations in Metals and Alloys. Oxford University Press, Oxford (1975)
95. Stanley, H.A.: Introduction to Phase Transitions and Critical Phenomena. Clarendon, Oxford (1971)
96. Mutaftschev, B.: The Atomistic Nature of Crystal Growth. Springer, Berlin (2001)
97. Schmelzer, J.W.P.: Phases, Phase Transitions, and Nucleation. In: Hubbard, A. (ed.) Encyclopedia of Surface and Colloid Science, pp. 4017–4029. Marcel Dekker, New York (2002)
98. Wu, D.T.: Nucleation theory. In: Ehrenreich, H., Spaepen, F. (eds.) Solid State Physics: Advances in Research and Applications, vol. 50, pp. 37–91. Academic, New York (1997)
99. Skripov, V.P., Koverda, V.P.: Spontaneous Crystallization of Undercooled Liquids. Nauka, Moscow (1984) (in Russian)
100. Skripov, V.P., Faizullin, M.Z.: Crystal-Liquid-Gas Phase Transitions and Thermodynamic Similarity. Wiley-VCH, Berlin/Weinheim (2006)

101. Baidakov, V.G.: Explosive Boiling of Superheated Cryogenic Liquids. Wiley-VCH, Berlin/Weinheim (2007)
102. Slezov, V.V.: Kinetics of First-Order Phase Transitions. Wiley-VCH, Berlin/Weinheim (2009)
103. Gusak, A.M., Lyashenko, Yu.A., Kornienko, S.V., Pasichnyy, M.O., Shirinyan, A.S., Zaporozhets, T.V.: Diffusion-Controlled Solid-State Reactions. Wiley-VCH, Berlin/Weinheim (2010)
104. Fokin, V.M., Yuritsyn, N.S., Zanotto, E.D.: Nucleation and Crystallization Kinetics in Silicate Glasses: Theory and Experiment. In: Schmelzer, J.W.P. (ed.) Nucleation Theory and Applications, pp. 74–125. Wiley-VCH, Berlin/Weinheim (2005)
105. Fokin, V.M., Yuritsyn, N.S., Zanotto, E.D., Schmelzer, J.W.P.: Homogeneous crystal nucleation in silicate glasses: a forty years perspective. J. Non-Cryst. Solids **352**, 2681 (2006)
106. van der Waals, J.D., Kohnstamm, Ph.: Lehrbuch der Thermodynamik. Johann-Ambrosius-Barth Verlag, Leipzig und Amsterdam (1908)
107. Cahn, J.W., Hilliard, J.E.: Free energy of a non-uniform system. I. Interfacial free energy. J. Chem. Phys. **28**, 258 (1958)
108. Cahn, J.W., Hilliard, J.E.: Free energy of a non-uniform system. III. Nucleation in a two-component incompressible fluid. J. Chem. Phys. **31**, 688 (1959)
109. Oxtoby, D.W.: Nucleation at first-order phase transitions. Acc. Chem. Res. **31**, 91 (1998)
110. Skripov, V.P., Skripov, A.V.: Spinodal decomposition. Usp. Fiz. Nauk **128**, 193 (1979)
111. Gunton, J.D., San Miguel, M., Sahni, P.S.: The dynamics of first-order phase transitions. In: Domb, C., Lebowitz, J.L. (eds.) Phase Transitions and Critical Phenomena, vol. 8, pp. 85–187. Academic, London/New York (1983)
112. Binder, K.: Theory of first-order phase transitions. Rep. Prog. Phys. **50**, 783 (1987)
113. Bagdassarian, C.K., Oxtoby, D.W.: Crystal nucleation and growth from the under-cooled liquid: a nonclassical piecewise parabolic free-energy model. J. Chem. Phys. **100**, 2139 (1994)
114. Shah, M., Galkin, O., Vekilov, P.: Smooth transition from metastability to instability in phase separating protein solutions. J. Chem. Phys. **121**, 7505 (2004)
115. Schmelzer, J.W.P., Schmelzer, J. Jr., Gutzow, I.: Reconciling Gibbs and van der Waals: a new approach to nucleation theory. J. Chem. Phys. **112**, 3820 (2000)
116. Baidakov, V.G., Boltachev, G.Sh., Schmelzer, J.W.P.: Comparison of different approaches to the determination of the work of critical cluster formation. J. Colloid Interface Sci. **231**, 312 (2000)
117. Ostwald, W.: Studien über die Bildung und Umwandlung fester Körper. Z. Phys. Chem. **22**, 289 (1897)
118. Scheil, E.: Bemerkung über die Konzentration von Keimen bei ihrer Ausscheidung aus übersättigten Mischkristallen. Z. Metallkunde **43**, 40 (1952)
119. Hobstetter, J.N.: Stable transformation nuclei in solids. Trans. Am. Inst. Min. (Metall.) Eng. **180**, 121 (1949)
120. Burke, J.: The Kinetics of Phase Transformations in Metals. Pergamon Press, New York (1965)
121. Gerlach, W.: Die heterogene Ausscheidung im System Gold-Nickel. Z. Metallkunde **40**, 281 (1949)
122. Masing, G.: Lehrbuch der Allgemeinen Metallkunde. Springer, Berlin (1950)
123. Becker, R.: Die Keimbildung bei der Ausscheidung in metallischen Mischkristallen. Ann. Phys. **32**, 128 (1938)
124. Schmelzer, J.W.P., Baidakov, V.G.: Kinetics of condensation and boiling: comparison of different approaches. J. Phys. Chem. **105**, 11595 (2001)
125. Schmelzer, J.W.P.: A new approach to nucleation theory and its application to phase formation processes in glass-forming melts. Phys. Chem. Glasses **45**, 116 (2004)
126. Schmelzer, J.W.P., Baidakov, V.G., Boltachev, G.Sh.: Kinetics of boiling in binary liquid-gas solutions: comparison of different approaches. J. Chem. Phys. **119**, 6166 (2003)
127. Schmelzer, J.W.P., Boltachev, G.Sh., Baidakov, V.G.: Is Gibbs theory of heterogeneous systems really perfect? In: Schmelzer, J.W.P. (ed.) Nucleation Theory and Applications, pp. 418–446. Wiley-VCH, Berlin/Weinheim (2005)

128. Schmelzer, J.W.P., Boltachev, G.Sh., Baidakov, V.G.: Classical and generalized Gibbs approaches and the work of critical cluster formation in nucleation theory. J. Chem. Phys. **124**, 194503 (2006)
129. Schmelzer, J.W.P., Gokhman, A.R., Fokin, V.M.: Dynamics of first-order phase transitions in multicomponent systems: a new theoretical approach. J. Colloid Interface Sci. **272**, 109 (2004)
130. Schmelzer, J.W.P., Abyzov, A.S., Möller, J.: Nucleation versus spinodal decomposition in phase formation processes in multi-component solutions. J. Chem. Phys. **121**, 6900 (2004)
131. Abyzov, A.S., Schmelzer, J.W.P.: Nucleation versus spinodal decomposition in confined binary solutions. J. Chem. Phys. **127**, 114504 (2007)
132. Schmelzer, J.W.P.: Crystal nucleation and growth in glassforming melts: experiment and theory. J. Non-Cryst. Solids **354**, 269 (2008)
133. Schmelzer, J.W.P., Fokin, V.M., Abyzov, A.S., Zanotto, E.D., Gutzow, I.S.: How do crystals form and grow in glass-forming liquids: Ostwald's rule of stages and beyond. Int. J. Appl. Glass Sci. **1**, 16 (2010)
134. Abyzov, A.S., Schmelzer, J.W.P.: Comment on "minimum free-energy pathway of nucleation". J. Chem. Phys. **135**, 134508 (2011); J. Chem. Phys. **136**, 107101 (2012)
135. Rukeyser, M.: Willard Gibbs. Doubleday/Doran & Company, New York (1942)
136. Debenedetti, P.G., Reiss, H.: Reversible work of formation of an embryo of a new phase within a uniform mother phase. J. Chem. Phys. **108**, 5498 (1998)
137. Reguera, D., Reiss, H.: Nucleation in confined ideal binary mixtures: the Renninger-Wilemski problem revisited. J. Chem. Phys. **119**, 1533 (2003)
138. Boltachev, G.Sh., Schmelzer, J.W.P.: On the definition of temperature and its fluctuations in small systems. J. Chem. Phys. **133**, 134509 (2010)
139. Abyzov, A.S., Schmelzer, J.W.P., Kovalchuk, A.A., Slezov, V.V.: Evolution of cluster size-distributions in nucleation-growth and spinodal decomposition processes in a regular solution. J. Non-Cryst. Solids **356**, 2915 (2010)
140. Abyzov, A.S., Schmelzer, J.W.P.: Thermodynamic analysis of nucleation in confined space: generalized Gibbs approach. J. Chem. Phys. **134**, 054511 (2011)
141. Abyzov, A.S., Schmelzer, J.W.P.: On the theoretical description of nucleation in confined space. Am. Inst. Phys. Adv. **1**, 042160 (2011)
142. Abyzov, A.S., Fokin, V.M., Schmelzer, J.W.P.: Theory of pore formation in a "Stretched" diopside glass: generalized Gibbs approach. J. Non-Cryst. Solids **357**, 3474 (2011)
143. Fokin, V.M., Zanotto, E.D., Schmelzer, J.W.P.: Method to estimate crystal/liquid surface energy by dissolution of subcritical nuclei. J. Non-Cryst. Solids **278**, 24 (2000)
144. Fokin, V.M., Zanotto, E.D., Schmelzer, J.W.P., Potapov, O.V.: New insights on the thermodynamic barrier for nucleation in lithium disilicate glass. J. Non-Cryst. Solids **351**, 1491 (2005)
145. Fokin, V.M., Zanotto, E.D., Schmelzer, J.W.P.: On the thermodynamic driving force for the interpretation of nucleation experiments. J. Non-Cryst. Solids **356**, 2185 (2010)
146. Ulbricht, H., Schmelzer, J., Mahnke, R., Schweitzer, F.: Thermodynamics of Finite Systems and the Kinetics of First-Order Phase Transitions. Teubner, Leipzig (1988)
147. Kelton, K.F.: Crystal nucleation in liquids and glasses. Solid State Phys. **45**, 75 (1991)
148. Tatchev, D., Hoell, A., Kranold, R., Armyanov, S.: Size distribution and composition of magnetic precipitates in amorphous Ni-P Alloys. Physica **B 369**, 8 (2005)
149. Tatchev, D., Goerigk, G., Valova, E., Dille, J., Kranold, R., Armyanov, S., Delplancke, J.-L.: Investigation of the primary crystallization of Ni-17 at.% P alloy by ASAXS. J. Appl. Cryst. **38**, 787 (2005)
150. Granasy, L., James, P.: Nucleation and growth in cluster dynamics: a quantitative test of the classical kinetic approach. J. Chem. Phys. **113**, 9810 (2000)
151. Lewis, G.N., Randall, M.: Thermodynamics and the Free Energy of Chemical Substances. McGraw-Hill, New York (1923)
152. Schmelzer, J.W.P.: Generalized Gibbs thermodynamics and nucleation-growth phenomena. In: Rzoska, S., Drozd-Rzoska, A., Mazur, V. (eds.) Proceedings of the NATO Advanced Research Workshop Metastable Systems Under Pressure, Odessa, Ukraine, 4–8 Oct 2008, pp. 389–402. Springer (2009)

153. Gutzow, I., Kashchiev, D., Avramov, I.: Nucleation and crystallization in glass-forming melts: old problems and new questions. J. Non-Cryst. Solids **73**, 477 (1985)
154. Rusanov, A.I.: Phasengleichgewichte und Grenzflächenerscheinungen. Akademie-Verlag, Berlin (1978)
155. Stefan, J.: Über die Beziehung zwischen den Theorien der Capillarität und der Verdampfung. Wiedemanns Ann. Phys. Chem. **29**, 655 (1886)
156. Fokin, V.M., Zanotto, E.D.: Crystal nucleation in silicate glasses: the temperature and size dependence of crystal/liquid surface energy. J. Non-Cryst. Solids **265**, 105 (2000)
157. Baidakov, V.G.: On the temperature dependence of the surface free energy crystal-liquid. Zh. Fiz. Khim. **86**, 1–3 (2012) (in Russian)
158. Möller, J., Schmelzer, J.W.P., Gutzow, I.: Elastic stresses in surface crystallization of glasses: phase transformations at spike tips. J. Non-Cryst. Solids **219**, 142 (1997)
159. Möller, J., Schmelzer, J.W.P., Gutzow, I.: Elastic stress effects on critical cluster shapes. J. Non-Cryst. Solids **240**, 131 (1998)
160. Möller, J., Schmelzer, J.W.P., Gutzow, I.: Optimum growth shapes of clusters near planar interfaces. J. Non-Cryst. Solids **283**, 186 (2001)
161. Möller, J., Schmelzer, J.W.P., Gutzow, I.: Ostwald's rule of stages: the effect of elastic strains and external pressure. Z. Phys. Chem. **204**, 171 (1998)
162. Möller, J., Jacob, K., Schmelzer, J.W.P.: Ostwald ripening in porous viscoelastic materials. J. Phys. Chem. Solids **59**, 1097 (1998)
163. Möller, J., Jacob, K.: Instability in competitive crystallization in porous viscoelastic materials. J. Cryst. Growth **197**, 973 (1999)
164. Morozova, E.V.: Antimony oxide effect on phase separation in sodium-borosilicate glass. Fizika i Khimiya Stekla **17**, 717 (1991); Kinetic peculiarities of isothermal growth of disperse phase particle sizes in liquating sodium-borosilicate glass. Fizika i Khimiya Stekla **17**, 875 (1991)
165. Schmelzer, J.W.P., Müller, R., Möller, J., Gutzow, I.S.: Elastic stresses, stress relaxation, and crystallization: theory. Phys. Chem. Glasses **43 C**, 291 (2002)
166. Schmelzer, J.W.P., Müller, R., Möller, J., Gutzow, I.S.: Theory of nucleation in viscoelastic media: application to phase formation in glass-forming melts. J. Non-Cryst. Solids **315**, 144 (2003)
167. Schmelzer, J.W.P., Potapov, O.V., Fokin, V.M., Müller, R., Reinsch, S.: The effect of elastic stress evolution and relaxation on crystal nucleation in lithium disilicate glasses. J. Non-Cryst. Solids **333**, 150 (2004)
168. Möller, J., Schmelzer, J.W.P., Avramov, I.; Kinetics of segregation and crystallization with stress development and stress relaxation. Phys. Status Solidi **b 196**, 49 (1996); Kinetics of crystallization with stress development and stress relaxation. In: Proceedings V.-th Otto-Schott-Colloquium, Jena, Germany, July 1994
169. Schmelzer, J.W.P., Zanotto, E.D., Avramov, I., Fokin, V.M.: Stress development and stress relaxation during crystal growth in glass-forming melts. J. Non-Cryst. Solids **352**, 434 (2006)
170. Schmelzer, J., (under participation of Slezov, V.V., Gutzow, I.S., Todorova, S., Avramov, I., Schmelzer, J. Jr.): Bubble formation and growth in viscous liquids, project report for BASF Ludwigshafen, Rostock – Ludwigshafen, p. 203, 1998
171. Schmelzer, J.: On the kinetics of decomposition of dilute Al-(Zn,Mg) alloys. Phys. Status Solidi **b 161**, 173 (1990)
172. Schmelzer, J., Gutzow, I.: Ostwald ripening in elastic media, Wissenschaftliche Zeitschrift der Wilhelm-Pieck-Universität Rostock, Mathematisch-Naturwissenschaftliche Reihe **35**, 5 (1986); On the kinetic description of Ostwald ripening in elastic media. Z. Phys. Chem. (Leipzig) **269**, 753 (1988)
173. Pascova, R., Gutzow, I.: Model investigation of the mechanism of formation of phototropic silver halide phases in glasses. Glastech. Ber. **56**, 324 (1983)
174. Schmelzer, J., Pascova, R., Gutzow, I.: Cluster growth and Ostwald ripening in viscoelastic media. Phys. Status Solidi **a 117**, 363 (1990)

175. Schmelzer, J., Gutzow, I., Pascova, R.: Kinetics of phase segregation in elastic and viscoelastic media. J. Cryst. Growth **104**, 505 (1990)
176. Schmelzer, J.W.P., Möller, J.: Evolution of cluster size distribution function for Ostwald ripening in viscoelastic media. J. Phase Transit. **38**, 261 (1992)
177. Schmelzer, J., Möller, J., Slezov, V.V.: Ostwald ripening in porous materials: the case of arbitrary pore size distributions. J. Phys. Chem. Solids **56**, 1013 (1995)
178. Schmelzer, J.W.P., Slezov, V.V., Röpke, G., Schmelzer, J. Jr.: Shapes of cluster size distributions evolving in nucleation – growth processes. In: Schmelzer, J.W.P., Röpke, G., Priezzhev, V.B. (eds.) Nucleation Theory and Applications, pp. 82–129. Joint Institute for Nuclear Research Publishing House, Dubna (1999)
179. Abyzov, A.S., Schmelzer, J.W.P., Fokin, V.M.: On the effect of elastic stresses on crystallization processes in finite domains. In: Schmelzer, J.W.P., Röpke, G., Priezzhev, V.B. (eds.) Nucleation Theory and Applications, pp. 379–398. Joint Institute for Nuclear Research Publishing House, Dubna (2008)
180. Abyzov, A.S., Schmelzer, J.W.P., Fokin, V.M.: Elastic stresses in crystallization processes in finite domains. J. Non-Cryst. Solids **356**, 1670 (2010)
181. Fokin, V.M., Abyzov, A.S., Schmelzer, J.W.P., Zanotto, E.D.: Stress induced pore formation and phase selection in a crystallizing stretched glass. J. Non-Cryst. Solids **356**, 1679 (2010)
182. Schmelzer, J.W.P., Abyzov, A.S., Fokin, V.M.: Theory of pore formation in a "Stretched" diopside glass: generalized Gibbs approach. In: Proceedings International Congress on Glass 2010, Salvador de Bahia, Brazil
183. Gutzow, I., Pascova, R., Karamanov, A., Schmelzer, J.W.P.: The kinetics of surface induced sinter crystallization and the formation of glass-ceramic materials. J. Mater. Sci. **33**, 5265 (1998)
184. Karamanov, A., Perlino, M.: Sinter crystallization in the system diopside-albite. Part 1. Formation of induced crystallization porosity; Part 2. Kinetics of crystallization and sintering. J. Eur. Ceram. Soc. **26**, 2511, 2519 (2006)
185. Karamanov, A., Pelino, M.: Induced crystallization porosity and properties of sintered diopside and wollastonite glass ceramics. J. Eur. Ceram. Soc. **28**, 555 (2008)
186. Karamanov, A., Georgieva, I., Pascova, R., Avramov, I.: Pore formation in glass ceramics: influence of the stress energy distribution. J. Non-Cryst. Solids **356**, 117 (2010)
187. Karamanov, A., Avramov, I., Arrizza, L., Pascova, R., Gutzow, I.: Variation of avrami parameter during non-isothermal surface crystallization of glass powders with different sizes. J. Non-Cryst. Solids **358**, 1486 (2012)
188. Gutzow, I.: Kinetics of crystallization processes in glass forming melts. J. Cryst. Growth **48**, 589 (1980)
189. Pascova, R., Avdeev, G., Gutzow, I., Penkov, I., Ludwig, F.-P., Schmelzer, J.W.P.: Refractory alkali-free cristobalite glass-ceramics: activated reaction sinter-crystallization synthesis and properties. Int. J. Appl. Glass Sci. **3**, 75 (2012)
190. Dobreva, A., Gutzow, I.: Activity of substrates in the catalyzed nucleation of glass-forming melts. I. Theory. J. Non-Cryst. Solids **162**, 1 (1993)
191. Dobreva, A., Gutzow, I.: Activity of substrates in the catalyzed nucleation of glass-forming melts. II. Experimental evidence. J. Non-Cryst. Solids **162**, 13 (1993)
192. Gutzow, I., Todorova, S., Vassilev, Ts., Dobreva, A.: The activity of substrates in the catalyzed nucleation of under-cooled melts and aqueous aerosols. Cryst. Res. Technol. **32**, 893 (1997)
193. Gutzow, I., Dobreva, A., Schmelzer, J.: Nucleation catalysis in glass-forming systems. In: Prof. Norbert Kreidl Symposium 1994, Glastechnische Berichte: Glass Science and Technology **70**, 95 (1997)
194. Dobreva-Veleva, A., Vassilev, Ts., de Saja, J.A., Rodriguez, M.-A., Gutzow, I.: Unified thermodynamic approach for describing the nucleating activity of substrates in the induced crystallization of organic and inorganic under-cooled glass-forming melts. J. Non-Cryst. Solids **253**, 99 (1999)
195. Todorova, S., Schmelzer, J.W.P., Gutzow, I.: Nucleation catalysis in metastable liquids: inborn active sites. Cryst. Res. Technol. **35**, 515 (2000)

196. Reiss, H., Müller, M., Pascova, R., Gutzow, I.: Catalyzed nucleation under micro-gravity conditions: results with a model glass. J. Cryst. Growth **222**, 328 (2001)
197. Guencheva, V., Stoyanov, E., Gutzow, I., Günter, C., Rüssel, Ch.: Induced crystallization of glass-forming melts. Part 1. Heterogeneous nucleation. Effect of noble metal micro-crystals on the crystallization of calcium metaphosphate glasses. Glass Sci. Technol. **5**, 217 (2004)
198. Guencheva, V., Rüssel, C., Fokin, V.M., Gutzow, I.: The induced crystallization of glass-forming melts. Part 2. Influence of surfactants and non-surfactant soluble additives. Phys. Chem. Glasses **B 48**, 48 (2007)
199. Slezov, V.V., Schmelzer, J.W.P.: Kinetics of nucleation – growth processes: the first stages. In: Schmelzer, J.W.P., Röpke, G., Priezzhev, V.B. (eds.) Nucleation Theory and Applications, pp. 6–81. Joint Institute for Nuclear Research Publishing House, Dubna (1999)
200. Slezov, V.V., Schmelzer, J.W.P.: Kinetics of formation of a new phase with an arbitrary stoichiometric composition in a multi-component solid solution. Phys. Rev. **E 65**, 031506 (2002)
201. Nascimento, M.L.F., Fokin, V.M., Zanotto, E.D. Abyzov, A.S.: Dynamic processes in a silicate liquid from above melting to below the glass transition. J. Chem. Phys. **135**, 194703 (2011)
202. Schmelzer, J.W.P.: On the determination of the kinetic pre-factor in classical nucleation theory. J. Non-Cryst. Solids **356**, 2901 (2010)
203. Gutzow, I.: Mechanism of crystallization in under-cooled melts and glass-forming systems. In: Kaldis, E., Scheel, H.J. (eds.) Crystal Growth and Materials. North-Holland, Amsterdam, New York (1977)
204. Leko, V.K.: Crystallization of quartz glasses. In: Schmelzer, J.W.P., Röpke, G., Priezzhev, V.B. (eds.) Nucleation Theory and Applications, pp. 109–166. JINR Publishing Department, Dubna (2008)
205. Schmelzer, J.W.P., Schick, C.: Dependence of crystallization processes of glass-forming melts on prehistory: a theoretical approach to a quantitative treatment. Phys. Chem. Glasses **B 53**, 99 (2012)
206. Anderson, P.W.: Through the Glass Lightly. Science **267**, 1615 (1995)

References

1. Abbe, Y., Mori, K., Naruse, A.: Proceedings of the 10-th International Congress on Glass, Kyoto, p. 17 (1974)
2. Abbe, Y., Mori, K., Naruse, A.: Yogue-Kyokai-Shi **84**, 111 (1976)
3. Abyzov, A.S., Schmelzer, J.W.P.: Nucleation versus Spinodal Decomposition in Confined Binary Solutions. J. Chem. Phys. **127**, 114504 (2007)
4. Abyzov, A.S., Schmelzer, J.W.P., Kovalchuk, A.A., Slezov, V.V.: Evolution of cluster size-distributions in nucleation-growth and spinodal decomposition processes in a regular solution. J. Non Cryst. Solids **356**, 2915 (2010)
5. Adam, G., Gibbs, J.H.: J. Chem. Phys. **43**, 139 (1965)
6. Adams, L.H.: J. Franklin Inst. **216**, 39 (1933)
7. Alfrey, T.: Mechanical Behaviour of High Polymers. Interscience Publishers, New York (1955)
8. Alfrey, T., Goldfinger, G., Mark, H.: J. Appl. Phys. **14**, 701 (1943)
9. Anderson, C.T.: J. Am. Chem. Soc. **59**, 1036 (1937)
10. Anderson, P.W.: Phys. Rev. **109**, 1492 (1958)
11. Anderson, E., Story, L.G.: J. Amer. Chem. Soc. **45**, 1102 (1923)
12. Anderson, P.W., Halperin, B.I., Varma, C.M.: Phil. Mag. **25**, 1 (1972)
13. Andrade, E.N.: Nature **125**, 309 (1930); Phil. Mag. **17**, 698 (1934)
14. Andreev, N.S., Mazurin, O.V., Porai-Koshits, E.A., Roscova, G.P., Filipovich, V.N.: Liquid Phase Separation in Glasses. Nauka, Moscow (1974, in Russian)
15. Angell, C.A., Rao, K.J.: J. Chem. Phys. **57**, 470 (1972)
16. Angell, C.A., Sichina, W.: Thermodynamics of the glass transition: empirical aspects. In: Goldstein, M., Simha, R. (eds.) The Glass Transition and the Nature of the Glassy State, vol. 279, p. 53. Annals New York Academy of Sciences, New York (1976)
17. Arayo, R.J.: Contemp. Phys. **21**, 77 (1980)
18. Arcimovich, L.A.: Elementare Plasmaphysik. Akademie-Verlag, Berlin (1972)
19. Avrami, M.: J. Chem. Phys. **7**, 1103 (1939); **8**, 212 (1940); **9**, 177 (1941)
20. Avramov, I.: Phys. Stat. Solidi **a120**, 133 (1990)
21. Avramov, I.: J. Chem. Phys. **95**, 4439 (1991)
22. Avramov, I.: J. Mater. Sci. Lett. **13**, 1367 (1994)
23. Avramov, I., Gutzow, I.: Mater. Chem. **5**, 315 (1980)
24. Avramov, I., Gutzow, I.: J. Non Cryst. Solids **104**, 148 (1988)
25. Avramov, I., Milchev, A.: Fiz. i Khim. Stekla **10**, 649 (1984)
26. Avramov, I., Milchev, A.: J. Non Cryst. Solids **104**, 253 (1988)
27. Avramov, I., Pascova, R., Samouneva, B., Gutzow, I.: Phys. Chem. Glass. **20**, 91 (1979)
28. Avramov, I., Grantcharova, E., Gutzow, I.: J. Non Cryst. Solids **52**, 111 (1981)
29. Avramov, I., Grantcharova, E., Gutzow, I.: J. Non Cryst. Solids **91**, 386 (1987)

I.S. Gutzow and J.W.P. Schmelzer, *The Vitreous State*,
DOI 10.1007/978-3-642-34633-0, © Springer-Verlag Berlin Heidelberg 2013

30. Avramov, I., Grantcharova, E., Gutzow, I.: J. Cryst. Growth **87**, 305 (1988)
31. Avramov, I., Grantcharova, E., Gutzow, I.: J. Non Cryst. Solids **104**, 148 (1988)
32. Avramov, I., Grudeva, S., Gutzow, I.: Thin Solid Films **185**, 91 (1990)
33. Avramov, I., Gnappi, G., Montenero, A.: Phys. Chem. Glass. **33**, 140 (1992)
34. Baidakov, V.G.: Explosive Boiling of Superheated Cryogenic Liquids. WILEY-VCH, Berlin-Weinheim (2007)
35. Balta, P., Balta, E.: Introduction to the Physical Chemistry of the Vitreous State. Editura Academiei, Bukarest. Abacus Press, Kent (1976)
36. Barker, J.A., Hoare, M.R., Finney, J.L.: Nature **257**, 120 (1975)
37. Barlow, W.: Proc. R. Soc. (Dublin) **8**, 527 (1898)
38. Barrett, P.: Cinetique Heterogene. Gauthier-Villars, Paris (1973)
39. Bartels, J.: Zur Theorie von Keimbildung und Keimwachstum in kondensierten Systemen. Dissertation A, Rostock (1991)
40. Bartels, J., Schmelzer, J.: Phys. Stat. Solidi **a132**, 361 (1992)
41. Bartels, J., Schmelzer, J., Schweitzer, F.: Non-stationary nucleation and the Johnson-Mehl-Avrami equation. In: Ebeling, W., Ulbricht, H. (eds.) Irreversible Processes and Selforganization, p. 47 ff. Teubner Texte zur Physik, Leipzig (1989)
42. Bartels, J., Schweitzer, F., Schmelzer, J.: J. Non Cryst. Solids **125**, 129 (1990)
43. Bartels, J., Lembke, U., Pascova, R., Schmelzer, J., Gutzow, I.: J. Non Cryst. Solids **136**, 181 (1991)
44. Bartenev, G.M.: Doklady Akademii Nauk SSSR **76**, 227 (1951)
45. Bartenev, G.M.: Structure and Mechanical Properties of Inorganic Glasses. Building Materials Press, Moscow (1966, in Russian)
46. Bartenev, G.M.: Strength and Mechanism of Fracture of Polymers. Chemistry State Press, Moscow (1984, in Russian)
47. Bartenev, G.M., Frenkel, S.Y.: Physics of Polymers. Chemistry State Press, Leningrad (1990, in Russian)
48. Bartenev, G.M., Sanditov, D.S.: Relaxation Processes in Glass-forming Systems. Nauka, Moscow (1986, in Russian)
49. Bartenev, G.M., Sanditov, D.S., Rasumovskaya, I.V., Lukyanov, I.A.: Ukr. Fiz. Zhurnal **14**, 1529 (1969)
50. Batchinski, J.: Phys. Z. **13**, 1157 (1912); Z. Phys. Chem. **84**, 643 (1913)
51. Battezatti, L., Garrone, E.: Z. Metallkunde **75**, 305 (1984)
52. Bauer, E.: Zs. Kristallografie **110**, 372 (1958)
53. Bazarov, I.P.: Thermodynamics. Higher Education Press, Moscow (1976, in Russian)
54. Beal, R.J., Dean, R.P.: Phys. Chem. Glass. **9**, 125 (1968)
55. Beaman, R.: J. Polym. Sci. **9**, 470 (1952)
56. Beaver, M.B.: Encyclopedia of Materials Science and Engineering. Mechanical Properties of Polymers, vol. 4. Pergamon Press, Oxford (1986)
57. Becker, R.: Ann. Phys. **32**, 128 (1938)
58. Becker, R.: Theorie der Wärme. Springer, Berlin-Göttingen-Heidelberg (1964)
59. Becker, R., Döring, W.: Ann. Phys. **24**, 719 (1935)
60. Behrnd, K.: J. Vac. Sci. Technol. **7**, 385 (1970)
61. Bekkedahl, N.: J. Res. Natl. Bureau Stand. **13**, 411 (1934); Rubbber Chem. Technol. **8**, 5 (1935)
62. Belkevich, P.I.: Overview on topochemical equations and their applicability to the kinetics of thermal decomposition of solid bodies. In: Collected Works of the Belorussian Academy of Sciences, Institute of Chemistry, p. 21. Academy of Sciences Publishers, Minsk (1956, in Russian)
63. Belov, N.B.: Structure of Ionic Crystals and Metallic Phases. Academy of Sciences USSR Publishers, Moscow (1947, in Russian)
64. Bengtzelius, U., Sjögren, L.: J. Chem. Phys. **84**, 1744 (1986)
65. Bengtzelius, U., Götze, W., Sjölander, A.: J. Phys. **C17**, 5915 (1984)
66. Bennett, C.H.: Demons, engines and the second law. Sci. Am. **257**, 108–116 (1987)

67. Berezhnoi, A.I.: Sitals and Photositals. Mashinostroenie Publishers, Moscow (1981, in Russian)
68. Berger, E.: Glastech. Ber. **8**, 339 (1930)
69. Bergmann, C., Avramov, I., Zahra, C.Y., Mathieu, J.K.: J. Non Cryst. Solids **70**, 367 (1985)
70. Berman, I., Patterson, M.S.: J. Appl. Chem. **11**, 369 (1961)
71. Bernal, J.D.: Science in History. C. A. Watts, London (1957)
72. Bernal, J.D.: Nature **183**, 141 (1959)
73. Bernal, J.D.: Sci. Am. **8**, 908 (1960)
74. Bernal, J.D.: Proc. R. Soc. **280**, 299 (1964)
75. Bernal, J.D., Mason, J.: Nature **188**, 908 (1960)
76. Berry, R.S., Burdett, J., Castleman, A.W. (eds.): Proceedings VI-th International Meeting on Small Particles and Inorganic Clusters, Chicago, USA, September 1992, Z. Phys. **D 26** (1993)
77. Bertocci, U.: Surf. Sci. **15**, 286 (1969)
78. Bestul, A.B., Blackburn, D.H.: J. Chem. Phys. **33**, 1274 (1960)
79. Bestul, A., Chang, S.: J. Chem. Phys. **40**, 3731 (1964)
80. Bezborodov, M.A.: Viscosity of Silicate Glasses. Science and Technology Press, Minsk (1975, in Russian)
81. Bienenstock, A.: Radial distribution function in EXAFS-studies of amorphous materials. In: Gaskall, P.H. (ed.) The Structure of Non-crystalline Materials. Symposium Proceedings, Cambridge, England, p. 5. Taylor and Francis, London (1977)
82. Binder, K.: Spinodal Decomposition. In: Materials Science and Technology. VCH-Verlagsgesellschaft, Weinheim (1992)
83. Binder, K., Stauffer, D.: Adv. Phys. **25**, 343 (1976)
84. Bliznakov, G.: Fortschritte der Mineralogie **36**, 149 (1958)
85. Blumberg, B.Y.: Introduction into the Physical Chemistry of Glasses. Chemistry State Publishers, Leningrad (1939, in Russian)
86. Bokii, G.P.: Crystal Chemistry. Moscow University Press, Moscow (1960, in Russian)
87. Boltzmann, L.: Vorlesungen über die kinetische Gastheorie. Johann-Ambrosius-Barth Verlag, Leipzig (1896–1898)
88. Bonch-Bruevich, V.L. (ed.): Theory and Properties of Disordered Materials, p. 5. Mir Publishers, Moscow (1977, in Russian)
89. Bondi, A.: Physical Properties of Molecular Crystals, Liquids and Glasses. Wiley, New York, 1968
90. Bonissent, A., Mutaftschiev, B.: J. Phys. Chem. **56**, 580 (1973)
91. Borissov, M., Kirov, N., Vavrek, A. (eds.): Disordered Structures and New Materials, Proceedings of the V.-th International School on Condensed Matter Physics, Varna, Bulgaria, 1988; World Scientific, Singapore/New Jersey/London/Hong Kong (1989)
92. Borovinski, L.A., Zindergosen, A.N.: Investigation of Processes of Crystallization. In: Scientific Papers of the Herzen State College of Education, Novgorod, p. 27 (1969)
93. Botet, R., Jullien, R.: Ann. Phys. (France) **13**, 153 (1988)
94. Botvinkin, O.H.: Introduction into the Physical Chemistry of Silicates. State Press Lechkoi Promyschlennosti, Moscow, Leningrad (1938, in Russian)
95. Boucher, E.A.: Nucleation in the atmosphere. In: Zettlemoyer, A.C. (ed.) Nucleation, p. 527 ff. Marcel Decker, New York (1969)
96. Boyer, R.F., Spencer, R.S.: J. Appl. Phys. **15**, 398 (1944)
97. Boyer, R.F., Spencer, R.S.: J. Appl. Phys. **16**, 594 (1945)
98. Boyer, R.F., Spencer, R.S.: Advances in Colloid Science, vol. II. Interscience Publishers, New York (1946)
99. Bragg, W.I., Williams, E.J.: Proc. R. Soc. **145A**, 699 (1934)
100. Brandes, H.: Z. Phys. Chem. **126**, 196 (1927)
101. Bray, P.J.: Proceedings of the 3-rd International Otto-Schott-Kolloquium. Jena, 1987. Wissenschaftliche Zeitschrift der Friedrich-Schiller-Universität Jena, Mathematisch-Naturwissenschaftliche Reihe **36**, 735 (1987)
102. Bray, P.J., Silver, A.H.: Nuclear magnetic resonance adsorption in glass. In: Mackenzie, J.D. (ed.) Modern Aspects of the Vitreous State, p. 92. Butterworths, London (1960)

103. Bray, P.J., Loui, M.L., Hintenlang, D.E.: Proceedings of the 2-nd International Otto-Schott-Kolloquium, Jena, 1983. Wissenschaftliche Zeitschrift der Friedrich-Schiller-Universität Jena, Mathematisch-Naturwissenschaftliche Reihe **32**, 409 (1983)
104. Bresler, S.F.: Acta Physicochim. (USSR) **10**, 491 (1939)
105. Brizke, E.W., Kapustinski, A.F. (eds.): Caloric Constants of Inorganic Substances. Academy of Science Press, Moscow, Leningrad (1949, in Russian)
106. Buckley, H.E.: Crystal Growth. Wiley, New York/London (1951)
107. Budewski, E., Bostanoff, W., Vitanov, T., Stoinov, Z., Kotzewa, A., Kaischew, R.: Phys. Stat. Solidi **13**, 577 (1966)
108. Budurov, S., Spassov, T., Marchev, K.: J. Mater. Sci. **22**, 3485 (1987)
109. Bueche, F.: Physical Properties of Polymers. Interscience Publishers, New York (1962)
110. Buff, F.P., Kirkwood, J.G.: J. Chem. Phys. **18**, 991 (1950)
111. Burckhardt, H.G., Trömel, M.: Acta Cryst. **C 39**, 1322 (1981)
112. Burnett, D.G., Douglas, R.W.: Phys. Chem. Glass. **12**, 117 (1971)
113. Burton, W.K., Cabrera, N.: Discuss. Faraday Soc. **5**, 33 (1949)
114. Burton, W.K., Cabrera, N., Frank, F.C.: Phil. Trans. R. Soc. (Lond.) **A 243**, 299 (1951)
115. Cahn, J.W.: Acta Met. **8**, 554 (1960)
116. Cahn, R.W.: Nature **257**, 356 (1975)
117. Cahn, R.W.: Alloys rapidly solidified from the melt. In: Cahn, R.W., Haasen, P. (eds.) Physical Metallurgy, 3rd edn, pp. 2399–2500. North-Holland Physics Publishing House, Amsterdam/Oxford/New York/Tokyo (1983)
118. Cahn, R.W., Haasen, P. (eds.): Physical Metallurgy, 3rd edn. North-Holland Physics Publishing House, Amsterdam/Oxford/New York/Tokyo (1983)
119. Cahn, J.W., Hilliard, J.E.: J. Chem. Phys. **28**, 258 (1958); **31**, 688 (1959)
120. Cahn, J.W., Hillig, W.B., Sears, G.W.: Acta Met. **12**, 1421 (1964)
121. Calef, D.F., Deutch, J.M.: Ann. Rev. Phys. Chem. **34**, 493 (1983)
122. Cargill, G.S.: Structure of metallic alloy glasses. In: Ebenreich, H., Seitz, F. (eds.) Solid State Physics, vol. 30, p. 227. Academic, New York (1975)
123. Cargill, S.: Recurring Themes in the Structure of Glassy Solids. In: Goldstein, M., Simha, R. (eds.) The Glass Transition and the Nature of the Glassy State, vol. 279, p. 208. Annals New York Academy of Sciences, New York (1976)
124. Cernuschi, F., Eyring, H.: J. Chem. Phys. **7**, 547 (1939)
125. Chalmers, B., King, R. (eds.): Progress in Metal Physics, vol. 6. Pergamon Press, London/New York (1956)
126. Chandrasekhar, S.: Rev. Mod. Phys. **15**, 1 (1943)
127. Charles, R.J.: Glass Technol. **12**, 24 (1971)
128. Chen, H.S., Turnbull, D.: J. Appl. Phys. **38**, 3646 (1967)
129. Chen, H.S., Turnbull, D.: J. Chem. Phys. **48**, 2560 (1968)
130. Chen, H.S.: J. Non Cryst. Solids **22**, 135 (1976)
131. Chen, H.S.: Structure and properties of metallic glasses. In: Gaskall, P.H. (ed.) The Structure of Non-crystalline Materials. Symposium Proceedings, Cambridge, England, p. 79. Taylor and Francis, London (1977)
132. Chernov, A.A.: Formation of crystals. In: Modern Crystallography, vol. 3. Nauka Publishers, Moscow (1980, in Russian)
133. Chernov, A.A.: Z. Phys. Chem. (Leipzig) **269**, 941 (1988)
134. Chopra, K.L.: Thin Film Phenomena. McGraw Hill, New York (1962)
135. Christian, J.W.: The Theory of Transformations in Metals and Alloys. Oxford University Press, Oxford (1975)
136. Christov, S.G.: Collision Theory and Statistical Theory of Chemical Reaction. Lecture Notes in Chemistry, Ser. Ed. G. Berthier et al., Springer, Berlin/Heidelberg/New York (1980)
137. Cohen, M., Turnbull, D.: J. Chem. Phys. **59**, 3639 (1959)
138. Cohen, M., Turnbull, D.: Nature **189**, 131 (1961)
139. Collins, F.C.: Z. Elektrochem. **59**, 404 (1955)
140. Cornelissen, J., van Leeuwen, J., Waterman, H.-I.: Chem. et. Ind. **77**(1), 69 (1957)

141. Cook, H.E.: Acta Met. **18**, 297 (1970)
142. Cooper, A.: J. Non Cryst. Solids **95–96**, 24 (1971)
143. Cooper, A.: Crystal growth in network liquids by structure rearrangement. In: Freeman, S.W., Hench, I.I. (eds.) Advances in Nucleation and Crystallization in Glasses, p. 123. American Chemical Society, Columbus (1971)
144. Cooper, A.R.: Internal parameters, ordering parameters, history and the glass transition. In: Frischat, G. (ed.) The Physics of Non-crystalline Solids, p. 384. Aedermansdorf, Switzerland (1977)
145. Cooper, A.R.: J. Non Cryst. Solids **49**, 1 (1982)
146. Cooper, A., Gupta, A.: Phys. Chem. Glass. **23**, 44 (1982)
147. Cormia, R.L., Mackenzie, J.D., Turnbull, D.: J. Appl. Phys. **34**, 2239 (1963)
148. Courtney, W.G.: J. Chem. Phys. **36**, 2018 (1962)
149. Coxeter, H.S.M.: Introduction to Geometry. Wiley, New York (1961)
150. Crank, J.: The Mathematics of Diffusion. Clarendon Press, Oxford (1975)
151. Danilov, V.I., Malkin, V.I.: Zh. Fiz. Khim. **28**, 1837 (1934)
152. Daragan, G.: Glass Ind. **33**, 307 (1952)
153. Davies, R.O., Jones, G.O.: Adv. Phys. **2**, 370 (1953); Proc. R. Soc. (Lond.) **A217**, 26 (1953)
154. de Bolt, M.A., Easteal, A.J., Macedo, P.M., Moynihan, C.T.: J. Am. Ceram. Soc. **59**, 16 (1976)
155. De Donder, T.: Bull. Acad. Roy. Belg. (Cl.Sc.) **23**, 936 (1937); **24**, 15 (1938)
156. De Donder, T., van Rysselberghe, P.: Thermodynamic Theory of Affinity. Stanford University Press, Menlo Park (1936)
157. de Groot, S.R.: Thermodynamics of Irreversible Processes. North-Holland Publishers, Amsterdam (1952)
158. de Guzman, J.: Ann. Soc. Espan. Fis. Quim. **11**, 353 (1913)
159. de Reaumur, R.: Memoires l' Academie des Sciences, Paris (1739)
160. Debye, P., Menke, H.: Ergebnisse der technischen Röntgenkunde **11** (1931)
161. Defay, R., Prigogine, I., Bellemans, R., Everett, D.H.: Surface Tension and Adsorption. Longmans, London (1966)
162. Dehlinger, U.: Theoretische Metallkunde. Springer, Berlin (1955)
163. Demkina, L.I.: Investigation of the Dependence of Glass Properties on Composition. Gosizdat, Oboronprom Publishers, Moscow (1958, in Russian)
164. Demo, P., Kozicek, Z.: Phys. Rev. **B 48**, 3620 (1993)
165. Deryaguin, B.V., Fedosseev, V.D.: Carbon **11**, 299 (1973)
166. Dietzel, A.: Glastech. Ber. **22**, 212 (1949)
167. Dietzel, A.: Silikattechnik **7**(7), 318 (1956)
168. Dietzel, A., Brückner, R.: Glastech. Ber. **28**, 455 (1955)
169. Dietzel, A., Brückner, R.: Glastech. Ber. **30**, 73 (1957)
170. Dietzel, A., Deeg, E.: Glastech. Ber. **30**, 282 (1957)
171. Dietzel, A., Poegel, H.J.: Naturwissenschaften **40**, 604 (1953)
172. Dietzel, A., Wiekert, H.: Glastech. Ber. **29**, 1 (1956)
173. Dobreva, A.: Non-steady state effects in the kinetics of crystallization of polymer melts. Ph.D. thesis, Bulgarian Academy of Sciences, Sofia (1992)
174. Dobreva, A., Gutzow, I.: J. Cryst. Res. Tech. **20**, 863 (1991)
175. Dobreva, A., Gutzow, I.: J. Non Cryst. Solids **162**, 1, 13 (1993)
176. Dobreva, A., Gutzow, I.: Bulg. Chem. Commun. **27**, 103 (1994)
177. Dobreva, A., Gutzow, I.: J. Non Cryst. Solids **162**, 235 (1997)
178. Doi, M.: J. Polym. Sci. (Polym. Phys.) **18**, 1005 (1980)
179. Donth, E.-J.: Glasübergang. Wissenschaftliche Taschenbücher Mathematik-Physik, Bd. 271, Akademie-Verlag, Berlin (1981)
180. Doolittle, H.: J. Appl. Phys. **22**, 1471 (1951); **23**, 236 (1952)
181. Dubey, K.S., Ramanchandrao, P.: Inter. J. Rapid Solid. **11**, 1 (1984/1985)
182. Echt, O., Recknagel, E. (eds.): Small Particles and Inorganic Clusters, ISSPIC5, September 1990; Springer Verlag, 1991; see also the Proceedings of the previous symposia on small particles and inorganic clusters

183. Ehrenfest, P.: Commun. Leiden Univ. **20**(Suppl. b75), 628 (1933)
184. Eitel, W.: Thermochemical Methods in SilicateInvestigation. Rutgers University Press, New Brunswick (1952)
185. Eitel, W.: The Physical Properties of the Silicates. University of Chicago Press, Chicago (1954)
186. Eitel, W., Pirani, M., Scheel, K.: Glastechnische Tabellen. Springer, Berlin (1932)
187. Einstein, A.: Annalen der Physik **17**, 549 (1905)
188. Einstein, A.: Verh. Dtsch. Phys. Ges. **16**, 820 (1914)
189. Eldrigde, M.D., Madden, P.A., Frenkel, D.: Nature **365**, 35 (1993)
190. Erofeev, B.V.: Dispersity of solid phases in connection with the kinetics of their formation. In: Collected Works of the Belorussian Academy of Sciences, Institute of Chemistry. Academy of Sciences Press, Minsk, p. 13 (1956, in Russian)
191. Everett, D.H. (ed.): Colloid Science, vol. 2. Chemical Society, Burlington House, London (1975)
192. Evstropyev, K.S.: Crystallite theory of the structure of glass. In: Lebedev, A.A. (ed.) Structure of Glass, Proc. Conf. on Glass, Leningrad, Nov. 1953, p. 9. Soviet Acad., Moscow-Leningrad (1955)
193. Eyring, H.: J. Chem. Phys. **4**, 283 (1936)
194. Fajans, K.: Ceram. Age **54**, 288 (1949)
195. Fanderlik, I., Prodhomme, L.: Verres et. Refract. **27**, 97 (1973)
196. Farkas, L.: Z. Phys. Chem. **125**, 236 (1927)
197. Farley, F.J.M.: The theory of the condensation of supersaturated ion-free vapour. Proc. R. Soc. (Lond.) **A 212**, 530 (1952)
198. Feder, J., Russell, K.C., Lothe, J., Pound, G.M.: Adv. Phys. **15**, 117 (1966)
199. Feder, J.: Fractals. Plenum Press, New York/London (1988)
200. Feenstra, T.P., de Bryun, P.L.: J. Colloid Interface Sci. **84**, 66 (1981)
201. Feenstra, T.P., van Straaten, H.A., de Bryun, P.L.: J. Colloid Interface Sci. **80**, 255 (1981)
202. Feltz, A.: Amorphe und Glasartige Anorganische Festkörper. Akademie-Verlag, Berlin (1983)
203. Fermi, E.: Thermodynamics. Prentice-Hall, New York (1937)
204. Ferry, J.D.: Viscoelastic Properties of Polymers. Wiley, New York (1961)
205. Fichtenholz, G.M.: A Course in Differential and Integral Calculus, vol. 1. Nauka Publishers, Moscow (1966, in Russian)
206. Filipovich, V.N.: Initial stages of the crystallization of glasses. In: The Vitreous State, p. 9. Academy of Sciences Publishers USSR, Moscow-Leningrad (1963, in Russian)
207. Filipovich, V.N.: The crystallization of glass-ceramics. In: Structural Changes of Glasses at Elevated Temperatures, p. 30. Nauka Publishers, Moscow/Leningrad (1965, in Russian)
208. Filipovich, V.N.: Proceedings of the 3rd International Otto-Schott-Kolloquium, Jena, 1987; Wissenschaftliche Zeitschrift der Friedrich-Schiller-Universität Jena, Naturwissenschaftliche Reihe **36**, 809 (1987)
209. Finney, G.L., Bernal, J.D.: Nature **213**, 1079 (1967)
210. Finney, G.L.: Structural modelling of non-crystalline materials In: Gaskall, P.H. (ed.) The Structure of Non-crystalline Materials. Symposium Proceedings, Cambridge, England, p. 35. Taylor and Francis, London (1977)
211. Fischer, E.W.: Naturforschung **12a**, 753 (1957)
212. Fisher, I.Z.: Statistical Theory of Liquids. State Publishing House Physico-Mathematical Literature, Moscow (1961, in Russian)
213. Fletcher, N.: J. Chem. Phys. **29**, 572 (1958)
214. Fletcher, N.: The Physics of Rainclouds. Cambridge University Press, Cambridge (1962)
215. Flory, P.J.: J. Am. Chem. Soc. **58**, 1877 (1936)
216. Flory, P.J.: J. Am. Chem. Soc. **62**, 1057 (1940)
217. Flory, P.J.: J. Chem. Phys. **10**, 51 (1942)
218. Flory, P.J.: Principles of Polymer Chemistry. Cornell University Press, Ithaca (1943)
219. Flory, P.J.: J. Chem. Phys. **17**, 223 (1949)
220. Flory, P.J.: Proc. R. Soc. **A234**, 60 (1956)

221. Flory, P.J.: Statistical Mechanics of Chain Molecules. Moscow, Mir (1971, in Russian)
222. Fokin, V.M., Kalinina, A.M., Filipovich, V.N.: Fiz. i Khim. Stekla **3**, 129 (1977)
223. Fokin, V.M., Kalinina, A.M., Filipovich, V.N.: Fiz. i Khimia Stekla **6**, 148 (1980)
224. Fokin, V.M., Zanotto, E.D., Yuritsyn, N.S., Schmelzer, J.W.P.: Homogeneous Crystal Nucleation in Silicate Glasses: A Forty Years Perspective. J. Non Cryst. Solids **352**, 2681 (2006)
225. Fowler, R.H., Guggenheim, E.A.: Statistical Thermodynamics. Cambridge University Press, Cambridge (1939)
226. Fox, T.J., Flory, P.J.: J. Appl. Phys. **21**, 581 (1950)
227. Frank, F.C.: Discuss. Faraday Soc. **33**, 40 (1949)
228. Frank, F.C.: Proc. R. Soc. (Lond.) **A215**, 43 (1952)
229. Frank, F.C., Tosi, M.: Proc. R. Soc. (Lond.) **A 263**, 323 (1961)
230. Frank, F.C., van der Merwe, J.H.: Proc. R. Soc. (Lond.) **A 198**, 205 (1949)
231. Frank-Kamenetzki, D.A.: Plasma: The Fourth State of Aggregation of Matter. Gosatomizdat, Moscow (1963, in Russian)
232. Frenkel, Y.I.: The Theory of Solid and Liquid Bodies. Russian Academy of Sciences, Leningrad (1934, in Russian)
233. Frenkel, Y.I.: The Kinetic Theory of Liquids. Oxford University Press, Oxford (1946)
234. Frenkel, Y.I.: Uspechi Fiz. Nauk **32**, 294 (1947)
235. Freudenthal, A.M.: Inelastic Behaviour of Engineering Materials and Structures. Wiley, New York (1955)
236. Frisch, K.L., Carlier, C.C.: J. Chem. Phys. **54**, 4326 (1971)
237. Frischat, G.H.: Ionic Diffusion in Oxide Glasses. Transtech Publications, Aedermannsdorf (1975)
238. Frischauer, L.: Sur une influence du radium sur la vitesse de cristallisation. Comptes Rendus Acad. Sci. Paris **148**, 1251 (1909)
239. Fulcher, G.S.: J. Am. Chem. Soc. **77**, 3701 (1925)
240. Gaskall, P.H. (ed.): The Structure of Non-crystalline Materials. Symposium Proceedings, Cambridge, England. Taylor and Francis, London (1977)
241. Gaskall, P.H.: Novel Aspects of the Structure of Glasses, Proceedings 16-th International Congress on Glass, Madrid, 1992. Bull. Soc. Esp. Ceram. Vid. **31c**, 1, 25 (1992)
242. Gaskall, P.H., Gibson, J.M., Howie, A.: Construction of a Polytetrahedral Model for Amorphous Tetrahedral Materials. In: Gaskall, p. 181 (1977)
243. Gattef, E., Dimitriev, Y.: Phil. Mag. **B 40**, 231 (1979)
244. Gattef, E., Dimitriev, Y.: Phil. Mag. **43**, 331 (1981)
245. Gattef, E., Dimitriev, Y.: Internat. J. Electron. **62**, 757 (1987)
246. Gebhardt, W., Krey, U.: Phasenübergänge und kritische Phänomene, Braunschweig (1980)
247. Geil, P.: Polymer Single Crystals. Interscience Publishers, New York (1963)
248. Gerngross, O., Herrmann, K., Abitz, W.: Z. Phys. Chem. (Leipz.) **B 10**, 371 (1930)
249. Gibbs, J.W.: On the equilibrium of heterogeneous substances. Trans. Conn. Acad. Sci. **3**, 108, 343 (1875–78); see also: Gibbs, J.W.: The collected works. Thermodynamics, vol. 1. New York/London/Toronto (1928)
250. Gibbs, J.H.: Nature of the glass-transition and the vitreous state. In: Mackenzie, J.P. (ed.) Modern Aspects of the Vitreous State. Butterworths, London (1960)
251. Gibbs, J.H., DiMarzio, E.A.: J. Chem. Phys. **28**, 370 (1958)
252. Gibson, G.E., Giauque, W.F.: J. Am. Chem. Soc. **45**, 93 (1923)
253. Giessen, B.C., Wagner, C.N.J.: Structure and properties of non-crystalline metallic alloys produced by rapid quenching. In: Beer, S.Z. (ed.) Liquid Metals, p. 633. Marcel Decker, New York (1972)
254. Gindt, R., Kern, R.: Ber. Bunsenges. für Phys. Chem. **72**, 459 (1968)
255. Glasstone, S., Laidler, H.J., Eyring, H.: The Theory of Rate Processes. Princeton University Press, New York/London (1941)
256. Gmelins Handbuch der anorganischen Chemie, 8. Auflage, Nr. 10, Verlag Chemie GmbH (1942)

257. Gmelins Handbuch der anorganischen Chemie, 8. Auflage, Nr. 17, Verlag Chemie GmbH 1952
258. Goethe, J.W.: Die Schriften zur Naturwissenschaft, Bd. 9, H. Böhlhaus Verlag, Weimar, 1954, p. 335
259. Goetz, J., Hoebbel, D., Wieker, W.: J. Non Cryst. Solids **20**, 413 (1977)
260. Goetz, J., Mason, C.R., Casteliz, L.M.: Crystallization of lead silicate glass as studied by chromatographic separation of the anionic constituents. In: Douglas, R.W., Ellis, B. (eds.) Amorphous Materials. Proceedings of the 3rd International Conference on Physics of Non-crystalline Solids, p. 317. Sheffield, 1970, Wiley Interscience, London (1972)
261. Götze, W.: Z. Phys. Chem. NF **156**, 3 (1988); Götze, W., Sjögren, L.: Rep. Prog. Phys. **55**, 241 (1992)
262. Goldschmidt, V.M.: Skrifter Norske Videnskaps Akad. (Oslo) I, Mathematisch-Naturwiss. Klasse **1**, 7 (1926)
263. Goldstein, M., Simha, R. (eds.): The Glass Transition and the Nature of the Glassy State, vol. 279. Annals New York Academy of Sciences, New York (1976)
264. Goodman, C.H.L.: Nature **257**, 370 (1975)
265. Goodman, C.H.L.: Mixed clusters, viscous melts and glass-formation. In: Gaskall, p. 197 (1977)
266. Gordon, J.M., Gibbs, J.H., Fleming, P.D.: J. Chem. Phys. **65**, 2771 (1976)
267. Gorski, N.: Z. Phys. Chem. (Leipzig) **270**, 817 (1989)
268. Grantcharova, E., Gutzow, I.: J. Non Cryst. Solids **81**, 99 (1986)
269. Grantcharova, E., Gutzow, I.: Cryst. Res. Technol. **25**, 991 (1990)
270. Grantcharova, E., Gutzow, I.: Vapour pressure of glasses: a thermodynamic and kinetic approach. In: Nicoletti, F. (ed.) Proceedings 2nd Conference on Science and Technology of Glass, Venice, Italy, 1993, Venice (1994)
271. Grantcharova, E., Avramov, I., Gutzow, I.: Thermochimica Acta **102**, 249 (1986)
272. Grantcharova, E., Avramov, I., Gutzow, I.: Naturwissenschaften **73**, 95 (1986)
273. Green, H.S.: The Molecular Theory of Fluids. North-Holland, Amsterdam/Interscience Publishers Inc., New York (1952)
274. Greer, A.L.: Mater. Sci. Eng. **97**, 285 (1988)
275. Greer, A.L. et al.: J. Cryst. Growth **99**, 38 (1990)
276. Greet, R.J., Turnbull, D.: J. Chem. Phys. **47**, 2185 (1967)
277. Großberg, A.Y., Chochlov, A.R.: Statistical Physics of Chain Molecules. Nauka, Moscow, (1989, in Russian)
278. Grunze, H.: Silikattechnik **7**, 143 (1956)
279. Grudeva, S., Kanev, M.: Vacuum **10**, 599 (1986)
280. Grunze, H., Thilo, E.: Sitzungsberichte der Deutschen Akademie der Wissenschaften, Kl. Mathematik-Allgemeine Naturwissenschaften **5**, p. 1 (1953); Grunze, H., Thilo, E.: Paper Chromatography of Condensed Phosphates. Akademie, Berlin (1955)
281. Guggenheim, E.A.: Mixtures. Oxford University Press, Oxford (1952)
282. Gul, N.E., Kulesnev, V.N.: In: Structure and Mechanical Properties of Polymers. High School Publishers, Moscow (1966, in Russian)
283. Gunton, J.D., San Miguel, M., Sahni, P.S.: The dynamics of first-order phase transitions. In: Domb, C., Lebowitz, J.L. (eds.) Phase Transitions and Critical Phenomena, vol. 8. Academic, London/New York (1983)
284. Güntherodt, H.-J., Beck, H. (eds.): Metallic Glasses. Springer, Berlin/Heidelberg/New York (1981)
285. Gupta, P.K., Cooper, A.R.: Topologically Disordered Networks of Rigid Polytops. Proceedings of the 16-th International Congress on Glass, Madrid, 1992. Bol. Sociedad Espanola de Ceram. Vidio **31c**(3), 15 (1992)
286. Gusak, A.M. et al.: Diffusion-Controlled Solid-State Reactions. WILEY-VCH, Berlin-Weinheim (2010)
287. Gutzow, I.: Z. Anorgan. Allg. Chem. **302**, 18, 259 (1959)
288. Gutzow, I.: Z. Phys. Chem. (Leipzig) **221**, 152 (1962)
289. Gutzow, I.: Commun. Inst. Phys. Chem. (Bulgarian Academy of Sciences) **2**, 31 (1962)

290. Gutzow, S.: Technology of Glass. Tekhnika Publishers, Sofia (1963, in Bulgarian)
291. Gutzow, I.: Relationship between the Structure of a Substance in the Glassy State and the Zero-Point Entropy. In: Porai-Koshits, E.A. (ed.) Proceedings of the IV-th All-Union Conference on the Glassy State, Leningrad, 1964. The Structure of Glass, vol. 6, part 1, p. 55. Consultants Bureau, New York (1966)
292. Gutzow, I.: Crystallization Processes in Viscous Glass-forming Melts. Doctoral thesis, Bulgarian Academy of Sciences, Sofia (1970)
293. Gutzow, I.: Z. Phys. Chem. (Leipzig) **81**, 195 (1972)
294. Gutzow, I.: The thermodynamic functions of super-cooled glass-forming liquids and the temperature dependence of their viscosity. In: Douglas, R.W., Ellis, B. (eds.) Amorphous Materials, Proceedings of the Third International Conference, Sheffield, 1970, p. 159. Wiley, London (1972)
295. Gutzow, I.: Glastech. Ber. **46**, 219 (1973)
296. Gutzow, I.: Compte Rend. Acad. Sci. Bulg. Chim. phys. **27**(7), 945 (1974)
297. Gutzow, I.: Fiz. i. Khim. Stekla **1**, 431 (1975)
298. Gutzow, I.: Thermodynamical and model-statistical treatment of the glassy solidification. In: Frischat, G. (ed.) The Physics of Non-crystalline Solids, Proceedings 4-th International Conference Clausthal, 1976, p. 356. Transtech, Aedermansdorf (1977)
299. Gutzow, I.: Mechanism of crystallization in undercooled melts and glass-forming systems. In: Kalwis, E., Scheel, H.J. (eds.) Crystal Growth and Materials. North-Holland, Amsterdam (1977)
300. Gutzow, I.: J. Cryst. Growth **42**, 15 (1977)
301. Gutzow, I.: J. Cryst. Growth **48**, 569 (1979)
302. Gutzow, I.: Proceedings of the 1-st International Otto-Schott Kolloquium, Wissenschaftliche Zeitschrift der Friedrich-Schiller Universität Jena, Mathematisch-Naturwissenschaftliche Reihe **28**, 243 (1979)
303. Gutzow, I.: Contemp. Phys. **21**, 121, 243 (1980)
304. Gutzow, I.: J. Non Cryst. Solids **45**, 301 (1981)
305. Gutzow, I.: Thermodynamic properties of glass-forming systems. In: Borissov, M., Kirov, N., Vavrek, A. (eds.) Disordered Systems and New Materials, Proceedings of the V-th International School on Condensed Matter Physics, Varna, Bulgaria, 19–27 September, 1988, p. 11. World Scientific, Singapore/New Jersey/London/Hong Kong (1989)
306. Gutzow, I., Avramov, I.: J. Non Cryst. Solid **16**, 128 (1974)
307. Gutzow, I., Avramov, I.: Thin Solid Films **85**, 203 (1981)
308. Gutzow, I., Dobreva, A.: J. Non Cryst. Solids **129**, 266 (1991)
309. Gutzow, I., Dobreva, A.: Kinetics of nucleation and crystallization in polymer melts. In: Proceedings of the Atlanta Meeting of the American Ceramic Society on Nucleation and Crystallization in Glasses and Liquids, Atlanta, July, 1992, p. 151, American Ceramic Society, Columbus, Ohio (1992)
310. Gutzow, I., Dobreva, A.: Polymer **33**, 451 (1992)
311. Gutzow, I., Grantcharova, E.: Commun. Dep. Chem. (Bulgarian Academy of Sciences) **18**(1), 102 (1985)
312. Gutzow, I., Kashchiev, D.: Commun. Dep. Chem. (Bulgarian Academy of Sciences) **3**, 645 (1970)
313. Gutzow, I., Kashchiev, D.: The kinetics of overall crystallization of undercooled melts in terms of the non-steady state theory of nucleation. In: Hench, L.L., Freiman, S.W. (eds.) Kinetics of Overall Crystallization in Terms of the Non-Steady State Theory of Nucleation. Advances in Nucleation and Crystallization of Glasses, p. 116. American Ceramic Society, Columbus Ohio (1971)
314. Gutzow, I., Konstantinov, I.: Comptes Rend. Acad. Sci. Bulg. **23**, 1107 (1970)
315. Gutzow, I., Pancheva, E.: Krist. Tech. **11**, 793 (1976)

316. Gutzow, I., Penkov, I.: Proceedings of the 3-rd International Otto-Schott Kolloquium, Wissenschaftliche Zeitschrift Friedrich-Schiller Universität Jena, Naturwiss. Reihe **36**, 907 (1987)
317. Gutzow, I., Slavtschev, P.: Kristall und Technik **6**, 593 (1971)
318. Gutzow, I., Toschev, S.: Kristall und Technik **3**, 485 (1968)
319. Gutzow, I., Toschev, S.: J. Cryst. Growth **7**, 215 (1970)
320. Gutzow, I., Toschev, S.: The kinetics of nucleation and the formation of glass-ceramic materials. In: Hench, L.L., Freiman, S.W. (eds.) Advances in Nucleation and Crystallization of Glasses, p. 10. American Ceramic Society, Columbus Ohio (1971)
321. Gutzow, I., Toschev, S., Marinov, M., Popov, E.: Kristall und Technik **3**, 337 (1968)
322. Gutzow, I., Popov, E., Toschev, S., Marinov, M.: Crystallization of sodium metaphosphate glass on metallic condensation cores with a cubic lattice. In: Growth of Crystals; Proceedings of the 7-th International Congress on Crystallography, Moscow, July 1966, vol. 8, part 2, p. 95. Nauka, Moscow (1968, in Russian)
323. Gutzow, I., Streltzina, M.W., Popov, E.: Commun. Dep. Chem. (Bulgarian Academy of Sciences) **1**, 19 (1968)
324. Gutzow, I., Razpopov, A., Kaischew, R.: Phys. Stat. Solidi **a1**, 159 (1970)
325. Gutzow, I., Konstantinov, I., Kaischew, R.: Commun. Dep. Chem. (Bulgarian Academy of Sciences) **5**, 433 (1972)
326. Gutzow, I., Razpopov, A., Pancheva, E., Kaischew, R.: Krist. Tech. **7**, 769 (1972)
327. Gutzow, I., Kitova, S., Marinov, M., Tzakin, L.: Glastech. Ber. **49**, 144 (1976)
328. Gutzow, I., Zlateva, E., Alyakov, S., Kovatscheva, T.: J. Mater. Sci. **12**, 1190 (1977)
329. Gutzow, I., Donchev, V., Panchev, E., Dimov, K.: J. Polym. Sci. (Phys.) **16**, 1155 (1978)
330. Gutzow, I., Kashchiev, D., Avramov, I.: J. Non Cryst. Solids **73**, 477 (1985)
331. Gutzow, I., Avramov, I., Kästner, K.: J. Non Cryst. Solids **123**, 97 (1990)
332. Gutzow, I., Dobreva, A., Schmelzer, J.: J. Mater. Sci. **28**, 890 (1993)
333. Gutzow, I., Dobreva, A., Schmelzer, J.: J. Mater. Sci. **28**, 901 (1993)
334. Gutzow, I., Pascova, R., Karamanov, A., Schmelzer, J.: Kinetics of Surface Induced Sinter Crystallization, Proceedings of the V-th Otto-Schott-Colloquium, Jena, Germany, July 1994
335. Gutzow, I., Pye, D., Dobreva, A.: J. Non Cryst. Solids **180**, 107, 117 (1994)
336. Gutzow, I., Pascova, R., Karamanov, A., Schmelzer, J.: Kinetics of Surface Induced Sinter Crystallization, Proceedings of the VI-th International Otto-Schott Colloquium, Jena, July, 1994
337. Gutzow, I., Pascova, R., Schmelzer, J.W.P.: The Generic Phenomenological Theory of Vitreous Matter: Principles and Ideas. Springer (2013, in preparation)
338. Haase, R.: Thermodynamik der Mischphasen. Springer, Berlin (1956)
339. Haase, R.: Thermodynamik der Irreversiblen Prozesse. Verlag D. Steinkopf, Darmstadt (1963)
340. Haberland, H. (ed.): Clusters of Atoms and Molecules – Theory, Experiment, and Clusters of Atoms. Springer, Berlin/Heidelberg (1994)
341. Hackenberg, D., Scholze, H.: Glastech. Ber. **43**, 488 (1970)
342. Haeckel, E.: Kristallseelen-Studien über das anorganische Leben. A. Kröner-Verlag, Leipzig (1917)
343. Hägg, G.: J. Chem. Phys. **3**, 42 (1935)
344. Halpern, V.: Br. J. Appl. Phys. **18**, 163 (1967)
345. Hammel, J.J.: J. Chem. Phys. **46**, 2234 (1967)
346. Hänggi, P., Talkner, P., Borkovec, M.: Rev. Mod. Phys. **62**, 251 (1980)
347. Hanszen, K.J.: Z. Phys. **157**, 523 (1960)
348. Harvey, K.B., Boase, C.A.: Phys. Chem. Glass. **28**, 11 (1987)
349. Harvey, K.B., Litke, C.D., Boas, C.A.: Phys. Chem. Glass. **27**, 15 (1986)
350. Haynes, J.M.: Porous media-structures and models. In: Everett, D.H. (ed.) Colloid Science, vol. 2, p. 101. Chemical Society, Burlington House, London (1975)
351. Hegel, G.W.F.: (1817) Encyclopadie der philosophischen Wissenschaft. Heidelberg. Translated by William Wallace, The Encyclopedia of Philosophical Sciences. Oxford University Press, Oxford (1892)

352. Heinicke, G.: Tribochemistry. Akademie-Verlag, Berlin (1984)
353. Heinrich, M., Ulbricht, H.: Mechanik der Kontinua, Wissenschaftliche Taschenbücher Mathematik-Physik, Bd. 128. Akademie-Verlag, Berlin (1981)
354. Henderson, D.W.: J. Non Cryst. Solids **30**, 301 (1979)
355. Hicks, F.G.: Science **155**, 459 (1966)
356. Hilbert, D., Cohn-Vossen, S.: Anschauliche Geometrie. Springer, Berlin (1932)
357. Hill, T.L.: J. Phys. Chem. **56**, 526 (1952)
358. Hill, T.L.: Statistical Mechanics. Principles and Selected Applications. McGraw Hill, New York/Toronto/London (1956)
359. Hill, W.L., Faust, G.T., Hendricks, S.B.: J. Am. Chem. Soc. **65**, 794 (1943)
360. Hillig, W.B.: A Theoretical and experimental investigation of nucleation leading to uniform crystallization of glass. In: Reger, M.K., Smith, G., Insley, A. (eds.) Symposium on Nucleation and Crystallization in Glasses and Melts. American Ceramic Society, Columbus, Ohio (1962)
361. Hillig, W.B.: Acta Met. **14**, 1868 (1966)
362. Hillig, W., Turnbull, D.: J. Chem. Phys. **24**, 914 (1956)
363. Hinz, W.: Silikate: Grundlagen der Silikatwissenschaft und Silikattechnik, Bd. 1, S.158–S.171. Verlag für Bauwesen, Berlin (1970)
364. Hirai, N., Eyring, H.: J. Appl. Phys. **29**, 810 (1958)
365. Hirai, N., Eyring, H.: J. Polym. Sci. **37**, 51 (1959)
366. Hirschfelder, J.O., Curtiss, C.F., Bird, R.B.: Molecular Theory of Gases and Liquids. Wiley, New York/Chapman and Hall, London (1954)
367. Hirth, J.P.: Acta Met. **7**, 755 (1959)
368. Hirth, J.P., Pound, G.M.: Condensation and Evaporation. Pergamon Press, London (1963)
369. Hoare, M.R.: Stability and Local Ordering in Simple Amorphous Packings. In: Goldstein, M., Simha, R. (eds.) The Glass Transition and the Nature of the Glassy State, vol. 279, p. 186. Annals New York Academy of Sciences, New York (1976)
370. Hoare, M.R., Barker, J.A.: Tammann revisited: cluster theories of glass-transition with special Reference to Soft Packings. In: Gaskall, P.H. (ed.) The Structure of Non-crystalline Materials. Symposium Proceedings, Cambridge, England, p. 175. Taylor and Francis, London (1977)
371. Hoare, M.R., Pal, P.: Adv. Phys. **20**, 161 (1971)
372. Hodgdon, J.A., Stillinger, F.H.: Phys. Rev. **E48**, 207 (1993)
373. Hodge, I.M.: J. Non Cryst. Solids **169**, 211 (1994)
374. Hodgson, A.W.: Adv. Colloid Interface Sci. **21**, 303 (1984)
375. Hoffman, J.D.: J. Chem. Phys. **29**, 1192 (1958)
376. Hoffman, J.D.: SPE Trans. **4**(6), 1 (1964)
377. Hollomon, D.N., Turnbull, D.: Nucleation at phase transitions. In: Chalmers, B. (ed.) Progress of Metal Physics, vol. 4, p. 304. Butterworths, Pergamon Press, London (1953)
378. Honigmann, B.: Gleichgewichts- und Wachstumsformen von Kristallen. Steinkopff, Darmstadt (1958)
379. Hoover, W.G., Ree, F.H.: J. Chem. Phys. **18**, 380 (1968)
380. Hosemann, R.: Z. Phys. **113**, 751 (1939)
381. Houwink, R.: Elastizität, Plastizität und Struktur der Materie. Verlag Th. Steinkopff, Dresden (1957)
382. Hu, H., Ma, F., Mackenzie, J.D.: J. Non Cryst. Solids **55**, 169 (1983)
383. Hübert, Th., Müller, R., Kirsch, M.: Silikattechnik **39**, 183 (1988)
384. Hülsenberg, D.: Elektrotechnische Verfahren für Glass und Keramik, Sitzungsberichte der Sächsischen Akademie der Wisssenschaften zu Leipzig, Mathem.-Naturwissenschaftliche Klasse, Bd. 124, Heft 1. Akademie Verlag, Berlin (1993)
385. Hunt, A.: J. Non Cryst. Solids **160**, 183 (1993)
386. Iler, R. K.: The Chemistry of Silica: Solubility, Polymerization, Colloid and Surface Properties and Biochemistry of Silica. Wiley, Chichester (1979)
387. Ivanov, D.Y.: Critical Behavior of Non-Ideal Systems. WILEY-VCH, Berlin-Weinheim (2008)

388. Ivanova, Z., Boncheva-Mladenova, Z.: Annuaire Chem. Technol. Inst. Sofia **26**(4), 61 (1979)
389. Izard, J.O.: J. Phys. Chem. **14**, 144 (1974)
390. Izard, J.O.: Phil. Mag. **36**, 817 (1977)
391. Jäckle, J.: Phil. Mag. **B 44**, 533 (1981)
392. Jäckle, J.: Rep. Prog. Phys. **49**, 171 (1986)
393. Jackson, K.A.: Liquid metals and solidification. In: Doremus, R.H., Roberts, B.W., Turnbull, D. (eds.) Normal Mode of Crystal Growth. Growth and Perfection of Crystals, p. 319. Wiley, New York (1958)
394. Jackson, K.A.: J. Cryst. Growth **50**, 13 (1969)
395. Jackson, K.A.: Mater. Sci. Eng. **65**, 7 (1984)
396. Jackson, K.A.: Kinetic Processes: Crystal Growth, Diffusion, and Phase Transitions in Materials. WILEY-VCH, Weinheim (2004)
397. Jacobs, P., Tompkins, F.: Classification and theory of reactions in the solid state. In: Garner, W.E. (ed.) Chemistry of the Solid State. Butterworths, Lomdon (1955)
398. Jackson, K.A., Uhlmann, D.R., Hunt, J.D.: J. Cryst. Growth **1**, 1 (1967)
399. Jahn, W., Thilo, E.: Z. Anorg. Chem. **274**, 72 (1953)
400. James, P.F.: Phys. Chem. Glass. **15**, 95 (1974)
401. James, P.: J. Mater. Sci. **10**, 1802 (1975)
402. James, P.F.: Transient Nucleation. In: Simmons, G.H., Uhlmann, D.R., Beal, G.H. (eds.) Advances in Ceramics. Nucleation and Crystalliation in Glasses, vol. 4, p. 5. American Ceramic Society, Columbus, Ohio (1982)
403. Jarič, M., Benneman, K.H.: Phys. Rev. **A27**, 1228 (1983)
404. Jarič, M.: Phys. Rev. **A28**, 1179 (1983)
405. Jayanth, C.S., Nash, P.: J. Mater. Sci. **24**, 3041 (1989)
406. Jena, P.S., Khanna, S.N., Rao, B.K.: Physics and Chemistry of Finite Systems: From Clusters to Crystals, vol. 1. Kluwer Academic Publishers, Dordrecht/Boston/London (1992)
407. Jenckel, E.: Rheology of non-Newtonion flow. In: Stuart, A.A. (ed.) Die Physik der Hochpolymere, vol. 3, p. 620. Springer, Berlin (1955)
408. Jenckel, E., Gorke, K.: Z. Naturforsch. **7a**, 630 (1952)
409. Jones, G.O., Simon, F.: Endeavour **8**, 174 (1949)
410. Johari, G.P.: Phil. Mag. **B 24**, 41 (1980)
411. Johari, G.P.: J. Chim. Phys. **89**, 2073 (1992)
412. Johnson, W.A., Mehl, R.F.: Reaction kinetics in processes of nucleation and growth. Trans. Am. Inst. Min. Metall. Eng. **135**, S. 416-458 (1939)
413. Jost, K.H.: Macromol. Chem. **55**, 203 (1962)
414. Jost, K.H., Wodtcke, F.: Macromol. Chem. **53**, 1 (1962)
415. Kahlweit, M.: Z. Phys. Chem. (NF) **28**, 245 (1961)
416. Kaischew, R.: Z. Phys. Chem. **40**, 273 (1938)
417. Kaischew, R.: Bull. Acad. Bulg. Sci. (Phys) **1**, 100, 191 (1952)
418. Kaischew, R.: Acta Phys. Hung. **8**, 75 (1957)
419. Kaischew, R.: On the Further Development of the Molecular-Kinetic Theory of Crystal Growth. In: Rost Kristallov, vol. 5. Nauka Publishers, Moscow (1965, in Russian)
420. Kaischew, R.: J. Cryst. Growth **51**, 643 (1981)
421. Kaischew, R., Budewski, E.: Contemp. Phys. **8**, 489 (1967)
422. Kaischew, R., Mutaftschiev, B.: Bull. Inst. Chim. Bulg. Acad. Sci. **7**, 177 (1959)
423. Kaischew, R., Krastanov, K.: Z. Phys. Chem. **B 23**, 158 (1933)
424. Kaischew, R., Stoyanov, S.: Commun. Dep. Chem. (Bulgarian Academy of Sciences) **2**, 127 (1969)
425. Kaischew, R., Stranski, I.N.: Z. Phys. Chem. **A 170**, 295 (1934); **B26**, 317 (1934)
426. Kaischew, R., Budewski, E., Malinowski, J.: Z. Phys. Chem. **204**, 248 (1955)
427. Kalinina, A.M., Fokin, V.M., Filipovich, V.N.: Fiz. Khim. Stekla **2**, 298 (1976)
428. Kanai, E., Satoh, T.: J. Phys. Chem. (Japan) **9**, 117 (1954); **10**, 1002 (1955)
429. Kanno, H.: J. Non Cryst. Solids **37**, 203 (1980)
430. Kantrowitz, A.: J. Chem. Phys. **19**, 1097 (1951)

431. Karamanov, A., Gutzow, I., Bogdanov, B., Chomakov, I., Kostov, A.: Glastech. Ber. (Glass Sci. Technol.) **67**, 202, 227 (1994)
432. Karapetyanz, M.H.: Chemical Thermodynamics. Chemistry State Press, Moscow (1975, in Russian)
433. Kaseev, S.A.: Kinetics in Application to Metallurgy. State Publishers Oboronnoi Promyschlennosti, Moscow (1956, in Russian)
434. Kashchiev, D.: Surf. Sci. **14**, 209 (1969); **18**, 389 (1969)
435. Kashchiev, D.: J. Cryst. Growth **13–14**, 128 (1972)
436. Kashchiev, D.: J. Chem. Phys. **76**, 5098 (1982)
437. Kashchiev, D.: Cryst. Res. Technol. **19**, 1413 (1984)
438. Kashchiev, D.: Krist. Tech. **20**, 723 (1985)
439. Kashchiev, D.: Nucleation: Basic Theory and Applications. Butterworth-Heinemann, Oxford (2000)
440. Kauzmann, W.: Chem. Rev. **43**, 219 (1948)
441. Kawasaki, K.: Enomoto, Y.: Physica **A 150**, 463 (1988)
442. Keinath, S.E., Miller, R.L., Rieke, J.K. (eds.): Order in the Amorphous "State" of Matter. Plenum Press, New York/London (1987)
443. Keller, A.: Phil. Mag. **2**, 1171 (1957)
444. Keller, A.: Macromol. Chem. **34**, 1 (1959)
445. Keller, A.: Chain folded crystallization of polymers from discovery to present day: a personalized journey. In: Chambers, R.G., Enderby, J.E., Hilger, A. (eds.) Sir Charles Frank: An 80s Birthday Tribute, p. 256. Hilger Publications, Bristol (1991)
446. Kelley, E.C.: Education for What is Real. Harper and Brothers, New York (1947)
447. Kelley, K.H.: J. Am. Chem. Soc. **51**, 779 (1929)
448. Kelton, K.F., Greer, A.L.: J. Non Cryst. Solids **79**, 295 (1986)
449. Kelton, K.F., Greer, A.L.: Phys. Rev. **B38**, 10089 (1988)
450. Kelton, K.F., Greer, A.L.: Nucleation in Condensed Matter: Applications in Materials and Biology. Elsevier, (2010)
451. Kelton, K.F., Greer, A.L., Thompson, C.V.: J. Chem. Phys. **72**, 6261 (1983)
452. Kessler, D.A., Koplik, J., Levine, H.: Adv. Phys. **37**, 255 (1988)
453. Kirkaldy, J.S., Young, D.J.: Diffusion in the Condensed State. The Institute of Metals, London (1987)
454. Kirkwood, J.: J. Chem. Phys. **18**, 380 (1950)
455. Kirkwood, J.G., Buff, F.P.: J. Chem. Phys. **17**, 338 (1949)
456. Kitaigorodski, A.I.: *X*-Ray Analysis of Polycrystalline and Amorphous Bodies. State Publishing House for Theoretico-Technical Literature, Moscow, Leningrad (1952, in Russian)
457. Kitaigorodski, A.I.: Organic Crystallochemistry. Academy Sciences Press, Moscow (1955, in Russian)
458. Kittel, C.: Thermal Physics. Wiley, New York (1969)
459. Knacke, O., Stranski, I.N.: Ergebnisse der exakten Naturwissenschaften **26**, 383 (1952)
460. Knacke, O., Stranski, I.N.: Mechanisms of evaporation. In: Chalmers, B., King, R. (eds.) Progress of Metal Science, vol. 6. Pergamon Press, London/New York (1956)
461. Kobeko, P.P.: Amorphous Materials. Academy of Sciences USSR Press, Moscow, Leningrad (1952, in Russian)
462. Kohlrausch, F.: Poggendorffs Annalen der Physik und Chem. **8**, 332 (1876)
463. Kolb, E. D.: In: W. Charles Cooper (ed.) The Physics of Selenium and Tellurium, p. 155. Pergamon Press, Oxford (1969)
464. Kolmogorov, A.N.: Izv. Acad. Sci. USSR, Ser. Math. **1**, 355 (1937)
465. Konobejewski, S.: Z. Phys. Chem. **171**, 25 (1939)
466. Kondoguri, W.: Einfluss des elektrischen und magnetischen Feldes auf die Kristallisation unterkühlter Flüssigkeiten. Z. der Russischen Physikalisch-Chemischen Gesellschaft B **58**, 279 (1926), **62**, 451 (1930); Z. Physik **47**, 589 (1928)
467. Korn, G.A., Korn, T.M.: Mathematical Handbook. McGraw-Hill Book Company, New York/San Francisco/Toronto/London/Sydney (1968)

468. Korshak, V.V.: Progress in Polymer Chemistry. Mir Publishers, Moscow (1965, in Russian)
469. Koslovski, M.I.: The Influence of Electric Fields on Nucleation. In: Sirota, N.N. (ed.) Crystallization and Phase Transformations. Academy of Sciences of Belorussian SSR, Minsk (1962, in Russian)
470. Koslovski, M.I., Burtschakova, V.I., Melentiev, I.I.: Electric Fields and Crystallization. Stiintsa Publishers, Kischinev (1976, in Russian)
471. Kossel, W., Nachrichten Gesellschaft Wiss, p. 135. Göttingen, Math.-Phys. Klasse (1927)
472. Köster, U.: Phys. Stat. Solidi **a 48**, 313 (1978)
473. Köster, U.: Metallkunde **75**, 691 (1984)
474. Köster, U.: Mater. Sci. Eng. **97**, 233 (1988)
475. Köster, U., Herold, U.: Crystallization of Metallic Glasses. In: Güntherodt, H.-J., Beck, H. (eds.) Glassy Metals I (Ionic Structure, Electronic Transport and Crystallization). Springer, Berlin/Heidelberg/New York (1981)
476. Kouchi, A.: Nature **330**, 550 (1987)
477. Kouchi, A., Kuroda, T.: Jpn. J. Appl. Phys. **29**, 807 (1990)
478. Kovacs, A.J., Hutchinson, J.M., Aklonis, J.J.: Isobaric Volume and Enthalpy Recovery of Glasses. A Critical Survey of Recent Phenomenological Approaches. In: Gaskall (ed.), p. 153 (1977)
479. Kovacs, A.J., Aklonis, J.J., Hutchinson, J.M., Ramos, A.R.: J. Polym. Sci. **17**(7), 1097 (1979)
480. Kozisek, Z.: Non-steady state nucleation kinetics. In: Chvoj, Z., Sestak, J., Triska, A. (ed.) Kinetic Phase Diagrams, p. 277. Elsevier Science Publishers, New York (1991)
481. Kozisek, Z., Demo, P.: J. Cryst. Growth **132**, 491 (1993)
482. Kramers, H.A.: Physica **7**, 284 (1940)
483. Krastanov, L.: Hydrologiya i Gidrologiya USSR (Moscow) **12**, 16 (1957, in Russian)
484. Krebs, H.: Angew. Chem. **70**, 1615 (1958)
485. Krikorian, E., Sneed, R.J.: J. Appl. Phys. **37**, 3665 (1966)
486. Kritchevski, I.R.: Notions and Basic Concepts of Thermodynamics. Nauka, Moscow (1970, in Russian)
487. Kubo, R.: Thermodynamics. North-Holland, Amsterdam (1968)
488. Kuhrt, F.: Z. Phys. **131**, 185, 205 (1952)
489. Kuznetsov, V.D.: Crystals and Crystallization. State Publishing House of Technical Literature, Moscow (1954, in Russian)
490. Kuznetsov, W.D., Bolschanina, M.A.: Z. der Russischen Physikalisch-Chemischen Gesellschaft B **57**, Hefte 1-2 (1925)
491. Lai, S.K., Chou, M.H., Chen, H.C.: Phys. Rev. **E48**, 214 (1993)
492. Landau, L.D., Lifshitz, E.M.: Mechanics of Continuous Media. Nauka, Moscow (1953, in Russian)
493. Landau, L.D., Lifschitz, E.M.: Elektrodynamik der Kontinua. Akademie-Verlag, Berlin (1967)
494. Landau, L.D., Lifschitz, E.M.: Statistische Physik. Akademie-Verlag, Berlin (1969)
495. Landau, L.D., Lifschitz, E.M.: Elastizitätstheorie. Akademie-Verlag, Berlin (1976)
496. Landoldt-Börnstein, A.: Zahlenwerte und Funktionen, Physikalische Chemie, Astronomie, Technik, Bd. II, 2b, 6. Auflage, Springer, Berlin (1962)
497. Langer, J.S., Bar-on, M., Miller, H.-D.: Phys. Rev. **A 11**, 1417 (1975)
498. Lauritzen, J.I., Hoffman, J.D.: J. Chem. Phys. **31**, 1680 (1959)
499. Lauritzen, J.I., Hoffman, J.D.: J. Res. Natl. Bur. Stand. **64 a**, 73 (1960)
500. Lebedev, A.A.: Arbeiten des Staatlichen Optischen Instituts Leningrad **2**(10) (1921)
501. Lebedev, A.A.: Izv. Akad. Nauk, Otdel. Matem. Estestven. Nauk, Ser. Fiz., No. **3**, 381 (1937)
502. le Chatelier, H.L.: Compte. Rend. Acad. Sci., Paris **179**, 517, 718 (1924)
503. Lennard-Jones, J.E., Devonshire, A.F.: Proc. R. Soc. **A139**, 317 (1939); **A170**, 464 (1939)
504. Leontowitsch, M.A.: Einführung in die Thermodynamik. Deutscher Verlag der Wissenschaften, Berlin (1953)
505. Levich, V.G.: Introduction into Statistical Physics. State Publishers Technico-Theoretical Literature, Moscow (1954, in Russian)

506. Lewis, B.: Thin Solid Films **1**, 85 (1967)
507. Lewis, G.N., Gibson, G.E.: J. Am. Chem. Soc. **42**, 1529 (1920)
508. Li, J.H., Uhlmann, D.R.: J. Non Cryst. Solids **3**, 127 (1970)
509. Lifshitz, I.M., Slezov, V.V.: J. Exper. Theor. Phys. (USSR) **35**, 479 (1958)
510. Lifshitz, I.M., Slezov, V.V.: Fiz. Tverd. Tela (USSR) **1**, 1401 (1959)
511. Lifshitz, I.M., Slezov, V.V.: J. Phys. Chem. Solids **19**, 35 (1961)
512. Lillie, H.R.: J. Am. Ceram. Soc. **16**, 619 (1933)
513. London, F.: Z. Phys. Chem. **11**, 22 (1930)
514. Lothe, J., Pound, G.M.: J. Chem. Phys. **36**, 2080 (1962)
515. Lothe, J., Pound, G.M.: J. Chem. Phys. **45**, 630 (1966)
516. Luborsky, F.E.: In: Cahn, R.W., Haasen, P. (eds.) Physical Metallurgy, 3rd edn. North-Holland Physics Publishing, Amsterdam/Oxford/New York/Tokyo (1983)
517. Lyubov, B.Y.: In: Growth and Defects of Metallic Crystals, p. 5. Naukova Dumka Publishers, Kiev (1966, in Russian)
518. Lyubov, B.Y., Roitburd, A.L.: On the rate of nucleation of the new phase in one-component systems. In: Problems of Metal Science and Metal Physics, vol. 5, p. 91. State Publishers of Metallurgy, Moscow (1958, in Russian)
519. Lucas, J.: Halide Glasses: Recent Developments. In: Disordered Systems and New Materials; Proceedings 5-th International Summer School on Condensed Matter Physics, Varna 1988, p. 186. World Scientific Publishers, Singapore/London/New York (1989)
520. Ludwig, F.-P.: On the kinetics of phase transformations in condensed systems. M.Sc. Thesis, University of Rostock (1993)
521. Ludwig, F.-P., Schmelzer, J., Bartels, J.: J. Mater. Sci. **29**, 4852 (1994)
522. Ludwig, F.-P., Schmelzer, J., Milchev, A.: Phase Transit. **48**, 237 (1994)
523. Lungu, S., Popescu, H.D.: Industria usoara **4**, 26 (1954)
524. Macedo, B., Litovitz, T.A.: J. Chem. Phys. **42**, 245 (1965)
525. Mackenzie, J.D. (ed.): Structure of some inorganic glasses from high temperature studies. Modern Aspects of the Vitreous State, p. 188. Butterworths, London (1960)
526. Mackenzie, J.D., Zheng, H.: Oxide-nonoxide glasses. In: Proceedings of the 16-th International Congress on Glass, Bull. Soci. Esp. Ceram. Vid. **31c** 1, 1 (1992)
527. Mampel, K.: Z. Phys. Chem. **A 187**, 43, 225 (1940)
528. Mandelkern, L.: Crystallization of Polymers. McGraw-Hill, New York (1964)
529. Manning, J.: Diffusion Kinetics for Atoms and Crystals. van Nostrand, Princeton (1968)
530. Marder, M.: Phys. Rev. **A36**, 858 (1987)
531. Markov, I., Kashchiev, D.: J. Cryst. Growth **13–14**, 131 (1972)
532. Markov, I., Kaischew, R.: Kristall und Technik **11**, 685 (1973)
533. Markov, I., Stoyanov, S.: Contemp. Phys. **28**, 267 (1987)
534. Markov, I.: Crystal Growth for Beginners: Fundamentals of Nucleation, Crystal Growth and Epitaxy. World Scientific, Singapore (2002)
535. Marqusee, J., Ross, J.: J. Chem. Phys. **79**, 373 (1983); **80**, 536 (1984)
536. Mason, B.J.: The Physics of Clouds. Clarendon Press, Oxford (1957)
537. Matheson, A.J.: J. Phys. Chem. **7**, 2569 (1974)
538. Matox, D.: J. Am. Ceram. Soc. **50**, 683 (1967)
539. Matusita, K., Tashiro, M.: J. Non Cryst. Solids **11**, 471 (1975)
540. Maurer, R.D.: J. Appl. Phys. **29**, 1 (1958)
541. Mayer, J., Goeppert-Mayer, M.: Statistical Mechanics. Wiley, New York (1946)
542. Mazurin, O.V.: J. Non Cryst. Solids **25**, 130 (1977)
543. Mazurin, O.V.: Vitrification. Nauka, Leningrad (1986)
544. Mazurin, O.V. (ed.): Glass '89: Survey of Papers of the XV-th International Congress on Glass. Nauka, Leningrad (1989)
545. Mazurin, O.V.: Principles and methods of collection of glass property data and analysis of data reliability. In: Schmelzer, J.W.P., Gutzow, I.S. (eds.) Glasses and the Glass Transition, chap.6, WILEY-VCH, Weinheim (2011)

546. Mazurin, O.V., Streltzina, M.V., Shveiko-Shveikovskaya, T.P.: Properties of Glasses and Glass-forming Melts, vol. 1–9. Nauka, Leningrad (1973–1995, in Russian); Mazurin, O.V., Streltsina, M.V., Shvaiko-Shvaikovskaya, T.P., Handbook of Glass Data, 5 vols. Elsevier, Amsterdam (1980–1990).
547. Mazurin, O.V., Filipovich, V.N., Shultz, M.N.: Fiz. i Khim. Stekla **3**, 3 (1977)
548. Mc Donald, J.E.: Am. J. Phys. **30**, 870 (1962); **31**, 31 (1963)
549. McMillan, P.W.: Glass-Ceramics. Academic, London (1964)
550. Meakin, P.: Fractal Aggregates. Adv. Colloid Interface Sci. **28**, 249 (1988)
551. Meiling, G.S., Uhlmann, D.R.: Phys. Chem. Glass. **8**, 62 (1967)
552. Meisel, J.: Wissenschaftliche Zeitschrift der Friedrich-Schiller Universität Jena (Physikalisch Mathematische Reihe) **20**, 185 (1972)
553. Meiwes-Broer, K.H., Lutz, H.O.: Phys. Blätter **47**, 283 (1991)
554. Meixner, J.: Changements de Phases, Paris 432 (1952)
555. Meixner, J.: Kolloid Z. Z. Polym. **134**, 3 (1953)
556. Meixner, J.: Z. Naturforsch. **9A**, 654 (1954)
557. Milchev, A.: Comp. Rend. **36**(11), 1415 (1983)
558. Milchev, A.: Electrocrystallization: Fundamentals of Nucleation and Growth. Kluwer, Dordrecht (2002)
559. Milchev, A., Avramov, I.: Phys. Stat. Solidi **b 120**, 123 (1983)
560. Milchev, A., Gutzow, I.: Phys. Chem. Liq. **11**, No 1, 25 (1981)
561. Milchev, A., Gutzow, I.: J. Macromol. Sci. Phys. B **21(4)**, 583 (1982)
562. Milchev, A., Stoyanov, S.: J. Electroanal. Chem. **72**, 33 (1976)
563. Milchev, A., Stoyanov, S., Kaischew, R.: Thin Solid Films **22**, 255, 267 (1974)
564. Milchev, A., Gerroff, I., Schmelzer, J.: Z. Phys. **B 94**, 101 (1994)
565. Mitcherlich, E.: J. Prakt. Chem. **66**, 257 (1855)
566. Mitkova, N., Boncheva-Mladenova, Z.: J. Non Cryst. Solids **90**, 789 (1987)
567. Moelwyn-Hughes, E.: Physical Chemistry. Pergamon Press, Oxford (1972)
568. Möller, J.: Zur theoretischen Beschreibung von Phasenumwandlungen in elastischen und viskoelastischen Medien. Ph.D. thesis, University of Rostock (1994)
569. Möller, J., Schmelzer, J.: Phys. Stat. Solidi **b180**, 331 (1993)
570. Möller, J., Schmelzer, J., Gutzow, I., Pascova, R.: Phys. Stat. Solidi **b180**, 315 (1993)
571. Möller, J., Schmelzer, J., Avramov, I.: Kinetics of Segregation and Crystallization with Stress Development and Stress Relaxation. Phys. Stat. Solidi **b 196**, 49 (1996)
572. Möller, J., Schmelzer, J.W.P., Gutzow, I.: Ostwald's Rule of Stages: The Effect of Elastic Strains and External Pressure. Z. Phys. Chem. **204**, 171 (1998)
573. Monnerie, I., Suter, U.W.: Atomistic Modeling of Physical Properties of Polymers. Springer, Berlin (1994)
574. Morey, G.W.: The Properties of Glass. Reinhold Publishers, New York (1938, 1954)
575. Morgan, L.B.: Phil. Trans. R. Soc. (Lond.) **A 247**, 13 (1954)
576. Mott, N.F.: Proc. R. Soc. (Lond.) **A146**, 465 (1934)
577. Moynihan, C.T., Gupta, P.K.: J. Non Cryst. Solids **29**, 143 (1978)
578. Moynihan, C.T., Lesikar, A.V.: Ann. N. Y. Acad. Sci. **371**, 151 (1981)
579. Moynihan, C.T., Sasabe, H., Tucker, J.: Kinetics of the glass transition in a calcium-potassium nitrate melt. In: Molten Salts, pp. 182–194. Electrochemical Society Publications, Princeton (1976)
580. Moynihan, C.T. et al.: Structural relaxation in vitreous materials. In: Goldstein, Simha, p. 15 (1976)
581. Moynihan, C.T., Easteal, A.J., DeBolt, M.A.: J. Am. Ceram. Soc. **54**, 491 (1971); **59**, 12 (1976); **59**, 12 (1978)
582. Müller, R.: J. Therm. Anal. **35**, 823 (1989)
583. Müller, R., Hübert, T., Kirsch, M.: Silikattechnik **37**, 111 (1986)
584. Müller, R., Thamm, D.: In: Proceedings of the 4-th Otto-Schott Kolloquium, Jena 1990, p. 86. Wissenschaftliche Zeitschrift der Universität Jena (1990)

585. Mutaftschiev, B.: Nucleation Theory. In: Hurle, T.D.J. (ed.) Handbook of Crystal Growth, p. 187. Elsevier Science Publishers B.V., Amsterdam (1993)
586. Mutaftschiev, B.: The Atomistic Nature of Crystal Growth. Springer, Berlin (2001)
587. Mutaftschiev, B., Bonissent, A.: J. Phys. Colloid **38**, C4, 82, (1977)
588. Nabarro, F.R.: Proc. R. Soc. (Lond.) **A 175**, 519 (1940)
589. Nacken, R.: FIAT **N641**, 11 (1945)
590. Nanev, C., Kaischew, R.: Kristallwachstum und Kristallgitterstörungen. In: Reinststoffe in Wissenschaft und Technik, Proceedings 3-rd International Symposium, Dresden (1979)
591. Nanev, C.: Prog. Cryst. Growth Character. **4**, 3 (1994)
592. Narayanaswami, O.S.: J. Am. Ceram. Soc. **54**, 491 (1971)
593. Narsimhan, G., Ruckenstein, E.: J. Colloid Interface Sci. **128**, 549 (1989)
594. Neely, J.E., Ernsberger, F.M.: J. Am. Ceram. Soc. **49**, 396 (1966)
595. Nemilov, S.V.: Zh. Prikl. Khimii **37**, 1020 (1964)
596. Nemilov, S.V.: Fiz. Khim. Stekla **2**, 97 (1976)
597. Nemilov, S.V.: Fiz. Khim. Stekla **3**, 423 (1977)
598. Nemilov, S.V.: Thermodynamic content of the prigogine-defay ratio and the structural difference between glasses and liquids. In: Porai-Koshits, E.A. (ed.) The Vitreous State, p. 15. Nauka, Leningrad (1988, in Russian)
599. Nenov, D.: Prog. Cryst. Growth Character. **9**, 185 (1984)
600. Nenov, D., Trayanov, A.: Surf. Sci. **213**, 488 (1989)
601. Nernst, W.: Die theoretischen und experimentellen Grundlagen des neuen Wärmesatzes. Verlag W. Knapp, Halle (1918)
602. Neumann, K., Döring, W.: Z. Phys. Chem. **186 A**, 193, 203 (1940)
603. Nielsen, E.A.: Kinetics of Precipitation. Pergamon Press, Oxford (1964)
604. Nishii, J., Kaite, Y., Yamagishi, T.: J. Non Cryst. Solids **74**, 411 (1985)
605. Novick, A.S.: Comment. Solid State Phys. **2**, 155 (1970)
606. Novikov, N.V., Fedosseev, D.V. et al.: Synthesis of Diamonds. Kiev, Naukova Dumka (1987, in Russian)
607. Novikova, S.I.: Thermal Expansion of Solids. Nauka, Moscow (1974, in Russian)
608. Nowakowski, B., Ruckenstein, E.: J. Chem. Phys. **94**, 1397 (1991)
609. Oblad, A.G., Newton, R.F.: J. Am. Chem. Soc. **59**, 2495 (1937)
610. Ohlberg, S.M., Hammel, J.J.: Formation and structure of phase separated soda-lime silica glass. In: Proceedings of the 7-th Congres Internationale du Verre, p. 32 28.6.–3.7.1965
611. Onsager, L.: Phys. Rev. **65**, 117 (1944)
612. Ono, B., Kondo, S.: Molecular theory of surface tension in liquids. In: Flügge, S. (ed.) Handbuch der Physik, vol. 10. Springer, Berlin (1960)
613. Oono, Y., Puri, S.: Phys. Rev. **A 38**, 434 (1989)
614. Ornstein, G.E., Uhlenbeck, L.S.: Phys. Rev. **36**, 823 (1930)
615. Ostwald, W.: Z. Phys. Chem. **22**, 282 (1897)
616. Ostwald, W.: Lehrbuch der Allgemeinen Chemie. Engelmann, Leipzig (1896–1901)
617. Ostwald, W.: Analytische Chemie. Engelmann, Leipzig (1901)
618. Ostwald, W.: Kolloid Z. **36**, 99 (1925); **47**, 176 (1929)
619. Oxtoby, D.W., Kashchiev, D.: J. Chem. Phys. **100**, 7665 (1994)
620. Palatnik, L., Papirov, I.: Oriented Crystallization. Metallurgy Publishers, Moscow (1964, in Russian)
621. Palatnik, L., Zorin, V.: Zh. Fiz. Khim. **33**, 191 (1959)
622. Pamplin, B.R.: Crystal Growth. Pergamon Press, New York (1975)
623. Parks, G.S.: J. Am. Chem. Soc. **47**, 338 (1925)
624. Parks, G.S., Huffman, F.E.: Z. Phys. Chem. **31**, 1842 (1927)
625. Parlange, J.I.: J. Cryst. Growth **6**, 311 (1970)
626. Pascova, R., Gutzow, I.: Atomistic model for crystal nucleation in glassforming melts. In: Proceedings of the 2-nd International Conference on Fundamentals of Glass Science and Technology, Venice, Italy (1993)
627. Pascova, R., Gutzow, I., Tomov, I.: J. Mater. Sci. **25**, 913 (1990)

628. Pascova, R., Gutzow, I., Schmelzer, J.: J. Mater. Sci. **25**, 921 (1990)
629. Pauling, L.: The Nature of Chemical Bonding. Cornell University Press, Ithaca (1948)
630. Pauling, L., Tolman, R.C.: J. Am. Chem. Soc. **47**, 2148 (1925)
631. Pavlushkin, H.M.: Basic Principles of the Technology of Sitals. Stroitelstvo Publishers, Moscow (1970, in Russian)
632. Penkov, I., Gutzow, I.: J. Mater. Sci. **19**, 233 (1984)
633. Petrov, Ju. I.: Physics of Small Particles. Nauka Publishers, Moscow (1982, in Russian)
634. Petroff, B., Milchev, A., Gutzow, I.: J. Macromol. Sci. Phys. **B 35**, 763 (1996)
635. Philips, W.A.: J. Low Temp. Phys. **7**, 351 (1972)
636. Planck, M.: Vorlesungen über Thermodynamik, 10. Auflage, de Gruyter, Berlin (1954)
637. Poisson, S.D.: Resherches sur la Probalite des Judgment (en Materies Criminelles et Civiles), Paris, p. 206 (1837)
638. Polk, D.: Scr. Metall. **4**, 117 (1970)
639. Popoff, K.: Comptes Rend. Acad. Sci. (Paris) **237**, 698 (1953); **238**, 331 (1954); **239**, 1152 (1954)
640. Porai-Koshits, E.A.: Possibilities and Results of X-ray Investigations of Glass-Forming Substances. Academy of Sciences Press, Moscow-Leningrad (1955)
641. Porai-Koshits, E.A.: Genesis of Modern Concepts on Structure of Inorganic Glasses. In: Glass '89, p. 7 (1989)
642. Porai-Koshits, E.A., Golubkov, V.V.: Proceedings of the 1-st International Otto-Schott-Colloquium, Jena, 1979, Wissenschaftliche Zeitschrift der Friedrich-Schiller-Universität Jena, Mathematisch-Naturwissenschaftliche Reihe **28**, 265 (1979)
643. Poulain, M.: Nature **293**, 279 (1981)
644. Prandtl, L.: ZAMM **8**, 85 (1928)
645. Preston, E.: J. Soc. Glass Technol. **24**, 104, 139 (1940)
646. Price, F.P.: Mechanism of Polymer Crystallization. In: Zettlemoyer, A.C. (ed.) Nucleation, p. 405. Dekker, New York (1969)
647. Prigogine, I.: Molecular Theory of Solutions. North-Holland Publishing Company, Amsterdam/ Interscience Publishing Company, New York (1957)
648. Prigogine, I., Bellemans, A.: Statistical mechanics of surface tension and adsorption. In: Lee, L.H. (ed.) Adhesion and Adsorption of Polymers. Part A. Plenum Press, New York (1980)
649. Prigogine, I., Defay, R.: Chemical Thermodynamics. Longmans, London (1954)
650. Privalko, V.P.: J. Phys. Chem. **84**, 3307 (1980)
651. Probstein, R.J.: J. Chem. Phys. **19**, 619 (1951)
652. Pugatchev, V.S.: Theory of Probability Functions. Fizmatgiz, Moscow (1960, in Russian)
653. Pye, L.D., O'Keefe, J.A., Frechette, V.D. (eds.): Natural Glasses. North-Holland Physics Publishing, Amsterdam (1984)
654. Rabinovich, E.M.: Influence of crystallochemical matching on the process of heterogeneous nucleation of glasses. In: Toropov, I.A. (ed.) The Glassy State: vol. 1, Catalyzed Crystallization of Glass, p. 29. Academy of Sciences of the USSR Publishers, Moscow, Leningrad (1963, in Russian)
655. Randall, G.T., Ruxby, H.P., Cooper, B.S.: J. Soc. Glass Technol. **14**, 219 (1930)
656. Rao, K.J., Angell, C.A.: Thermodynamic and relaxational aspects of a glass-transition from a bond-lattice model. In: Douglas, R.W., Ellis, B. (eds.) Amorphous Materials, Proceedings Third International Conference on Physics of Non-crystalline Solids, Sheffield, 1970, p. 171; Wiley Interscience, New York (1972)
657. Rawson, H.: Inorganic Glass-Forming Systems. Academic, London/New York, 1967
658. Rehage, G., Borchardt, W.: The thermodynamics of the glassy state. In: Haward, R.N. (ed.) The Physics of Glassy Polymers, chapter 1, p. 54. Applied Science Publishers, London (1973)
659. Reiner, M.: Phenomenological Macrorheology. In: Eirich, F.R. (ed.) Rheology, Theory, and Applications, vol. 1, chapter 6, p. 23. Academic, New York (1956)
660. Reiner, M.: Phys. Today **17**, 62 (1964)
661. Reiss, H.: J. Chem. Phys. **18**, 840 (1950)

662. Rekhson, S.M., Mazurin, O.V.: J. Am. Ceram. Soc. **57**, 327 (1974)
663. Rhodin, T.H., Walton, D.: Nucleation of oriented films. In: Francombe, M.H., Sato, H. (eds.) Single Crystal Films; Proceedings of the International Conference, p. 31, Blue Bell, PA, May 1963; Pergamon Press, New York (1964)
664. Richter, H.: J. Non Cryst. Solids **8–10**, 388, 394 (1972)
665. Rindone, G.E.: J. Am. Ceram. Soc. **45**, 7 (1962)
666. Ringer, A.: Z. Anorg. Chem. **32**, 212 (1912)
667. Ritland, H.N.: J. Am. Chem. Soc. **37**, 370 (1954)
668. Röpke, G.: Statistische Mechanik des Nichtgleichgewichts. Deutscher Verlag der Wissenschaften, Berlin (1987)
669. Rouse Ball, W.W., Coxeter, H.S.M.: Mathematical Recreations and Essays, 12th edn. University of Toronto Press, Toronto (1974)
670. Rowlinson, J.S.: Translation of J.D. van der Waals' The thermodynamic theory of capillarity under the hypothesis of a continuous variation of density. J. Stat. Phys. **20**, 197 (1979)
671. Rowlinson, J.S., Curtiss, C.F.: J. Chem. Phys. **19**, 1519 (1951)
672. Rowlinson, J.S., Widom, B.: Molecular Theory of Capillarity. Clarendon Press, Oxford (1982)
673. Roy, D., Roy, R., Osborn, E.: J. Am. Ceram. Soc. **33**(3), 85 (1950)
674. Ruckenstein, E., Nowakowski, B.: J. Chem. Phys. **94**, 1397 (1991)
675. Rukeyser, M.: Willard Gibbs. E.P. Dutton and Co., Inc., New York (1964)
676. Rusanov, A.I.: Phasengleichgewichte und Grenzflächenerscheinungen. Akademie-Verlag, Berlin (1978)
677. Russew, K., Stoyanova, L.: J. Mater. Sci. **A 123**, 80 (1990)
678. Sack, W.: In: Schott, E. (ed.) Beiträge zur Angewandten Glasforschung, p. 111. Universität Mainz, Stuttgart (1959)
679. Sadoc, J.F., Dixmier, J., Guinier, A.: J. Non Cryst. Solids **12**, 46 (1973)
680. Sakka, S., Mackenzie, J.D.: J. Non Cryst. Solids **6**, 145 (1971)
681. Salmang, H.: Die physikalischen und chemischen Grundlagen der Glasfabrikation. Springer, Berlin-Göttingen-Heidelberg (1957)
682. Samwer, K., Ettl, C.: Physikalische Blätter **50**, 465 (1994)
683. Sanditov, D.S., Bartenev, G.M.: Physical Properties of Disordered Structures. Nauka, Moscow (1982, in Russian)
684. Schaefer, H.: Chemische Transportreaktionen. Verlag Chemie GmbH, Weinheim (1962)
685. Scherer, G.W.: J. Am. Ceram. Soc. **67**, 504 (1984)
686. Scherer, G.W.: Relaxation in Glass and Composites. Wiley, New York (1986)
687. Schischakov, N.A.: Structure of Silicate Glasses. Academy of Sciences USSR Publishers House, Moscow (1954, in Russian)
688. Schmelzer, J.: Z. Phys. Chem. **266**, 1057 (1985)
689. Schmelzer, J.: Thermodynamik finiter Systeme und die Kinetik von thermodynamischen Phasenübergängen 1. Art. Dissertation B, Rostock (1985)
690. Schmelzer, J.: J. Chem. Soc. Faraday Trans. I **82**, 1421 (1986)
691. Schmelzer, J.: Phys. Stat. Soldi **b161**, 173 (1990)
692. Schmelzer, J.: Repetitorium der klassischen theoretischen Physik. Aula-Verlag, Wiesbaden (1992)
693. Schmelzer, J.W.P.: Comments on the nucleation theorem. J. Colloid Interface Sci. **242**, 354 (2001)
694. Schmelzer, J.W.P.: Some additional comments on the nucleation theorem. Russian J. Phys. Chem. **77**(Suppl. 1), S 143 (2003)
695. Schmelzer, J.W.P. (ed.): Nucleation Theory and Applications. WILEY-VCH, Berlin-Weinheim (2005)
696. Schmelzer, J.W.P.: Crystal Nucleation and Growth in Glassforming Melts: Experiment and Theory. J. Non Cryst. Solids **354**, 269 (2008)
697. Schmelzer, J.W.P.: Generalized Gibbs thermodynamics and nucleation-growth phenomena. In: Rzoska, S., Drozd-Rzoska, A., Mazur, V. (eds.) Proceedings of the NATO Advanced

Research Workshop Metastable Systems under Pressure, Odessa, Ukraine, 4.-8. October 2008, pp. 389–402, Springer (2009)
698. Schmelzer, J.W.P.: On the Determination of the Kinetic Pre-factor in Classical Nucleation Theory. J. Non Cryst. Solids **356**, 2901 (2010)
699. Schmelzer, J.W.P.: Structural Order Parameters, Relaxation and Crystallization, Proceedings International Congress on Glass 2010, Salvador de Bahia, Brazil
700. Schmelzer, J.W.P.: Kinetic criteria of glass-formation and the pressure dependence of the glass transition temperature. J. Chem. Phys. **136**, 074512 (2012)
701. Schmelzer, J.W.P. (ed.): Glass and Crystallization of Glass-Forming Melts. de Gruyter (2014, in preparation)
702. Schmelzer, J.W.P., Abyzov, A.S.: Generalized Gibbs' approach to the thermodynamics of heterogeneous systems and the kinetics of first-order phase transitions. J. Eng. Thermophys. **16**, 119 (2007)
703. Schmelzer, J.W.P., Abyzov, A.S.: Thermodynamic analysis of nucleation in confined space: generalized gibbs approach. J. Chem. Phys. **134**, 054511 (2011)
704. Schmelzer, J.W.P., Abyzov, A.S.: Comment on "minimum free-energy pathway of nucleation". J. Chem. Phys. **135**, 134508 (2011); **136**, 107101 (2012)
705. Schmelzer, J., Gutzow, I.: Z. Phys. Chem. **269**, 753 (1988)
706. Schmelzer, J.W.P., Gutzow, I.: The Prigogine-Defay ratio revisited. J. Chem. Phys. **125**, 184511 (2006)
707. Schmelzer, J.W.P., Gutzow, I.S.: Glasses and the Glass Transition. WILEY-VCH, Berlin-Weinheim (2011)
708. Schmelzer, J., Mahnke, R.: J. Chem. Soc. Faraday Trans. I **82**, 1413 (1986)
709. Schmelzer, J., Milchev, A.: Phys. Lett. **A 158**, 307 (1991)
710. Schmelzer, J., Möller, J.: J. Phase Trans. **38**, 261 (1992)
711. Schmelzer, J.W.P., Schick, C.: Dependence of crystallization processes of glass-forming melts on prehistory: A theoretical approach to a quantitative treatment. Phys. Chem. Glass. **53**, 99–106 (2012)
712. Schmelzer, J., Ulbricht, H.: J. Colloid Interface Sci. **117**, 325 (1987)
713. Schmelzer, J., Gutzow, I., Pascova, R.: J. Cryst. Growth **104**, 505 (1990)
714. Schmelzer, J., Pascova, R., Gutzow, I.: Phys. Stat. Solidi **a117**, 363 (1990)
715. Schmelzer, J., Pascova, R., Möller, J., Gutzow, I.: J. Non Cryst. Solids **162**, 26 (1993)
716. Schmelzer, J., Möller, J., Gutzow, I., Pascova, R., Müller, R., Pannhorst, W.: J. Non Cryst. Solids **183**, 215 (1995)
717. Schmelzer, J., Möller, J., Slezov, V.V.: J. Phys. Chem. Solids **56**, 1013 (1995)
718. Schmelzer, J., Slezov, V.V., Milchev, A.: Phase Trans. **54**, 193 (1995)
719. Schmelzer, J., Gutzow, I., Schmelzer, J. Jr.: J. Colloid Interface Sci. **178**, 657 (1996)
720. Schmelzer, J.W.P., Röpke, G., Priezzhev, V.B. (eds.): Nucleation Theory and Applications, 5 vols. Joint Institute for Nuclear Research Publishing Department, Dubna, Russia (1999, 2002, 2005, 2008, 2011)
721. Schmelzer, J., Röpke, G., Mahnke, R. (eds.): Aggregation Phenomena in Complex Systems. WILEY-VCH, Weinheim (1999)
722. Schmelzer, J.W.P., Schmelzer, J. Jr., Gutzow, I.S.: Reconciling Gibbs and van der Waals: A new approach to nucleation theory. J. Chem. Phys. **112**, 3820 (2000)
723. Schmelzer, J.W.P., Müller, R., Möller, J., Gutzow, I.S.: Elastic Stresses, Stress Relaxation, and Crystallization: Theory. Phys. Chem. Glass. **43 C**, 291 (2002)
724. Schmelzer, J.W.P., Potapov, O.V., Fokin, V.M., Müller, R., Reinsch, S.: The effect of elastic stress evolution and relaxation on crystal nucleation in lithium disilicate glasses. J. Non Cryst. Solids **333**, 150 (2004)
725. Schmelzer, J.W.P., Gokhman, A.R., Fokin, V.M.: On the dynamics of first-order phase transitions in multi-component systems. J. Colloid Interface Sci. **272**, 109 (2004)
726. Schmelzer, J.W.P., Abyzov, A.S., Möller, J.: Nucleation vs. spinodal decomposition in phase formation processes in solutions. J. Chem. Phys. **121**, 6900 (2004)

727. Schmelzer, J.W.P., Zanotto, E.D., Avramov, I., Fokin, V.M.: Stress development and stress relaxation during crystal growth in glass-forming melts. J. Non Cryst. Solids **352**, 434 (2006)
728. Schmelzer, J.W.P., Fokin, V.M., Abyzov, A.S., Zanotto, E.D., Gutzow, I.: How do crystals form and grow in glass-forming liquids: Ostwald's rule of stages and beyond. Int. J. Appl. Glass Sci. **1**, 16 (2010)
729. Schmelzer, J.W.P., Boltachev, G.Sh., Baidakov, V.G.: Classical and generalized Gibbs' approaches and the work of critical cluster formation in nucleation theory. J. Chem. Phys. **124**, 194503 (2006)
730. Schmolke, A.: Z. Phys. Chem. **64**, 714 (1931)
731. Schönborn, H.: Silikattechnik **6**, 367 (1955)
732. Scholze, H.: Glas: Natur, Struktur und Eigenschaften, 2nd edn. Vieweg, Braunschweig, 1965; Springer, Berlin (1977)
733. Scholze, H., Gliemeroth, G.: Naturwissenschaften **51**, 431 (1964)
734. Schott, O.: Z. Instrumentenkunde **11**, 330 (1891)
735. Schottky, W.: Phys. Z. **22**, 1 (1921)
736. Schreiber, M., Ottomeier, M.: J. Phys. Condens. Matter. **4**, 1959 (1992)
737. Schulz, G.V.: Z. Phys. Chem. **32**, 27 (1936); **43**, 25, 47 (1937); **47**, 155 (1940)
738. Schulz, G.V.: Angew. Chem. **50**, 767 (1937)
739. Schulz, A.K.: J. Chim. Phys. Biol. **51**, 324 (1954)
740. Schulz, I., Hinz, W.: Silikattechnik **6**, 235 (1955)
741. Scott, G.D.: Nature **188**, 908 (1960)
742. Scott, M.G., Ramachandrao, P.: Mater. Sci. Eng. **29**, 137 (1977)
743. Secrist, D., Mackenzie, J.D.: Unusual methods of glass-formation. In: Modern Aspects of the Vitreous State, vol. 3, p. 149. Butterworths, London (1964)
744. Semenov, N.N.: J. Russ. Phys. Chem. Soc. **61**, 117 (1930)
745. Shambadal, P.: Evolution et Applications du Concept d'entropie. Dunod Publisher, Paris (1963)
746. Shneidman, V.A.: J. Technol. Phys. (USSR) **58**, 2202 (1988)
747. Shneidman, V.A.: Transient kinetics of nucleation. A review of russian papers. In: proceedings of the 13-th International Conference on Nucleation and Atmospheric Aerosols, Salt Lake City, Utah, 22—28 August, 1992
748. Shneidman, V.A., Hänggi, P.: Phys. Rev. **E49**, 82 (1994)
749. Shneidman, V.A., Weinberg, M.: J. Chem. Phys. **97**, 3621 (1992)
750. Shneidman, V.A., Weinberg, M.: J. Non Cryst. Solids **160**, 89 (1993)
751. Shi, G., Seinfeld, J.H.: J. Mater. Res. **6**, 2091, 2097 (1991)
752. Shi, G., Seinfeld, J.H., Okuyama, K.: Phys. Rev. **A41**, 2101 (1990); J. Chem. Phys. **93**, 9033 (1990)
753. Simha, R., Boyer, R.F.: J. Chem. Phys. **37**, 1003 (1962)
754. Simon, F.: Die Bestimmurg der freien Energie. In: Geiger, H., Scheel, H. (eds.) Handbuch der Physik, 350, 352 pp., vol. 10. Springer, Berlin (1926)
755. Simon, F.: Z. Phys. **41**, 806 (1927)
756. Simon, F.: Ergebnisse der exakten Naturwissenschaften **9**, 222 (1930)
757. Simon, F.: Z. Anorg. Allg. Chem. **203**, 219 (1931)
758. Simon, F.: Physica **4**, 1089 (1937)
759. Simon, F.: 40-th Gutrie Lecture, Year Book Physical Society (London), **1** (1956)
760. Simon, F., Lange, F.: Z. Phys. **38**, 227 (1926)
761. Simon, I., Litke, A.D.: Infrared studies of glass. In: Mackenzie, J.D. (ed.): Modern Aspects of the Vitreous State, p. 120. Butterworths, London (1960)
762. Sirota, N.N.: On the theory of crystallization. In: Sirota, N.N. (ed.) Mechanism and Kinetics of Crystallization. Nauka i Tekhnika Publisher, Minsk (1969, in Russian)
763. Sirota, N.N.: Proceedings of the International Conference on Crystallography, Moscow (1967)
764. Skapski, A.S.: The surface tension of liquid metals. J. Chem. Phys. **16**, 389 (1948)

765. Skapski, A.S.: A theory of surface tension of solids – I application to metals. Acta Met. **4**, 576 (1956)
766. Skapski, A.S.: A next-neighbors theory of maximum undercooling. Acta Met. **4**, 583 (1956)
767. Skornyakov, M.M.: On the viscosity of glasses above and below liquidus temperatures. In: Lebedev, A.A. (ed.) Structure of Glasses, p. 256. Sov. Acad. Sci Publ., Moscow-Leningrad (1955)
768. Skripov, V.P., Baidakov, V.G.: Teplofizika Vysokikh Temperatur **10**, 1226 (1972) (English Translation: High Temperatures **10**, 1102 (1972)
769. Skripov, V.P., Faizullin, M.Z.: Comparison between solid-liquid and liquid-vapor phase transitions: thermodynamic aspects. In: Schmelzer, J.W.P., Röpke, G., Priezzhev, V.B. (eds.) Nucleation Theory and Applications, Workshop Proceedings 2000–2002, pp. 4–18. Joint Institute for Nuclear Research Publishing Department, Dubna, Russia (2002)
770. Skripov, V.P., Faizullin, M.Z.: Solid-Liquid-Gas Phase Transitions and Thermodynamic Similarity. WILEY-VCH, Berlin-Weinheim (2006)
771. Skripov, W.P., Koverda, V.P.: Spontane Kristallisation unterkühlter Flüssigkeiten. Nauka, Moskau (1984, in Russian)
772. Slavianski, V.T.: Gases in Glass. Gosizdat-Oboronprom-Publishers, Moscow (1957)
773. Slezov, V.V.: Kinetics of First-Order Phase Transitions. WILEY-VCH, Berlin-Weinheim (2009)
774. Slezov, V.V., Sagalovich, V.V.: Uspekhi Fiz. Nauk **151**, 67 (1987)
775. Slezov, V.V., Schmelzer, J.: J. Phys. Chem. Solids **55**, 243 (1994)
776. Slezov, V.V., Schmelzer, J.W.P.: Kinetics of formation of a new phase with an arbitrary stoichiometric composition in a multi-component solid solution. Phys. Rev. **E 65**, 031506 (2002)
777. Slezov, V.V., Schmelzer, J., Möller, J.: J. Cryst. Growth **132**, 419 (1993)
778. Slezov, V.V., Schmelzer, J.W.P., Kinetics of Nucleation – Growth Processes: The First Stages, J. W. P. Schmelzer, V. V. Slezov, G. Röpke, J. Schmelzer, Jr.: Shapes of cluster size distributions evolving in nucleation - growth processes. In: Schmelzer, J.W.P., Röpke, G., Priezzhev, V.B. (eds.) Nucleation Theory and Applications, pp. 6–81, 82–129. Joint Institute for Nuclear Research Publishing House, Dubna (1999)
779. Slezov, V.V., Schmelzer, J.W.P., Abyzov, A.S.: A new method of determination of the coefficients of emission in nucleation theory. In: Schmelzer, J.W.P. (ed.), Nucleation Theory and Applications, pp. 49–94. WILEY-VCH, Berlin-Weinheim (2005)
780. Smakula, A.: Einkristalle, p. 163. Springer, Berlin (1962)
781. Sloope, B.W., Tiller, C.O.: J. Appl. Phys. **36**, 3174 (1965)
782. Smirnov, A.A.: Molecular-Kinetic Theory of Metals. Nauka, Moscow (1966, in Russian)
783. Smith, G.S., Rindone, G.E.: J. Am. Ceram. Soc. **44**, 72 (1961)
784. Smyth, H.T.: In: Alpern, A.M. (ed.) High Temperature Oxides, part 4, p. 209. Academic, London (1971)
785. Sobotka, Z.: Rheology of Materials and Engineering. Academia, Prague (1984)
786. Sommerfeldt, A.: Thermodynamik und Statistik. Akademische Verlagsgesellschaft, Leipzig (1937)
787. Soules, T.F.: J. Non Cryst. Solids **123**, 48 (1990)
788. Spaepen, F.: Solid State Phys. **47**, 1 (1994)
789. Spaepen, F., Fransaer, J.: Adv. Eng. Mat. **2**(9), 593–596 (2000)
790. Spassov, T., Budurov, S.: Cryst. Res. Technol. **23**, 1225 (1988)
791. Springer, G.S.: Adv. Heat Transf. **14**, 281 (1978)
792. Stanworth, J.E.: J. Soc. Glass Technol. **30**, 54T (1946)
793. Stanworth, J.E.: Physical Properties of Glass. Clarendon Press, Oxford (1953)
794. Stanhouse, B.J., Grout, P.J.: J. Non Cryst. Solids **27**, 247 (1978)
795. Staverman, A.: Physica **10**, 1141 (1937)
796. Stefan, J.: Wiedemanns Annalen der Physik und Chemie **29**, 655 (1886)
797. Steinike, U., Ebert, I., Geissler, H., Hening, H.P., Kretzschmar, U.: Kristall und Technik **13**, 597 (1978)

798. Stern, O.: Annalen der Physik **49**(4), 823 (1916)
799. Sternberg, A.A., Mironova, G.S., Zvereva, O.V., Molovina, M.V.: In: Crystal Growth, p. 142, vol. 17. Nauka Publishers, Moscow (1989, in Russian)
800. Stevels, G.M.: J. Non Cryst. Solids **6**, 307 (1971)
801. Stewart, H.R. (ed.): Die Physik der Hochpolymere, Bd. 2. Springer, Berlin-Göttingen-Heidelberg 1953; Bd. 3 (1955)
802. Stookey, S.D.: Nucleation. In: Kingey, W.D. (ed.) Ceramic Fabrication Processes. Wiley, New York (1957)
803. Stookey, S.D.: Glastech. Ber. **32K**, 1 (1959)
804. Stoyanov, S.: Thin Solid Films **18**, 91 (1973)
805. Stoyanov, S.: J. Cryst. Growth **24/25**, 293 (1974)
806. Stoyanov, S., Kashchiev, D., Georgiev, M.: Phys. Stat. Solidi **41**, 387, 395 (1970)
807. Stoycev, N., Budurov, S., Kovatchev, P., Kovatchev, M.: Krist. Tech. **8**, 21 (1973)
808. Storonkin, A.W.: Thermodynamics of Heterogeneous Systems. Leningrad University Press, Leningrad (1967)
809. Stranski, I.N.: Z. Phys. Chem. **336 A**, 259 (1928)
810. Stranski, I.N., Totomanov, D.: Z. Phys. Chem. **A163**, 399 (1933)
811. Stranski, I.N., Wolf, G.: Research **4**, 15 (1951)
812. Strnad, Z.: Glass-Ceramic Materials. Elsevier, Amsterdam (1986)
813. Stricland-Constable, R.F.: Kinetics and Mechanism of Crystallization. Academic, London/New York (1968)
814. Swift, H.R.: J. Am. Ceram. Soc. **30**, 165 (1947)
815. Szilard, L.: Z. Phys. **53**, 840 (1929)
816. Tabata, K.: J. Am. Ceram. Soc. **10**, 6 (1927)
817. Tammann, G.: Kristallisieren und Schmelzen. J.A. Barth-Verlag, Leipzig (1903)
818. Tammann, G.: Die Aggregatzustände. Leopold Voss Verlag, Leipzig (1922)
819. Tammann, G.: Ann. Phys. **5**(5), 107 (1930)
820. Tammann, G.: Der Glaszustand. Leopold Voss Verlag, Leipzig (1933)
821. Tammann, G., Jenckel, E.: Z. Anorg. Allg. Chem. **193**, 76 (1930)
822. Tammann, G., Hesse, W.: Z. Anorg. Allg. Chem. **156**, 245 (1926)
823. Tammann, G., Starinkevich, J.: Z. Phys. Chem. **85**, 573 (1913)
824. Tarassov, V.V.: Dokl. Akad. Nauk USSR **46**, 22 (1945); **46**, 117 (1945); **54**, 803 (1946)
825. Tarassov, V.V.: New Problems of the Physics of Glass. Gosstroiizdat, Moscow (1956, in Russian)
826. Tashiro, M.: Nucleation and Crystal Growth in Glasses. In: Proceedings of the 8-th International Congress on Glass, London, 1968, Society Glass Technology, Sheffield, p. 113 (1969)
827. Tashiro, M.: J. Non Cryst. Solids **73**, 575 (1985)
828. Temkin, D.E.: In: Sirota, N.N. (ed.) Crystallization and Phase Transitions, p. 249. Academy of Sciences of Belorussia Press, Minsk (1962, in Russian)
829. Thilo, E.: Forschungen und Fortschritte **29**, 161 (1955)
830. Thilo, E.: Silikattechnik **6**, 1 (1955)
831. Thilo, E.: Chem. Technol. **10**, 70 (1958)
832. Thilo, E., Wicker, C., Wicker, W.: Silikattechnik **15**, 109 (1964)
833. Thomfor, E., Volmer, M.: Ann. Phys. **33**, 109, 124 (1938)
834. Thomson, W.: Proc. R. Soc. Edinb. **7**, 63 (1870); Phil. Mag. **42**, 448 (1871)
835. Thomson, J.J.: Conduction of Electricity Through Gases, 2nd edn. Cambridge University Press, Cambridge (1906)
836. Tilton, L.W.: J. Natl. Bur. Stand. **59**, 139 (1957)
837. Timura, S., Yokogawa, T., Niwa, K.: J. Chem. Thermodyn. **7**, 633 (1975)
838. Tobolsky, A.V.: Properties and Structure of Polymers. Wiley, New York (1960)
839. Tobolsky, A., Powel, P., Eyring, H.: In: Kargin, V.A. (ed.) The Chemistry of High Polymer Molecules, vol. 2. Inostrannaya Literature Publishers, Moscow (1948, in Russian)
840. Todes, O.M.: Zh. Fiz. Khim. (USSR) **14**, 1224 (1940)
841. Tokuyama, M., Kawasaki, K.: Physica **A 123**, 386 (1984)

842. Tolman, R.C.: J. Chem. Phys. **16**, 758 (1948)
843. Tolman, R.C.: J. Chem. Phys. **17**, 333 (1949)
844. Tool, A.Q.: J. Am. Ceram. Soc. **29**, 240 (1946)
845. Tool, A.Q., Eichlin, C.: J. Am. Ceram. Soc. **14**, 276 (1931)
846. Tool, A.Q., Hill, E.F.: J. Soc. Glass Technol. **9**, 185 (1925)
847. Toschev, S.: Processes of phase formation in electrolytic deposition of metals. Ph.D. thesis, Bulgarian Academy of Sciences, Sofia (1969)
848. Toschev, S.: Equilibrium forms. In: Hartmann, P. (ed.) Crystal Growth: An Introduction, p. 328. North-Holland, Amsterdam (1973)
849. Toschev, S., Gutzow, I.: Phys. Stat. Solidi **21**, 683 (1967)
850. Toschev, S., Gutzow, I.: Phys. Stat. Solidi **24**, 349 (1967)
851. Toschev, S., Gutzow, I.: Krist. Tech. **7**, 43 (1972)
852. Toschev, S., Paunov, M., Kaischew, R.: Commun. Dep. Chem. (Bulgarian Academy of Sciences) **1**, 119 (1968)
853. Treloar, L.: The Physics of Rubber Elasticity. Clarendon Press, Oxford (1949)
854. Trinkaus, H., Yoo, M.H.: Philos. Mag. **A55**, 269 (1987)
855. Trömel, M.: Z. Kristallogr. **183**, 15 (1988)
856. Tropin, T.V., Schmelzer, J.W.P., Schick, C.: On the dependence of the properties of glasses on cooling and heating rates: II. Prigogine-Defay ratio, fictive temperature and fictive pressure. J. Non Cryst. Solids **357**, 1303–1309 (2011)
857. Tropin, T.V., Schmelzer, J.W.P., Gutzow, I., Schick, C.: On the theoretical determination of the Prigogine-Defay ratio in glass transition. J. Chem. Phys. **136**, 124502 (2012)
858. Turnbull, D.: J. Appl. Phys. **20**, 411 (1949)
859. Turnbull, D.: J. Appl. Phys. **21**, 1022 (1950)
860. Turnbull, D.: J. Chem. Phys. **20**, 411 (1952)
861. Turnbull, D.: Phase Changes. In: Seitz, S., Turnbull, D. (eds.) Solid State Physics, vol. 3, p. 225. Academic Press, New York (1965)
862. Turnbull, D.: Contemp. Phys. **10**, 473 (1969)
863. Turnbull, D., Cech, R.I.: J. Appl. Phys. **21**, 804 (1950)
864. Turnbull, D., Cohen, M.H.: J. Chem. Phys. **29**, 1049 (1958)
865. Turnbull, D., Cohen, M.H.: Crystallization kinetics and glass-formation. In: Mackenzie, J.D. (ed.): Modern Aspects of the Vitreous State, p. 38. Butterworths, London (1960)
866. Turnbull, D., Fisher, J.C.: J. Chem. Phys. **17**, 71 (1949)
867. Turnbull, D., Vonnegut, B.: Ind. Eng. Chem. **44**, 1292 (1952)
868. Turski, L.A.: Acta Phys. Pol. **A75**, 111 (1989)
869. Überreiter, K., Bruns, W.: Ber. Bunsenges. Phys. Chem. **68**, 541 (1964); **70**, 17 (1966)
870. Überreiter, K., Bruns, W., Brenner, A.B.: Naturwissenschaften **49**, 466 (1962)
871. Ubbelohde, A.R.: Melting and Crystal Structure. Clarendon Press, Oxford (1965)
872. Uhlmann, D.R.: J. Non Cryst. Solids **7**, 337 (1972)
873. Uhlmann, D.R.: J. Non Cryst. Solids **25**, 42 (1977)
874. Ulbricht, H., Schmelzer, J., Mahnke, R., Schweitzer, F.: Thermodynamics of Finite Systems and the Kinetics of First-Order Phase Transitions. Teubner, Leipzig (1988)
875. Umanski, Y.S. et al.: Physical Metallurgy. Metallurgy Press, Moscow (1955, in Russian)
876. Urnes, S.: Trans. Br. Ceram. Soc. **60**, 85 (1961)
877. van Laar, J.: Die Thermodynamik einheitlicher Stoffe und binärer Gemische. Noordhoff, Groningen (1936)
878. van der Merwe, J.: In: Hermann, H. (ed.) Treatise on Materials Science and Technology. Academic, London (1973)
879. van der Waals, J.D.: Thesis, Leiden (1873)
880. van der Waals, J.D.: Die Kontinuität des gasförmigen und flüssigen Zustandes, 2. Auflage. Johann Ambrosius Barth, Leipzig (1899–1900). The first Dutch edition of this book was published in 1893
881. van der Waals, J.D., Kohnstamm, P.: Lehrbuch der Thermodynamik. Johann Ambrosius Barth, Leipzig und Amsterdam (1908 and 1912, 2 volumes)

882. van Wazer, J.R.: Phosphorus and its Compounds, vol. 1. Interscience Publishers, New York (1958)
883. Ventzel, E.S.: Theory of Probability. Nauka, Moscow (1969, in Russian)
884. Verma, A.R.: Crystal Growth and Dislocations. Butterworth Science Publishers, London (1953)
885. Vergano, P.J., Uhlmann, D.R.: Phys. Chem. Glass. **11**, 30, 39 (1970)
886. Vetter, K.J.: Electrochemical Kinetics. Academic, New York (1967)
887. Vogel, W.: Phys. Z. **22**, 645 (1921)
888. Vogel, W.: Struktur und Kristallisation der Gläser. Deutscher Verlag für Grundstoffindustrie, Leipzig, (1965, 1971)
889. Vogel, W.: Glaschemie. Deutscher Verlag fürGrundstoffindustrie, Leipzig (1979)
890. Vogelsberger, W.: J. Colloid Interface Sci. **88**, 17 (1982)
891. Volkenstein, M.V.: Configurational Statistics of Polymer Chains. Academy of Sciences USSR Publishing House, Moscow, Leningrad (1959, in Russian)
892. Volkenstein, M.V., Ptizyn, O.B.: JETF (USSR) **26**, 2204 (1956)
893. Volkmann, K.G., Knorr, K.: Surf. Sci. **221**, 379 (1989)
894. Volmer, M.: Kinetik der Phasenbildung. Th. Steinkopff, Dresden (1939)
895. Volmer, M., Marder, M.: Z. Phys. Chem. **A 154**, 97 (1931)
896. Volmer, M., Weber, A.: Z. Phys. Chem. **119**, 227 (1926)
897. von Neumann, J.: Mathematische Grundlagen der Quantenmechanik. Springer, Berlin (1932)
898. von Smoluchowski, M.: Phys. Z. **17**, 557, 585 (1916)
899. von Smoluchowski, M.: Z. Phys. Chem. **92**, 129 (1917)
900. von Weimarn, P.P.: Chem. Rev. **2**, 217 (1926)
901. Voorhees, P.W.: J. Stat. Phys. **38**, 231 (1985)
902. Voorhees, P.W., Glicksman, M.E.: Acta Met. **32**, 2001, 2013 (1984)
903. Vukalovich, M.P., Novikov, I.I.: Technical Thermodynamics. Energy State Press, Moscow/Leningrad (1952, in Russian)
904. Wagner, C.: Z. Elektrochem. **65**, 581 (1961)
905. Wagstaff, F.F.: J. Am. Ceram. Soc. **52**, 650 (1969)
906. Wakeshima, H.: J. Chem. Phys. **22**, 1614 (1954)
907. Walton, D.: J. Chem. Phys. **37**, 2182 (1962)
908. Walton, A.G.: Nucleation in Liquids and Solutions. In: Zettlemoyer, A.C. (ed.): Nucleation, p. 225. Marcel Decker, New York (1969)
909. Warren, B.E.: J. Appl. Phys. **8**, 645 (1937)
910. Warren, B.E.: J. Am. Ceram. Soc. **24**, 256 (1941)
911. Warren, B.E., Biscoe, J.: J. Am. Ceram. Soc. **21**, 259 (1938)
912. Wäsche, R., Brückner, R.: J. Non Cryst. Solids **27**, 80 (1968)
913. Waterton, H.J.: J. Soc. Glass Technol. **16**, 244 (1932)
914. Wegener, P.P., Parlange, J.Y.: Naturwissenschaften **57**, 525 (1970)
915. Wells, A.F.: Structural Inorganic Chemistry, 4th edn. Clarendon Press, Oxford (1975)
916. Westerhoff, T., Feile, R.: Ramann scattering from CN orientational glasses. In: Hunklinger, S. et al. (eds.) Phonons, p. 603. World Scientific, Singapore (1990)
917. Westmann, A.E.R., Crowther, J.: J. Am. Ceram. Soc. **37**, 420 (1954)
918. Westmann, A.E.R., Krishnamurthy, M.: Kinetics of reorganization, nucleation and crystallization in sodium phosphate glasses. In: Reger, M.K., Smith, G., Insley, A. (eds.) Symposium on Nucleation and Crystallization in Glasses and Melts, p. 91. American Ceramic Society, Columbus, Ohio (1962)
919. Weyl, W.A., Marboe, E.C.: The Constitution of Glasses, vol. 1. Interscience Publishers, New York-London, (1962); vol. II/1 (1964); vol. II/2 (1967)
920. Whittaker, E.J.W.: Geochimica et. Cosmochimica Acta **31**, 2275 (1967)
921. Wiekert, H., Maus, E., Knorr, K.: Jpn. J. Appl. Phys. **26**(suppl. 263), 889 (1987)
922. Wilkinson, W.L.: Non-Newtonian Fluids. Pergamon Press, New York (1960)
923. Wilks, J.: The Third Law of Thermodynamics. Oxford University Press. Oxford (1961)
924. Williams, M.L., Landel, R.F., Ferry, J.D.: J. Am. Chem. Soc. **77**, 3701 (1955)

925. Williamson, E.D., Adams, L.H.: J. Franklin Inst. **190**, 597, 835 (1920)
926. Winkelmann, A., Schott, O.: Ann. Phys. **51**, 697 (1894); **51**, 730 (1894)
927. Winkler, C.: J. Prakt. Chem. (2), 31, 247 (1885)
928. Winter, A.: J. Am. Ceram. Soc. **40**, 54 (1957)
929. Winter-Klein, A.: J. Am. Ceram. Soc. **26**, 189 (1943)
930. Witzel, R.: Z. Anorg. Allg. Chem. **64**, 71 (1921)
931. Woodcock, L.V.: J. Chem. Soc. Faraday Trans. **72**, 1667 (1976)
932. Woodruff, D.P.: The Solid-Liquid Interface. Cambridge University Press, Cambridge (1973)
933. Wu, D.T.: J. Chem. Phys. **97**, 2644 (1992)
934. Wunderlich, B.: J. Phys. Chem. **64**, 1052 (1960)
935. Wunderlich, B.: Macromolecular Physics, vol. 1–3. Academic, New York/San Francisco/London (1973, 1976, 1980)
936. Yinnon, H., Uhlmann, D.R.: J. Non Cryst. Solids **54**, 253 (1983)
937. You, H., Faine, S.C., Satiga, S., Passell, L.: Phys. Rev. Lett. **56**, 244 (1986)
938. Young, D.: Decomposition of Solids. Pergamon Press, London (1966)
939. Yourgreau, W., van der Merwe, A., Raw, G.: Treatise on Irreversible and Statistical Thermophysics. Dover, New York/London (1966)
940. Yuritsyn, N.S., Fokin, V.M., Kalinina, A.M., Filipovich, V.N.: In: Proceedings Symposium of the American Ceramical Society on Nucleation and Crystallization in Glasses and Liquids, Atlanta (1992)
941. Zachariasen, W.H.: J. Am. Chem. Soc. **54**, 3841 (1932)
942. Zachariasen, W.H.: Phys. Rev. **(2), 39**, 185 (1932)
943. Zachariasen, W.H.: Glastech. Ber. **11**, 120 (1933)
944. Zakis, Y.P.: Defects in the Vitreous State of Matter. Zinatne Publishers, Riga (1984, in Russian)
945. Zanotto, E.D., James, P.F., Craevich, A.F.: Bull. Miner. **106**, 169 (1983)
946. Zanotto, E.D., James, P.F.: J. Non Cryst. Solids **74**, 373 (1985)
947. Zanotto, E.D.: J. Non Cryst. Solids **129**, 183 (1991)
948. Zanotto, E.D., Müller, E.: J. Non Cryst. Solids **130**, 220 (1991)
949. Zeldovich, Y.B.: Sov. Phys. JETP **12**, 525 (1942); Acta Physicochim. USSR **18**, 1 (1943)
950. Zeldovich, Y.B., Myschkis, A.D.: Elements of Applied Mathematics. Nauka, Moscow (1965)
951. Zeller, R.C., Pohl, R.O.: Phys. Rev. **B 4**, 2029 (1971)
952. Zener, C.: J. Appl. Phys. **20**, 950 (1949)
953. Zernicke, F., Prins, J.: Z. Phys. **41**, 184 (1927)
954. Zettlemoyer, A.C. (ed.): Nucleation. Marcel Decker, New York (1969)
955. Zettlemoyer, A.C. (ed.): Nucleation Phenomena. Adv. Colloid Interface Sci. **7** (1977)
956. Zhdanov, G.S.: Physics of Solids. Moscow University Press, Moscow (1961, in Russian)
957. Zhurkov, S., Levin, B.: Special volume of papers dedicated to the 70th birthday of Academician A.F. Joffe, Izd, p. 260. AN SSSR (1950)
958. Zhuravlev, E., Schmelzer, J.W.P., Wunderlich, B., Schick, C.: Kinetics of Nucleation and Crystallization in Poly(ε-Caprolactone) (PCL). Polymer **52**, 1983–1997 (2011)
959. Ziabicki, A.: J. Chem. Phys. **48**, 4368 (1968)
960. Ziman, J.M.: Models of Disorder. Cambridge University Press, Cambridge (1979)
961. Zschimmer, E., Dietzel, A.: Z. Techn. Phys. **278**, 6 (1926)
962. Zvetkov, V.N., Eskin, V.E., Frenkel, C.Y.: Structure of Macromolecules in Solutions. Nauka, Moscow (1964, in Russian)

Index

I.S. Gutzow and J.W.P. Schmelzer, *The Vitreous State*,
DOI 10.1007/978-3-642-34633-0, © Springer-Verlag Berlin Heidelberg 2013